2
11/27/95 (8)

DOE/METC-95/1017, Vol. 2
(DE95009704)
CONF-950494--Vol.2

Proceedings of the Natural Gas RD&D Contractors Review Meeting Volume II

Rodney D. Malone

April 1995

Co-Hosted by

U.S. Department of Energy
Office of Fossil Energy
Morgantown Energy Technology Center

and

Southern University and
Agricultural and Mechanical College

DISTRIBUTION OF THIS DOCUMENT IS UNLIMITED

Disclaimer

This report was prepared as an account of work sponsored by an agency of the United States Government. Neither the United States Government nor any agency thereof, nor any of their employees, makes any warranty, express or implied, or assumes any legal liability or responsibility for the accuracy, completeness, or usefulness of any information, apparatus, product, or process disclosed, or represents that its use would not infringe privately owned rights. Reference herein to any specific commercial product, process, or service by trade name, trademark, manufacturer, or otherwise does not necessarily constitute or imply its endorsement, recommendation, or favoring by the United States Government or any agency thereof. The views and opinions of authors expressed herein do not necessarily state or reflect those of the United States Government or any agency thereof.

This report has been reproduced directly from the best available copy.

Available to DOE and DOE contractors from the Office of Scientific and Technical Information, 175 Oak Ridge Turnpike, Oak Ridge, TN 37831; prices available at (615) 576-8401.

Available to the public from the National Technical Information Service, U.S. Department of Commerce, 5285 Port Royal Road, Springfield, VA 22161; phone orders accepted at (703) 487-4650.

DOE/METC-95/1017, Vol. 2
(CONF-950494)--Vol. 2
(DE95009704)
Distribution Category UC-109
UC-110
UC-131
UC-132
UC-133

Proceedings of the Natural Gas RD&D Contractors Review Meeting Volume II

Editor
Rodney D. Malone

Co-Hosted by

U.S. Department of Energy
Morgantown Energy Technology Center
P.O. Box 880
Morgantown, WV 26507-0880
(304) 285-4764
FAX (304) 285-4403/4469

and

Southern University and
Agricultural and Mechanical College
Southern Branch Post Office
Baton Rouge, LA 70813

April 4-6, 1995

MASTER

DISTRIBUTION OF THIS DOCUMENT IS UNLIMITED

Contents

Volume I

Volume II

Session 3B — Natural Gas Upgrading: Low-Quality Natural Gas

Session 4B — Natural Gas Storage

Poster Session

Session 7 — Drilling, Completion, and Stimulation

Appendices

Session 3B

Natural Gas Upgrading — Low-Quality Natural Gas

3B.1 Upgrading Low-Quality Natural Gas By Means of Highly Performing Polymer Membranes

CONTRACT INFORMATION

Contract Number	**DE-FG21-91MC28072**
Contractor	**Syracuse University** **Dept. of Chemical Engineering and Materials Science** **Syracuse, New York 13244-1190** **(315) 443-4469 (Telephone)** **(315) 443-2559 (Fax)**
Other Funding Sources	**Gas Research Institute, Chicago, IL**
Contractor Project Manager	**S. Alexander Stern**
Principal Investigators	**S. A. Stern (PI)** **B. Krishnakumar** **A.Y. Houde**
METC Project Manager	**V. Venkataraman**
Period of Performance	**March 1, 1994 - February 28, 1995**

ABSTRACT

The objective of the present study is to assess the potential usefulness of membrane separation processes for removing acid gases (CO_2 and H_2S) from low-quality natural gas. Nonporous "dense" (homogeneous) membranes made from new, highly gas-selective polymers are being evaluated for this purpose. The project comprises gas permeability and separation measurements with CH_4/CO_2 and $CH_4/CO_2/H_2S$ mixtures having compositions in ranges found in low-quality natural gas. Process design studies and economic evaluations are also being made to determine the cost of upgrading low-quality natural gas with the most promising membranes. Until recently, the membranes used in this study were made from new types of polyimides synthesized in our laboratory. The polyimide membranes were found to exhibit a very high CO_2/CH_4 selectivity but a relatively low H_2S/CH_4 selectivity. Therefore, different types of polymers that exhibit a high H_2S/CH_4 selectivity are also being evaluated.

In studies performed up to now, binary CH_4/CO_2 mixtures containing 10 to 46 mole-% CO_2 and ternary $CH_4/CO_2/H_2S$ mixtures also containing up to 8 mole-% H_2S were used in the permeability and separation measurements with the polyimide membranes. All measurements were made at 95°F (35°C) and at "upstream" pressures ranging from 59 to 800 psia (4 to 54 atm). All polyimides are much more permeable to CO_2 and H_2S than to CH_4. As a result, CO_2

and H_2S are concentrated in the permeate whereas CH_4 is concentrated in the retentate.

A considerable amount of information was obtained on the CO_2/CH_4 and H_2S/CH_4 selectivity and on the permeability to CH_4, CO_2, and H_2S of the new polyimides. The CO_2/CH_4 selectivity of six of the eight polyimides studied so far is 2-3 times higher than that of cellulose acetate (CA), while the permeability to CO_2 of these polyimides is similar or higher than that of CA under comparable conditions. Asymmetric CA membranes are being widely used at present for upgrading crude natural gas and for separating CO_2 from mixtures with hydrocarbons in enhanced oil recovery operations.

The CO_2/CH_4 selectivity of the new polyimides decreases with increasing concentration of acid gases (CO_2 and H_2S) in the feed. For example, a CO_2/CH_4 selectivity of 94 was obtained with one of the polyimides at 95°F (35°C) and 147 psia (10 atm) when measured with a feed mixture containing (in mole-%) 87.5% CH_4, 9.7% CO_2, and 2.8% H_2S; this selectivity decreased by only about 15% when the concentration of acid gases in the feed was increased to 36.7% CO_2 and 8% H_2S. Interestingly, the CO_2/CH_4 selectivity is somewhat lower in the absence of H_2S. The CO_2/CH_4 selectivity either decreases slightly or in some cases is unaffected by an increase in the total feed pressure. However, the CO_2/CH_4 selectivity of the polyimides studied was in all cases significantly higher than that of CA under comparable conditions. The presence of H_2O vapor at concentrations of up to 0.75% (54% relative humidity) in feed mixtures did not affect the CO_2/CH_4 selectivity of the polyimides tested.

The extent of separation of binary CH_4/CO_2 and ternary $CH_4/CO_2/H_2S$ mixtures achievable with one of the most promising polyimide membranes was also measured at 95°F (35°C) and at 147 psia (10 atm) as a function of the "stage cut" (the fraction of the feed allowed to permeate through the membrane). In a typical measurement with a $CH_4/CO_2/H_2S$ feed mixture containing 10% CO_2 and 2.8% H_2S, the CO_2 concentration in the retentate could be reduced to the pipeline specification of 2% CO_2 at a stage cut of only 0.1. The H_2S concentration could not be reduced to pipeline specification (4 ppm) at this stage cut.

Process design studies and economic evaluations of membrane processes for upgrading low-quality natural gas were made using the selectivity and permeability data obtained with four of the most promising polyimide membranes examined thus far. Single-stage processes as well as multistage processes with product recycle were considered. Upgrading processes utilizing membranes fabricated from any of four polyimides considered in the process design study were found to be significantly more economical than a comparable process using CA membranes. The estimated savings in feed processing costs range from 30% to 60%. These savings result from lower capital investment costs, lower CH_4 losses, and lower compressor power requirements.

As shown above, several polyimides synthesized in this laboratory are very promising membrane materials for the removal of CO_2 from low-quality natural gas. However, these polymers have a relatively low H_2S/CH_4 selectivity of 15-19 at 95°F (35°C), and hence are not as effective in removing H_2S from natural gas. Therefore, a new membrane separation process capable of effectively removing both CO_2 and H_2S is now being studied experimentally and by process design simulations. This process will consist of two membrane permeation stages

connected in series, one stage containing a highly CO_2-selective membrane, such as made from the new polyimides, and the other from a highly H_2S-selective membrane. Such a process configuration will yield two permeate streams, one enriched in CO_2 and the other in H_2S, which would be amenable to further processing. The CH_4 will be enriched, as before, in the retentate. Preliminary process design simulations and economic assessments show that:

(1) At low concentrations of CO_2 (< 20 mole-%) in the feed, it is more cost-effective for the CO_2-selective membrane stage to precede the H_2S-selective stage. The opposite is true in cases where the CO_2 concentration in the feed is ≥ 20 mole-%, i.e., processing costs are lower when the H_2S-selective stage is the first of the two stages, and

(2) The cost for upgrading natural gas using either of the two configurations *decreases* with increasing concentration of CO_2 in the feed.

These simulations assumed that the H_2S-selective membrane is made from a block copolymer of polyether and polyamide reported to have a H_2S/CH_4 selectivity of 190 (1). Membrane processes using CA membranes are not economical for upgrading natural gas streams containing more than about 1 mole-% of H_2S to pipeline specifications.

(1) J. Pinnau, S.V. Segelke, R.P. Castro, and J.G. Wijmans, Paper presented at 5th Annual Meeting of the North American Membrane Society, Lexington, KY, May 17-20, 1992.

3B.2 Evaluation of High Efficiency Gas-Liquid Contactors for Natural Gas Processing

CONTRACT INFORMATION	DE-FC21-92MC28178
Contractor	Institute of Gas Technology 1700 S. Mt. Prospect Road Des Plaines, Illinois 60018
Other Funding Sources	Gas Research Institute IGT's Sustaining Membership Program
Contractor Project Manager	Anthony L. Lee
Principal Investigators	Nagaraju Palla Anthony L. Lee
METC Project Manager	Harold D. Shoemaker
Period of Performance	October 1, 1992 to September 30, 1995

Schedule and Milestone

FY 95 Program Schedule

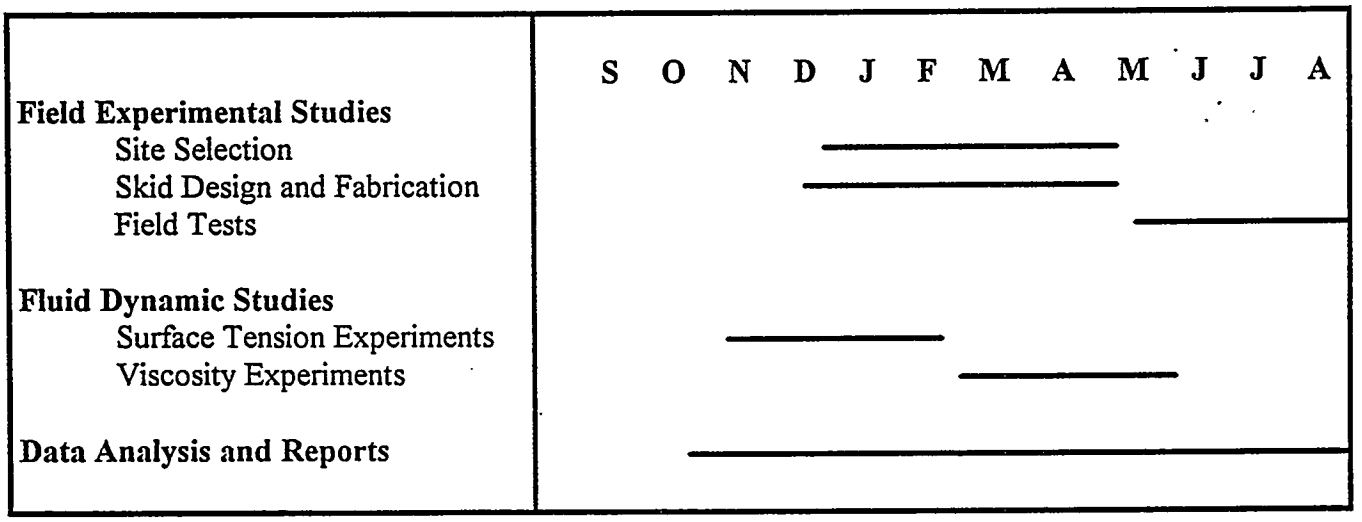

OBJECTIVES

The objectives of this program are to develop and evaluate advanced processing technologies that can reduce the cost of upgrading sub quality natural gas to pipeline standards. The successful application of cost-effective, new technologies will facilitate the production of sub quality natural gas that otherwise would be too expensive to produce. The overall program is focused on the following activities:

- evaluation of the potential of structured packing for the removal of acid gases from natural gases,

- expansion of the currently available database of the fluid dynamics of rotating gas liquid contactors.

BACKGROUND INFORMATION

Almost all of the natural gas produced in the United States is subjected to some form of processing before it is introduced into the pipeline system. Approximately 50% of the gas processed requires only dehydration while the processing for the remainder is more extensive and dependent upon the constituents that must be removed to meet pipeline standards. Currently, there are more than 1200 natural gas dehydration facilities in operation in the United States and over 600 other natural gas processing plants being operated to do gas treating and sulfur recovery. It has been estimated that during the period 1995 - 2000, approximately 600 new dehydration facilities will be required along with an additional 200 gas treating and sulfur recovery plants will be placed in operation to meet the meet the demand for natural gas and accommodate the new resources being produced (1). A survey conducted in 1993 indicated that the expenditure of approximately $1.7 Billion would be required for new facilities over the next 10 year period to meet the projected natural gas demands (1). New technologies that can reduce the cost of gas processing will help insure the availability of natural gas at prices competitive with other energy options.

In addition to the requirement for new facilities, frequently there are needs for revamping or debottlenecking the existing plants as the requirements for processing change because of such factors as increased demand, changes in feed gas composition or changes in feed gas pressure.

Because most of the constituents (i.e. carbon dioxide, hydrogen sulfide and water vapor) being removed from natural gas are themselves gaseous at usual process conditions, gas-liquid contacting is a fundamental step in most processes. Higher efficiency gas-liquid contacting elements can have a marked impact on the size of processing elements, the weight of the units, the operating limits of these elements, solvent selection, operating costs and capital costs.

Structured Packing

Structured packings, in contrast to random packings, provide for the organized contacting of the liquid and gas streams throughout a column. Liquid flows as a thin film down individual surfaces set at a constant angle to the gas flow where the capillary action of the material or surface treatment of the material contributes to the uniform spreading of the liquid. As a result of these flow patterns, intimate contact is provided between the gas and liquid phases, "by-pass" is minimized, mass transfer is enhanced, the onset of flooding is delayed, there is reduced gas-liquid drag and, as a result, lower pressure drops than that required for a random packing.

The capacity of structured packings is higher than the capacity of tray contactors or dumped packing for a given efficiency. Depending on the

physical properties of the solvent and the operating conditions, the structured packings can offer capacity increases of 80% or more (2). An important aspect of this increased efficiency is that equilibrium conditions can be more closely approached which can translate into a reduction in the circulation rate of the absorption media.

The potential benefits of expanding the use of structured packings for natural gas processing is demonstrated by the information available from two different applications.

In a natural gas dehydration plant, ARCO Oil and Gas Company achieved excellent performance with structured packing at pressure of 1000 psig and higher. For this application, ARCO was able to reduce the column size by 62%, vessel weights by 50%, internal weights by 50%, and costs by 30% compared to conventional contactors.

The application of structured packings to the processing of natural gas containing both CO_2 and H_2S at a combined concentration of approximately one percent has been examined in a study considering both a structured packing design and a tray column design. They concluded that the height of the tray column would be 52.5 feet with a diameter of 3.6 feet. The column with the structured packing would be 36.1 feet with a diameter of 2.3 feet. For both designs, the H_2S concentration in the exit gas was 2 ppm. However, the structured packing column had slipped 90% of the CO_2 while the tray column had slipped only 60% (3).

While the use of structured packings has been incorporated into some gas processing applications, it has yet to be successfully applied in the United States for natural gas sweetening. This application is one of the focal points of the current R&D program in progress at the INSTITUTE OF GAS TECHNOLOGY (IGT).

Rotating gas-liquid contactor

The rotating gas-liquid contactor was conceived by Colin Ramshaw of Imperial Chemical Industries (ICI) of Great Britain in the mid-1970's. The original work investigated the validity of a modified Sherwood Correlation to predict flooding in enhanced gravity contactors and demonstrated that significant enhancements of mass transfer coefficients could be realized under same flow and rotational conditions. In 1984, Glitsch Inc. was granted exclusive rights to develop and market the ICI rotating contactor technology on a world wide basis.

A rotary contactor, depicted in Figure 1, uses a rotating bed of high specific surface area and high voidage packing to promote intense gas-liquid mixing and disengagement in a counter current flow configuration. Liquid is introduced at the inner radius and accelerated outward through the packing. Gas is introduced at the outer radius and flows inwardly across the rotor, exiting at the inner radius. Packings with specific surface areas as high as 40 cm^2/cm^3 and void fractions of 0.92 have been studied. Rotational speeds providing centrifugal forces up to the equivalent of 100 g's have been investigated.

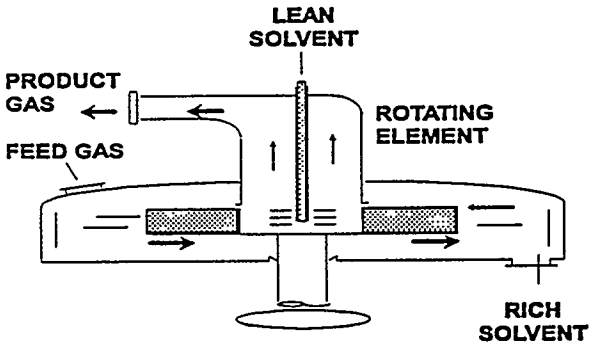

Figure 1. Schematic Diagram of Rotating Contactor

Rotating gas-liquid contactors have been successfully used by the U.S. Coast Guard to air-strip aromatics from ground water at atmospheric pressure and proprietary experiments have been carried out to evaluate the possible application of the technology to bulk CO_2 removal from natural gas, natural gas dehydration and selective H_2S removal from natural gas containing both CO_2 and H_2S. In addition, the use of a rotating contactor for distillation operations is under investigation at the University of Texas. Currently, rotating gas-liquid contactors are not in use in the natural gas processing industry.

Mass transfer studies with a centrifugal contactor have shown that the operational environment provided in the contactor result in transfer heights of 2.5 **centimeters** compared to the transfer heights of 1.25 to 2 **feet** for conventional column contactors. These significantly smaller heights of transfer units lead to large reductions in the physical size of a unit to effect a given separation. A preliminary engineering design study indicated that a processing duty requiring a conventional packed column diameter of 4.5 feet and height of 45 feet (715 cubic feet of packing) could be accomplished using a rotor with an outer diameter of 39 inches, an inner diameter of 14 inches and an axial length of 18 inches (10 cubic feet of packing).

Based on the studies to date and the available data, rotary contacting devices appear to offer the following advantages over conventional contactors:

- Small size, low profile
- Low weight
- Low liquid hold-up
- Insensitive to motion and orientation
- Rapidly attains steady state
- Easily emptied and cleaned
- Easily transported

While a number of applications have been explored experimentally, a review of the available information and the data in the open literature has indicated that an expansion of the existing data base will facilitate the optimization of rotating gas-liquid contactors for natural gas processing application. Expansion of this data base to better characterize the fluid dynamic behavior of a rotating contactor as a function of operating variables and liquid properties is part of the overall objectives of the program now in progress at IGT.

PROJECT DESCRIPTION

Structured Packing

The effectiveness of using structured packing for acid gas removal in natural gas sweetening applications is being evaluated through a series of field tests. A 10 GPM skid-mounted amine unit has been designed and is under construction. The skid will incorporate a nominal 8 inch diameter structured packing absorption column. The unit will have a gas processing capacity ranging from 0.25 - 1.25 million SCFD depending on the acid gas content of the feed gas.

A team consisting of the program sponsors (DOE, GRI and IGT's SMP), a structured packing manufacturer (KOCH) and a solvent manufacturer (Huntsman) has been formed to both oversee the planned tests and provide materials for the program. It is anticipated that testing will be conducted at three different sites - each site providing a different quality of natural gas for testing. Three sites located in Texas are currently under consideration. These sites would provide a range of sub quality natural gas for processing with low acid gas concentrations (2 to 5%), medium acid gas concentration (5 to 15%), and a high acid gas concentration (>15%).

In conjunction with the structured packing field tests, a series of experiments will be conducted to evaluate the effectiveness N-formyl morpholine as an absorbent for acid gas removal from sub quality natural gas. N-formyl-morpholine (NFM), a potential physical absorbent for acid gases, is being studied at IGT under a program jointly funded by the Gas Research Institute and the IGT SMP program. Laboratory experiments indicate that NFM/H_2O mixtures have the potential to be cost effective solvents for removing CO_2 and H_2S from natural gas under same process conditions. By conducting parallel experiments, the performance of NFM as an absorbent can be compared directly with the amine solvents being used in the structured packing field tests.

Rotating gas-liquid contactor

Expansion of the available data base on the hydraulic characteristics of a rotating gas-liquid contactor is being pursued through a series of laboratory experiments. A 100 GPM, low pressure rotary contactor system has been assembled at IGT's Energy Development Center to examine the fluid dynamic behavior of this type of contactor. The studies are determining the effects of liquid viscosity, liquid surface tension and operating conditions on liquid residence times and flooding limits.

The rotor has an outer diameter of 80 cm, an inner diameter of 25.4 cm and an axial height of 12.7 cm. The rotor packing is metallic with a specific surface area of 25 cm^2/cm^3 and a volume void fraction of 0.95. The unit can be operated at rotational speeds in the range of 600-1200 RPM and can provide induced accelerations of the order of 100 g's at the inner radius.

The unit is equipped with two conductivity probes which respond to the presence of a pulse of a salt solution when it is injected into the liquid stream. One probe is located in close proximity to the inner radius of the rotor and the other is located immediately adjacent to the outer radius of the rotor. The conductivity transients detected by each probe, as the salt-liquid pulse passes, are continuously recorded by the data acquisition system.

Over 60 experiments have been conducted to determine the flooding characteristics of the unit as a function of rotational speed. Other experiments have been conducted to determine residence time data using simulated solvents ranging from 40 - 70 dynes/cm.

RESULTS

Structured packing

The natural gas sweetening, structured packing field tests are scheduled to be conducted in calendar year 1995. Design, procurement and construction of the field test unit, shown in Figure 2, is proceeding on schedule. The results of these tests will be presented at a subsequent contractors' project review meeting.

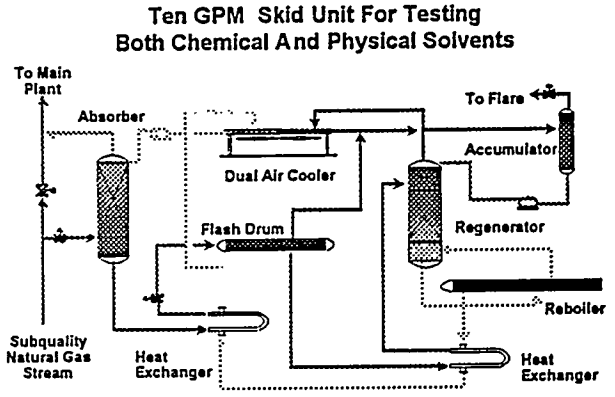

Figure 2. Flow Diagram for Field Skid

Rotating gas-liquid contactor

Flooding experiments

Flooding points were systematically determined by observing the pressure drop across the rotor for varying gas flow rates at a fixed liquid rate and a preset spin rate. The onset of flooding at the inner radius of the contactor is manifested in a change in the slope of the pressure drop vs. gas flow rate curve. Figure 3 is a typical plot of data obtained during a flooding point experiment.

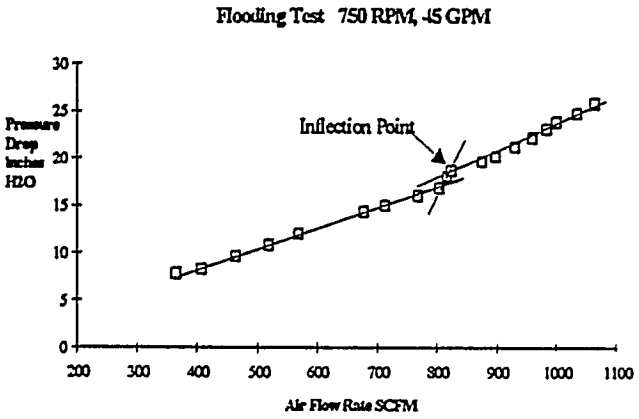

Figure 3. Typical Flooding Curve

The results of the flooding experiments have been compared with flooding predictions using the Sherwood flooding correlations and the experimental data reported by Singh (4). In his experimental studies, Singh used a rotor with internal dimensions and packing characteristics similar to those of the rotor used in the IGT experiments.

Figure 4 shows the experimental data obtained at spin rates of 750, 900 and 1200 RPM for the range of liquid flow rates and surface tensions investigated. The data are presented using the dimensionless groups associated with the Sherwood relationship where

$$F1 = \frac{U_G^2 \, a_p}{r_i \, \omega^2 \, \varepsilon^3}\left(\frac{\rho_G}{\rho_L}\right)\left(\frac{\upsilon_L}{\upsilon_W}\right)^{0.2}$$

where U_G = superficial gas velocity at ID

a_p = packing specific surface area

r_i = inner radius

ω = radians / s

ρ = density

υ = viscosity

ε = void fraction

subscripts L, G and W refer to liquid, gas and water

and $F2 = \frac{L}{G}\sqrt{\frac{\rho_G}{\rho_L}}$

where L and G denote liquid and gas mass flow rates per unit area at the inner radius.

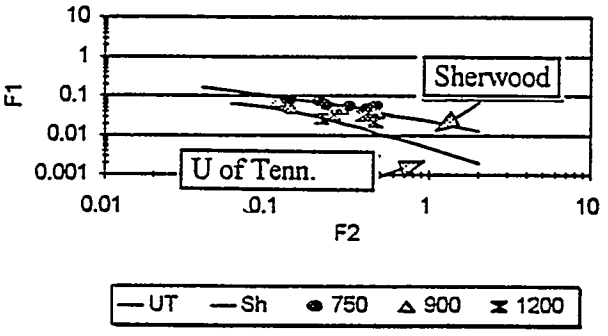

Figure 4. IGT Experimental Flooding Data, Operating Limit Curves

The data in the figure show that the Sherwood relationship considering the data for "dumped rings" effectively represents the IGT experimental

flooding at a spin rate of 750 RPM. However, at the higher spin rates the observed experimental flooding conditions fall below those associated with the "dumped ring" data and approach the operating curve developed by Singh as the spin rate increases to 1200 RPM.

Figure 5 compares the IGT experimentally determined gas flow rates associated with flooding and the gas flow rates predicted by the "dumped ring " flooding correlation for the experimental liquid rate and spin rate. At a spin rate of 750 RPM, the experimental data and the predicted gas flow rates are in good agreement. At the higher spin rates of 900 and 1200 RPM, the experimentally observed gas flow rates are significantly lower than those predicted by the "dumped ring" data.

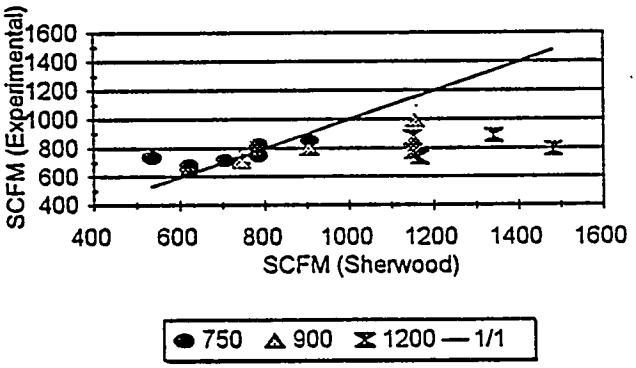

Figure 5. Flooding Data Comparison IGT vs. SHERWOOD

When examining these data, both the nature of the experiment and the parameters associated with the flooding correlations need to be considered. The term designated as "F1" assumes that the liquid is experiencing the centrifugal force associated with the rotating rotor. Once the liquid reaches and is, in effect, "captured" by the rotor, it will be accelerated by the centrifugal force. However, since there is a finite distance between the injector and the rotor face, there will be a short time during which the liquid is exposed to the high velocity gases without the benefit of the centrifugal forces associated with the rotor. In this initial volume, the liquid is likely to be in the form of droplets with diameters distributed over some range which is dependent on the geometry of the injector, the pressure drop across the injector orifices, the viscosity of the liquid and the surface tension of the liquid. As lower liquid flow rates are considered, the Sherwood flooding correlation would indicate that the system will accommodate higher gas throughputs. If entrainment of the liquid begins to occur in the space between the liquid injector and the inner radius of the rotor, overall system pressure drop variations will be encountered at gas velocities below those predicted by the Sherwood type correlations. Both the initial droplet diameter and the initial droplet velocity would be important in determining when this entrainment would occur.

Figure 6 presents the flooding data with spin rate as the parameter. Flooding boundaries, as defined by the Sherwood correlation, are shown as continuous line. The IGT experimental data are super imposed as individual data points. A comparison of the experimental data with the predicted flooding curves shows that as the liquid rate is decreased and, therefore, as the momentum of the liquid stream decreases, the difference between the expected gas velocity at flooding and the experimentally observed gas velocity increases. This difference becomes more pronounced at higher spin rates.

A series of tests was carried out to investigate the effect of surface tension on flooding. Liquid surface tensions were varied by the addition of a surfactant or the use of deionized tap water which could provide a liquid stream with a surface tension as high as 72 dynes/cm. The results of these tests are summarized in the following Table 1.

Table 1. Flooding Points

RPM	GPM	SCFM*	in H_2O
	49.0 dynes/cm		
900	30	995	19.5
900	90	750	23.3
1200	88	735	20.6
	61.2 dynes/cm		
900	30	845	17.1
900	90	710	21.5
1200	90	775	20.5

* denotes conditions at flood

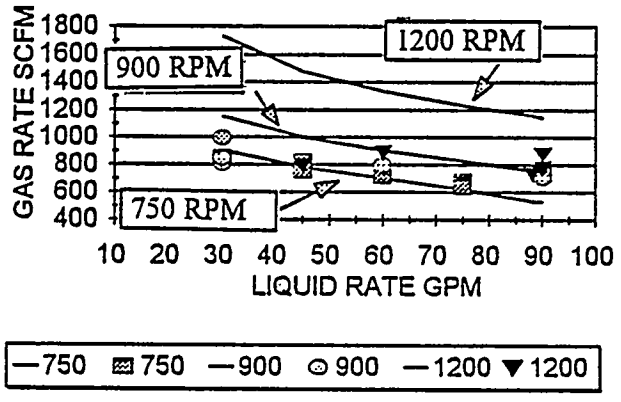

Figure 6. Flooding Data Comparison IGT vs SHERWOOD

While this data set is limited, the data suggest that the increase in surface tension from 49 dynes/cm to 61.2 dynes/cm resulted in the onset of flooding at lower gas rates with the attendant lower pressure drop at flood. Additional analyses is required to determine the extent of any relationship that may exist between liquid surface tension and flooding conditions.

Residence times

Figure 7 shows a typical set of the pulse records that are obtained during the liquid residence time experiments. With these records, it is possible to identify several characteristic times to describe the data. These include the differences in the times associated with initial changes in conductivity at each of the two probes (i.e. a first-to-first time), the differences in the times associated with the achievement of the maximum conductivity at each of the probes, a time that is characteristic of the dilution process and the difference in the concentration weighted average times for each of the pulses. The concentration weighted time for each pulse is computed according to the following:

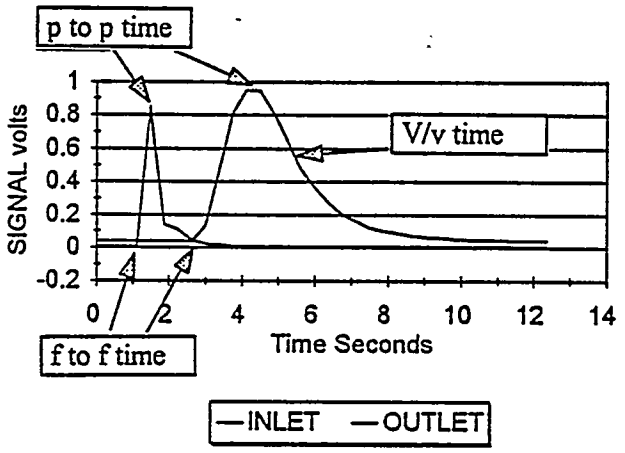

Figure 7. Typical Residence Time Tracing Curve

$$t_{avg} = \int (ct)dt \Big/ \int (c)dt$$

where t_{avg} = average time

and c and t denote concentration and time respectively.

The dilution process which represents the removal of the salt pulse from the rotor can be viewed in the context of a well stirred reactor.

This simplified model provides the following expression:

$$Log(C_r) = -\left(\frac{v}{V}\right)t + k$$

where C_r = salt concentration in rotor volume
v = volumetric flow rate
V= the volume being diluted
t = time
k = constant of integration

It should be noted that the term (v/V) is the reciprocal of the "plug flow" residence time for the volume V.

This expression suggests that the slope of the concentration (or conductivity) pulse plotted as the logarithm of the concentration vs. time will be related to the "plug flow" time provided the semi logarithmic relationship is linear. Figure 8 presents semi logarithmic plots for two of the downstream pulse that were recorded. For each pulse, a reasonably linear segment can be seen after the maximum voltage has been recorded. In almost all cases, a linear segment can be identified covering a period of several seconds. A linear regression analysis of these data segments included 10 to 20 data points and provided a basis for calculating (v/V) values. Correlation coefficients were in the range of 0.98 to >0.99 indicating a very high level of correlation.

During the experiments, each electrode was set to a different sensitivity in order to capture the conductivities on the same scale. As a result, no conclusions can be drawn with respect to the relative values of the two pulses. However, both electrodes were recording against the same time scale.

The overall reproducibility of the experimental data was found to be excellent. Six independent runs were carried out at 900 RPM, 90 GPM and gas flow rates of approximately 637 SCFM. An analysis of the integral residence times from these runs yielded a mean residence time of 3.3 seconds and indicated there was a 95.45 percent probability that the "true integral residence time" was between 3.28 and 3.39 seconds.

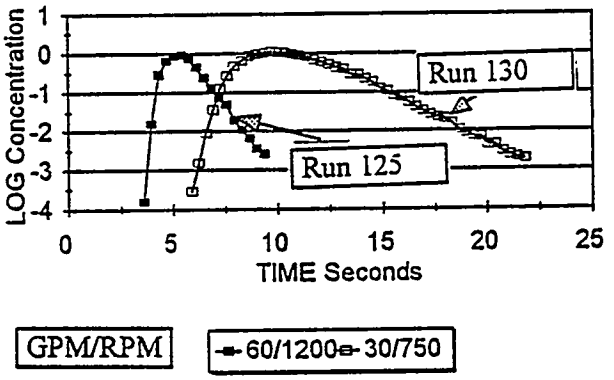

Figure 8. Tracer Response Logarithm Curve

The characteristic times obtained during residence time experiments are summarized in the Table 2 at the end of this paper. All duplicate runs have not been included. However, several are included and the general reproducibility of the data is apparent.

Figure 9 shows experimental characteristic times at constant spin rates and liquid flows as a function of gas flow rate. Both the integral times and the V/v times are presented. These data indicate that the integral times may have a weak, inverse dependence on gas flow rate over the range of flow rates studied; this dependence being more pronounced at the lower spin rates and lower liquid rates. The V/v times do not suggest any dependency on gas flow rates. This second order, or lack of, dependency of times on gas flow rate allows gas flow rate variations to be disregarded to a first approximation when examining the influence of other parameters on liquid residence times.

The pulse records shown in Figure 7 are typical of all conductivity traces in that each of the different characteristic times can be readily determined. The characteristics of these traces are such that they suggest the liquid, as it flows through the contactor has both a "plug flow" character and a "well stirred volume" character. If the liquid volume in the rotor responds to flow variations as a plug flow volume, the "first-to-first" times will represent the residence times and, for a square wave disturbance, the response pulse will also be square. However, if the liquid volume responds as a well stirred volume, a flow disturbance will be sensed immediately and the "first-to-first" time will be zero. The liquid residence time will the be characterized by the V/v time.

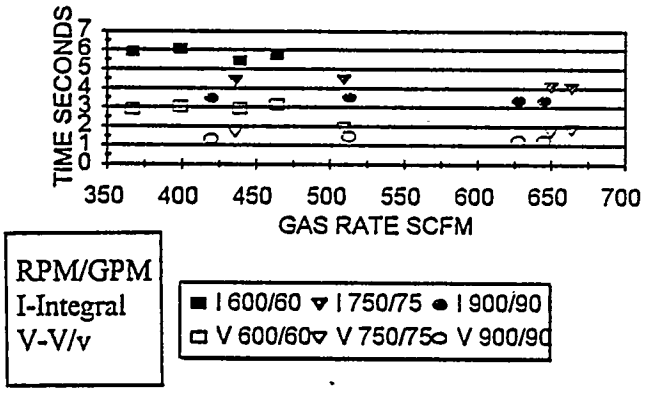

Figure 9. "L" Times vs Gas Rate (Integral & V/v Times)

Figure 10 compares the experimentally determined V/v times and the "first-to-first" times with liquid flow rate as the parameter. A one-to-one correlation line is included. This figure indicates that there are conditions where the "first-to-first" plug flow time and the V/v plug flow time are in good agreement. Data points to the right and below the "one-to-one" line are associated with experimental conditions which tend to produce lower liquid velocities and more back mixing occurring in the rotor.

Assuming that the V/v times can be interpreted as the characteristic plug flow time in the rotor, liquid hold up volumes can be calculated directly. These liquid hold up volumes are shown in Figure 11. Knowledge of the liquid holdup volumes is important because the holdup volumes will affect the mass transfer process, the pressure drop through the rotor and impact the effectiveness of any selective absorption application.

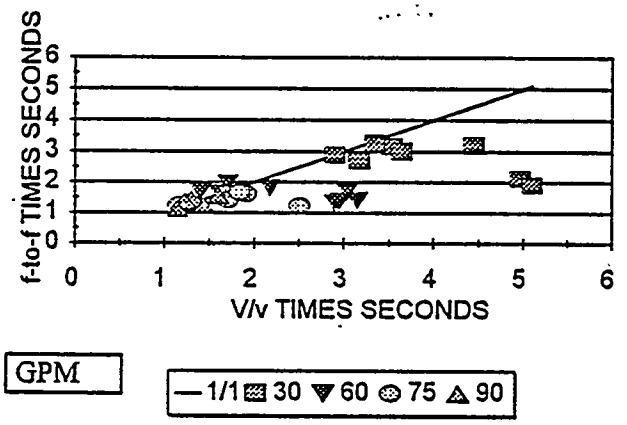

Figure 10. Residence Time Comparison (V/v vs f to f)

Currently, there are no detailed analytical models for adequately predicting the residence time characteristics and holdup volumes of a rotating gas-liquid contactor. Analyses have been carried out to examine the hydrodynamics of fluids on rotating blades or spinning disks (5). However, use of these analyses may be limited because of the assumptions that are made. These analyses assume that the thickness of spreading liquid films can continuously decrease as the liquid flows across the rotor without regard to surface tension effects, that all surfaces are fully wetted at any liquid rate and that the liquid flow is not effected by the counter current gas flow. With these assumptions, a relationship for the liquid film thickness can be derived with the form:

downstream response. Both of these differences suggest that the lower surface tension liquids will experience more dispersion and better mixing in the rotary contactor.

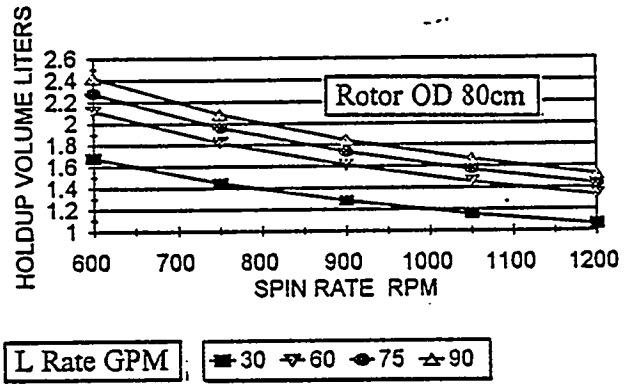

Figure 13. Holdup Volumes Spinning Disk Model

Integral residence time data as influenced by liquid surface tension is summarized in the following Table 3:

Table 3. Effects of the Surface Tension on Residence Time

		Residence Time		
	Dynes/cm	41.9	50	72
RPM	GPM			
900	60	4.31	4.42	4.53
900	90	2.68	3.22	3.29
900	30	6.98	7.87	8.11
1200	90	1.99	2.11	2.49
750	75	4.11	3.88	4.05
600	60	5.01	5.00	5.41

A comparisons of these times indicates that higher residence result from higher surface tension liquids. This, in turn, will translate into higher liquid holdup volumes in the rotor.

FUTURE WORK

The following tasks are planned for the third year of the project:

- Field Experiment Site Selection
- Field experimental studies to evaluate high efficiency gas-liquid contactors using structured packing for acid gas removal applications.
- Fluid Dynamic Studies- Expansion of the currently available database of the fluid dynamics (effects of surface tension and viscosity on residence time) of rotating gas liquid contactors.
- Data Analysis and reports

REFERENCES

1. Tannehill, C.C., and Gibbs, J.E., "Gas Processing Industry, Lower 48 States", July 1991, Purvin & Gertz, Inc., GRI-911/0232

2. Bomio, P., Laso, M., Breu, K., "Improving Selectivity, Capacity and Efficiency of Hydrogen Sulfide/Carbon Dioxide Removal Columns with Sulzer Structured Packing", International Conference on Sulfur, Vienna, Austria, November 1988

3. Bonio, P., Saner, B., Breu, K., "Experience with Structured Packing in High Pressure Gas Absorption", AIChE Spring National Meeting, March 1993

4. Singh, S.P., "Air Stripping of Volatile Organic Compounds from Groundwater: An Evaluation of a Centrifugal Vapor-Liquid Contactor", a dissertation, University of Tennessee, Knoxville, August 1989

5. Munjal, S., "Fluid Flow and Mass Transfer in Rotating Packed Beds with Countercurrent Gas-Liquid Flow", a dissertation, Washingt on University, St. Louis, Missouri, December 1986

Table 2. Time Characterization of Residence Time Pulse Experiments

RUN #	GPM	SCFM	Int (sec)	V/v (sec)	p to p (sec)	f to f (sec)
600 RPM						
57	30	659	8.91	5.10	5.38	1.91
121	30	582	8.31	4.97	6.81	2.12
92	60	367	5.93	2.90	3.57	1.33
96	60	399	6.07	3.03	3.80	1.68
69	60	439	5.41	2.95	4.03	1.39
58	60	464	5.76	2.51	3.86	1.42
109	75	507	4.91	4.45	3.57	1.21
750 RPM						
61	30	666	10.24	4.45	7.35	3.20
129	30	662	8.61	3.54	7.25	3.17
130	30	666	8.45	3.65	6.81	3.01
60	60	653	5.40	2.18	3.84	1.81
104	75	436	4.36	1.68	3.25	1.61
105	75	509	4.43	1.91	3.31	1.61
59	75	650	4.05	1.71	3.30	1.40
106	75	664	3.99	1.84	3.26	1.67
110	90	558	3.89	1.61	2.94	1.55
900 RPM						
103	30	558	8.11	3.34	6.55	3.28
63	60	623	4.83	1.70	3.71	1.96
107	90	669	3.46	1.30	2.71	1.45
108	90	420	3.50	1.45	2.60	1.25
126	90	513	3.36	1.26	2.73	1.35
64	90	628	3.36	1.24	2.74	1.39
1200 RPM						
66	30	768	7.81	3.18	6.38	2.71
132	30	754	7.44	2.91	6.41	2.90
125	60	685	4.01	1.40	3.31	1.69
67	60	714	4.07	1.61	3.38	1.67
111	75	505	3.47	1.30	2.79	1.28
131	75	516	3.35	1.16	2.68	1.23
68	90	668	2.49	1.15	2.38	1.14

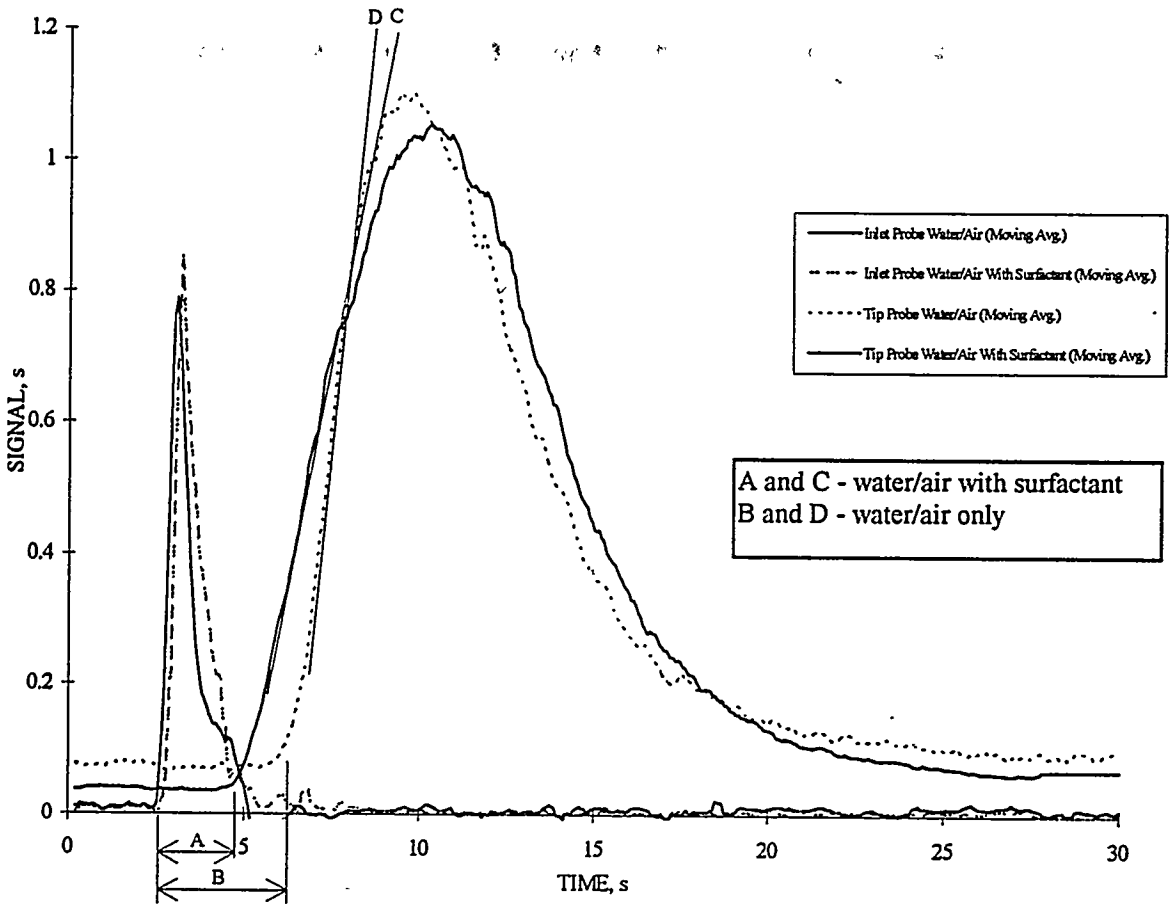

Figure 14. Surface Tension Effects on Residence Time

3B.3 Membrane Process for Separating H_2S from Natural Gas

CONTRACT INFORMATION

Contract Number	DE-AC21-92MC28133
Contractor	Membrane Technology and Research, Inc. 1360, Willow Road, Ste 103 Menlo Park, CA 94025 (415) 328-2228 (telephone) (415) 328-6580 (telefax)
Contractor Project Managers	Kaaeid A. Lokhandwala Johannes G. Wijmans
Principal Investigator	Richard W. Baker
METC Project Manager	Harold Shoemaker
Period of Performance	September 29, 1992 to October 29, 1995

Schedule and Milestones

FY95 Program Schedule

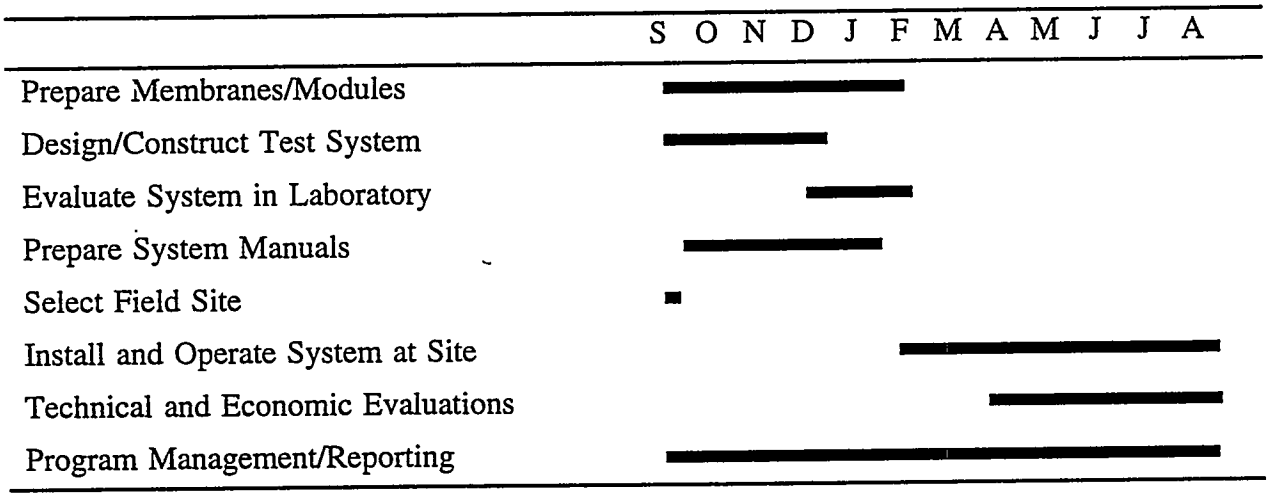

OBJECTIVES

The overall objective of this program is to develop a membrane process for the separation of hydrogen sulfide and other impurities (carbon dioxide and water vapor) from low-quality natural gas. The specific objectives of the program are as follows:

- Develop membranes/membrane processes for H_2S removal from natural gas
- Optimize membranes
- Optimize spiral-wound modules
- Study suitable process designs
- Perform economic analysis
- Address scale-up issues in membrane and module production
- Perform bench-scale demonstrations
- Construct a field test system
- Conduct field test

BACKGROUND INFORMATION

Production of natural gas in the Lower-48 states is expected to increase significantly to meet the rising demand. Natural gas supply is projected to increase by 25% between 1991 and 2010 with 70% of the increased production after 1995 coming from the Lower-48 gas fields[1]. Recent studies of U.S. natural gas reserves have shown that an increasing fraction of the gas produced will be from smaller gas fields at remote locations, and will be subquality on hydrogen sulfide, carbon dioxide, and nitrogen specifications. More than 13% of current reserves are known to be contaminated with hydrogen sulfide[2]. It is projected that, when these subquality reserves are brought into production, between $30-40 million will be invested every year in the new treatment facilities that will be required[3]. Alternatives to currently available absorption-based technologies are being sought for processing gas streams to pipeline specifications in an environmentally and economically acceptable manner.

Conventional amine processes are energy-intensive, and, because they are prone to problems such as corrosion in the reboiler, and foaming and solvent losses in the absorption column, require constant supervision and maintenance. Also, spent amines must increasingly be disposed of as hazardous wastes, which increases operating costs. Membrane processes are simple and modular, and offer greater operational reliability and lower maintenance costs. Membrane processes require almost no operator supervision and are, therefore, ideally suited for operation in remote locations. Membrane processes would be very cost-competitive with conventional amine processes, especially for gas streams with high acid gas concentrations and low flow rates.

PROJECT DESCRIPTION

Phase I Status

The Phase I portion of the project was completed during the 1994 Fiscal year. All the milestones of the Phase I project were fully achieved. During the Phase I program, we selected an appropriate membrane material from a family of copolymers. Membrane screening tests were performed at three feed pressures, 400, 600 and 1,000 psia, and with a feed gas containing 0.1% H_2S, 4% CO_2 and balance methane. Based on the screening test results, we selected two membrane materials for further evaluation in a parametric test plan.

The two membrane materials were tested as 3-inch-diameter stamps over a wide range of feed compositions, pressures and temperatures. The test plan covered the wide range of feed compositions anticipated in produced natural gas.

The effect of water vapor in the feed gas was also evaluated. Based on the tests of these two materials, we selected one polymer, Pebax 4011, for further development in the subsequent Phase II program.

In Phase I we also conducted an extensive survey of H_2S-prone formations, utilizing existing databases and reports by the Gas Research Institute. Further, we made a preliminary technical and economic evaluation of the membrane process. This included evaluation of the feasibility of different membrane process designs, and membrane hybrid processes. Economic evaluations were also performed for a conventional DEA amine absorption process for comparison with the membrane process. The results of this analysis are discussed in a subsequent section. A Phase I final report was prepared and submitted.

Phase II Status

In Phase II of the program, we scaled up the production of the Pebax 4011 membrane to commercial-size 40-inch-wide membrane rolls. For commercial applications involving large gas flow rates, a substantial membrane area is required; MTR incorporates flat-sheet membrane into spiral-wound modules. Pebax 4011 membrane modules were prepared and tested. The issues involved in the scale-up process are discussed in subsequent sections, and the module test results are also discussed.

During Phase II, we have also designed and constructed a field test system incorporating two 3-inch module housings. This unit is currently being tested in the laboratory and will be sent to a field site in June 1995.

MTR's Composite Membrane

Figure 1 shows a diagram of the membrane produced by MTR. The composite membrane has at least three layers. The optimized membrane for the separation of hydrogen sulfide from natural gas consisted of the following components:

- Support fabric
- Polymeric microporous support layer
- Rubbery gutter layer (not shown)
- Selective Pebax layer
- Rubbery top protective layer (not shown)

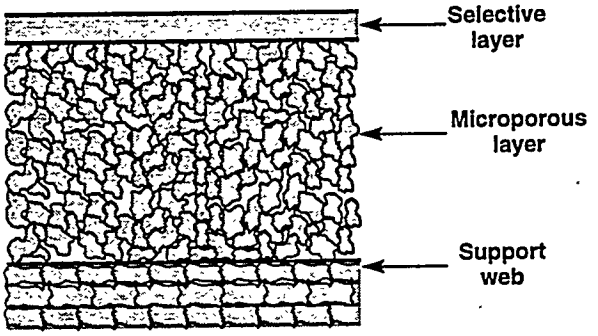

Figure 1. MTR's Composite Membrane

Each component plays an important part in the overall function of the membrane. The support fabric characteristics affect the support membrane structure. The choice of appropriate material for the support layer is important because this layer provides the mechanical strength of the membrane. The selective layer is responsible the separation of hydrogen sulfide and methane. The top layer provides protection during handling and module rolling. Each of these layers was optimized during Phase II.

MTR's Spiral-Wound Module

A schematic diagram of MTR's spiral-wound module is shown in Figure 2. The module

consists of a central product tube, around which are wrapped a number of membrane envelopes. Each membrane envelope consists of two sheets of membrane separated by a feed spacer. The permeate side of the membrane envelopes are separated by a permeate spacer. The entire assembly is rolled tightly around the central product tube and locked in place with adhesive tape.

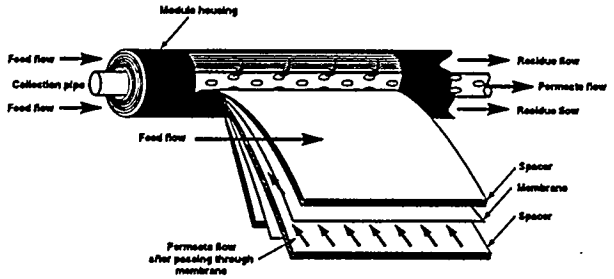

Figure 2. MTR's Spiral-Wound Module

The spiral-wound module has one inlet for the feed gas and two outlets. One outlet is for the permeate stream, which is enriched in the faster permeating component, in this case H_2S. The other stream, which is depleted in H_2S, is removed through the residue stream outlet. The driving force for the separation is the difference between the feed and permeate pressures.

In natural gas applications, the feed gas is typically at high pressure, while the permeate is held at a lower pressure. MTR's commercial modules usually operate at pressures up to 200 psig. For this program we developed modules capable of withstanding pressures up to 1,200 psig. This involved optimizing various parts of the module, including:

- feed spacer material
- product pipe material, and
- membrane envelope dimensions.

Another important issue that was addressed in Phase II was the protocols used in manufacturing the spiral-wound module. The result of the optimization effort was a high-pressure spiral-wound module able to withstand high pressure operation and pressure cycling, and at the same time have separation performance matching that of the membrane stamps.

Bench-Scale Test System

The modules have been continuously tested in our bench-scale test system. This test system was built specifically for this project, and contains a two-stage diaphragm compressor to recompress the residue and permeate gas to feed pressure. The system operate in a full recycle mode, i.e., the residue and permeate streams are fully recycled. The system can be used for feed pressures as high as 1,500 psig and at feed flow rates of up to 11 scfm.

RESULTS

Bench-Scale Module Tests

Figure 3 shows the results obtained with several spiral-wound modules. In Figure 3, the module selectivity is plotted as a function of feed pressure. The module selectivity is defined as the ratio of the permeation flux of H_2S to that of CH_4 through the membrane in the module.

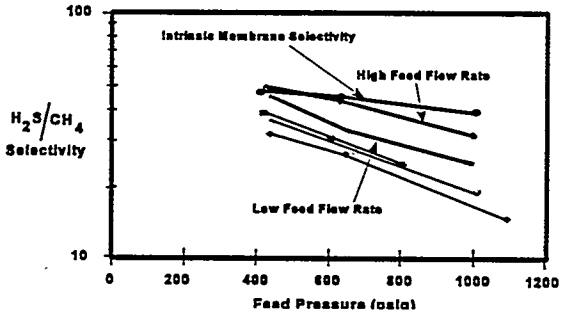

Figure 3. Bench-Scale Test Results

For comparison, Figure 3 shows the intrinsic H_2S/CH_4 selectivity of the optimized membrane. Ideally the module selectivity will match the membrane selectivity, provided the module design is such that mass transfer effects on the feed side are completely eliminated and there is no permeate side pressure drop. Figure 3 shows that progressively better modules were developed during the program as optimization of the module internals and the manufacturing protocols was carried out, so that the H_2S/CH_4 selectivity in the module approached that of the membrane.

Figure 3 also shows the data for the final optimized module, at low and high feed flow rates. At higher flow rates and lower pressures, the module selectivity matches that of the membrane. At lower flow rates, the module selectivity is somewhat lower. This difference can be explained by the concentration polarization effect common in membrane separations. If an adequate velocity cannot be developed at the membrane surface in the module, and the membrane is highly selective for the faster permeating component, a boundary layer is formed adjacent to the membrane. In this layer the concentration of the faster permeating component is greatly depleted. This effect leads to a reduction in the separation performance of the module. At higher flow rates, such as those expected in commercial operation, the problem of inadequate flow velocity is much less.

Overall Process Design

The membranes designed in this project will be used to separate hydrogen sulfide from natural gas. A schematic of the acid gas removal process is shown in Figure 4. The overall process consist of an initial separation step in which the H_2S is removed from the feed and concentrated in the acid gas stream. The sweetened natural gas then enters an optional polishing step to remove the H_2S to pipeline specifications of 4 ppm or less. The H_2S-enriched acid gas stream then enters a sulfur recovery stage. This will be a process for converting the H_2S to elemental sulfur, such as the Claus process, or a redox process depending on the composition and volume of the feed stream entering the sulfur plant.

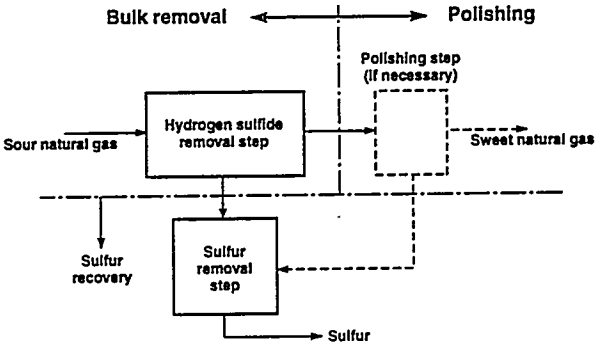

Figure 4. An Overall Schematic Diagram For Treating H_2S-Bearing Natural Gas

A membrane process would be used in the initial separation step to remove hydrogen sulfide from sour natural gas. The membrane process design will also remove the CO_2 to pipeline specification. The membrane process design used in this portion of the plant will depend on the specific requirements of the operator. Three such designs are shown in Figure 5.

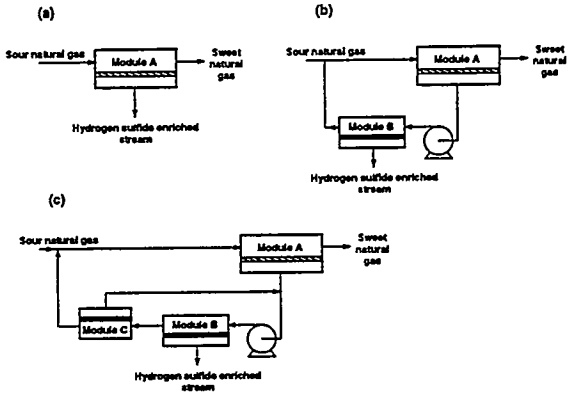

Figure 5. Membrane Process Designs For Separation of Hydrogen Sulfide From Natural Gas

Economic Analysis

A preliminary economic analysis of the membrane/Sulfatreat hybrid process was performed. The module permeation properties used for this calculation were those obtained from the optimized modules in the bench-scale tests. A cost comparison of this process was made with amine absorption. The cost of the amine system was obtained from a GRI study based on calculations performed by M. W. Kellogg. For a 2-MMscfd stream containing 6.3% CO_2 and 2.7% H_2S, the capital costs of the membrane hybrid system were $430,000, whereas those of the amine system as reported by GRI were $1.5 million. The processing cost for the membrane process is $0.57/MMBtuf, compared to $0.83/MMBtuf for the amine absorption process. Although the costs of the membrane process and the amine process are dependent on number of site specific variables, a few general observations can be made. Membrane processes are most economical for treating feed gas at low flow rates and high acid gas concentrations. Based on our economic evaluations, for a wide range of feed H_2S and CO_2 concentrations we prepared an applications envelope for the region of feasibility of membrane processes. This application envelope is shown in Figure 6.

As can be seen in Figure 6, the Pebax membranes developed in this program would be suitable for treating subquality natural gas for which the economics are not viable or marginal. Also, the Pebax membranes are best used for low to medium gas flows and for H_2S contents in the feed gas exceeding 1,000 ppm up to about 5%. Interestingly, a significant proportion of H_2S contaminated subquality natural gas fits this category. The applications envelope also shows that absorption processes would be economical at flow rates more than about 10-15 MMscfd, mainly because they show good economies of scale compared to membrane processes. Also, at high acid gas concentrations, a combination of the amine and the membrane process may be the most economical, because the membrane process removes most of the acid gases and the amine plant removes the remainder separation. This allows both processes to operate in their most effective range.

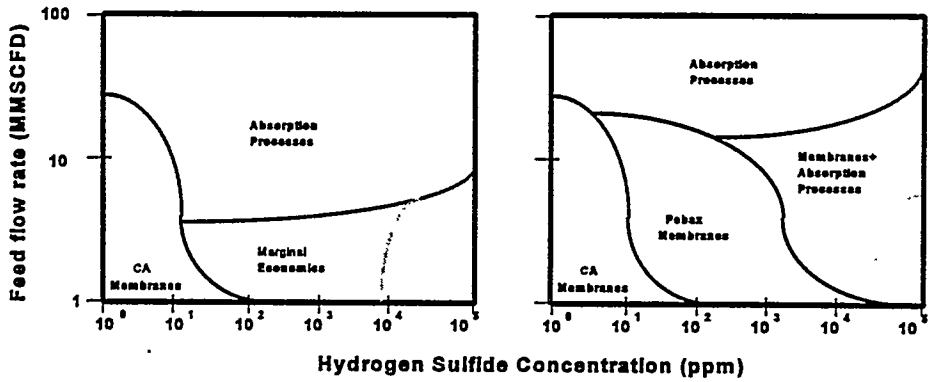

Figure 6. Application Envelope for the Membrane-Based H_2S and CO_2 Removal Process

ACCOMPLISHMENTS

The major accomplishments of the program to date are listed below:

- Identified membrane material exhibiting very high H_2S/CH_4 selectivity in the range of 40-60.
- Scaled up membrane production to commercial size rolls.
- Completed high-pressure membrane and module development and optimization.
- Achieved a membrane permeation flux for CH_4 of about 4×10^{-6} $cm^3/s \cdot cm^2 \cdot cmHg$, which is about twice as high as state-of-the-art cellulose acetate gas separation membranes.
- Demonstrated separation at bench-scale with laboratory-scale modules.
- Developed process designs and economics.
- Prepared applications envelope.
- Constructed field test system.

FUTURE WORK

The following work is planned within the project period:

- Test pilot skid in laboratory
- Conduct field test
- Update economics based on field data

We also anticipate a subsequent cost-shared Phase III commercial demonstration program. In this phase, we expect to perform the following work.

- Scale up modules to 8-inch
- Build demonstration system
- Conduct demonstration field tests

REFERENCES

1. The Clean Fuels Report, J.E. Sinor Consultants, Inc., Nivot, CO 80544, 5(3), June 1993.

2. "Chemical Composition of Discovered and Undiscovered Natural Gas in the Lower-48 - Executive Summary," R.M. Hugman, E.H. Vidas, and P.S. Springer, Energy and Environmental Analysis, Inc., prepared for the Gas Research Institute, Chicago, IL March 1993.

3. "Gas Research Institute in Natural Gas Processing," D. Leppin and H.S. Meyer, presented at SPE Gas Technology Symposium, Houston, TX January 23-25, 1991.

3B.4 Low Quality Natural Gas Sulfur Removal/Recovery

CONTRACT INFORMATION

Contract Number
DE-AC21-92MC29470

Contractor
CNG Research Company
CNG Tower / 625 Liberty Avenue
Pittsburgh, Pennsylvania 15222-3199

Contractor Project Manager
David A Damon
(412) 227 1464, FAX (412) 456 7603

Principal Investigators
Lawrence A Siwajek
Acrion Technologies, Inc
9099 Bank Street / Cleveland, Ohio 44125
(216) 573 1185

Larry Kuehn
BOVAR Corp., Western Research
3130 Rogerdale, Suite 110, Houston, TX 77042
(713) 789 1084 Ext. 255

METC Project Manager
Harold D Shoemaker
(304) 291 4715

Period of Performance
October 1, 1992 - December 31, 1995

Schedule/Milestones

FY95 Program Schedule

	O	N	D	J	F	M	A	M	J	J	A	S
3. Bench-Scale Testing	✓	✓	✓	✓	✓	✓	✓	✓	✓	✓	✓	✓
3.1 Triple Point Crystallizer	✓	✓	✓	✓		✓	✓	✓	✓	✓	✓	✓
3.2 Sulfur Recovery Unit Testing	✓	✓	✓	✓	✓	✓	✓	✓	✓	✓	✓	✓
3.3 Final Report												✓

OBJECTIVES

1. Develop the CFZ and CNG-Claus process for treatment of low quality natural gas having a high carbon dioxide content (>10%) and hydrogen sulfide.
2. Test the carbon dioxide triple point crystallizer and the modified high pressure thermal Claus sulfur reactor at a bench scale.

BACKGROUND

Low Quality Natural Gas (LQNG)

Natural gas is generally categorized as low quality if its acid gas content or inert content is above the minimum specifications of a natural gas transmission company. Pipeline specifications for acid gas content are usually a maximum of ¼ grain H_2S per 100 SCF (4 ppm H_2S) and less than 2%

CO_2. Hugman's [1] definition of low quality gas appears as suitable as any other: " . . . *any volume of gas containing levels of carbon dioxide above 2 percent or of nitrogen above 4 percent or gas with carbon dioxide plus nitrogen above 4 percent, or significant (more than trace) quantities of H_2S.*"

Motivation to Tap LQNG Reserves

Increased use of natural gas (methane) in the domestic energy market will force the development of large domestic non-producing gas reserves now considered low quality.

New Federal regulations embodied in the Clean Air Act of 1990, Title III and Title V, are creating strong new market opportunities for natural gas. These include natural gas co-firing and reburn in coal-fired power plants to help reduce SO_2 and NOx emissions; natural gas fired turbines for peak-shaving and on-site generation of electrical power and steam; and natural gas as an alternative clean transportation fuel. The American Gas Association forecasts these new markets will increase the annual demand for natural gas by 2 TCF, more than 13% of current production. To meet these anticipated gas supply demands, domestic production of natural gas must begin to exploit the large reserves of low quality gas available but not now produced for technical, economic, or environmental reasons.

Target LQNG

The target high acid gas LQNG for processing with the CFZ-CNG-Claus Process contains more than 10% CO_2, is contaminated with H_2S, possibly COS and other sulfur compounds, and may contain nitrogen and other inerts such as helium. Conventional gas treatment in the form of amine based chemical solvents, physical solvents, and newer membrane based processes, is accustomed to processing LQNG contaminated with only modest levels of acid gas, e.g., up to several percent of H_2S and CO_2. With the possible exception of physical absorption processes such as Selexol, existing technologies do not now process high acid gas LQNG in an economic, environmentally acceptable manner.

The major proven non-producing reserve of high acid gas LQNG is located in the LaBarge reservoir of southwestern Wyoming; the amount of gas is large, dwarfing all other proven reserves combined. Estimates place the LaBarge reservoir recoverable gas at 167 TCF (trillion cubic feet), of which at least 33 TCF is methane. The LaBarge reservoir is high in CO_2 and prone to other contaminants such as H_2S, COS, N_2 and He [1,2].

The CFZ/CNG-Claus process is designed to treat the relatively large quantity of LQNG containing >10% CO_2 which may also contain either or both of H_2S and COS and which cannot be economically treated on a large scale by other known technologies.

LQNG Production Barriers

There are many technical and economic barriers which now prevent the up-grade of LQNG to pipeline standards [3] These include but are not limited to:

- removal of H_2S to pipeline specification of 4 ppm H_2S;
- removal of N_2 to increase heating value, decrease transportation cost;
- regeneration of separating agents [4];
- degradation of polymeric membrane materials;
- poor selectivity for CH_4 in presence of acid gases, or for H_2S in presence of CO_2;
- separation of isolated acid gases into pure CO_2 and concentrated H_2S;
- recovery of sulfur from separated H_2S;
- dissipation of high CO_2 partial pressure available in high-CO_2 LQNG;
- recompression of CO_2 for commodity use or sales.

The above list mentions explicitly only the three major contaminants (aside from water) of LQNG: nitrogen, hydrogen sulfide, and carbon dioxide. The presence of additional contaminants,

especially sulfur species such as carbonyl sulfide (COS) and mercaptans (RSH), increases the difficulty of treating LQNG.

CFZ-CNG LQNG Process

The technology comprises four process technologies integrated to produce pipeline methane from LQNG by efficient separation of relatively large amounts of hydrogen sulfide and carbon dioxide. These process technologies are:

- Exxon's Controlled Freeze Zone (CFZ) Process
- CNG's Liquid CO_2 Absorption of Sulfur Contaminants
- CNG's Triple-Point Crystallization (TPC) Process, and
- CNG's High Pressure Sulfur Recovery Process (HPSRU).

Exxon developed the CFZ process to separate methane from acid gases in a single cryogenic distillation operation. CNG Research Company developed the TPC process to purify carbon dioxide and concentrate hydrogen sulfide by alternately freezing and melting CO_2 at or near its triple point conditions (-69.9°F, 75.1 psia). The CNG HPSRU combines the high initial conversion obtained in a Claus thermal reactor with recycle of unconverted H_2S to effectively remove all sulfur components in the HPSRU feed gas. Liquid CO_2 is used to absorb sulfur compounds from HPSRU tail gas, and can be used to absorb sulfur containing contaminants from LQNG in a process variant which does not use CFZ to separate methane from acid gases.

The conceptual designs developed in the Base Program separate hydrogen sulfide and large amounts of carbon dioxide (>20%) from methane, convert hydrogen sulfide to elemental sulfur, produce a substantial portion of the carbon dioxide as EOR or food grade CO_2, and vent residual CO_2 virtually free of contaminating sulfur containing compounds.

CFZ-CNG Process Features

Controlled Freeze Zone

- Acid gas removal in single distillation step,
- No solvents or additives necessary,
- Contaminant insensitivity,
- High pressure acid gas,
- Synergy with cryogenic NRU, LNG product,
- Non-corrosive process streams.

Liquid Carbon Dioxide Contaminant Absorption

- Attractive physical properties (density/viscosity/mol weight),
- Favorable contaminant equilibrium,
- High stage efficiency,
- No solvents or additives necessary, available from raw gas,
- Not combustible

Triple-Point Crystallization

- Concentrated hydrogen sulfide,
- Commercially pure LCO_2 for market or absorption of H_2S
- Sharp separation of trace contaminants
- No solvents or additives necessary,
- Direct contact heat exchange,
- Small pressure changes cause phase changes.

CNG High Pressure Claus Sulfur Recovery

- Claus thermal stage at elevated pressure,
- Eliminates catalytic stages, tail gas unit, and incinerator,
- Oxygen or enriched air,
- No solvents or additives necessary,
- High sulfur recovery, low sulfur emissions.

PROJECT DESCRIPTION

The project comprises a Base Program and an Optional Program. The Base Program, which included NEPA reporting, process design and an experimental research plan for the optional program, was completed August 31, 1993 with submission of the Task 2 Final Report. The Optional Program, Task 3, began in July 1994. The project goal is to further develop and demonstrate two of the component technologies of the CFZ-CNG Process: 1) pilot-scale triple-point crystallization of carbon dioxide, producing commercially pure carbon dioxide from contaminated carbon dioxide at the rate of 25 ton/day, and 2) bench-scale modified high pressure Claus technology, recovering elemental sulfur from hydrogen sulfide at the rate of 200 lb/day.

RESULTS AND DISCUSSION

A complete discussion of Base Program results is contained in Task 2 Final Report [5] and Research Plan [6], Contract DE-AC21-92MC29470. Optional program work is ongoing.

Base Program Results

CFZ Process

The Controlled Freeze Zone (CFZ) Process is a cryogenic technology for the separation of carbon dioxide from natural gas by distillation. CFZ is a proprietary process developed and wholly owned by Exxon Production Research Company [7]. The CFZ concept has been successfully demonstrated in a 600 MSCFD pilot plant at Clear Lake, near Houston, Texas [8,9]. CFZ is the most fully developed of the component technologies comprising the CFZ-CNG LCNG Process. As such, further development of Exxon's CFZ process is not a contract objective, and no DOE funds are allocated for that purpose.

Natural gas processing involves the separation and recovery of valuable hydrocarbon components, and the removal of undesirable components such as H_2S, CO_2 and water. Low temperature physical separations, based on turbo-expander and Joule-Thomson (J-T) operations, and direct fractionation are the preferred methods for processing natural gas whenever possible. However, cryogenic fractionation of a gas containing more than about 5% CO_2 can lead to solidification of CO_2 at an intermediate point in a cryogenic demethanizer rendering such tower inoperative [10]. Thus alternative technologies, using solvents or freeze-prevention additives, have been utilized in the past. The CFZ process, in contrast, achieves a direct cryogenic separation of methane and CO_2. In an otherwise conventional distillation tower, solid CO_2 is confined to a special section of the tower, *the CFZ section*, specifically designed to control the formation and melting of solid CO_2.

TPC Process

Acid gas removal from gases with a high CO_2 to H_2S ratio requires the separation of CO_2 and H_2S to produce a CO_2 byproduct or vent stream free of sulfur compounds and a concentrated H_2S Claus feed. Distillation of CO_2 and H_2S to produce a pure CO_2 product is not practical due to the low relative volatility of CO_2 to H_2S and high CO_2 purity requirements at the pure CO_2 end (top) of the distillation column.

The continuous triple point crystallizer separates pure carbon dioxide from a variety of contaminants such as H_2S, COS, CH_3SH and hydrocarbons. The process has been developed and patented by Consolidated Natural Gas Company (CNG Research Company) [11,12,13,14,15,16]. The crystallizer operates at or near the triple point of CO_2. Solid CO_2 crystals are formed by adiabatic flashing at pressures slightly *below* the CO_2 triple point, and melted by adiabatic contact with CO_2 vapor at pressures slightly *above* the CO_2 triple point. No solid CO_2 is formed on heat exchange surfaces by indirect heat exchange; all solid CO_2 is formed and melted by direct contact heat exchange.

Experimental operation of a laboratory crystallizer has demonstrated that a very high

degree of separation can be achieved in a single stage of crystallization. Experimentally measured separation factors, the ratios of contaminant concentrations in the flash zone (solid forming) to the melt zone, are 1000 to 1500 for H_2S and over 3000 for COS [16]. Pure CO_2 containing less than 1 ppm by volume H_2S has been produced by triple point crystallization from contaminated CO_2 mixtures. In this particular low quality natural gas processing application, two stages of triple point crystallization produce pure CO_2 and a concentrated H_2S product.

The triple point crystallizer has been tested extensively in the laboratory at bench-scale (up to 6-inch vessel diameters) [16]. With the laboratory bench-scale equipment continuous runs of up to 72 hours duration were achieved and terminated routinely. A large scale flash vessel (18-inch diameter) built to test rates of solid carbon dioxide production and slurry pumping characteristics was operated in continuous runs of up to 40 hours duration at production rates of 25 tons of solid CO_2 per day [17]. No unusual wear or abrasion on the slurry pump was observed after many tests totaling hundreds of hours. Slurries of 25 wt% solid CO_2 were routinely pumped.

HPSRU Process

A new sulfur recovery process [18] based on the Claus thermal reaction, with no catalytic stages or conventional tailgas cleanup, is made possible by TPC's ability to separate hydrogen sulfide and other contaminants from carbon dioxide. The high pressure sulfur recovery unit (HPSRU) comprises four operations: 1) Claus thermal reaction to convert hydrogen sulfide to sulfur, 2) waste heat exchange and sulfur condensation, 3) hydrogenation of sulfur and SO_2 in the Claus reactor effluent to hydrogen sulfide, and 4) quench and dehydration. All hydrogen sulfide is recycled to the TPC which concentrates acid gases by rejecting carbon dioxide and other inert species such as nitrogen

To recover 99+% sulfur, the conventional Claus plant normally comprises a thermal reactor, several catalytic reactors in series, and a tail gas cleanup unit. As noted by Hyne [19], "more than 50% of the conversion of hydrogen sulfide to elemental sulfur takes place in the front end reaction furnace; (while the) downstream components do no more than convert that part of the sour gas feed stream that is not converted to product sulfur in the front end reaction furnace." The high conversion of hydrogen sulfide to sulfur achieved in the front end reaction furnace is achieved at relatively modest cost -- about 20% of the total Claus plant capital cost. The downstream components, which accomplish roughly 40% of hydrogen sulfide conversion to sulfur, account for about 80% of the capital cost.

The new HPSRU process retains the high recovery/low cost of the Claus thermal reactor, but eliminates the low recovery/high cost catalytic stages and tailgas cleanup unit. Unreacted hydrogen sulfide is recycled to the thermal reactor inlet via the TPC section; this tail gas recycle approach enables essentially 100% sulfur recovery, free of thermodynamic and kinetic limitations imposed by the Claus reaction.

Aside from the Claus thermal reactor, the remaining equipment is more conventional. Concern for corrosion should be limited to the quench tower where liquid water and hydrogen sulfide are present. However, quench towers performing comparable service are presently used in the SCOT and Beavon tail gas cleanup processes. Also, sulfur dioxide, which is much more acidic in aqueous solution than hydrogen sulfide, is not present in the quench tower because of upstream hydrogenation.

Contaminant Absorption with Liquid CO_2

Sulfur contaminants in the HPSRU tail gas, H_2S and COS, are absorbed with pure liquid CO_2 from the TPC. These sulfur contaminants are recycled to the TPC. Liquid CO_2's low molecular weight (44) and high density (1.18 g/cm^3 at -70°F)

provide high absorption capacity per unit volume of solvent. Liquid CO_2's low viscosity (0.25 cp at -70°F) promotes high stage efficiency. Liquid CO_2 absorption of H_2S and COS has been measured experimentally in a pilot absorption unit processing 20 MCFD of gas [16].

Liquid CO_2 is an effective absorbent for removal of contaminants from raw gas streams which contain CO_2. Favorable contaminant equilibrium data has been measured for many compounds which contain sulfur, chlorine, or an aromatic ring structure. Liquid CO_2 absorption efficiently cleans landfill gas because of its high CO_2 content and the many, often unknown, contaminants which are present [20].

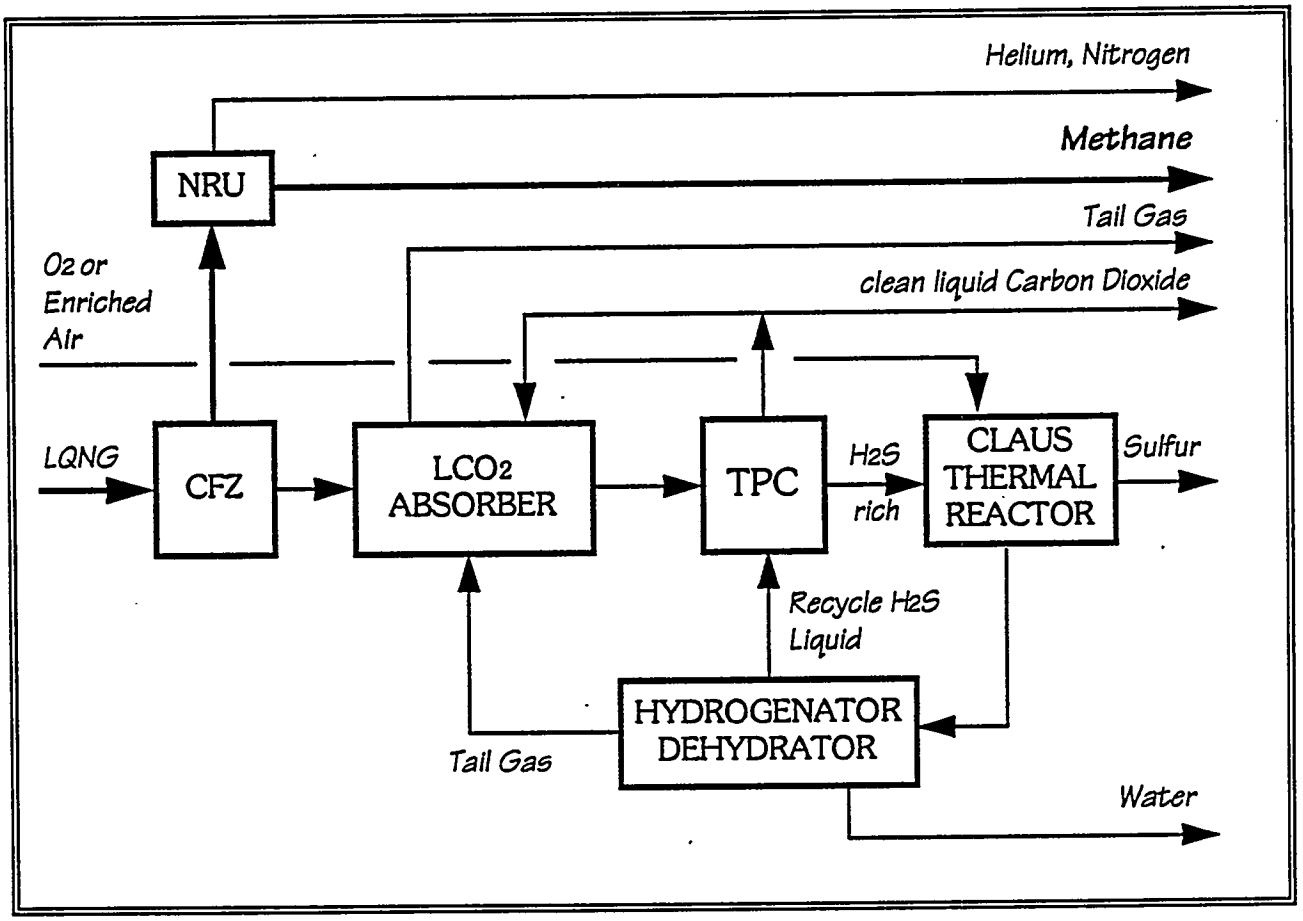

Figure 1. Conceptual CFZ/CNG Claus LQNG Treatment Process

Conceptual CFZ-CNG LQNG Process

The integrated process is shown in Figure 1. After dehydration and cooling the feed gas is sent to the CFZ tower which separates the CH_4 and other light components such as He and N_2 from CO_2, H_2S and other trace heavy components such as COS and C_2H_6. If the CH_4 overhead product contains significant amounts of N_2 it is sent to a cryogenic nitrogen rejection unit (NRU). The CO_2 rich bottoms product is sent to the TPC section of

the process.

The TPC section contains an absorber-stripper which strips out small amounts of CH_4 (approximately 1%) and C_2H_6 carried over in the CFZ bottoms. H_2S in the vent stripping gas is re-absorbed with clean liquid CO_2 from the crystallizer. The vent gas also contains the inert components N_2, argon, and hydrogen brought to the TPC with the HPSRU recycle stream. The stripped CO_2 is sent to the TPC which produces pure CO_2 and a CO_2 stream concentrated in H_2S. Pure CO_2 product can be used for EOR or commodity CO_2 applications. H_2S rich TPC product is further enriched by stripping out CO_2 and is sent to the Claus plant. Tail gas from the HPSRU is returned to the TPC for reconcentration of the unreacted H_2S.

Two feed gas mixtures, each 200 million SCF/day, were studied having CO_2 contents covering a wide range of process applicability. One case is a high CO_2 gas now processed at Exxon's Shute Creek facility near LaBarge, Wyoming. The feed gas for the second case is a lower CO_2 content generic subquality gas. These crude gas streams are more fully described below.

The LaBarge case examines treatment of LQNG produced from the LaBarge field in southwestern Wyoming. The formation is estimated to contain 167 TCF of low Btu raw gas [1]. This crude gas is characterized below in Table 1. The product slate includes methane (pipeline gas), elemental sulfur, helium, and EOR grade carbon dioxide. The CFZ methane product has 50 ppm CO_2 and less than 4 ppm H_2S (¼ grain/SCF). The low CO_2 content of the methane prevents formation of solid CO_2 in the cryogenic NRU. The final methane product specification after nitrogen and helium rejection and recompression is 97% CH_4 at 1000 psia. The EOR-grade liquid CO_2 product, at 2000 psia, contains less than 16 ppm H_2S.

The generic case examines treatment of LQNG with composition shown in Table 1. Product specifications for the generic case include a methane product with 4 ppm H_2S (¼ grain/SCF) and less than 2% CO_2 (0.25% CO_2 is achieved as dictated by the controlling spec on H_2S). In the design of this case, no market was assumed to exist for CO_2. Pipeline methane and a small stream of elemental sulfur are the only salable products produced from this generic subquality gas.

Process economics, evaluated for high and low product price scenarios, were developed on the basis of a breakeven allowance per MSCF of raw gas, i.e., the raw gas cost per MSCF at which plant net revenues become zero. Plant net revenue is positive for raw gas cost below the breakeven allowance, negative above. Breakeven allowances range from 20¢ to $2.14/MSCF of raw gas for low and high product price scenarios, assuming a simple five year capital payout. Capital and operating costs estimated for the conceptual process compare favorably with costs derived for the Selexol process treating low quality LaBarge gas [21]. Comparable breakeven allowances derived for the Selexol process are 8¢ and 73¢.

Optional Program Unit Operation Testing and Demonstration

The Optional Program goal is to further test and demonstrate two of the most technologically advanced component technologies of the CFZ-CNG Process, the pilot-scale carbon dioxide triple-point crystallizer, and the bench-scale modified high pressure Claus reactor.

The triple point crystallizer pilot unit has been constructed by Acrion in Cleveland OH. The unit occupies a space 15' wide by 60' long by 10' high in Acrion's laboratory. The feed to the unit is a contaminated liquid carbon dioxide stream. The unit operates in a total recycle mode with the products, purified liquid CO_2 and contaminant enriched liquid CO_2 being returned as feed. The unit has three stainless steel vessels with diameters of 12 to 18 inches. They are the solid forming vessel or flasher, the solid melting vessel (melter) and a storage vessel for purified liquid CO_2 or boiler. The solid is transported by a slurry pump

from the flasher to the bottom of the melter. Cooling for solid formation is provided by vaporizing a portion of the flasher liquid. This vapor is compressed in a reciprocating compressor, condensed in an aluminum plate fin heat exchanger and recycled to the flasher. On the opposite side of the heat exchanger, liquid from the boiler is vaporized to provide melting gas to the top of the melter. The pilot unit also includes a 3 ton refrigeration system for startup and to compensate for heat leaks in the system.

During a crystallizer test run the pressures, temperatures, levels, mass flows and slurry density are recorded. Contaminant concentrations are measured with a gas chromatograph. Up to now, the crystallizer pilot unit has been operated with contaminants less toxic than H_2S, e.g. propane, acetone and toluene, at contaminant concentrations of from 1 % to 4%(mole%). Carbon dioxide purities 100 to 1000 times greater than the feed liquid have been measured. Most recent efforts have looked at ways of modifying the melter and flasher internals to improve the production rate and operability of the unit.

The modified high pressure Claus reactor consists of a ceramic lined reactor furnace capable of operating at up to 2500F and 100 psig, a waste heat exchanger and a sulfur condenser. Also included are a feed metering system to adjust the acid gas composition (H_2S to CO_2 ratio), acid gas flow, oxygen flow and startup fuel gas flow from the gas cylinders to the reactor and the sampling system to measure the concentrations in the reactor, and the feed and product streams. The reactor will be tested over a range of residence times, acid gas compositions(50% to 90% H_2S), and percentage of stoiciometric oxygen (40% to 90%). Since the reactor is adiabatic, the acid gas composition and percent stoiciometric oxygen determine the reactor temperature (1500 to 2500F). Test data to be measured includes the amount of sulfur produced, the gas composition, pressures and reactor temperature. This will allow determination of the sulfur conversion and the amount of reducing gas (H_2 and CO) available for the hydrogenation of SO_2.

The Claus reactor system is being designed and constructed by Bovar in Houston TX. After initial testing the system will be transported to CNG's Southwest Davis Gas Plant in Davis OK. The reactor system will be connected to the flare at the site for disposal of H_2S. All test runs will be conducted on site.

FUTURE WORK

Operation of the one-stage triple point crystallizer will continue. Test runs will determine the maximum production rate and purity of the CO_2 product. The goal of the TPC demonstration is production at a scale of 25 ton/day.

The HPSRU design is based on an equilibrium model of the thermal reactor. The model has been shown valid for many systems with a similar array of reacting components. Reaction kinetics may have an effect on conversion efficiency, reaction temperature and the extent of side reactions such as hydrogen or carbon monoxide formation. These effects will be quantified by operation of the bench scale high pressure Claus reactor. The HPSRU scale will be 200 lb sulfur/day.

REFERENCES

1. Hugman, R.H., E.H. Vidas, and P.S. Springer, "Chemical Composition of Discovered and Undiscovered Natural Gas in the Lower 48 United States," GRI Contract 5088-222-1745, GRI 90/0248, November, 1990.
2. Meyer, Howard S., Presentation, Chemical Process Research Department, Gas Research Institute, October 3, 1990.
3. Kohl, Arthur, and Fred Riesenfeld, *Gas Purification,* Gulf Publishing Company, Houston, 1974.
4. Rosseau, R.W., et al, "Regeneration of Physical Solvents in Conditioning Gases from Coal," in *Acid and Sour Gas Treating,* Stephen A. Newman, Ed., Gulf Publishing Company, Houston, 1985, p 131.

5. Cook, W. Jeffrey, Marina Neyman, Wm R. Brown, Bruce W. Klint, Larry Kuehn, John O'Connell, Harold Paskall, and Peter Dale "TASK 2 REPORT, Low Quality Natural Gas Sulfur Removal/Recovery," US Department of Energy, Morgantown Energy Technology Center, Contract DE-AC21-92MC29470, August 16, 1993.

6. Siwajek, Lawrence A., Clark C. Turner, Sheldon Asnien, Bruce W. Klint, Larry Kuehn, John O'Connell, Harold Paskall, and Peter Dale, "RESEARCH PLAN, Low Quality Natural Gas Sulfur Removal/Recovery," US Department of Energy, Morgantown Energy Technology Center, Contract DE-AC21-92MC29470, August 16, 1993.

7. Valencia, J. A. and Denton, R. D., "Method and Apparatus for Separating Carbon Dioxide and Other Acid Gases from Methane by the Use of Distillation and a Controlled Freeze Zone", U.S. Patent 4,533,372, August 6, 1985.

8. Victory D. J., and J. A. Valencia, "The CFZ Process: Direct Methane-Carbon Dioxide Factionation," *Hydrocarbon Processing*, 66 (5) 1987.

9. Haut, R. C., et. al., "Development and Application of the Controlled Freeze Zone Process," SPE Production Engineering, p 265, August 1989.

10. Donnelly, H. G. and Katz, D. L., "Phase Equilibria in the Carbon Dioxide - Methane System", *Ind & Eng Chem*, Vol. 46, No. 3, p. 511, March 1954.

11. Brown, W.R., et al, "Gas Separation Process," U.S. Patent 4,270,937, June 2, 1981.

12. Brown, W.R., et al, "Gas Separation Process," U.S. Patent 4,581,052, April 8, 1986.

13. Brown, W.R., et al, "Gas Separation Process," U.S. Patent 4,609,388, September 2, 1986.

14. Brown, W.R., Cook, W.J., et al, "Crystallization Process," U.S. Patent 4,623,372, November 18, 1986.

15. Brown, W.R., et al, "Triple-Point Crystallization Separates and Concentrates Acid Gases," presented at AIChE Spring National Meeting, March 27-31, 1983, Houston, Texas.

16. Siwajek, L.A., et al, "CNG Acid Gas Removal Process," Final Technical Report, US Department of Energy, Morgantown Energy Technology Center, Contract DE-AC21-83MC20230, July, 1986.

17. Siwajek, L.A., Brown, W.R., et. al., "CNG Gas Separation Process," Final Technical Report, Gas Research Institute Contract 5086-222-1429, September 1988.

18. Hise, Ralph E., and Jeffrey Cook, "Sulfur Recovery Process," US Patent 5,021,232, June 4, 1991.

19. Hyne, J.B., "Design and Chemistry of Front End Reaction Furnaces," *Canadian Gas Journal*, March-April 1972, pp 12-16.

20. Siwajek, Lawrence. A., Clark C. Turner, W. Jeffrey Cook, and William R. Brown, "Landfill Gas Recovery for Compressed Natural Gas Vehicles and Food Grade Carbon Dioxide," SBIR Phase I Final Report, Contract No DE-FG02-91ER81223, May 4, 1992.

21. Johnson, John E., and Arthur C. Homme, Jr., "Selexol Solvent Process Reduces Lean, High-CO2 Natural Gas Treating Costs," Paper 65c, AIChE 1983 Summer National Meeting, Denver, August 29, 1983.

Table 1. Gas Compositions and Process Conditions

	Case 1: LaBarge		Case 2: Generic	
Specie:	mol%	lb mol/hr	mol%	lb mol/hr
CH_4	20.50	4,494	80.50	17,679
CO_2	66.50	14,578	19.00	4,172
H_2S	5.00	1,096	0.50	110
N_2	7.35	1,644		
COS	0.05	10		
C_2H_6	0.01	2		
He	0.60	132		
TOTAL	100.00	21,956	100.00	21,961
Pressure	1,060 psia		715 psia	
Temperature	60°F		90°F	
Gas Flow	200 MMSCF/day		200 MMSCF/day	
Water	10 lb/MMSCF		75 lb/MMSCF	
Claus Plant	High Pressure Oxygen		High Pressure Oxygen	
Oxygen	90% O_2 210 Ton/day		90% O_2 21 Ton/day	
EOR CO_2	16 ppm H_2S 2,000 psia		None	
Methane	50 ppm CO_2 undetectable H_2S 40 MMSCFD		0.25% CO_2 4 ppm H_2S 160 MMSCFD	
Sulfur	375 LT/day 99.9% recovery		38 LT/day 99.9% recovery	
CO_2 Vent	16 ppm H_2S 13 Ton H_2S/yr		16 ppm H_2S 8.5 Ton H_2S/yr	

3B.5 Microbially-Enhanced Redox Solution Reoxidation for Sweetening Sour Natural Gas

CONTRACT INFORMATION

Contract Number:	DE-FG21-94MC31162
Contractor:	Texas A&M University-Kingsville Department of Chemical & Natural Gas Engineering Campus Box 193 Kingsville, Texas 78363 (512) 595-2090 (telephone) (512) 595-2106 (FAX)
Other Funding Sources:	Gas Research Institute 8600 West Bryn Mawr Ave. Chicago, Illinois 60631
Contractor Project Manager:	Charanjit Rai
Principal Investigator:	Charanjit Rai, Ph.D., P.E.
METC Project Manager:	Harold D. Shoemaker
Period of Performance:	June 1, 1994 - May 31, 1996
Schedule and Milestones:	FY'95-96 Program Schedule

Task No. and Activity	By Quarters Year 1 1	2	3	4	Year 2 1	2	3	4
TASK 1 - Fe^{3+}•EDTA/NTA Oxidation of H_2S and Regeneration	━━	━━	━━	━━				
TASK 2 - LO-CAT 310 and LO-CAT 340 Experimentation					━━	━━	━━	━━
TASK 3 - LO-CAT 310/340 and Fe^{3+}•EDTA/NTA Degradation Experimentation							━━	━━

OBJECTIVES

About twenty five percent of natural gas produced in the United States is sour containing significant volumes of hydrogen sulfide and other contaminants (1, 2). Liquid redox processes remove hydrogen sulfide from natural gas. Aqueous solution of chelated ferric ions oxidize the hydrogen sulfide to elemental sulfur. The reduced iron chelate is then oxidized by contact with air and recycled. This requires expensive equipment for regeneration, costly chemicals and the process is usually energy intensive (3, 4, 5).

Recent studies by Rai et.al (12, 16) show that the ferric ion regeneration rates are substantially enhanced in presence of acidophilic bacteria. The specific objectives of this project are to advance the technology and improve the economics of the commercial iron-based chelate processes utilizing biologically-enhanced reoxidation of the redox solutions used in these processes, such as LO-CAT II and SulFerox.

BACKGROUND INFORMATION

The Liquid Redox Sulfur Recovery Processes absorb hydrogen sulfide from the sour gas stream and produce elemental sulfur. The liquid redox processes may use vanadium, iron or a mixture of iron and quinone as the primary catalysts interacting with hydrogen sulfide. The iron-based processes have been most successful because of their superior performance, simple operation, greater reliability and environmental acceptability (6). However, the process conditions promote the oxidation reactions that accelerate the decomposition of metal-chelate catalysts resulting in high processing costs, and recirculation power requirements. Moreover, in all the commercial liquid redox processes, expensive redox solution is lost via salt formation and inadequate washing of the sulfur cake produced (7).

Redox Process Chemistry:

The iron-based redox processes employ iron in the ferric state (Fe^{3+}) to oxidize hydrogen sulfide to the elemental sulfur (S^o). The ferric ion is reduced to the ferrous state (Fe^{2+}), which is then regenerated to the ferric state by oxidation with air as follows:

$$H_2S_{(l)} + OH^- \leftrightarrow HS^- + H_2O$$
$$HS^- + OH^- \leftrightarrow S^= + H_2O$$
$$S^= + 2\,Fe^{3+} \leftrightarrow S^o + 2Fe^{2+}$$
$$2Fe^{2+} + \tfrac{1}{2}O_2 + H_2O \leftrightarrow 2Fe^{3+} + 2OH^-$$

Typical iron concentrations in the chelated catalysts range from 500 to 2500 ppm as determined by economics involving pumping and chemical costs. The LO-CAT chelated catalysts can handle concentrations of H_2S as high as 100% and there appears to be no lower limits (9).

Neither ferrous nor ferric ions are stable in aqueous solutions at neutral or alkaline pH levels and ordinarily will precipitate either as ferrous or ferric hydroxide. This precipitation is prevented by complexing the iron with organic chelates which are capable of holding both forms of iron in solution. These organic chelates are classified into two groups: Type A chelates such as ethylenediaminetetraacetic acid (EDTA) or nitrilotriaectic acid (NTA) which are powerful chelating agents at low pH's; and the type B chelates, consisting of polyhydroxylated sugars such as sorbitol that are effective at pH above 8. Combination of both types of chelates makes the catalyst stable at any pH from 5 to 9.0.

The selection of a chelant is dependent on the reaction rate of Fe^{3+} - chelate with H_2S, Fe^{3+} - chelate with oxygen and the rate of degradation of the chelate. The chelate degradation occurs through the oxidation of the chelate by Fe^{3+} ion and the free radical induced oxidation (8). Other variables that control the oxidative degradation are: pH, temperature, chelant concentration, chelant to iron ratio, and the type of degradation products formed.

The LO-CAT™ process was originally developed by ARI Technologies, now Wheelabrator Clean Air Systems, Inc., to treat sour gas in the absorber at feed gas pressure, relatively low iron concentrations (1000 to 1500 ppmw) and high circulation rates. This system referred to as conventional LO-CAT works well for many low-pressure plants, however it results in excessive equipment and pumping costs for high pressure applications. The ARI-LO-CAT II process as shown in Figure 1, was developed for the high pressure direct treat applications (9). The process uses

substoichiometric iron chelated catalyst in the absorber and an oxidizer unit that circulates liquid through density differences. The process is described in greater detail in the literature (9, 10). The process also uses a separate sulfur settler vessel. These features reduce the chemical and operating costs.

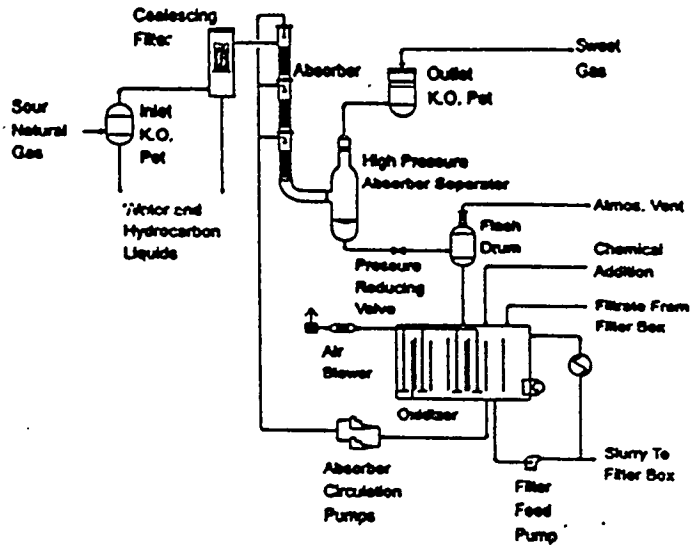

Figure 1. Process Flow Diagram for the ARI-LO-CAT II System

PROJECT DESCRIPTION

The iron-oxidizing bacteria are capable of oxidizing ferrous ions to the ferric state at low pH. According to the literature references these microbes are capable of oxidizing Fe^{2+} to Fe^{3+} state at 500,000 times faster rate than the purely chemical oxidation process in the absence of bacteria (11). The regeneration of Fe^{3+} chelate in the presence of acidophilic microbes under mild conditions at 25-45°C, and atmospheric pressure would minimize the chelate degradation process and thus help in improving the economics of hydrogen sulfide oxidation in the natural gas sweetening process. The Fe^{3+}-chelates are also capable of oxidizing the mercaptans to the insoluble disulfides (12). It is proposed to use these microbes for achieving enhanced ferric ion reoxidation rates in ARI-LO-CAT II process thereby improving the overall sour gas processing economics.

The basic objective of this study, jointly sponsored by U.S Department of Energy and Gas Research Institute, is to develop information and technology to improve the economics of the commercial iron-based redox processes such as ARI-LO-CAT II and SulFerox, with emphasis on the biologically-enhanced reoxidation of the redox solution used in these processes. In this study, a mixed culture of iron oxidizing bacteria are used to regenerate the commercially used iron chelates for reoxidation of reduced redox solutions. There are more than forty gas processing units nationwide using liquid redox technology. These gas processing plants could use the new technology being developed in this project and thus lower the gas processing costs of sub-quality sour natural gas substantially.

Mechanism of Microbial Oxidation of Ferrous Iron:

The iron oxidizing bacteria derive the energy required for their growth from the oxidation of reduced sulfur compounds and from the oxidation of Fe^{2+} to Fe^{3+} ions, using air as an oxidant. The major electron transfer components of the respiratory chain of the iron oxidizing bacteria have been postulated by Ingledew et.al (13) and Cox et.al (14). These components are organized in the cytoplasmic membrane in such a way as to couple Fe^{2+} oxidation to generate a transmembrane proton electrochemical potential. This potential is the main driving force for electron transfer. A diagrammatic representation of electron transfer mechanism is shown in Figure 2. The major electron transfer components of the respiratory system of the bacteria are comprised of: a cytochrome oxidase, cytochrome c, cytochrome a and a blue colored copper protein, rusticyanin (15). Ferrous ion oxidation takes place at the cell wall and generates a transmembrane electrochemical potential of 250 mV. The reduction of molecular oxygen is catalyzed by a cytochrome oxidase at a pH of 6.5 on the inside of the cytoplasmic membrane (16).

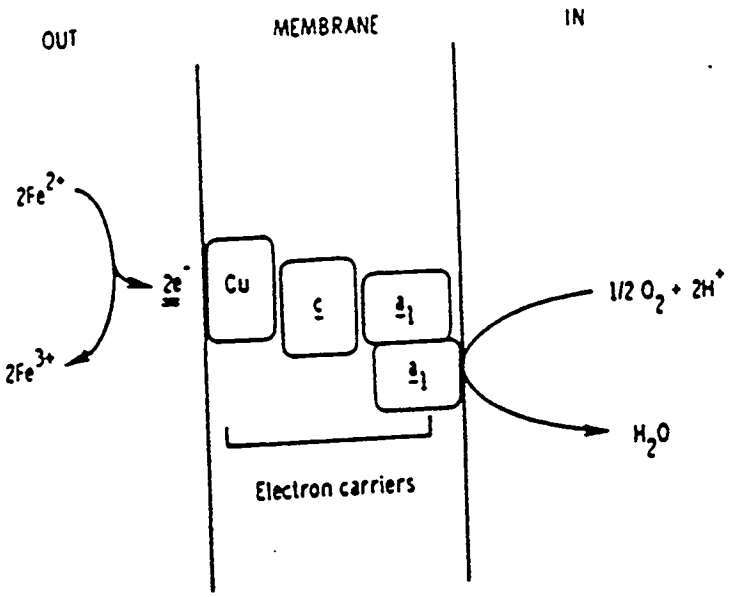

Figure 2. Components of the iron oxidase are identified by their prosthetic groups and are arranged from left to right in order of increasing redox potential (Cobley and Haddock, 1975; Ingledew and Cobley, 1980). "Out" and "in" refer to the bulk phase and cytoplasm, respectively.

Materials and Methods

a.Growth Characteristic of Iron Oxidizing Bacteria

The proprietary iron oxidizing bacteria used in this study were maintained in basal salt solutions at a low pH prior to their use in these experiments. One bacteria (Bacteria A) was grown in 9K media and the other bacteria (Bacteria B) was grown in a high pH nutrient media. These bacteria were also grown in a redox solution system for three to five days prior to use in a high pH media maintained at 25° to 45°C in a controlled temperature shaker bath. The composition of nutrient media is shown in Table I. The iron oxidizing bacterial mixed cultures used in this study were initially obtained from American Type Culture Collection (ATCC), however, they were cultivated either in a high pH media or grown in the redox solution used for the hydrogen sulfide oxidation studies. The cultures were grown separately and then mixed and also were grown in the same media. The maximum cell growth typically occurred in 25 to 50 hours resulting in a cell density of 1.5×10^{11} cells/l in high pH media. The cell densities of 1.0 to 2.0×10^{11} cells/l were achieved in the redox system solutions. Cell densities of $(1.0\text{-}1.5) \times 10^9$ cells/l were used in the experiments carried out in the presence of the bacteria. Bacterial cell counts were determined using a Petroff-Hauser bacterial cell counter under a phase contrast microscope.

Table I

High pH Medium for Iron Oxidizing Bacteria

Composition per liter:

$Na_2S_2O_3 \cdot 5H_2O$.....	10.0g
$Na_2HPO_4 \cdot 7H_2O$.....	7.9g
Sodium formate.....	6.8g
Glucose.....	3.6g
KH_2PO_4.....	1.5g
NH_4Cl.....	0.3g
$MgSO_4 \cdot 7H_2O$.....	0.1g
Trace metals solution.....	5.0mL

pH 7.6-8.5 at 25°C

b. Gas Samples and Chemicals:

Synthetic sour gas samples used in this study were blended by Alphagaz Inc. of LaPorte, Texas. The synthetic sour gas had the following composition:

H_2S - 0.5 (v/v)
CO_2 - 5% (v/v)
N_2 - 94.5%

Two types of commercial catalysts, Catalyst A and Catalyst B, were used in this study. These catalysts contain chelated ferric ion complexes. Precipitation of ferric hydroxide is prevented by chelating the ferric ions with organic chelates. Two types of chelates: type A, such as ethylene diaminetetraacetic acid (EDTA) or nitrilotriacetic acid (NTA) and type B, such as polyhydroxylated sugars keep the catalyst stable at any pH and were used in the commercial chelated catalyst formulations. This paper presents data using catalyst A only. All other chemicals used were obtained from Sigma Chemical Company.

c. Experimental Procedure:

The oxidation of hydrogen sulfide present in the synthetic sour gas blend was studied in a two-liter Virtis Omni Culture Bioreactor shown in Figure 3 (17, 18). The hydrogen sulfide is readily oxidized by the chelated ferric ions present in the commercial catalyst A used in this study. The ferric ions (Fe^{3+}) are reduced to the ferrous state (Fe^{2+}) and hydrogen sulfide is oxidized to elemental sulfur. The elemental sulfur is removed by filtration or centrifuging and the ferric ion is regenerated by bubbling air through the reduced redox solution under controlled experimental conditions. The rate of hydrogen sulfide oxidation is a function of the pH, temperature, concentration of Fe^{3+} chelate, the gas/liquid ratio and the degree of agitation. These variables were carefully controlled and optimized. Likewise, the rate of ferric ion regeneration is a function of the pH of the redox solution, the temperature, the concentration of chelated iron, air to redox solution ratio and the degree of agitation. The progress of the reaction was monitored by measuring the concentration of Fe^{2+}, Fe^{3+}, pH, temperature, and redox potential of the reaction medium in the Virtis Omni Culture Bioreactor. Two sets of experiments were conducted in each case, one in absence of bacteria (blank) and the other one in presence of a single bacteria or a mixed culture.

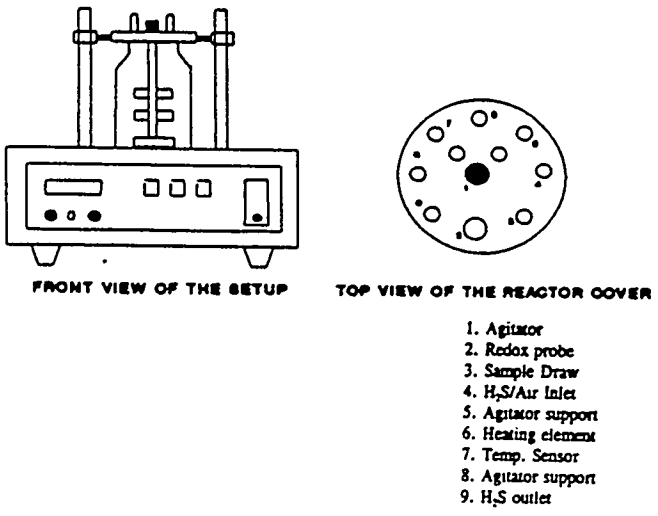

Figure 3. Omni Culture Bio-Reactor

1. One-Cycle Experiments Using Commercial Chelated Catalysts. (Absence of Bacteria) -Baseline.

A set of experiments was conducted at 30°C to 45°C and a pH varying from 3, 5 and 7.6 using 1000 ppm solution of commercial iron-chelate Catalyst A in absence of iron oxidizing bacteria (baseline). A cycle consists of oxidation of hydrogen sulfide by bubbling it through redox solution, filtration of elemental sulfur followed by reoxidation of ferrous ions with air. In a typical experiment, hydrogen sulfide was oxidized by passing the synthetic sour gas mixture through one liter of redox solution in Virtis Omni-Culture Bioreactor, the redox solution was regenerated by bubbling air through it in absence of bacterial cells (blank run) and elemental sulfur was centrifuged after each cycle. The data on these experiments is shown in Figures 4 to 6. The redox solution regeneration rates were fairly constant, for a specific pH, temperature and gas to liquid ratio in the control (baseline) experiments and the quantity of elemental sulfur recovered ranged from 35 to 50% of the theoretical amount.

2. One Cycle Experiments Using Commercial Chelated Catalyst A in Presence of Iron Oxidizing Bacteria.

In this set of one-cycle experiments the iron oxidizing bacterial cells of bacteria A, B or a mixed culture were used in the redox solution containing 1000 ppm of commercial chelated Catalyst A at 30°C to 45°C and a pH of 3.0 or 7.5. In a typical experiment, hydrogen sulfide was oxidized by bubbling the synthetic sour gas mixture through one liter of redox solution contained in the Virtis Omni-Culture Bioreactor, the redox solution was regenerated by bubbling air through the solution containing iron oxidizing bacteria or a mixed culture at a cell concentration of 1 to 7.5 x 10^9 cells/liter and elemental sulfur produced was filtered (not centrifuged) after each cycle. The data are presented in Figures 4, 5 and 6 and compared with the baseline experimental data obtained in absence of bacteria. The data show a ferric ion regeneration rate enhancement of 50 to 150% and an increased production of elemental sulfur, 80 to 98% recovery as compared to 35 to 50% recovery in absence of bacteria. The data on rate

enhancement is shown in Figures 7 and 8 and the data on sulfur recovery is given in Figures 9 and 10.

RESULTS

The oxidation of hydrogen sulfide present in the synthetic sour gas mixture blended by Alphagaz of LaPorte, Texas has been studied using a commercial chelated iron catalyst in a two-liter Virtis Omni-Culture Bioreactor. The rate of hydrogen sulfide oxidation was found to be primarily influenced by the pH, temperature, gas/liquid ratio and the concentration of iron chelate in the redox solution. Essentially all hydrogen sulfide was oxidized to elemental sulfur in the presence of commercial iron-chelate catalysts at a pH of 7.5 and 30 to 45°C. There was a 20% rate enhancement in hydrogen sulfide oxidation in the presence of mixed cultures.

The regeneration of the ferric ions in the chelated catalysts could be accomplished by bubbling air through the reduced chelated catalyst in the bioreactor. The air regeneration of the chelated ferric ions was dependent on the pH, temperature, air/redox solution ratio and the bacterial cell concentration. Single cycle experiments were carried out both in absence of iron oxidizing bacteria (blank), as well in presence of the bacterial cells. The ferric ion regeneration rates in the reduced redox solution were found to be 50% to 150% higher in presence of bacterial cells at typical cell density of 1 to 5 x 10^9 cells/l under optimum operating conditions. The data are presented in Figures 7 and 8 with a commercial chelated catalyst in one-cycle experiments.

The sulfur recovery was also studied in single cycle experiments. Invariably, 35 to 50% sulfur was recovered by centrifuging in the controlled blank runs, whereas in presence of mixed cultures of iron oxidizing bacteria the sulfur recovery ranged from 80 to 100% of the theoretical values. It was observed that filtration was preferred technique for sulfur recovery in presence of iron-oxidizing bacteria, since centrifuging affected the bacterial cell densities in the redox system. The sulfur recovery data for one-cycle experiments are shown in Figures 9 and 10.

FUTURE WORK

One of the bacterial strain (Bacteria A) was readily grown in 9K media and the other iron-oxidizing bacteria (Bacteria B) used in this study was grown in a high pH medium containing trace metals. Cell densities as high as 2 x 10^{11} cells/l could be achieved in twenty to fifty hours. Moreover, the high pH medium could be easily replaced by the used redox solution of the commercial catalyst evaluated in this study without adversely affecting the growth characteristics and the bacterial cell densities of the iron-oxidizing bacteria and the mixed cultures. The conditions for maximizing bacterial cell densities in the redox solutions will be studied and optimal parameters will be investigated.

These experiments conclusively show that in the presence of iron oxidizing bacteria, Bacteria A, or B or the mixed cultures, the rates of hydrogen sulfide oxidation are enhanced by about 20%, the ferric ion reoxidation rates in the redox system of the commercial chelated redox catalyst are enhanced by 50% to 150% as compared to blank runs in absence of bacterial cells at an operating pH of 7.5 and the redox solution temperature varying from 30° to 45°C. Moreover, the iron oxidizing bacteria also induce higher elemental sulfur recoveries ranging from 80 to 100% of theoretical as compared to 35 to 50% in absence of bacteria. The mechanism of bacterial action on sulfur recoveries will be investigated.

During processing of sour natural gas there is excessive degradation of the aminopolycarboxylic acid chelating agents such as Fe^{3+}•EDTA, Fe^{3+}•NTA and the commercial chelants used in the industry. Chelate degradation occurs through the oxidation of the chelate by Fe^{3+} ions, and the free radical induced oxidation (8). During the regeneration of Fe^{3+} chelate, hydroxy radicals are formed that degrade the Fe^{3+} chelate. Attempts will be made to determine the mechanism of chelate degradation more precisely and the role of bacterial cells in preventing such degradation. It has been observed in our preliminary laboratory study that the degree of chelate degradation is minimal in presence of bacterial cells (22).

ACKNOWLEDGEMENTS:

This study was sponsored by U.S. Department of Energy, Contract Number DE-FG21-94MC31162 and by Gas Research Institute, Contract Number 5094-220-3037. The author is grateful to USDOE and GRI and appreciate the keen interest of the Project Managers, Harold Shoemaker and Dennis Leppin. Author is also indebted to other members of Texas A&M University-Kingsville research team: Martin Taylor, Ajay Singh, Jaisimha Rao, Lora Lopez, Dr. James R. Pierce, (Microbiologist) for their contributions and also Mrs. Conchetta Heath for typing the manuscript and meeting all the project deadlines in a timely fashion.

REFERENCES

1. Kohl, Arthur and Reisenfeld, F.C.; Gas Purification, Gulf Publishing, Houston, Texas. 1979.

2. Hugman, R.H., Vidas, E.H. and P.S. Springer, (Energy and Environmental Analysis, Inc.), "Chemical Composition of Discovered and Undiscovered Natural Gas in the Lower-48 United States - 1993 Update, Volume I. Report No. GRI-93/0456.1.

3. Leppin, D. & Meyer, H.S. "Gas Research Institute Program in Natural Gas Processing." Paper SPE 21505 presented at SPE Gas Technology Symposium, Houston, TX, January 1991.

4. Dalrymple, D.A., Trofe, T.W. and Evans, J.M., "An Overview of Liquid Redox Sulfur Recovery", Chemical Engineering Progress, 43-49, (March, 1989).

5. Quinlan, M.P., "Technical and Economic Analysis of the Iron-Based Liquid Redox Processes." Proceedings of the 71st Annual Gas Processors Association Convention, Anaheim, CA, March 1992.

6. Leppin, D. "Update on GRI Sulfur Recovery Research." Proceedings of the 1992 Liquid Redox Sulfur Recovery Conference, Austin, TX, October 1992, GRI Report No. GRI-93/0129.

7. Leppin, D., Evans, J.M. & Krist, K. "Gas Research Institute Program in Sulfur Recovery Research." Proceedings of the 1991 Liquid Redox Recovery Conference, Austin, TX, May 1991. GRI Report No. GRI-91/0188.

8. Kundu, K.P. and N. Matsuura. Internat. J. Radiation Phys. Chem. Vol. 3, 1971, 1.

9. Hardison, L.C. "LO-CAT II - A Big Step Forward in Iron Redox Chemistry." Proceedings of the 1991 Liquid Redox Sulfur Recovery Conference, Austin, TX, May 1991. GRI Report GRI-91/0188.

10. Hardison, L.C. (ARI Systems, Inc.), "Early Experience with ARI-LO-CAT II for Natural Gas Treatment," paper presented at AIChE Spring National Meeting, March 29 -April 2, 1992, New Orleans, Louisiana.

11. Lacey, D.T. and Lawson, F., "Kinetics of Liquid Phase Oxidation of Acid Ferrous Sulfate by the Bacterium Thiobacillus ferrooxidans, Biotechnology and Bioengineering, xii, 29-50, (1987).

12. Agumadu, P.N. and Rai, C., "Microbial Sweetening of Sour Gas", 1991 GRI Liquid Redox Sulfur Recovery Conference, May 5-7, 1991, Austin, Texas. GRI Report No., GRI-91/0188.

13. Ingledew, W.J., "Ferrous Ion Oxidation by Thiobacillus ferrooxidans". Biotechnology and Bioengineering Symposium No. 16, p. 23-32 (1986).

14. Cox, J.C., and M.D. Brand, "Iron Oxidation and Energy Conservation in Chemoautotroph Thiobacillus ferrooxidans". p. 31-46. In W.R. Strohl and O.H. Touvinen (ed.), Microbial Chemoautotrophy. Ohio State University Press, Columbus, Ohio (1984).

15. Rawlings, D.E., and Kusano, T., "Molecular Genetics of Thiobacillus ferrooxidans" Microbiological Reviews 58 (1), p. 39-55. (March 1994).

16. Rai, C. and Rao, J., "Biologically-Enhanced Redox Solution Reoxidation". Proceedings of the GRI 1994 Sulfur Recovery Conference, Austin, Texas, p. 199-214, May 15-17, 1994.

17. Gokarn, R.R. August 1993. "Process Optimization for Microbial Sweetening of Sour Natural Gas." M.S. Thesis, Texas A&I University, TX 140 pp.

18. Dinesh-Mohan, H.K. 1992. A Novel Microbial Sweetening Process for Sour Natural Gas Upgrading. M.S. Thesis, Texas A&I University, TX. 97 pp.

19. Rai, C. "Microbial Desulfurization of Coals in a Slurry Pipeline Reactor Using Thiobacillus ferrooxidans, Biotechnology Progress, 1, 200-205 (1985).

20. Satoh, H., Yoshizawa, J. & Kametani, S. "Bacteria Help Desulfurize Gas." Hydrocarbon Processing, May 1988, pp 76-D to 76-F.

21. Leppin, D., (Gas Research Institute), GRI Program in Sulfur Removal and Recovery from Natural Gas - 1994 Update, paper presented at GRI Sixth Sulfur Recovery Conference, Austin, Texas, May 15-17, 1994.

22. Rai, C., and Taylor, M., "Microbial Sweetening of Sour Natural Gas Using Mixed Cultures". Presented at 1995 AIChE Spring National Meeting, Houston, Texas, March 19-23, 1995.

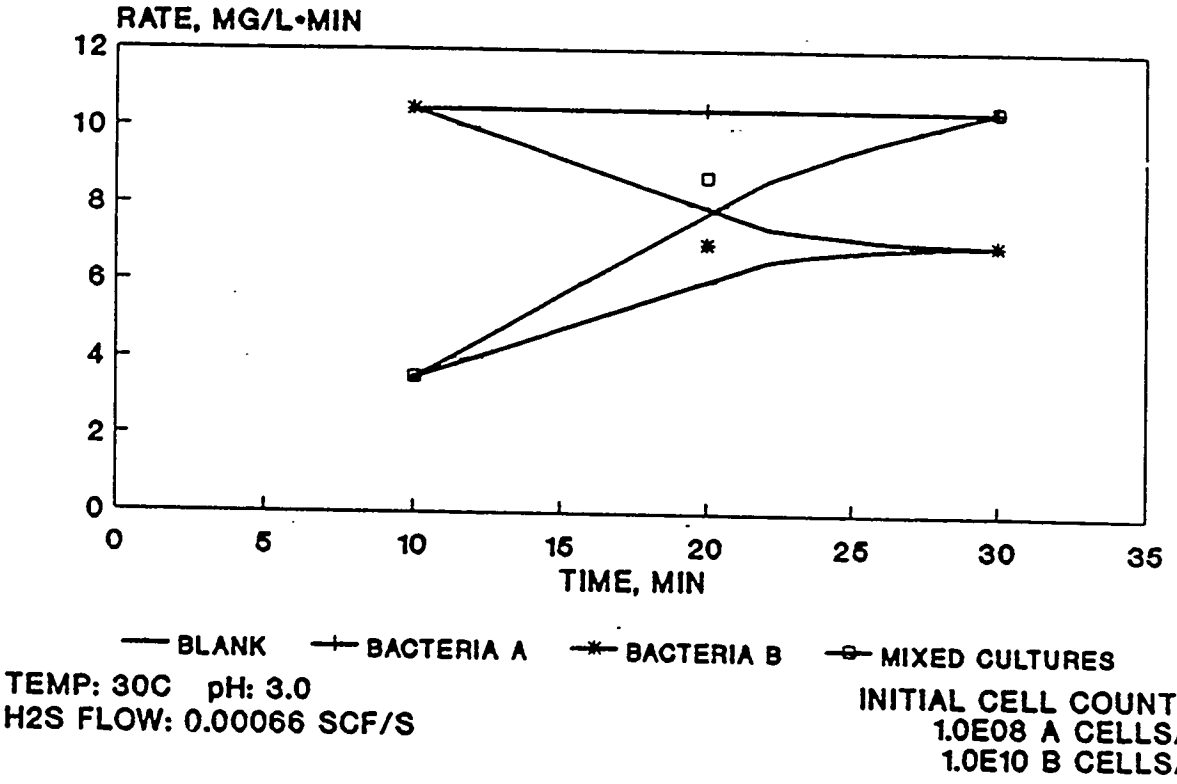

Figure 4A. Comparison of H_2S Oxidation Rates With and Without Bacteria at 30°C and pH, 3.0

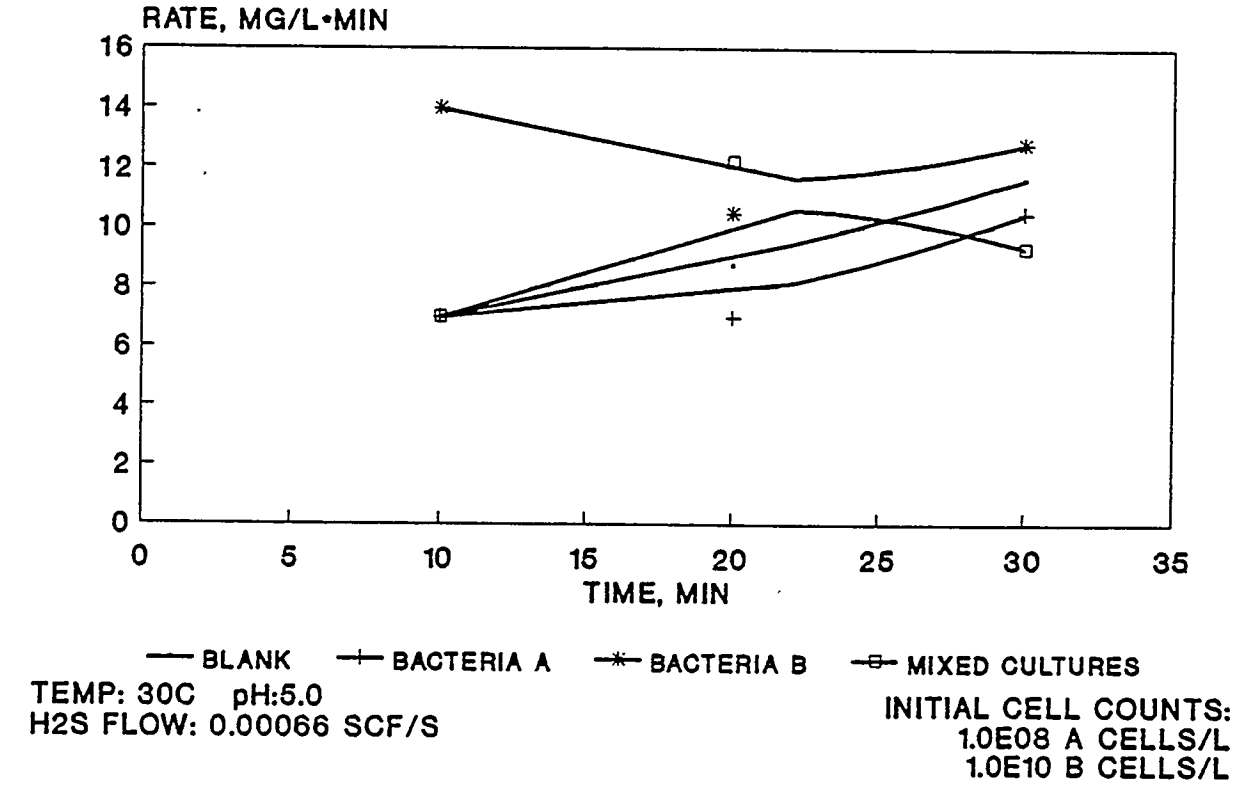

Figure 4B. Comparison of H_2S Oxidation Rates With and Without Bacteria at 30°C and pH, 5.0

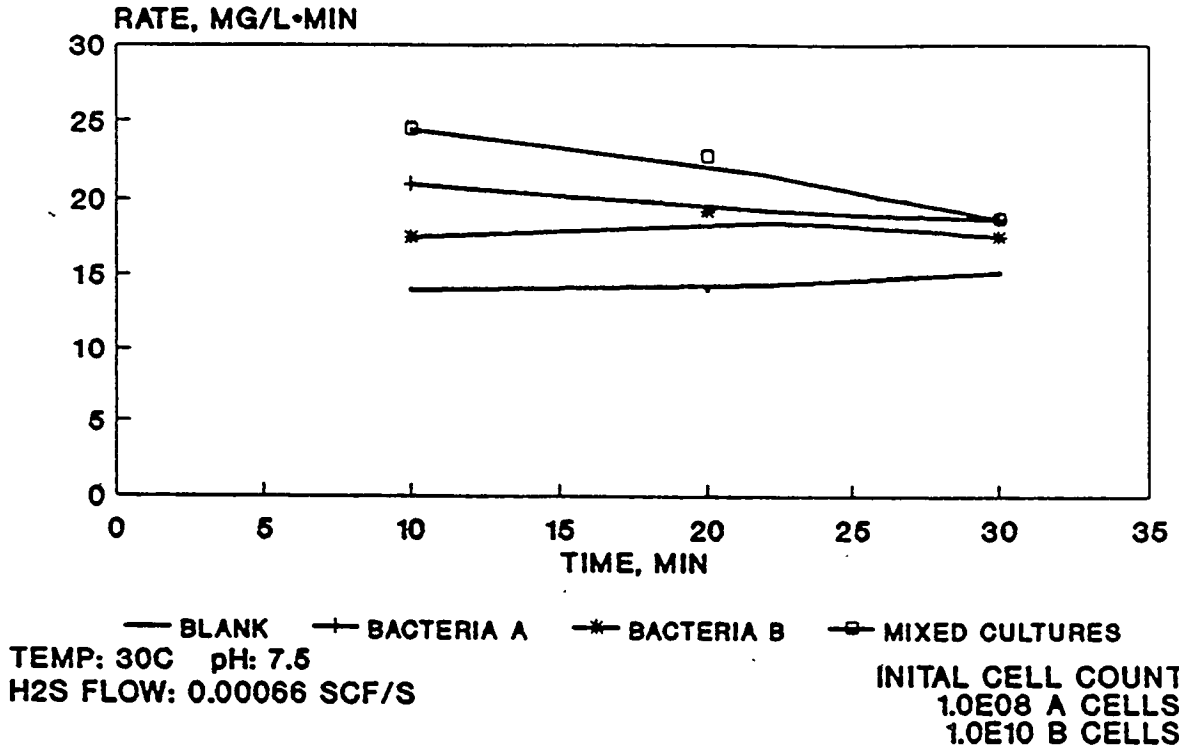

Figure 5. Comparison of H_2S Oxidation Rates With and Without Bacteria at 30°C and pH, 7.5

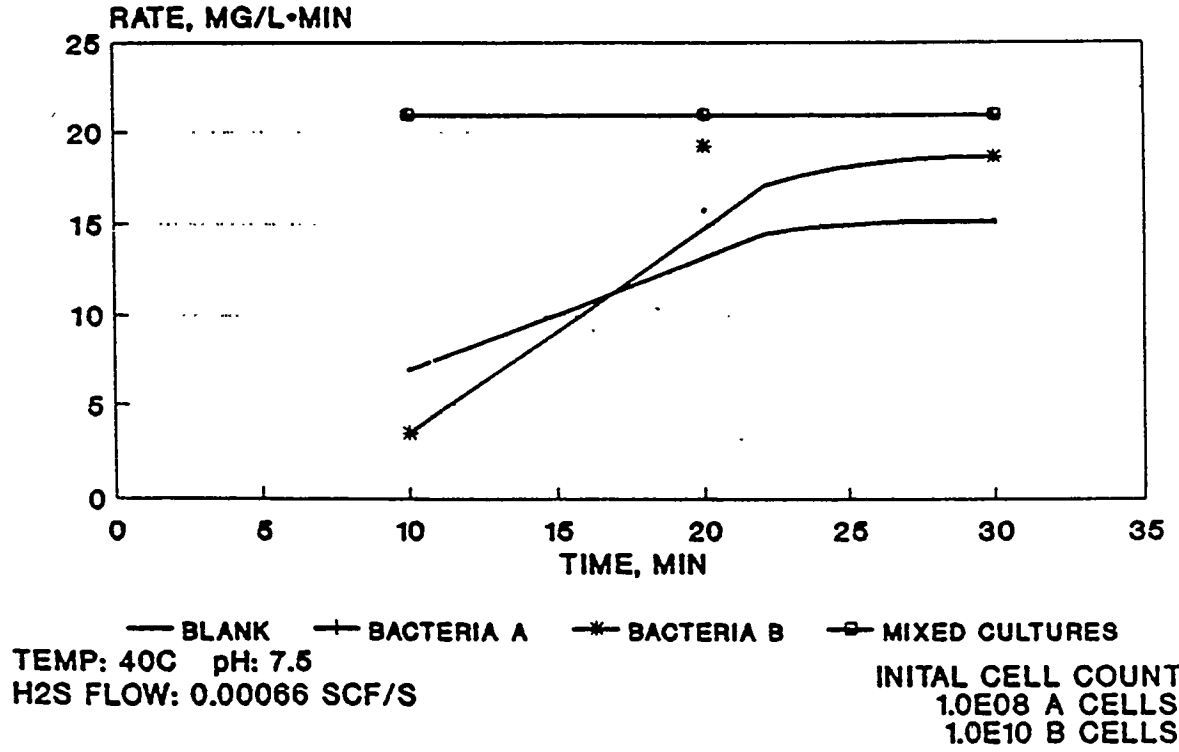

Figure 6. Comparison of H_2S Oxidation Rates With and Without Bacteria at 40°C and pH, 7.5

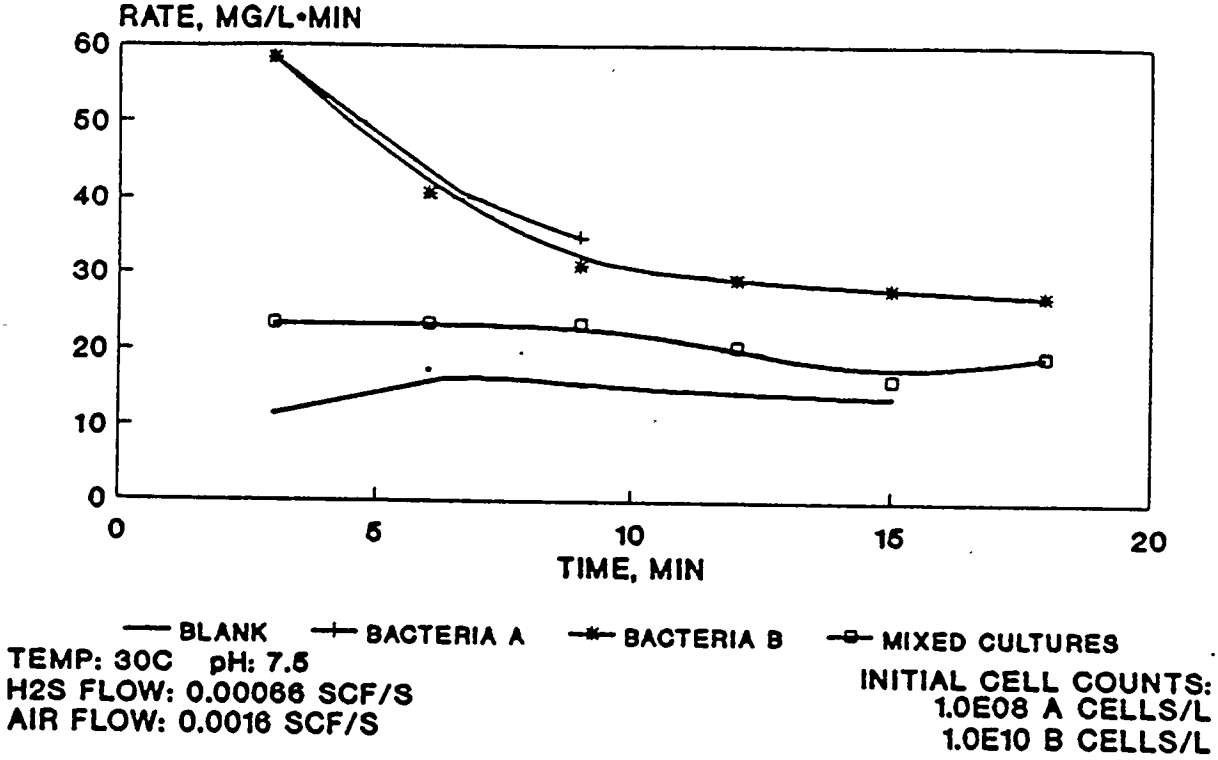

Figure 7. Comparison of Regeneration Rates With and Without Bacteria at 30°C and pH, 7.5

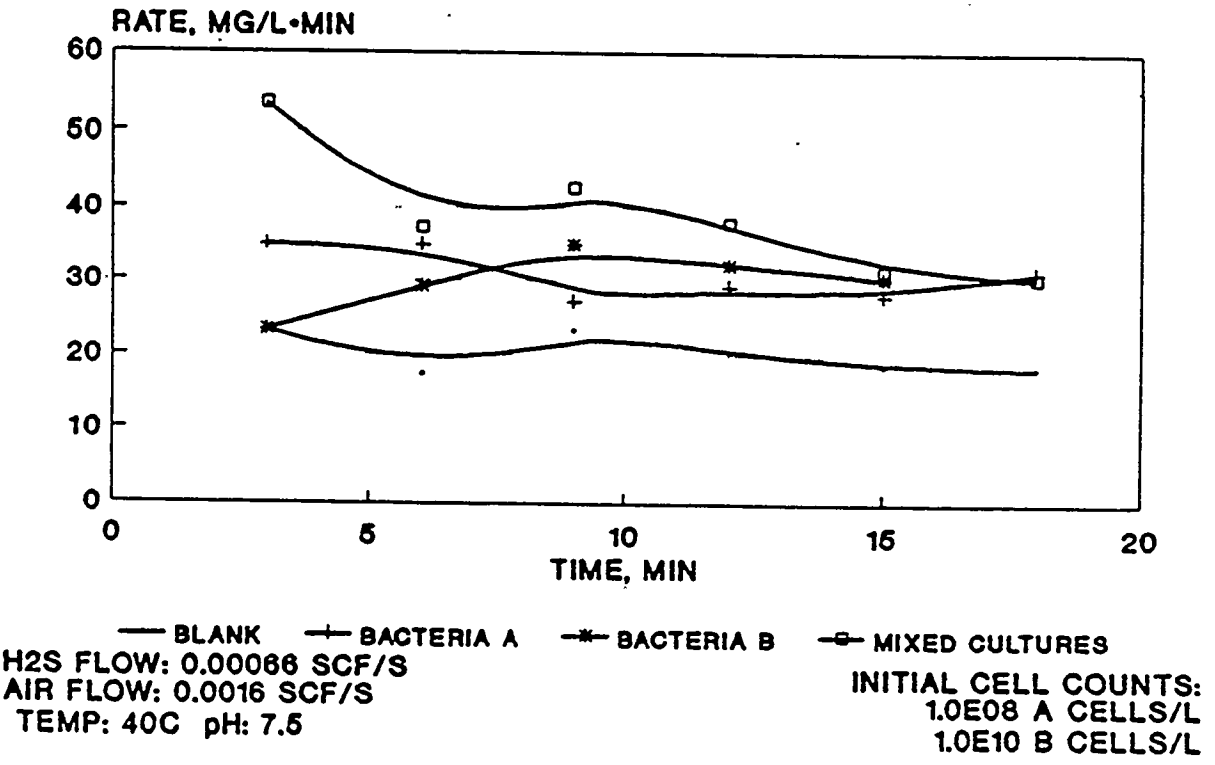

Figure 8. Comparison of Regeneration Rates With and Without Bacteria at 40°C and pH, 7.5

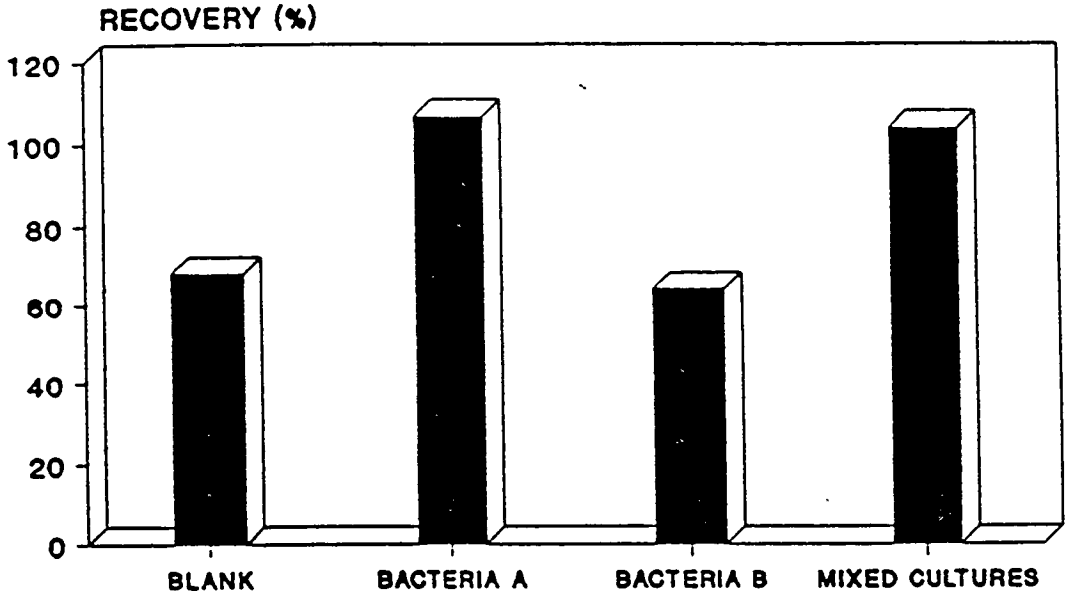

TEMP: 30C pH: 7.5
H2S FLOW: 0.00066 SCF/S
AIR FLOW: 0.0016 SCF/S

INITIAL CELL COUNTS:
1.0E08 A CELLS/L
1.0E10 B CELLS/L

Figure 9. Comparison of Sulfur Recovery With and Without Bacteria at 30°C and pH, 7.5

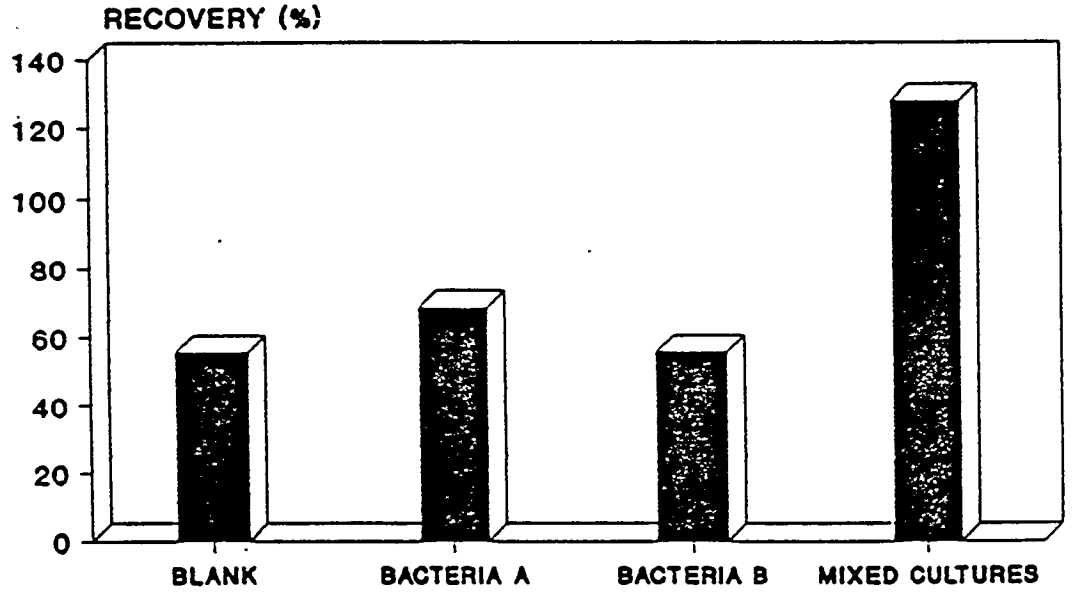

TEMP: 40C pH: 7.5
H2S FLOW: 0.00066 SCF/S
AIR FLOW: 0.0016 SCF/S

INITIAL CELL COUNTS:
1.0E08 A CELLS/L
1.0E10 B CELLS/L

Figure 10. Comparison of Sulfur Recovery With and Without Bacteria at 40°C and pH, 7.5

Session 4B

Natural Gas Storage

4B.1 Natural Gas Storage and End User Interaction A Progress Report

CONTRACT INFORMATION

Contract Number	DE-AC21-94MC31114
Contractor	ICF Resources Incorporated 9300 Lee Highway Fairfax, VA 22031-1207 (703) 934-3869 FAX (703) 691-3349
Contractor Project Manager	Leonard R. Crook, Jr.
Principal Investigators	Leonard R. Crook, Jr. Steven Reich Michael L. Godec
METC Project Manager	Anthony M. Zammerilli
Period of Performance	September 30, 1994, to March 31, 1995

In late 1994, ICF Resources began a contract with the Morgantown Energy Technology Center ("METC") to conduct a study of natural gas storage and end user interaction. This study is being conducted in three phases: the first phase is an assessment of the market requirements for natural gas storage and in particular to identify those end user requirements for storage that could benefit from METC-sponsored research and development ("R&D") in storage technology; the second phase will address the particular technical and economic feasibility for expanding conventional storage; and the third phase will address alternative, unconventional technologies.

ICF is approaching the conclusion of the first phase of the study and the second phase has begun. This paper summarizes the scope of the study and reports some of the preliminary findings of the first phase. We begin by providing an overview of the goals of the effort and of natural gas storage. We will address the evolving market requirements for storage and the regulatory and institutional changes that are having a major impact on the use of natural gas storage. We address the demand for storage and the alternatives for meeting this demand, with specific reference to regional and end use issues.

Overview of the Project

The overall objective of this contract is to identify whether there is a need for METC-sponsored RD&D into alternative gas storage technologies with that need specified in terms of the requirements of the users of gas storage, now and in the future. The contract is designed to identify where such storage may be needed, when it would be needed, and what the characteristics of such storage should be to meet end user requirements.

The contract is divided into two phases. The first phase is intended to identify the regional needs for storage and the capability of the current and planned storage infrastructure to meet these needs. This involves an assessment of storage markets (Task 1), the various alternatives to storage currently being pursued, and the physical and technological capabilities of existing conventional storage to meet these market requirements (Task 3). Because it is anticipated that a major source of new market demand will be for electricity generation, METC has specified that the analysis specifically address the storage requirements of this market segment. The product of Task 3 will be the specification, by region, of potential barriers to the more efficient use of gas storage, and the potential role of government in addressing these barriers.

The second phase (Task 5) is intended to characterize the technical possibilities for alternative storage. Conventional storage consists of underground storage situated in the traditional storage media: depleted oil/gas fields, salt formations, aquifers and reefs. Liquified natural gas using current liquefaction/vessel technologies can also be considered conventional storage. Alternative storage could include a broad array of new storage technologies or innovative uses of conventional storage, along with non-traditional storage reservoirs such as tight fractured formations, thin bedded salts, and non-reservoir rock formations.

Expected Results of the First Phase Effort

At the conclusion of the first phase, ICF will provide METC with the following:

- A description of the end user requirements for gas storage on a regional basis for the period 2000 through 2010. These requirements will consist of the following elements:
  - seasonal storage capacity for meeting seasonal demand variations
  - cycling storage capacity for meeting short term, operational demand for gas
  - estimates of the value of storage in each region and for each type of use
- A data base of storage reservoir characteristics consistent with production reservoir characteristics currently in GSAM.
- A complete representation of storage in GSAM, including demand and supply characteristics on a regional basis, for both seasonal and short-term cycling operations.
- An evaluation of capabilities of the current and planned storage projects to meet demand with an identification of the key technical parameters that may affect the performance characteristics of storage.
- An initial assessment of the need for RD&D to enhance capabilities from conventional storage formations and a characterization of possible alternative storage requirements.

Expected Results of the Second Phase Effort

This phase is designed to identify alternative (i.e., unconventional) storage possibilities and provide METC with the capability to analyze near and long term RD&D strategies for assessing these possibilities. Such unconventional storage may consist of (1) storage performance capabilities for meeting end user requirements at substantially lower costs than current technologies; (2) enhanced storage performance for meeting anticipated new demands for storage-type services; (3) identification of new unconventional storage media that can increase the availability of storage in regions where conventional storage (or its alternatives) is inadequate. From this task we will provide the following:

- A description of a range of possible alternative storage technologies.

- An assessment of storage technology possibilities in the GSAM framework to provide an initial analysis of realistic near-term and long-term R&D goals.

- A benefit/cost study of alternative storage R&D actions based on regional storage and gas market economics.

- Development of feasibility criteria for evaluating alternative storage RD&D activities.

Overview of the Storage Industry

Underground natural gas storage has long been an integral part of the interstate natural gas delivery system. Storage has served several purposes in the gas system. Market area storage is used to meet seasonal peak demand, provide control for pipeline operations and assure the availability of gas for incremental sales. Supply area storage serves as a backup gas supply, a supply aggregation facility and a control for pipeline and production operations. Storage is also used midway along pipelines also as a control for operations and as a supplemental source of supply.

Underground storage is typically in geological formations with different operational characteristics. These include:

- depleted gas and oil reservoirs which are the most common type, located in the northeast, midcontinent and west coast

- aquifers, mainly in the upper midwest and Pacific northwest

- salt formations which are quite widespread but where most of the development to date has been in the Gulf coast

- marine reefs, located mainly in Michigan

In addition to these formations typical of U.S. storage, there are storage possibilities in underground caverns associated with mining. Finally, liquified natural gas facilities ("LNG") provide storage peaking capacity in a number of locales.

There are approximately 375 underground storage sites in the U.S. with a working gas capacity of approximately 4 Tcf. On a peak day, these storage reservoirs can deliver approximately 60 Bcf. As our figure indicates, most of the storage capability is located in the northeastern quadrant of the country. The largest concentrations of storage are in the producing areas throughout the midcontinent and gulf coast, and in former oil and gas production areas in the upper midwest (Illinois, Michigan) and the northeast in Pennsylvania.

As of late 1994, there were approximately 80 new storage developments announced. Of these, 47 were classified as "new" greenfield storage and 34 as expansions of existing storage.

The trend in new projects has been towards the development of high deliverability salt cavern projects, which constitute about 58 percent of the new projects proposes. Thirty-eight percent of the new projects are in depleted oil and gas reservoirs, with the rest proposed in aquifers. If all these projects are developed (and they will not be), they would contain about 495 Bcf of working gas capacity and 21,000 MMcf per day of deliverability. Almost 70 percent of the new deliverability will come from the salt cavern projects. Most of the proposed projects are located in the producing regions, although some are in the upper midwest and the northeast.

The trend in development reflects the changing market needs for storage. This market places high value on high deliverability relative

to storage capacity and to a quick responsiveness to demand. The popularity of salt cavern storage is its ability to be drawn dawn and refilled several times per year. Traditional storage can only be drawn down over an entire heating season.

Market Trends

The focus of the first phase in this research effort has been on end user interaction. This interaction comes about in several ways. First, is to identify those growth areas for gas consumption that can benefit from storage services. That is, where new markets are developing, can storage enhance the ability of the gas system to meet these market requirements? This also involves understanding how patterns of energy consumption affect fuel choices and choices between gas services. In addition it is necessary to understand how the market is evolving in response to institutional and regulatory changes.

The basis of the market trends analysis has been the 1994 GRI Baseline Forecast. The 1994 forecast shows a natural gas market of just over 21 Tcf in 2000 and a market of about 24 Tcf by 2010. Gas prices over the period increase fairly moderately, reaching $2.50 in 2000 and $3.20 in 2010 (1994 dollars). Growth in consumption is expected to occur in all sectors, but major growth is expected in the electric generation and industrial markets. (In the GRI forecast, industrial consumption includes cogeneration.) As such, gas for electricity generation will be the major source of growing gas consumption in the GRI forecast. This view is generally held by most forecasters. By the year 2010, GRI expects about 80,000 MW of new gas fired generation.

Much of this new electric capacity will be combined cycle ("CC") plants and in gas/oil turbines. Gas fired CCs are becoming increasing attractive to electric system planners. Improvements in gas turbine technology has brought about great advances in CC heat rates. Many operate well below 8,000 Btu/Kwh down to 6,500 Btu/Kwh in some units, which depending on gas prices can make gas-fired CCs competitive with coal plants. Lower environmental impacts and certification costs of CCs also make these units more attractive than coal units. The shorter lead times and lower costs per MW of installed capacity (currently around $600 to $800 per MW) make CC investment less risky given the uncertainties of electricity demand and pricing. Finally, CCs typically have superior load following characteristics and can be brought on and off line quicker than other units.

As such, CCs typically operate at intermediate load factors of between 25 and 60 percent, although in some cases CCs can be operated as base load. The singular characteristic of CCs relevant to gas system planning is the fact that they can be stopped and started many times over the course of a year, month or week. Ramp up times usually are 2 to 3 hours. Thus, when the CCs are brought on line, the gas must be available on short notice.

Gas turbines have very low load factors, operating in some cases less than 100 hours per year. Turbines are used to meet needle peaks in electric demand. As such, the turbines are less cost sensitive than CCs or other steam plants. If gas is not available, turbines can use higher priced distillate oil without penalty.

Growing gas consumption in the generation of electricity will have an impact on the natural gas delivery system. Each region has a distinctive electric generation load profile. As more gas fired generation is added, gas consumption will increase consistent with that profile. An example of this is shown in this graph of national patterns. More gas fired generation will add considerably to summer gas demand, but should also add to gas demand in the winter. On a region by region basis, this will result in

additional demand for transportation and possibly storage requirements. At the same time, as more CCs are added, there will be a greater need for quick cycling storage capabilities.

Industrial gas consumption growth is largely driven by cogeneration demand. This will tend to have similar patterns to electric generation consumption to the extent that cogenerators sell power into the grid as opposed to simply serving as "inside the fence" steam/electric providers. Looking at industrial patterns of gas consumption suggests that while there is some seasonality associated with industrial uses, industrial demand tends to be flatter over the course of the year.

Turning to residential and commercial gas consumption -- the firm, core demand for gas services -- the forecasts indicate very modest growth in consumption. This, however, masks the effect of even small amounts of growth in this sector on deliverability. As this figure indicates, the growth in gas demand when viewed over the entire year shows winter peak month consumption increasing by about 200 Bcf. This assumes that conservation and improvements in technology do not reduce peak consumption or alter patterns significantly. (This may be the case, as most such technologies tend to lower gas consumption over the entire year and not on the peak.) Indeed, in many utilities that are experiencing residential growth, peak day sendout is also increasing, leading to more interest in storage or other peaking options.

The implications of these forecast trends are twofold:

- additional seasonal deliverability may be required in some regions as seasonal demand for gas increases

- additional rapid response deliverability may be necessary for winter and non-winter demands to enhance deliverability

The demand for additional storage services is being identified in our project on a regional basis. For each region within the GSAM structure, we have developed a load duration curve as represented in this slide. This load profile arranges the months of the year in four seasons. Average daily consumption is presented from the highest month to the lowest month in the respective seasons. This load profile is for the South Atlantic region in 2000. For each month we have identified the end use sectors, stacking these from the least seasonal variation to the most variation. This figure illustrates several points we have found.

First, as noted above, industrial consumption of gas tends to be less seasonal than other uses. This pattern is fairly consistent across all regions. Second, the peak day send out estimate does not distinguish among sectors; we have not been able to estimate on a regional basis which sectors may be on system during the peak besides the firm, core loads. Third the optimal pipeline/storage configuration is suggested by the comparison of summer and winter loads relative to average daily demand. Pipeline capacity should be sufficient to meet daily requirements in the summer and refill storage, while in the winter demand must be met by the combination of pipeline and storage withdrawals. Therefore, to identify where additional storage capacity would be required, we are comparing current and propose storage capacity and pipeline capacity to seasonal patterns of gas consumption. We are also identifying on a regional basis how much combined cycle and combustion turbine capacity is planned. From both of these comparisons, we should begin to be able to identify in a general way how much seasonal storage capacity and how much cycling storage capacity may be required.

This in a general way describes how we have been proceeding. The storage question is, however, much more complicated as anyone who has examined the economics and demand

for storage can attest. One indicator of this is the current diversity of opinion as to whether there is an excess of storage capacity in today's market. In addition, while a great many storage projects have been announced, not all of these are coming on line as planned. One of the major factors is the absence in some cases of adequate market interest and commitment to storage projects in light of the uncertainties of today's gas market and the alternatives available to storage.

Institutional and Regulatory Changes

FERC's Order 636 has had a major impact on storage planning and operations. Indeed, the changing rules in the gas marketplace have had by far the larger effect on storage than market growth or changing demand patterns.

Prior to FERC's Order 636, storage was a service provided by the pipelines as a bundled aspect of their merchant, contract demand service. While buyers could purchase storage service separately from regular CD service in some cases, the choices were limited. In the main, storage service was a relatively expensive, seasonal supply of gas used to supplement winter CD gas supply.

Order 636 made major changes in several areas that affect the need for storage services:

- It required the unbundling of pipeline services and the separate pricing of those services. Pipelines were no longer gas merchants, becoming suppliers of transportation and related services. Buyers could select from among the services they wanted to best meet their individual requirements. In unbundling their services, pipelines were required to transfer or assign ownership of storage and upstream pipeline capacity to customers. For storage, this has led many users to begin making their own independent judgements about filling and withdrawal.

- The imposition of straight-fixed-variable rates fundamentally changed the price signals to purchasers of storage and pipeline capacity. Under previous rate regimes, modified-fixed-variable rates, the Seaboard and United formulas, more or less of the pipelines' fixed costs were recovered in the commodity charge. Under SFV all fixed cost are paced in the demand charge. The effect of this, as shown in the slide, is to penalize low load factor users of capacity. This in effect makes storage, or some equivalent a critical element in the local distribution company system planners' decision making.

- The order allows holders of pipeline capacity and storage capacity to remarket that capacity. Pipelines are no longer the sole providers of pipeline capacity. The impact of this is still being worked out. The initial observation, however, is that the price of spare capacity has collapsed in many regions to the variable cost of transportation. At the same time, this is leading to a more intensive use of the pipeline system, as new customers seek out assigned capacity deals rather than new constructed capacity. As the system is more efficient employed, the need for new construction has diminished.

- While not a direct requirement of Order 636, a major consequence of the order has been a proliferation of pipeline and related services. These include the market hub services, balancing, no notice services, seasonal swing services and alternative storage services (i.e., Columbia's Storage in Transit Service). In particular, the pipelines' new restrictions on balancing have enhanced the value of short term storage

access. At the same time, some of the services compete with new, third party storage offerings.

Other market changes are also affecting the uses of and need for gas storage. These include the volatility of gas prices and the success of the futures market for managing commodity risk in the industry. The result of this is that storage is now used in many cases to "park" gas, either to take advantage of gas price changes or to meet other operational needs.

Options Analyses

What is becoming apparent in this new regime is that gas storage can be used in a wide variety of ways. The value of storage depends on how it is used and the alternatives for that use. In sorting out the kinds of possible uses of storage for R&D planning, we have focused on the uses of storage that require the delivery of natural gas. We have found the following construct helpful for identifying the market uses of storage and how to begin to evaluate the enhancements that R&D can make.

This figure shows the cost of storage compared with the major physical delivery alternatives. These include, pipeline capacity, propane air or LNG, and distillate fuel oil. What we see in this picture is that the economics of storage vary relative to the other options depending on the capacity factor or length of time the option is available. That is over a range of low capacity uses, storage is more economic than new, full cost pipeline capacity. On the other hand, traditional storage is more costly than propane air/LNG for very low capacity factor uses. Similarly, it can be less costly to interrupt some dual fuel customers with distillate backup than it is to supply those needs with storage (depending on the cost of fuel oil). We have identified three market segments useful for characterizing storage and its physical substitutes relative to end user requirements and for establishing the value of storage in each region.

- Short term peak shaving -- this is storage used to supplement peak day requirements or daily swing requirements on the pipeline system. This form of storage requires high deliverability. Traditional storage can meet this albeit at relatively high cost since the amount of gas in inventory necessary to support high deliverability is considerable: typically 100 or greater to one. The substitutes for this form of storage can be interruption, propane air, LNG, and in some cases cheap pipeline expansion. Salt cavern storage is aimed at this market.

- Intermediate winter service -- this is thought of as 30 to 90 day services. This is probably the dominant storage market since propane air or fuel oil can be expensive over this period due to high variable costs. Such storage is vulnerable to pipeline capacity, especially where excess capacity may exist or substantial amounts of capacity can be controlled by a single entity. Traditional storage fields can meet these requirements. In addition, large, baseload LNG plants such as Cove Point and Distrigas can compete with underground storage in this market segment.

- Full winter service -- this is the full 151 day winter service for which traditional storage services were designed. The value of storage in this market is set by the gas pipeline alternative and in the east by the costs of LNG.

Our study is working through these markets in each of the GSAM region. The intent is to identify the value of storage in these markets as an indicator of how R&D can reduce the cost of storage and enhance the overall deliverability of the gas system.

Possible generic RD&D initiatives include increasing the short term deliverability from existing reservoirs by increasing flow rates, decreasing base gas costs by substituting lower cost gases or increasing allowable pressures without causing additional migration, reducing reservoir costs to improve the economics of low inventories by allowing greater deliverability per Mcf of gas stored. Research can help in a greater diversity of storage sites by reducing the costs of smaller facilities or identifying new potential storage media.

4B.2 Field Verification of New and Novel Fracture Stimulation Technologies for the Revitalization of Existing Underground Gas Storage Wells

CONTRACT INFORMATION

Contract Number DE-AC21-94MC31112

Contractor

Advanced Resources International, Inc.
1110 North Glebe Road, Suite 600
Arlington, Virginia 22201
(703) 528-8420 (telephone)
(703) 528-0439 (telefax)

Other Funding Sources

Contractor Project Manager Scott R. Reeves

Principal Investigators Scott R. Reeves

METC Project Manager James R. Ammer

Period of Performance September 27, 1994 to September 26, 1998

Schedule and Milestones

FY95 Program Schedule

	S	O	N	D	J	F	M	A	M	J	J	A
Provide NEPA Information						—						
Review Existing Technology		—	—	—								
Locate Gas Storage Cos.		—	—	—								
Obtain Test Site Approvals					—	—	—					
Develop Work Plans							—	—	—			
Execute & Report on Field Tests										—	—	—

OBJECTIVES

The objective of this research project is to demonstrate improved, less costly means for restoring injection and withdrawal capability in existing gas storage wells. This will be accomplished by field testing alternative fracture stimulation techniques that incorporate the latest in technology with a concentration on cost-effective, small-scale well treatments.

BACKGROUND INFORMATION

An improved, more efficient natural gas transmission and deliverability system will be essential for supporting the expected growth in U.S. gas demand in the coming decades. The role of gas storage in this system will be particularly important as much of the new natural gas use will be cyclic in nature, coming from the residential sector of the north-east with high winter season gas needs, and from new power generation facilities throughout the U.S. with high peak-day requirements. The most cost-effective means for providing this additional seasonal storage capacity and peak-day deliverability is to improve the efficiency of the existing gas storage system. Recognizing the economic realities of FERC Order 636 and an unbundled storage system, the National Petroleum Council clearly set forth industry's views on this issue when they stated[1]:

> *The first step in reducing costs is "minimizing new facility requirements through the more efficient use of existing facilities and the utilization of new technology."*

Thus, a high priority is to improve the efficiency of the 370 gas storage facilities and the 17,000 existing gas storage wells. These facilities and wells currently contain almost 4 Tcf of working gas, 24 Bcf per day of seasonal capability and 54 Bcf per day of peak-day deliverability[2]. The goal is to increase current capability, and, importantly, to counteract the persistent 5.2% loss in annual well deliverability that is being observed by industry[3].

With these annual deliverability losses, it is now becoming obvious to gas storage operators that most wells are not physically performing up to their deliverability potential, but they currently do not have an entirely effective remediation solution. Industry's current deliverability enhancement techniques focus mainly on simple well remediation methods and infill drilling. The typical remediation treatment involves cleaning the wellbore by mechanical means or by blowing/washing, acidizing, and/or re-perforating. Field evidence suggests that these treatments, at best, temporarily restore gas deliverability. As a result, costly infill drilling is the main approach used to offset the decline in gas storage deliverability, which requires annual capital expenditures of $65 to $70 million[2]. Alternative, more effective and durable stimulation methods would significantly lower these costs.

Fracturing technologies, now routinely employed in the oil and gas production industry as a means of stimulating well performance, hold great potential to meet this need. These technologies have not been widely utilized by the gas storage industry, however, because of concerns that created fractures may penetrate the reservoir seal and promote leakage. Through the utilization and advanced treatment design and implementation procedures, these methods can be safely applied to gas storage reservoirs.

The economic impact of successfully transferring these well revitalization techniques to the gas storage industry would be substantial. If the average decline rate of storage well deliverability could be cut by one-third, from 5.2% to 3.5% per year (by effectively fracturing existing wells), such that infill well drilling could be curtailed, the industry would save one-half to two-thirds of what it currently spends offsetting deliverability decline, translating into an industry savings of $50-70 million per year. Hence a substantial RD&D opportunity exists to promote and accelerate the transfer of this technology.

DOE/METC has responded to this industry priority and RD&D opportunity by recognizing it in their Natural Gas Plan and by initiating a major, multi-year field demonstration program designed to demonstrate the application of fracturing to revitalize deliverability from existing gas storage wells. The program's key features are its broad consideration of various new and novel fracturing technologies and its joint effort with and co-funding by industry.

PROJECT DESCRIPTION

The approach that will be utilized for this RD&D project is to test up to five new and novel well stimulation technologies in a series of field demonstrations. A total of nine such tests will be performed during 1995, 1996 and 1997, with each project examining one specific technique. By incorporating three test wells and one control well into each test site, we will be able to rigorously evaluate the five well stimulation technologies being investigated in this project:

- Tip screen-out hydraulic fracturing
- Hydraulic fracturing with liquid carbon dioxide
- Hydraulic fracturing with (proppantless) gaseous nitrogen
- Propellant fracturing
- Nitrogen pulse fracturing

In order to achieve the objectives and requirements of this project, the RD&D effort must possess four key elements (Figure 1):

- A clear demonstration of the effectiveness of fracturing to revitalize the deliverability of gas storage wells, as compared to conventional industry well remediation practices, and the durability of deliverability improvement.

- State-of-the-art fracture treatment design procedures to maximize the potential for stimulation success and to predict the potential for caprock damage.

- A diagnostics program that identifies possible damage to the reservoir seal, both during fracturing (such that it can be immediately arrested) and afterwards.

- Effective deployment of the technology to industry.

These elements, and ARI's approach to providing them, are described below.

Evaluating Deliverability Improvement

A key objective of this RD&D project is to demonstrate the effectiveness of fracturing technologies to improve the deliverability of gas storage wells. Well deliverability is primarily a function of reservoir permeability and wellbore skin effect, the skin being a theoretical measure of the degree of damage or stimulation existing around a wellbore. Since bulk reservoir permeability is unlikely to change significantly with time, skin is the fundamental determinant for deliverability in gas storage wells. Pressure transient testing, which involves the injection or withdrawal of fluids at either a constant pressure or rate, followed by a shut-in period, can be used to quantify the skin value. This technique, therefore is our proposed approach to well deliverability evaluation.

ARI will utilize gas injection/falloff and/or production/buildup testing as evaluation methods, depending upon which technique best suits the needs of each cooperative research partner. Both methods are equally applicable to the needs of this RD&D project, and the flexibility to utilize either approach will allow ARI better to integrate this project with the routine operations of operators. Pre- and post-treatment testing will be performed to evaluate stimulation effectiveness, as well as one year later to measure the durability of the stimulation.

To be successful this project must also compare the deliverability enhancement achieved with the new and novel fracturing technologies to traditional gas storage well remediation techniques in a clear, direct manner. Such clarity between the effectiveness of different stimulation treatments can only be adequately achieved in a controlled, carefully monitored environment in which all wells are evaluated using consistent diagnosis methodologies. Therefore to meet this objective, a control well will be incorporated into each test site, which will be stimulated using the operator's current practices, for direct comparison to the fracturing test wells. This control well

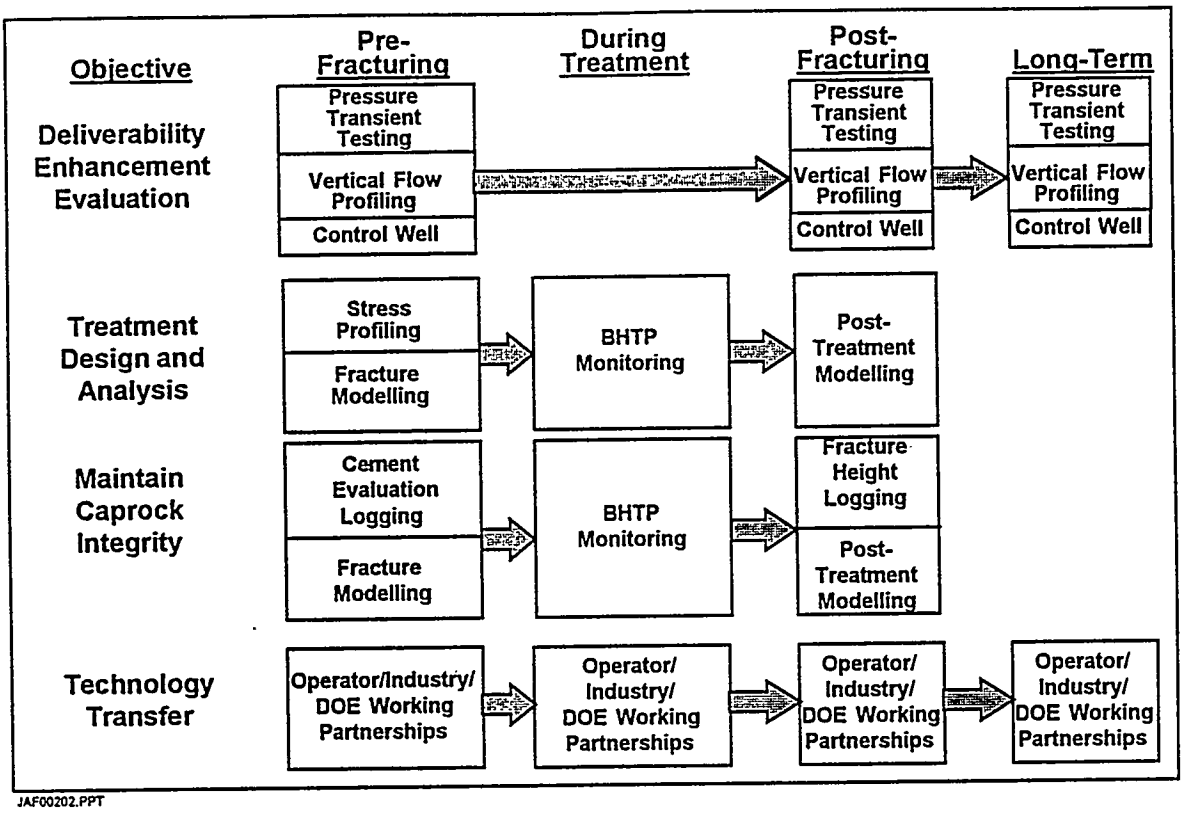

Figure 1. Key Elements of ARI's Technical Approach

will be fully tested and studied in a parallel manner as the fracture test wells, which includes pre- and post-stimulation pressure transient testing to quantify immediate deliverability enhancement as a result of the treatment, as well as testing one year later to evaluate any longer-term changes in well deliverability.

Implementation of Advanced Fracturing Technologies

A critical aspect of this project will be to provide expert design and analysis capabilities for these advanced fracturing technologies. Mike Smith, the pioneer of tip screenout fracturing, the co-developer of the industry-standard Nolte-Smith procedure for the analysis of treatment pressures, and author of the pseudo-3D fracturing simulator STIMPLAN and the mini-frac analysis software FRACTEST, brings unparalleled design and analysis expertise in the area of novel hydraulic fracturing technology. In addition, John Schatz, as author of the leading pulse fracturing simulator PULSFRAC, and a pioneer in the analysis of pulse fracturing treating pressures brings similar expertise in the area of fracturing technology. These intellectual and software resources will be utilized to demonstrate that each fracturing technology being evaluated as part of this project can be confidently and safely designed and implemented.

Maintaining Caprock Integrity

As mentioned previously, the potential for caprock damage is the industry's number one concern with fracturing technology, and the prevention of caprock damage and its detection if it does occur, a priority of this RD&D program. The prevention of caprock damage will be firstly achieved through careful treatment design and modelling. An understanding of rock mechanical

properties and in-situ state of stress will be of critical importance during this process. To obtain these parameters at each test site acoustic logs will be obtained and processed to determine these parameters. Available fracturing, stress test and rock mechanical properties data will be used to correlate the log information to observed values. Fracture simulation studies will be performed to determine how likely an occurrence of fracture breakout is.

Deploying Technology to Industry

Deploying the findings of this RD&D effort to industry will be an equally important element of the program. Without this, DOE's objective of reducing the cost of deliverability enhancement will not be achieved.

This project, being a field verification and demonstration effort, by its very nature possesses an excellent technology transfer component. By working cooperatively with industry in the field, operators will gain a firsthand knowledge of the technology and its application for gas storage. For this reason, the overall project will involve many different operators, as opposed to a select few. Due to the relatively small gas storage community, the nine field tests proposed in this project have the potential to impact of a large percent of the gas storage capacity of the U.S.

RESULTS

Work performed to date has been primarily related to acquisition of test sites for the 1995 RD&D program. To facilitate this, all gas storage companies were contacted and asked if they were interested in providing a test site. Industry response was strong. Forty one companies representing 71% of all U.S. working gas capacity and 75% of all I/W wells indicated an interest to participate in the project. A preliminary screening of potential sites resulted in a list of twelve from which to select the three sites needed for the 1995 RD&D program (Table 1).

A number of technical criteria were then used to further screen the test sites, including consistency with overall project objectives, and simplicity (both geologic and operational) for this first year of the project. Six test sites were deferred on this basis, as shown in Table 2.

From the resulting immediate list of six potential sites, final screening yielded three primary sites and two back-up sites as presented in Table 3, with two planned for demonstrating tip-screenout fracturing and one for fracturing with liquid carbon dioxide. The criteria for final screening included indications that the field would respond positively to fracturing (i.e., has a high permeability and the wells were "damaged"), availability of pre-existing data which would benefit the project, and the consistency of the work plan with the operator's intentions for the field.

Relevant data on the three test sites are presented in Table 4. This mix of projects will provide a comparison of tip-screenout and liquid carbon dioxide fracturing in the sandstone storage formations of Pennsylvania, and a comparison of tip-screenout fracturing in high and low deliverability gas storage fields.

FUTURE WORK

During 1995, the two tip-screenout and one liquid carbon dioxide fracturing RD&D programs presented above will be performed and reported upon. Additional test sites will also be selected for further demonstrating the application of these and other fracture technologies (e.g., propellant, nitrogen, pulse) in 1996 and 1997.

Table 1. Initial List of Potential Test Sites

Company	Field	State
Columbia Natural Gas	Crawford Victory "B" Donegal	Ohio W. Virginia Pennsylvania
KN Energy	Huntsman Wolf Creek Loop	Nebraska Colorado Texas
Consumers Power	Overisel	Michigan
National Fuel Gas Supply	Galbraith	Pennsylvania
Natural Gas Pipeline	Cooks Mills Sayre North Lansing	Illinois Oklahoma Texas
Southern California Gas	West Montebello	California

Table 2. Test Sites Deferred from 1995 Program

Field	Reason
Crawford	Proposed treatment were for new wells
Wolf Creek	Complex geology; faulted, low permeability, naturally fractured
Loop	Horizontal well, not representative of older well population
Sayre	Problem was with injection, not withdrawal
North Lansing	Facilities limitations restricted deliverability enhancement opportunity
West Montebello	Dual completions, operational complexity

Table 3. Final 1995 Test Site Selections

	Field	Company	Initial Treatment Selection
Primary Sites	Donegal	Columbia Gas Transmission	Tip-Screenout
	Galbraith	National Fuel Gas Supply	Liquid Carbon Dioxide
	Huntsman	KN Energy	Tip-Screenout
Secondary Sites	Cooks Mills	Natural Gas Pipeline	Tip-Screenout
	Overisel	Consumers Power	Undecided

Table 4. 1995 Test Site Descriptions

	Donegal (Tip-Screenout)	Galbraith (Liquid CO_2)	Huntsman (Tip-Screenout)
State	Pennsylvania	Pennsylvania	Nebraska
Formation	Gordon Stray	1st Sheffield	Third Dakota "J"
Lithology	Sandstone	Sandstone	Sandstone
Age	Devonian	Devonian	Cretaceous
Reservoir Type	Depleted Gas	Depleted Gas	Depleted Gas
Depth	2600 ft.	2800 ft.	4800 ft.
Thickness	10 ft.	25 ft.	30 ft.
No. I/W wells	112	26	18
Ultimate Storage Capability (Bcf)	9.9	1.9	39.5
Maximum Field Deliverability (MMCF/day)	223	20	101
Maximum Per-Well Deliverability (MMCF/day/well)	2.0	0.8	5.6
Maximum Storage Pressure (psi)	1260	620	1170

REFERENCES

1. Potential for Gas in the United States, Washington, D.C.; National Petroleum Council, 1992.

2. Survey of Gas Storage Facilities in the United States and Canada, 1993, Arlington, VA; American Gas Association, Operating Section Report, 1993.

3. State of Technology Assessment and Evaluation of Gas Storage Well Productivity Techniques, Maurer Engineering, Inc. and T. Joyce Associates, Inc., GRI 93/0001, December 1993.

4B.3 Underground Natural Gas Storage Reservoir Management

CONTRACT INFORMATION

Contract Number	DE-AC21-94MC31113
Contractor	**UEDC** United Energy Development Consultants, Inc. 2301 Duss Ave. Suite 12 Ambridge, PA 15003 1-412-266-8833 1-412-266-9002 fax
Other Funding Sources	----
Contractor Project Manager	Isaias Ortiz
Principal Investigators	Isaias Ortiz Robin V. Anthony
METC Project Manager	Anthony M. Zammerilli
Period of Performance	Phase I -- Sept. 23, 1994 -- April 30, 1995
Schedule and Milestone	

Program Schedule

Phase I	**FY95** S	O	N	D	J	F	M	A	M	J	J	A
Electronic Data												
Research Storage Losses												
Summarize Losses												
Evaluate Financial Impact												
Write Report												

OBJECTIVES

The objective of this study is to research technologies and methodologies that will reduce the costs associated with the operation and maintenance of underground natural gas storage. This effort will include a survey of public information to determine the amount of natural gas lost from underground storage fields, determine the causes of this lost gas, and develop strategies and remedial designs to reduce or stop the gas loss from selected fields.

Phase I includes a detailed survey of US natural gas storage reservoirs to determine the actual amount of natural gas annually lost from underground storage fields. These reservoirs will be ranked, the resultant will include the amount of gas and revenue annually lost. The results will be analyzed in conjunction with the type (geologic) of storage reservoirs to determine the significance and impact of the gas loss. A report of the work accomplished will be prepared. The report will include; 1) a summary list by geologic type of US gas storage reservoirs and their annual underground gas storage losses in ft^3; 2) a rank

by geologic classifications as to the amount of gas lost and the resultant lost revenue; and 3) show the level of significance and impact of the losses by geologic type.

Phase II includes a determination of the mechanisms and causes of lost gas due to migration and related causes shall be summarized. Correlation's among storage reservoir types, locations, characteristics such as trap type, and gas loss mechanisms that are common to all U. S. storage reservoirs surveyed will also be included. For each type of storage field identified, screen, rank, and evaluate the source causes of gas migration. Strategies for prevention of gas loss as a result of the analysis, strategies and remedial designs to reduce or stop the gas loss from the highest ranked fields identified will be evaluated.

BACKGROUND

Gas storage operators are facing increased and more complex responsibilities for managing storage operations under Order 636 that requires that storage be unbundled from other pipeline services. Low cost methods that improve the accuracy of inventory verification are needed to optimally manage stored natural gas. Gas loss is costly to the operator as well as to the consumer.

Migration of injected gas out of the storage reservoir is a problem that has not been well documented by industry. The two types of gas losses that occur are those due to mechanical communication with adjacent formations or migration of gas out of the storage reservoir due to unknown faults or poor reservoir traps. The goal of this investigation is to estimate the amounts of natural gas annually lost from underground storage fields and determine the significance and impact of the lost gas, and resultant revenue loss.

Storage reservoir types, regional locations, characteristics such as depth, pressure, trap types, and vintage of U. S. storage reservoirs are discussed. Correlation's between certain types of storage fields and commonly found mechanisms of gas leakage are elaborated. The impact of this gas loss is assessed from available databases, which, due to the sensitive nature of the information, is reported on an aggregate basis. Once this impact is quantified, the source causes of gas migration and gas loss mechanisms can then be evaluated in order to develop strategies to mitigate these losses.

For northern climates' storage gas represent some 20% of the annual sales; while on a cold day, storage gas may reach some 50-70% of gas sold. By providing continuous fuel service to residences, hospitals, and commercial buildings, underground gas storage has been a vital part of natural gas distribution systems.

Historically, underground storage, which was first practiced in 1915, experienced a remarkable growth starting in 1950 resulting in nearly 7.5 trillion cubic feet in storage in more than 400 pools in 25 states by 1979. Currently, gas storage operators are facing increased responsibilities for managing these storage operations under Order 636 that requires that storage be unbundled from other pipeline services.

Energy supply and demand over the last twenty years are shown on Figure No. 1. As shown, the net amount of energy imported has increased steadily, while the relative contribution of US production to domestic supply requirements has steadily declined. Figure No. 2 shows only US gas consumption and production; similarly, consumption has exceeded supply.

Concurrently, the amount of storage activity has increased in conjunction with the net increase of natural gas imports as shown on Figure No. 3. Storage is playing an ever increasing importance in supplying the domestic energy requirements.

Natural gas was first stored underground successfully in 1915 in Canada, where a depleted gas reservoir was developed for peak requirements. In 1916 the first successful underground storage project in the United States was developed by Iroquois Gas Company (a National Fuel affiliate). That project, the depleted Zoar Field, is still in use today.

The first depleted oil and gas field developed for natural gas storage was Fink Field in Lewis County, West Virginia, in 1941 by Hope Natural Gas Company (Consolidated Gas Supply Corporation). Historic records show that gas storage began by allowing depleted gas reservoirs produced in the winter to be recharged in summer by pipeline gas. As the intercontinental pipeline systems spread rapidly in the post war period, reservoirs were selected and refurbished for full utilization as underground storage reservoirs. Figure No. 4 shows the development of storage in the US since 1916.

The first depleted oil reservoir used for natural gas storage was started by Lone Star Gas Company, which developed the New York City Field in Clay County, Texas, in 1954. Eventually a number of depleted oil fields were converted to gas storage. Oil recovery was part of the objective in the early years of operation. Oil in reservoirs however, added complications over dry gas storage fields due to liquids in the well bore, possible enrichment of the gas, and condense formation in pipelines. Also, gas could go into solution in crude oil in amounts that made it difficult to assess the volume of stored gas in the reservoir.

In the 1950's, aquifer storage was developed by injecting gas into structures filled with water. Here water movement and caprock quality became focal points of interest for research and technical development. Louisville Gas and Electric Company first started experimenting with the storage of natural gas in a water-bearing sand aquifer in 1931 and developed the Doe Run Field in 1946. This Meade County, Kentucky, project is the oldest aquifer storage field operating in the United States, although it no longer exhibits the water-drive characteristics of an aquifer.

Porous and permeable rock provided by nature was the only storage host of natural gas until 1961, when cavities in bedded salt were developed by Southeastern Michigan Gas Company in St. Clair County, Michigan. Leached cavern storage in salt dome intrusions was developed by Transcontinental Gas Pipe Line Corporation in 1970 in Covington County, Mississippi. Currently, salt domes, which occur principally in the Gulf Coast region of the United States, account for 1% of gas stored underground.

In 1959 mined cavern storage of natural gas was introduced by the Public Service Company of Colorado, which converted an abandoned coal mine in Jefferson County, Colorado, into a storage reservoir. No mine has yet been excavated solely for natural gas storage, although extensive studies have been conducted.

The relative contribution of these types of storage reservoirs as shown on Figure No. 6. Regional storage capacity is summarized on Figure No. 5. The largest amount of storage is located in the Northeast and Mid-west.

Low cost methods that improve the accuracy of inventory verification are needed to optimally manage stored natural gas. Gas loss is costly to the operator as well as to the consumer. Migration of injected gas out of the storage reservoir is a problem that has not been well documented by industry.

The types of gas losses that occur are those due to mechanical communication with adjacent formations or migration of gas out of the storage reservoir due to unknown faults or poor reservoir traps. This study was undertaken to address the problem of this gas loss. The source causes of gas migration (Table No. 1) and gas loss mechanisms need

to be identified and evaluated in order to develop strategies to mitigate these losses.

PROJECT DESCRIPTION

Sources of information used in this report include textbooks, journal articles, American Gas Association (AGA) and Gas Research Institute (GRI) reports, and Federal Energy Regulatory Commission (FERC) and Energy Information Administration (EIA) databases. Underground storage fields, operators and geologic formations were identified and categorized and the available databases were analyzed. A summary of the sources of information is tabled below: (Table No. 2)

A database search was conducted in order to identify sources of detailed and comprehensive information on the storage field reservoirs in the United States. Databases and reports are available from a number of public sources, including both private and government institutions. Non-government sources include the Gas Research Institute (GRI) and the American Gas Association (AGA). The Federal Regulatory Commission (FERC) public databases were also accessed. In addition, certain restricted information was also made available through the Energy Information Administration (EIA). Results from the analysis of the EIA data are reported in a manner consistent with the regulations regarding the use of this information. The types of information contained in the databases used for analysis are summarized below.

FERC

Public reports on underground gas storage are available through the Federal Energy Regulatory Commission (FERC). Data from 1988 onward has been submitted to the FERC by companies under the FERC's jurisdiction, via electronic media and has been incorporated into computer databases. The following FERC reports were initially examined:

- Form 2: Annual Report of Major Natural Gas Companies, filed by about 45 interstate and natural gas pipeline companies with combined gas sold for resale and gas transported or stored for a fee exceeding 50 billion cubic feet. The 132-page report contains general corporate information, financial statements and supporting schedules, and engineering statistics.
- Form 2-A: Annual Report of Non-major Natural Gas Companies, filed by about 86 interstate natural gas pipeline companies, with annual sales or volume transactions of more than 200 million cubic feet but less than 50 billion cubic feet. The 19-page report contains corporate information, financial statements and supporting schedules, and engineering statistics.
- Form 8: Underground Gas Storage Report, five-page report filed monthly by about 40 natural gas companies that operate natural gas storage fields in the United States.
- Form 11: Natural Gas Pipeline Company Monthly Statement, filed by about 35 natural gas pipeline companies that sold and/or transported, for a fee, more than 50 billion cubic feet of gas during the previous calendar year. The 7-page report contains data on revenues, income, operating and maintenance expenses, and gas supplies.

Three-quarters of the volume of gas stored underground are in fields operated by companies reporting in FERC Form 2. Therefore, a detailed analysis was conducted on FERC Form 2 data. Data from this form was sorted and comparisons between data sets were graphed in order to identify potentially useful relationships.

An in-house FERC report, "The Semi-Annual Report on Jurisdictional Underground Natural Gas Storage Fields in the United States" was also obtained, along with the supporting electronic database and graphs covering a ten-year period. Monthly injection

and withdrawal cycles of gas from underground storage are reported by each pipeline company subject to the jurisdiction of the FERC. (Figure No. 7) The gas volumes represent around 70% of the volume of gas stored underground in the United States. Reported as an aggregate of all active storage fields operated per company, this database does not discern individual storage field volumes. The report is based on the compilation of present and past information, technical interpretation and analysis by the Supply Analysis Branch staff (currently reorganized under the FERC's Office of Pipeline Regulation).

AGA

The 1992 AGA Operating Section Report-Survey of Underground Gas Storage Facilities in the United States and Canada was also used for this study. The information in this report contains individual storage field summaries, including: the company, reservoir name, formation, type of trap, reservoir characteristics, base and working gas, etc. Once again, however, monthly volumes per field are not available. A total of 425 reservoirs is listed in the AGA report, with cumulative gas volumes, wells, acreage and horsepower, and average thickness, depth and pressure, are summarized below. The US has around 400 storage reservoirs. Figure No. 8 shows the number of storage operators versus the total capacity as a percentage. Only 20% of the storage operators operate about 80% of the total underground storage capacity. Two major operators operate nearly 25% of the underground storage capacity in the US.

EIA

The Energy Information Administration (EIA) collects monthly individual storage field data on working and base gas volumes, total gas in storage and injections and withdrawals that they report on their Form 191. This detailed information allows for a more thorough examination of changes in storage field conditions. Gas losses that may be concealed through aggregate reporting methods may become more apparent when viewed on a monthly basis by field. Access to this report is necessarily restricted due to the confidential nature of the material reported. This information was used, in conjunction with the publicly available data, to better determine actual gas loss, define general field characteristics that may be indicative of gas loss and quantify overall trends concerning gas migration.

All of these databases were imported into a spreadsheet format. This format allows for manipulation of the databases and sorting by category, such as company or geologic formation, that will allow for rapid characterization of, and correlation among, the various storage fields. For example, a preponderous amount of lost gas among a particular geologic formation or type of trap may indicate a geologic cause of migration (such as natural fracturing or incomplete seal) as opposed to a correlation with date of storage conversion, which may indicate a mechanical mechanism, especially in older vintage wells. Mechanical problems, such as pipe corrosion, can cause leakage, while repeated injection and withdrawal (perhaps with prior repeated hydraulic stimulation to improve deliverability), could result in eventual damage to the formation.

RESULTS

Current Status Of Underground Storage

The AGA database lists a total of 83 operators in the United States who maintain active storage fields with a total capacity of around 7 trillion cubic feet (TCF) of gas. Roughly 72% of this gas are under the jurisdiction of the Federal Energy Regulatory Commission (FERC). Approximately 45% of gas stored underground is working gas, with the remaining 55% forming the base gas.

The number of storage operators that represent a large percentage of the total

storage capacity is relatively small. One quarter of storage field operators maintains three quarters of the US underground storage capacity. Half of the storage capacity is operated by ten percent of the active storage operators. Nearly one-quarter of the storage capacity in the US is operated by only two companies.

Underground natural gas storage facilities in the United States are located in only 25 of the lower 48 states. Even there, almost half the total storage capacity is concentrated in only three of these states as illustrated by the chart below. (See Figure No. 9.)

The majority of underground natural gas storage capacity, facilities and deliverability in United States is located primarily in the Eastern and Midwestern geographical areas.

Types Of Storage

Storage reservoirs can be classified by several parameters. Common classification schemes include: drive mechanism, type of geologic trap, lithology, permeability and initial fluid content. In working with available databases and reports, an attempt was made to determine the common parameters addressed in each of the databases. Three types of underground storage recognized by the FERC, EIA, GRI and AGA are

1) Depleted reservoir,
2) Aquifer, and
3) Cavern or mine.

The three storage classifications are defined by drive mechanism, type of geologic trap, lithology, and initial fluid content. (Permeability is another important parameter that strongly influences well deliverability; however, the value of field permeability is often uncertain or unknown.) Drive mechanism can usually be described as one of two readily determinable states: water drive or pressure drive. Drive mechanism has an important effect on the productivity of a well. All of the caverns and most (around 85%) of the depleted reservoirs are classified as pressure drive. Pressure drive has also been referred to as pressure depletion or volumetric expansion. All aquifers have water drive mechanisms. The term aquifer refers to a water-bearing zone. Thus, the initial fluid content of all aquifers is water. Figure No. 6 shows the total number of US storage reservoirs in each of these classifications:

Depleted reservoirs are the only type of storage field found in the Northeast. Aquifers are most common in the Midwest, while most salt caverns are found along the Gulf Coast. Half of the salt caverns are located in Texas. The one storage reservoir in an abandoned coal mine is located in Colorado.

Another parameter known to have a significant influence on the production and maintenance of a gas well is the trap type. Many geologic trap descriptions are given in Table No. 3, below. Lithology is another important and easily determined categorization parameter. All known underground gas storage reservoirs consist of porous formations of sandstone (or carbonate) or are salt dome associated. Although a variety of geological terms are used by the operators, four descriptions can be used to generically specify any of the geologies listed below. These are:

1) salt cavern
2) stratigraphic
3) structural
4) combination of stratigraphic/structural

Gas Loss -- Comparative Database Analysis

The FERC, EIA, and AGA databases contain gas volume information. This gas volume information was analyzed for evidence of gas loss.

Gas losses are reported directly in the FERC Form 2 report and indirectly through the accounting and financial data of this report.

The indirect and reported gas losses were summarized, compared and added in order to

arrive at an estimate of the magnitude of total gas loss occurring. Gas-in-Place for storage fields is calculated by the following equation. Losses are reported directly in the FERC Form 2 report and indirectly through the accounting and financial data of this report.

GIP = NATIVE + BASE + WORK +ADD – LOSS

Where GIP = (gas-in-place)
NATIVE = native gas originally in place
WORK = working gas
ADD = additions to storage and
LOSS = gas losses

The EIA reports end of year (EOY) and beginning of year (BOY) GIP volumes. The amount of GIP and associated storage losses can be calculated by the following:

EOY(GIP) =BOY(GIP) + INJ – WITH + ADD - LOSS

Where INJ = injected volumes during the year
WITH = withdrawals during the year

Gas Loss Reporting

Gas losses from storage reservoirs can be reported in several ways by virtue of the reporting method. FERC Form 2 gas losses are reported as transportation losses' 98% of the time, vs. other forms of gas loss, such as reservoir.

Gas storage losses are often reported as an increase in cushion gas, particularly for gas storage in aquifers (FERC-personal communication). Migration of gas, into tighter areas of the formation, or solution of gas in the water or the creation of isolated non-recoverable pockets of gas are the primary mechanisms of gas loss in these instances. Aquifers are used for gas storage exclusively in the Midwest. Approximately 25%, or one-quarter of the storage fields have an active water drive. Of these, half are aquifers.

The largest gas losses appear, from FERC Form 2 data, to be from conventional depleted gas reservoir storage fields in the Northeast. These fields are primarily sandstone with either structural or stratigraphic trapping mechanisms. In certain instances, these apparent losses are reported in FERC Form 2 as gas removed from storage or as a negative addition to gas storage. This type of loss tends to be reported over one or two months in one calendar year, although the loss may actually be cumulative ongoing. Pressure depletion (gas expansion) reservoirs account for 72%, or almost three-quarters, of active storage fields. Two-thirds of these reservoirs are in sandstone. Therefore, depleted sandstone reservoirs account for half of all storage reservoirs.

Table No. 4 (and Figure No. 10) Summarize the gas-in-place volumes from EIA data. The end-of-year, injected and withdrawn gas volumes are reported. Also, shown on this table are the net gas losses and additions associated with storage. The total gas loss/additions to storage from 1989 to 1994 is 530 BCF. This number also includes additions to storage during that time period.

It appears that, except for salt cavern storage, most fields, for various mechanical and geological reasons, will experience a certain amount of ongoing gas loss. Certain cases have demonstrated that a leak from the reservoir does not necessarily prevent it from serving a market very effectively.

The impact of this loss may be offset by other factors, such as geographical location and proximity to market, the size of the company and the number of fields it operates, the size of the storage field, the availability, or lack, of a suitable replacement field, the costs of maintaining vs. developing a storage field, the cost of various mitigation measures, and whether these measures will prove effective in eliminating or containing the problem.

While the economics may vary, in general, some of the smaller fields that experience a large percentage of inventory decline due to gas loss may be effectively abandoned. Conversely, mitigate measures may be sought for larger, more critically important fields, before a decision to abandon the field is sought.

The effectiveness of mitigation measures and the types of fields to which they apply along with new technologies and the use of new reservoir types (such as salt caverns) need to be compared for an effective overall storage strategy to be implemented in the wake of Order 636.

FUTURE WORK

The work presented here in Phase I incorporates information obtained solely from public sources. A detailed analysis of EIA Form 191 data, which tabulates individual reservoir data also has to be incorporated into this analysis along with the Form 2 financial information to arrive at the impact of losses categorized by storage type.

Remaining work includes:

- detailed loss estimate for 400 reservoirs
- categorization of these losses by geologic type
- categorization of losses by drive mechanism
- Estimation of the financial losses for each reservoir

The results of Phase I will be reviewed and incorporated in Phase II of this study.

REFERENCES

DOE/ EIA

1. EIA, Natural Gas Annual 1992, Volume I, US DOE/EIA-131(92)/1, Washington, DC, Nov. 1993, p. 40-41.
2. USDOE, Natural Gas Strategic Plan and Multi-year Program Crosscut Plan, FY 1994-1999, DOE/FE-0297P, Washington, DC, Dec. 1993, p. 4:159-4:185.
3. EIA, Emissions of Greenhouse Gases in the United States, 1985-1990, US DOE/EIA-0573, Washington, DC, Sept. 1993, p. 29-30.
4. EIA, Energy Facts, 1992, USDOE/EIA-0469(92), Washington, DC, Oct. 1993, p. 40-41.

BOOKS & OTHER PUBLICATIONS

5. Tek, M.R., Underground Storage of Natural Gas, Contributions in Petroleum Geology & Engineering Series, Volume 3, Gulf Publishing Company, Houston, TX 1987, 389p. ISBN 0-87201-913-6
6. Katz, D. L. and K. H. Coats, Underground Storage of Fluids, Ulrichs Book Store, Inc., Ann Arbor, Michigan, 1968.
7. Duann, D.J., Nagler, P.A., et al., Gas Storage: Strategy, Regulation, And Some Competitive Implications, The National Regulatory Research Institute, September 1990
8. Pennsylvania Public Utility Commission, "Statements of Policy, Recovery of FERC Order 636 Transition Costs," Pennsylvania Bulletin, Vol. 23, No. 13, March 27, 1993, p. 1478-1484
9. Anderson, D., Report Of The Commission Of Inquiry Into Fraser Valley Petroleum Exploration, Province of British Columbia Jan. 1991.
10. Ball, D. and Burnett, P. G., "Storage of Gas in Water Sands." In Beebe, B. W., Natural Gases of North America, V. 2. Tulsa: American Association of Petroleum Geologists, 1890-1898 (1968).
11. Bamds, R.M., Playa Del Rey Oil Field, Los Angeles County, California Natural Gas Storage. Mem. – Am. Assoc. Pet. Geol. 1: 9, 169-173 (1968).

A.G.A /GRI

12. Ball, D. and Burnett, P. G., "The Storage of Gas in Water Sands." Proceedings of American Gas Association, Operating Section, 1959, T63-T48, (GSTS-59-9) New York, N. Y., 1959.
13. Balogh, D.R., "Detection and Monitoring of Gas Bubble Growth in Underground Gas Storage Field Through the Use of High Resolution Reflection Seismology." Evergreen, CO: Evergreen Geophysical Association, Inc. (1985) February. AGA Research Project PR-160-154.

14. Fogler, H.S. and Crain, E.R., "Stimulation of Gas Storage Fields to Recovery Deliverability." A.G.A. Oper. Sect. Proc. T403-411 (1980).
15. Gas Research Institute. Critical Performance Parameters for Horizontal Well Applications in Gas Storage Reservoirs, Chicago (PB94-103793.)
16. Gas Research Institute. The Deliverability Issue, Final Report. November 1990--March 1991, Chicago
17. Gas Research Institute. The Load Balancing Issue Final Report November 1990-June 1991, Chicago
18. Katz, D. L. and Tek, M. R., "Storage of Natural Gas in Saline Aquifers." Trans. Paper No. H69, 50th Annual AGA Meeting, April 21-25, 1969.
19. Katz, D. L., Tek, M. R. and Ibrahim, M. A., "Threshold Displacement Pressure in Gas Storage." AGA Oper. Sect. Proc. -- 1969, 69-T-33.
20. Martinson, E. V., "Review of Aquifer Gas Storage Projects." A.G.A. Oper. Sect. Proc., GSTS-61-23 (1961).
21. Pandey, G. N., Tek, M. R., and Katz, D. L., "Studies of Front-End Threshold Pressure Measurements," A.G.A. Operating Section Proceedings, T-112 (1973).
22. Tek, M. R., et al., Inventory-Migration-Deliverability In Underground Storage. Arlington, VA: American Gas Association (1987).
23. Colonna, J. and Carriere J-F, "Cushion Gas and Working Volume: for Each Geological Structure, Its Optimal Management." A. G. A. Operating Section Proceedings, 665 (1985.)
24. Kelley, W. M., "Underground Storage of Gas in the United States." AGA Oper. Sect. Proc., 64-T-184 -- 64-T-185, (1964).
25. Tek, M. R. et al., "New Concepts in Underground Storage of Natural Gas." AGA Monograph on Project P050, New York (1966).
26. Byrne, J. J. and Lu, T. A., "Fully Automated Gas Storage Field." A.G.A. Oper. Sect. Proc., T16-T21 (1975).
27. Clark. W. H., "Use of Storage Field Automation by the Reservoir Engineer." A.G.A. Operating Section Proceedings, T-230 (1975).
28. Wallis, G. B., Slug Frequency in Horizontal Gas-Liquid Flow. Arlington, VA: American Gas Association (1990).
29. Katz, D. L., "A Look Ahead in Gas Storage Technology." A. G. A. Oper. Sect. Proc., T283-90 (1981).
30. Hardy, H. Reginald, Jr., et al., A Study to Evaluate the Stability of Underground Gas Storage Reservoirs, (project 12-43), American Gas Association, Inc., Arlington, VA, 1972.
31. Underground Storage Volume I-Supply, Gas Engineering and Operating Practices Series, American Gas Association (AGA) *printed in USA*, 1990.

J.P.T. /OIL GAS JOURNAL/ S.P.E.

32. Aronofsky, J. S. and Jenkins, R., "A Simplified Analysis of Unsteady Radial Gas Flow." J. Pet. Tech. 6, 23 (1954) July.
33. Bagrodia, V. and Katz, D. L., "Gas Migration by Diffusion in Aquifer Storage." J. Petrol. Tech. 29, 121-122 (1977) February.
34. Bailey, P. E., "Accident Field Proves No Accident to Texas Eastern." Pipeline Eng. 41:1, 50, 52, 54 (1969) January.
35. Baird, J. L., "Clay Basin Storage Project -- Development of a Nearly Depleted Gas Reservoir (Dakota Reservoir) to Gas Storage." In Society of Petroleum of AIME. Rocky Mountain Regional Meeting, Cody, Wyoming, May 17-18, 1978, (SPE-7171) Dallas: Society of Petroleum Engineers, 1978.
36. Batten, R.B. and Elenbaas, J. R., "Giant Storage Enables Sendouts Ranging from 150 to 1,270 MMCFD." Oil Gas J. 57, 164-168 (1959) March 9.
37. Bell, A.H., "Underground Gas Storage in Illinois." Paper presented at Illinois Geological Survey & Illinois Basin Chapter of the S.P.E. of the A.I.M.E. Petroleum Engineering Conference, Urbana, Illinois, May, 1961.
38. Bell, J. S. and J.M. Shepherd; "Pressure Behavior in the Woodbine Sand," Trans. AIME, Vol. 92, p 19 (1952).
39. Berger, L.C., Arnoult, J. R., "Production of Inert Gas for Partial Replacement of Natural Gas Trapped in an Underground Aquifer Storage Reservoir." Proceedings: 1989 SPE Gas Technology Symposium, Dallas, TX (June 7-9, 1989) p. 309-320. Bernard, G. G. et al., "Model Study of Form as a Sealant for Leaks in Gas Storage Reservoirs." Soc. Pet. Eng. J., 10, 9-16 (1970) March.
40. Bond, D.C. and Cartwright, K., "Pressure Observations and Water Densities in Aquifers and Their Relation to Problems in Gas Storage." J. Pet. Tech. 22, 1492-1498 (1970) December.
41. Briggs, J. E. et al., "Water Drainage From Sand in Developing Aquifer Storage." Oil Gas J. 66, 61-66 (1968) December.
42. Coats, K. H. and others. "Calculation of gas recovery upon ultimate depletion of aquifer storage." Proceedings of 42 Annual SPE of AIME Fall Meeting, Oct. 1-4, 1967. 1967. Preprint No. SPEC-1815. 8 pp.
43. Coats, K. H. and Richardson, J. G., "Calculation of Water Displacement by Gas in Development of

Aquifer Storage." Soc. of Pet. Eng. J., 7, 105-112 (1967) June.
44. Coats, K. H. et al., "Determination of Aquifer Influence Functions from Field Data." J. Pet. Tech. 16, 1417-1424 (1964) December.
45. Coats, K. H. "Some Technical and Economic Aspects of Underground Gas Storage." J. Pet. Tech. 18, 1561-1566 (1966) December.
46. Collier, R. S. Monash, E. A. and Hultquist, P. F., "Modeling Natural Gas Reservoirs – A Simple Model." Soc. Pet. Eng. J. 21, 521-26 (1981) Oct.
47. Ellington, D. M., "Frac Plan Pays Off in Gas Storage." Pet. Eng. 13, No. 33, 75-80 (1961) December.
48. Kumar, A. and Kimbler, D. K., "The Effect of Mixing and Gravitational Segregation Between Natural Gas and Inert Cushion Gas on the Recovery of Gas From Horizontal Storage Aquifers." SPE Paper 3866, 4th Biannual Natural Gas Technology Symposium of SPE, Omaha, 1972.
49. Mayfield, J. F., "Inventory Verification of Gas Storage Fields." J. Pet. Technol. 33, 1730-34 (1981) Sept.,
50. McMinn, R. E., "Production Techniques for Aquifer-Type Gas Storage Fields." Paper No. SPE 1685, SPE of AIME Northern Plains Sect. Reg. Gas Technol. Symp. 1966.
51. Bleakley, W. B., "Old Coal Mine Converted to Gas Storage." Oil Gas J. 59, No. 51, 88-94 (1961) December 18.
52. Katz, D. L. and Tek, M. R., "Overview on Underground Storage of Natural Gas." J. Pet. Technol. 33, 943-51 (1981) June.
53. Knepper, G. A. and Cuthbert, J. F. "Gas Storage Problems and Detection Methods," AIME, SPE Paper No. 8412, Dallas, 1979.
54. Van Horn, H.G. and Wienecke, D. R., "A Method for Optimizing the Design of Gas Storage Systems." Preprint No. SPE-2966, presented at 45th Annual SPE of AIME, Fall Meeting, 1970.
55. "How Northern Natural Operates Aquifer Storage." Oil Gas J. 59, No. 6, 116-117 (1961) March 13.
56. Shotts, S.A, J. R. Neal, R.J. Solis, "Spindletop Salt-Cavern Points Way for Future Natural-Gas Storage," Oil & Gas Journal, Vol. 92, No. 37, Sept. 12, 1994, p. 68-75
57. Barron, Thomas F. "Regulatory., technical pressures prompt more U. S. Salt-cavern gas storage," Oil & Gas Journal, Sept. 12, 1994, p. 55-67
58. "Underground Natural Gas Storage Fields, Table 1," Pipeline Report Issue, Oil & Gas Journal, Vol. 92, No. 37, Sept. 12, 1994, p. 47-54.
59. Katz, D. L. and Tek, M.R., "Overview On Underground Storage Of Natural Gas." SPE Paper No. 9390, presented at the 55th Annual Fall Tech. Conf. and Exhibition of the SPE and AIME; Dallas, TX, Sept., 21-24, 1980.
60. Mayfield, J.E., "Inventory Verification Of Gas Storage Fields." SPE Paper No. 9391 presented at the 55th Annual Fall Tech. Conf. Exhibition of the SPE of AIME held in Dallas, TX. Sept. 21-24 1980
61. Shikari, Y.A., "Gas Research Institute Underground Gas Storage Program; An Overview." SPE Paper No. 17739 presented at the SPE Gas Technology Symposium, Dallas, TX; June 13-15. 1988.
62. Misra, B.R., and Foh, S. E., Shikari, Y.A., Berry, R.M., Labaune, F. "The Use of Inert Base Gas in Underground Natural Gas Storage." SPE Paper No. 17741 presented at the SPE Gas Technology Symposium, held in Dallas, TX, June 13-15, 1988.
63. Weaver, J.D., and Morgan, J.A., "Furan Resin Process Replaces Workovers in Gas Storage Reservoirs." SPE Paper No. 17742 presented at the SPE Gas Technology Symposium, held in Dallas, TX, June 13-15, 1988.
64. Gomm, H. and Quast, P., "Status of Gas Storage in Salt Caverns in West Germany." SPE Paper No. 19084 presented at the SPE Gas Technology Symposium held in Dallas, Texas, June 7-9, 1989.
65. Toneyl, J.B., Morgan, J.A., Barnetter, J.C., and Bieleckil, D.L., "Completion Planning for Elimination of Sand Production in Thinly Bedded Aquifer Gas Storage Wells." SPE Paper No. 19756, presented at the 64th Annual Technical Conference and Exhibition of the Society of Petroleum Engineers held in San Antonio, TX October 8- 11 , 1989.
66. Hower, I., Fugate; M. Wand Owens, R. W., "Improved Performance in Aquifer Gas Storage Fields Through Reservoir Management." SPE Paper No. 26172.
67. Bergin, and Shikari, Y.A., "A Horizontal Well in Gas Storage: A Case Study." SPE Paper No. 26165 presented at the SPE Gas Tech. Symposium, Calgary, Alberta, Canada.
68. Chierici, Gottardi, G., and Guidorzi, R., "Identified Models For Gas Storage Dynamics." SPE Paper 8862 (unsolicited).

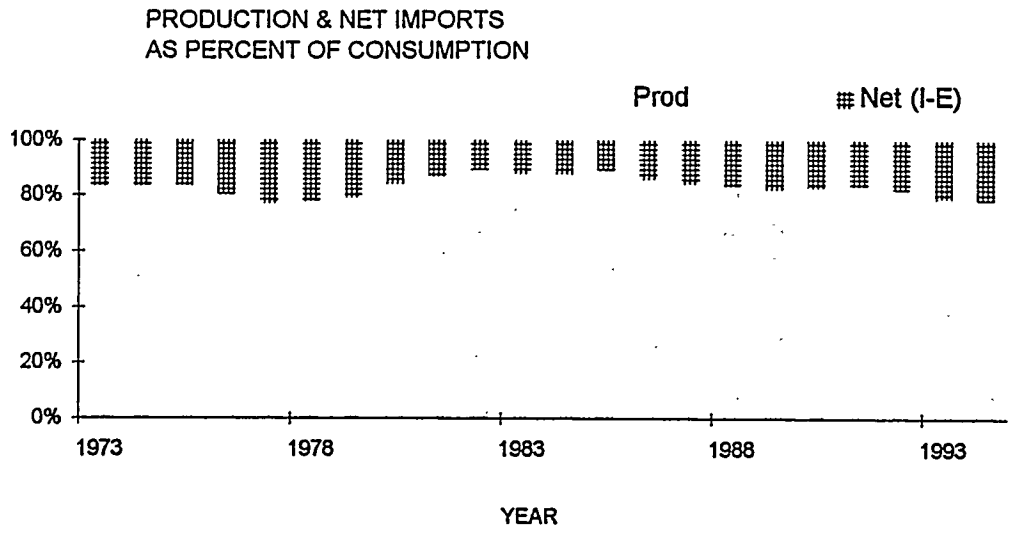

Figure 1. US Total Production and Net Imports as Percent of Consumption (1973-94)
source: Table 1.2 Energy Overview EIA

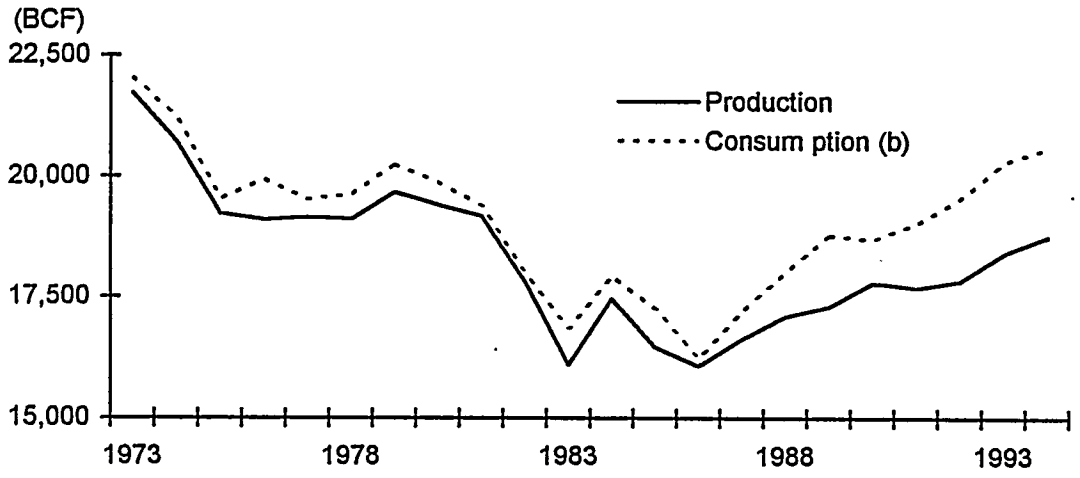

Figure 2. US Total Gas Consumption and Production (1973-94)

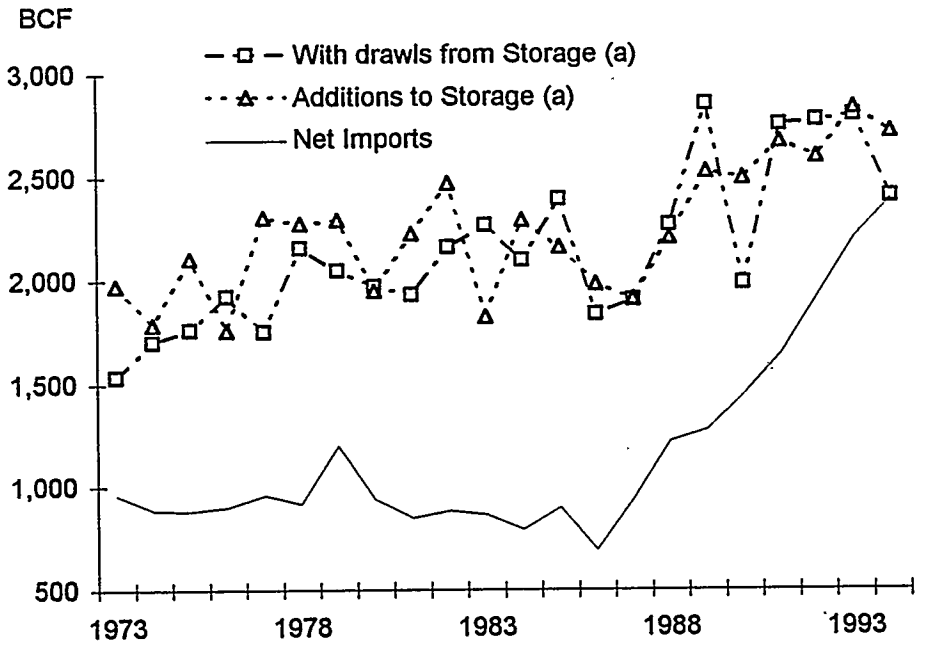

Figure 3. US Underground Natural Gas Storage Activity and Net Imports Gas (1973-94)

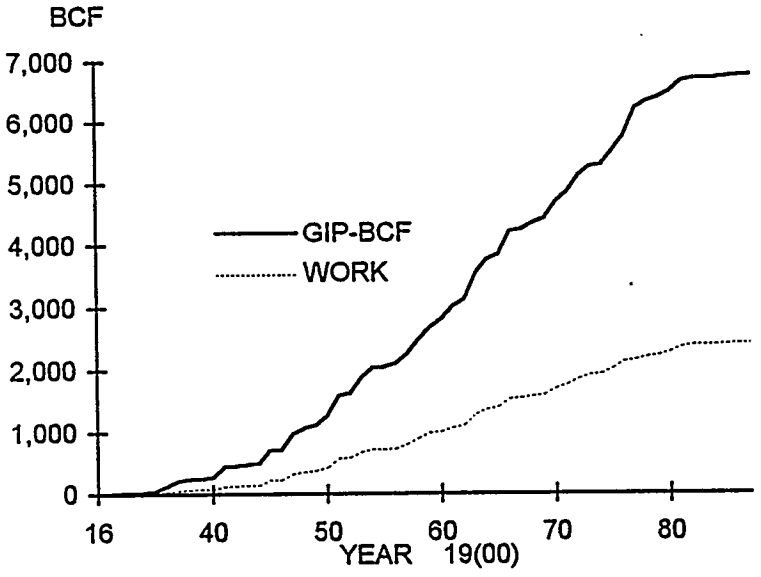

Figure 4. Underground Natural Gas Storage Development (1916-92)

source: AGA 1992 database

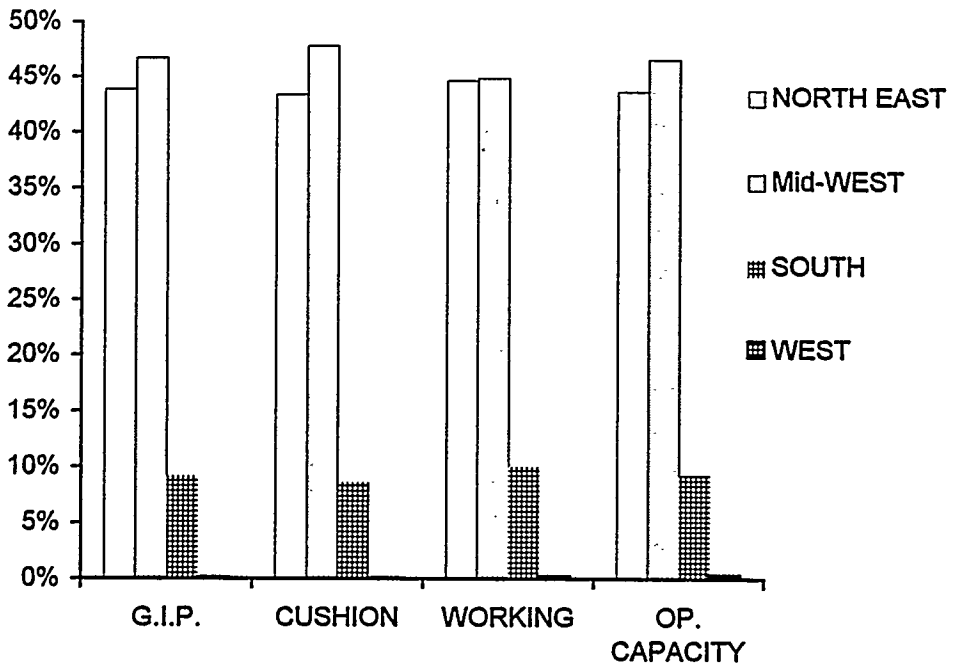

Figure 5. Total US Regional Storage Distribution -1994

source: FERC 1994 semi-annual report

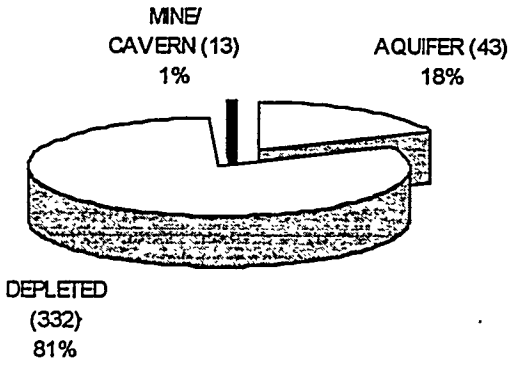

Figure 6. Distribution of Storage Reservoir Types

source: AGA 1992 database

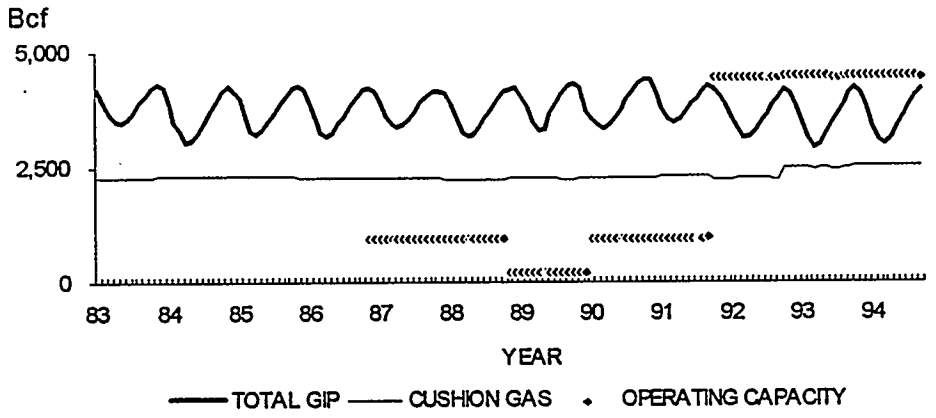

Figure 7. US Underground Natural Gas Storage Capacity (1983-94)

source: FERC 1994 database Form 2.

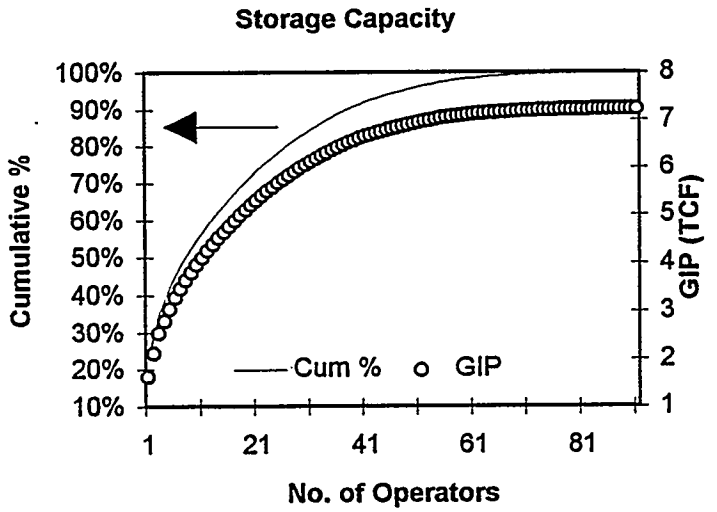

Figure 8. Storage Capacity in the US Vs Number of Operators

source: AGA 1992 database

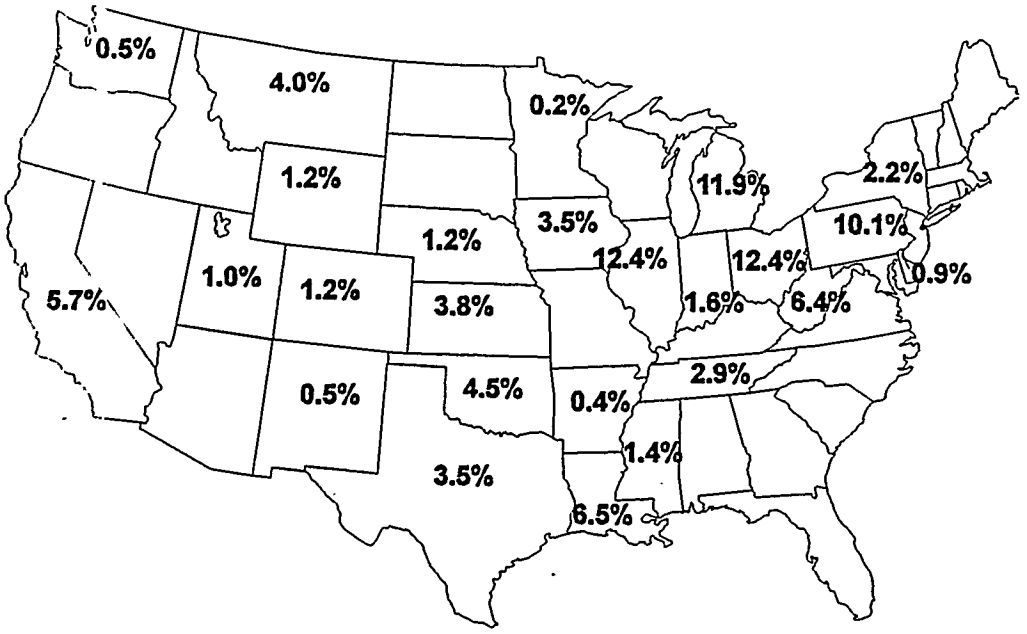

Figure 9. US Storage Capacity % of Total 1992

source: AGA 1992 database

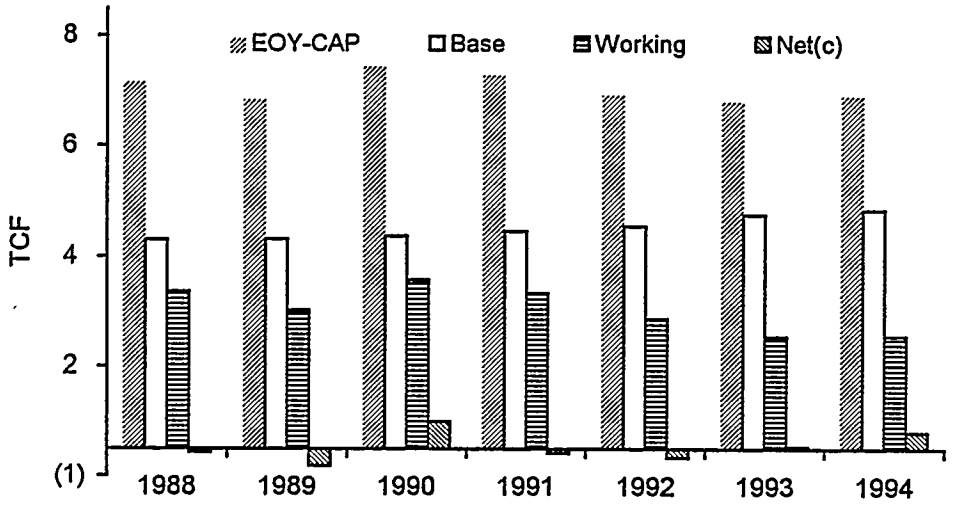

Figure 10. Underground Natural Gas Bar Chart (1988-94)

source: Energy Information Administration, Natural Gas Monthly, Table 13.

WELLHEADS	WELLBORES	RESERVIORS
Christmas Tree	Casing Collars (mechanical)	Fractures
Gathering System	Corrosion (internal and/or external)	Faults
Surface Equipment	Cement Bond	Areas of Minimum Structural Closure
Compressor	Leaks	Caprock Thresholds
Pipeline	Blowouts	Down Structure
		Gas Fingering (in aquifers)
		Areas of Lower Permeability

Table 1. Causes and Areas for Unmetered Loss of Inventory

(after Tek, M.R., Underground Storage of Natural Gas, Gulf Publishing Co., Houston, TX, 1987.)

TEXTBOOKS & PAPERS	JOURNAL ARTICLES	GRI	AGA	FERC	EIA
Textbooks: Katz Tek Papers from: SPE AGA GRI AAPG	Journal of Petroleum Technology Oil & Gas J.	topical report	Annual Survey of Underground Storage (US/Canada)	Jurisdictional Report & Database Form 2 Form 2A Form 8 Form 11	Form 191

Table 2 Information Sources

STRUCTURAL	STRATIGRAPHIC	STRATIGRAPHIC/STRUCTURAL	SALT
faulted structural	sand lens	faulted stratigraphic	salt intrusion
faulted anticline	terrace lens	reef-anticline	salt caverns
structural lens	porosity lens	anticlinal pinch-out	
anticline	permeability trap		
dome	permeability pinch-out		
domal anticline	stratigraphic draping		
anticlinal dome	bioherm		
closed anticline	reef		
elongated anticline	pinnacle reef		
plunging anticline			
truncated anticline			

Table 3. Underground Natural Gas Reservoir Geologic Types

(from GRI report)

	(TCF) EOY GIP =	BOY GIP +	INJ -	WITH	+ ADD - LOSS
	EOY GIP -	BOY GIP -	INJ	+ WITH	= ADD /LOSS
1988	6.7	-	2.17	2.24	
1989	6.3	6.7	2.49	2.80	(0.01)
1990	6.9	6.3	2.43	1.93	0.11
1991	6.8	6.9	2.61	2.69	(0.08)
1992	6.4	6.8	2.56	2.72	(0.20)
1993	6.3	6.4	2.76	2.72	(0.16)
1994	6.4	6.3	2.72	2.41	(0.20)
					Total (0.53)

Table 4. Underground Natural Gas Storage Operation Summary (1988-1994)

source: Energy Information Administration, Natural Gas Monthly, Table 13.

Underground Natural Gas Storage Reservoir Management

Isaias Ortiz
Robin V. Anthony
United Energy Development Consultants, Inc.
Pittsburgh, PA

Contract DE-AC21-94MC31113
METC Project Manager : Anthony M. Zammerilli

Natural Gas RD&D Contractors Review Meeting
April 4-6-1995
Baton Rouge, LA

Project Objectives

- *Phase I*
  - » *summarize gas loss*
    - *volume and dollar impact*
- *Phase II*
  - » *evaluate gas loss mechanisms*
  - » *develop gas strategies for prevention*

Total U.S. - Production/Consumption

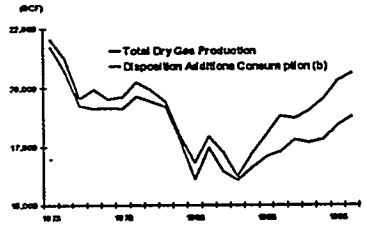

Total U.S. - Storage Inj/With & Net Imports (BCF)

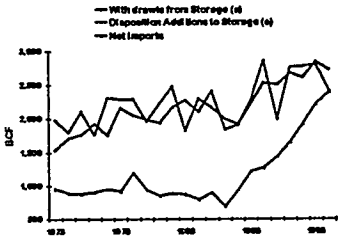

Overview

- *Underground Storage Background*
- *Project Status*
- *Key Issues*
- *Summary*

Underground Storage Background

- *Cavern (salt / coal mine)*
- *Matrix porosity*
  - *depleted gas, oil fields, aquifers*

Terminology

- *GIP (Gas in Place)*
- *Native Gas*
- *Cushion Gas / Base Gas*
- *Working Gas*
- *Operating Capacity*

Geologic formation matrix porosity

- *Geologic trap types (carbonates/sandstones)*
  - *» structural*
  - *» stratigraphic*
- *Pressure Mechanisms*
  - *» volumetric depletion*
  - *» aquifer/waterdrive*

Storage Mechanisms

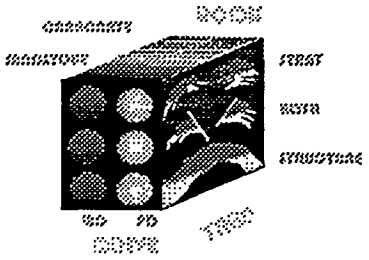

Pressure Response

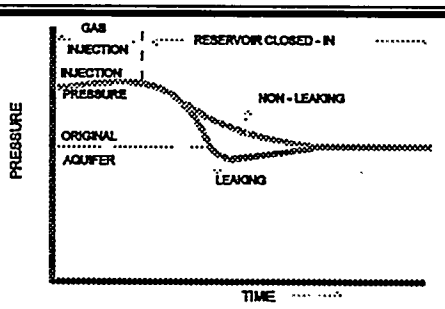

Storage Calculations

GIP = NATIVE + BASE + WORK

EOY GIP = BOY GIP + INJ - WITH +ADD - LOSS

Storage Loss Reported As:

- *Storage Loss*
- *Transportation Loss*
- *Revision to base gas (addition)*
- *Not reported*

Storage Operators

- *92 Operators*
- *388 Storage Fields*

No. of Storage Fields

Depleted	332
Aquifer	43
Cavern	13
Total	388

Storage Types

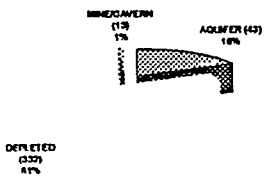

Ratio Working/ Base Gas

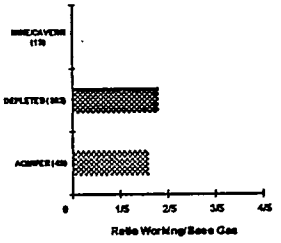

Average Working Gas - Mcf/well

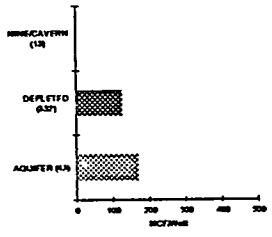

Location of Storage Fields

Regional Storage Capacity

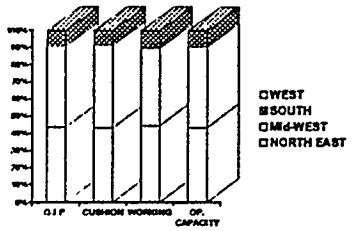

US STORAGE CAPACITY

1983 - 94 (BCF) FERC

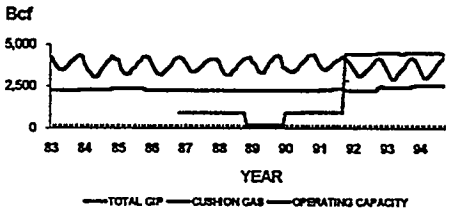

Data Sources

- *FERC (U.S. jursidictional)*
- *EIA (U.S. juridictional & LDC's)*
- *AGA (U.S. & Canadian Members Co.)*

Data Sources

- *Data Collection*
  - » *FERC*
    - Form 8 & 11
    - Form 2
    - Staff Data
    - Rate Cases
  - » *EIA*
    - F 191
  - » *AGA*
    - Computer Diskette

FERC - AGA DATA

	TOTAL WELLS	TOTAL BASE GAS	TOTAL WORKING GAS	GRAND TOTAL
		(TCF)	(TCF)	(TCF)
TOTAL - AGA	18,485	4.57	2.67	7.24
TOTAL - US	18,035	4.35	2.41	6.76
TOTAL - FERC	12,988	3.21	1.76	4.97
% FERC OF AGA - US	72%	74%	73%	73%

Storage Loss Reported As:

- *Storage Loss*
- *Transportation*
- *Revision to base gas (addition)*
- *Not reported*

U.S. Storage Activity 1988 - 94

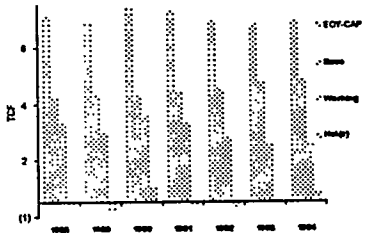

AGA Data

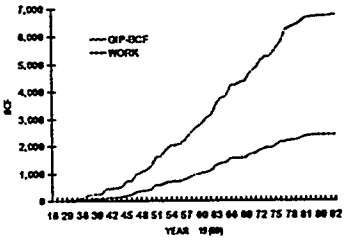

EIA - Year End Summary (TCF)

Year	GIP	INJ	WITH
1988	6.65	2.17	2.24
1989	6.33	2.49	2.80
1990	6.94	2.43	1.93
1991	6.78	2.61	2.69
1992	6.41	2.56	2.72
1993	6.30	2.76	2.72
1994	6.41	2.72	2.41

EIA - Storage Changes

(TCF)	EOY GIP =	BOY GIP +	INJ -	WITH	+ ADD -	LOSS
	EOY GIP -	BOY GIP -	INJ	+ WITH	= ADD / LOSS	
1988	6.65	-	2.17	2.24		
1989	6.33	6.65	2.49	2.80		(0.01)
1990	6.94	6.33	2.43	1.93		0.11
1991	6.78	6.94	2.61	2.69		(0.09)
1992	6.41	6.78	2.56	2.72		(0.20)
1993	6.30	6.41	2.76	2.72		(0.18)
1994	6.41	6.30	2.72	2.41		(0.20)
					TOTAL=	(0.53)

System Gas Losses F-2 (BCF)

	PROD	STORAGE	TRANS	DISTRIB	OTHER	TOTAL UNACCOUNTED
1990	0	2.64	51	5	20	79
1991	0	(5.39)	125	6	24	149
1992	0	1.00	109	2	16	129
1993	0	0.13	120	(0)	32	152
		(1.63)	406	14	91	510

Status

- ***Accomplishments***
  - ***» AGA & FERC data***
- ***Issues***
  - ***» Classification of losses***
- ***What was learned during period of report***
  - ***» losses greater than reported***

FERC DATA

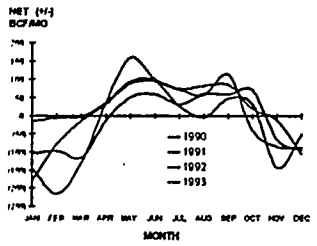

Poster Session

P1

Fundamental Studies for Sol-Gel Derived Gas-Separation Membranes

CONTRACT INFORMATION

Contract Number	91MC-28074
Contractor	Sandia National Laboratories P.O. Box 5800 Albuquerque, NM 87185-5800 (505) 272-7627 (telephone) (505) 272-7304 (telefax)
Contractor Project Manager	Harold D. Shoemaker
Principle Investigators	C. Jeffrey Brinker R. Sehgal
METC Project Manager	Venkat K. Venkataraman Margaret Kotzalas
Period of Performance	July 1, 1994 to Sept. 30, 1995

Schedules and Milestones

FY 95 Program Schedule

	S O N D J F M A M J J A S
pore size reduction of microporoussilica membranes	———
deposition of titania modified silica membranes	———
single and two gas transport measurements of silica and titania modified silica membranes as a function of temperature	———
Stability analysis of the membranes	———

ABSTRACT

We prepared silica membranes using sol-gel techniques and explored the effects of post-deposition sintering, capillary stresses developed during drying, and surface derivatization of the membranes with titanium iso-propoxide. We observed that both partial sintering of membranes and development of larger capillary stresses during membrane formation lead to consolidation of the membrane structure as evidenced by increased ideal separation factors, e.g. $\alpha_{CO_2/CH_4} > 250$ over the temperature range of 160 to 220 °C. Surface derivatization was also shown to be an effective

tool to reduce the membrane pore size in an angstrom by angstrom fashion, resulting in comparable separation factors. What's more, the altered pore surface chemistry of TiO_2 derivatized membranes may lead to improved stability and impart catalytic properties to the membrane surface.

OBJECTIVES

The primary objective of this study is to prepare supported inorganic membranes suitable for gas separation/gas purification applications in the processing of natural gas. The design criteria for such membranes include: high selectivity and high flux combined with excellent chemical, thermal and mechanical stability.

BACKGROUND INFORMATION

In the processing of natural gas, membranes have been proposed as replacements for more energy intensive purification processes for the removal of H_2O, CO_2, H_2S, and higher hydrocarbons from methane. Due to their inherent thermal, mechanical, and chemical stability, inorganic membranes are attractive for such applications. For practical gas separations, an inorganic membrane must combine high flux J with a high selectivity factor α. The membrane flux for Knudsen transport is proportional to the pore radius r_p divided by the film thickness h:

$$J_K(\text{cm/s}) \propto \frac{\varepsilon r_p}{\tau^* h}\sqrt{\frac{1}{RT}}\Delta P \qquad (1)$$

where ε is the porosity, ΔP is the pressure drop across the membrane, and τ^* is the tortuosity. Membrane selectivity is related to pore size and pore size distribution. When the pore size is reduced below the mean free path of a gas molecule, gas transport occurs by Knudsen diffusion, and the separation factor for a binary gas mixture depends on the inverse ratio of the respective molecular weights. For example, the Knudsen selectivity factor α_K for a He/N_2 mixture is 2.65. Much greater separation factors (approaching ∞) are achieved when the pore size is reduced sufficiently and the pore size distribution is sufficiently narrow to admit and exclude molecules on the basis of size, a mechanism referred to as molecular sieving. Thus to combine high flux with high selectivity it is necessary to prepare extremely thin, porous films with a narrow distribution of extremely small pores (r_p ~ molecule size) and no cracks or other imperfections that would serve as large pores and diminish selectivity.

The traditional approach to the preparation of thin inorganic membranes with controlled pore sizes is to deposit (slip-cast and/or dip-coat) particulate sols with narrow particle size distributions on porous supports.[1,2,3] If aggregation is avoided, the pore size of the membrane is controlled by the particle size of the sol - smaller particles yield smaller pores. An advantage of this approach is that the porosity of the membrane, which dictates its flux (Eq. 1) is independent of the particle size. So-called Knudsen membranes prepared from particulate sols have been successfully demonstrated by many research groups and are now commercially available.[4] However due to problems with cracking[5] and pore size coarsening at elevated temperatures,[6] it has proven difficult to prepare molecular sieving membranes using this traditional approach.

This paper considers the use of polymeric silicate sols to prepare thin supported membranes, where the distinction between particles and polymers, made on the basis of NMR and SAXS measurements,[6] is that the polymeric sols contain no regions of fully condensed silica. The idea of this alternative approach is to utilize the fractal properties of polymeric sols to favor polymer interpenetration during membrane deposition. This concept is qualitatively understood on the basis of the following relationship describing the mean number of intersections $M_{1,2}$ of two mass fractal objects of size R placed in the same region of space:[7]

$$M_{1,2} \propto R^{D1+D2-d} \qquad (2)$$

where D1 and D2 are the respective mass fractal dimensions and d is the dimension of space, 3. From Equation 2, we see that if D1 + D2 < 3, the probability of intersection decreases indefinitely with R. This suggests that as D is reduced polymers should more easily interpenetrate as they are concentrated during slip-casting/dip-coating. If

compliant, such interpenetrating networks should collapse during drying to create pores of molecular dimensions appropriate for molecular sieving.

As reported in last year's Natural Gas R & D Contractors Review Meeting report, a practical advantage of this polymer approach with respect to the preparation of supported membranes is that the final pore size should be independent of the polymer size. Thus aging can be used to grow the polymers large enough to be trapped on the support surface during membrane deposition (avoiding the creation of thick often imperfect membranes by so-called "pore plugging" (see Figure 1)) without detrimentally increasing the pore size. Also a broadening of the polymer molecular weight distribution should not necessarily be manifested as a broadening of the pore size distribution.

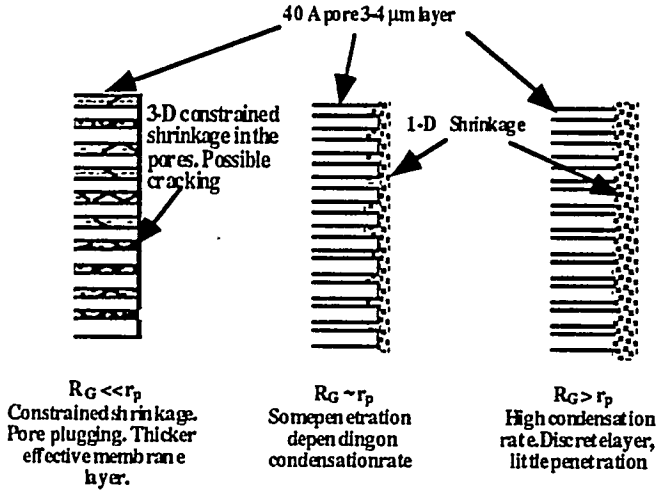

Figure 1. Schematic illustration of the effect of the relative sizes of polymer and support pores on membrane formation

A second advantage of this approach is that polymeric sols generally lead to the formation of amorphous membranes that do not exhibit grain growth or phase transformations during heating (as is often observed for particulate sols). Thus compared to particulate membranes, the pore dimensions of polymeric membranes should exhibit improved thermal stability.

A possible disadvantage of this approach is that small pore sizes are achieved at the expense of pore volume. This limitation may be overcome by the use of organic molecules or ligands as pore templates.

Last year we reported on the effects of sol-aging conditions and condensation rates on the microstructure and transport behavior of supported silica membranes and demonstrated a template strategy as a means of independently controlling pore size and pore volume. This year we report on the effects of post-deposition sintering, capillary stress during membrane deposition and a derivatization technique designed to develop truly molecular sieving membranes.

Partial Sintering

Partial sintering of an amorphous silica membrane is expected to further collapse the structure at higher sintering temperatures, leading to a narrower pore size distribution and/or smaller pore sizes. The collapse of the structure is accompanied by a large reduction in porosity and a loss of hydroxyl coverage on the silica structure.[6] The loss of hydroxyl coverage is also expected to make the structure slightly hydrophobic and thus more stable to attack by a humid environment.

Drying Stress

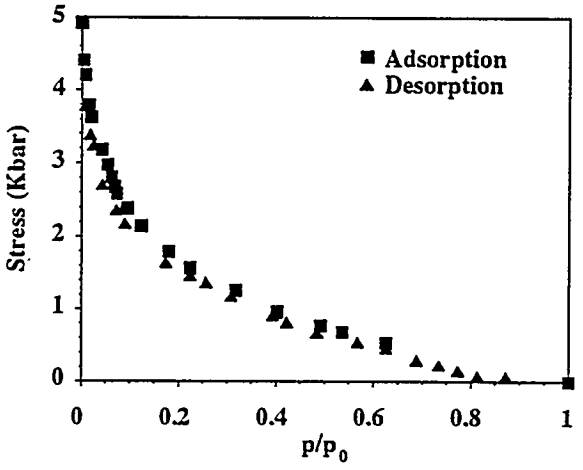

Figure 2. Stress generated in an 'as deposited' A2 film vs relative pressure

Recently Josh Samuel[8] quantified the capillary stress development in microporous sol-gel derived

silica films. The results shown for an 'as deposited' A2 film in Figure 2 indicate that very large capillary stresses (of the order 5 kbar) are developed at low relative pressures of water in the overlying gas. These pressures are exerted on the solid phase during film deposition causing collapse of the gel network and as we report in the Results section a reduction in pore size and/or narrowing of the pore size distribution leading to enhanced separation factors.

Surface Derivatization

Reaction of a hydroxylated silica surface with a dilute solution of Ti (O i-Pr)$_4$ can lead to two possible reactions: 1) alcohol condensation between the surface hydroxyl and the alkoxy group (Equation 3) and 2) alcoholysis of the siloxane (Si-O-Si) bonds (Equation 4).

$$\equiv Si\text{-}OH + i\text{-}Pr\text{-}O\text{-}Ti\equiv \rightarrow \equiv Si\text{-}O\text{-}Ti\equiv + i\text{-}Pr\text{-}OH \quad (3)$$

$$\equiv Si\text{-}O\text{-}Si\equiv + i\text{-}Pr\text{-}OH \rightarrow \equiv Si\text{-}OH + i\text{-}Pr\ O\text{-}Si\equiv \quad (4)$$

Titanium alkoxides are sufficiently electropositive to undergo reaction 3 even in the absence of a catalyst. Furthermore, the alcoholysis reaction is relatively slow.[6] As a result, the reaction with Ti(O i-Pr)$_4$ will presumably lead to the deposition of a Si-O-Ti layer on the silica surface according to Reaction 3.[9] Apart from the above two reactions some isopropoxide may be adsorbed on the hydrogen bonded surface hydroxyls associated with the silica membranes. These adsorbed molecules can subsequently condense during the calcination stage to form Si-O-Ti bonds similar to Reaction 3 with the hydrogen bonded intermediate step.

According to Srinivasan et. al.[9] silica surfaces with a larger fraction of hydrogen bonded hydroxyls have a higher loading of titania due to the condensation of adsorbed precursor. The hydrogen bonded surface hydroxyls were found to be the preferred adsorption sites for the precursor as per infrared spectroscopy.

This titania layer has the potential to improve the separation properties and the hydrothermal stability of the membrane.[10] The titania membrane also imparts catalytic properties to the membrane, or alternatively, this membrane can be used as a high surface area support for other catalysts such as vanadia.[9] These modified membranes are very good candidates for membrane reactor applications.

PROJECT DESCRIPTION/EXPERIMENTAL DETAILS

Preparation of Coating Solutions

The silica sols were prepared in a two step process referred to as A2**.[11] In the first step an A2** stock solution was prepared with TEOS:EtOH:H_2O:HCl ratio of 1:3.8:1.1:5 X 10^{-5}. and refluxed for 90 min. at 60 °C. Prior to the second step of sol formation, the stock solution was maintained in a freezer at ~ -30 °C. In the second step additional water and acid was added at room temperature, resulting in final molar ratios of TEOS:EtOH:H_2O:HCl of 1.0:3.8:5.1:0.004. The sol was shaken for 15 minutes using a wrist action shaker and aged in a 50 °C oven to determine the gel time. The coating sol was prepared by diluting the A2** sol aged for $t/t_{gel} = 0.24$ (t_{gel} = 99 hours), with twice the volume of 200 proof ethanol soon after removal from the oven. The coating sols are stable for over 2 months when stored at -30 °C.

The titania modification solution for the silica membranes was prepared by mixing 5 vol. % Ti (O i-Pr)$_4$ in tetrahydrofuran (THF). Hexane and toluene are used for removal of excess precursor after the titania modification step. The Ti (O i-Pr)$_4$, THF, hexane and toluene must be freshly distilled to remove any trace amounts of water as the precursor is highly susceptible to hydrolysis.

Membrane Deposition

Membranes were deposited on commercially available Membralox® supports (supplied by U. S. Filter in 25 cm lengths). Supports were cut into 5 cm sections, using a diamond wafering saw. Each uncoated support was pre-calcined to 400 °C or 550 °C depending on the final membrane calcination temperature.

Before coating, the supports were cleaned with CO_2 snow using a SNOGUN™ cleaner. The silica membranes were deposited using a Compumotor™

linear translation stage in a glove box, which was continuously backfilled with dry N_2 from a liquid N_2 dewar to maintain a clean and dry environment. Purging time of the dry box was used to control the relative pressure of water. The support was dip-coated at a constant immersion and removal rate of 20 cm/min. The support was held immersed in the sol for 100 seconds prior to removal. After dip-coating the membrane was allowed to dry for 15 minutes in the glove box before calcination in air to 400 °C or 550 °C for 3 hours with a heating and cooling rate of 1 °C/min. After calcination the membranes were always stored in air at 150 °C.

Titania modification was performed on A2** membranes calcined to 550 °C. For the modification experiments the dry box was maintained at < 10 ppm of water. The water content in the box is checked with a $TiCl_4$ solution by opening the bottle periodically while the box is being purged with dry nitrogen. The chamber has less than 10 ppm water when the $TiCl_4$ solution no longer fumes when opened. At this stage, the container of the modification solution is opened and the membrane is lowered into the solution. The membrane is allowed to react with the solution for five minutes and then withdrawn. The reaction is followed by repeated hexane and toluene washing.

The membrane was subsequently removed from the dry box and calcined at 400 °C for 3 hours using heating and cooling rates of 1 °C/min.

Characterization

Membranes. The membranes were characterized using a manual or an automated single gas permeability measurement system. The automated system is capable of measuring the permeance of six different gases in succession at various temperatures and pressures. The system is set-up to measure the membrane transport properties over the temperature range 25-220 °C and pressure range of 12 to 92 psia. The series of gases used in the permeability experiments was He, H_2, N_2, C_3H_6, CO_2, CH_4, and SF_6. In case the permeance was below the accurate detection range of the mass flow controllers (MFCs) connected to the system, the flow data was collected by running the system in a semi-automated mode in which gas flux was measured manually with bubble meters.

Adsorption. To obtain the adsorption measurements on bulk silica and modified samples, freshly gelled silica sols were dried in an explosion proof oven at 50 °C. The gel was allowed to dry for approximately 1 day and subsequently calcined to 400 or 550 °C for 3 hours with a heating and cooling rate of 1 °C/min. The calcined xerogels thus obtained were used for N_2 adsorption measurements at 77 K. The bulk gels were modified with titania following the same procedure outlined earlier.

The adsorption data was collected over the relative pressure range of 10^{-6} to 1 using a Micromeritics ASAP 2000.

Ellipsometry. Companion coatings to supported membranes were prepared on dense <100> single crystal silicon wafers for ellipsometry analysis. A Gaertner® model L116C ellipsometer, with a He-Ne laser light source, was used to derive the thickness and refractive indices of the silica films. The film porosity was calculated using the Lorentz-Lorenz model[5] (equation 5) assuming a skeletal refractive index of 1.46 for silica,

$$V_S = \frac{(n_f^2-1)}{(n_f^2+2)} \frac{(n_s^2+2)}{(n_s^2-1)} \qquad (5)$$

where n_f is the film refractive index, V_S is the volume fraction solids, and n_s is the refractive index of the solid skeleton.

RESULTS

Effect of sintering

Sintering was studied as means of reducing pore size and narrowing pore size distribution for bulk, thin film and membrane specimens. Figure 3 plots the adsorption isotherms for bulk A2** xerogels calcined to two different temperatures under similar conditions. The isotherms clearly indicate a sharp decrease in the surface area and volume % porosity for the 550 °C sample compared to the 400 °C sample. The sharper isotherm for the A2** sample calcined to 550 °C also indicates the loss of the larger pores,

consistent with a narrower pore size distribution. Similar results were observed in case of thin A2** films deposited on dense silicon wafers as summarized in Table 1. We see that the film thickness as well as the volume % porosity is reduced with increasing calcination temperature indicative of a more consolidated structure.

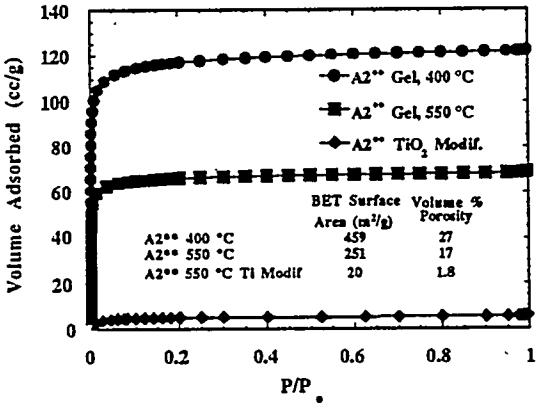

Figure 3. Surface area and porosity comparison, pure silica A2 and modified A2** Gels**

Table 1. Film Thickness and Porosity comparison of single coated A2 films Sintered at Different Temperatures**

Film Sintering Temperature (°C)	Thickness (Å)	Refractive Index	% Porosity
400	1550	1.375	16.0
550	1300	1.410	9.5

Table 2. Permeability Results on A2 Membranes Sintered at Different Temperatures**

	He Perm.	He/ N_2	He/ CO_2	He/ CH_4	He/ SF_6	CO_2/ CH_4
Ideal Knudsen	-	2.65	3.31	2.0	6.0	0.6
Single layer membrane, calc. 400 °C	0.0085	2.0	2.4	1.6	4.0	0.66
Double layer membrane, calc. 400 °C	0.0021	6.9	0.74	2.6	11.8	3.5
Single layer membrane, calc. 550 °C	0.0028	9.0	4.4	6.8	16.8	1.6

Single or double layer membranes were prepared using the A2** sol composition and calcined to 400 °C or 550 °C. Table 2 summarizes the permeability results obtained at 25 °C. We can clearly see that the second A2** coating calcined to 400 °C leads to a four fold loss in He permeance accompanied by an increase in gas selectivities above the ideal Knudsen values for the various gas pairs. The second coating presumably acts as a healing layer for the first membrane coating and leads to blockage of the defects or larger pores in the first coating. Instead if a single coating of the A2** sol is calcined to 550 °C we obtain ideal separation factors larger than for the double-layer A2** membrane calcined to 400 °C along with higher permeance.

These observations lead to the following conclusions: 1) Partial sintering is effective in reducing pore size and/or narrowing PSD resulting in greater selectivity and lower flux. 2) Partial sintering enables the achievement of molecular sieving using a single membrane layer, obviating the need of a second layer and resulting in greater flux than observed for double layer membranes.

Effect of Drying Chamber Humidity

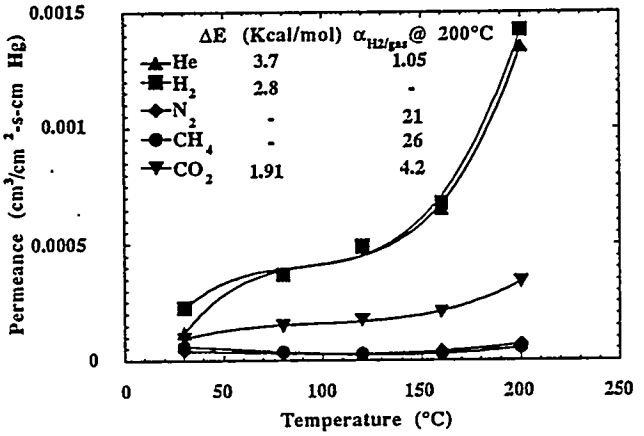

Figure 4. Permeability vs temperature, A2 membrane deposited in drying chamber with > 10 ppm water**

Figure 4 plots the typical permeance of the various gases through an A2** membrane calcined to 550 °C versus measurement temperature over the

temperature range, 30 to 220 °C. This membrane was prepared in the dry box with a short purge time causing > 10 ppm of water in the box. The average pressure across the membrane for all the data points is 52 psia with a pressure drop of 80 psi. Ideal separation factors determined at 200 °C are indicated on the plot along with the apparent activation energies for transport. The large activation energies for He and H_2 indicate a very narrow pore size distribution for the membrane. The high separation factors are also an indication of a narrow PSD and suggest that the membrane has a very small fraction of pores larger than the size of a methane molecule. If we can further reduce the pore size and narrow the pore size distribution we expect to achieve membranes that exhibit perfect molecular sieving behavior.

We have discussed earlier that, one of the ways to collapse the silica structure, is by increasing the capillary stress at the time of membrane formation. We have also discussed in Figure 2 that the stress can be increased by reducing the drying chamber humidity.

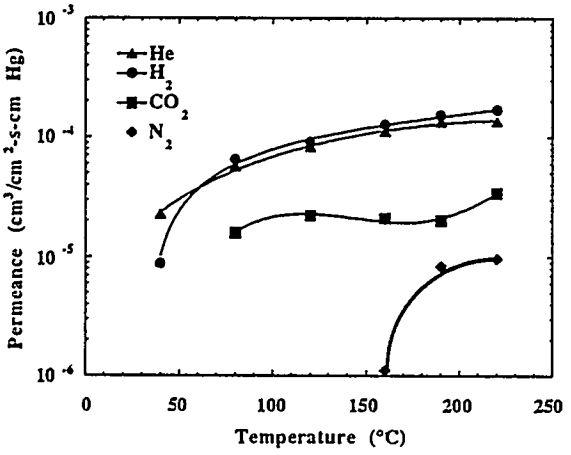

Figure 5. Permeability vs temperature, A2 membrane deposited in drying chamber with < 10 ppm water**

Figure 5 and 6 plot the permeance and selectivity results for an A2** membrane prepared when the water content in the coating chamber was reduced below 10 ppm before membrane deposition. The two plots indicate some very significant results. We see that there is no CH_4 flux through the membrane over the complete temperature range. There is no N_2 flux through the membrane below 180 °C and no CO_2 flux below 80 °C. The flow of these gases was much below the minimum detection limit of the instruments (< ~ 10^{-7} cm^3/cm^2-s-cm Hg). Thus we can easily separate various sets of gases by operating the membrane at selected temperatures and achieve almost perfect selectivity. An order of magnitude

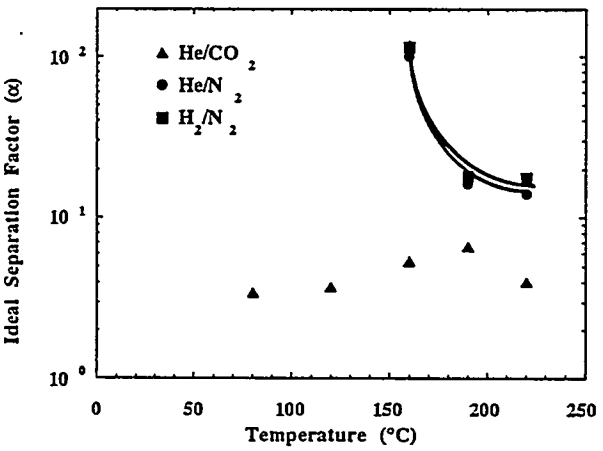

Figure 6. Ideal separation factor vs temperature, A2 membrane deposited in drying chamber with < 10 ppm water**

increase in N_2 permeance between 160 and 190 °C indicates that the activation energy for transport is very large over this temperature range. A similar result is seen for the case of H_2 over the temperature range, 40 to 80 °C.

We have therefore been able to prepare membranes in a one step process which have true molecular sieving properties.

A comparison of He flux through this membrane at 40 °C (2 x 10^{-5} cm^3/cm^2-s-cm Hg) with the baseline He flux through vitreous silica at 27 °C (7 x 10^{-9} cm^3/cm^2-s-cm Hg) indicates that the flux through our membrane is about 4 orders of magnitude greater than the flux through dense silica. This comparison indicates that the fluxes that we are measuring for our membranes must be due to the presence of well defined molecular-sized pores.

Titania Modified Silica Membranes

The comparison of the N_2 adsorption isotherms of an A2** bulk gel and an A2** bulk gel modified with TiO_2 in Figure 3 indicates that the TiO_2 modification step causes a greater reduction in porosity than partial sintering.

Figure 7 shows permeance versus temperature for an A2** membrane deposited at >10 ppm water and modified twice with TiO_2. For this membrane we have completely excluded CH_4 and N_2 over the temperature range 30 - 220 °C. CO_2 flux is not detectable below 180 °C, and H_2 flux is not detectable below 160 °C.

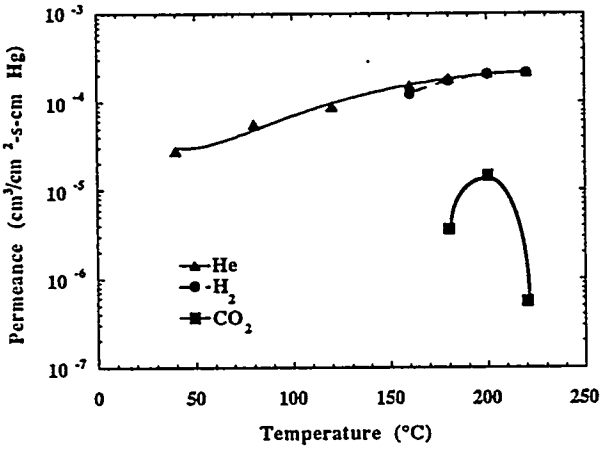

Figure 7. Permeability vs temperature, titania modified A2 membrane, with two TiO_2 modifications**

A closer comparison of this membrane with the membrane in Figure 5 indicates that He permanence through the two membranes over the complete temperature range are comparable. The difference is in the flux of the other gases. The titania modified membrane seems to have a smaller number of large pores (we observe a larger N_2 permeance through the pure silica membrane). The activation energies of the gases through these membranes are similar to the activation energies for most zeolites and carbon molecular sieves with pore diameters of the order of 4 to 5 Å.

SUMMARY/FUTURE WORK

Improvements to the membrane deposition process have led to significant increases in membrane performance this year. Through reduction of the relative pressure of water used in the membrane deposition and drying ambient, we have increased the drying stress exerted on the gel network leading to a reduction in pore size and/or a narrowing of the pore size distribution of the resulting membranes. This is evident from the improvements noted in the performance of single-layer membranes processed to 550 °C (α_{He/N_2} > 250 below 160 °C compared to 9.0 (last year) and α_{CO_2/CH_4} > 250 over the temperature range 80-220 °C compared to α_{CO_2/CH_4} = 1.54 (last year) with He permeance 2 x 10^{-5} cm^3/cm^2-s-cm Hg at 40 °C). We have also demonstrated a surface derivatization technique whereby a hydroxylated silica membrane is reacted with a monomeric titanium alkoxide to reduce the pore size and modify the pore surface chemistry of a thin region of the membrane surface. This approach has resulted in α_{CO_2/CH_4} > 250 above 160 °C with He permeance = 3 x 10^{-5} cm^3/cm^2-s-cm Hg at 40 °C.

The stability of the membranes presented in this paper are currently being studied. The titania modified membranes seem to be a better candidate for membrane application due to the known instability of sol-gel derived ultramicroporous silica structures.

In future we will continue working with the strategies presented in this paper to further optimize the conditions for membrane deposition and improve the permeance of the faster permeating gases.

ACKNOWLEDGEMENTS

Portions of this work were supported by the National Science Foundation, the Electric Power Research Institute, the Gas Research Institute, Morgantown Energy Technology Center, and the Department of Energy Basic Energy Sciences Program. We are grateful to Jan Ellison for building the automated gas permeability system. Sandia National Laboratories is a U. S. Department of Energy facility supported by Contract Number DE-AC04-76-DP00789.

REFERENCES

1 A.F.M. Leenaars, K. Keizer and A.J. Burggraaf, J. Mat. Sci., 10, 1077-1088 (1984).

2 A. Larbot, J.A. Alary, J.P. Babre, C. Guizard and L. Cot, "Better Ceramics Through Chemistry II", Eds. C.J. Brinker, D.E. Clark and D.R. Ulrich, Mat. Res. Soc. Symp. Proc., Vol. 73, Mat. Res. Soc., Pittsburgh, PA (1986), 659.

3 M.A. Anderson, M.J. Gieselman and Q. Xu, J. Membrane Sci., 39, 243-258 (1988).

4 J. Guibaud in ICIM-89, "The First International Conference on Inorganic Membranes, eds. L. Cot and J. Charpin, Montpellier, France, 1989.

5 T.J. Garino, Ph.D. Dissertation, MIT., Cambridge, MA, 1986.

6 C.J. Brinker and G.W. Scherer, "Sol-Gel Science", Academic Press, San Diego (1990).

7 B.B. Mandelbrot, "The Fractal Geometry of Nature", Freeman, San Francisco (1982).

8 J. Samuel, private communications 1995.

9 S. Srinivasan, A.K. Datye, M.H. Smith, and C.H.F. Peden, "Interaction of titanium isopropoxide with surface hydroxyls on silica", J. Catalysis 145, 565-573 (1994).

10 A. Matsuda, Y. Matsuno, S. Katayama, T. Tsuno, "Weathering resistance of glass plates coated with sol-gel derived $9TiO_2.91SiO_2$ films", J. Mater. Sci. Lett., 8, (1989), 902-904.

11 R. Sehgal, "Preparation and Characterization of Ultrathin Sol-gel Derived Silica Membranes for Gas Separation Applications," M.S. Thesis, The University of New Mexico, 1993.

P2 Atlas of Major Appalachian Basin Gas Plays

CONTRACT INFORMATION

Contract Number	DE-FC21-91MC28176
Contractor	Appalachian Oil and Natural Gas Research Consortium P.O. Box 6064 Morgantown, WV 26506-6064 Voice: (304) 293-2867 Fax: (304) 293-3749
Contractor Project Manager	Douglas G. Patchen
Principal Investigators	Kashy Aminian Katharine Lee Avary Mark T. Baranoski Kathy Flaherty Matt Humphreys Richard A. Smosna
METC Project Manager	Harold D. Shoemaker
Period of Performance	October 1, 1991 to September 30, 1995

Schedule and Milestones

FY 96 Program Schedule

	O	N	D	J	F	M	A	M	J	J	A	S
Finish manuscripts				X								
Finish illustrations					X							
Complete review and edit							X					
Receive field data						X						
Complete data base									X			
Submit atlas to printer										X		
Received printed atlases											X	

OBJECTIVES

This regional study of gas reservoirs in the Appalachian basin has four main objectives: to organize all of the gas reservoirs in the Appalachian basin into unique plays based on common age, lithology, trap type and other geologic similarities; to write, illustrate and publish an atlas of major gas plays; to prepare and submit a digital data base of geologic, engineering and reservoir parameters for each gas field; and technology transfer to the oil and gas industry during the preparation of the atlas and data base.

BACKGROUND

This project was designed in 1991 in response to DOE's "Gas Research Program Implementation Plan" (April 1990). In that document DOE stressed the need to develop an appropriate reservoir classification scheme that assigned gas reservoirs in a basin into groups with common geologic and engineering characteristics as a preliminary step before consolidating existing data bases and producing gas atlases. However, DOE envisioned a close linkage among the three endeavors, with data flowing among all three projects as they were being performed concurrently.

Using the play concept is a logical approach to developing a reservoir classification scheme that ultimately will result in a data base of field-specific parameters and a gas atlas of a basin. Plays are defined as a group of geologically similar drilling prospects having basically the same source, reservoir, and trap controls of gas migration, accumulation and storage (modified from White, 1980; 1988). Thus, they share some common elements of risk with respect to the possible occurrence of natural gas. Plays are commonly designated by their reservoir lithology (the Oriskany Sandstone Play), although play names can be modified by reference to trap type (the Oriskany Pinchout Play) and other geologic similarities (the Knox Unconformity Play). The play approach has been used to prepare an atlas of major gas plays in the Texas Gulf Coast (Kosters, et al, 1989) and other areas. In the Appalachian basin the U.S. Geological Survey defined seven broad plays in their first approach to preparing a resource assessment of the basin. The USGS currently is preparing a revision in which they have organized reservoirs into more than 20 oil and gas plays. Our approach has been to define stratigraphically and geographically restricted geologic plays based largely on age, lithology and deposition of reservoir rocks under similar environments of deposition that have undergone similar structural and diagenetic histories. The end result should be a set of reservoirs with common geologic and engineering characteristics.

PROJECT DESCRIPTION

The Appalachian Oil and Natural Gas Research Consortium (AONGRC) organized a research team that is familiar with the geology and oil and gas fields in each of the Appalachian basin states that will be covered by the atlas. This team included members of the Oil and Gas Sections at the Kentucky, Maryland, Ohio, Pennsylvania and West Virginia Geologic Surveys; Research Professors in the departments of Geology and Petroleum and Natural Gas Engineering at West Virginia University; professionals at the U.S. Geological Survey; and private consultants. All of the gas reservoirs in each of these states were listed in stratigraphic order, correlated with reservoirs in other states, and then grouped together in plays based on age, lithology, environments of deposition, degree and type of structural control, or a combination of stratigraphic and structural control. Preliminary maps were prepared showing production fairways for each of these plays to define the initial study area for each play description.

Once plays had been defined, authors were recruited to write and illustrate each play, and two tasks were performed concurrently: a geologic and engineering study of each play; and data collection for every field and reservoir in each play. Play descriptions were subjected to sequential internal reviews by project team members, external reviews by industry geologists, review by geologists and engineers at the Morgantown Energy Technology Center, and technical edit by a professional editor hired to guarantee standardization of the final products.

RESULTS

Play Designation

Thirty-one unique gas plays were defined, ranging in age from Middle Pennsylvanian to Late Cambrian. These plays can be further organized by reservoir lithology, depositional environment of the reservoir rock, structural control, importance of fractures, and combination of stratigraphic and structural control. In general, plays in younger reservoir rocks (Pennsylvanian through Devonian) are confined to the center of the basin in northeast to southwest trends, whereas plays in older reservoirs rocks (Silurian to Cambrian) are confined to the northern and western sides of the basin where these rocks occur at shallower drilling depths.

Initially, plays were organized geologically by depositional environments, fractured reservoirs, and structural plays with the intent of presenting them in that order in the atlas. However, it was determined that a straight forward approach would be more user friendly. Thus, plays will be organized and presented in the atlas based on increasing geologic age, and will be named, whenever possible, after stratigraphic units familiar to most geologists and engineers working in the basin.

Play Descriptions

Play descriptions follow a standard format that includes these major headings: Location, Production History, Stratigraphy, Structure, Reservoir, Key Fields, Resources and Reserves, and Future Trends (Table 1). Required illustrations include: a pool map on a standard basin base map with play outline (Figure 1); a regional map with all key fields identified (Figure 2); a stratigraphic column with both formal and drillers' terms (Figure 3); a correlation chart (Figure 4); an isopach of the reservoir unit or structure map on the unit (Figure 5a and 5b); a cross section (either stratigraphic or structural; Figure 6); a type log for key fields (Figure 7); and a pay or porosity map for key fields (Figure 8). Other illustrations that are encouraged are models of depositional systems or environment, types of traps, and decline curves (Figure 9a and 9b). An attempt has been made to reduce text whenever possible and increase the number of maps and illustrations.

All 31 play descriptions have been written and have passed through internal review. However, several have not yet passed through the required external review stage prior to revision and submission to the Technical Editor. The Technical Editor has received and read 25 play descriptions, and has completed nine of them. He is working with the authors on various versions of the other descriptions.

Final scale mock-ups have been prepared of 15 of the 31 plays and all 15 have been reviewed by METC. In every case a second version is prepared that incorporates all changes suggested by METC reviewers and is resubmitted to METC and the authors.

Each play description also includes a table of geologic and engineering data for key fields within the play (Table 2). Data are organized into basic reservoir data (depth, age, formation, lithology, environment, trap type, drive mechanism, etc); reservoir parameters (pay thickness, porosity,

temperature, pressure); fluid and gas properties (Rw, gravity, saturations, Btu's); and volumetric data (original gas in place and reserves, production, remaining gas in place and reserves).

Data Base

Table 1 in each play description contains average values for key fields described or mentioned in the play description. A separate deliverable is a digitized data base that contains the same parameters as well as a few additional parameters for all, or nearly all, of the fields in each play. Data entered into this data base were gathered from the literature, from industry, and from the oil and gas files and data bases at the various state geological surveys. In most cases data were collected for a representative set of wells for each reservoir in each field and used to estimate average field values. These included original data from log and core analyses made specifically for this project.

Technology Transfer

During the past three and a half years numerous papers and posters have been presented and exhibits have been taken to professional and trade association meetings to describe the project and its products. These meetings include DOE Contractor meetings in Morgantown; meetings of the Independent Oil and Gas Associations in Ohio, Kentucky and West Virginia; the Eastern Section of the American Association of Petroleum Geologists in Champaign, IL, Williamsburg, VA, and East Lansing, MI; and the 25th Appalachian Petroleum Geology Symposium (APGS) in Morgantown, WV. During the two-day APGS meeting, papers or posters were presented on each of the 31 gas plays.

FUTURE WORK

All figures for the atlas are being computer drafted and prepared for printing in the Publications Section of the West Virginia Geological Survey. Many of these illustrations are being modified for standardization using digital files submitted electronically by the other state surveys. However, because the atlas will contain more than 600 illustrations, computer drafting and quality control have been major tasks. Much remains to be done between this writing and the deadline of June 1, 1995.

Several of the manuscripts are still out for external review. These must be retrieved and authors' changes made so that they can be submitted to the Technical Editor, the Publication Editor, and METC for review. The remaining manuscripts are in the technical edit process. Various versions are being circulated between the Technical Editor and the authors for final revisions.

Digital data submitted by four state surveys and two consultants are being combined into one data base at the West Virginia Geological Survey. Validation of these data has not been completed as yet. In some cases, data have had to be returned to the surveys to be corrected. We still expect to meet the June 1 deadline for completion of this task.

REFERENCES

Kosters, E.C., and others. 1989. Atlas of Major Texas Gas Reservoirs. Gas Research Institute and Texas Bureau of Economic Geology, Austin, TX., 161 p., 4 plates.

White, D.A. 1980.Assessing oil and gas plays in facies-cycle wedges. American Association of Petroleum Geologists Bulletin, v. 64, p. 1158-1178.

White, D.A. 1988. Oil and gas play maps in exploration and assessment. American Association of Petroleum Geologists Bulletin, v. 72, p. 944-949.

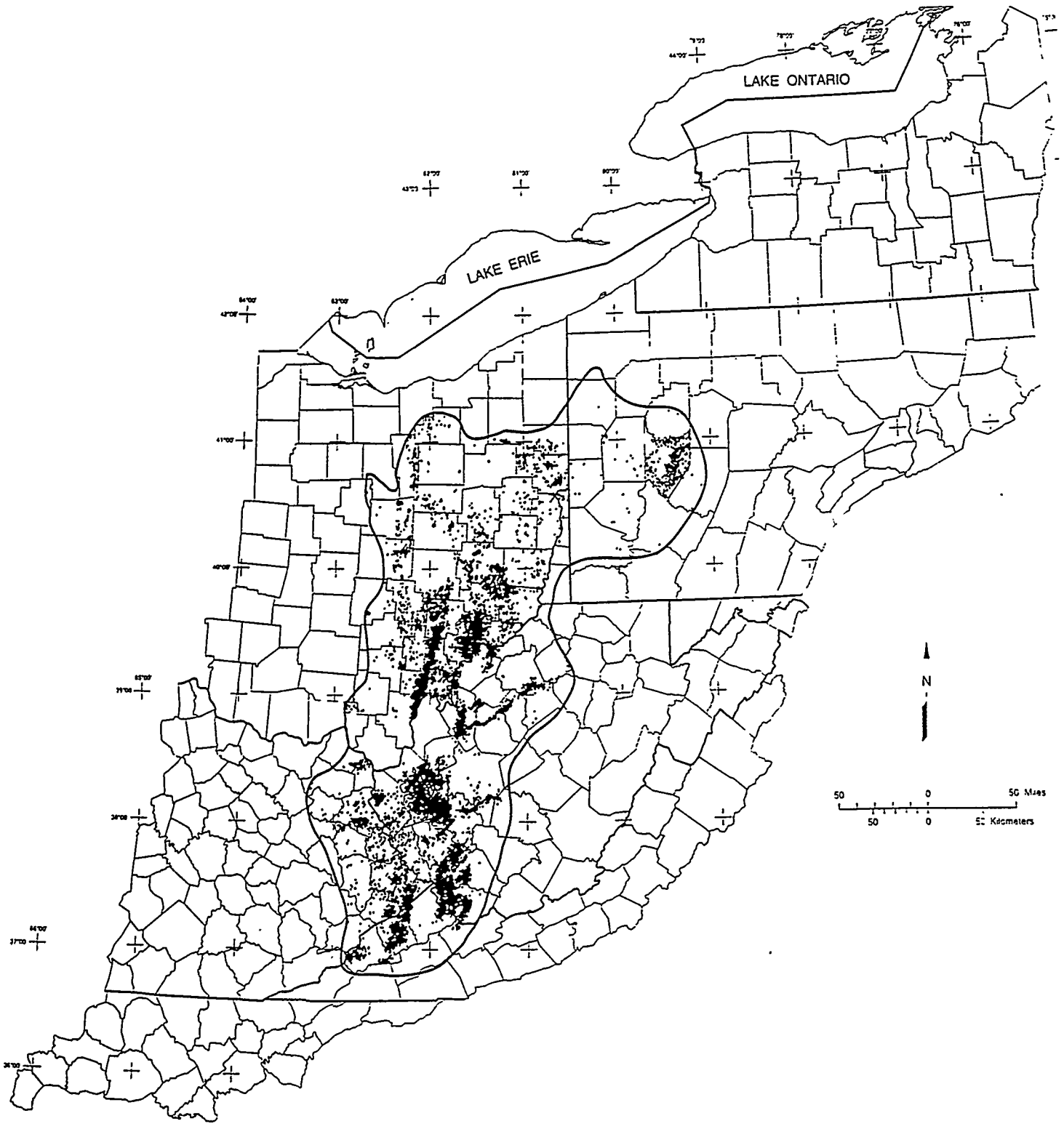

Figure 1. Outline of the Lower Mississippian-Upper Devonian Berea and equivalent sandstones play in the Appalachian basin. Dots represent individual gas wells; areas where dots have merged represent fields.

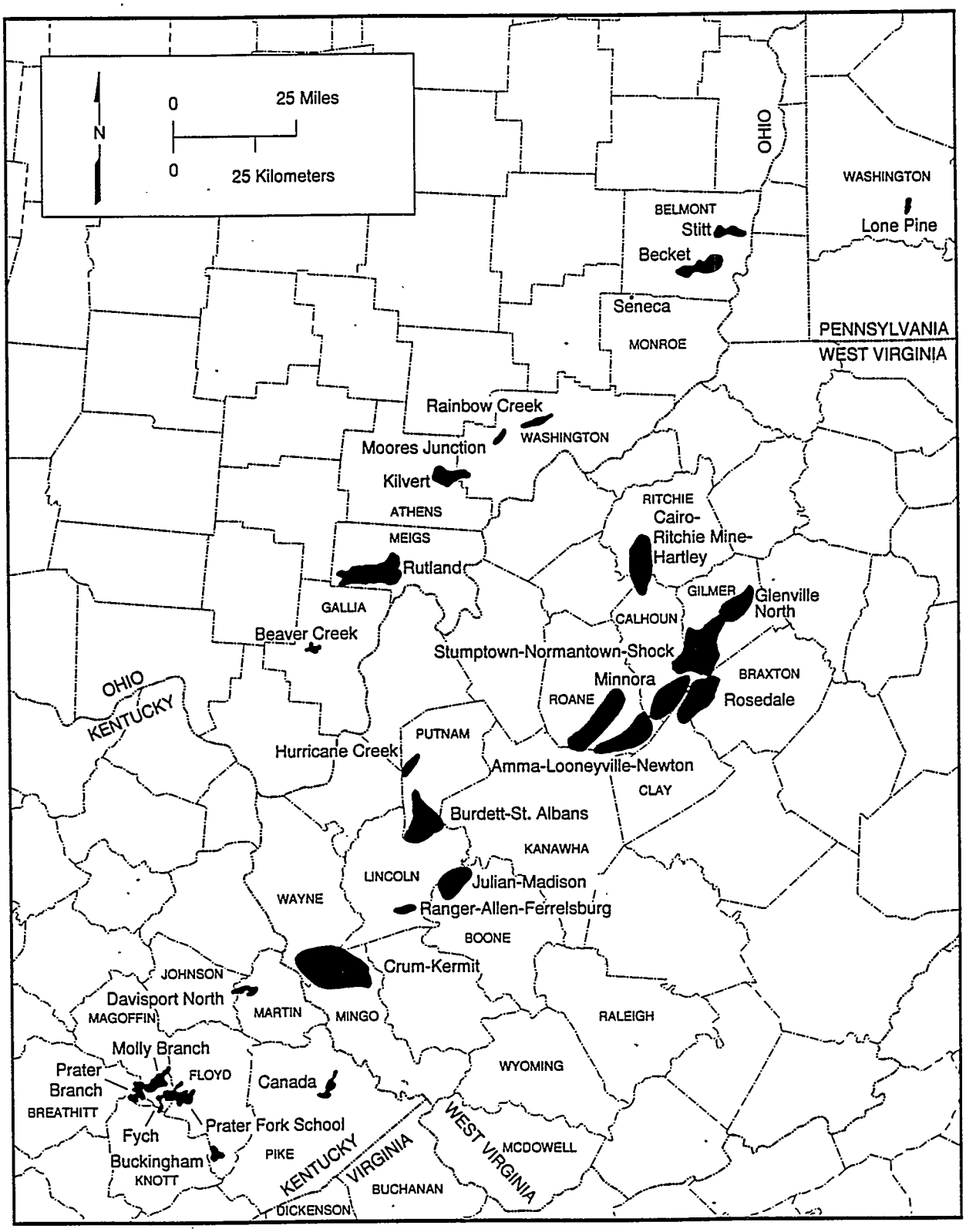

Figure 2. Locations of Lower and Middle Pennsylvanian fields discussed in text or listed in Table 1. Other productive areas illustrated in Figure 1 are not shown.

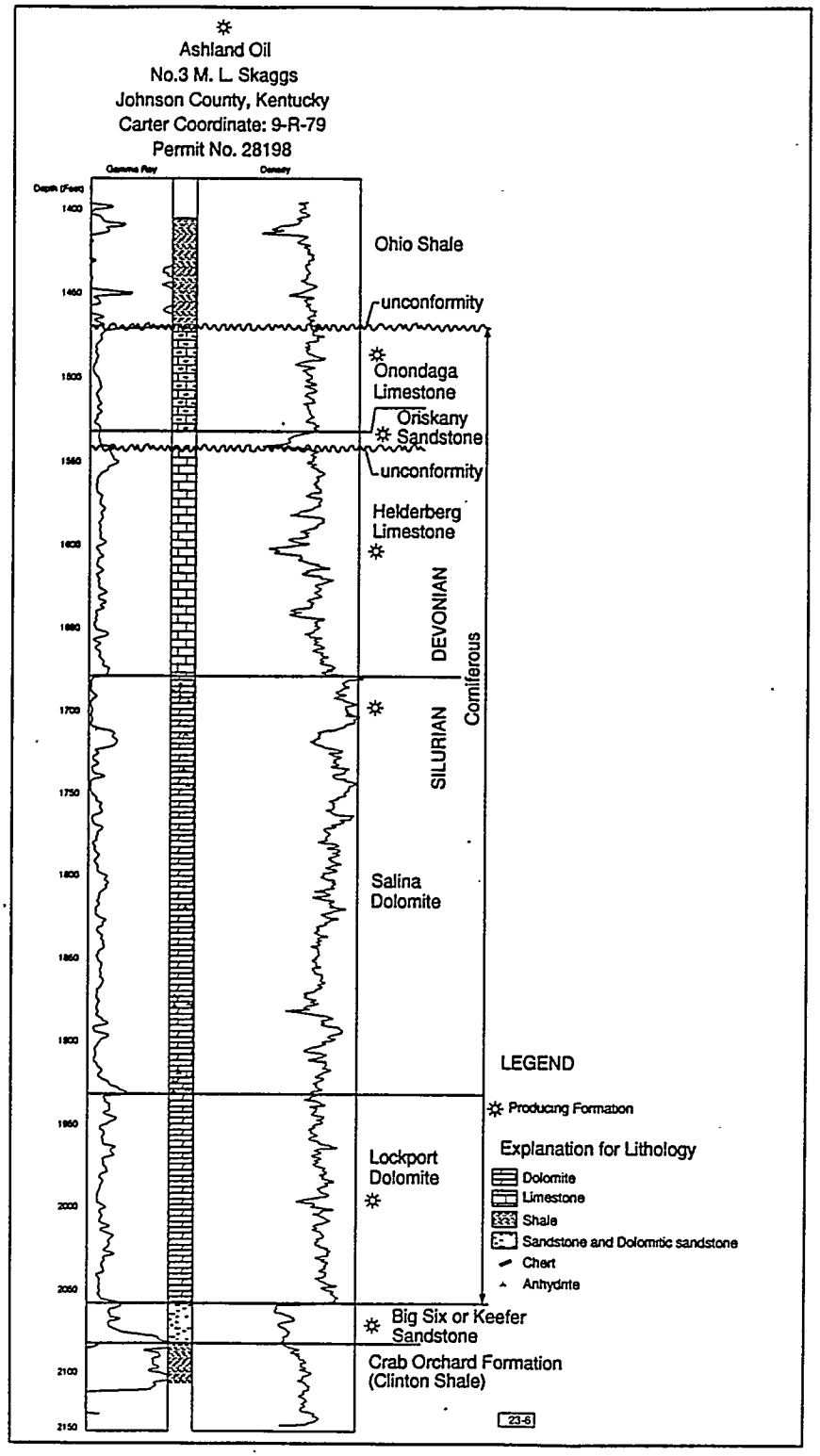

Figure 3. Type log from the Ashland Oil, No. 3 M.L. Skaggs, Johnson County, Kentucky, showing the vertical succession of formations from the Ohio Shale to the Crab Orchard Formation. The gamma-ray curves, density curves, and interpreted lithologies are also shown. The intervals representing the drillers' terms Corniferous and Big Six are also shown.

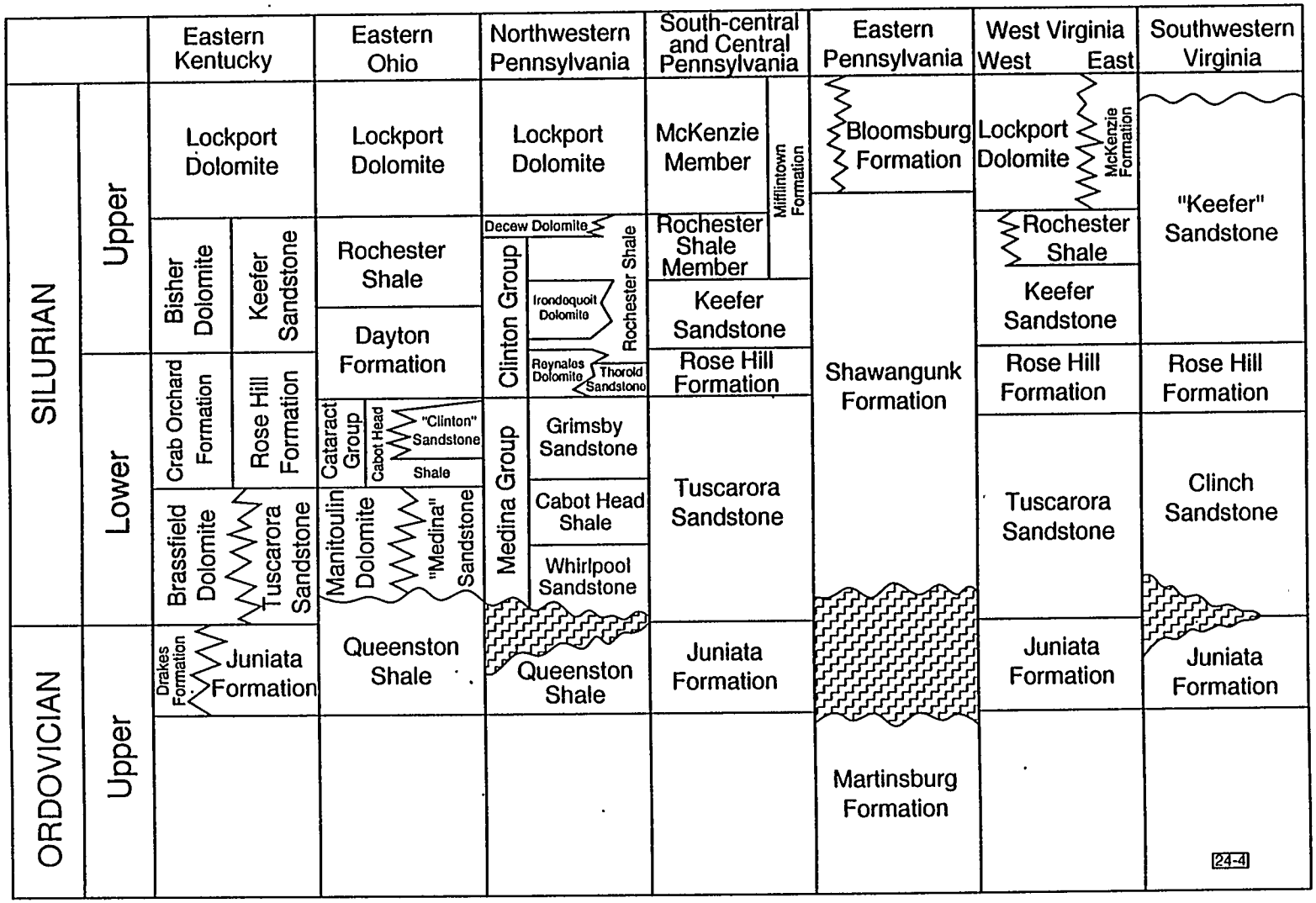

Figure 4. Stratigraphic correlation chart showing the Tuscarora Sandstone and its stratigraphic equivalents.

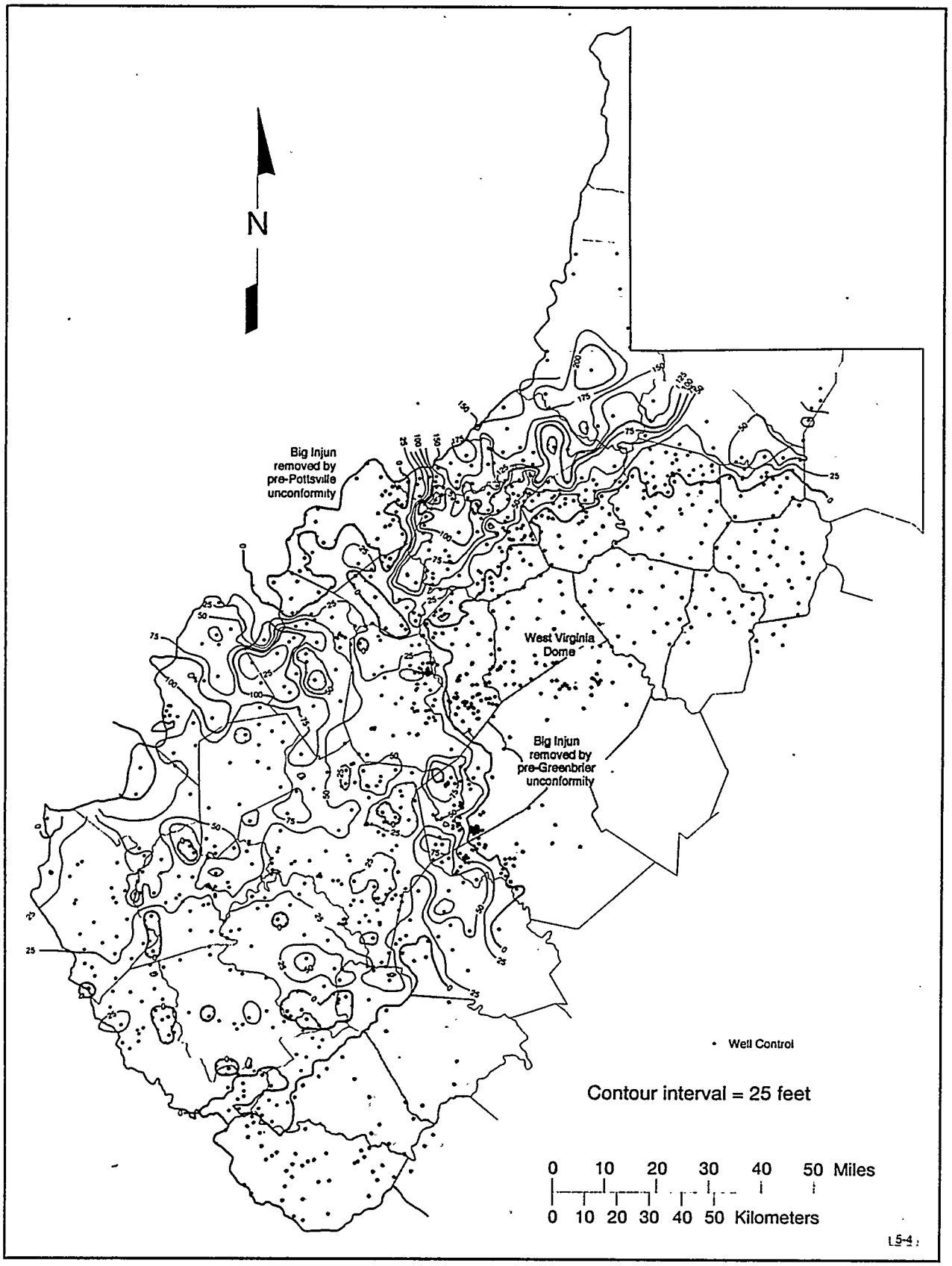

Figure 5a. Isopach map of the Big Injun sandstone in West Virginia. The effect of the pre-Greenbrier unconformity on the Big Injun sandstone is evident, particularly around the West Virginia Dome. This map was compiled by the authors using wireline logs represented by control points.

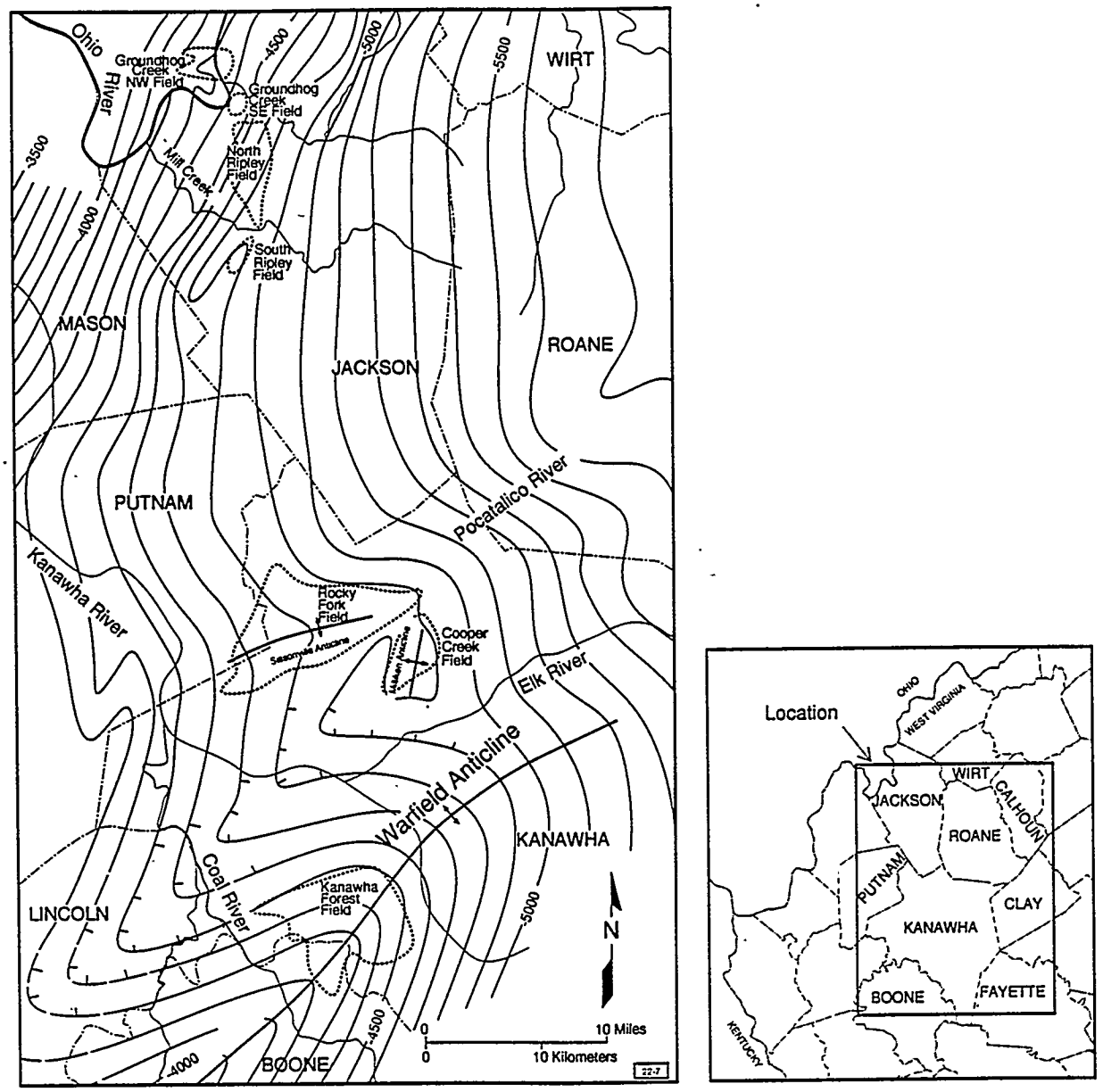

Figure 5b. Regional structure mapped on the top of the Newburg sandstone, and locations of Newburg gas fields. Locations of at least five of the seven gas fields are controlled by structure. With the exception of Cooper Creek field, updip loss of permeability is a second trapping mechanism. From Cardwell (1971).

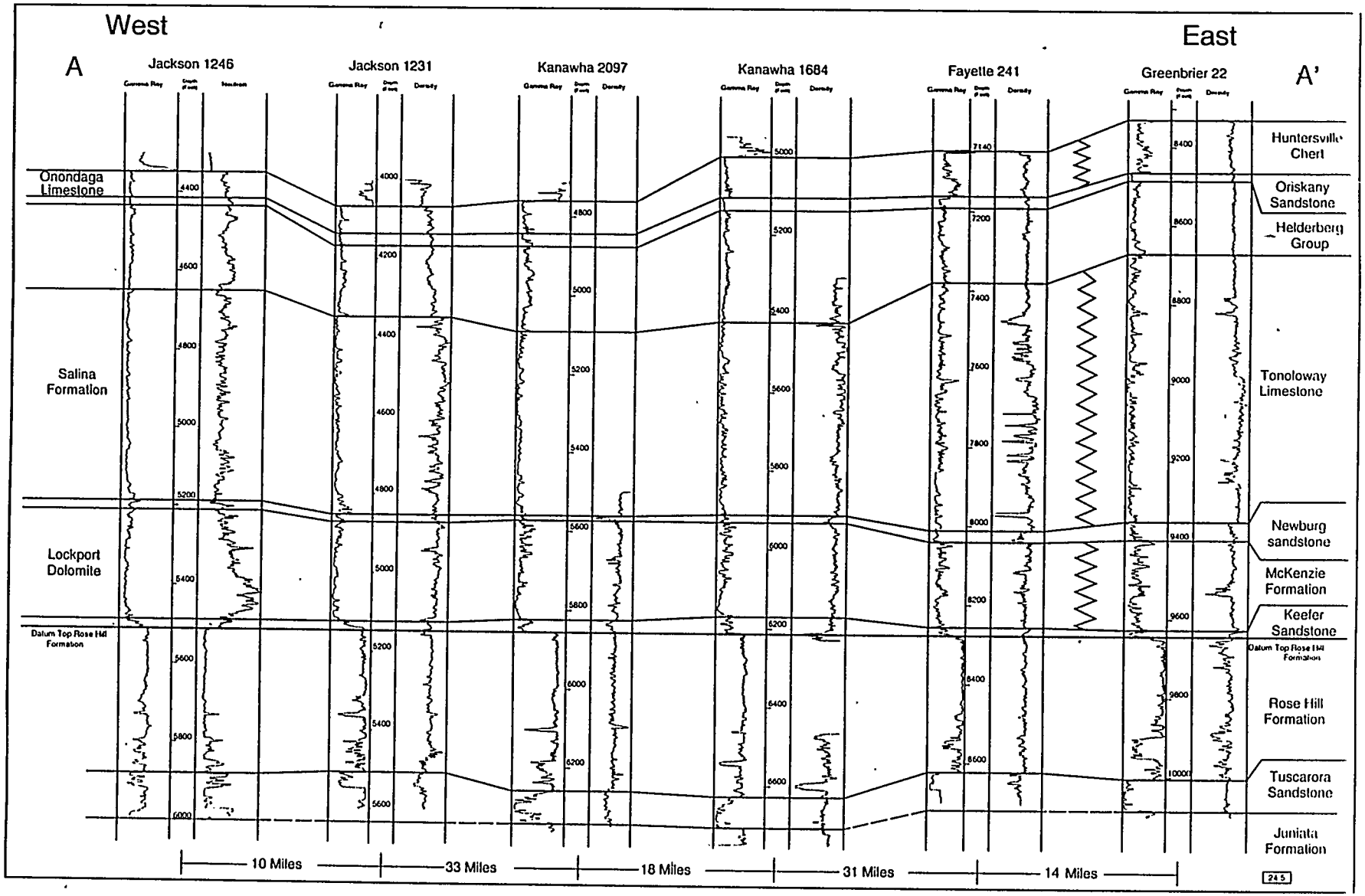

Figure 6. Tuscarora stratigraphic cross section across southern West Virginia showing the increase in shale content and decrease in thickness of the Tuscarora Sandstone from east to west. The upper part of the Lockport interval also includes the Salina "A" and "B" at the top. Columbia Gas Transmission Corporation No. 8804 Fee (Kanawha 1684) is the well designated as the discovery for Indian Creek field.

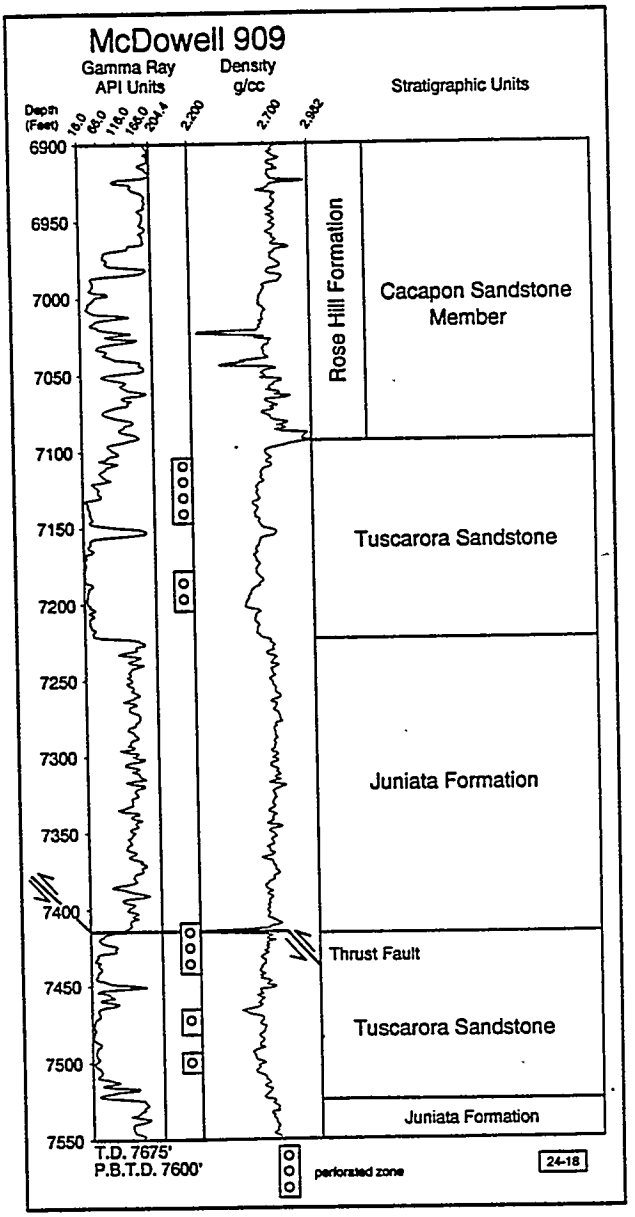

Figure 7. Portion of the gamma-ray and bulk density logs for Conoco, Inc., No. 1 Clarence Billups (McDowell 909), Cucumber Creek field discovery well, McDowell County, West Virginia, showing repetition of the Tuscarora Sandstone by thrust faulting.

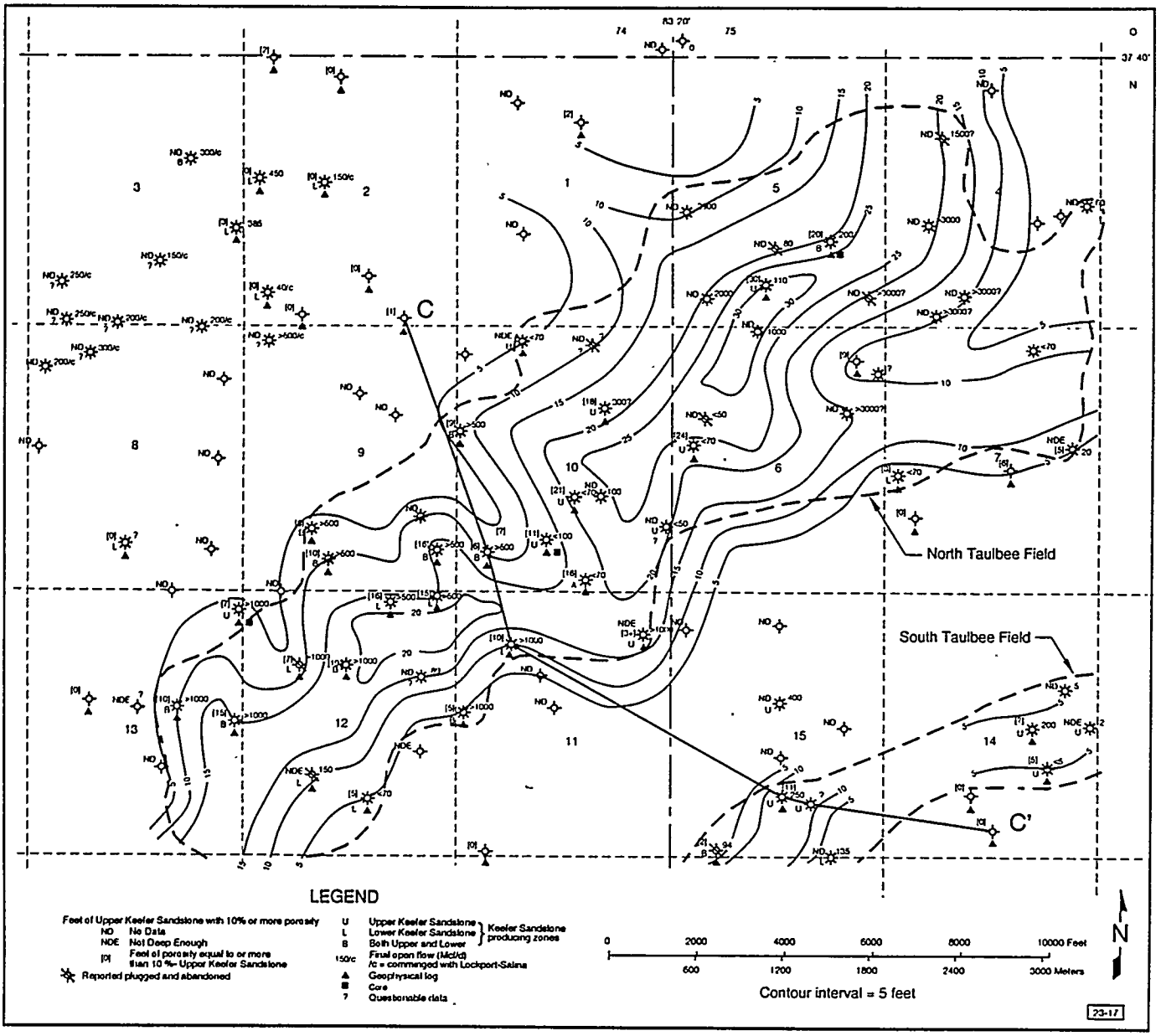

Figure 8. Isopach map of the upper Keefer Sandstone at North Taulbee field, Breathitt County, Kentucky, showing net feet of porosity greater than or equal to 10 percent.

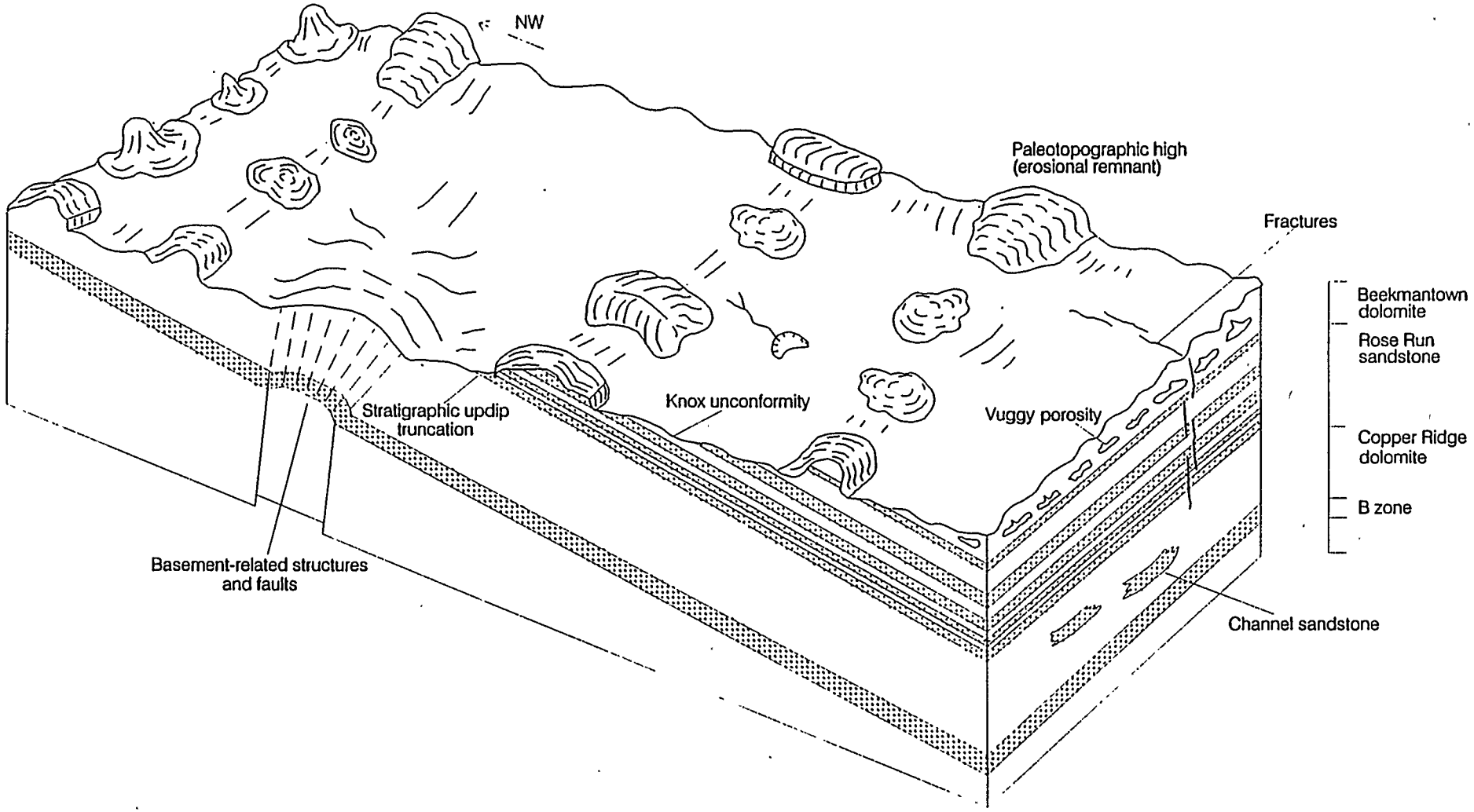

Figure 9a. Block diagram illustrating trapping mechanisms for the knox unconformity play.

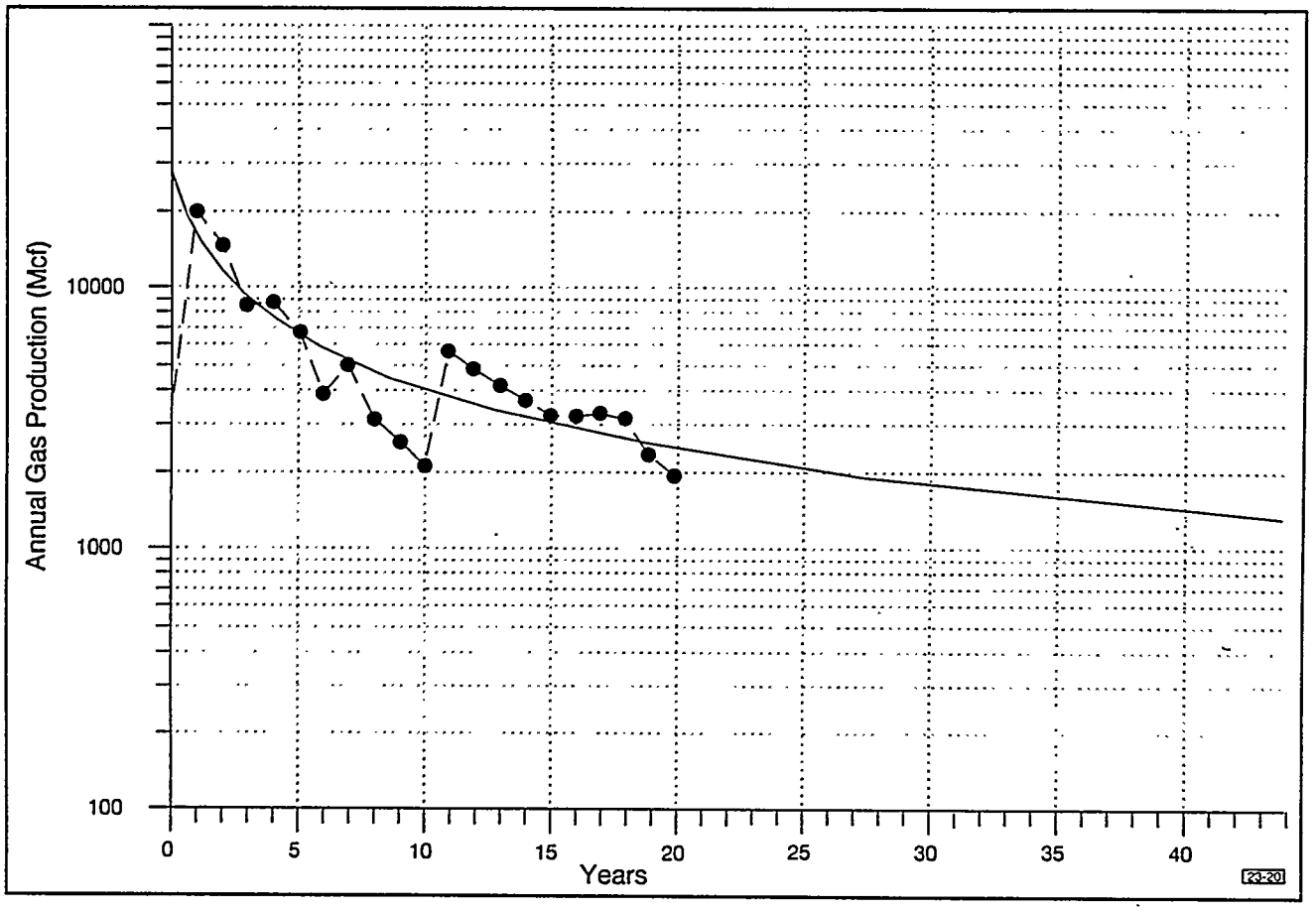

Figure 9b. Production decline curves for an average Keefer Sandstone well in Breathitt County, Kentucky. Actual data curve (shown as small dots) and best fit curve (shown as continuous line) are shown.

Table 2. Reservoir Data for Key Fields in the Newburg Play

TABLE Sns-1		Kanawha Forest WV	Rocky Fork WV	Cooper Creek WV	South Ripley WV	North Ripley WV	Greenbrier Creek NW WV	Greenbrier Creek SE WV
BASIC RESERVOIR DATA	POOL NUMBER	305	312	331	311	342	337	
	DISCOVERED	1964	1,966	1968	1966	1970	1969	1970
	DEPTH TO TOP RESERVOIR	5,430	5,575	5,690	5,575	5,530	4,945	5,030
	AGE OF RESERVOIR	Late Silurian	Late Silurian	Late Silurian	Late Silurian	Late Silurian	Late Silurian	Late Silurian
	FORMATION	Salina	Salina	Salina	Salina	Salina	Salina	Salina
	PRODUCING RESERVOIR	Newburg	Newburg	Newburg	Newburg	Newburg	Newburg	Newburg
	LITHOLOGY	sandstone	sandstone	sandstone	sandstone	sandstone	sandstone	sandstone
	TRAP TYPE	combination	combination	structural	combination	stratigraphic	combination	stratigraphic
	DEPOSITIONAL ENVIRONMENT	shallow shelf	shallow shelf	shallow shelf	shallow shelf	shallow shelf	shallow shelf	shallow shelf
	DISCOVERY WELL IP (Mcf)	7,838	63,000	7,100	6,782	22,000	6,200	10,000
	DRIVE MECHANISM	salt water	salt water	salt water	salt water	salt water	salt water	salt water
	NO. PRODUCING WELLS	48	133	30	7	48	18	9
	NO. ABANDONED WELLS							
	AREA (acreage)	16,000	32,800	6,000	2,200	12,000	2,900	1,600
	OLDEST FORMATION PENETRATED	Juniata	Juniata	Juniata	McKenzie	Juniata	Juniata	Juniata
	EXPECTED HETEROGENEITY DUE TO	stratigraphy diagenesis	stratigraphy diagenesis	stratigraphy diagenesis	structure stratigraphy diagenesis	structure stratigraphy diagenesis	structure stratigraphy diagenesis	structure stratigraphy diagenesis
RESERVOIR PARAMETERS	AVERAGE PAY THICKNESS (ft.)	8	5	6	4	7	3	4
	AVERAGE COMPLETION THICKNESS (ft.)							
	AVERAGE POROSITY-LOG (%)	11	18	15	8	14	11	11
	MINIMUM POROSITY-LOG (%)							
	MAXIMUM POROSITY-LOG (%)							
	NO. DATA POINTS	38	58	15	10	30	5	1
	POROSITY FEET	0.88	0.90	0.90	0.32	0 98	0.33	0.44
	RESERVOIR TEMPERATURE (°F)	130	130	130	130	130	130	130
	INITIAL RESERVOIR PRESSURE (psi)	2,070	2,240	2,260	2,180	2,145	2,110	
	PRODUCING INTERVAL DEPTHS (ft.)	4,940-5,940	5,220-6,000	5,560-6,150	5,400-5,700	5,010-5,780	4,800-5,300	5,000-5,300
	PRESENT RESERVOIR PRESSURE (psi) / DATE							
FLUID & GAS PROPERTIES	Rw (SLM)							
	GAS GRAVITY (g/cc)	0.602			0 615	0.648	0.642	
	GAS SATURATION (%)	84						
	WATER SATURATION (%)	16						
	COMMINGLED							
	ASSOCIATED OR NONASSOCIATED	nonassociated	nonassociated	nonassociated	associated	associated	nonassociated	nonassociated
	Btu / Mcf	1,064			1,060	1,134	1,108	
VOLUMETRIC DATA	STATUS (producing, abandoned, storage)							
	ORIGINAL GAS IN PLACE (Mcf)	59,320,000	160,170,000	21,274,000	107,648,000		14,750,000	
	ORIGINAL GAS RESERVES (Mcf)	53,388,000	144,153,000	19,147,000	96,881,000		13,280,000	
	PRODUCTION YEARS	1964-1973	1966-1973	1968-1973	1966-1973	1970-1973	1969-1973	1970-1973
	REPORTED CUMULATIVE PRODUCTION (Mcf)	49,185,000	138,451,000	17,752,000	86,654,000 combined	86,654,000 combined	10,177,000 combined	
	NO. WELLS REPORTED							
	ESTIMATED CUMULATIVE PRODUCTION (Mcf)							
	REMAINING GAS IN PLACE (Mcf)/DATE	10,135,000	23,718,000	3,522,000	20,992,000		4,573,000	
	REMAINING GAS RESERVES (Mcf)/DATE	4,203,000	7,702,000	1,395,000	10,227,000		3,103,000	
	RECOVERY FACTOR (%)	90	90	90	90	90	90	90
	INITIAL OPEN FLOW (Mcf/d)	1,294	12,866	13,464	1,113	12,393	8,008	10,392
	FINAL OPEN FLOW (Mcf/d)	5,845	31,012	38,852	5,584	40,464	10,242	20,857

P3 Atlas of Northern Gulf of Mexico Gas and Oil Reservoirs—Play Analysis Procedures and Examples of Resource Distribution

CONTRACT INFORMATION

Cooperative Agreement	14-35-0001-30683
Contractor	The University of Texas at Austin Bureau of Economic Geology University Station, Box X Austin, TX 78713-8924
Other Funding Sources	Minerals Management Service Gas Research Institute
Contractor Project Manager	Steven J. Seni
Principal Investigators	Steven J. Seni Robert J. Finley
METC Project Manager	Harold Shoemaker
Period of Performance	October 1, 1992, to September 30, 1996

Schedule and Milestones

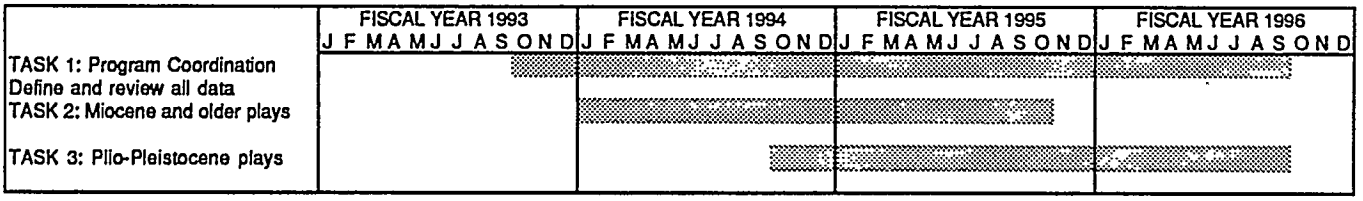

OBJECTIVES

The objective of the program is to produce a reservoir atlas series of the Gulf of Mexico that (1) classifies and groups offshore oil and gas reservoirs into a series of geologically defined reservoir plays, (2) compiles comprehensive reservoir play information that includes descriptive and quantitative summaries of play characteristics, cumulative production, reserves, original oil and gas in place, and various other engineering and geologic data, (3) provides detailed summaries of representative type reservoirs for each play, and (4) organizes computerized tables of reservoir engineering data into a geographic information system (GIS). The primary product of the program will be an oil and gas atlas series of the offshore northern Gulf of Mexico and a computerized geographical information system of geologic and engineering data linked to reservoir location.

The oil and gas atlas of the Gulf of Mexico will provide a critically compiled, comprehensive

reference, which is needed to more efficiently develop reservoirs, to extend field limits, and to better assess the opportunities for intrafield exploration. The play atlas series will provide an organizational framework to aid development in mature areas and to extend exploration paradigms from mature areas to frontier areas deep below the shelf and into deep waters of the continental slope. In addition to serving as a model for exploration and education, the offshore atlas will aid resource assessment efforts of State, Federal, and private agencies by allowing for greater precision in the extrapolation within and between plays. Classification and organization of reservoirs into plays have proved to be effective in previous atlases produced by the Bureau, including the Texas oil (Galloway and others, 1983) and gas atlases (Kosters and others, 1989), the central and eastern Gulf Coast gas atlas (Bebout and others, 1992), and the Midcontinent gas atlas (Bebout and others, 1993).

BACKGROUND INFORMATION

The Offshore Northern Gulf of Mexico Oil and Gas Resource Atlas Series is a cooperative research effort managed by the Bureau of Economic Geology as lead technical contractor. Funding for the program is supplied by the Department of Energy (DOE) through the Morgantown Energy Technology Center (METC) and the Bartlesville Program Office (BPO), the Gas Research Institute (GRI), and the Department of the Interior's Minerals Management Service (MMS). The State of Louisiana Center for Coastal, Energy, and Environmental Resources and the Geological Survey of Alabama are subcontractors for research in their respective State waters. This report summarizes activities conducted during the second year of the Northern Gulf of Mexico Oil and Gas Resource Atlas Series program. Funded by the Gas Research Institute, the U.S. Department of Energy, and the U.S. Department of the Interior's Minerals Management Service, investigations began in October 1992, with the Bureau of Economic Geology as lead technical contractor.

The need to find additional hydrocarbons is directing exploration in the Gulf of Mexico toward historically productive areas on the shelf and frontier trends on the slope. Systematic synthesis of information on oil and gas resources for the offshore area is needed for the continued success of exploration, development, and resource assessment in the area. We are responding to this need through a coordinated research effort to develop a gas and oil atlas series about the offshore northern Gulf of Mexico. Efficient offshore development requires improved understanding of the controls on the location and distribution of gas and oil reservoirs for field extension and infill drilling.

PROJECT DESCRIPTION

Our play methodology includes identifying structural and depositional style, constructing composite type logs and type log cross sections, and integrating geologic data from type reservoirs. We emphasize progradational, aggradational, and retrogradational depositional styles and submarine-fan depositional facies because they strongly influence the distribution of reservoir-quality sands and sandstones. For example, submarine-fan reservoirs of the *Lenticulina* chronozone in the High Island Area of Texas State waters compose a play controlled by the distribution of reservoir sandstone. In contrast, structural style is typically the key determinant of the trapping mechanism. A play of middle Miocene reservoirs that is structurally controlled forms the Corsair trend in the Federal OCS of Brazos and Mustang Areas. The extent of hydrocarbon plays depends largely on the distribution of depositional and diagenetic facies containing favorable reservoir rocks. Hydrocarbons are trapped where structures

coincide with favorable facies. The lower Miocene of offshore Texas is a useful area in which to apply these concepts of play analysis because depositional style and facies are well described and the extensional structural style is relatively uniform.

This report includes three sections: (1) the first section describes the general play-analysis procedure and methodologies, (2) the second section describes three plays of reservoirs in Texas State waters of the Gulf of Mexico, and (3) the third section examines the resource distribution in terms of chronozones and depositional styles for the entire Gulf of Mexico.

Play-Analysis Procedure

White (1980) and Galloway and others (1983) defined a play as a group of reservoirs genetically related by depositional origin, structural style or trap type, and nature of source rocks and seals. The generalized play-analysis procedure we used for the offshore gas and oil atlas program is as follows: (1) define chronozones, (2) outline area of production for chronozones, (3) collect engineering and geologic data for each reservoir within chronozones, (4) identify reservoirs on field type logs, (5) correlate reservoirs, depositional styles, and chronozones on strike and dip cross sections with type logs, (6) outline plays by grouping depositionally and structurally similar reservoirs, (7) synthesize defining attributes of each play, (8) identify and describe type reservoirs within each play, (9) tabulate reservoir engineering data for each play, and (10) write play descriptions (Seni and others, 1994).

Chronostratigraphy

Play analysis begins with identification and correlation of chronozones. Chronozones provide a temporal framework for grouping reservoirs in the Gulf of Mexico. In the absence of formations, chronozones are typically defined on the basis of biostratigraphic zones. In order to correlate reservoirs within strata of the same age, we employ an MMS-based chronostratigraphic synthesis of the Gulf according to biostratigraphic zones (fig. 1) (Reed and others, 1987). Major flooding surfaces and their biostratigraphically rich faunal assemblages are important reference horizons for this chronostratigraphic subdivision. The 26 chronozones identified by the MMS are grouped into 16 chronozones for the Atlas program.

SYSTEM	SERIES	ATLAS CHRONO.	CHRONO-ZONES	BIOCHRONOZONES
QUATERNARY	Pleistocene	UPL	UPL-4	Sangamon Fauna
			UPL-3	*Trimosina* A 1st
			UPL-2	*Trimosina* A 2nd
			UPL-1	*Hyalinea b./Trimosina* B
		MPL	MPL-2	*Angulogerina* B 1st
			MPL-1	*Angulogerina* B 2nd
		LPL	LPL-2	*Lenticulina* 1
			LPL-1	*Valvulineria* H
TERTIARY	Plio-cene	UP	UP	*Buliminella* 1
		LP	LP	*Textularia* X
	Miocene	UM3	UM-3	*Robulus E/Bigeneria* A
			UM-2	*Cristellaria* K
		UM1	UM-1	*Discorbis* 12
		MM9	MM-9	*Bigenerina* 2
			MM-8	*Textularia* W
		MM7	MM-7	*Bigenerina humblei*
			MM-6	*Cristellaria* I
			MM-5	*Cibicides opima*
		MM4	MM-4	*Amphistegina* B
			MM-3	*Robulus* 43
			MM-2	*Cristellaria* 54/*Eponides* 14
			MM-1	*Gyroidina* K
		LM4	LM-4	*Discorbis b.*
			LM-3	*Marginulina ascensionensis*
		LM2	LM-2	*Siphonina davisi*
		LM1	LM-1	*Lenticulina hanseni*
PALEOGENE	Oligocene	FA1	Oligocene Frio-Anahuac	*Marginulina idiomorpha*

Figure 1. Chronostratigraphic subdivisions and biostratigraphic zones used in Gulf of Mexico. Modified from Reed and others (1987)

Depositional Style

Three depositional styles used as primary defining attributes of plays in the offshore Gulf atlas are retrogradation (transgression), aggradation, and progradation (fig. 2). These depositional styles define the large-scale patterns of basin fill in the Gulf of Mexico and provide a framework for predicting sand-body trends, reservoir distribution, and reservoir quality. We identify the depositional styles by using spontaneous potential (SP) log patterns as well as water depth, paleoecological depth zones, seismic lines, and structure. We also identify submarine fans as a primary depositional defining attribute and substitute depositional style. Although submarine fans are not confined to a single depositional style, they are identified uniquely because they are important reservoirs on the slope and below the shelf.

We chose to identify depositional styles instead of depositional facies or systems tracts because styles (1) capture the appropriate scale of geologic variability for a basinwide resource investigation, (2) dovetail with the existing chronostratigraphic divisions in the Gulf, (3) are readily interpreted from logs, and (4) avoid the complications inherent in local depositional events. Although a basinwide analysis of sequence stratigraphic systems tracts or genetic stratigraphic sequences would be useful, such an analysis is beyond the scope of this project. The depositional styles correlation grid is an important first step to such a study.

We recognize that in some fields nearly every sandstone is a hydrocarbon reservoir, and in those instances the structural style is more important than depositional style in controlling reservoir distribution. Examples of reservoirs that are structurally controlled include middle Miocene reservoirs associated with the Corsair trend and various reservoirs in the Louisiana OCS over salt structures. Plays based solely on structural style are of limited exploration utility in mature areas where all such structures are well mapped. Depositional style remains a robust attribute of plays where reservoirs are structurally controlled as well as in areas where reservoirs are depositionally stratified. Plays defined on the basis of depositional style thus remain suitable for hydrocarbon exploration in structurally dominated areas.

SP LOG SHAPE	DEPOSITIONAL STYLE/FACIES	CHARACTER
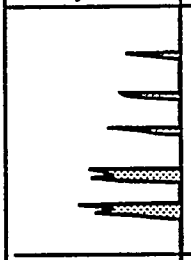	RETROGRA-DATIONAL	Commonly upward-fining log character, rarely upward-coarsening; thin sandstone bodies, upward-thickening retrogradational package of sandstone bodies separated by thicker mudstones
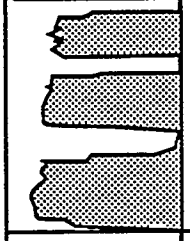	AGGRA-DATIONAL	Thick, blocky to upward-fining log character; stacked sandstone bodies separated by thinner mudstones
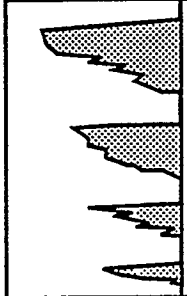	PROGRA-DATIONAL	Commonly upward-coarsening log character, rarely upward-fining; thin to thick sandstone bodies; upward-thickening, progradational package of sandstone bodies separated by subequally thick mudstones
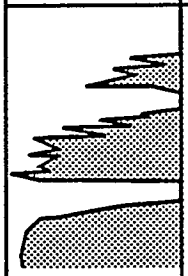	DEEP-SEA FAN	Variable sandstone body thickness patterns; includes thick to thin, blocky to upward-fining log character, sharp-based sandstones; also, serrated, thin to thick sandstones; thick mud-stone at top; singular or stacked package of sandstone bodies; commonly upward-fining package

Figure 2. Depositional styles, sand-body characteristics, and associated idealized SP log shapes

Depositional styles are important elements of two common models that organize packages of reservoir-quality strata: (1) sequence stratigraphic systems tracts (Vail, 1987; Van Wagoner and others, 1988) and (2) genetic stratigraphic sequences (Galloway, 1989). The internal architecture of both models is similar; the difference lies in the choice of sequence boundaries. Sequence stratigraphic systems tracts (Vail, 1987; Van Wagoner and others, 1988) are unconformity-bounded packages comprising highstand systems tracts, lowstand systems tracts, and transgressive systems tracts. In contrast, genetic stratigraphic sequences (Galloway, 1989) are bounded by flooding surfaces and comprise progradational systems tracts, lowstand progradational complexes, and retrogradational systems tracts.

For the atlas program, we use flooding surfaces as primary genetic boundaries because (1) the abundance of biostratigraphic information typically coincides with the boundaries of most MMS chronozones in the Gulf of Mexico and (2) major flooding surfaces in the Gulf of Mexico are more readily identified on type logs and seismic lines than are unconformities. The chronozones do not correspond to sequence stratigraphic cycles because they are one-half cycle out of phase and chronozones typically include two or three third-order cycles (Haq and others, 1987).

Type Logs

Type logs were chosen for each field to identify the style and position of all reservoirs. All productive reservoirs, chronozones, biozones, paleobathymetric zones, and depositional styles are identified on each type log (fig. 3). Large fields may require a composite type log in order to capture all reservoirs because of expanded sections across growth faults and intrafield stratigraphic variations.

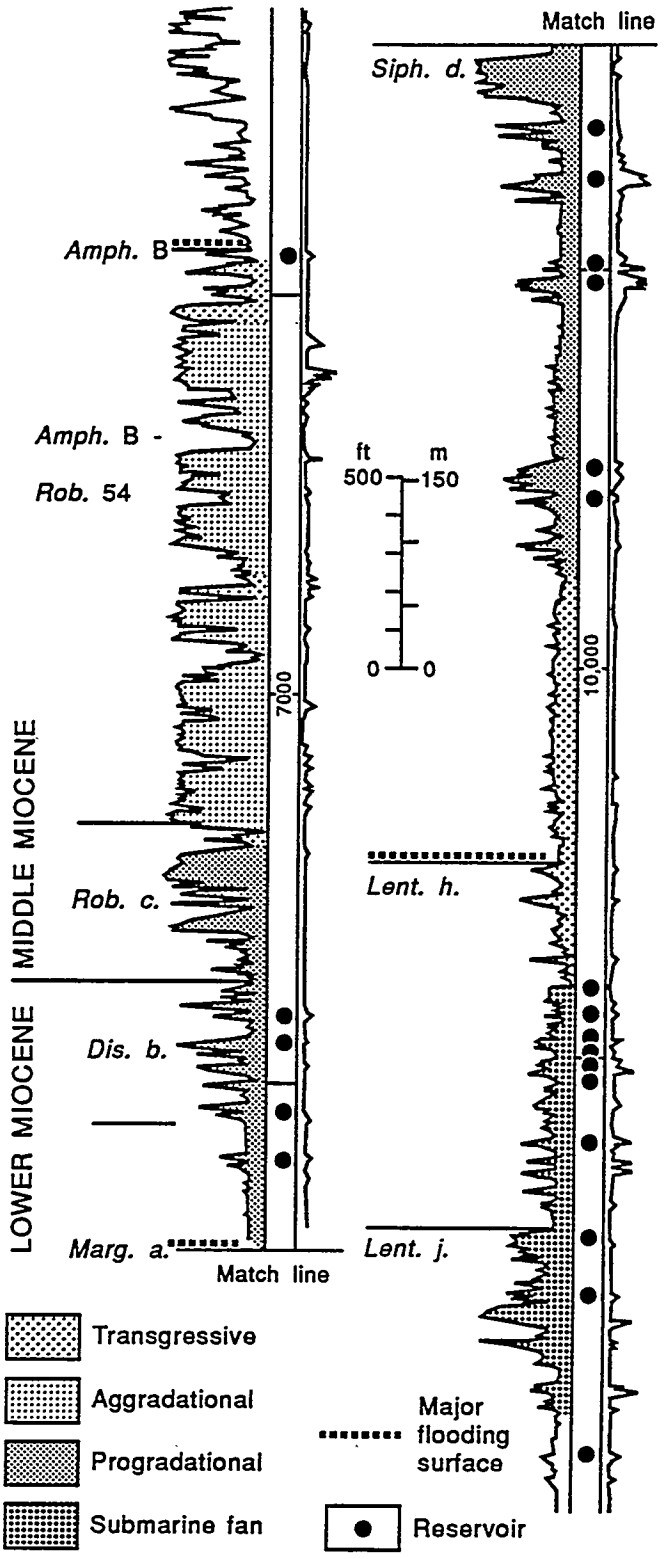

Figure 3. Type log showing depositional styles, major flooding surfaces, reservoirs, and biozones for High Island Block 24-L field

RESULTS

Cross sections based on type logs are used to correlate reservoirs within a chronostratigraphic and depositional style framework and form one basis for grouping reservoirs into plays. A strike-oriented cross section of the upper Texas coast illustrates the depositional styles and reservoir distribution of the Miocene section (MM-4 to LM-1) (fig. 4). Depositional styles include submarine-fan *Lenticulina* sandstones, progradational *Lenticulina*, *Siphonina d.*, and *Discorbis b.* sandstones and mudstones, aggradational *Amphistegina* B to *Robulus c.* sandstones, and transgressive sandstones and mudstones of *Amphistegina* B (fig. 4). The progradational depositional style and the submarine-fan facies contain abundant reservoirs, whereas the aggradational and retrogradational (transgressional) styles are relatively barren.

Twenty-four plays and two subplays of Miocene and Oligocene reservoirs have been identified in the Texas State offshore area. Offshore Oligocene (Frio–Anahuac Formations) reservoirs are present in two regions of the Texas offshore (Hamlin, 1989): a southern region of Mustang and Matagorda Areas and a northern region of Galveston Area. Distal Frio reservoirs, currently productive offshore, include shelf and slope sandstones associated with extensive shelf-margin progradation. Miocene reservoirs are present in Texas State waters from South Padre Area to High Island Area and extend south into the Federal OCS and east into Louisiana State waters.

Miocene Plays

The lower Miocene is the primary hydrocarbon-producing zone in the Texas State offshore area, and gas is the dominant hydrocarbon. Lower Miocene production extends a short distance into the Federal OCS. In the Federal OCS, middle Miocene strata are highly productive in rollover structures associated with the Corsair trend just downdip of the State–Federal boundary (Morton and others, 1988). Three examples of major lower Miocene plays in the Galveston and High Island Areas will be discussed. Miocene plays in offshore Texas State waters have produced 3.1 Tcf of gas and 37.6 MMbbl of oil. Miocene reservoirs below the *Amphistegina* B chronozone are the most productive in the Texas State offshore waters. Lower Miocene production is predominantly gas; subordinate volumes of oil are associated with salt domes in updip plays. The structural style is characterized by major extension of the lower Miocene shelf margin. Rollover anticlines and listric growth faults are the primary traps.

High Island and Galveston Areas host three examples of lower Miocene plays: LM-1A1, LM-1A2, and LM-2B (fig. 5). The defining attributes of submarine-fan *Lenticulina* play LM-1A1 are listed in table 1. Plays LM-2B and LM-1A2 comprise progradational reservoirs from the *Siphonina davisi* and *Lenticulina* chronozones, respectively. Annual production of all reservoirs in each play shows the long-term temporal trend of increasing production from deeper reservoirs (fig. 6). The shallow play LM-2B had an initial increase in gas production from 1970 to 1974 and a second higher peak from 1979 to 1981. Production from the play LM-1A2—progradational *Lenticulina*—peaked from 1977 to 1980. The latest surge in production, from 1980 to 1983, came from the deeply buried LM-1A1, the submarine-fan *Lenticulina* play.

Lower Miocene Play LM-1A1—Submarine-Fan *Lenticulina*. Lower Miocene play LM-1A1 includes the oldest lower Miocene reservoirs and extends across the High Island Area and into State waters of western Louisiana. Production is from *Lenticulina* submarine-fan sandstones in Texas and from *Planulina* sandstones in Louisiana State waters (Caughey, 1981). The structural style is characterized by fault blocks in rollover anticlines. Gas is the dominant type of hydrocarbon.

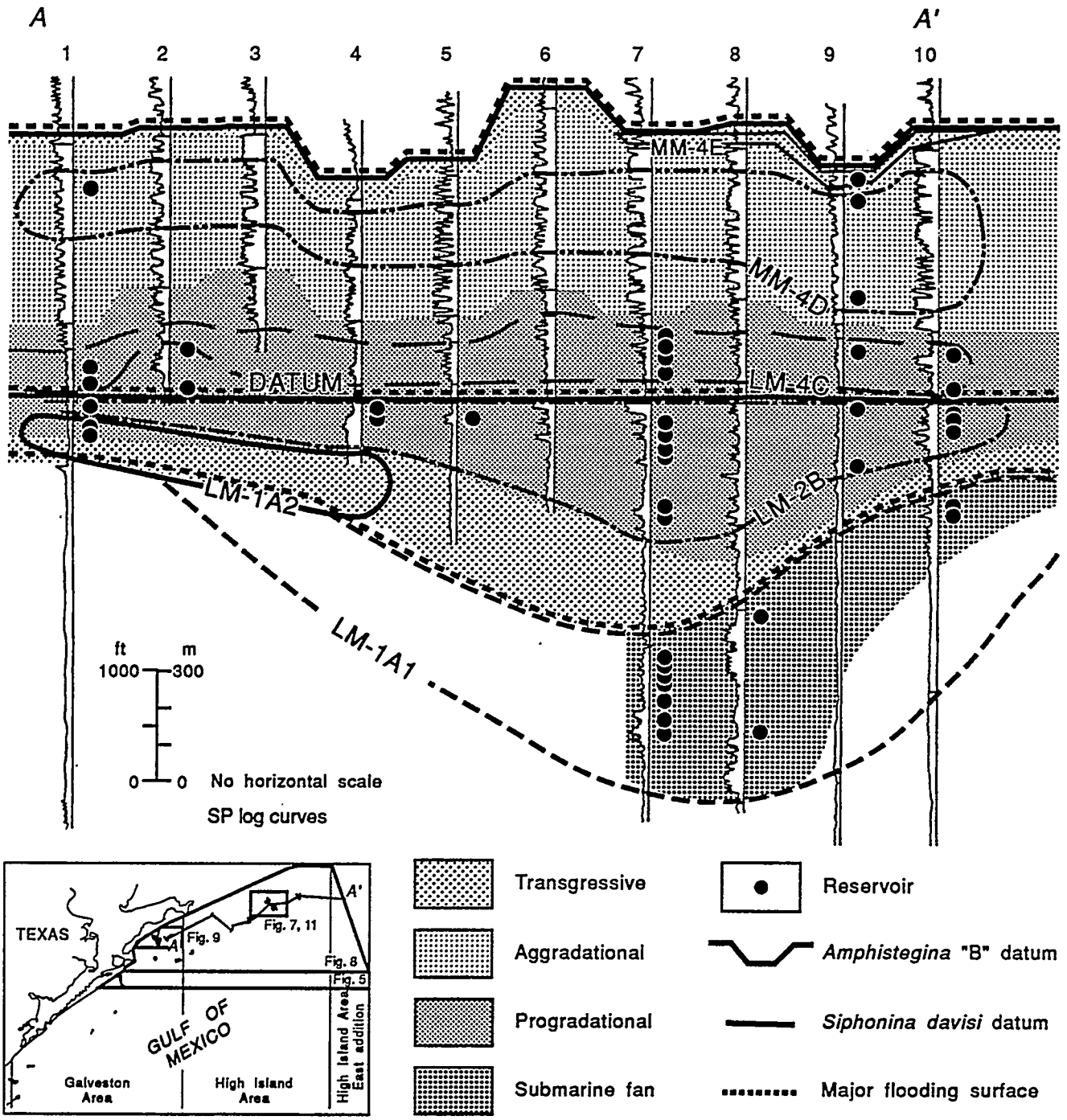

Figure 4. Strike-oriented type log cross section showing depositional styles for Galveston and High Island Areas. The progradational depositional style and submarine-fan facies contain the most numerous and largest reservoirs. Inset map shows location of figures 4, 5, 7, 8, 9, and 11

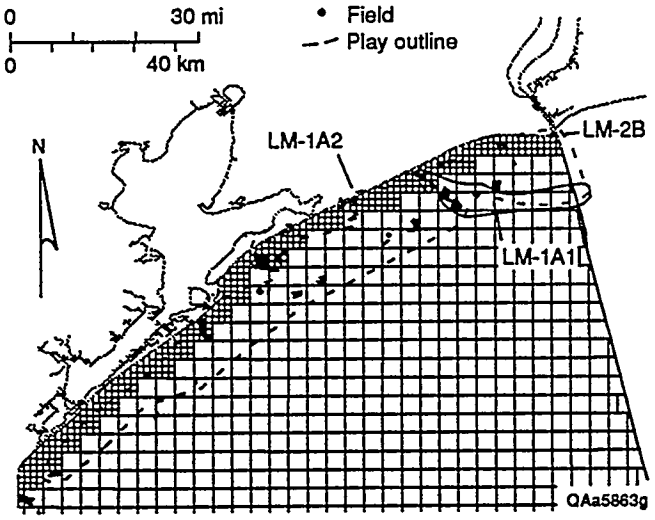

Figure 5. Map of lower Miocene plays (LM-1A1, LM-1A2, and LM-2B) in the Texas State offshore and the High Island and Galveston Areas. Map location is indicated on inset map of figure 4

High Island Block 24-L field produces gas from a series of *Lenticulina* reservoir sandstones (I, J, J-SER, KC, KG, and KL reservoirs) in seven individual fault blocks. The configuration of *Lenticulina* reservoir sandstones at High Island Block 24-L field indicates production from J-SER and KG reservoirs in fault blocks D and K (fig. 7). High Island Block 30-L field, which has produced 119 Bcf, contains the most productive reservoirs in the play.

Exploration for submarine-fan sandstones of the *Lenticulina* chronozone has been hampered by significant depth of burial (12,000 to greater than 18,000 ft) and by erratic distribution of reservoir sandstone bodies. A map of maximum sandstone illustrates the thickness of the single thickest sandstone body in the *Lenticulina* chronozone in a part of the High Island and Galveston Areas (fig. 8). The updip thinning and downdip coalescence of thick maximum sandstone supports the submarine-fan interpretation. The accumulation of thick *Lenticulina* sandstone is related to submarine canyon and fan lobe

Table 1. Defining attributes of lower Miocene play LM-1A1

Defining attribute—Deep-water, gas-rich, submarine-fan facies of middle to upper slope associated with submarine canyon, submarine fan, or failed embayment of continental margin during *Lenticulina* chronozone. Two *Lenticulina* chronozone plays are differentiated on basis of depositional environment: LM-1A1 (updip progradational deltaic play) and LM-1A2 (downdip submarine-fan play).

Hydrocarbon type—Geopressured gas.

Reservoir facies—Aggradational submarine-fan channel and overbank facies along State/Federal boundary. Reservoirs in submarine-fan systems are very fine to fine sandstone of two types: (1) blocky, sharp-based, channel facies and (2) serrated mudstone and very fine sandstone of overbank and levee facies. Reservoirs are often perforated throughout entire sand body. Trends of thick sandstone are dip oriented.

Structural style—Fields and reservoirs are associated with major rollover anticlines and growth faults along the lower Miocene continental margin.

Trapping mechanism—Downthrown fault blocks of rollover anticlines associated with growth faults; also upthrown and tilted fault blocks between growth faults.

Possible hydrocarbon source—Subjacent slope mudstones and underlying Frio/Anahuac shelf and slope mudstones.

Exploration maturity—Relatively immature in submarine-fan subplay because of burial depths of 12,000 to 16,000 ft.

Frontiers—Stratigraphic traps in updip pinch-out of slope sandstones; deeper pool extensions.

Intraplay limitations—Deep burial, increase in depth of reservoirs downdip.

Boundaries—Loss of reservoir sandstone away from localized embayed or failed margin; loss of reservoir sandstone downdip, updip, to southwest, and northeast; and loss of high-quality thick net sandstone away from dip-oriented axes.

deposition or to failure of the *Lenticulina* shelf margin and filling of a submarine embayment (Morton, 1993).

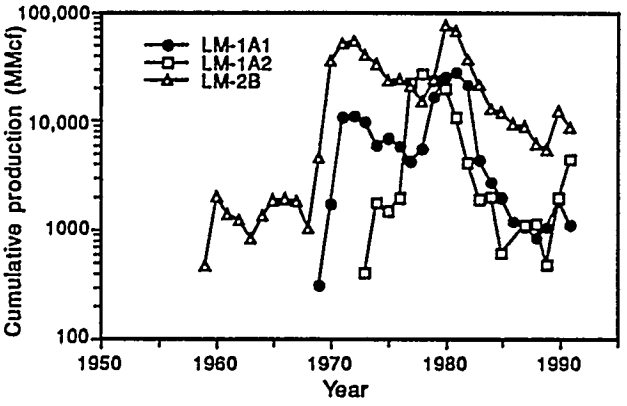

Figure 6. Graph of annual production from all reservoirs in lower Miocene plays LM-1A1, LM-1A2, and LM-2B

Lower Miocene Play LM-1A2—Progradational *Lenticulina.* Lower Miocene play LM-1A2 also extends across the High Island Area into State waters of western Louisiana. Gas is the dominant type of hydrocarbon that is produced. Peak play production was 26 Bcf in 1978; however, production has climbed in the 1990's as a result of recent discoveries on subtle structures in nearshore Texas State land at Pirate's Cove and State Tract 60 fields. Block 176-S (L-1 and L-2A), Galveston 175-S (L-1), and Shipwreck (L-1 and L-2) fields and reservoirs produce gas from progradational reservoirs in fault traps and rollover anticlines in the Galveston Area (fig. 9). Shipwreck (L-1 and L-2) reservoirs have produced 107 Bcf and are the most productive *Lenticulina* reservoirs. The structural style of this play is dominated by rollover anticlines and expansion-zone listric normal faults (fig. 10). The salt dome in the center of figure 10 is a relatively isolated structure rooted at the zone of décollement in the Oligocene.

Lower Miocene Play LM-2B—Progradational *Siphonina davisi.* Lower Miocene play LM-2B extends across High Island Area into Galveston Area and from western Louisiana State waters into the Federal OCS. Gas is the dominant type of hydrocarbon that is produced. The depositional style is progradational facies of shelf-margin deltas. The *Siphonina davisi* chronozone comprises two to three progradational packages that are 200 to 500 ft thick. Toward the southwest, *Siphonina davisi* sandstones thin and pinch out from the major deltaic lobe centered in the State part of the High Island Area. Downdip in the Federal OCS, *Siphonina davisi* reservoirs compose a submarine-fan play.

The structural style of this play is characterized by extension and listric growth faults at the lower Miocene continental margin. Tilted fault blocks and rollover anticlines form most of the traps. Flank traps against salt domes, as at Galveston Block 104-L, form a secondary structural style. In addition to structurally controlled traps, stratigraphic entrapment of hydrocarbons is affected by sand-body pinch-outs at High Island 30-L, High Island 31-L, and Galveston 102-L.

The HC reservoir of High Island Block 24-L field is the type reservoir of play LM-2B (fig. 11). Cumulative production from the HC reservoir totals 185 Bcf from four separate fault blocks. *Siphonina davisi* sandstones form laterally continuous wave-dominated, shelf-margin deltaic sand bodies that are segmented by normal faults into a series of fault-block reservoirs (fig. 10).

Hydrocarbon Resource Distribution

The distribution of hydrocarbons in the Gulf of Mexico is not uniform in terms of location, age of reservoir, or depositional environment of reservoir. In the Federal OCS, recoverable in

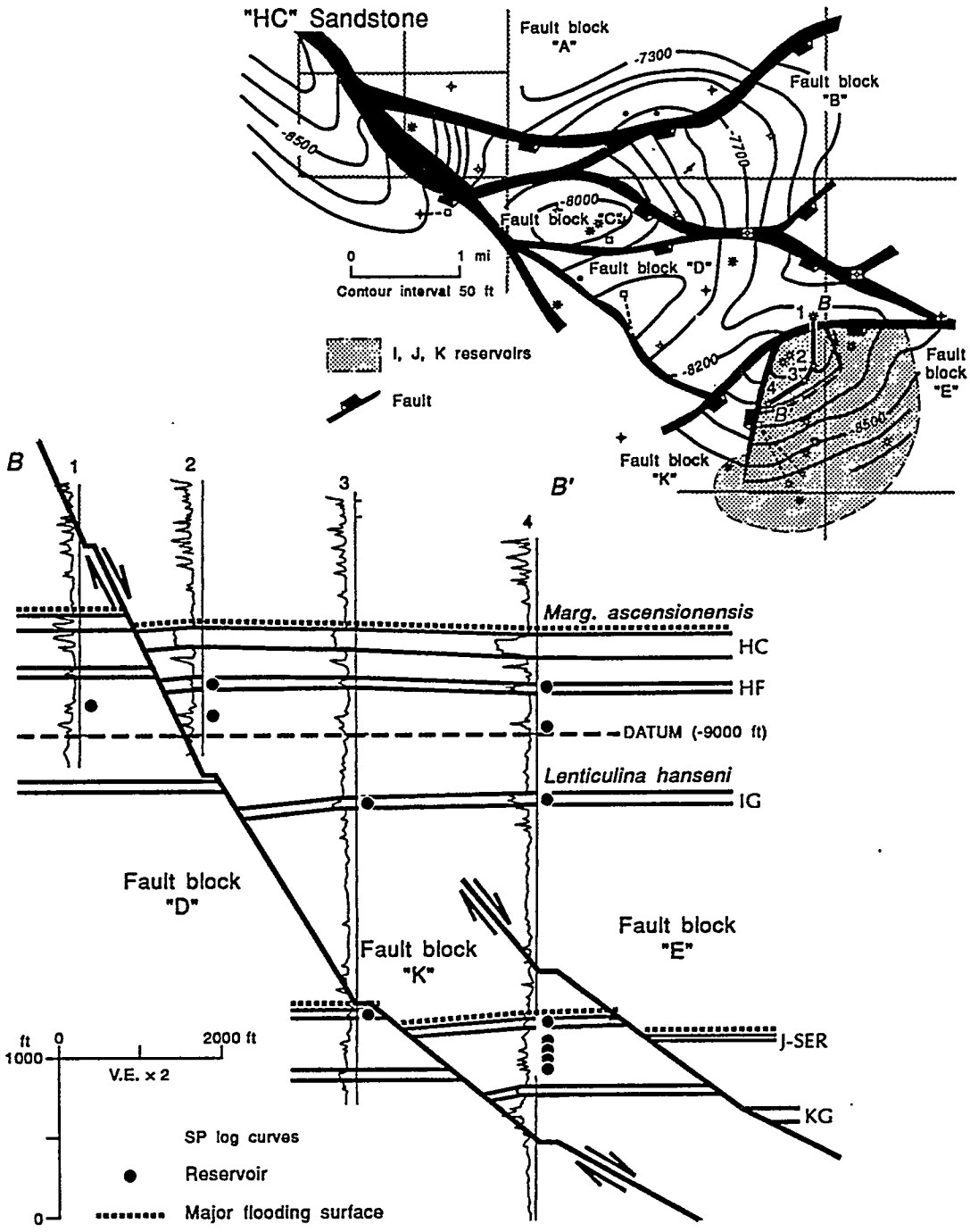

Figure 7. Structural cross section of submarine-fan *Lenticulina* play LM-1A1 at High Island Block 24-L, J-SER, and KG reservoirs in fault blocks D and K. Note that the structure-contour map indicates the location of I, J, and K reservoirs, but the structure of the HC reservoir is illustrated because of greater well control. Map location is indicated on inset map of figure 4. Structure-contour map modified from Fowler and others (1986)

place hydrocarbons are apportioned 40 percent to Pleistocene reservoirs, 20 percent to Pliocene reservoirs, 39 percent to Miocene reservoirs, and 1 percent to Mesozoic reservoirs. The relative smoothness of this distribution is masked by the relatively short age span of Pleistocene (1.7 to 2.8 Ma) and Pliocene (2.6 to 3.7 Ma) in comparison with that of the Miocene era (18.6 to 21.1). This age distribution is favorable for future discoveries because Plio-Pleistocene reservoirs have a greater amount of strata within the hydrocarbon window in lightly explored regions of the deep water Gulf of Mexico.

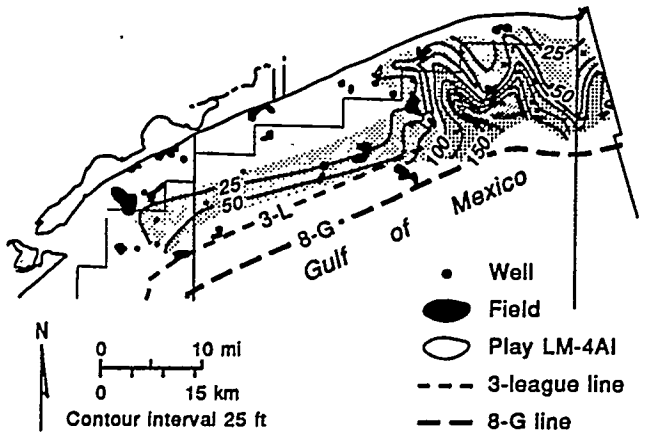

Figure 8. Map of maximum thickness of individual sand bodies in *Lenticulina* chronozone in High Island Area. Log character, ecological zonations, and sharp-based SP character indicate that thick *Lenticulina* sandstones probably represent submarine-fan and canyon sandstones. Map location is indicated on inset map of figure 4

Resource Distribution by Chronozone. The distribution and production status of hydrocarbon resources in the northern Gulf of Mexico Federal OCS reveals additional insights when disaggregated by chronozone (fig. 12). Both recoverable in place and cumulative production generally increase with decreasing age of the reservoir. The Lower Pleistocene chronozone (*Lenticulina* to *Buliminella* 1) hosts the greatest recoverable in place, cumulative production, and reserves of any chronozone. The concentration of over 7 billion boe of hydrocarbons in relatively young and thermally immature reservoirs indicates tremendous migration of hydrocarbons from older strata in deeper parts of the basin into Plio-Pleistocene reservoirs.

The distribution of gas and oil resources reveals interesting patterns of segregation with respect to reservoir age (figs. 13 and 14). Oil resources are concentrated in Plio-Pleistocene reservoirs (fig. 13). In contrast, gas resources are distributed more uniformly between Mesozoic, Miocene, and Plio-Pleistocene reservoirs. Thus, the hydrocarbon resources that exist within Miocene and Mesozoic reservoirs are predominantly gas (fig. 14). Several chronozones are almost exclusively gas producers, including the Jurassic Norphlet and LM1, LM2, LM4, and MM4 chronozones. Significant gas resources are concentrated in state waters (not tabulated in these graphs) for these chronozones. Gas and oil are more equally distributed within Plio-Pleistocene reservoirs.

Distribution by Depositional Style. The depositional style of the reservoir exerts a powerful control on the distribution of hydrocarbon resources in the northern Gulf of Mexico (fig. 15). As previously discussed in the section Play-Analysis Procedure, we emphasized progradational, aggradational, and retrogradational depositional styles and submarine-fan depositional facies because they strongly govern the distribution of reservoir-quality sands and sandstones and provide a basis for predicting reservoir location. For the entire Federal OCS, recoverable in place hydrocarbons are apportioned to three primary depositional styles: progradational (60 percent), submarine fan (19 percent), and aggradational (15 percent). Minor amounts of recoverable in place

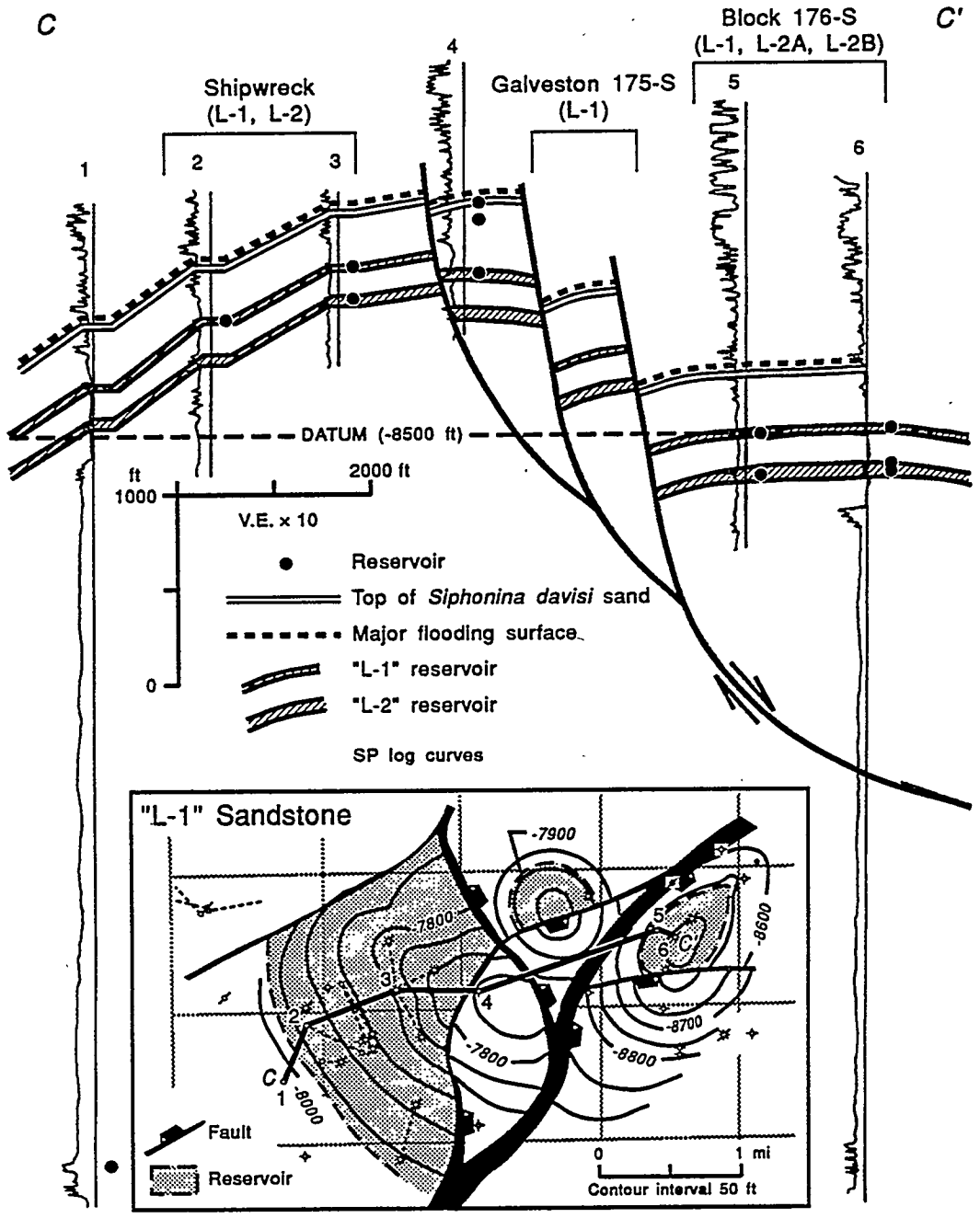

Figure 9. Structural configuration of progradational *Lenticulina* play LM-1A2 at Shipwreck L-1 and L-2 reservoirs, Galveston 175-S L-1 reservoir, and Block 176-S L-1, L-2, and L-2B reservoirs. Map location is indicated on inset map of figure 4

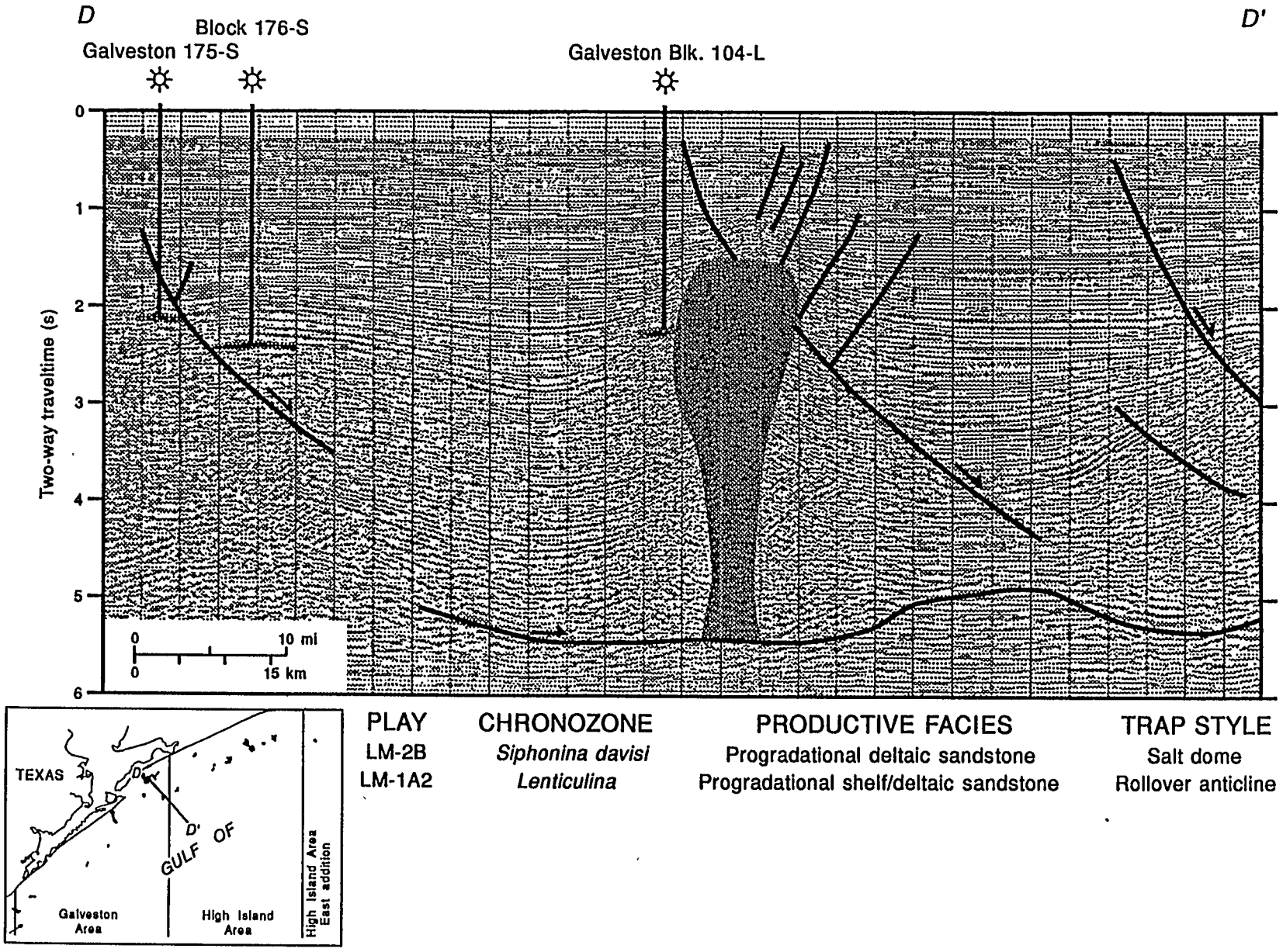

Figure 10. Seismic line illustrating structural style associated with listric growth faults trapping reservoirs in progradational *Lenticulina* play LM-1A2 and salt dome structure in progradational *Siphonina davisi* play LM-2B

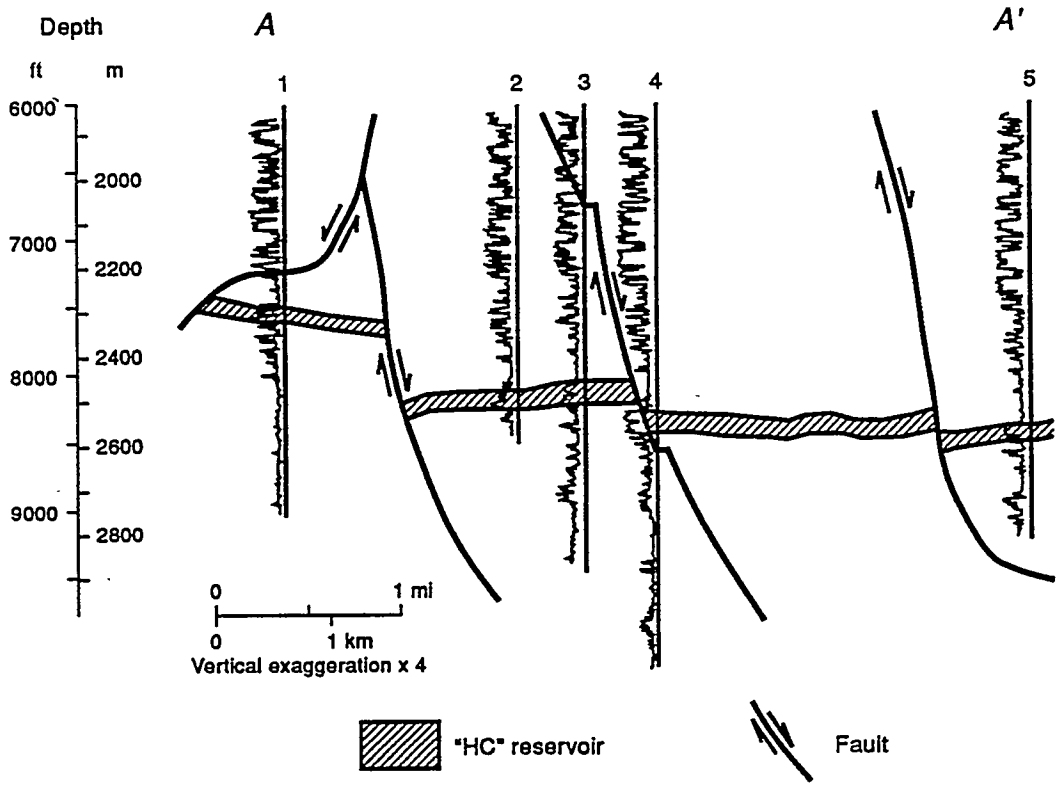

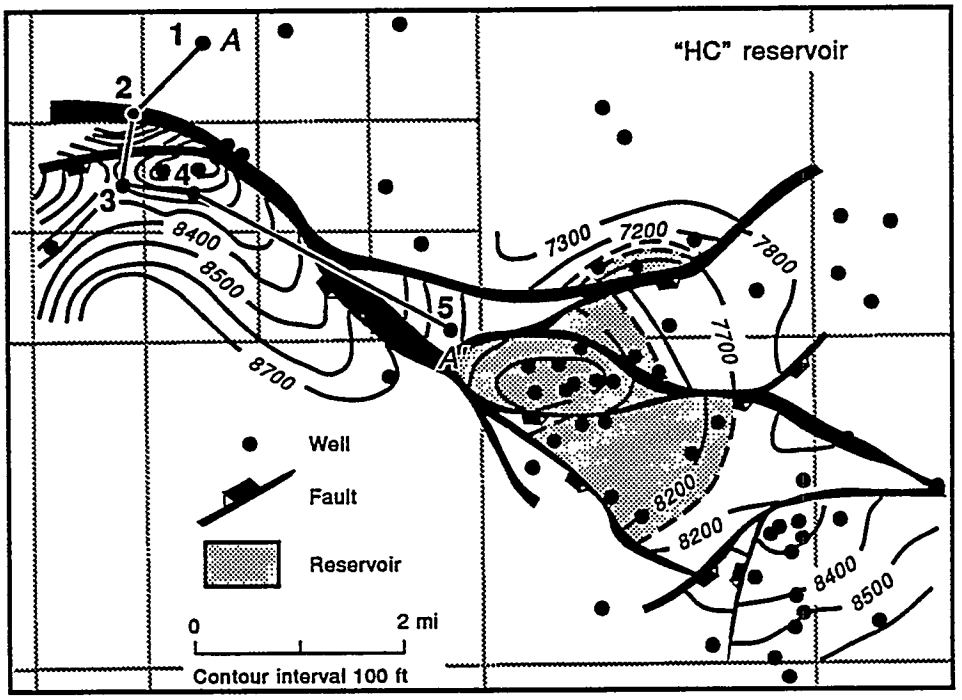

Figure 11. Structural cross section and structure-contour map of progradational *Siphonina davisi* play LM-2B at High Island Block 24-L HC reservoir. Map location is indicated on inset map of figure 3. Structure map modified from Fowler and others (1986)

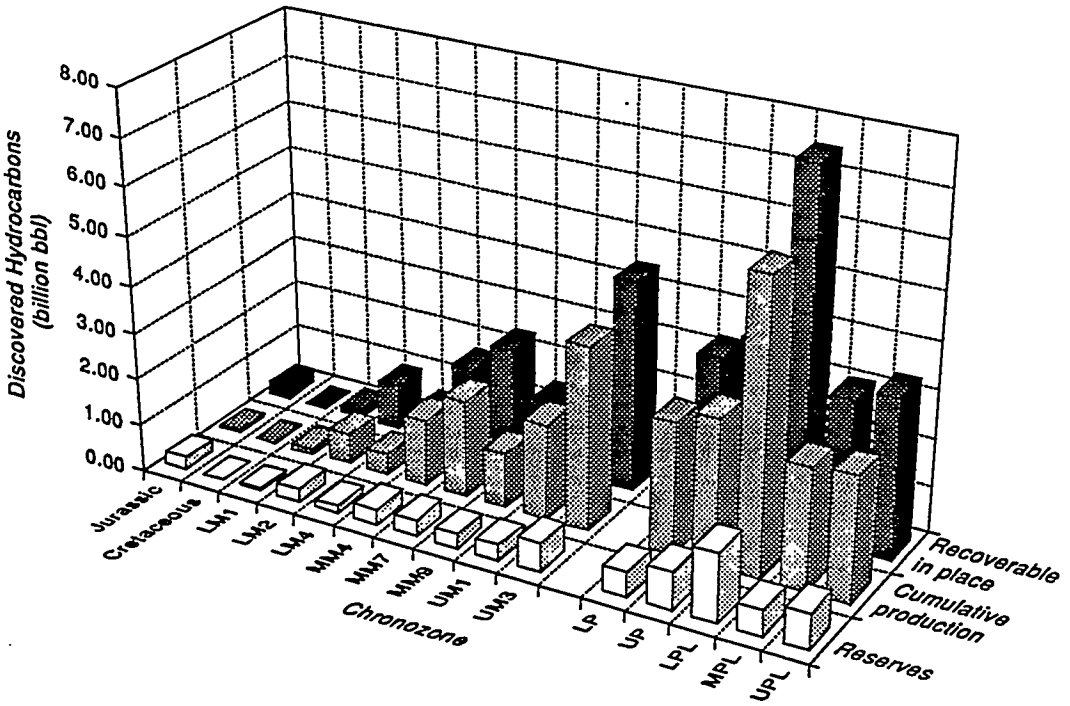

Figure 12. Histogram of recoverable in place, cumulative production, and reserves for hydrocarbons in the Federal OCS segregated by atlas chronozones

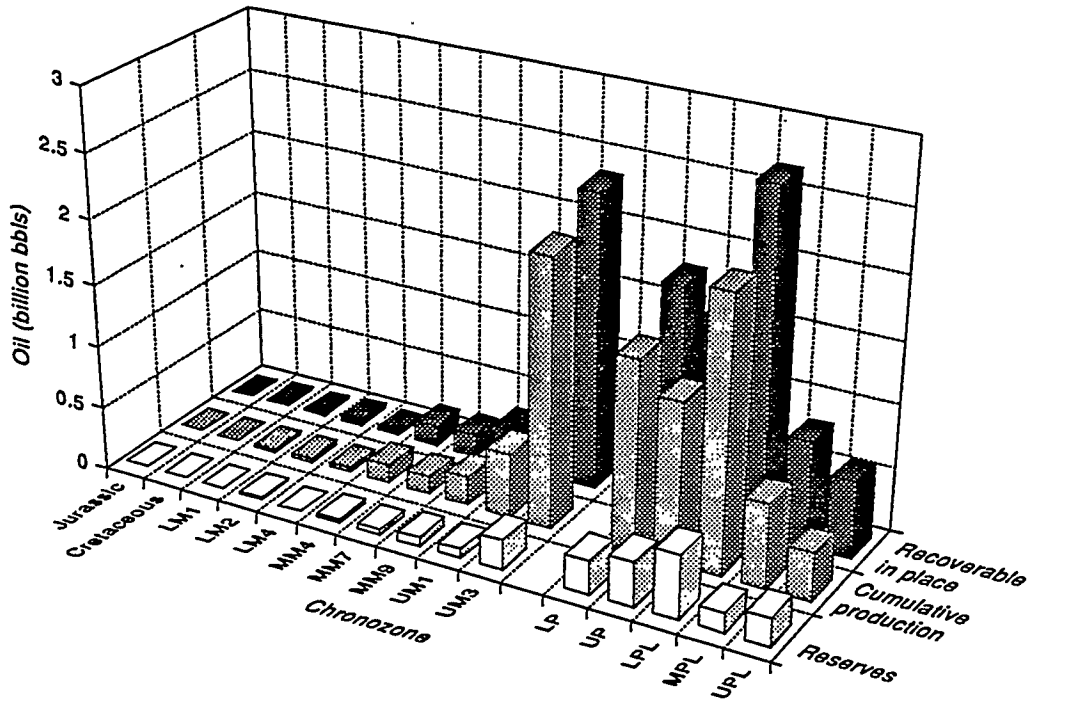

Figure 13. Histogram of recoverable in place, cumulative production, and reserves for oil in the Federal OCS segregated by atlas chronozones

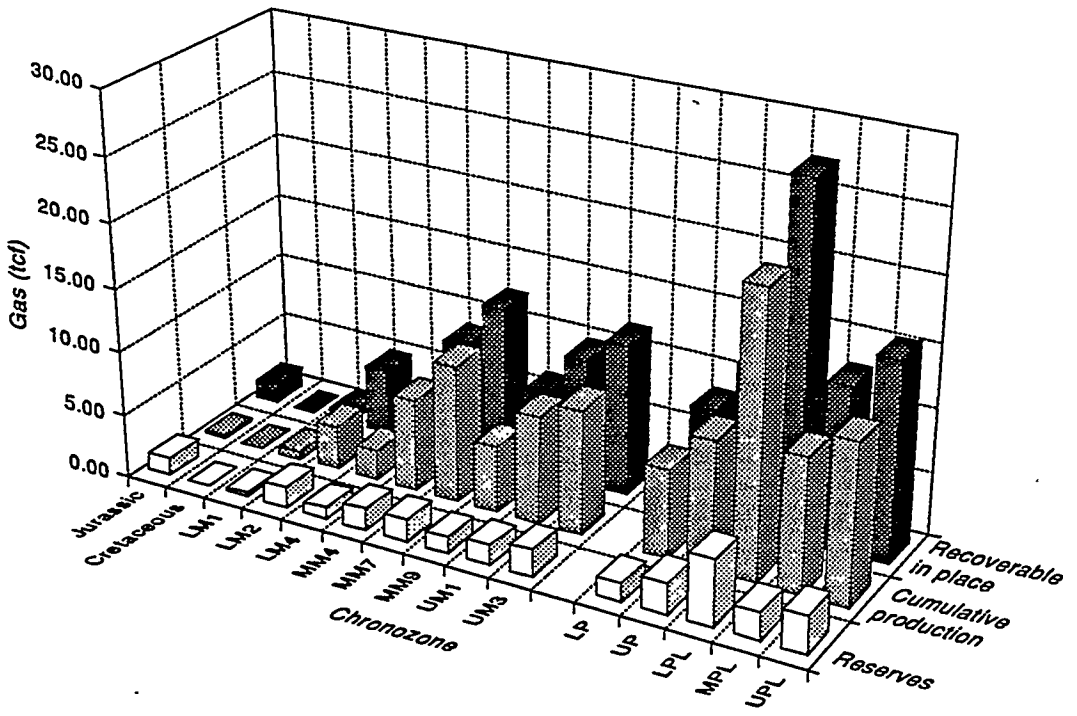

Figure 14. Histogram of recoverable in place, cumulative production, and reserves for gas in the Federal OCS segregated by atlas chronozones

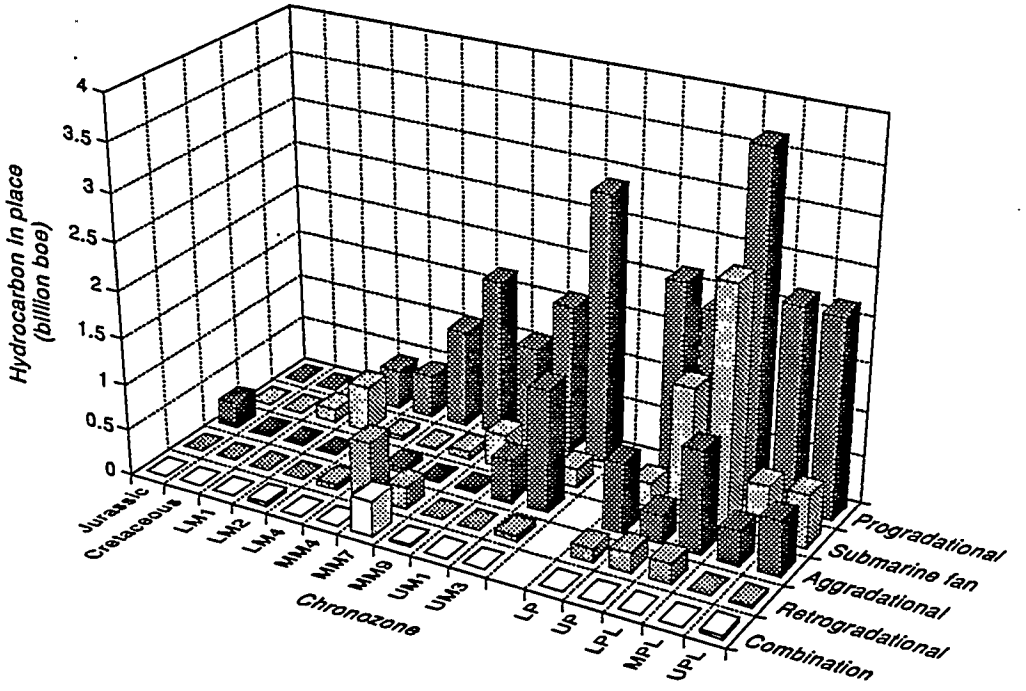

Figure 15. Histogram of producible in place hydrocarbons in the Federal OCS segregated by depositional style for atlas chronozones

hydrocarbons are apportioned to retrogradational (5 percent) and combination (1 percent) styles. The distribution of hydrocarbon reserves by depositional style reveals an interesting shift. Progradational style still contains the most reserves at 47 percent, but no longer a majority. Submarine-fan reservoirs host 32 percent of the hydrocarbon reserves, an increase of 68 percent coming almost exclusively from the progradational style. The increase in oil reserves for submarine-fan reservoirs is even more dramatic. Forty-four percent of oil reserves are hosted by submarine-fan reservoirs, versus forty-three percent for progradational reservoirs. These figures reflect the increasing importance of submarine-fan reservoirs as exploration continues the shift to deep water reservoirs. In addition, the proportionally greater concentration of oil reserves in submarine-fan reservoirs indicates that the newer fan reservoirs are oil prone.

FUTURE WORK

Future work will emphasize computer application of the tremendous volume of data from hydrocarbon reservoirs in the northern Gulf of Mexico. We envision an electronic atlas that will integrate within a single application many data sets available from the Gulf of Mexico. Such integrated data sets will include, as well as field and play data in the atlas, additional type logs, seismic data, core data, engineering and production data, and maps of net sandstone, structure, faults, and salt structures. A long-term goal is to make the data available on the Internet.

REFERENCES

Bebout, D. G., White, W. A., Garrett, C. M., and Hentz, T. F., eds., 1992, Atlas of major central and eastern Gulf Coast gas reservoirs: The University of Texas at Austin, Bureau of Economic Geology, 88 p.

Bebout, D. G., White, W. A., Hentz, T. F., and Grasmick, M. K., eds., 1993, Atlas of major Midcontinent gas reservoirs: The University of Texas at Austin, Bureau of Economic Geology, 85 p.

Caughey, C. A., 1981, Deltaic and slope deposits in the *Planulina* trend (basal Miocene), southwestern Louisiana (abs.), *in* Recognition of shallow-water versus deep-water sedimentary facies in growth-structure affected formations of the Gulf Coast Basin: Society of Economic Paleontologists and Mineralogists, Gulf Coast Section 2d Annual Research Conference, Abstracts, p. 20–21.

Fowler, J., Houston, J., Mitchell, D., and Slater, J. A., 1986, High Island Block 24-L field, Jefferson County, *in* Typical oil and gas fields of southeast Texas V, part II: Houston Geological Society, p. 291–294.

Galloway, W. E., 1989, Genetic stratigraphic sequences in basin analysis 1: architecture and genesis of flooding-surface bounded depositional units: American Association of Petroleum Geologists Bulletin, v. 73, no. 2, p. 125–142.

Galloway, W. E., Ewing, T. E., Garrett, C. M., Tyler, Noel, and Bebout, D. G., 1983, Atlas of major Texas oil reservoirs: The University of Texas at Austin, Bureau of Economic Geology, 139 p.

Hamlin, H. S., 1989, Hydrocarbon production and exploration potential of the distal Frio Formation, Texas Gulf Coast and offshore: The University of Texas at Austin, Bureau of Economic Geology Geological Circular 89-2, 47 p.

Haq, B. U., Hardenbol, L., and Vail, P. R., 1987, Chronology of fluctuating sea levels since the Triassic (250 million years ago to present): Science, v. 235, p. 1156–1167.

Kosters, E. C., Bebout, D. G., Seni, S. J., Garrett, C. M., Jr., Brown, L. F., Jr., Hamlin, H. S., Dutton, S. P., Ruppel, S. C., Finley, R. J., and Tyler, Noel, 1989, Atlas of major Texas gas

reservoirs: The University of Texas at Austin, Bureau of Economic Geology, 161 p.

Morton, R. A., 1993, Attributes and origins of ancient submarine slides and filled embayments: examples from the Gulf Coast Basin: American Association of Petroleum Geologists Bulletin, v. 77, no. 6, p. 1064–1081.

Morton, R. A., Jirik, L. A., and Galloway, W. E., 1988, Middle–upper Miocene depositional sequences of the Texas coastal plain and continental shelf: geologic framework, sedimentary facies, and hydrocarbon plays: The University of Texas at Austin, Bureau of Economic Geology Report of Investigations No. 174, 40 p.

Reed, J. C., Leyendecker, C. L., Khan, A. S., Kinler, C. J., Harrison, P. F., and Pickens, G. P., 1987, Correlation of Cenozoic sediments, Gulf of Mexico Outer Continental Shelf: U.S. Department of the Interior, Minerals Management Service, OCS Report MMS 87-0026, variously paginated.

Seni, S. J., Desselle, B. A., and Standen, Allan, 1994, Scope and construction of a gas and oil atlas series of the Gulf of Mexico: examples from Texas offshore lower Miocene plays: Gulf Coast Association of Geological Societies Transactions, v. 44, p. 681–690.

Vail, P. R., 1987, Seismic stratigraphy interpretation using sequence stratigraphy, part 1, seismic stratigraphic interpretation procedure, *in* Bally, A. W., ed., Atlas of seismic stratigraphy: American Association of Petroleum Geologists Studies in Geology 27, v. 1, p. 1–10.

Van Wagoner, J. C., Posamentier, H. W., Mitchum, R. M., Vail, P. R., Sarg, J. F., Louitit, T. S., and Hardenbol, J., 1988, An overview of the fundamentals of sequence stratigraphy and key definitions, *in* Wilgus, C. K., and others, eds., Sea-level changes: an integrated approach: Society of Economic Paleontologists and Mineralogists Special Publication 42, p. 39–45.

White, D. A., 1980, Assessing oil and gas plays in facies-cycle wedges: American Association of Petroleum Geologists Bulletin, v. 64, no. 8, p. 1158–1178.

P4

Natural Gas Supply SBIR Program

Harold D. Shoemaker
William J. Gwilliam
Morgantown Energy Technology Center

INTRODUCTION

The Small Business Innovation Research (SBIR) program was created in 1982 by Public Law 97-219 and reauthorized in 1992 until the year 2000 by Public Law 102-564. The purposes of the new law are to (1) expand and improve the SBIR program, (2) emphasize the program's goal of increasing private sector commercialization of technology developed through Federal R&D, (3) increase small business participation in Federal R&D, and (4) improve the Federal Government's dissemination of information concerning the SBIR program.

Eleven agencies, those with extramural R&D budgets of more than $100 million, were required to establish a SBIR program using a set-aside of a stated percentage of that budget. The percentage has grown from an initial 0.2 percent in Fiscal Year (FY) 1983 to 1.25 percent in FYs 1986-1992 for the civilian agencies. Public Law 102-564 increases the set-aside gradually, beginning with 1.5 percent in FYs 1993-1994 and attaining a maximum of 2.5 percent in FY 1997.

The funding for the DOE SBIR program has totaled $384 million over the first 12 years. The program's budget for FY 1995 was $70 million, based on a set-aside of 2 percent. These funds are used to support an annual competition for Phase I awards of up to $75,000 for about 6 months to explore the feasibility of innovative concepts. Phase II is the principal research or R&D effort, and the awards are up to $750,000 for a 2-year period. Phase III is the commercial application of the research and R&D effort by small businesses with non-Federal capital and may also involve follow-on, non-SBIR funded Federal contracts for products or services intended for use by the U.S. Government. To date, the DOE has funded an average of about 145 Phase I applications and about 55 Phase II applications per year. Success ratios for applications have been about 12 percent in Phase I and 45 percent in Phase II.

Each agency issues at least one annual solicitation for Phase I grant applications. DOE's solicitation contains topics in technical areas such as the following: Basic Energy Sciences, Health and Environmental Research, High Energy and Nuclear Physics, Magnetic Fusion Energy, Energy Efficiency and Renewable Energy, Nuclear Energy, Fossil Energy, Environmental Management, and Nonproliferation and National Security. Each year about 45 topics are allocated among the technical areas in proportion to their contributions to the budget. These funds are placed in a common pool, and applicants are selected competitively for awards on scientific and technical merit.

DOE's SBIR program has two features that are unique:

- It provides for uninterrupted funding between Phases I and II for those awardees that choose to submit their Phase II applications 6 weeks before the end of their Phase I grants. Funding continuity has been provided to these awardees for 12 consecutive years.

- To assist awardees in seeking follow-on funding for Phase II, DOE has sponsored a Commercialization Assistance Project (CAP) for the past 6 years. This effort has provided individual assistance in developing business plans and in preparation of presentations to potential investment sponsors. In the 1993 CAP, awardees made presentations to about 55 sponsors from venture capital firms and large corporations. Forty-three percent of the companies that participated in the 1991 CAP achieved further funding for their projects, resulting in a total of more than $14 million in private sector support toward commercialization, with an additional $24 million expected from option agreements over the next 4 years.

In the 1995 DOE SBIR solicitation, the DOE Fossil Energy topics were

- Environmental Technology for Natural Gas, Oil, and Coal.
- Advanced Recovery of Oil.
- Natural Gas Supply.
- Natural Gas Utilization.
- Advanced Coal-Based Power Systems.
- Advanced Fossil Fuels Research.

The subtopics for this solicitation's Natural Gas Supply topic are (1) Drilling, Completion, and Stimulation; (2) Low-Permeability Formations; (3) Delivery and Storage; and (4) Natural Gas Upgrading.

The 1995 DOE SBIR solicitation was mailed to prospective proposers on December 1, 1994, and the proposals were due to DOE March 1, 1995. The FY 1996 SBIR solicitation will be issued in the Fall of 1995. Questions about the DOE SBIR program, or if you want to be placed on the SBIR mailing list, may be addressed with Mrs. Kay Etzler, Program Spokesperson, c/o SBIR Program Manager, ER-16, U.S. Department of Energy, Washington, DC 20585, telephone (301) 903-5867.

A Fossil Energy natural gas topic has been a part of the DOE SBIR program since 1988. To date, there has been 65 Phase I SBIR natural gas applications that were funded (15 in 1994). Of the initial 50 Phase I applications, 30 were successful in obtaining Phase II SBIR funding (the 15 in 1994 have not competed yet). The current Phase II natural-gas research projects awarded under the SBIR program and managed by METC are presented below by award year. The presented information on these 2-year projects includes project title; awardee company, address, and telephone number; principal investigator; project abstract; anticipated results/potential commercial applications; and a project schematic (grouped together at the end of article).

1993 PHASE II PROJECTS

Process for Sweetening Sour Gas by Direct Thermolysis of Hydrogen Sulfide -- Bend Research, Inc., 64550 Research Road, Bend, Oregon 97701-8599; (503) 382-4100
Dr. David J. Edlund, Principal Investigator

About 25 percent of the natural gas produced in the U.S. contains excessive amounts of hydrogen sulfide (see Exhibit 1). Current methods for treating this sour natural gas (e.g., amine scrubbing coupled with flaring or the Claus process, and liquid redox systems) produce environmentally objectionable by-products. As increasingly stringent environmental regulations are legislated and enforced, current gas-sweetening technology will become inadequate for economically utilizing the nation's sour-gas reserves --estimated to be 135 trillion cubic feet.

Continued development of a membrane-reactor-based process to sweeten sour natural

gas without releasing sulfur compounds (such as SO_x) to the atmosphere or producing other toxic or polluting by-products appears promising. The membrane-reactor process will be energy- and cost-efficient relative to currently used processes. The membrane-reactor achieves high efficiency in the direct conversion of hydrogen sulfide in the sour-gas feed to elemental sulfur and hydrogen, by employing a platinum-coated, hydrogen-permeable metal membrane that catalyzes the decomposition of hydrogen sulfide and simultaneously separates hydrogen as it is produced.

In Phase I, it was demonstrated that the hydrogen sulfide thermolysis reaction catalyzed by the membrane surface was very rapid, and that the rate of conversion of hydrogen sulfide to hydrogen and elemental sulfur (beyond the equilibrium value) was proportional to the rate of hydrogen removal via the metal membrane. Tests at realistic operating conditions showed that the formation of coke and other byproducts on the membrane surface was insignificant.

Phase II is directed at increasing hydrogen flux by reducing the thickness of the Pt coating on the feed surface of the membrane. Using a prototype reactor that utilizes this high-flux membrane, a synthetic sour natural gas feed (at 1,000 psi) will be treated by reducing hydrogen sulfide from an initial concentration of about 0.5 percent down to ≤4 parts per million (pipeline specifications).

Anticipated Results/Potential Commercial Applications as described by the awardee: The membrane-reactor process is expected to sweeten sour natural gas without producing SO_x (a leading cause of acid rain), toxic metal and sulfide wastes, or other pollutants. Processing costs equal to or less than that of current methods for treating sour gas are projected. Projected processing costs for the membrane-reactor process are ≤$0.20/1,000 standard cubic foot for streams containing ≤0.5 percent H_2S (about 80 percent of the H_2S-bearing gas currently in production in the U.S.). In addition, the process could also find application in treating H_2S in refinery streams -- replacing the current reliance on the Claus process and associated tail-gas clean-up systems.

Remote Leak Survey Capability for Natural Gas Transport, Storage and Distribution Systems -- Deacon Research, 2440 Embarcadero Way, Palo Alto, California 94303;
(415) 493-6100
Dr. Anthony O'Keefe, Principal Investigator

The detection of natural gas and coal mine methane leakage is important for both worker safety as well as for environmental considerations (see Exhibit 2). The accepted techniques for the detection of such leaks are based upon slow air sniffing systems which detect the major constituent of natural gas (methane) by chemical means. While such techniques are sensitive, they are slow and must be employed in the immediate vicinity of the suspected leak. Remote optical detection of methane has been demonstrated, but such systems have been too complicated for field use.

Phase I developed a small and rugged remote optical sensor for the detection of dilute gaseous methane in air which utilizes a proprietary stabilization scheme. The approach is considerably less complicated than other schemes, such as distributed feedback frequency stabilization, and will be inexpensive enough to manufacture for several commercial areas. The sensitivity, ruggedness, and simplicity of this approach was demonstrated in Phase I.

Phase II will develop a prototype system design suitable for field testing for performance and regulatory certification.

Anticipated Results/Potential Commercial Applications as described by the awardee: This project will develop a commercial detector of methane gas leaks. The device will be used in

the transportation, storage, and distribution phases of gas handling to prevent explosions, to reduce the impact of greenhouse gas emissions by early detection of methane sources, and as safety instrumentation in coal mining.

Electrochemical Natural Gas Reduction to Alcohols -- Eltron Research, Inc., 2830 Wilderness Place, Boulder, Colorado 80301-5455; (303) 440-8008
Dr. Anthony F. Sammells, Principal Investigator

This project aims toward the development of advanced electrolytic technology for the purpose of promoting methane hydroxylation at practical rates, selectivities, and efficiencies leading to the synthesis of commercially significant alcohols (see Exhibit 3).

Phase I identified advanced electrocatalyst and catalyst sites which were incorporated into gas diffusion electrodes, demonstrating high activity toward promoting initial oxygen reduction, from a methane/oxygen reactant gas mixture. Subsequent proton abstraction from the methane intermediate was found to be followed by reaction to yield methanol and ethanol. Experimental conditions were identified which gave high efficiencies for this process and provided a technical foundation for optimization. Methanol synthesis rates observed during Phase I, using electrodes which were not yet optimized, were up to three orders of magnitude greater than those for conventional heterogeneous methanol synthesis.

Phase II will include (1) preparing selected electrocatalysts and catalysts; (2) performing an in-depth electrochemical study of electrocatalyst and catalyst optimization for improved selective methane hydroxylation; (3) incorporating preferred dispersed electrocatalysts and catalysts into gas diffusion electrodes, compatible for application with aqueous and polymer electrolyte-based electrolytic technology; and (4) fabrication and performance testing of electrolytic stack technology. The application of mature technology for methane hydroxylation leading to alcohol synthesis will be expected to proceed with higher selectivity, efficiency, and rate than for related heterogeneous reactions leading to the same reaction products.

. *Anticipated Results/Potential Commercial Applications* as described by the awardee: Successful completion of this program will result in the development of technology for achieving methane activation under ambient or near ambient conditions, leading to the synthesis of condensed species such as methanol. This technology would provide an option for lowering costs associated with methane conversion to methanol, and consequently, will be of value to the chemical feedstock industry. A plentiful supply of low cost methanol could then be used as a feedstock for gasoline synthesis on an industrial scale, thereby reducing dependency on foreign energy sources.

Reinterpretation of Existing Wellbore Log Data Using Neural-Based Pattern Recognition Processes -- Jason Associates Corporation, 1500 West Canal Court, Suite 400, Littleton, Colorado 80120; (303) 798-8032
Mr. Curtis L. Morgan, Principal Investigator

A significant portion of known gas reserves is contained within heterogeneous reservoirs for which well logging, using current analytical techniques, often can only provide information of a qualitative type (see Exhibit 4). This is due to the indeterminate nature of geologic signal processing, combined with the inherent limitation of utilizing mechanistic approaches to analyze the interrelationships of multiple signals in complex geologic formations.

Hydrocarbon Signature Logs (HSLs) identify producing zones with a greater degree of accuracy than can be derived using conventional wellbore analysis. This can substantially increase the hydrocarbon discovery rate for

obscure reservoirs. HSLs are created using a proprietary process termed PROWLS (Pattern Recognition for Wellbore Log Suites). PROWLS is based upon an emergent pattern recognition technology called neural computing which has been developed primarily through Department of Defense sponsored research to address the problems of identifying military targets in difficult environments.

Phase I successfully adapted this technology which can be used to identify oil-producing zones in a well, using a suite of conventional wellbore logs. Proof of concept was initially demonstrated using the Silurian Interlake formation, an Upper Interlake Subgroup of the central Williston Basin, which produced oil and gas from sequences of thinly interbedded peritidal dolomites and calcareous dolomites. On the Nesson Anticline, the Silurian interval is recognized as an area with a high potential for bypassed production because of the extreme difficulty of identifying pay zones using conventional log analysis. HSLs developed for wells in this formation identified producing intervals to a high degree, which were not achievable with conventional analysis.

Phase I demonstrated that PROWLS can reliably estimate production of tight gas sands based upon patterns contained within the log suites. Further, PROWLS accurately identified all of the dry wells within the study field. HSLs were produced that showed definitive signatures indicating downhole porosity and permeability of the producing sand. Maps were produced that identified producing trends for the study field.

Phase II will define process capabilities and limitations. Procedures for model verification and validation will be designed. The PROWLS process will be imbedded into an existing commercial well log software system. Extensive demonstration cases will be developed to show system capabilities.

Anticipated Results/Potential Commercial Applications as described by the awardee: PROWLS will be a software product that will allow oil and gas professionals, with no prior experience in neural computing, to take advantage of this state-of-the-art pattern recognition technology. Innovative applications of this technology will facilitate additional gas production from depleted or nearly depleted fields, enhance development of new production, and create new reserves through discovery of bypassed pay or oil and gas.

An Advanced Liquid Membrane System for Natural Gas Purification -- LSR Technologies, Inc., 898 Main Street, Acton, Massachusetts 01720; (508) 635-0123
Dr. Zhen Wu Lin, Principal Investigator

The cost associated with contaminant removal from natural gas is considerable. Impurities such as hydrogen sulfide, carbon dioxide, nitrogen, moisture, and natural gas liquids must be removed in order for the gas to be suitable for pipeline transport (see Exhibit 5). Hydrogen sulfide removal and recovery in particular can involve costly processing steps, due to the low selectivity of this contaminant by chemical solvents which also have an affinity for carbon dioxide.

This project will develop a novel Moving Liquid Membrane System (MLMS) for the selective removal of hydrogen sulfide. The MLMS combines absorption and regeneration in the same processing unit. Its design utilizes a large surface area for high mass transfer in a compact control volume. Also, the liquid circulation rate is much lower than that of conventional absorption systems. Phase I has shown that the MLMS has the ability to produce very high hydrogen sulfide permeability and hydrogen sulfide/carbon dioxide selectivity. The bench-scale membrane apparatus has also proven to be completely stable with no evidence of membrane dryout or degradation. The concept

needs further refinement of its design through additional laboratory and pilot-scale testing.

Phase II will focus on further testing for hydrogen sulfide removal using simulated feed gases. It is also important that new gas processing technology be brought to the field to validate its operability with real gas. Therefore, a larger pilot-scale unit will be constructed to evaluate the long-term operability of the system with industrial gas. A key aspect of the research will be to bring the technology to the demonstration stage.

Anticipated Results/Potential Commercial Applications as described by the awardee: The MLMS is well-suited to treating gases with significant H_2S concentrations (up to the percent range), especially when the CO_2 to H_2S concentration ratio is high. Projection from the gas industry indicate that new reserves will likely be smaller, of lower quality, and at remote locations. The simplicity and performance of the MLMS will make it an attractive choice in these applications.

1994 PHASE II PROJECTS

Application of Exploration and Advanced Well Completion Technology to High Productivity Coalbed Methane Fairways --
Advanced Resources International, Inc., 165 South Union Boulevard, Suite 816, Lakewood, Colorado 80228; (303) 986-2121
Mr. A. David Decker, Principal Investigator

The growth of coalbed methane has been dramatic and highly valuable to the gas and oil industry (see Exhibit 6). Looking across all of coalbed methane production, one quickly grasps a startling observation -- the majority of U.S. coalbed methane production, 1.2 billion cubic feet per day out of 2 billion cubic feet per day, is provided by less than 10 percent of the producing wells, the highly prolific open-hole cavity wells located in the San Juan basin cavity fairway. Finding and efficiently developing other coalbed methane cavity fairways are the top priority for a healthy, growing coalbed methane industry.

During Phase I, the controlling parameters for highly productive cavity completions and the set of geologic processes responsible for these favorable reservoir properties were documented. An exploration rationale and a set of geological/geophysical tools were set forth to "rediscover" the San Juan basin "cavity fairway." Using this exploration strategy in conjunction with exploration tools, the San Juan basin was specifically high-graded with a final partition that accurately defined the fairway location and outlined an area within which 80 percent of the wells produce at a rate of 1 million cubic feet per day or greater. Using the same exploration strategy, a preliminary geologic evaluation suggests that cavity-type fairways are likely to exist in other North American coal basins.

In Phase II, the two basins most suitable for cavity well completions will be screened. The Phase I exploration strategy will be used to identify the cavity fairways in these basins and to locate specific drilling sites. The wells will be tested and then cavitated to determine the economic feasibility of cavitation in these new basins.

Anticipated Results/Potential Commercial Applications as described by the awardee: This project should demonstrate that coalbed methane production economics can be substantially improved by the utilization of the cavity completions in coal basins where this technique has not been attempted. Widespread utilization of the technology should be a natural outgrowth when the economic benefit has been demonstrated in Phase II.

Liquid Absorbent Process for Removing Nitrogen from Natural Gas -- Bend Research, Inc., 64550 Research Road, Bend, Oregon 97701-8599; (503) 382-4100
Dr. David K. Lyon, Principal Investigator

Domestic natural gas provides an increasingly important portion of the U.S. energy supply (see Exhibit 7). Estimated U.S. gas reserves are about 1,000 trillion standard cubic feet (scf), or about 1,000 quads. About 25 percent of the estimated reserves are contaminated with nitrogen to the extent that the gas cannot be used without nitrogen removal. No technology exists today for the cost-effective removal of nitrogen from natural gas at the wellhead while keeping gas losses during treatment below a 3 percent limit imposed by environmental and economic constraints.

Over the past 3 years, a process has been developed for purifying nitrogen-contaminated natural gas at the wellhead. In this process, the nitrogen is separated from the rest of the natural gas using a regenerable absorbent based on aqueous solutions of transition-metal complexes. The final nitrogen absorbent ideally will have the following characteristics: (1) rapid absorption of nitrogen at the pressure and temperature of the natural gas feed stream (high pressure and ambient temperature), (2) rapid desorption of nitrogen under mild conditions (ambient pressure and moderate temperature), (3) extremely high selectivity for nitrogen over methane, and (4) appropriate kinetics and lifetime properties.

During Phase I, the understanding of the relationship between the molecular structure of the nitrogen-binding compounds and their properties was advanced, and the performance of candidate nitrogen absorbents was substantially increased. Specifically, the feasibility of identifying new absorbents with solubilities and nitrogen-binding capabilities that met Phase I targets was demonstrated. A computer model was developed that predicted process economics at the current level of performance of $0.55/1,000 scf, based on reasonable absorbent cost and lifetime assumptions. This level of performance would enable economical treatment of a small percentage of the nitrogen-contaminated U.S. gas reserves, and this progress sets the stage for continued collaborative funding from a commercialization partner and for an accelerated Phase II project.

The goal of this project is to prepare new nitrogen absorbents (based on Phase I results) that exhibit superior nitrogen-binding properties, and (when their production is scaled up) can lead to process costs approaching the target of $0.25/1,000 scf. This level of performance would allow for economical treatment of virtually all known nitrogen-contaminated U.S. gas reserves.

Anticipated Results/Potential Commercial Applications as described by the awardee: An economical process for purifying nitrogen-contaminated natural gas should render up to 250 trillion scf (250 quads) of low-grade natural gas saleable. This gas, at today's prices, is valued at $7-8 billion each year over a 50-year period. In addition, this project should serve as the groundwork for development of other liquid-absorbent-based separation processes, such as separation of olefins from paraffins, and fractionation of olefin isomers.

A Pressure Swing Adsorption Process for Nitrogen Rejection from Natural Gas -- Northwest Fuel Development, Inc., 4064 Orchard Drive, Lake Oswego, Oregon 97035; (503) 699-9836
Dr. Peet M. Soot, Principal Investigator

The technical and economic feasibility of the pressure swing adsorption (PSA) process was demonstrated in Phase I (see Exhibit 8). The laboratory work demonstrated that activated carbons affect the desired separation between methane and nitrogen. Some commercially available activated carbons were shown to have

a selectivity of methane to nitrogen of three or more. A kinetics test demonstrated that these materials adsorb methane very rapidly, a major unexpected positive result. Because the PSA process can be cycled so quickly, the activated carbon adsorbents are much better than the more expensive carbon molecular sieve materials used by other developers.

Based on laboratory test results and on mathematical modeling, a conceptual PSA process was developed and a preliminary demonstration plant was designed. The plant is expected to produce pipeline quality methane gas (exceeding 97 percent methane) from a feed stream containing only 83 percent methane. The plant recovers 57 percent of the feed methane. Some of the unrecovered methane is used as fuel for the necessary compressors, and the balance is reinjected into the producing formation at some distance from the producing well.

The demonstration plant, planned for Phase II, could process 300 Mcfd (thousands of cubic feet per day) of raw natural gas. This should yield 149 Mcfd of product gas at a cost of $1.40/Mcf. Even this small plant should produce an economically competitive product since present day natural gas prices at the well-head are generally in excess of $2.00/Mcf. A larger plant, capable of producing 1 MMcfd of pipeline quality gas, should have a processing cost of only $0.70-1.00/Mcf.

The Phase II process demonstration unit should provide the foundation for rapid commercial deployment of this technology in Phase III.

Anticipated Results/Potential Commercial Applications as described by the awardee: The Nation has nearly 250 trillion cubic feet of sub-quality natural gas. Successful development of this process should provide economic, national security, and environmental benefits. Cost estimates show that this process could provide gas at lower prices than current levels. It uses a domestic resource -- not an imported one. Environmental benefits arise from the capture of a greenhouse gas: methane.

HSHOEM\2:950971

Exhibit 1

Process for Sweetening Sour Gas by Direct Thermolysis of Hydrogen Sulfide

Company: Bend Research, Inc., Bend, OR

About 25% of the natural gas produced in the U.S. contains excessive amounts (≥ 4 ppm) of H_2S

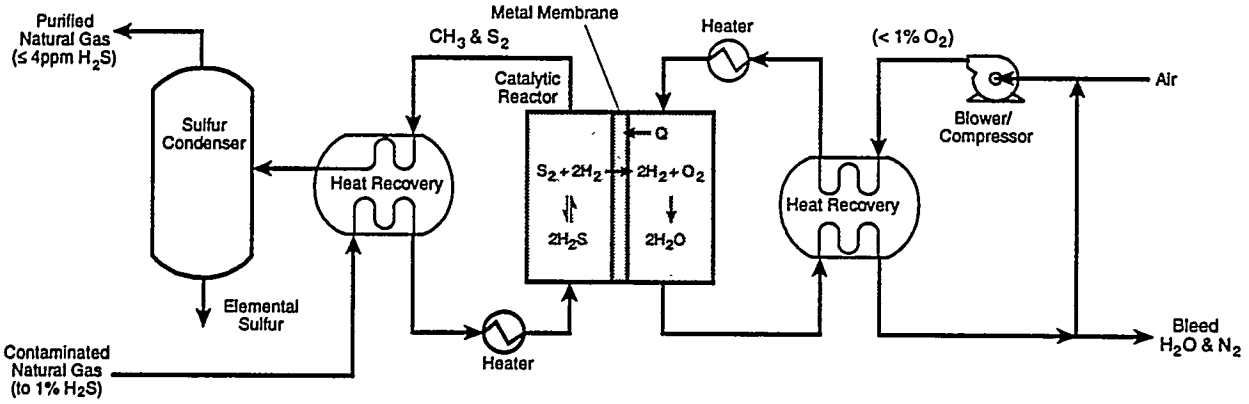

Economics

- The estimated processing cost for reducing H_2S from 0.5% to pipeline specifications is < $0.20/1000 standard cubic feet (scf) for a 30 million scf/day natural gas stream

Benefits:

- No atmospheric release of sulfur containing compounds of SO_x
- Environmentally benign byproducts: sulfur and water
- Minimal energy requirements due to catalytic combustion of H_2 on the permeate side of the membrane

M94000072

Exhibit 2

Remote Leak Survey Capability for Natural Gas Transport, Storage and Distribution Systems

Company: Deacon Research, Palo Alto, CA

Objective:

- Demonstrate the viability of remotely determining methane concentration in air with a diode laser based sensor. This device addresses mining and natural gas market needs for making measurements under new safety regulations at greater distances than can be done with present technology

Characteristics:

- The device is hand-held
- The device will produce a reading of the methane concentration
- The device will also indicate the distance to the reflecting target wall to provide for normalization

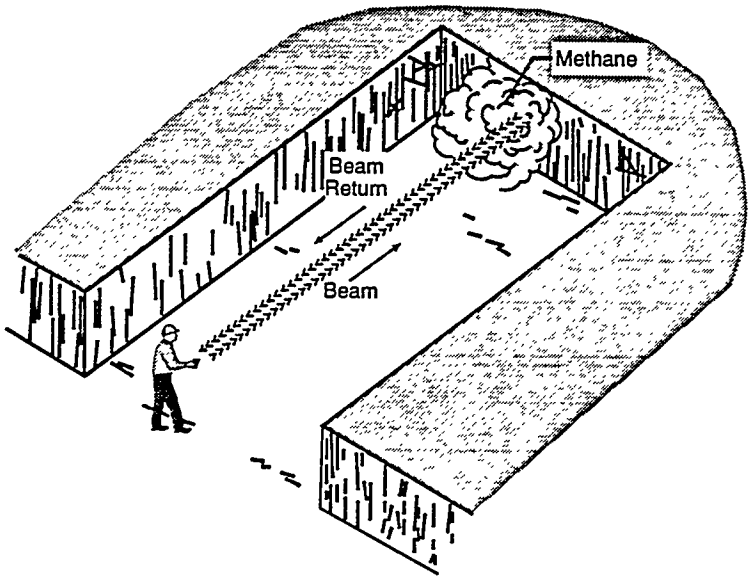

This approach provides readings in units of: Concentration x Distance

M94000075

M95002317W

Exhibit 3

Electrochemical Natural Gas Reduction to Alcohols

Company: Eltron Research, Inc., Boulder, CO

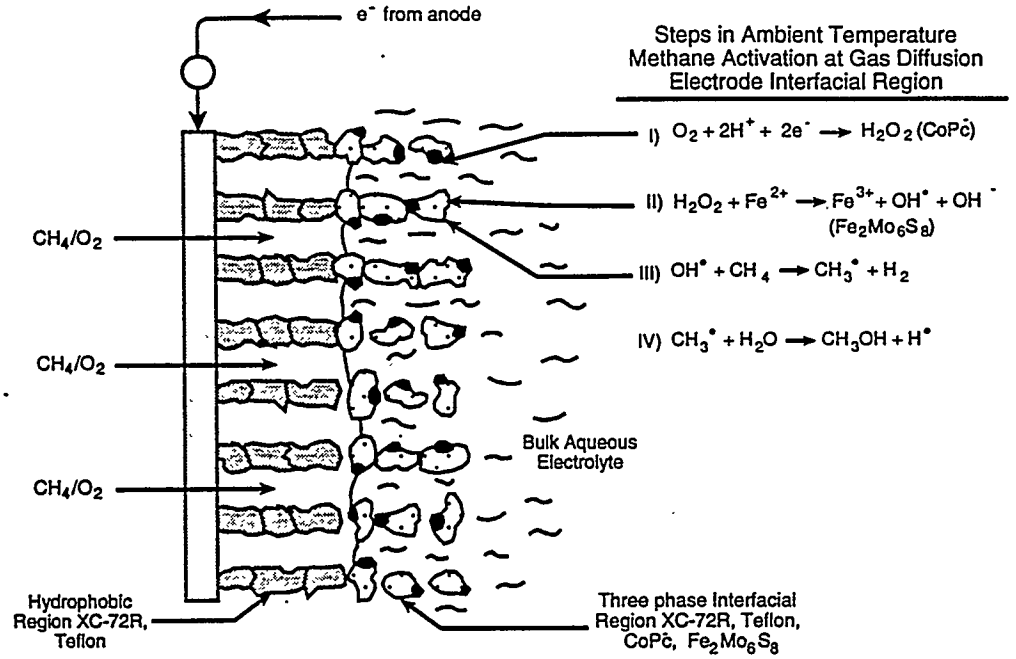

Findings:

- Ambient temperature electrochemical conditions found for the Faradaic conversion of methane to methanol at > 10 $^{-3}$moles/cm ^{2}/hr

M94000070

Exhibit 4

Reinterpretation of Existing Wellbore Log Data Using Neural-Based Pattern Recognition Processes

Company: Jason Associates Corporation, Littleton, CO

Objective:

- Develop broadly applicable pattern recognition techniques that substantially enhance the qualitative and quantitative information that can be derived from suites of conventional wellbore logs

Benefits:

- PROWLS will allow oil and gas professionals, with no prior experience in neural computing, to take advantage of state of the art pattern recognition
- Application of this tool may enhance production from existing fields and aid in recovery of reserves for new fields

PROWLS

Pattern Recognition for Wellbore Log Suites

PROWLS is a neural network based process that identifies patterns, contained within wellbore log suites and geologic data, that are indicative of the presence of hydrocarbons

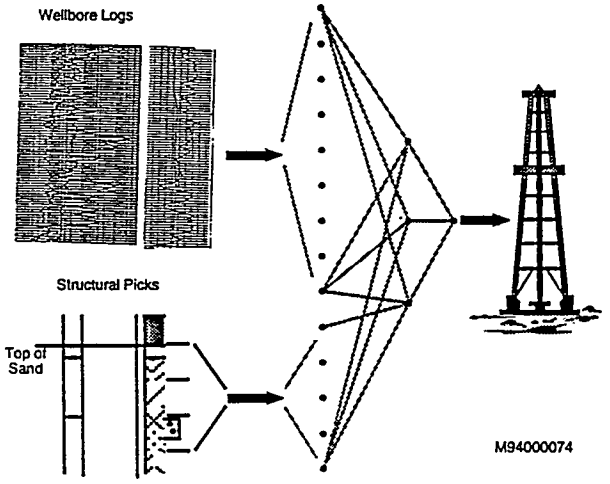

M94000074

Exhibit 5

An Advanced Liquid Membrane System for Natural Gas Purification

Company: LSR Technologies, Inc., Acton, MA

Objective:

- Develop a moving liquid membrane system that combines absorption and regeneration into a single unit which can also be selective towards H_2S over CO_2

Benefits:

- The moving liquid membrane system can achieve high H_2S over CO_2 selectivity and high mass transfer
- The moving liquid membrane system demonstrates advances in energy efficiency
- The moving liquid membrane system is compact and stable

Moving Liquid Membrane System Configuration

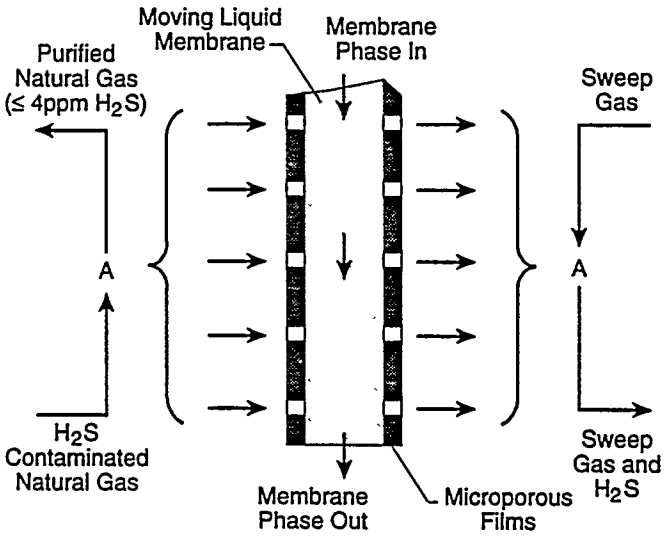

M95001189W

Exhibit 6

Application of Exploration and advanced Well Completion Technology to High Productivity Coalbed Methane Fairways

Company: Advanced Resources International, Inc., Denver, CO

Technical Objectives:

Identify portions of coal basins suitable for cavity completions

Develop model that will predict cavity performance

Phase I Results:

Developed exploration strategy for identifying coal reservoirs capable of high-gas rate cavity completions

Phase II Activities:

Apply exploration strategies within Appalachian and Western coal basins

Development of well bore stability numerical simulator

Target well locations to demonstrate exploration and engineering cavitation technologies

Economic Benefits:

Establish low-cost natural gas supply from underdeveloped coalbed methane resources

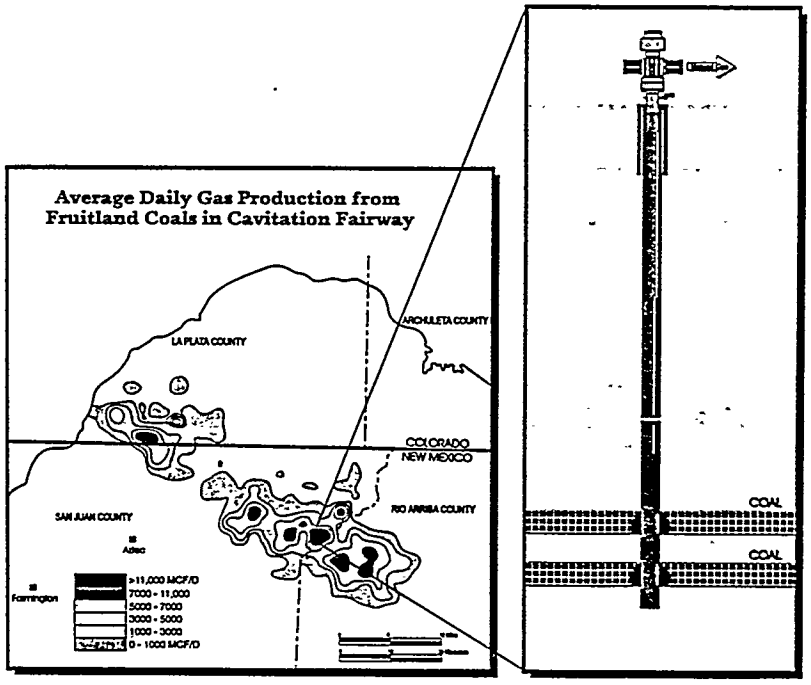

M95001930C

M95002319W

Exhibit 7

Liquid Absorbent Process for Removing Nitrogen from Natural Gas

Company: Bend Research, Inc., Bend, OR

About 16% of the natural gas reserves in the U.S. contain excessive amounts (≥4%) nitrogen

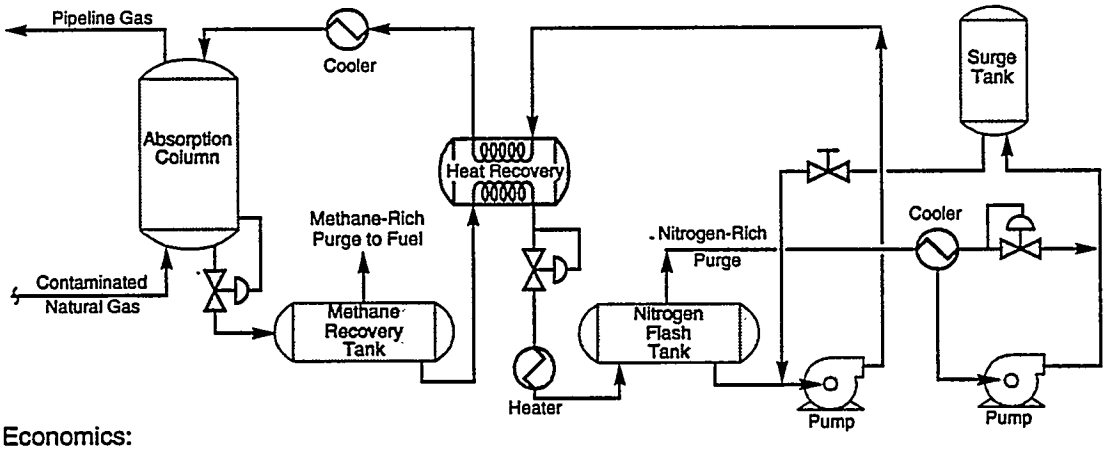

Economics:

- The estimated processing costs using Bend's current generation of liquid absorbents is $0.35 - $0.45/Mscf for reducing 15% nitrogen contaminated methane to 4% nitrogen pipeline gas at flow rate of 5 MMscf/d with projected methane losses of less than 3%
- The estimated processing costs using optimized absorbents is $0.25/Mscf

M95001183W

Exhibit 8

A Pressure Swing Adsorption Process for Nitrogen Rejection from Natural Gas

Company: Northwest Fuel Development, Inc., Lake Oswego, OR

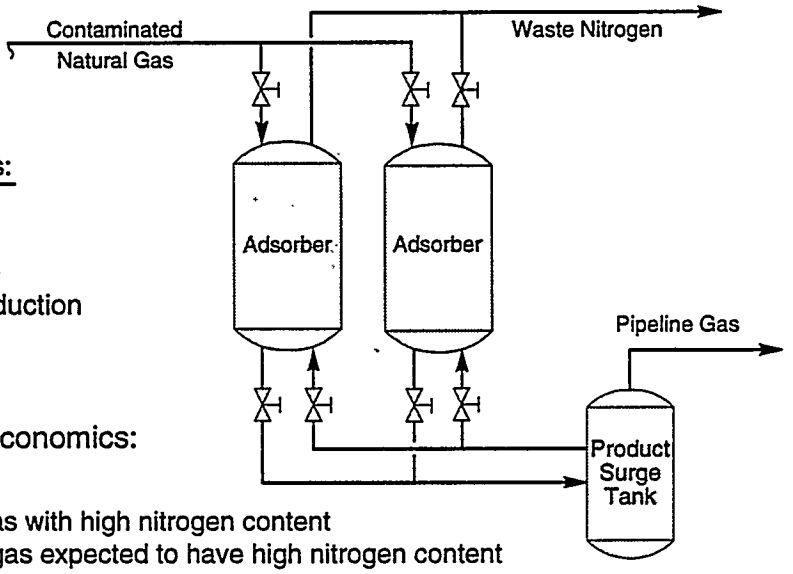

Process Cycle Steps:

A - Pressurization
B - Adsorption
C - Methane Rinse
D - Blowdown/Production

Technology Applications and Economics:

Subquality Natural Gas

- U.S. Reserves: 23 Tcf of gas with high nitrogen content
- U.S. Reserves: 250 Tcf of gas expected to have high nitrogen content

Coal Mine Methane

- Gob Wells: 0.1 Bcf per day of methane lost to the atmosphere

Economics

- 1 MMcfd Plant: $0.70/Mcf of natural gas products

M95001184W

M95002320W

P5

Methodology for Optimizing the Development and Operation of Gas Storage Fields

James C. Mercer
James R. Ammer
Thomas H. Mroz
Morgantown Energy Technology Center

SUMMARY

The Morgantown Energy Technology Center is pursuing the development of a methodology that uses geologic modeling and reservoir simulation for optimizing the development and operation of gas storage fields. Several Cooperative Research and Development Agreements (CRADAs) will serve as the vehicle to implement this product. CRADAs have been signed with National Fuel Gas and Equitrans, Inc. A geologic model is currently being developed for the Equitrans' CRADA. Results from the CRADA with National Fuel Gas are discussed here.

The first phase of the CRADA, based on original well data, was completed last year and reported at the 1993 Natural Gas RD&D Contractors Review Meeting. Phase 2 analysis was completed based on additional core and geophysical well log data obtained during a deepening/relogging program conducted by the storage operator. Good matches, within 10 percent, of wellhead pressure were obtained using a numerical simulator to history match 2 1/2 injection withdrawal cycles.

Projections of storage deliverability and field performance were made based on the rate schedule and new vertical well locations designed by the storage operator. Results from these projections were compared to results where the new vertical wells were replaced by horizontal wells. These projections showed that the field performance can be significantly enhanced by replacing the 14 planned new vertical wells with 4 horizontal wells.

Future work on both CRADAs includes surface facility modeling to optimize gathering line size, compression, etc., and to show the importance of including surface facility effects during the reservoir simulation. Economic analyses will also be conducted to show the profitability of the various field/facility designs. The CRADA results will show the importance of geologic modeling and reservoir simulation to design storage operations and the cost savings and field improvement that can be obtained from field development using horizontal wells.

OBJECTIVES

- Develop a geologic/reservoir modeling methodology for optimizing the development and operation of gas storage fields.
  - Use CRADAs as the vehicle.
  - Develop one CRADA for each important geologic storage environment (sandstones, aquifers, reefs, fractured systems, etc.).
  - Primary interest in using horizontal wells in gas storage fields.
  - CRADAs require that partners provide horizontal well data for at least two storage cycles in order to validate predictions.
- Transfer technology of CRADA results.

- Distribute methodology to simulation industry for commercialization.

EXPECTED OUTPUT FROM THE METHODOLOGY

- Reservoir description.
  - Type and quantity of data needed.
  - Best processing techniques.
  - Sensitivity of predicted outcomes to measured values of reservoir fluid and rock properties.
- Storage system optimization.
  - Maximize field deliverability.
  - Minimize base gas requirements.
  - Minimize development and operation costs.
- Confidence levels for model predictions.
- Cost benefit of using geologic modeling and reservoir simulation.
- Economic analysis.

STATUS OF RESEARCH

- Work nearing completion of National Fuel Gas CRADA.
  - History matching completed.
  - Simulation forecasts of vertical and horizontal wells completed.
  - Awaiting field development.
- Equitrans, Inc., CRADA underway.
  - Geologic model developed.
- Integrated reservoir/surface facility modeling being conducted by Scientific Software-Intercomp.

FUTURE WORK

- Put CRADAs in place for each major storage geologic environment.
- Redo existing history matches and predictions with updated data set.
- Determine best geostatistical techniques for describing important distributions such as permeability, porosity, saturation, pressure, etc.
- Improve the modeling capability of existing simulators.
- Validate predictions with data from horizontal wells.
- Investigate the importance of modeling surface facilities.
- Develop techniques for optimizing field development.
- Technology transfer and commercialization.

Location Map

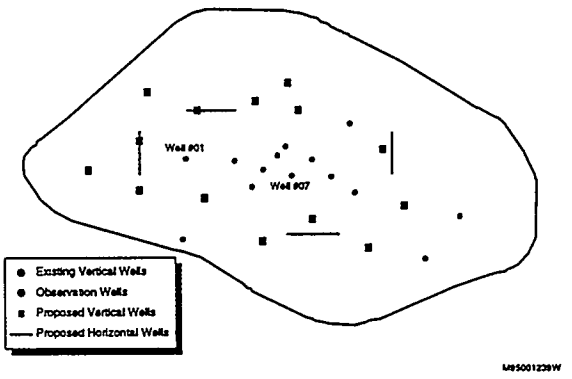

Percentage of Injection/Withdrawal

Case	Existing 11 Vertical Wells	14 New Vertical Wells	4 Horizontal Wells
Existing 11 Vertical Wells	100.0	---	---
Existing 11 Vertical Wells Plus 14 Vertical Wells	55.5	45.5	---
Existing 11 Vertical Wells Plus 4-2,000 ft Horizontal Wells	36.0	---	64.0

M95001247W

Comparison of Base Gas Requirements and Working Gas Turnaround for Various Forecasts

Case	Base Gas (Bcf)	Working Gas (Bcf)	Percentage of Base Gas to Total Gas
Existing 11 Vertical Wells	9.6	3.1	75.6
Existing 11 Vertical Wells Plus 14 Vertical Wells	8.6	5.3	61.9
Existing 11 Vertical Wells Plus 4-2,000 ft Horizontal Wells	7.3	7.0	51.0

M95001248W

History Match of Wellhead Pressure - Well 01

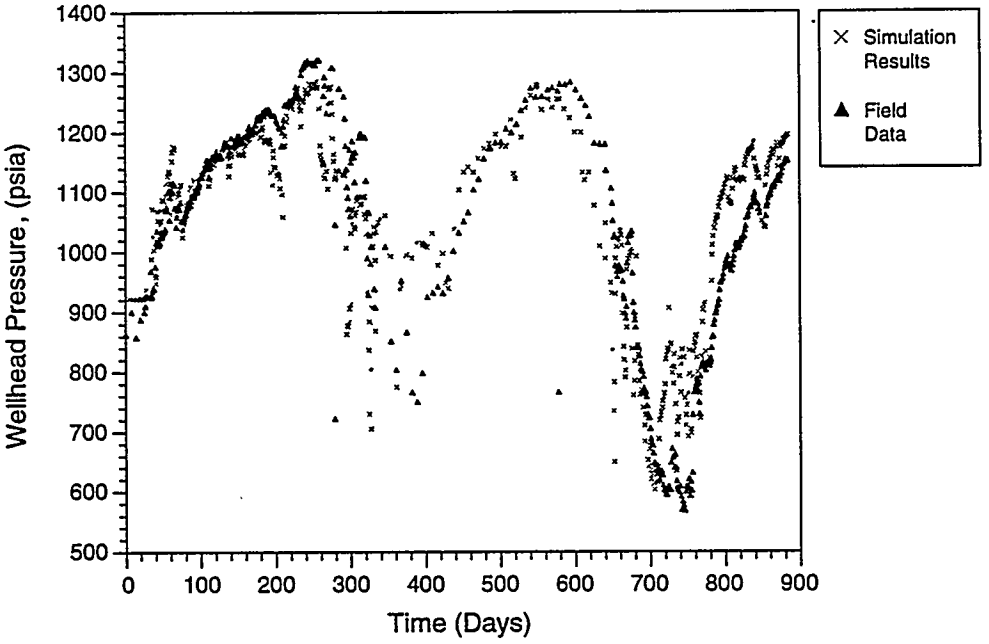

M94000437

History Match of Wellhead Pressure - Well 07

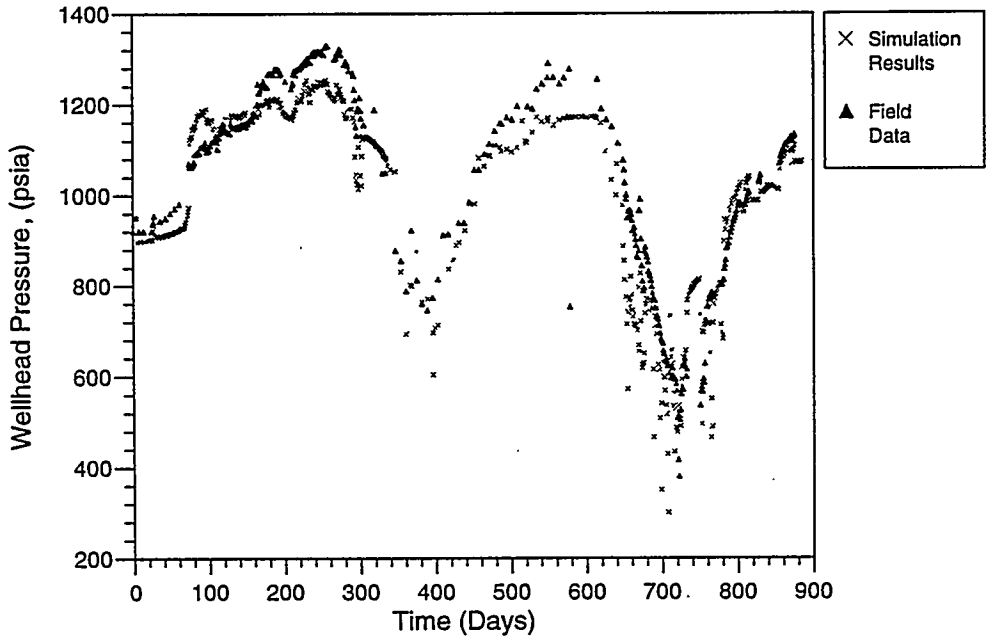

M94000438

JAMMER\951256

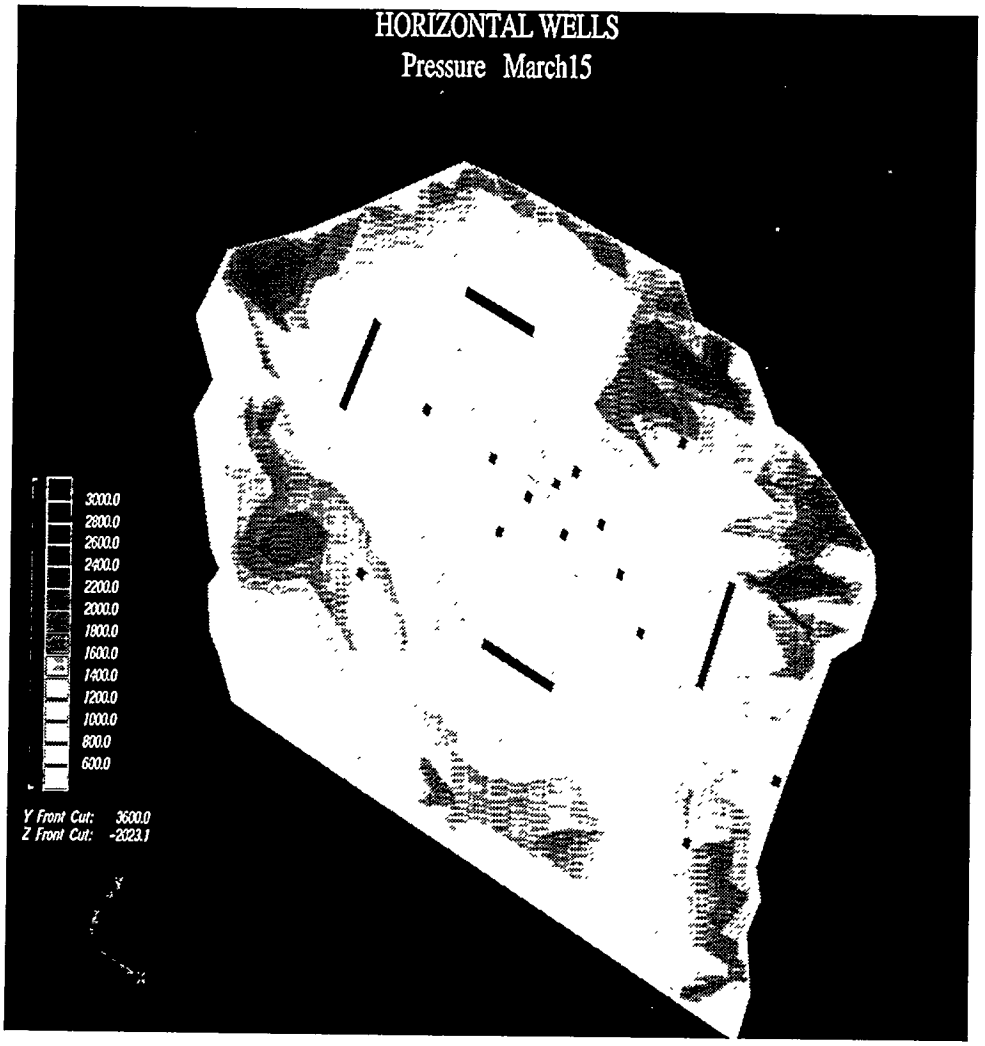
HORIZONTAL WELLS
Pressure March15
3000.0
2800.0
2600.0
2400.0
2200.0
2000.0
1800.0
1600.0
1400.0
1200.0
1000.0
800.0
600.0
Y Front Cut: 3600.0
Z Front Cut: -2023.1

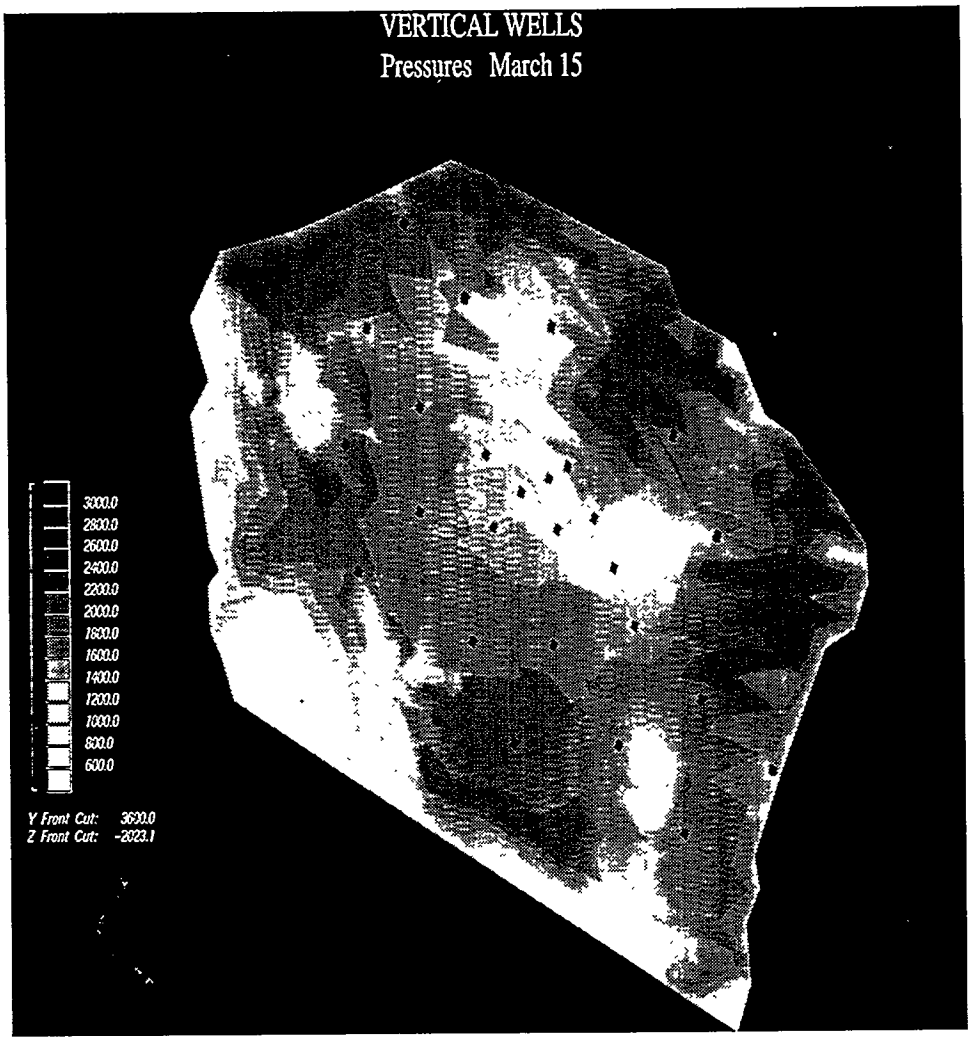
VERTICAL WELLS
Pressures March 15
3000.0
2800.0
2600.0
2400.0
2200.0
2000.0
1800.0
1600.0
1400.0
1200.0
1000.0
800.0
600.0
Y Front Cut: 3600.0
Z Front Cut: -2023.1

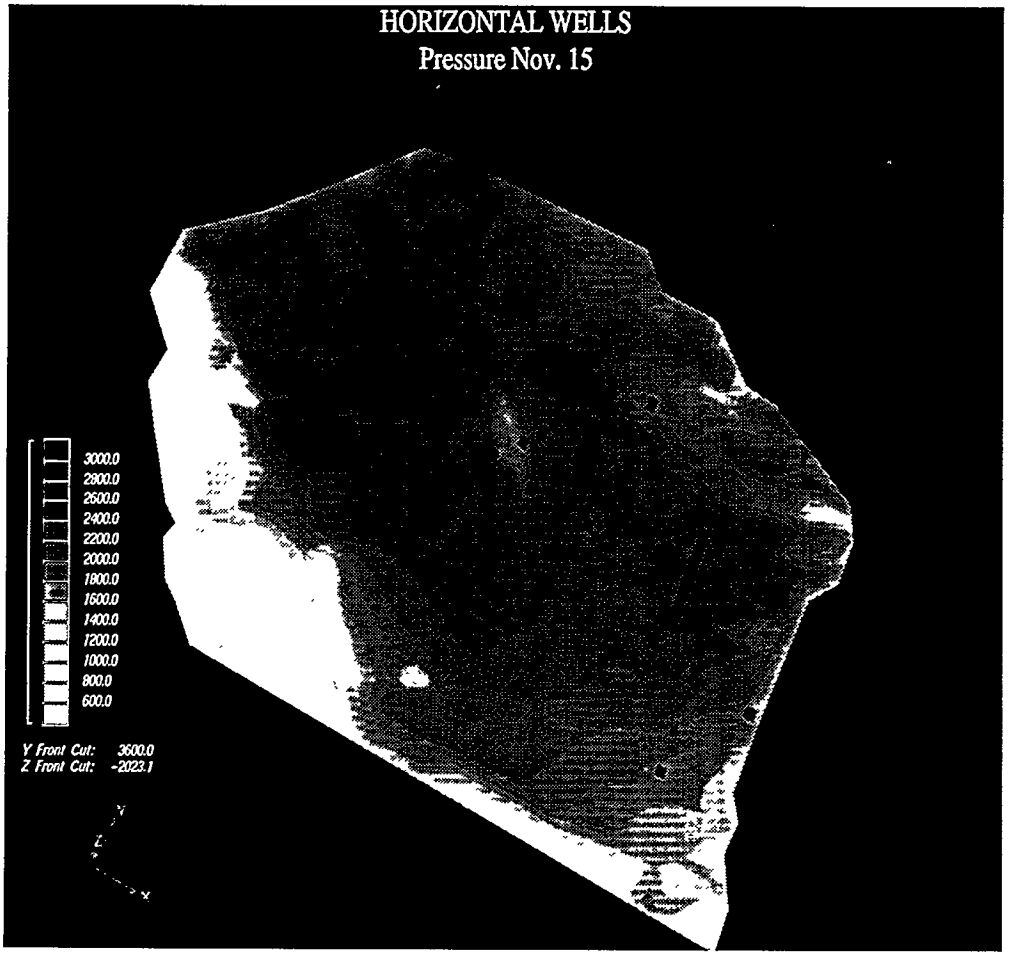
HORIZONTAL WELLS
Pressure Nov. 15
3000.0
2800.0
2600.0
2400.0
2200.0
2000.0
1800.0
1600.0
1400.0
1200.0
1000.0
800.0
600.0
Y Front Cut: 3600.0
Z Front Cut: -2023.1

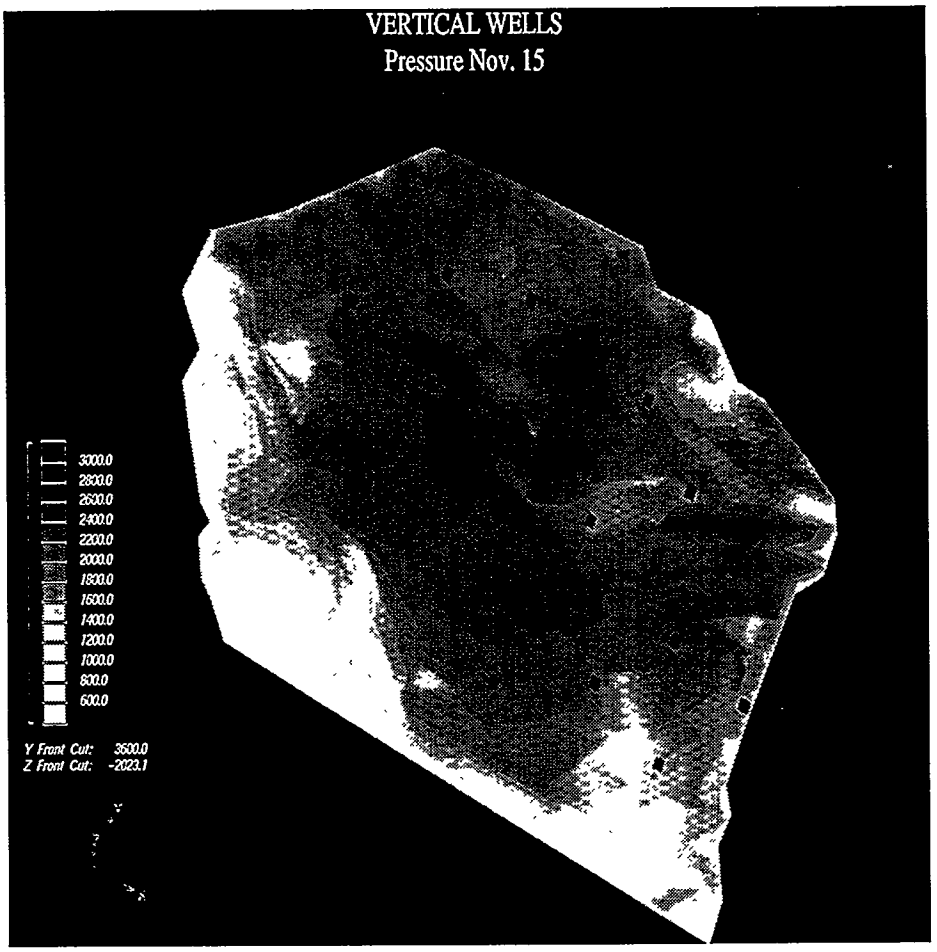
VERTICAL WELLS
Pressure Nov. 15
3000.0
2800.0
2600.0
2400.0
2200.0
2000.0
1800.0
1600.0
1400.0
1200.0
1000.0
800.0
600.0
Y Front Cut: 3600.0
Z Front Cut: -2023.1

P6 The Synthesis and Characterization of New Iron Coordination Complexes Utilizing an Asymmetric Coordinating Chelate Ligand

CONTRACT INFORMATION

Contract Number	FEW0003
Contractor	Lawrence Livermore National Laboratory 7000 East Avenue, L-365 Livermore, CA 94550 (510) 422-5717
Contractor Project Manager	David Baldwin
Principal Investigators	Bruce E. Watkins Joe H. Satcher
METC Project Manager	Rodney D. Malone
Period of Performance	Open

OBJECTIVES

We are investigating the structure/activity relationships of the bacterial enzyme methane monooxygenase, which catalyzes the specific oxidation of methane to methanol. We then utilize this information to design and synthesize inorganic coordination complexes that mimic the function of the native enzyme but are more robust and have higher catalytic site density. We envision these catalysts to be useful in process catalytic reactors in the conversion of methane in natural gas to liquid methanol.

BACKGROUND INFORMATION

The catalytic oxidation of light hydrocarbons, especially methane derived from natural gas, is an important research area attracting considerable attention. The potential for methane processing will depend on the development of catalyzed routes directly converting methane to higher valued products (heavier

hydrocarbons, olefins, and alcohols). However, methane is chemically quite inert and has not proved easy to convert to liquid hydrocarbons. Modeling studies suggest that a theoretical ceiling in overall yield exists as the rate constant of a catalyst is increased[1]. The rate constant of the catalyst must be sufficient to overwhelm the non-specific gas phase reactions but low enough to prevent over oxidation. In theory this limits the yield to about 35%. As a result, no technologies are currently available to process methane economically.

It is well-known that a select group of aerobic soil/water bacteria called methanotrophs can efficiently and selectively utilize methane as the sole source of their energy and carbon for cellular growth.[2] The first reaction in this metabolic pathway is catalyzed by the enzyme methane monooxygenase (MMO) forming methanol. Methanol is a technologically important product from this partial oxidation of methane since it can be easily converted to liquid hydrocarbon transportation fuels, used directly as a liquid fuel itself, or serve as a feedstock for fine chemicals production.

Microorganisms can produce MMO in two distinct forms: a membrane-bound particulate form or a discrete soluble form. The soluble form contains an oxygenase subunit, whose active site includes a binuclear iron center.[3,4,5] The X-ray crystal structure of the oxidized form has recently been determined,[6] and reveals a carboxylato and hydroxo bridging system between the two iron atoms. There is also a semi-bridging carboxylate which leads to coordination number asymmetry for the two metals (Figure 1). The remaining ligands are derived from adjacent amino acid residues and the Fe-Fe distance is 3.4 Å. Recent Mössbauer and EPR studies on the reduced form of soluble MMO[7] have demonstrated that coordination number asymmetry occurs about the two metal centers similar to that found in the related binuclear iron oxygen transport enzyme, hemerythrin. X-ray crystallography has clearly shown a 5,6 coordination sphere about the iron atoms in hemerythrin and reaction studies reveal that oxygen binding occurs at the five coordinate iron.[8]

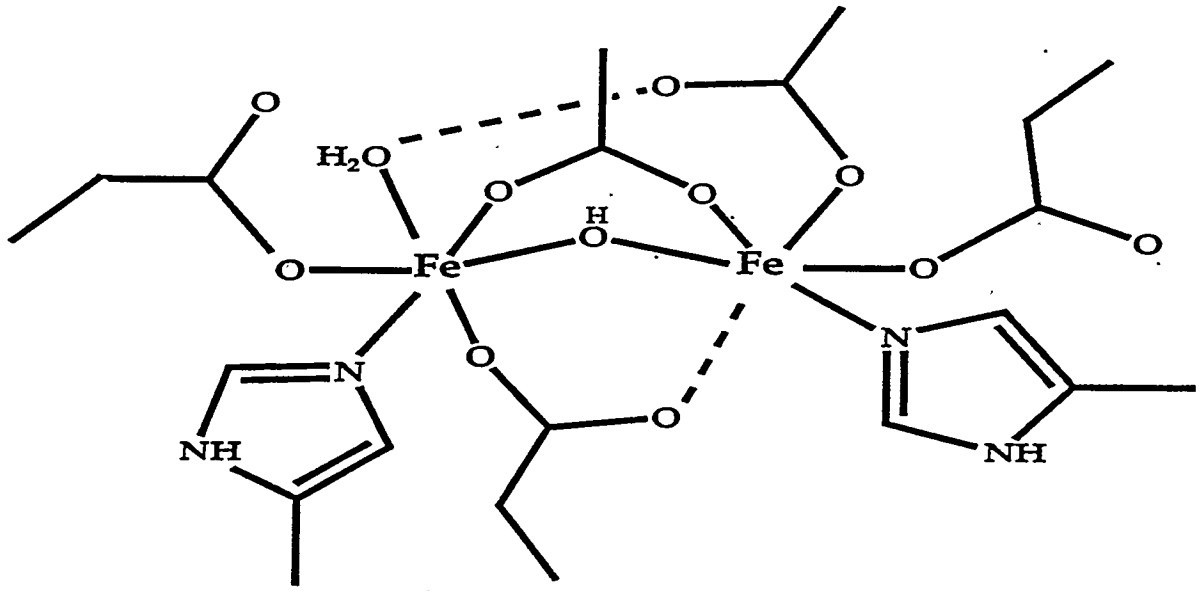

Figure 1. Schematic representation of MMO active site.

It is speculated that the active site of particulate form of the enzyme is similar to the soluble form, except that the coordinated metal is copper. We have previously reported on the synthesis of asymmetrically coordinated copper complexes and their ability to catalyze the oxidation of cyclohexane to a mixture of cyclohexanol and cyclohexanone[9,10].

PROJECT DESCRIPTION

Our work centers on the synthesis and characterization of inorganic/organic chemical models of the active site of MMO. We have focused on the synthesis of an asymmetrical, binuclear chelating ligand possessing an alkoxo group that can serve as a bridging ligand. The advantage of such a ligand system is twofold: (a) metal complexes of an asymmetric binucleating ligand will provide coordinative unsaturation at only one metal resulting in focused substrate reactivity at that site and (b) a single ligand with binuclear coordination provides a more robust environment for metal oxidation state changes and accompanying chemical reactivity.

We report here the synthesis of new prototype asymmetric iron complexes, and characterization of oxidized chelate compounds. This work provides the first proof-of-concept for the formation of binuclear iron complexes with different coordination

at each metal ion. Such complexes are relevant to the development of model systems for the active site of MMO.

RESULTS

Synthesis of the chelating ligand HMeL obtained by a five step procedure has been described previously.[10] When HMeL was allowed to react with iron(II)tetrafluroborate and sodium benzoate in methanol under anaerobic conditions, yellow crystals of $[Fe_2(OBz)(MeL)][BF_4]_2$ (1) were deposited in 65% yield. In the crystal structure (Figure 2) one iron is five coordinate (distorted trigonal bipyramidal) utilizing three nitrogen donor atoms and an alkoxy oxygen atom from the chelate and an oxygen atom from a bridging benzoate group. The other iron atom is six coordinate (distorted octahedral) with nitrogen and oxygen donation from chelate and benzoate moieties and an additional donation from two methanol solvent molecules making a 5,6 coordinate pair. The ease of solvent removal (confirmed by elemental analysis) indicates that the molecule may be more appropriately considered 5,4 coordinate system. Attempts to demonstrate chemical reactivity at the coordinatively unsaturated iron center have led to crystalline adducts with thiocyanate and phosphate. These materials have been characterized by X-ray crystallography, and verify that exogenous ligand attachment occurs at the lower coordinated iron center.

The study of the reaction of binuclear iron(II) complexes with molecular oxygen is essential in the development of model compounds. The oxidation of complex (1) with molecular oxygen in acetonitrile was found to conform to a 1:1 stoichiometry. When an acetonitrile solution of (1) is exposed to air and subsequently layered with ether a crystalline material $[Fe_4(O)(MeL)(OH)_5][BF_4]_3$ (2) is formed (Figure 3). The structure reveals a tetrameric iron(III) unit supported by an alkoxo oxygen (intra-molecular) as well as oxo and hydroxo (inter-molecular) bridges, the bridging benzoate moiety has been eliminated. In addition there is a terminal hydroxy anion bound to two of the iron centers making all iron atoms six coordinate. It has not been determined at this point if the oxygen bridges are formed from molecular oxygen, however, in the oxidation of other binuclear iron(II) complexes the oxo bridges have been shown to be derived from molecular oxygen.[11] The lack of a benzoate bridge in this structure led to the investigation of the oxidation behavior in the presence of excess sodium benzoate. When an acetonitrile solution of (1) and five equivalents of sodium benzoate is exposed to air, single crystals of $[Fe_2(OBz)_3(MeL)][BF_4]$ (3) were formed in 55% yield (Figure 4). In this case the binuclear system remains intact supported by an endogenous alkoxo and two exogenous bidentate benzoate bridges. There is also a monodentate benzoate bound to one iron atom again making a 6,6

coordinate pair of metals. The crystal structure difference map shows only one tetrafluoroborate anion in the unit cell leading to Fe(II)/Fe(III) oxidation state assignment for charge balance. In both of the above oxidation structures the central core of the ligand remains intact and the metal:ligand ratio remains constant.

The importance of the formation of the oxidized binuclear complex (3) can be understood by considering the balanced reactions with and without excess benzoate. For the reaction of complex (1) without additional benzoate in acetonitrile we have:

$$2[Fe_2(OBz)(MeL)][BF_4]_2 + O_2 + 4H_2O \Rightarrow [Fe_4(O)(MeL)(OH)_5][BF_4]_3 + 2HOBz + HBF_4$$

In contrast, a balanced reaction in the presence of excess benzoate to yield complex (3) can be represented by:

$$2[Fe_2(OBz)(MeL)][BF_4]_2 + O_2 + 4NaOBz \Rightarrow 2[Fe_2(MeL)(OBz)_3][BF_4] + Na_2O_2 + 2NaBF_4$$

In the first reaction, the atoms of molecular oxygen (as well as some from adventitious water) are incorporated into the tetranuclear complex (2). In the second reaction the reduced oxygen species does not become part of the oxidized molecule, being represented as Na_2O_2 for the purpose of chemical balance. Thus, by inhibiting the formation of higher nuclearity complexes, the reduced oxygen species is available to participate in other reaction chemistry. The identity of the reduced species and fate of molecular oxygen is currently under investigation.

CONCLUSIONS

A binuclear, unsymmetric coordinating ligand that is an effective metal chelator has been designed and synthesized. The new ligand has been shown to react readily with iron(II)/(III) forming a variety of coordination complexes. The binuclear complexes are of significant interest since they represents proof-of-principle for the development of coordinatively asymmetric, binuclear metal chelate compounds. Although this structural type of chelator now appears to be common in biological systems, it has not been previously described for inorganic coordination chemistry. The isolation of oxidation products will be helpful in establishing reaction mechanism(s) of these complexes with molecular oxygen. It is expected that this ligand and derivatives of it will play an important role in the development of bioinorganic complexes that aim to mimic enzyme active sites that function by substrate interaction at only one metal site of a multimetal active site.

Work performed under the auspices of the US Department of Energy by the Lawrence Livermore National Laboratory under contract No. W-7405-ENG-48

REFERENCES

1. Hair, L.M., Pitz, W.J.; Droege, M.W.; and Westbrook, C.K. Preprint, ACS National Meeting, April 6-10, 1992, San Francisco, CA
2. Dalton, H. *Adv. Appl. Microbiol.* 1980, *26*, 71-87.
3. (a) Woodland, M.P.; Dalton, H. *J. Biol. Chem.* 1984, *259*, 53-59. (b) Green, J.; Dalton, H. *J. Biol. Chem.* 1985, *260*, 15795-15801. (c) Fox, B.G.; Froland, W.A.; Dege, J.E.; Lipscomb, J.D. *J. Biol. Chem.* 1989, *264*, 10023-10033.
4. (a) Woodland, M.P.; Patil, D.S.; Cammack, R.; Dalton, H. *Biochim. Biophys. Acta* 1986, *873*, 237-242. (b) Fox, B.G.; Surerus, K.K.; Munck, E.; Lipscomb, J.D. *J. Biol. Chem.* 1988, *263*, 10553-10556.
5. Prince, R.C.; George, G.N.; Savas, J.C.; Cramer, S.P.; Patel, R.N. *Biochim. Biophys. Acta* 1988, *952*, 220-229.
(6) Rosenzweig, A. C.; Frederick, C. A.; Lippard, S. J.; Nordlund, P. Nature 1993, 366, 537.

(7) Fox, B. G.; Hendrich, M. P.; Surerus, K. K.; Andersson, K. K.; Lipscomb. J. D. J. Am. Chem. Soc. 1993, 115, 3688.

8. (a) Stenkamp, R.E.; Sieker, L.C.; Jensen, L.H. *Proc Natl Acad Sci. U.S.A* 1976, *73*, 349. (b) Stenkamp, R.E.; Sieker, L.C.; Jensen, L.H. *J. Mol. Bio.* 1978, *126* , 457.
9. B.E.Watkins, M.W. Droege, R.T. Taylor, and J.H. Satcher Biommimetic methane oxidation, Preprint, IGRC meeting, Orlando, FL, November 16-19, 1992.
10. (a) Satcher, Jr., J. H.; Weakley, T. J. R.; Taylor, R. T.; Droege, M. W. Inorg. Chem. submitted, (b) Droege, M.W.; Satcher, J.H.; Reibold, R.A.; Weaklely, T.J.R. Preprint, ACS National Meeting, April 6-10, 1992, San Francisco, CA.
11. See for example: Tolman, W. B.; Liu, S.; Bentsen, J. G.; Lippard, S. J. *J Am Chem Soc* 1991, *113*, 152-164.

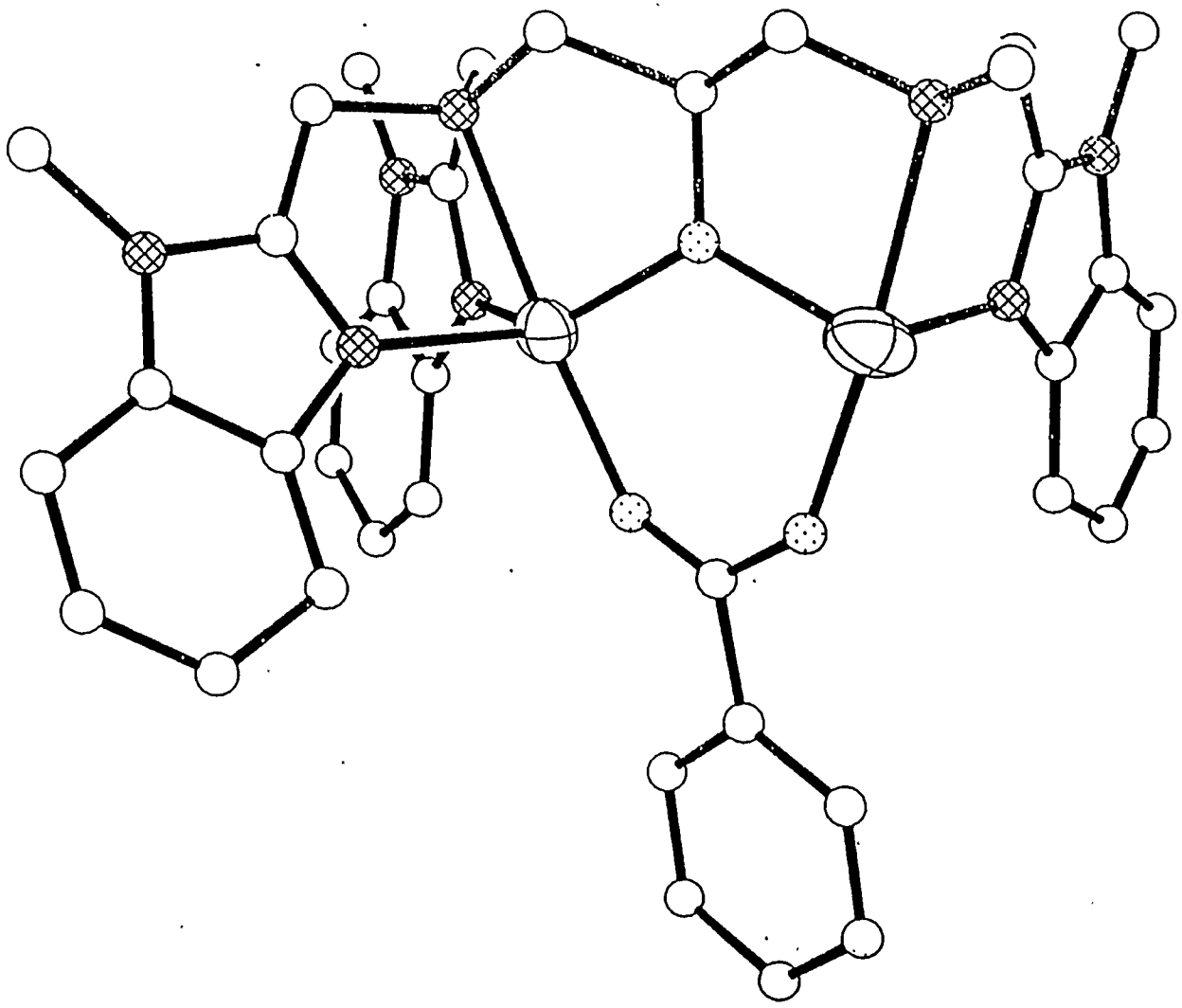

Figure 2. **Cation of $[Fe_2(OBz)(MeL)][BF_4]_2$ (1). Bound solvent and hydrogen atoms omitted for clarity. Thermal ellipsoids-Iron; Open circles-Carbon; Dotted circles-Oxygen; Cross-hatched circles-Nitrogen.**

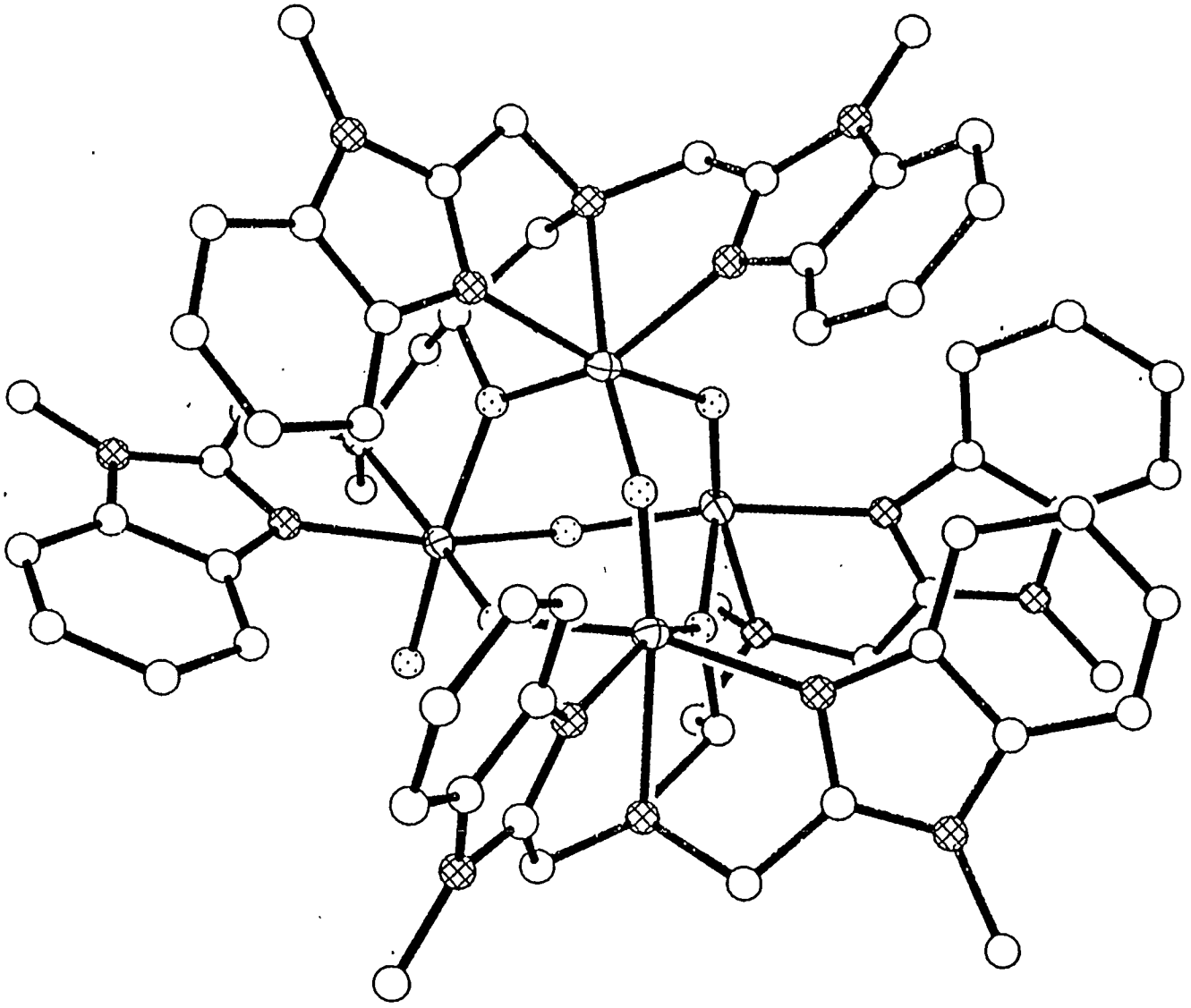

Figure 3. Cation of $[Fe_4(O)(MeL)(OH)_5][BF_4]_3$ (2). Hydrogen atoms omitted for clarity. Thermal ellipsoids-Iron; Open circles-Carbon; Dotted circles-Oxygen; Cross-hatched circles-Nitrogen.

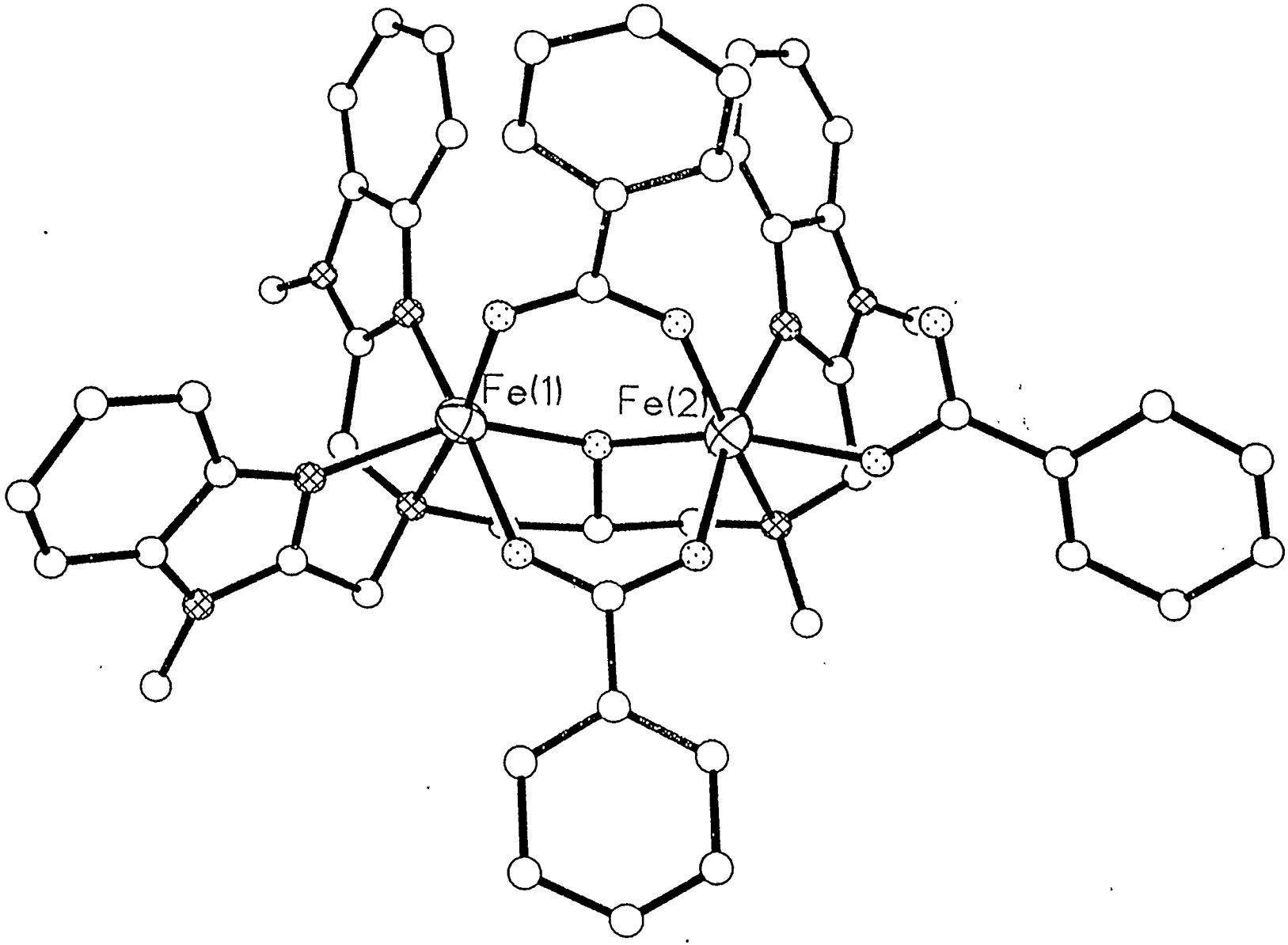

Figure 4. Cation of $[Fe_2(OBz)_3(MeL)][BF_4]$ (3). Hydrogen atoms omitted for clarity. Thermal ellipsoids-Iron; Open circles-Carbon; Dotted circles-Oxygen; Cross-hatched circles-Nitrogen.

P7 GASIS Demonstration

CONTRACT INFORMATION

Contract Number DE-AC21-93MC28139

Contractor Energy and Environmental Analysis, Inc.
1655 North Fort Myer Drive, Suite 600
Arlington, VA 22209
(703) 528-1900 (telephone)
(703) 528-5106 (fax)

Other Funding Sources

Contractor Project Manager E. Harry Vidas

Principal Investigators E. Harry Vidas
Robert H. Hugman
Peter S. Springer

METC Project Manager Harold D. Shoemaker

Period of Performance May 17, 1993, to May 16, 1996

ABSTRACT

A prototype of the GASIS database and retrieval software has been developed and is the subject of this poster session and computer demonstration. The prototype consists of test or preliminary versions of the GASIS Reservoir Data System and Source Directory datasets and the software for query and retrieval. The prototype reservoir database covers the Rocky Mountain region and contains the full GASIS data matrix (all GASIS data elements) that will eventually be included on the CD-ROM. It is populated for development purposes primarily by the information included in the Rocky Mountain Gas Atlas.

The software has been developed specifically for GASIS using Foxpro for Windows. The application is an executable file that does not require Foxpro to run. The reservoir database software includes query and retrieval, screen display, report generation, and data export functions. Basic queries by state, basin, or field name will be assisted by scrolling selection lists. A detailed query screen will allow record selection on the basis of any data field, such as depth, cumulative production, or geological age. Logical operators can be applied to any numeric data element or combination of elements. Screen display includes a "browse" display with one record per row and a detailed single record display. Datasets can be exported in standard formats for manipulation with other software packages. The Source Directory software will allow record retrieval by database type or subject area.

P8 Development of a Gas Systems Analysis Model (GSAM)

CONTRACT INFORMATION

Contract Number	DE-AC21-92MC28138
Contractor	ICF Resources Incorporated 9300 Lee Highway Fairfax, Virginia 22033 (703) 934-3000 (703) 691-3349
Contractor Manager	Michael L. Godec
Principal Investigators	Alan B. Becker William J. Pepper
METC Project Manager	Anthony Zammerilli
Period of Performance	June 22, 1992 - July 21, 1995

Schedule and Milestones

	Prior FY	FY95 Program Schedule O N D J F M A M J J
Review Models	1994	
Review Technologies	1994	
Model Design	1994	
Model Development	1994	----------C
Data Development		S---------C
Peer Review		X
Document, Test, and Validate		S----------P
Final Report		S----------P

S = Start
P = Planned Completion
C = Complete

OBJECTIVES

The objectives of developing a Gas Systems Analysis Model (GSAM) are to create a comprehensive, non-proprietary, PC based model of domestic gas industry activity. The system is capable of assessing the impacts of various changes in the natural gas system within North America. The individual and collective impacts due to changes in technology and economic conditions are explicitly modeled in GSAM. Major gas resources are all modeled, including conventional, tight, Devonian Shale, coalbed methane, and low-quality gas sources.

The modeling system assesses all key components of the gas industry, including available resources, exploration, drilling, completion, production, and processing practices, both for now and in the future. The model similarly assesses the distribution, storage, and utilization of natural gas in a dynamic market-based analytical structure. GSAM is designed to provide METC managers with a tool to project the impacts of future research, development, and demonstration (RD&D) benefits in order to determine priorities in a rapidly changing, market-driven gas industry.

BACKGROUND AND INTRODUCTION

The North American gas marketplace is rapidly evolving. Most forecasters believe the future growth of gas prices will be relatively modest. The historical surplus of gas deliverablity has ended, new markets for gas are forming, and open access transportation is changing the way gas gets to market and the costs associated with getting it there. At the same time, the characteristics of U.S. gas supplies are changing. Environmental and economic pressures are increasing the need for expanding gas supplies. The primary source of U.S. gas reserve additions has shifted from new discoveries to the more extensive development of known resources, which will continue to come from increasingly more complex and technically challenging settings. Consequently, the U.S. must expand its sources of low-cost gas supplies, and technology will play a key role in achieving this expansion.

However, traditional approaches for modeling the North American gas market cannot explicitly examine the role of specific future technology opportunities throughout this complex system. These approaches have not been based on an explicit, reservoir-by-reservoir characterization of the domestic gas resource base. This type of characterization is essential for performing explicit assessments of the potential of technology advances, while simultaneously accounting for the site-specific characteristics of the resource and the constraints imposed by the marketplace. Also, economic decision making in these traditional approaches is often inconsistent with true operator behavior, especially as it relates to representing operator responses to specific government policies and available technological opportunities.

DOE's objective for developing the Gas Systems Analysis Model (GSAM) was to create a comprehensive, non-proprietary, PC-based model of the domestic gas industry capable of assessing the impacts of various changes in the natural gas system within the entire North America system. DOE required that GSAM be capable of modeling individual and collective impacts due to changes in technology, policy, environmental requirements, and economic conditions, considering the entire North American gas market, from reservoir to burner tip.

PROJECT DESCRIPTION

DOE developed GSAM to assist in program planning and R&D evaluations related to discovery, development, production, transportation, storage, and end-use of natural gas. The three year development effort included evaluation of other models, various technologies, and numerous data sources to determine which of various options should be included in GSAM.

By design, GSAM was developed to focus on the details associated with specific gas resource characteristics, at the reservoir level. Of critical importance was technical and economic evaluations of extraction technologies which could be used, now and in the future, to develop and produce this resource. GSAM is designed to provide METC with a tool to project the impacts of future technology developments in a rapidly changing, market-driven gas industry. Figure 1 shows the overall structure of GSAM and the key modules that make up the system.

GSAM evaluates each exploration, development, and production activity as investment opportunities at the unit of analysis of the reservoir. These evaluations integrate detailed information on reservoir geology, technology applications, productivity, costs, and market prices -- the same information an operator uses in the field to evaluate projects.

Exploration is evaluated on a fully-risked prospect basis. For exploration to be conducted, the expected value of each discovery must exceed the full cost of finding hydrocarbons (including dry holes), and ultimately developing and producing the potential discovered reservoir(s). Once a reservoir has been discovered, development and production from that reservoir must generate expected revenues to cover the investments, operating costs, and risks of development. Each investment decision is approached from the view point of an operator determining if the investment is warranted.

GSAM integrates these discrete decisions into a market framework. Investment decisions over time are justified based on contemporary market conditions (e.g., capital and rig availability, wellhead prices) consistent with the supply and demand of gas and the availability of infrastructure in various regions. Based on aggregate activities in various supply and demand regions, GSAM equilibrates regional markets and prices over the forecast period. GSAM explicitly addresses seasonal demand fluctuations that influence gas infrastructure, storage, and utilization capacity. This comprehensive market framework ensures that the estimated impacts of technology advances and policy initiatives on E&P activities appropriately and credibly reflect market realities.

GSAM has been designed on a modular basis. This design was selected to speed the analysis by allowing each segment of the model to be run independently. Intermediate results can be used for many analytical requirements, reducing the time and manpower needed to complete model runs. Each module can also be individually tested and validated against other systems and modules.

The system was reviewed by a panel of industry experts last fall. Based on their favorable comments and recommendations, key aspects of GSAM have been enhanced. Additional modifications and enhancements have been identified and are being pursued.

Data Requirements

Since model results are only as useful as the data on which they are based, the GSAM methodology places a high priority on using validated information characterizing domestic natural gas resources. GSAM relies on accurate and available resource descriptions, at the level of individual reservoirs. Each reservoir is explicitly characterized by rock and fluid properties, depth, pressure, and temperature, as well as resource type, play, location, and current development status. These data, plus carefully selected defaults when required, are used to evaluate the productivity and costs of each reservoir for a variety of alternative technologies and policy scenarios.

Other information is needed to fully evaluate a gas reservoir's productivity and economics relative to other investments. Various capital and associated operating and maintenance (O&M) costs are estimated in the model as a function of specified technologies, location, and producing characteristics. Information on regional or national trends in drilling and completion costs, dry hole costs, and gas processing and waste disposal costs, along with other gas industry factors, are incorporated to reflect the dynamics of evolving capital and energy markets. Additional data on local, state, and federal tax structures, depletion, depreciation, and royalties, as they relate to gas producers and reservoir location and types, are used to provide fully costed reservoir evaluations on an explicit project discounted cashflow basis.

Current and advanced technology performance and cost assumptions and various policy conditions are defined as user-specified parameters. GSAM evaluates the evolution of decision parameters in response to constantly changing procedures and technologies as they are developed, tested, and implemented by operators in the field and as the character of the remaining resource base changes.

Finally, macroeconomic variables, infrastructure constraints and costs, and gas industry characterizations are required to fully represent the market within which investment decisions are made. These market parameters strongly affect investments in new gas supplies, as well as end-use demand, by imposing realistic limits on regional supplies and inter-regional transportation volumes. These downstream factors are derived from historic industry practices and adjusted for changes in industry structure and recent regulations.

The analysis of data and development of reservoir level resource descriptions are critical to the functioning of GSAM. As shown in Figure 2, the modeling system has a resource module that analyzes available data from several sources and produces consistent databases for the known and undiscovered reservoirs in each geologic play.

The initial GSAM database was developed using information on known domestic gas reservoirs provided in the commercially available *Significant Oil and Gas Fields of the United States* database by NRG Associates[1]. Other sources of gas reservoir data could also be incorporated into GSAM if desired. The NRG data contain reservoir specific rock and fluid properties, production histories, and location information of over 10,000 non-associated gas reservoirs nationwide.

This information was supplemented by data from the U.S. Geological Survey (USGS)[2] on resources that remain to be discovered, and by information from the National Petroleum Council (NPC)[3], as elaborated below. Based on the information available, a detailed description of the gas

resource can be developed, with this resource defined in terms that allows for the explicit and unique evaluation of potential technology performance in each individual resource setting where it may be applied.

An important feature of GSAM's gas reservoir database is that each reservoir is described in terms of *total gas resource in place*, rather that the traditional specification in terms of *technically recoverable resource.* Characterization of the gas resource base in terms of gas in place is crucial for credibly using GSAM to assess the potential of explicit advances in gas extraction technologies.

The NRG data provided another important element to the database; the assignment of all reservoirs to unique geologic-based plays[4]. This data element was used to develop default elements based on representative properties for reservoirs in each play. This provided a method for determining reasonable values for key missing data elements.

Additionally, using the data available from the NRG file and cross-walking to information from the USGS, an undiscovered resource database was initially constructed for use in GSAM. These data use average properties for known reservoirs to describe reservoirs that remain to be discovered in each play. Additional reservoir descriptions for zones in hypothetical or frontier plays were developed based on plays with similar geologic characteristics.

For selected offshore and unconventional resources, and where data were otherwise not available from the sources described above (e.g., Canada and Appalachia) reservoir data sets were created to calibrate the model. This step involved using information developed for the 1992 NPC study *The Potential for Natural Gas in the United States*[5], as well as data available from the National Energy Board[6] of Canada. These data are intended to serve as a surrogate until additional information on these resources can be collected and analyzed.

A key feature of GSAM is the source databases. These files contain information on the origin and evaluation of each element in the resource databases. This information is used to update and validate the data, assumptions, and analytical procedures resident in the resource module.

Upstream Model Components

Figure 3 shows the logic flow of the upstream segment of GSAM, which consist of four distinct activities -- resource analysis, analytical preprocessor, current resource status, and supply analysis. The model consists of consistent, parallel, but independent modules to assess the annual production levels, recovery potential, project costs, and summary economic results for individual reservoirs nationwide. All available raw resource data (Box 1 in Figure 3) are incorporated into a resource module (Box 2) to be processed, analyzed, and validated into full reservoir descriptions. The module consists of more than simple screens, instead using the distribution of properties within plays to confirm information and estimate missing data. The full characterization of known producing, discovered but undeveloped, and undiscovered reservoirs in the United States also draws on resource assessments available from USGS and MMS (including data from the current national assessment of undiscovered gas resources), and other private and public sources. Additional segments of these modules check for data consistency among reservoirs within plays by size and depth. This evaluation allows

data default values to be determined and appropriately incorporated where reservoir data are inconsistent or missing. The completed reservoir descriptions are stored in one database for undiscovered/ undeveloped reservoirs (Box 3) and another database for reservoirs for which initial development and significant production have occurred (Box 4).

The number of full individual technical, and economic reservoir evaluations required to fully characterize alternative resource, technology, and policy scenarios could exceed 100,000. Therefore, preprocessed evaluations of potential reservoir performance for each reservoir under alternative scenarios are necessary to improve the speed and flexibility of GSAM. The Resource Evaluation Modules estimate initial production and conduct economic analyses that are used later in the Upstream Model to sequence natural gas resource development. These modules incorporate reduced form reservoir models (type curves) that transform discrete reservoir properties and technology assumptions into reservoir development and production profiles and ultimate gas recovery.

Figure 4 displays the characteristics of the six reservoir performance (type-curve) models used in GSAM. These models use reservoir-level rock and fluid properties to determine the technically feasible production response for various reservoir types.

Table 1 shows how certain types of technologies can be represented in these type curves by adjusting specific parameters in the gas flow equation.

Each reservoir evaluation uses appropriate costs and economic values to determine discounted net cashflows and project profitability. The economically optimum technology scenarios are flagged and reservoirs that are never likely to be economic are excluded from further analysis. This preprocessor refines the list of reservoirs to the minimum set appropriate for the scenario being analyzed. The preprocessor design feature allows numerous technology scenarios to be evaluated prior to the demand for rapid scenario analysis, vastly reducing the analysis turnaround time.

The Current Resource Status function consists of three reservoir banks generated by the Resource Evaluation modules. It provides a current description of the producibility and the relative economic viability and profitability of the undiscovered resource (Box 7), the probable contribution of reservoirs recently discovered and under development (Box 8), and known producing reservoirs (Box 9). The banks only contain economically viable reservoirs within the range of fiscal and technology scenarios being considered. The GSAM resource status is only regenerated when significant shifts in technology, costs, or available reservoir data could significantly alter the character of the reservoir banks.

GSAM model decisionmaking for upstream investments is evaluated in five individual modules for exploration (Box 11), initial reservoir development (Box 12), production (Box 14), additional development (Box 13), and additional sources (Box 15; LNG, Canadian imports, and associated gas). These modules evaluate preprocessed, project-specific production and financial summary data against user-specified decision criteria for contemporary market conditions to determine the production from available reservoirs given a projected gas price track. Again, the modules consider options from the viewpoint of the operator, deciding whether to implement or defer various investment opportunities. For example, the additional development module evaluates investment options for infill drilling or

recompletion of initial development wells to maintain reservoir deliverability. The evaluations are based on reservoir-specific evaluations and consider the direct and secondary impacts of changing technology on future production, costs, and reservoir access.

The GSAM design also emphasizes the importance of proper accounting of resources by describing, quantifying, and evaluating the remaining domestic gas resource (Box 16) after production by selected technologies. The modular design provides an easy tracking capability within the model to monitor how technology is influencing gas recovery from various resource segments (Figure 5). The Remaining Resource Database will provide a balanced, accountable description of gas remaining to be recovered in various reservoir settings. These resources are targets for more aggressive R&D to overcome key physical or economic barriers to production.

The summary information is then used to determine the probable timing of development for each reservoir based on regional and national prices and cost factors. The system consists of intermediate databases that allow analyses to be completed without running the entire analytical system. The results of the upstream model flow to the integrating model to determine market conditions and timing of development.

Downstream Model Components

GSAM goes beyond evaluating gas supplies to explicitly model the full impact of technology and policy changes on the timing and magnitude of technology commercialization. Natural gas cost reductions due to improved technology may have limited value if they fail to stimulate production to meet market demand. Despite lower costs of producing specific segments of the resource, these supplies may ultimately be higher in cost to the end-user. To correctly and completely evaluate the market impact of various competing technologies and policies, GSAM includes a comprehensive model of the downstream (gas demand) segment.

Figure 6 illustrates schematically the market logic of the GSAM system and how it balances competing resources, R&D outcomes, policy considerations, and market realities to arrive at a single, comprehensive description of future gas potential. This evaluation can be run for a single gas price forecast, or in integrated mode to solve for regional and sectoral prices which balance end-use and production.

Inter-fuel competition is also explicitly analyzed within GSAM. End-users in the industrial and utility sectors have substantial fuel switching capacity, capable of using natural gas, oil, or coal as needed. GSAM explicitly analyzes the future impact of inter-fuel competition on regional and sectoral demand, and on gas prices, by modeling the decisions made by end-users in selecting the least-cost fuel. The methodology for assessing natural gas demand provides the most realistic assessment possible of demand and prices, and is consistent with most robust gas market models and provides for linkage with existing databases and models for calibration.

Integrating Model Components

The ability of existing infrastructure to cost-effectively move gas to market is modeled by GSAM as numerous transport links between supply and demand regions. GSAM provides for the evaluation of adding capacity or new service pipelines when market limitations and economics dictate,

accounting for seasonal demand fluctuations and storage and other peaking options. The explicit evaluation of seasonality provides an opportunity to evaluate storage reservoir performance and the need for additional capacity.

GSAM's Integrating Model also performs important accounting and equilibration of investments and available infrastructure, observing existing and probable future constraints. Similar to the Upstream and Downstream Models that provide input to it, the Integrating Model approaches decisions from an investor's viewpoint. It attempts to balance supply and demand in each region by the least-cost strategy that balances (fully risked) producer or consumer surplus, as appropriate.

The system was reviewed by a panel of industry experts last fall. Based on their favorable comments and recommendations, key aspects of GSAM have been enhanced. Additional modifications and enhancements, beyond the initial scope of the development phase, have been identified. Final model development work, including expanded data analysis capability, is being reviewed by METC.

RESULTS

Resource Data Development

The initial database developed for GSAM contains information on known conventional and unconventional reservoirs representing around 95% of the total U.S. non-associated gas production. Additionally, pseudo-reservoir data sets have been developed for Canada, Appalachia, and regions where, based on historic production levels, the database had missing reservoir units. The resulting database provides a detailed description of gas production from all regions in North America.

GSAM development also resulted in construction of data representing undiscovered reservoirs, consistent with the USGS assessment of remaining undiscovered gas resources. Key reservoir properties were assigned based on play average values. The database contains information on 175 major gas plays, representing over 10,000 undiscovered reservoir units.

The resource description in GSAM provides a starting point for initial analyses and final model development. As additional data is collected, GSAM provides the framework to incorporate, validate, and utilize it for R&D planning. Additional work is warranted to document the data and fully develop the GSAM resource files.

Supply Model Results

The initial analyses using GSAM indicate significant remaining resource recovery potential in domestic reservoirs. Consistent with the findings of recent national analyses, the availability of natural gas in most regions seems to be assured in the foreseeable future. The initial GSAM findings indicate an increase in production from the Rockies region and a somewhat smaller contribution from the Gulf Coast and offshore reservoirs.

Technology can substantially increase recovery potential and lower the overall cost of delivering natural gas. GSAM's detailed performance and cost assessment of individual reservoirs allows technology to be evaluated in detail. Figure 7 shows how new technology, e.g. longer fracture lengths in tight reservoirs, could lower the required wellhead price by increasing recovery from the zone. However, lower costs for fracturing operations combined with better

completion and stimulation technology may be required to allow operators to cost-effectively develop many tight and unconventional gas reservoirs.

Integrated Market Results

GSAM results indicate that, consistent with current conditions, regional gas price differentials will continue into the future. However, imports from Canada could be limited over the next twenty years unless new, lower cost technologies are applied to the diverse resources in Alberta and elsewhere.

Coalbed methane, shale gas, tight sands, and naturally fractured zones will play an increasingly important role in meeting future gas needs. As associated gas production declines and non-associated, conventional resources mature, more production must come from complex unconventional sources to meet demand. Additional research in drilling, completion, and processing to improve current practices and limit costs and risks will be needed to develop and produce these resources at reasonable gas prices.

Green River Basin Examples

Production from tight sands, especially in the Rockies, will need to increase in the future as gas demand expands and transportation infrastructure matures. The Green River Basin in southern Wyoming is a key area for application of new technologies for tight gas sands. With 56 to 83 TCF of estimated technically recoverable resource[6], this basin is a key future supply source for tight gas production.

Preliminary GSAM analysis indicates that current drilling, completion, stimulation, and production practices will limit economic recovery of the resource to only 7 to 8 TCF including reserves developed through the year 2010. Most critical seems to be the need for cost-effective hydraulic fracturing technology.

Technology improvements could substantially increase productivity, reserve potential, and economic attractiveness of Green River reservoirs. New techniques must provide economic incentives to develop the resource at prevailing regional gas prices. If stimulation processes can be improved and costs reduced by 30% of current costs, reserve potential in the basin could increase to around 10 TCF based on current GSAM resource description.

Figure 8 shows the potential impact on future production from reservoirs in the Eastern Green River Basin. As shown, the application of new technology to improve recovery or lower costs could have a profound impact on future production levels. However, the application of new technologies will have a downward impact on gas prices in the Rockies, Canada, and elsewhere.

METC research must overcome economic limitations to production from Green River reservoirs under level to slightly rising gas prices likely to be seen by operators. This figure also shows the effect of the combined impact of improved fracture technology and lower stimulation costs relative to current practices.

This initial basin analysis shows that cost-effective stimulation techniques must be developed and demonstrated in key reservoir settings in Green River. Development of more efficient fracture stimulation methods, providing longer, more conductive fractures at comparable costs are required.

GSAM analyses provide the capability to

comprehensively analyze the impact of individual or combined technology improvements for E&P operations, evaluating the impact of improvements in reservoir performance, reductions in costs, and management of operator risk. The capability to analyze potential improvements in detail allow METC to plan and focus research on the most critical needs. By linking to the downstream demand estimates, GSAM provides a realistic projection of the economic conditions that will define future production activities.

FUTURE WORK

Initial GSAM development is complete and documentation is being reviewed and finalized. Additional deliverables will include a complete documentation of the modeling system, databases, and analytical procedures used. A comprehensive users' guide is also being prepared.

Additional testing and validation is being completed consistent with recommendations and initial plans. The full validation and model installation will be complete prior to July.

Additional work to improve GSAM is being considered by METC. In addition, enhancements to the environmental module to increase data coverage and streamline analyses of cost/benefits are being planned. Initial use of GSAM for policy and program planning will be initiated upon final development activity.

The GSAM design provides a solid framework for additional model development, data collection and analysis, and system refinements. The additional enhancements can be quickly integrated within the modeling system.

REFERENCES

1. United State Geologic Survey, *Estimates of Remaining Hydrocarbon Deposits*, Washington, DC, 1989.

2. National Petroleum Council, *The Potential for Natural Gas in the United States*, Volumes I-VI, Washington, DC, 1992

3. NRG Associates, *Significant Oil and Gas Fields of the United States Database*, 1994.

4. NRG Associates, *U.S. Oil and Gas Plays*, Colorado Springs, CO, 1993.

5. NPC, Volume II, Chapter 4.

6. NPC, Volume II, p. 104.

Figure 1. GSAM Structure

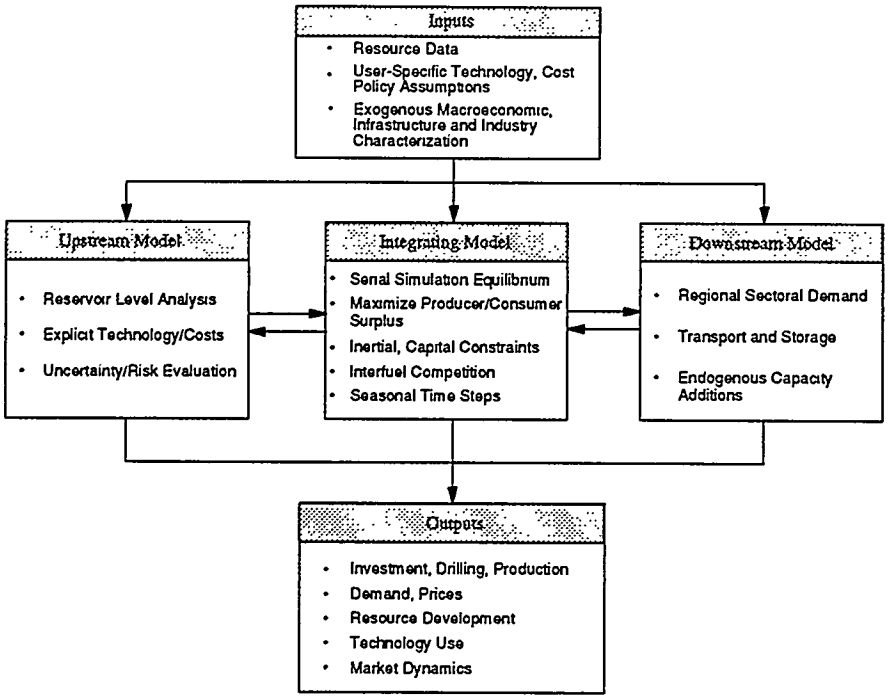

Figure 2. GSAM Resource Data Development Method

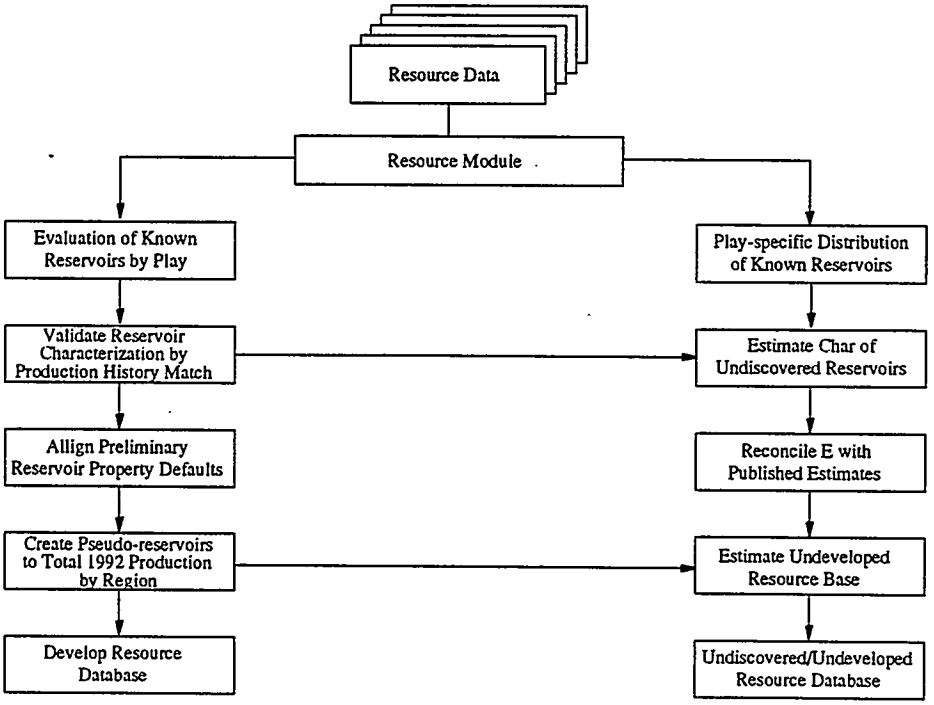

Figure 3. GSAM Upstream Model Flowchart

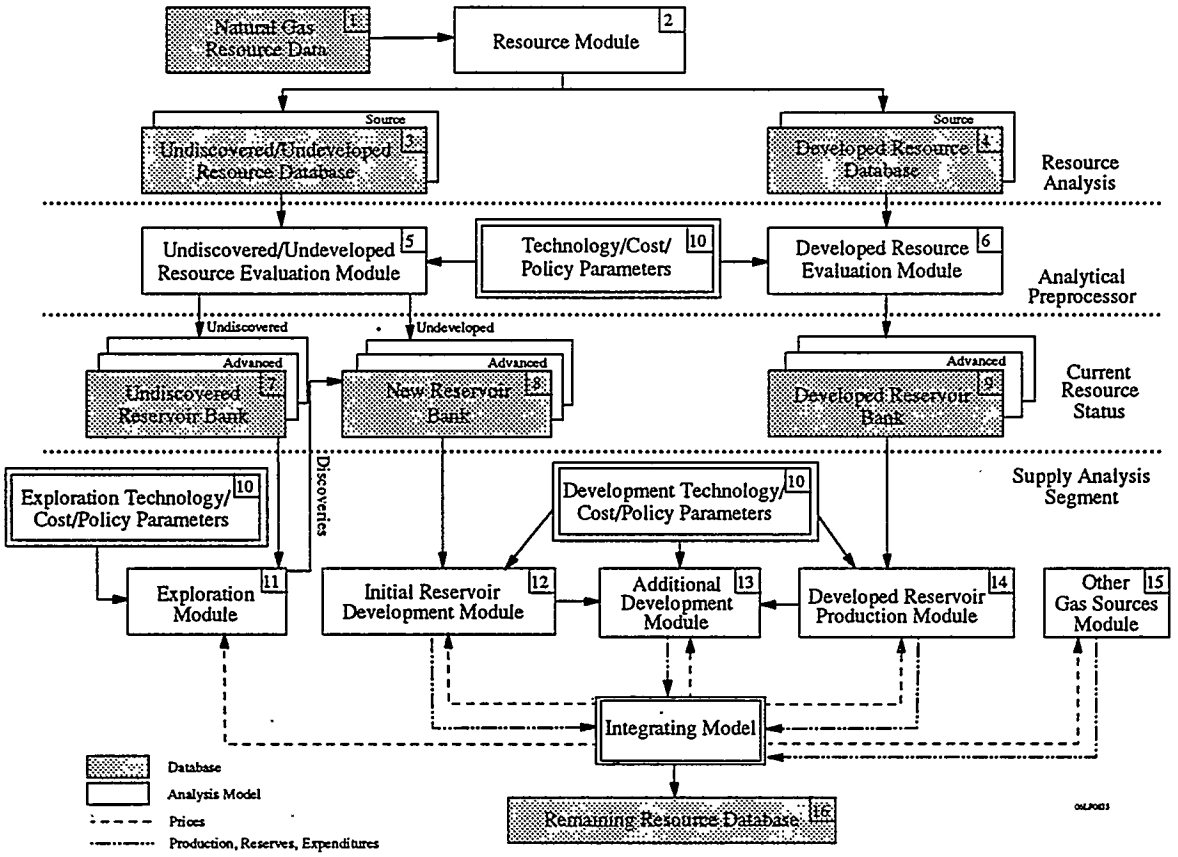

Figure 4. GSAM Reservoir Performance Models

Module	Reservoir Type	Drive Mechanism	Flow Geometry	Porosity Type	Number of Fluids
I	Conventional/ Tight	Fluid Expansion	Radial	Single	Single Fluid* (Gas)
II	Horizontal well/ Induced fracture	Fluid Expansion	Linear	Single	Single Fluid (Gas)
III	Conventional	Fluid Expansion	Radial	Dual	Single Fluid (Gas)
IV	Horizontal well/ Induced fracture	Fluid Expansion	Linear	Dual	Single Fluid (Gas)
V	Natural Fracture	Water-Drive	Radial	Single	Two Fluids (Gas & Water)
VI	Coal/Shale	Diffusion/ Desorption	Radial	Dual	1 or 2 Fluids (Gas or Water/Gas)
*Geopressured aquifers can be analyzed using Module I; mobile phase is water					

Figure 5. GSAM Logic Flow

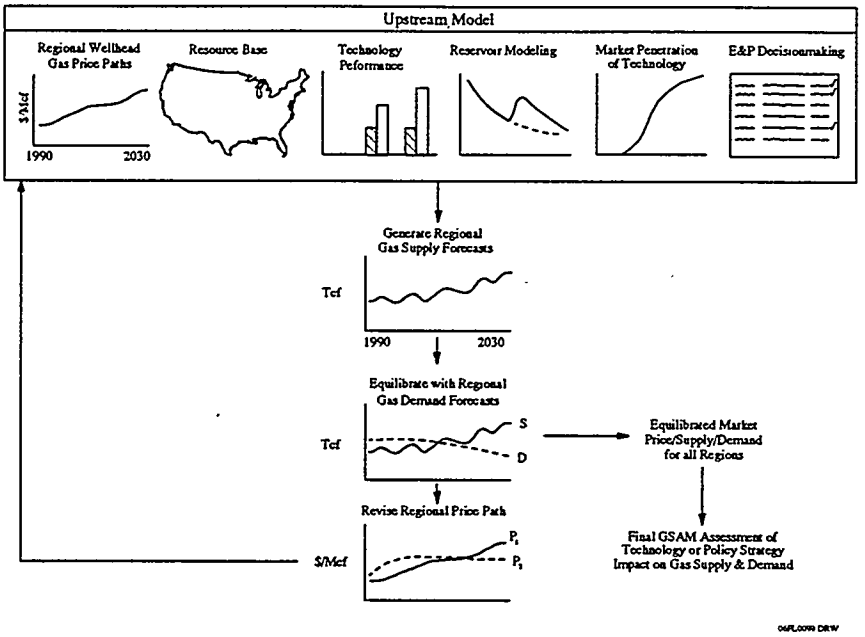

Figure 6. Analysis of Natural Gas Resources by GSAM Modules and Databases

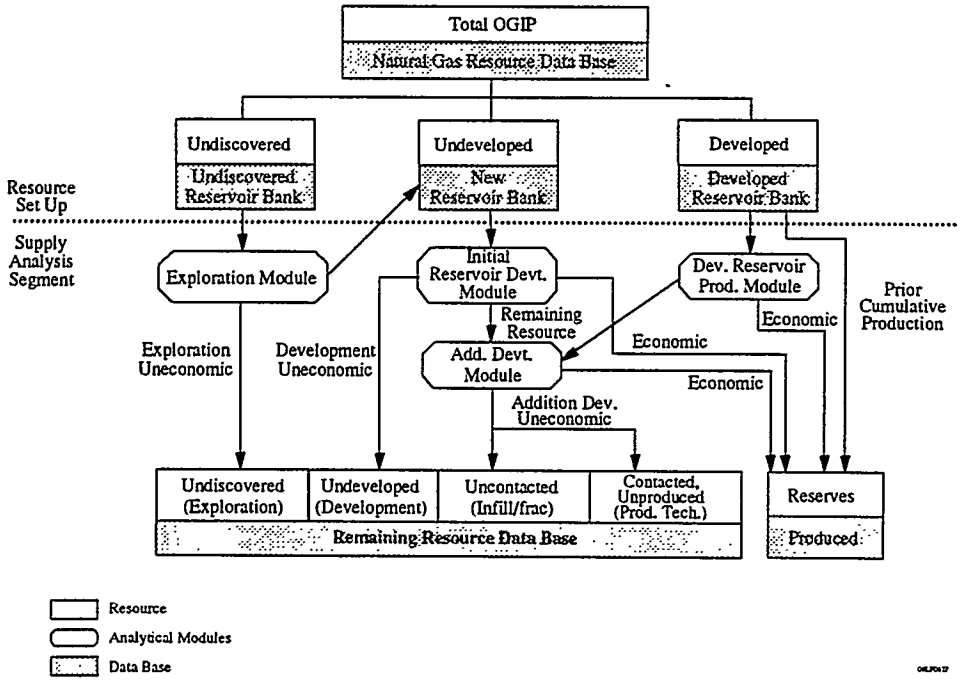

Figure 7. Economic Recovery May Require Improved Technology and Lower Cost

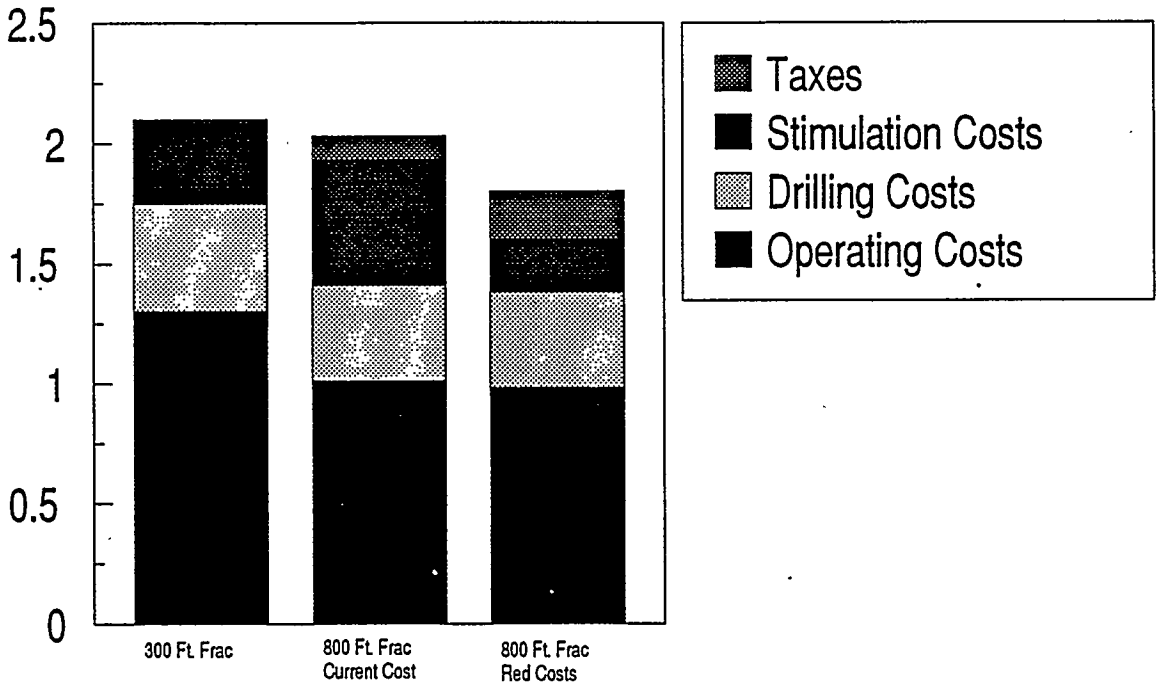

Figure 8. Gas Production Potential From Eastern Green River Basin

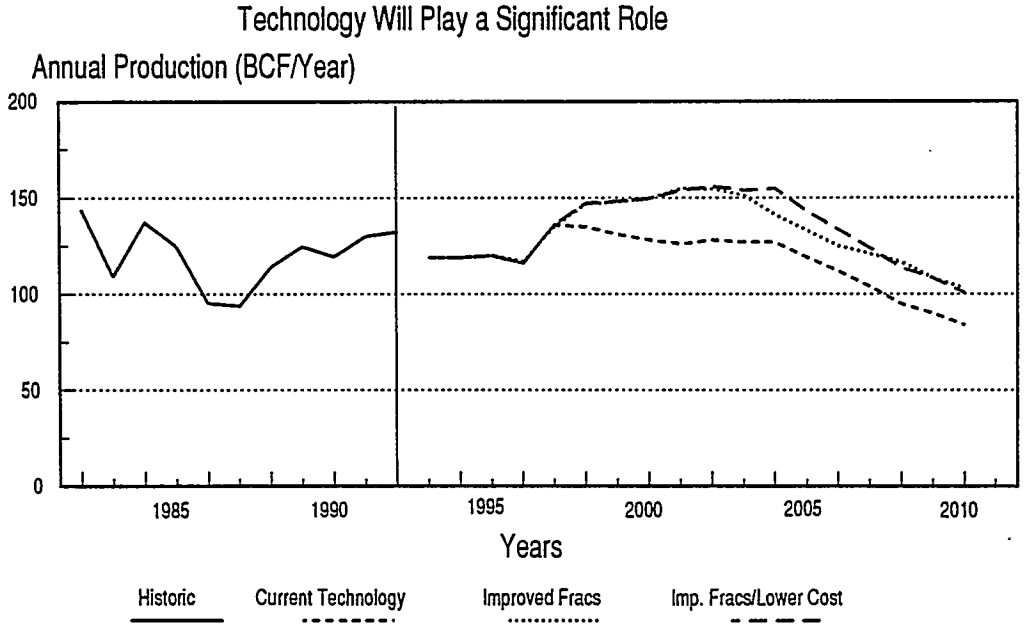

P10 Steady-State and Transient Catalytic Oxidation and Coupling of Methane

CONTRACT INFORMATION

Contract Number	DE-AC03-76SF00098
Contractor	Lawrence Berkeley Laboratory One Cyclotron Road Berkeley, CA 94720 (510) 642-9673 (510) 642-4778 (fax)
Contractor Project Manager	Enrique Iglesia
Principal Investigators	Enrique Iglesia Dale L. Perry Heinz Heinemann
METC Project Manager	Rodney D. Malone
Period of Performance	January 1, 1994 to January 31, 1995

Schedule and Milestones

Two papers have been published on calcium-nickel-potassium oxide catalytic thin films.[1,2] Three presentations,[3-5] including a keynote lecture at the 204th ACS meeting, were given in 1994 describing reaction-separation schemes using oxidative coupling of methane, and two more are scheduled for 1995.[6,7] Four quarterly reports have been written and submitted during this time.[8] These findings have led us to develop membrane and cyclic feed reactor designs for methane coupling. We have completed initial membrane trials using two methods of metal oxide film preparation, pulsed laser deposition and co-precipitation. In 1995, we will prepare non-porous membrane films using these techniques and test them in a membrane reactor.

OBJECTIVES

This project addresses the conversion of methane from natural gas into ethane, ethylene and higher hydrocarbons. Our research explores the mechanistic and practical implications of carrying out the methane oxidative coupling reaction in reactor designs other than conventional packed-beds with co-fed reactants. These alternate reactor designs are needed to prevent the full oxidation of methane, which limits C_{2+} yields in methane oxidative coupling reactions.

BACKGROUND INFORMATION

Oxidative coupling of methane (OCM) leads to ethane and ethylene as primary products and CO and CO_2 by primary direct oxidation of methane and by secondary combustion of C_2 products. The

oxidative coupling reaction combines methyl radical generation on various oxide surfaces with coupling and oxidation of alkyl radicals in the gas phase.

Maximum C_{2+} yields of about 25% have been achieved using single-pass catalytic reactors with mixed methane and O_2 feeds. Higher C_{2+} yields will require catalytic solids that activate methane but not ethane or ethylene, the existence of which appears improbable at this time.

PROJECT DESCRIPTION

The research strategy focuses on preventing contact between the O_2 reactant required for favorable overall thermodynamics and the C_{2+} products of methane coupling. The behavior of various reactor designs are simulated using detailed kinetic-transport models. These simulations have suggested that the best way to prevent high CO_2 yields is to separate the oxygen and hydrocarbon streams altogether. As a result, the project has focused on the experimental demonstration of proton transport membrane reactors for the selective conversion of methane into higher hydrocarbons.

RESULTS

Reaction-Transport Models of Oxidative Coupling

Kinetic-transport models of the oxidative coupling reactions have been used to predict the C_{2+} yields in various reactor configurations. These models combine a detailed gas phase kinetic network and surface reactions with rigorous descriptions of the convective and diffusive transport processes within catalytic reactors.[9,10] We have previously reported simulation results from staged oxygen injection and oxygen-transport membrane reactors.[9,10] More recently, we have used these models to simulate the behavior of two additional reactor designs:

1) tubular flow reactor with interstage separation of ethane and/or ethylene
2) recycle reactor with ethane and ethylene removal from the recycle stream

Figure 1 shows a tubular reactor with C_2 separators along its length. As the reaction proceeds, the gas stream is periodically diverted from the reactor into a separator with 100% C_2 removal efficiency. The function of this separator is to remove the C_2 products before they undergo complete oxidation, and to add a small amount of oxygen in order to satisfy the OCM reaction stoichiometry while maintaining low O_2 concentration.

Realistically, such a separator would require cooling (and subsequent re-heating) of the gas stream from reactor temperatures of 800°C to below 100°C, the lowest operating temperature of current C_2 adsorbents. These repeated heating/cooling cycles severely reduce the second-law efficiency of this process.

Figure 2 shows the predicted C_2 yield for ethylene or ethane/ethylene separation. As the number of separators

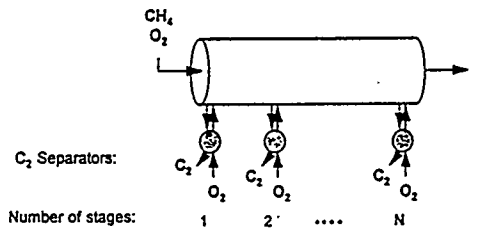

Figure 1. Staged C_2 Separation

increases, the overall reactor performance (and complexity) also increases. Fortunately, a small number of separators (<10) gives a significant improvement in C_2 yield. The maximum C_2 yield ($N = \infty$) is about 90%, corresponding to the selectivity of the surface methane oxidation reaction.

[800°C, $CH_4/O_2 = 2$, 1 bar total pressure]

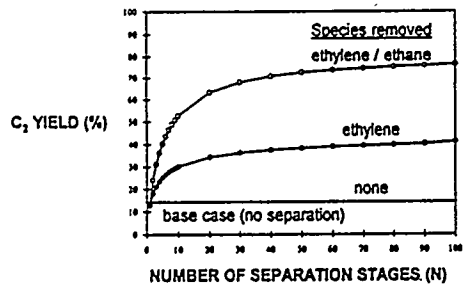

Figure 2. C_2 Yield Improves with an Increasing Number of Separators

This reactor is very similar to the simulated counter-current chromatographic moving-bed reactor reported by Tonkovich, et al.[11] Using an unpromoted Sm_2O_3 catalyst, and periodically removing both the ethane and ethylene product, they report a maximum C_2 yield of about 50% at a reactor temperature of 750°C. For large N, this value is between that predicted in figure 2 for ethane/ethylene removal and ethylene removal only. As noted by the authors,[11] this reactor could be optimized to achieve a C_2 yield closer to the 75% maximum predicted by our model for a large number of separators.

A more conventional reactor-separator design is the recycle reactor with C_2 removal from the recycle stream, as shown in figure 3. The recycle reactor operates on the same principle as the staged separation design: removal of the C_2 product before it can be completely oxidized. Figure 4 shows the simulated effect of increasing the recycle ratio on the overall C_2 yield, assuming the complete removal of both ethane and ethylene from the recycle loop. For a large recycle ratio (R=20), the C_2 yield is predicted to approach 60% at a methane conversion of 80%.

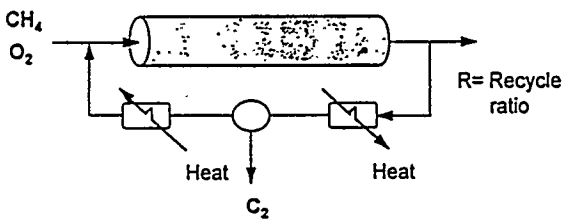

Figure 3. Recycle Reactor with C_2 Separation from Recycle Stream

Experimental results using a recycle reactor have been reported recently by Vayenas and coworkers.[12] Their reactor had a per-pass methane conversion of less than 3%. However, at steady-state, they report a maximum C_2 yield of 49%, at a CH_4 conversion of 65%. Furthermore, in batch operation ($R = \infty$), the reactor achieved a C_2 yield of 88%, the highest value reported to date for the oxidative coupling reaction. As

[800°C, $CH_4/O_2 = 2$, 1 bar total pressure]

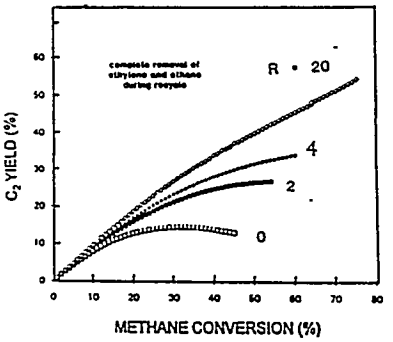

Figure 4. Predicted C_2 Yield in a Recycle Reactor with Increasing Recycle Ratio

noted by the authors[12] and demonstrated by our model, the dramatic C_2 yields attained were due to the separation of ethylene prior to oxidation, rather than any special aspect of the reactor design or the electrochemical catalyst employed.

A significant problem with these two reactor schemes is the availability of efficient C_1/C_2 separators. The low-temperature processes currently used to separate the light gases in an OCM product stream require efficient heat integration and cause large entropy losses (i.e., reduced second-law efficiency). Also, the dilution effect of a recycle stream leads to large reactors and high capital costs. Therefore, we are pursuing reaction-separation schemes that place less emphasis on the methane-C_2 gas separation process.

Hydrogen Transport Membranes for the Oxidative Coupling of Methane

An alternate approach that totally excludes contact between the hydrocarbon and oxygen components of the stoichiometric reaction mixture is the use of hydrogen transport membranes. Figure 5 shows the membrane reactor concept. One side of the membrane must activate the C-H bond in methane to generate methyl radicals and surface hydrogen. The hydrogen moves through the membrane under a concentration gradient developed by the removal of hydrogen from the opposite side by O_2 from air. The overall reaction is that of the OCM reaction, which is thermodynamically favorable and does not require an externally applied voltage.

The key to this reactor is the nature of the membrane and of the catalytic surface. Metal oxides with high protonic and electronic conductivity are appealing beacause they avoid the extensive fouling

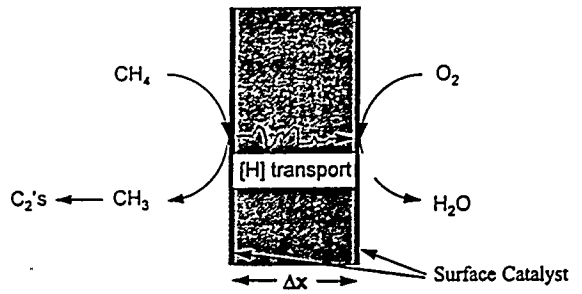

Figure 5. Methane Coupling in a Hydrogen Transport Membrane Reactor

inherent in the use of metal membranes (e.g. Pd alloys). These properties have been demonstrated in perovskites of composition $SrB_{1-x}B'_xO_{3-0.5x}$ (B=Ce, Zr; B'=Yb, Y; x=0.01-0.1).[13,14] In these materials, the B'^{3+} cation substitutes into the lattice position of the B^{4+} cation, creating lattice oxygen vacancies by charge compensation. Uchida et al, have shown that in the presence of oxygen these vacancies form electron holes (lattice O^- species), which can abstract hydrogen from gas phase molecules.[15] Within the oxide, the abstracted hydrogen forms a proton, which behaves as a point-charge interstitial species that can migrate among lattice oxygen ions.[16] At temperatures between 500 to 1000°C, these perovskites have a hydrogen diffusion coefficient of about 10^{-6} cm^2/sec, and practically no oxygen conductivity.[16]

The methane coupling reaction has been conducted using a $SrCe_{0.95}Yb_{0.05}O_{3-\delta}$ membrane in an electrochemical cell.[17] Although this configuration did enhance the conversion of methane to C_2 hydrocarbons, the rates were low due to slow transport of protons through the thick membrane and extensive coking on the metal electrodes at the high reaction temperature (900°C). Our goal is to demonstrate the feasibility of this approach, emphasizing thinner membrane films (<0.5 mm), more active and selective

surface catalysts, and much lower reaction temperatures (<700°C).

Membrane and Catalytic Thin Films of Metal Oxides

We are currently studying three methods of preparing ceramic thin films:

1) Pressed discs (~0.5 mm thick)
2) Pulsed laser deposition of a 1 μm film on a ceramic substrate,
3) Spin- or dip-coating of films (<0.1 mm) using dispersed precursors.

A general problem with preparing mixed metal oxides is the creation of a homogeneous mixture of the metal cations. The traditional method is to mix the (solid) metal salt precursors and sinter at high temperature to induce diffusion and formation of the desired phase in the solid state. We have prepared discs of various perovskite phases by grinding and calcining at 1000°C mixtures of the oxide precursors. This powder was then pressed to 30,000 psi and sintered at 1300°C in air, followed by another cold press and sintering at 1600°C overnight. These discs achieved 85-90% of the theoretical density. When we repeated the method, replacing the second cold press step with a hot press, we were able to achieve up to 95% theoretical density for some samples. These results are summarized in table 1.

We have attempted to test these membranes inside an alumina membrane reactor. Samples with less than 90% theoretical density proved to be permeable to methane. With the other samples, we have experienced cracking of the membranes and the zirconia cement used to attach the samples as the temperature is raised above 200°C. An alumina cement has been recently selected, to more closely match the thermal expansion of the reactor and perovskite discs.

Table 1. Per Cent of Theoretical Density of Perovskite Membrane Samples

Cold Press (30,000 psi, 25°C)	
$BaZr_{0.9}Y_{0.1}O_{2.95}$	85.3%
$CaZr_{0.9}Y_{0.1}O_{2.95}$	90.1
Hot Press (8,000 psi, 1600°C)	
$SrZr_{0.9}Y_{0.1}O_{2.95}$	93.8%
$SrCe_{0.9}Y_{0.1}O_{2.95}$	93.2
$BaCe_{0.9}Y_{0.1}O_{2.95}$	93.2

Using this technique, the minimum thickness for dense, unsupported ceramic membranes is about 0.5 mm.[17] Since a reduction in the membrane thickness will give a proportional increase in proton conductivity, we have begun to explore two alternate methods for the synthesis of thin films.

Pulsed-Laser Deposition of Thin Films

We have previously reported the preparation of $Ca_{1-x}Ni_xO$ catalytic thin films using pulsed laser deposition (PLD).[18] This technique involves the vaporization of a target by a high-energy pulsed laser beam, the formation of a plasma plume, and the deposition of the plume on a heated substrate. Recently, we have used an eximer laser with nanosecond pulses of 3-5 J/cm^2 energy density to deposit $SrZr_{0.9}Y_{0.1}O_{3-\delta}$ films of approximately 0.2 to 0.5 μm thickness on a porous Al_2O_3 substrate. (Coors Ceramics Company, average pore diameter <0.5 μm)

The resulting film was studied in a scanning electron microscope with energy dispersive spectroscopy (EDS) to examine the film composition and integrity. Figure 6 shows the EDS results. After film

deposition, the peaks due to impurities in the Al_2O_3 substrate have disappeared, being covered by peaks corresponding to $SrZr_{0.9}Y_{0.1}O_{3-\delta}$, in the same ratio as the target composition.

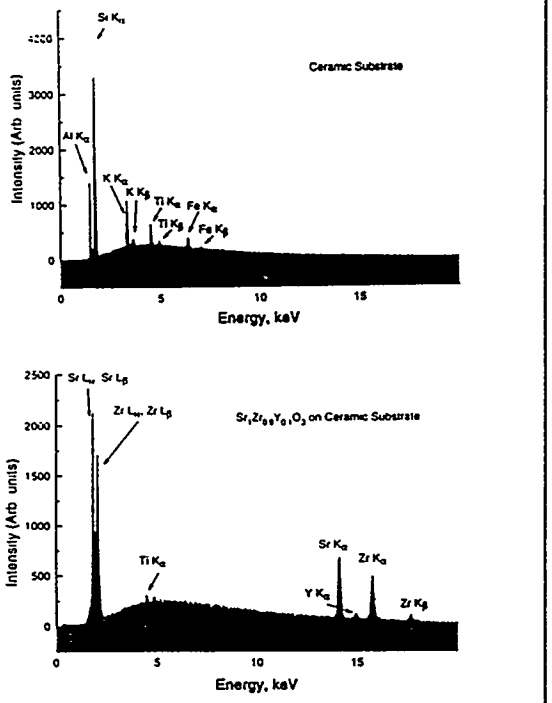

Figure 6. EDS Patterns of $SrZr_{0.9}Y_{0.1}O_{3-\delta}$ Film and Al_2O_3 Substrate

X-ray diffraction patterns of the substrate were taken before and after film deposition. Figure 7 shows the XRD pattern due to the film and substrate compared to the pattern of the substrate alone. The three strongest lines of $SrZrO_3$ at d = 2.91, 2.06, and 1.68 are the only peaks appearing after the film deposition, indicating the formation of a phase-pure film of $SrZrO_3$ in the distorted perovskite structure. As expected, the Y^{3+} cations have been substituted for Zr^{4+} cations with little alteration of the original lattice structure.

We are currently testing the film porosity in an alumina reactor at temperatures from 25 to 800°C. The earliest samples proved to be porous, allowing >14% gas flow (compared to the substrate alone) through the membrane. We have prepared samples with thicker films (~1 μm) in order to obtain a non-porous film for hydrogen transport and OCM studies.

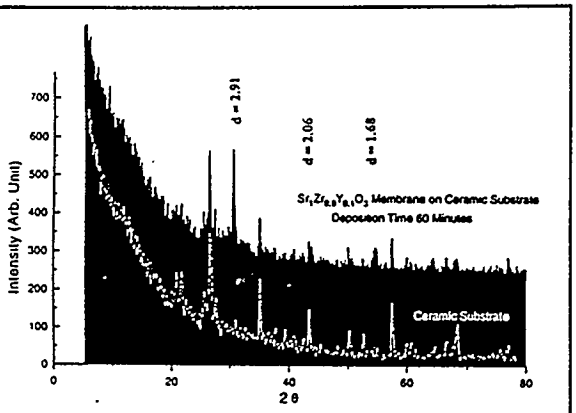

Figure 7. XRD Patterns of $SrZr_{0.9}Y_{0.1}O_{3-\delta}$ Film and Al_2O_3 Substrate

In pulsed-laser deposition, the target material and the substrate must fit inside an UHV chamber, which limits the utility of the method to small-scale applications. However, for experimental studies it provides a method to test the limit of improving the membrane concept via a reduction in the film thickness.

Preparation of Mixed Metal Oxide Precursors Via Co-Precipitation

The solid state reaction synthesis route for the Sr-Ce(Zr)-Yb(Y)-O perovskites requires reaction temperatures in excess of 1450 °C for 24 hours.[13] In order to form a dense perovskite phase at lower temperatures, we are exploring methods that allow the formation of high-surface area precursors with intimate contact among the desired metal cations.

Recently, high-temperature superconductors with the perovskite structure

have been prepared using precursors formed via co-precipitation.[19,20] This involves dissolving the appropriate metal salts in an acidic mixture, which is rapidly added to a basic solution to induce precipitation of the metals as hydroxides or carbonates. After thermal treatment, this method gives dense, homogenous sinters with the perovskite phase only. These sinters can then be sliced into thin discs or used as targets for pulsed laser deposition on a ceramic substrate. Alternately, the precursor can be dissolved and coated on a ceramic substrate prior to thermal treatment. Repeated coatings yield homogeneous thin films.[19]

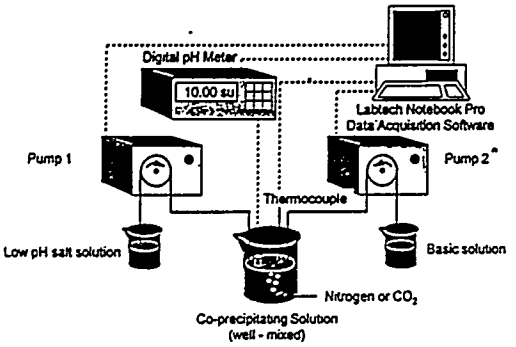

Figure 8. Constant pH Co-Precipitation

We have constructed a computer-controlled constant pH co-precipitation unit to prepare these precursors in a controlled and reproducible manner. The unit is shown in figure 8. In order to maintain stoichiometry and minimize waste, the precipitation is conducted at the pH value corresponding to the minimum solubility of the cations in solution. From potentiometric titration and solubility data for the cations Ce^{3+}, Yb^{3+}, and Y^{3+}, a pH of 9 was determined to be high enough to precipitate the metal hydroxides. This allows use of ammonium hydroxide as the base, which is readily removed upon heating. As expected from similar data for Ba^{2+}, $Sr(OH)_2$ is soluble at all values of pH. However, Sr^{2+} will precipitate as a carbonate over a wide range of pH. The addition of an excess amount of ammonium bicarbonate to the precipitating solution allows for the recovery of Sr^{2+} along with the other cations.

We have prepared several samples of mixed metal salts of stoichiometry $SrCe_{0.95}Yb_{0.05}$ at pH = 9. We are currently testing the effects of various heat treatments upon forming dense discs for eventual testing in the membrane reactor. We anticipate this method will allow the use of lower sintering temperatures in forming the perovskite phase.

FUTURE WORK

1. Test proton transport membranes prepared using pulsed-laser deposition and co-precipitation techniques.

2. Develop thin film deposition techniques and other fabrication methods for ceramic membranes.

3. Develop rigorous reaction-transport models of methane activation under medium temperature, non-oxidative (pyrolysis) conditions.

4. Screen potential surface catalysts for medium temperature, pyrolytic methane activation.

ACKNOWLEDGMENTS

The authors wish to acknowledge Sebastian C. Reyes of Exxon Research and Engineering (Annandale, NJ) for work on the OCM model, and Richard W. Borry III of the University of California at Berkeley

for work on the hydrogen transport membrane experiments.

REFERENCES

1. Perry, D.L., Thompson, A.C., Russo, R.E., and Mao, X.L., "Studies of Calcium-Nickel-Potassium Oxide Films by Synchrotron X-ray Fluorescence Microscopy", *Proceed. Fall Meet. Mat. Res. Soc.*, **375**, (1994)

2. Perry, D.L., Berdahl, P., Perrino, C., "Magnetic Characterization of Calcium-Nickel-Potassium Oxide Catalysts", *J. Mater. Res.* **9** (11), 2993 (1994)

3. Iglesia, E., and Reyes, S.C., "Reaction-Transport Models and the Design of Catalysts and Reactors for the Oxidation and Coupling of Methane", Keynote Lecture, *Symposium on Methane Conversion at the 204th Meeting of the American Chemical Society*, San Diego, CA, (1994)

4. Borry, R.W., and Iglesia, E., "Design of Reaction-Separation Schemes for the Oxidative Coupling of Methane", *California Catalysis Society Spring Meeting*, Lawrence Berkeley Laboratory, Berkeley, CA, (1994)

5. Heinemann, H., "Catalytic Natural Gas Conversion Research", *Fossil Energy/National Laboratory Joint Meeting*, Dulles Airport Marriot, (1994)

6. Iglesia, E., Borry, R.W., and Reyes, S.C., "Reaction-Separation Schemes for C_2 Yield Improvements in the Oxidative Coupling of Methane", Plenary Lecture, *International Natural Gas Conversion Symposium*, Johannesburg, Republic of South Africa, (1995)

7. Reyes, S.C., Borry, R.W., and Iglesia, E., "Reaction-Separation Schemes for C_2 Yield Improvements in the Oxidative Coupling of Methane", *North American Meeting of the Catalysis Society*, Snowbird, Utah, (1995)

8. LBL Reports: LBL-35485;

9. Reyes, S.C., Iglesia, E., and Kelkar, C.P., "Kinetic-Transport Models of Bimodal Reaction Sequences I. Homogeneous and Heterogeneous Pathways in Oxidative Coupling of Methane", *Chem. Eng. Sci.* **48**, 2643 (1993)

10. Reyes, S.C., Iglesia, E., and Kelkar, C.P., "Kinetic-Transport Models and the Design of Catalysts and Reactors for the Oxidative Coupling of Methane", *Catal. Lett.* **19**, 167 (1993)

11. Tonkovich, A.L., Carr, R.W., and Aris, R., "Enhanced C_2 Yields from Methane Oxidative Coupling by Means of a Separative Chemical Reactor", *Science* **262**, 221 (1993)

12. Jiang, Y., Yentekakis, I.V., Vayenas, C.G., "Methane to Ethylene with 85 Percent Yield in a Gas Recycle Electrocatalytic Reactor-Separator", *Science* **264**, (1994)

13. Iwahara, H., Esaka, T., Uchida, H., Maeda, N., "Proton Conduction in Sintered Oxides and its Application to Steam Electrolysis for Hydrogen Production", *Solid State Ionics* **3/4**, 359 (1981)

14. Shin, S., Huang, H., Ishigame, M., "Protonic Conduction in the Single Crystals of $SrZrO_3$ and $SrCeO_3$ Doped with Y_2O_3", *Solid State Ionics* **40/41**, 910 (1990)

15. Uchida, H., Maeda, N., Iwahara, H., "Relation Between Proton and Hole

Conduction in $SrCeO_3$ Based Solid Electrolytes Under Water Containing Atmospheres at High Temperatures", *Solid State Ionics* **11**, 117 (1983)

16. Norby, T., "Proton Conduction in Oxides", *Solid State Ionics* **40/41**, 857 (1990)

17. Hamakawa, S., Hibino, T., Iwahara, H., "Electrochemical Methane Coupling Using Protonic Conductors", *J. Electrochem. Soc.* **140**, 459 (1993)

18. Mao, X.L., Perry, D.L., and Russo, R.E., "$Ca_{1-x}Ni_xO$ Catalytic Thin Films Prepared by Pulsed Laser Deposition", *J. Mater. Res.* **8** (9), 2400 (1993)

19. Bunker, B.C., Voight, J.A., Lamppa, D.L., Doughty, D.H., Venturini, E.L., Kwak, J.F., Ginley, D.S, Headley, T.J., Harrington, M.S., Eatough, M.O., Tissot, R.G., Hammetter, W.F., "Chemical Preparation of Powders and Films for High Temperature Superconductors", Better Ceramics Through Chemistry III, *Mat. Res. Soc. Symp. Proc.* **121**, 373 (1988)

20. Spencer, N.D., "Alkali-Metal-Free Carbonate Coprecipitation: An Effective Synthetic Route to Bismuth-Based Oxide Superconductors", *Chem. Mater.* **2**, 708 (1990)

P11 Thermoacoustic Natural Gas Liquefier

CONTRACT INFORMATION

Contract Number MC32073

Contractor

Los Alamos National Laboratory
Mail Stop K764
Los Alamos, NM 87545
(505) 665-0640
FAX (505) 665-7652

Contractor Project Manager Robert J. Hanold

Principal Investigator Gregory W. Swift

METC Project Manager Rodney D. Malone

Period of Performance Beginning March or April 1995

Schedule and Milestones

December 1994: Shakedown test of half-scale model thermoacoustic driver system at Los Alamos
June 1995: First operation of 500-gal/day prototype at Cryenco
June 1995: Shakedown test of heat exchanger test bed at Los Alamos

OBJECTIVES

In collaboration with Cryenco, Inc., and NIST-Boulder, we intend to develop a natural gas-powered natural-gas liquefier which has absolutely no moving parts and requires no electrical power. It will have high efficiency, remarkable reliability, and low cost.

BACKGROUND INFORMATION

Although most natural gas is still carried from well to user as gas in pipelines, the use of liquefied natural gas (LNG) has been increasing 10 to 15 percent per year. Large liquefaction plants and cryogenic storage tanks exist throughout the U.S. close to major consumption centers for seasonal peakshaving. In this practice, relatively constant flow of gas through pipelines from the gas fields to load centers can be maintained throughout the year by liquefying and storing the excess when demand is low in summer and regasifying it as needed when demand increases in winter. LNG ocean transport vessels of 10^5 m^3 capacity are also commonplace, as are attendant coastal LNG facilities. Fleet vehicle use of LNG as fuel is increasing rapidly.

With a liquefaction temperature of only 110 Kelvin, natural gas has (until now) required rather sophisticated refrigeration machinery. A typical modern, large liquefaction plant costs up to a billion dollars, liquefies 10^9 scfd, uses 15 percent of its throughput to power itself, and has substantial operating and maintenance costs.

The need for reliable, inexpensive liquefaction equipment is clear.

Our recent invention of the thermoacoustically driven pulse-tube refrigerator follows a long development of related devices, each directed toward elimination of moving parts from heat engines and refrigerators.

Stirling-cycle refrigeration, over a century old, has always required two moving pistons, one of which is in contact with the cold temperature. In 1963, Gifford and Longsworth discovered a refrigeration technique which eliminated the cold piston. They called this new technique pulse-tube refrigeration. In 1984, Mikulin made a significant fundamental advance, adding a flow impedance; such "orifice" pulse-tube refrigerators, developed largely at NIST-Boulder, now routinely reach 50 K in a single stage. The addition of a bypass valve to the pulse-tube refrigerator, discovered by Zhu, Wu, and Chen in 1990, can bring the efficiency of pulse-tube refrigerators up to that of Stirling refrigerators. The pulse-tube refrigerator's importance is primarily due to the elimination of the cold piston, a significant simplification leading to high reliability.

Until recently, pulse-tube refrigerators still required one moving piston, at ambient temperature. We have eliminated this last moving part, substituting for it a thermoacoustic engine. Thermoacoustic engines produce pressure oscillation from heat in an acoustic standing wave resonating at the frequency of the desired pressure oscillation. Although thermoacoustic devices were discovered and explained qualitatively a century ago, research at Los Alamos (sponsored by DOE/BES) has led to quantitative understanding and the first attempts at practical applications.

In short, the invention uses acoustic phenomena to produce refrigeration from heat, with no moving parts. The required apparatus comprises nothing more than heat exchangers and pipes, made of common materials, without exacting tolerances.

Los Alamos and NIST built the first thermoacoustically driven pulse-tube refrigerator several years ago, sponsored by SDIO and, hence, ultimately directed toward cooling infrared sensors on satellites. It reached 90 Kelvin and produced 5 watts of refrigeration at 120 Kelvin. A Los Alamos-NIST-Tektronix collaboration began in late 1992, to develop a much smaller version suitable for routine cooling of cryogenic electronics.

Applied to the liquefaction of natural gas, our Thermoacoustic Natural Gas Liquefier (TANGL) will offer unsurpassed reliability, enabling routine unattended liquefaction of gas at remote sites and at sites with unskilled personnel. Because TANGL has no exotic materials or close tolerances anywhere, its cost will be very low. It will be economical at a size far smaller than that of existing LNG equipment. The efficiency of small TANGLs will be reasonable, although not as high as that of conventional large-scale liquefiers: we expect the first 500-gal/day TANGL to use 30 percent of its throughput to power itself, and the first 10,000-gal/day TANGL to use about 20 percent of its throughput to power itself. (Later research will lead to improved efficiency.) It will operate silently. It will eliminate the easement and environmental conflicts attending pipeline construction.

These features will permit economical recovery of natural gas from the 10^3 small wells presently capped, representing an increase of a few % in domestic gas supply. A 10^6 scfd TANGL will fit on a flatbed truck and would require no electrical or other auxiliary power. It will fill a LNG transport truck trailer in a day, so the gas can be taken to market everyday by simply hauling an empty trailer out to the well, exchanging it for a full trailer, and returning to a

central facility. It will also enable economical liquefaction of natural gas at fueling stations for fleet vehicles.

If, as we expect, TANGL is far less expensive to build and to operate than existing gas liquefaction equipment, it may also enable economic recovery of the gas from many other sources, ranging from coalbed gas (gob gas) and oil production waste gas to livestock manure. It could also simplify long-term storage of LNG for emergencies at sites such as hospitals in earthquake-prone locations, and provide inexpensive liquefaction of other cryogens such as nitrogen and oxygen.

PROJECT DESCRIPTION

To develop the TANGL, we have formed a three-way partnership comprised of Cryenco, Inc., in Denver, Colorado, the National Institute of Standards and Technology (NIST) in Boulder, Colorado, and Los Alamos National Laboratory in New Mexico. Cryenco is a manufacturer of large cryogenic equipment, including cryogenic tank trucks and LNG vehicle-fueling equipment. Their goal in this partnership is to turn TANGL into a major new product line, and their engineering skills are crucial for the success of the project. Los Alamos and NIST will help Cryenco get started with this new technology and will work to steadily improve the efficiency of TANGL. Los Alamos has been the national center for fundamental research in thermoacoustics and holds most of the patents in the field. NIST is similarly the center for research in pulse-tube refrigeration.

During 1994, Cryenco licensed the relevant patents from Los Alamos, and CRADAs were signed between Cryenco and Los Alamos, and between Cryenco and NIST.

The first task in our joint work is the design, construction, and testing of a 500-gal/day (50,000 scfd) TANGL at Cryenco. This size will be suitable for Cryenco to gain direct experience with TANGL and is suitable for fleet vehicle-fueling applications. Success in this task will be measured by timely demonstration of the technology and by meeting the targeted efficiency (70 percent liquefied, 30 percent burned). (Ultimately, success here will be measured by Cryenco's timely reduction of TANGL to routine use and production.) In this task, Los Alamos is providing overall design of the thermoacoustic parts of the system, design, filling, and testing of the sodium heat pipes required to bring heat from the burner to the engine, selection of instrumentation, assistance in testing, and other assistance as seems appropriate. NIST is playing similar roles with respect to the pulse-tube refrigerator. Cryenco is providing all detailed engineering, system-integration planning and execution, and construction.

A second task will be the construction and testing of a 10,000-gal/day prototype at Cryenco. This should follow easily on the experience gained with the smaller TANGL described above. Here, we expect the roles of Los Alamos and NIST will be less important since we will have trained Cryenco personnel during the 500-gal/day task.

In parallel with the first task, and with increasing emphasis as the first task is completed, Los Alamos and NIST will proceed with fundamental studies directed toward improving the efficiencies of thermoacoustic and pulse-tube processes, respectively. At Los Alamos, fundamental theoretical work on thermoacoustics will continue, and two experimental systems are being built for studies leading to improved thermoacoustic efficiency. Success in these studies will be measured by transfer of improvements to Cryenco (with attendant improvement in efficiency of their prototypes and production TANGLs), by publication of the results in peer-reviewed scientific journals, and by subsequent

efficiency improvements in other applications of thermoacoustics.

To get us started, Los Alamos National Laboratory internal funds (LDRD-PD) have supported this project at a modest level. We expect to receive our first funds from DOE/Fossil for the project in March or April 1995.

RESULTS

Progress on the liquefier to be constructed at Cryenco continues satisfactorily. The thermoacoustic driver is still ahead of the pulse-tube refrigerator because of NIST's schedule. We completed the thermoacoustics design in the fall of 1994, with Los Alamos providing physics input and checks of all aspects, and Cryenco providing engineering to ASME code, drafting, etc. Completion of this design represents a significant amount of work, especially in view of the many unexpected problems encountered.

The most serious unexpected problem was the realization that a serious bottleneck existed in the fin effectiveness in the hot heat exchanger in the thermoacoustic driver. This heat exchanger will deliver heat to the helium gas, thereby driving the thermoacoustic engine. The heat will be delivered to this heat exchanger from the burner via an array of 55 sodium heat pipes.

All materials for the thermoacoustic driver are now present at Cryenco, and construction of the most risky components -- the stack and the heat pipes -- has begun. The heat pipes are being fabricated and assembled at Cryenco and are being filled with sodium, "broken in," and tested at Los Alamos (with Cryenco personnel assisting in order to learn the process).

Meanwhile, Cryenco and NIST have almost completed the design of the pulse-tube refrigerator.

At Los Alamos, we have assembled a half-size scale model of the thermoacoustic portion of the 500-gal/day TANGL. This is an exactly meaningful scale model, in the same sense that model airplanes tested in wind tunnels are exactly meaningful: measurements on the model will be exactly, directly applicable to the full-size system. The model will be much easier to modify than the full-size system because of its size, because it will be heated electrically instead of by combustion, and because it will be able to operate driving a dummy load instead of a pulse-tube refrigerator. This scale model will enable easy experimentation in harmonic suppression techniques, new stack geometries, new heat exchanger geometries, resonator coiling, and other areas. As of March 1995, the scale model is complete, and we are performing routine debugging tests and modifications.

The greatest shortcoming of current understanding of thermoacoustics is in our ability to predict details of heat transfer in the heat exchangers. Therefore, the second test apparatus at Los Alamos is a large, well-instrumented model of a thermoacoustic heat exchanger. This model apparatus will permit simultaneous measurements of instantaneous pressure, velocity, temperature, and heat flow, as functions of time and position, throughout the inside of the heat exchanger and nearby regions. It will serve as a test bed against which new theories of these phenomena can be compared. As of March 1995, this system is partly completed and is undergoing very preliminary component testing.

We have succeeded in developing a new computation algorithm for the thermodynamic behavior of oscillatory flow through stacks of screens such are used for regenerators in pulse-tube refrigerators. Conventional methods for computing such behavior involve time-stepping through the differential equations until a periodic steady state is found. Our new approach essentially assumes a steady state and forces a sinusoidal (in time) approximation on all

variables so that the time dependence of each variable is reduced to just two numbers: a magnitude and a phase. The code runs about 10,000 times faster than time-stepping codes, with comparable accuracy. The enhanced speed is going to lead to great improvement in design of multi-stage pulse-tube refrigerators (TANGL's pulse tube will be two stage). We are in the process of writing an article about the method.

FUTURE WORK

At Cryenco, assembly of the 500-gal/day prototype will proceed as quickly as possible.

At Los Alamos, the half-scale model of the thermoacoustic driver was run for the first time in December. Immediate minor problems turned up which are now under repair. This system is designed for relatively quick and inexpensive tests in support of Cryenco's efforts, and ultimately for experiments directed at higher efficiency. It is much easier to modify than Cryenco's full-size unit because it is smaller, is indoors, operates at lower pressure, has O-ring sealed flanges instead of welded joints, and is heated electrically (without heat pipes!) instead of by combustion of gas.

We have picked five initial sets of measurements for the half-scale model. First will simply be a set of baseline measurements, with no load on the driver; these should be routine. Second will be baseline measurements with a dummy load to simulate the load that the pulse-tube refrigerator will put on the real system. During these measurements we will also test a method of measuring the acoustic power delivered from the driver to the load; if it works, it will be easy to install such a system at Cryenco as well. Third will be measurements to determine acoustic power losses in reducing cones. Fourth will be measurements to learn the efficiency penalty associated with coiling the resonator, both with smooth curves and with mitered joints.

Fifth will be testing a new design for carrying heat from the burner to the thermoacoustic engine. Apparently the sodium heat pipe array will be the most expensive and potentially troublesome component of the thermoacoustic driver. Hence, we have begun exploring a radically different design that needs no heat pipes. We expect design and debugging of this design will be a major project.

Heat exchangers remain the least understood components of thermoacoustic systems. Our large heat exchanger test stand is over half completed. It will contain movable hot-wire anemometers and tiny, fast thermometers for measurement of instantaneous values of velocity and temperature in and around thermoacoustic heat exchangers.

We are in the middle of several other fundamental thermoacoustics developments: measurements of dissipation in oscillatory flow in curved tubes under a broad range of conditions; a perturbation expansion of the equations of thermohydrodynamics to second order in amplitude and fourth order in power; computer calculations of flow patterns and thermodynamic behavior at the interface between open ducts and heat exchangers.

REFERENCES

"A review of pulse-tube refrigeration," Ray Radebaugh, Adv. Cryogenic Eng. **35,** 1191 (1990).

"Thermoacoustic engines," G. W. Swift, J. Acoust. Soc. Am. **84,** 1145 (1988).

"Acoustic Cryocooler," C. W. Swift, R. A. Martin, and Ray Radebaugh, U.S. Patent No. 4,953,366, September 4, 1990.

"Development of a thermoacoustically driven orifice pulse tube refrigerator," Ray Radebaugh, K. M. McDermott, G. W. Swift, and R. A. Martin, Proc. 1990 Interagency Meeting on Cryocoolers, Plymouth, MA, October 24, 1990 (David Taylor Research Center publication DTRC-91/003, 1991).

P12 Fractal Modeling of Natural Fracture Networks

Contract Information

Contract Number	DE-FG21-94MC31182
Contractor	Research Corporation P. O. Box 6845 West Virginia University Morgantown, WV 26506-6315
Contract Project Manager	Martin V. Ferer
Principal Investigators	Martin V. Ferer Bruce H. Dean Charles E. Mick
METC Project Manager	Duane H. Smith
Period of Performance	June 1, 1994 to June 1, 1995
Schedule and Milestones	**FY 94/95 Program Schedule**

	J	J	A	S	O	N	D	J	F	M	A	M
Outcrop Analysis	———											
Code Development		———	———	———	———	———	———					
Borehole Data Analysis								———	———			
Borehole Simulation										———	———	

Objectives

West Virginia University will implement procedures for a fractal analysis of fractures in reservoirs. This procedure will be applied to fracture networks in outcrops and to fractures intersecting horizontal boreholes. The parameters resulting from this analysis will be used to generate synthetic fracture networks with the same fractal characteristics as the real networks.

Background

Recovery from naturally fractured, tight-gas reservoirs is controlled by the fracture network.[1] Reliable characterization of the actual fracture network in the reservoir is severely limited. The location and orientation of fractures intersecting the borehole can be determined, but the length of these fractures cannot be unambiguously determined. Fracture networks can be

determined for outcrops, but there is little reason to believe that the network in the reservoir should be identical because of the differences in stresses and history. Seismic techniques do provide some large scale (resolution of tens or hundreds of feet) information about the fracture density and average fracture orientation, although there is some controversy about interpretation of the multi-component surface seismic data, especially regarding which layer is being probed.

Furthermore, independent of the assumption of fractal behavior, it is known that typical fractures in the second set should begin and end at fractures of the first set.[2] This effect is commonly observed in real fracture networks from outcrop studies, for example 92% of the secondary fractures in the MWX outcrop (Fig. 1) satisfy this criterion.[3] Imposing this constraint upon the secondary fractures increases the visual similarity between our networks and the real network over simulated networks from other fractal modeling schemes.[4]

Because of the lack of detailed information about the actual fracture network, modeling methods must represent the porosity and permeability associated with the fracture network, as accurately as possible with very little apriori information. Three rather different types of approaches have been used: i) dual porosity simulations, ii)'stochastic' modeling of fracture networks, and iii) fractal modeling of fracture networks. The dual porosity approach is a natural extension of the gridding schemes widely used in describing reservoirs, however in assuming mesoscopic scale (tens or hundreds of feet) averages of fracture porosities and permeabilities, they may be smoothing the very heterogeneities which control the recovery. This may limit reliability for strongly anisotropic fracturing. That is, even if fractures are located randomly throughout the grid-block so that an average porosity may be sensible, the conductivity of similar fractures differ widely invalidating assumptions of an average permeability.

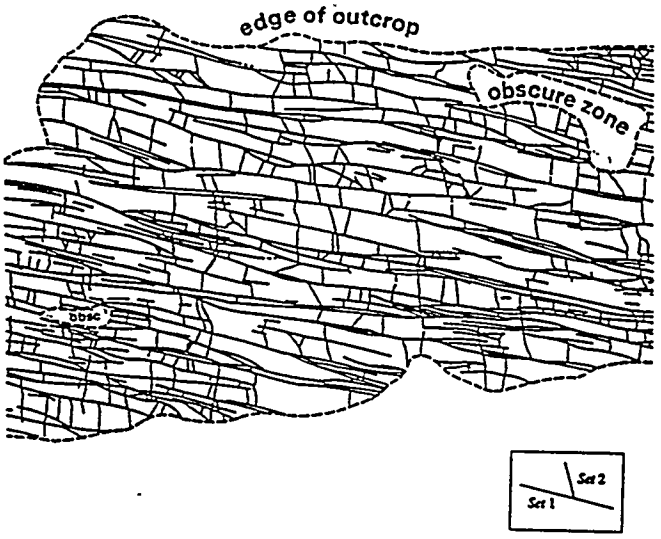

Figure 1 Outcrop Fractures at MWX site. Shows the primary fractures (set 1) and the secondary fractures (set 2).

Stochastic models which assume a variety of probability distributions of fracture characteristics have been used with some success in modeling fracture networks.[5-7] The advantage of these stochastic models over the dual porosity simulations is that real fracture hetero-geneities are included in the modeling process. On the other hand these

stochastic models need information about all features of the actual fracture network to provide the most accurate modeling. In the highest level (most accurate) model for each set of fractures with a given orientation, one needs to determine the probability distribution of i) the location of independent fractures ii) the location of fracture clusters or swarms iii) locations of fractures within clusters, iv) cluster lengths, v) fracture lengths, vi) fracture apertures, and vii) fracture orientations. The less reliable the information determining these probability distributions; the less reliable the fracture network. Reliable information about many aspects of the real fracture network is impossible to determine; the assumption of self-similar fractal behavior (if valid) enables us to predict features of one aspect of the distribution from other aspects of the distribution; i.e. i), ii), and iii) result from the box-counting along the borehole which, in turn, predicts features of the distributions for iv), v), and vi) for self-similar fractal networks.

Aspects of fractal geometry have been applied to mimic the heterogeneity associated with layering in real reservoirs for a number of years. In these cases, the variation in permeability with height at the borehole was found to obey fractal statistics,[8] and the correlations implicit in fractal geometries allowed them to interpolate between the known permeabilities at the borehole in such a way that results from flow models agreed with analyses of production logs and tracer breakthrough.[9] Examples in the open literature reporting the use of fractal geostatistics to treat naturally fractured reservoirs are less common.[4,10] If a set of natural fractures is described by a self-similar fractal geometry, the self-similar, scale invariance of the fracture network implies relationships among the fracture distribution, and the various length scales: clustering or fracture correlation, fracture aperture, and fracture length. Therefore, if fracture networks obey a self-similar fractal geometry, borehole data locating orientational sets of fractures, will enable a determination of the fractal dimension and 'lacunarity'. This along with relatively generic information about the typical aperture size and length of fractures,[1] will allow us to produce a self-similar fractal network. The clustering occurs naturally in the fractal network because of the correlations inherent in fractal geometries. The fractal parts of the aperture size and length distributions (even the fracture shape distributions) should be the same as the fractal parts of the fracture location vs. scale distributions.

In the sections following this introduction, we will i) present 'fractal' analysis of the MWX site, using the box-counting procedure[11,12]; ii) review evidence testing the fractal nature of fracture distributions and discuss the advantages of using our 'fractal' analysis over a stochastic analysis; iii) present an efficient algorithm for producing a self-similar fracture networks which mimic the real MWX outcrop fracture network.

Project Description-Fractal Analysis

Illustrative Example Before analyzing the MWX outcrop (Fig. 1), one must understand the box-counting

in our method for generating the fracture networks. As discussed later in this section, the box-counting procedure automatically reproduces the random aspects of the distribution of fractures in addition to reproducing the clustering obvious in Fig. 1.

For a simple example of the box-counting procedure consider the distribution of fractures intersecting a length of borehole. To determine the fractal dimension as well as the range of size scales over which the distribution is fractal, one covers the array of fractures by successively smaller and smaller rulers (one-dimensional 'boxes'), and then one counts the number of 'boxes' or rulers covering one or more fractures. If the distribution has a fractal dimension D_f over a range of sizes, then

$$N = A(\Delta)^{D_f}, \qquad (1)$$

where N is the number of rulers which cover fractures, the constant A is called the lacunarity, and the scale Δ determines the length of the rulers (L/Δ). If one covers the 24 fractures in Fig. (2) by a ruler of length L , (shown at the bottom of Fig. 2) one ruler covers the fractures; with two ruler of length L/2 (near the bottom of Fig. 2) both cover fractures; with four rulers of length L/4 all 4 cover fractures, but with 8 rulers of length L/8 only 6 cover fractures. This is continued down to 128 rulers of length L/128 as shown in Table 1.

Figure 2a Fractures intersecting a borehole.

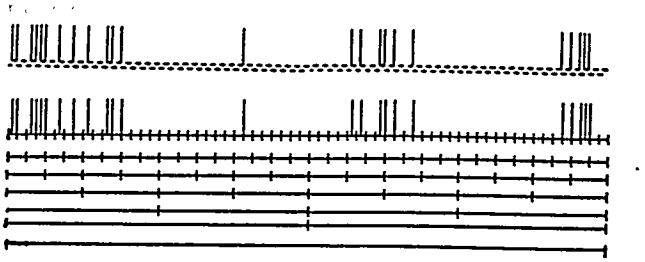

Figure 2b The lower half of the figure shows the fractures in Fig. 2a with the scale rulers 'covering' the set of fractures from a ruler of length L, proceeding upwards to rulers of length L/64 just below the fractures. The top half shows the same set of 'covering' rulers of length L/128. The rulers are left-justified so that the fractures at the right-end of the ruler are covered by the ruler.

Table I

Ruler Length	# of Rulers Covered
L/Δ	N
L	1
L/2	2
L/4	4
L/8	6
L/16	8
L/32	13
L/64	17
L/128	24
L/256	24
L/1024	24

Since there are only 24 fractures, at scales smaller than L/128, there will

only be 24 rulers covering fractures. A log-log plot of the box-counting for Fig. 2 is shown below

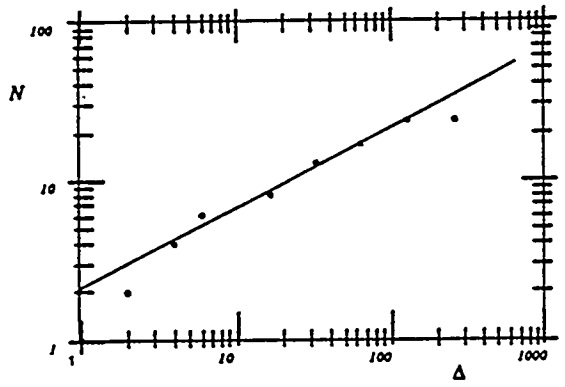

Figure 3 Fractal Plot for Fig. 2.

The fractal relationship is given by the solid line $N = 2.12\ \Delta^{0.5}$, except at large and small scales for the reasons that follow. At small Δ, (coarse scales L, L/2 and L/4), N equals the number of rulers ($N = \Delta$) because all the rulers cover fractures; in later sections, we refer to this as the initial covering regime. At very large Δ, (very fine scales L/256 and L/1024), only 24 rulers are covered because there are only 24 fractures and there is no more detail in the fracture pattern, so that the box-counting 'cuts-off' or 'saturates' at 24. Therefore, for this fracture pattern, the pattern is fractal between the initial covering and cutoff regimes (over the range of scales Δ = 8 to 128) with a fractal dimension of 1.5 and a lacunarity of 2.12. The ruler counting of this one-dimensional slice of the two-dimensional fracture network gives an exponent D_f - 1, i.e. the actual 2d fractal dimension minus one.

Before we continue, it should be pointed out that this fracture pattern was generated by our algorithm to have a lacunarity of 2.12 and a fractal dimension of 0.5 over the range of scales from L/8 to L/128. The algorithm which generated this pattern is described and used in a following section.

It is important to realize that if the distribution of fractures in Fig. 2 were completely random (i.e., if there were no clustering of fractures), the points from the box-counting would obey a linear relationship ($N = \Delta$) up to cutoff. That is, on the average, each box would contain one fracture up to the total number of fractures (in this case $N_{total} = 24$); at finer scales, the one fracture would randomly occupy one of the smaller boxes. However, because of clustering, groups of fractures are closer together than average. Therefore, when box-counting, the linear regime ends before $N = N_{total}$; and one enters the 'fractal' or clustering regime where some boxes are empty and others have several fractures much closer together than average. The box-counting provides a routine procedure for characterizing (and, thus, for reproducing) this clustering.

Results

MWX Outcrop First the primary set of fractures in Fig. 1 was analyzed. A series of eight lines (boreholes) of length L were drawn through the set of primary fractures, and the box-counting procedure was used on each of these boreholes. The results for the number of boxes covering fractures vs. the scale Δ is shown in Fig. 4. The initial covering regime persisted until scale 16. The cutoff regime began at scale 80. In-between the data are well represented

by the fractal power law $N = 4.9\ \Delta^{0.425}$, indicating a fractal dimension $D_f = 1.43$. It should be noted that scales intermediate to the simple doubling rule, $\Delta = 2^n$, (used in Figs. 2 & 3 and Table 1) were used to provide more data in the fractal regime.

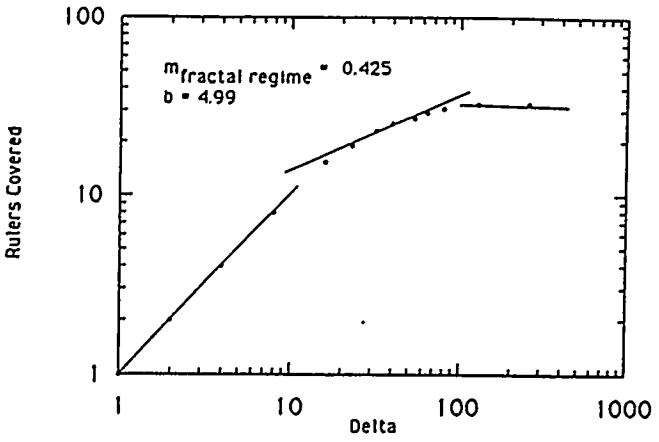

Figure 4. For the primary fractures, the box-counting from the 'boreholes' on the MWX outcrop (Fig. 1), shows the initial covering (the linear increase, $N = \Delta$, up to the clustering or fractal regime), the fractal regime, and the cutoff regime.

The secondary set of fractures in Fig. 1 were analyzed in the same way. A series lines of length L, perpendicular to these secondary fractures, were drawn through the secondary fractures, the box counting was performed and the values $N(\Delta)$ were averaged. Fig. 5 shows the plot of N vs. Δ and shows that for these secondary fractures the initial covering regime persists until scale 6 and that the cutoff regime begins at scale 40. In-between the number of rulers obeys the fractal power law $N = 3.47\ \Delta^{0.343}$, indicating a fractal dimension $D_f = 1.34$. Again, intermediate scales were used in the fractal regime to provide more data in the fractal regime.

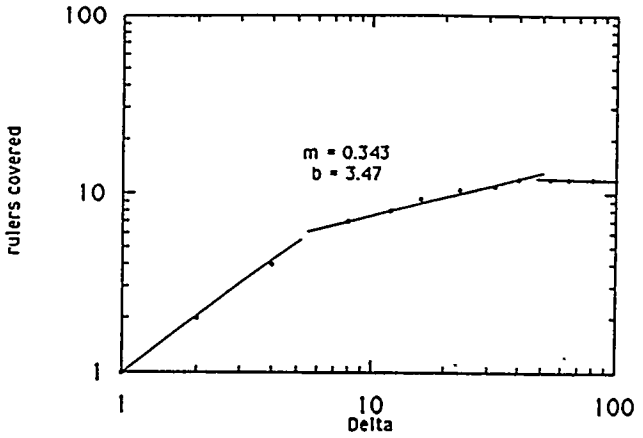

Figure 5. For the secondary fractures, the box-counting from the 'boreholes' on the MWX outcrop (Fig.1), shows the initial covering (the characteristic linear regime), the fractal regime, and the cutoff regime.

To determine the length distribution from the data provided by M. McKoy,[3] we plotted the total number of fractures with lengths greater than a given length L, N(L), vs. L. It should be noted that this total number N(L) with lengths $\ell > L$ is the integral of the number density of fractures $n(\ell)$ with length ℓ integrated from $\ell = L$ up to the one fracture of maximum length , i.e. $N(L) = \int_L^{L_{max}} n(\ell)\, d\ell$. This graph of the data is shown in Fig. 6. It is convincingly fit by the characteristic exponential cutoff for the greatest lengths (L>14), and by a fractal power law for the smallest lengths (4<L<14). For a self-similar fractal fracture network, the number density

should be given by $n(\ell)=\eta\ \ell^{-D_f}$ so that the total number should be given by $N(L)=\frac{\eta}{1-D_f} L^{1-D_f}$.[11] Therefore, the data are consistent with a fractal dimension $D_f=1.48$.

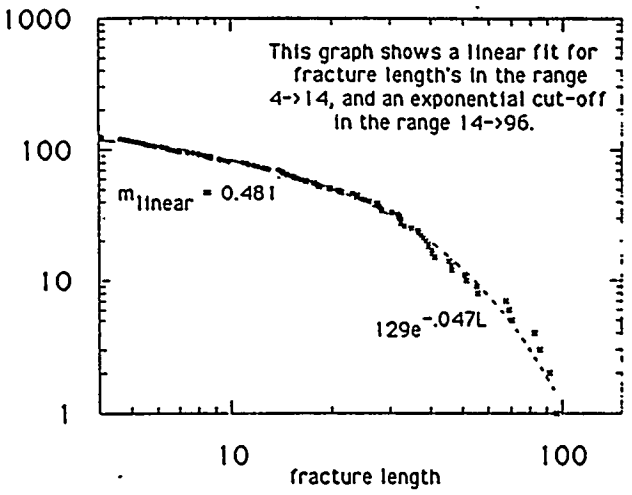

Figure 6. The number of fractures N(L) with lengths greater than L plotted against L. This shows the exponential cutoff for the larger lengths and the fractal regime for the smaller lengths.

These data do not decide unambiguously whether or not the clustering regime is rigorously fractal. That is, these data do not unambiguously favor a strictly power law regime (i.e. fractal behavior) between the linear, initial covering regime and cutoff. However, the power law assumption used to draw the lines does represent a good fit to the box-counting data. Therefore, at worst, by assuming that the intermediate regime is fractal, we may be merely providing a good approximation to the data. If the assumption of fractal clustering only provides a good approximation to the true clustering, our simulated fracture networks will represent a good approximation to the actual fracture network, which is all that is necessary.

On the other hand, it is encouraging that the power laws from the box counting and length distributions are all consistent with the same fractal dimension, $D_f=1.4\pm0.1$, to within a realistic uncertainty from the data fitting. This equality of fractal dimensions from all length measures is the hallmark of self-similar fracture networks.

A program to carry out the box-counting procedure and return the fractal dimension and lacunarity has been developed in order to process multiple sets of data from various boreholes. To test these programs as well as the routines for simulating the fracture networks, numerous trial runs have been performed to analyze the "borehole fractures" from simulated networks.

Are Fractures Fractal? There is evidence that real fracture networks are fractal both in outcrops where Barton and others found a fractal dimension of $D_f\approx1.55$, for different fracture systems,[13] as well as from underground data in the Fanay-Augères uranium mine[10] where they found a varying fractal dimension. The variation in their fractal dimension may result from use of too great a range of scales. As we saw for very large scales, all the rulers are covered so their finding a 'fractal dimension' of 2 at large scales is not surprising. Similarly, at very small scales one approaches a limit where the number of 'boxes' covered equals the number of fractures so the

fractal dimension approaches 1; this may be an artifact of the neglect of small aperture fractures (micro-cracks which may be significant in determining number at their 0.005 meter scale).

The length of the fractures has been found to be fractal,[14] and the shape of the fractures has also been determined to be fractal[15-17]. This suggests that all features of the fractures may be fractal: distributions of i) centers, ii) lengths, iii)widths, and iv) shapes. The evidence that the shapes are fractal suggests that porosities and permeabilities may also obey fractal statistics. If all geometrical aspects of the fracture distribution are fractal with the same fractal dimension, the fracture distribution is self-similar. This may seem to be a very unusual occurrence, but in fact many examples of development (or growth) which occur in random media (like the development of fractures in stressed rock formations) have a self-similar geometry. The first level of our geostatistical modeling will assume a self-similar fractal geometry for the fracture distribution. Higher levels of our geostatistical modeling could use actual measurements to determine the fractal distribution of (e.g.) the fracture widths.

Fracture Generation Algorithm

Here, we describe the implementation and design of an algorithm developed to generate a fracture network in 2-dimensions. The primary assumption in our model is that the network geometry is fractal - i.e. has a self-similar or scale invariant geometry. Using this information we have developed a program to generate complete 2-d fracture outcrop networks using only the lacunarity, fractal dimension, initial covering, and cutoff parameters obtained from MWX data.

In the broadest sense the program performs 2 tasks :

(1) Generates a horizontal fracture set.
(2) Generates a secondary fracture set consistent with the fracture set in (1)

To generate the primary fracture set the program first generates a 1-dimensional fracture set along a left-justified line

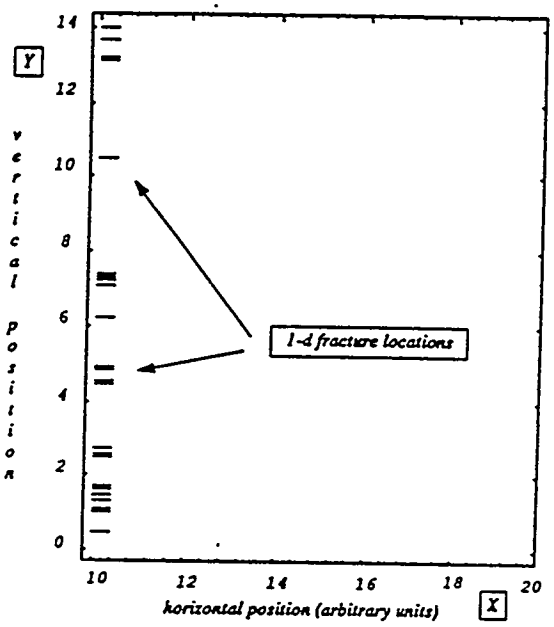

Figure 7. 1-d fracture generation output. The data are represented graphically by a series of small line segments in the x direction.

perpendicular to this fracture set, Fig. 7. This is accomplished by a procedure, the first step of which initializes the first row

in the 2-dimensional ruler array L[j,k], where i labels the scale and k labels the ruler. If a fracture is covered by a ruler, then the value of the array for this specific ruler is 1. Conversely, an empty ruler site is given the value 0.

Having initialized the L[1,i] array the procedure then divides each ruler into two new rulers and randomly chooses one of these 2 new rulers in L[2,k] for each of the covered rulers in L[1,i] and assigns this ruler a value of 1 while giving the other ruler a value of 0. The remaining rulers are randomly assigned fractures according to the distribution. This proceeds to finer and finer scale until saturation is reached.

Continuing with the generation of the primary fracture set, the program assigns a length to each fracture site according to the length distribution shown in Fig.6. Once the length of a fracture is chosen, the exact location of the origin (x=0) along the fracture is chosen randomly. The result is shown in Fig. 8.

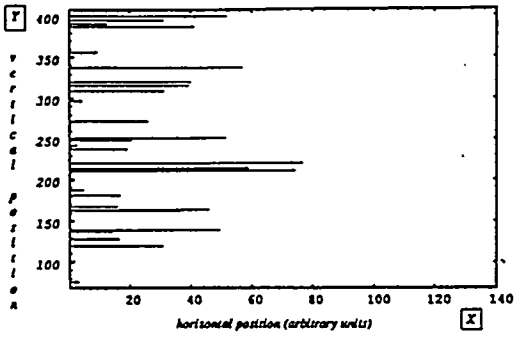

Figure 8. Lengths are assigned to the initial fracture set.

Having assigned lengths, the program will step forward by a specified amount in the x-direction (along the fractures). If any fractures have ended during the step, new fracture assignments must be made to maintain the distribution. To guarantee that the new fracture assignments produce a fractal distribution, we must reverse the ruler doubling process and re-assign fractures that have crossed the specified grid point to half as many rulers used in the final step of the initial 1-d fracture generation process. The unoccupied fracture sites are then assigned new fractures following the same procedure described for the initial fracture generation. The procedure continues stepping along in the x-direction until the full region is characterized.

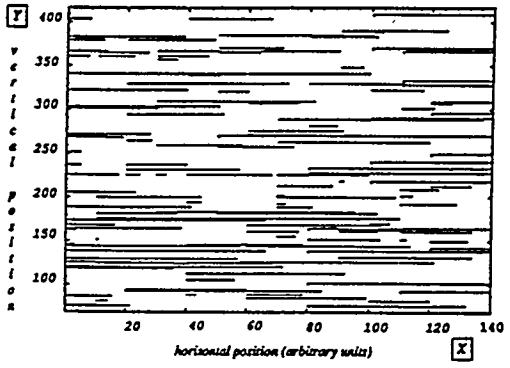

Figure 9. Primary Fractures-Simulated

The resulting output is given in Fig. 9 and can be compared with the MWX primary fractures shown in Fig. 1. The parameters used were those determined from the MWX outcrop using the box counting procedures described earlier.

To generate the secondary fracture set we first generate a fracture distribution along each of the horizontal fractures.

Starting in the upper left hand corner of Fig. 9 and proceeding downward, the program produces a fractal distribution (using a parameter set determined from the vertical fracture data) along the first fracture in the data set. In our model we assume that vertical fractures can only begin or end along a horizontal fracture. In this case, we need only find the next horizontal fracture below each vertical fracture site to determine the fracture endpoint and therefore its length.

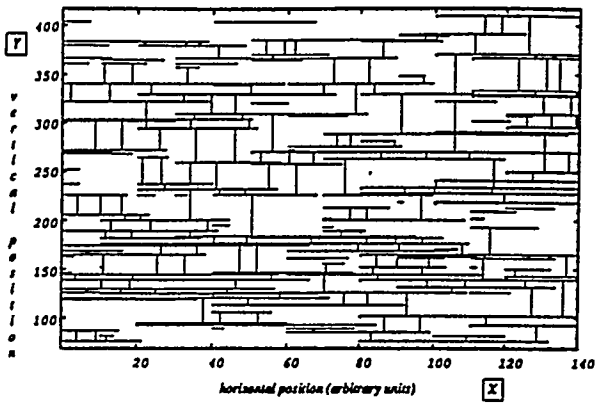

Fig. 10. MWX 2-d Fracture Outcrop Data

Conclusions & Future Work

To model the fracture outcrop networks occurring in naturally fractured tight-gas reservoirs we have taken an approach that incorporates:

A) Fractal Analysis of Available Data:
we characterized the MWX fracture data using four parameters (for the distribution of both horizontal and vertical fractures): i) Lacunarity, ii) Fractal Dimension, iii) Initial Covering Scale, and iv) Cutoff - determined from the distribution of fracture lengths.

B) Fracture Generation:
we generate self-similar fracture networks using data from I.) with an algorithm that incorporates fractal geostatistics.

From our work we have found that there are several advantages in an approach that uses fractal statistics:

i) The networks produced by our model appear to be in agreement with actual fracture networks but do not require extensive a-priori knowledge of the network. Using data from isolated borehole sites we can generate entire networks with an algorithm that assumes a self-similar or scale invariant geometry.

ii) We are able to generate horizontal and vertical fractures separately (although not independently) using distinct parameter sets in each case. The fractures can then be analyzed and combined later to produce complete self-consistent networks.

iii) Since the data is generated using a statistical approach, the algorithms require relatively little computer time to produce complete networks

iv) Evidence suggests that real fracture networks obey fractal statistics.

The characterization and analysis of the network data produced by our algorithms is not yet complete. By varying other parameters such as gridsize, fracture length, and the horizontal/vertical orientation of fractures, we believe that it will be

possible to generate fracture distribution patterns that are 'optimally similar' in the fractal/statistical sense - to real fracture networks occurring in nature.

We are in the process of analyzing the distribution of fractures along horizontal boreholes in the Austin Chalk and fracture lengths from nearby outcrops. The results from this analysis will be used to generate simulated fracture networks.

References

1. Skopec, R. A., JPT. December 1993, 1168, (1993).
2. Davidge, R. W. "Mechanical Behavior of Ceramics." 1979 Cambridge University Press. New York.
3. McKoy, M., private communication. (1994).
4. Xie, H. "Fractals in Rock Mechanics." Geomechanics Research Series. Kwasniewski ed. 1993 A. A. Balkema. Rotterdam.
5. McKoy, M., Development of Stochastic Fracture Porosity Models and Application to the Recovery Efficiency Test (RET #1) Well in Wayne County, West Virginia (1993).
6. Long, J. C. S. and D. M. Billaux, Wat. Resources Res. 23, 1201, (1987).
7. Billaux, D., J. P. Chilès, K. Hestir and J. C. S. Long, Int. J. Rock Mech., Min. Sci. & Geomech. Abstr. 26, 281, (1989).
8. Hewett, T. A. "SPE 15386 Fractal Geostatistics for reservoir hetero's." 1986 Soc. of Pet. Eng. Richardson,TX.
9. Matthews, J. L., A. S. Emanuel and K. A. Edwards, JPT. 1139, (1989).
10. Chilès, J., Math. Geol. 20, 631, (1988).
11. Feder, J. "Fractals." 1988 Plenum Press. New York.
12. Mandelbrot, B. B. "The Fractal Geometry of Nature." 1982 W. H. Freeman Publishers. New York.
13. LaPointe, P. R., Int. J. Rock Mech., Min. Sci. & Geomech. Abstr. . 25, 421, (1988).
14. Heffer, K. J. and T. G. Bevan, fracture length scaling (1990).
15. Roach, D. E., A. D. Fowler and W. K. Fyson, Geology. 21, 759, (1993).
16. Roach, D. E. and A. D. Fowler, Computers & Geosci. 19, 849, (1993).
17. Maloy, K. J., A. Hansen, E. L. Hinrichsen and S. Roux, Phys. Rev. Lett. 213, (1992).

P13 The Development of a Pulsed Laser Imaging System for Natural Gas Leak Detection

CONTRACT INFORMATION

Contract Number DE-AC04-94AL85000

Contractor

Sandia National Laboratories
PO Box 969 MS-9057
Livermore, CA 94551-0969
(510) 294-3676 (telephone)
(510) 294-2276 (fax)

Other Funding Sources Gas Research Institute

Contractor Project Manager Thomas J. Kulp

Principle Investigator Thomas J. Kulp

Metairie Project Manager Gene Pauling
(504) 734-4131

Gas Research Institute Project Manager Tom Altpeter
(312) 399-8196

Period of Performance October 1, 1994 - September 30, 1995

Schedule and Milestones

FY95 Program Schedule

	O	N	D	J	F	M	A	M	J	J	A	S
Focal-plane array survey	----------											
Evaluation plan formulation			--------									
Pulsed quantum efficiency test			----------									
Noise/background rejection test			----------									
Imaging wavelength selection			----------									
Camera purchase and breadboard assembly										----------		
Methane imaging tests in lab											--------->	
Range test model verification											--------->	
Differential imaging demonstration											--------->	

OBJECTIVES

In this co-funded DOE/GRI project we are developing a new technology that will produce dynamic video images of natural gas leaks. Based on laser remote sensing, it would be capable of operation from a stationary or moving platform while instantaneously detecting gas leaks at any

point within a large area. This gas leak imaging technology would be particularly useful in the gas industry, where complex or extensive gas piping must be routinely surveyed for leaks. This new approach would offer significant increases in leak survey speed and effectiveness over that attainable with state-of-the-art leak survey detectors. Potential benefits would include: (1) significant reduction in survey costs; (2) minimization of gas lost to leaks; and (3) further enhancement of the achievable level of safety within the gas industry. Industry-wide reductions in methane emissions would have a positive impact on the attainment of several national goals such as energy conservation and the mitigation of global warming. If the proposed technology can be successfully developed for natural gas detection, it should be possible to further extend the concept to the detection of other harmful or toxic gases and vapors in the environment.

A multi-phase program leading to the eventual transfer of this technology to industry for commercialization is envisioned. This project covers the first phase in which a demonstration of laboratory feasibility for the leak visualization technology would be accomplished. If successful, it is anticipated that the feasibility studies would be completed with subsequent field trials of a prototype instrument. Further efforts, if warranted, would lead to a preproduction prototype, final field testing, and technology transfer.

It is anticipated that the product of this advanced gas detection technology could operate from a stationary and/or a moving platform. The latter might include van-mounted systems for application in local utilities, or aerial-mounted systems for surveys of transmission pipelines. The remote sensing capability of the technology would also facilitate the inspection (from a stationary platform) of gas processing equipment and above-ground piping at locations such as metering stations, regulator stations, compressor stations, and LNG and storage facilities. Finally, the successful development of an improved gas leak detection technique should allow additional applications for the remote sensing of numerous other hazardous or harmful gases.

BACKGROUND INFORMATION

Status of Gas Imaging for Natural Gas Leak Detection

The detection of gas leaks represents a critical operation performed regularly by the gas industry to maintain the integrity and safety of its vast network of piping, both above and below the ground. Below-ground piping includes approximately 400,000 miles of transmission pipelines and 1.4 million miles of distribution piping, while above-ground piping is located mainly at 725-750 gas processing plants and some 8000 compressor stations. Whether addressing above or below ground gas sources, leak surveying with state-of-the-art gas detectors (i.e., flame ionization detector-based sniffers) can be a time-consuming operation of uncertain effectiveness.

To address the need for a more effective and efficient means of locating fugitive natural gas leaks, we are developing a technology that allows the real-time imaging of gas plumes in a television format. Termed backscatter absorption gas imaging (BAGI), the technique operates by illuminating a scene with infrared laser radiation having a wavelength that is absorbed by the gas to be detected (in this case, methane). Backscattered laser radiation is used to create a video image of the scene. If a leak of the target gas is present in the field-of-view of the camera, it attenuates a portion of the backscatter and creates a dark cloud in the video picture (see Figure 1).

The specific goal of this project is to investigate a new method of accomplishing BAGI using a pulsed laser source. Our motivation is to

Figure 1 - Photograph illustrating the operation of the first generation BAGI system imaging a leak of Freon 12.

ultimately generate a natural gas imager that has sufficient range and sensitivity to be useful to the gas industry. The efficacy of applying a first-generation BAGI technology to the detection of natural gas leaks has already been demonstrated in a program funded by the Gas Research Institute. That project used a first-generation gas imager that was developed at Lawrence Livermore National Laboratories (LLNL) [1-4] and transferred to Laser Imaging Systems (LIS, Punta Gorda, FL) where it was adapted for methane imaging. The first generation technology accomplishes laser-illuminated imaging by scanning a continuous-wave infrared laser (infrared helium-neon laser, emitting at 3.39 μm) across a scene at real-time video rates as the scene is imaged by a scanned infrared camera. The scanned BAGI imager was able to detect methane plumes at concentrations of ≥ 20 ppm-m in applications of interest to the natural gas industry. As will be described in following sections, the primary performance limitation of that system was its short imaging range (6 m) which resulted from the weak output energy of the helium neon laser and some undesirable aspects of the scanning optical arrangement.

Due to its use of more suitable laser sources and detection systems, the pulsed laser imager under development in this project is expected to have a range (≥ 40 m) and sensitivity (<10 ppm-m) that will surpass the respective attributes of the scanned imager. The pulsed system will operate by flooding (rather than scanning) the imaged scene with pulses of laser radiation. Imaging will be accomplished using a focal-plane array camera that operates in a snapshot format. The higher power of the pulsed laser source and the more effective collection optics of the focal-plane array-based receiver will allow the performance enhancements to be achieved.

First Generation Gas Imaging Technology

Figure 2 contains a diagram that illustrates the operation of the first-generation scanned BAGI technology. That system is essentially a flying-spot infrared imaging radiometer that was modified to scan the beam of a continuous-wave (cw) laser in synchrony with the scan of the instantaneous field-of-view (IFOV) of its single-element IR detector. As indicated in the figure, the scan occurs in a raster pattern that is carried out at video rates, thus providing a real-time laser-illuminated image of the scene. Gas plumes present in the scene absorb the laser light and generate dark cloud images in the video picture. The physical device that produces the raster scan consists of a pair of galvanometrically-swept scan mirrors. The horizontal mirror operates at a scan rate of 3933 Hz, providing the horizontal dimension of the video image while the vertical mirror sweeps at a frequency of 60 Hz, to produce the vertical dimension of the picture. The combined motion of the two mirrors produces the raster scan. The dimensions of the system field-of-view can be varied up to a full scan angle of 18° in the horizontal dimension. More specific

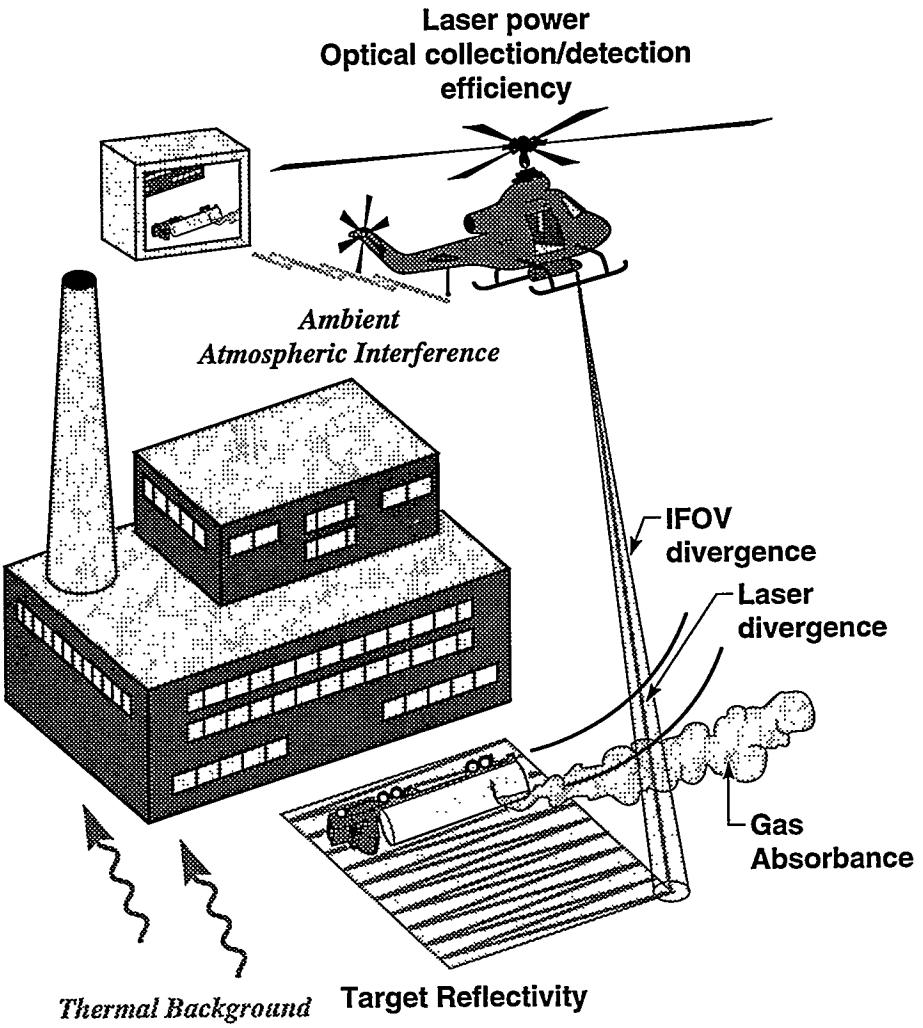

Figure 2 - Schematic of the first-generation scanned gas imager operation.

details regarding the imager hardware are provided in Refs. 1-4.

The original BAGI imager operated using a CO_2 laser emitting between 9 and 11 μm and was able to image ~80 gases at densities of ~ 1 to 100's of ppm-m. Because the imager detects gases via path integrated absorption, concentrations must be stated in ppm-m— i.e., a gas that is detectable at 1 ppm-m can be seen at a concentration of 1 ppm if the gas plume is 1 m thick, and 2 ppm if the plume is 0.5 m thick.

The scanned BAGI imager was converted by LIS to allow it to operate with a 3.39 μm wavelength (the absorption wavelength of methane) helium neon laser source. That imager was demonstrated to image methane at concentrations as low as 20 ppm-m and was successfully tested at a number of above and below ground leak locations. These included (1) a test at a sensor intercomparison trial coordinated by Pacific Gas and Electric (PG&E) involving the detection of leaks in below-ground pipes pressurized to 50 psi with natural gas, (2) a demonstration of the ability to image below-ground Class 3 or 4 leaks located in residential

natural gas distribution systems at Charleston, SC and Sarasota, FL, and (3) a demonstration of the ability to image above-ground leaks at compressor stations in Orlando, FL. Information regarding these trials can be obtained through GRI or LIS.

While extremely successful at short-range leak detection, the imager was found to be limited in certain aspects of its performance. These limitations arise from the use of the scanned imaging method and are enumerated as follows:

(1) The range is limited to 6-m because of the low power (30 mW) of the IR helium neon laser. This is the highest power cw laser that is currently available that operates at a methane absorption line. The scanned imager must operate with a cw laser.

(2) Range is also limited because the optical collection aperture of the scanner is constrained to a diameter of 1.2 cm, which is the size of the horizontal scan mirror. The aperture diameter determines the amount of light that is collected.

(3) The field-of-view of the imager cannot exceed 18 degrees, which is the maximum amplitude of the horizontal scan mirror.

(4) The spatial resolution of the imager is limited because the imager cannot achieve a true optical zoom. An effective zoom is accomplished by reducing the amplitude of the scan mirror motion. However, although this reduces the field-of-view, the size of the laser spot and IFOV remain the same. Thus, the spatial resolution is not increased when zooming the image field-of-view.

Limitations in range, resolution, and field-of-view directly influence the ability of the imager to rapidly search for gas leaks. Recognition of these limitations motivated the current research effort, in which a pulsed laser imager for natural gas leak detection is being developed. As described in the following section, we believe that the performance of an imager that operates in a pulsed mode can substantially exceed that of the cw system.

PROJECT DESCRIPTION

Our approach to improve the performance of methane imaging will be to create a new implementation of BAGI that uses a pulsed laser and a synchronously-gated focal-plane array (SGFPA) detector. The operation of this device is illustrated in Figure 3. Rather than use the scanning approach of the first imager, the pulsed 3.39-μm laser beam is expanded to flood the entire field-of-view of the SGFPA camera. The illuminated region is imaged directly on the focal-plane array sensor with a conventional lens. The initiation of the pulse emitted by the laser is synchronized with the opening of a gate on the SGFPA camera. The gate is effectively a shutter whose opening causes the camera to integrate the return signal and generate a frame of video. Thus, the operation of the pulsed system is analogous to that of a shuttered camera and a flashbulb. The frame acquisition will occur at 30 Hz to generate real-time video imagery. To accommodate this mode of operation, the SGFPA camera that is used must be capable of integrating the entire frame of pixels simultaneously with high efficiency (i.e., it must be a "snapshot" focal plane array). To prevent the collection of excessive levels of passive background radiation, it must also be capable of short integration times. The specification and construction of an appropriate SGFPA camera is the initial focus of the research in this project.

The advantages associated with a pulsed imager arise from attributes of both the pulsed laser transmitter and the SGFPA detector. A primary benefit of pulsed lasers is the facility with which they can be used to achieve nonlinear frequency conversion. Nonlinear conversions

allow new laser wavelengths to be generated via frequency multiplication, differencing, or parametric oscillation. The efficiency of nonlinear generation is directly related to the peak power of the pump beam and is, thus, vastly improved with high instantaneous power pulsed sources. Nonlinear conversion can be accomplished with cw beams—however, this usually requires intracavity methods that are highly sensitive to environment and in which continuously high intracavity power densities can easily damage optical crystals.

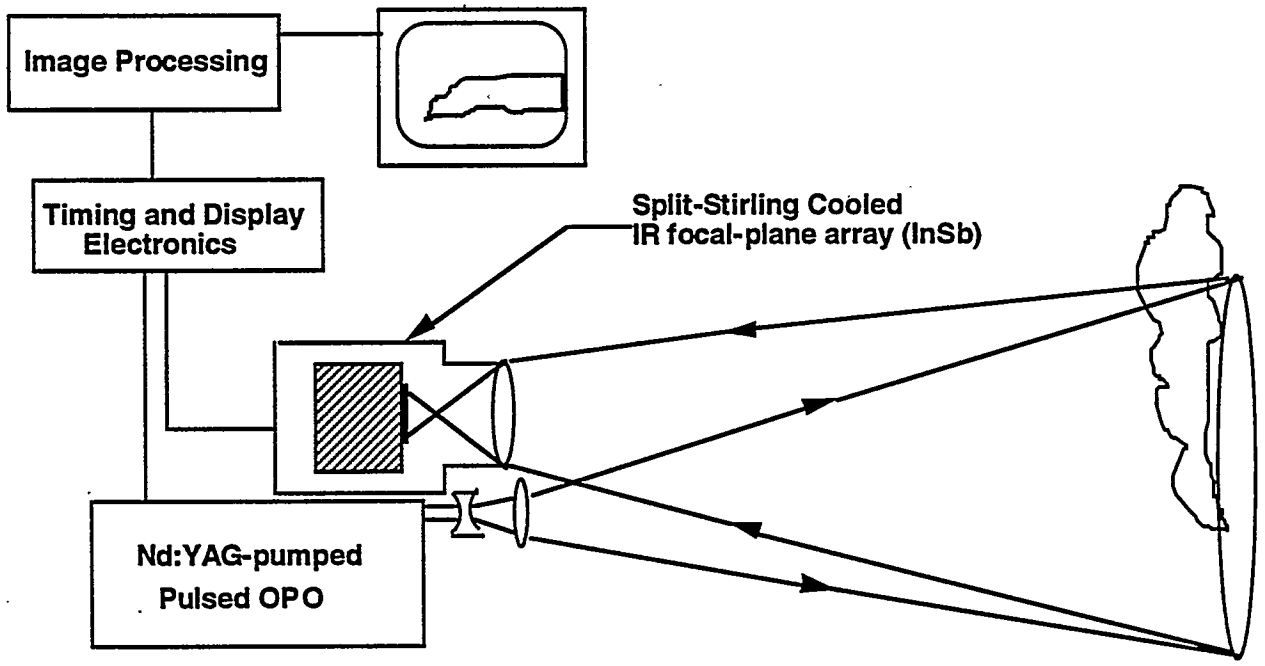

Figure 3 - Schematic of the pulsed BAGI imager, consisting of the beam expanded pulsed laser and the synchronously-gated focal-plane array camera. Arrows directed to the right indicate the footprint of the expanded laser beam, arrows to the left denote radiation collected by the focal-plane array imager. Note that the expanded beam covers the full imaged area.

The specific benefits of the pulsed approach to natural gas imaging can be summarized as follows:

(1) Nonlinear conversion will be used to generate a beam of high average power. The technology will be demonstrated using a commercially available optical parametric oscillator (OPO) laser source that is capable of generating average powers of 80-100 mW at wavelengths between 3 and 5 μm. This will increase the range of the system and expand its short range field-of-view. Both attributes are critical to the leak surveying process. It should be noted that higher power versions of mid-IR OPOs have been developed and should be available in the future.

(2) Beams generated via nonlinear conversion can be tuned to resonance with the peak of the methane absorption. The OPO that will be used will be continuously tunable over a spectral range that is wider than the methane absorption band. This will improve the detectivity of the system.

(3) The SGFPA can be configured with collection optics that allow a larger collection aperture than in the scanner. For example, an f/1.2 30-mm lens will allow a 25-mm aperture, which provides the same field-of-view as the scanned system. This can be contrasted with the 12-mm collection aperture of the scanned system. Conversely, if the 12-mm aperture of the scanned system is used, the field-of-view can be increased to about 35°. The scanned field-of-view is mechanically limited to 18°.

(4) The system under development will have a relatively simple configuration. Laser beam quality is not critical to its performance because the beam will be expanded to serve as a flood source. In the scanner, a low divergence, high mode quality laser beam is required. Alignment of the laser and detector are less critical in a pulsed system. Finally, the pulsed system will have no moving parts.

(5) The tuneability of the source offers the future potential of achieving simultaneous differential absorption lidar (DIAL) measurements, possibly in an imaging mode.

(6) Operation in a pulsed mode using short laser pulses (~10 nsec) will reduce image blurring, which can occur in a scanned system. This will facilitate operation from moving platforms.

(7) The rapidly evolving technology of diode-pumped solid state lasers offers the possibility of making a very compact and electrically efficient imager in the future. Similarly, the rapidly developing IR SGFPA technology will afford future improvements in sensitivity and resolution.

Figure 4 compares the performance that is expected with a pulsed imager operating using a 100 mW laser to that of the scanned methane imager. The triangles indicate the range and field-of-view of both systems. At the left is shown the performance of the scanned cw system; at the right the expected performance of the pulsed system (with three different lenses) is depicted. Clearly, the area of influence of the pulsed system is expected to greatly surpass that of the cw system.

RESULTS

This project began in October, 1994. Since that time, we have concluded a survey of candidate focal-plane array sensors for use in the pulsed imager, formulated an evaluation plan to determine the appropriate characteristics of the sensor that is required for this project, and have presented the results of the survey and the test plan to DOE and GRI. The first half of that evaluation plan has been completed. This constitutes the full completion of Tasks 1 and 2 and the 50% completion of Task 3-5. This is in full agreement with the program schedule.

FUTURE WORK

At the end of the evaluation phase (June, 1995), the optimal array will be purchased and the assembly of the breadboard pulsed imager will begin. Testing of the pulsed imaging system will begin in the fall of 1995 and will continue until June of 1996. This will include laboratory optimization of the system and range and sensitivity testing in an open-air test range. If feasibility is demonstrated at the end of the 19 month effort, a decision will be made to proceed to the development of a prototype instrument having an optimal focal-plane array and a field-hardened laser source.

REFERENCES

1.T.J. Kulp, R. Kennedy, D. Garvis, T. McRae, and J. Stahovec, "The Development of an Active Imaging System and Its Application to the Visualization of Gas Clouds,," in *Proceedings of SPIE, Laser Applications in Meteorology and Earth and Atmospheric Remote Sensing* (Society of Photo-Optical Instrumentation Engineers, Bellingham, WA, 1988), Vol. 1062, pp. 191-202.

2.T.J. Kulp, R. Kennedy, D. Garvis, L. Seppala, and D. Adomatis, "Further Advances in Gas Imaging," in Proceedings of the International Conference on Lasers '90 (Society for Optical and Quantum Electronics, McLean, VA, 1990), pp. 407-413 (1991).

3.T.G. McRae and T.J. Kulp, "Backscatter Absorption Gas Imaging — A New Technique for Gas Visualization," *Appl. Opt.* **32** 4037-4050 (1993).

4. T.J. Kulp, R. Kennedy, M. Delong, D. Garvis, and J. Stahovec, " The Development and Testing of a Backscatter Absorption Gas Imaging System Capable of Imaging at a Range of 300-m," in *Proceedings of SPIE, Applied Laser Radar Technology* (Society of Photo-Optical Instrumentation Engineers, Bellingham, WA, 1993), Vol. 1936, pp. 204-212.

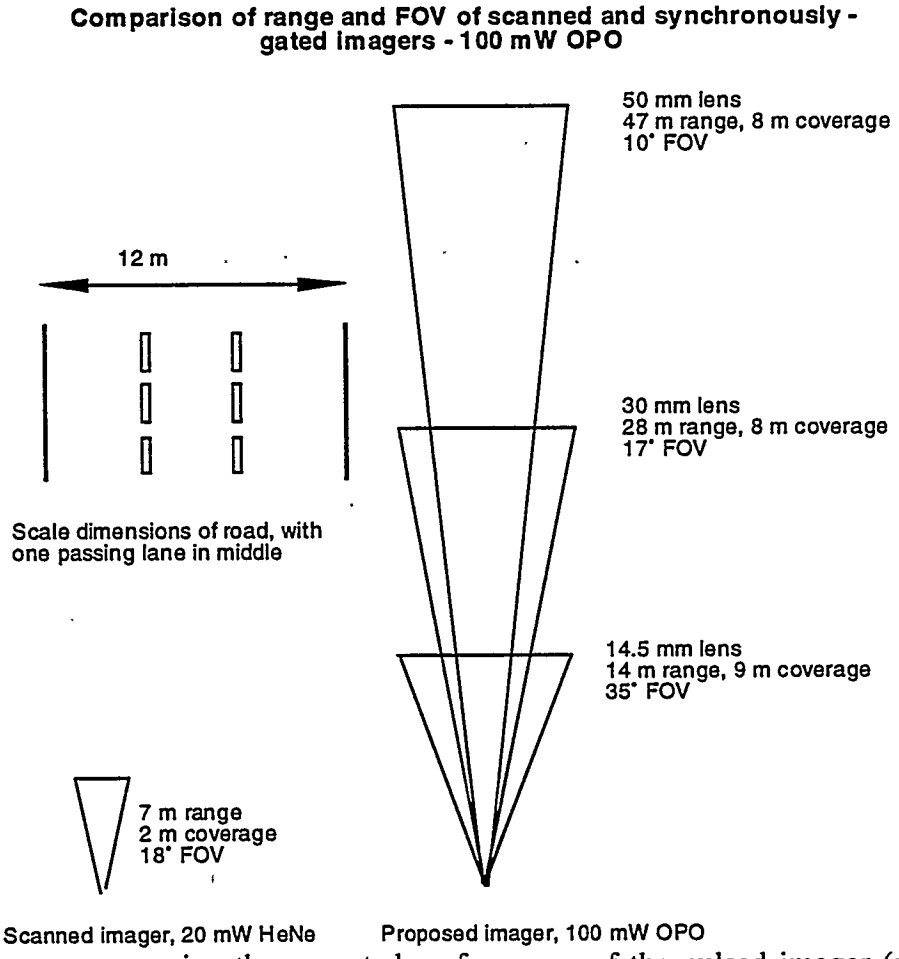

Figure 4 - Diagram comparing the expected performance of the pulsed imager (right) to that of the scanned imager (left). The triangles indicate the range and field-of-view under indicated condisions.

P14 Zeolite Membranes for Gas Separations

CONTRACT INFORMATION

Contract Number	DE-FG21-90MC27115
Contractor	Department of Chemical Engineering University of Colorado at Boulder Boulder, CO 80309-0424 (303)-492-7472 (telephone) (303)-492-4341 (telefax)
Other Funding Sources	Center for Separations using Thin Films Chevron Research and Technology Company
Contractor Project Manager	Richard D. Noble
Principal Investigators	John L. Falconer Richard D. Noble
METC Project Manager	Venkat K. Venkataraman
Period of Performance	July 19,1990 - 12/31/1994

OBJECTIVES

To form zeolite films on inorganic supports, and test them for CO_2/H_2, CO/H_2, and H_2O/H_2 separations. The separation conditions will be studied up to 773 K and 3 MPa pressure.

BACKGROUND INFORMATION

Gasification of coal and other organic fuel sources produces H_2 as well as CO, CO_2, and H_2O. The use of these gasification products as a source of H_2 for fuel cells requires gas separations at high temperatures and high pressures. The separation process must also be able to work in the presence of H_2S, COS and mercaptans. Zeolite membranes can meet these requirements.

Zeolites are crystalline inorganic materials with well-defined pore openings that are on the order of molecular dimensions. Zeolite particles are presently used as selective sorbents for various gas separations based on their sorptive and molecular sieving properties. They can tolerate very high temperatures and sulfur compunds due to their inorganic structure. A very recent developement is to fabricate a dense zeolite layer on a tubular support which can be used as a membrane. This configuration allows one to operate the separation step continuously. Also, a membrane structure allows one to vary the temperature, pressure and feed composition without interruption.

PROJECT DESCRIPTION

We proposed to demonstrate the effectiveness of a catalytic membrane reactor (a ceramic membrane combined with a catalyst) to selectively produce methanol by partial oxidation of methane. Methanol is used as a chemical feed stock, gasoline additive, and turbine fuel. Methane partial oxidation using a catalytic membrane reactor has been determined as one of the promising approaches for methanol synthesis from methane. Methanol synthesis and separation in one step would also make methane more valuable for producing chemicals and fuels. Another valuable fuel product is H_2. Its separation from gasification products would be very valuable as a chemical feedstock and a clean fuel for fuel cells.

RESULTS

Silicalite-alumina composite membranes prepared in our laboratory by an in-situ zeolite synthesis method were used in the gas permeation experiments. The preparation procedure is discussed elsewhere [1]. Silicalite-1 is a pure-silica zeolite with a cage size of 0.58 nm, and it was deposited on a tubular, asymmetric, γ-alumina support. The γ-alumina layer had a pore size of 5 nm. Both single-gas permeation and gas-mixture separation experiments were conducted.

As a first step in evaluating the membrane for gas separations, single gas permeation experiments with N_2, CH_4, and CO_2 were carried out, and permeation flux versus temperature data were obtained at 1.3 bar from 300-600 K. These data are plotted in Fig. 1. The data show that the permeance of each gas went through a minimum. The temperatures at which the minimum occurs are 400 K, 450 K, and 450 K for N_2, CH_4, and CO_2 respectively. Researchers at Kyushu university [2] also observed a minimum permeance of N_2 through silicalite-1 at 400 K, but they did not report minimums for the other gases. Transport of all gases was activated at higher temperatures, and the activation energies were 4.1, 3.8, and 6.3 kJ/mol for N_2, CH_4, and CO_2 respectively. Permeances at 600 K for CH_4 and CO_2 were lower than those at 300 K, and the N_2 permeances at 300 K and 600 K were the same. Therefore, to exceed the productivity at room temperature, temperatures higher than 600 K are required.

Separation experiments for N_2/CH_4 mixtures were also conducted. The feed mixtures contained 10 - 30 mol% N_2 in CH_4, because these are typical N_2 concentrations in natural gas. The separation selectivities were about 1.5, and CH_4 permeated faster than N_2 through the membrane.

Single-gas permeation of H_2, and separation of H_2/SF_6 mixture were also carried out with the silicalite-1 membrane. Flux of H_2 with the silicalite-alumina composite membrane was 8 times lower than the flux with the alumina membrane. Separation selectivity for H_2/SF_6 was 11.9, and the selectivity increased slightly as the temperature increased from 361 to 583 K.

Composite membranes of silicalite and Ni-SAPO-34 on the γ-alumina supports were also prepared. Initially, reproducible data for gas permeances could not be obtained. The stability of SAPO-34 membranes has been reported to be affected by H_2O vapor. When the feed gases were passed through $CaSO_4$, a desiccant made by Drierite, stable and reproducible permeances were obtained. Ratio of CO_2 to N_2 single-gas permeance was 4.3. When the gases were not dried, ratios as high as 9.5 were observed. Permeation experiments for CO_2 and H_2 were performed, but no significant single-gas selectivity was obtained. Compared to the reported promising selectivities for CO_2/N_2, this lack of selectivity was not expected.

FUTUER WORK

For better understanding of the single gas permeation, high pressure permeation experiments for N_2, CH_4 and CO_2 with the silicalite-1 membranes are planned. Pressure in these experiments will be up to 10 bar, and the temperature will be 300-600 K. Also, we plan to continue the preparation of Ni-SAPO-34 and silicalite-1 membranes using different gel compositions as well as other supports such as SAPO membranes, stainless steel, and silica. We will then perform permeation and separation experiments for these membranes for the following gas mixtures: CO_2/H_2,. CO/H_2, and H_2O/H_2.

REFERENCES

3. M. D. Jia, B. Chen, R. D. Noble, and J. L. Falconer, Ceramic-zeolite composite membranes and their application for separation of vapor/gas mixtures, J. Mem. Sci., 90 (1994) 1

2. Katsuki Kusakabe, Atsushi Murata, and Shigeharu Morooka, Permeation of Inorganic Gases Through Zeolite Membrane at High Temperature

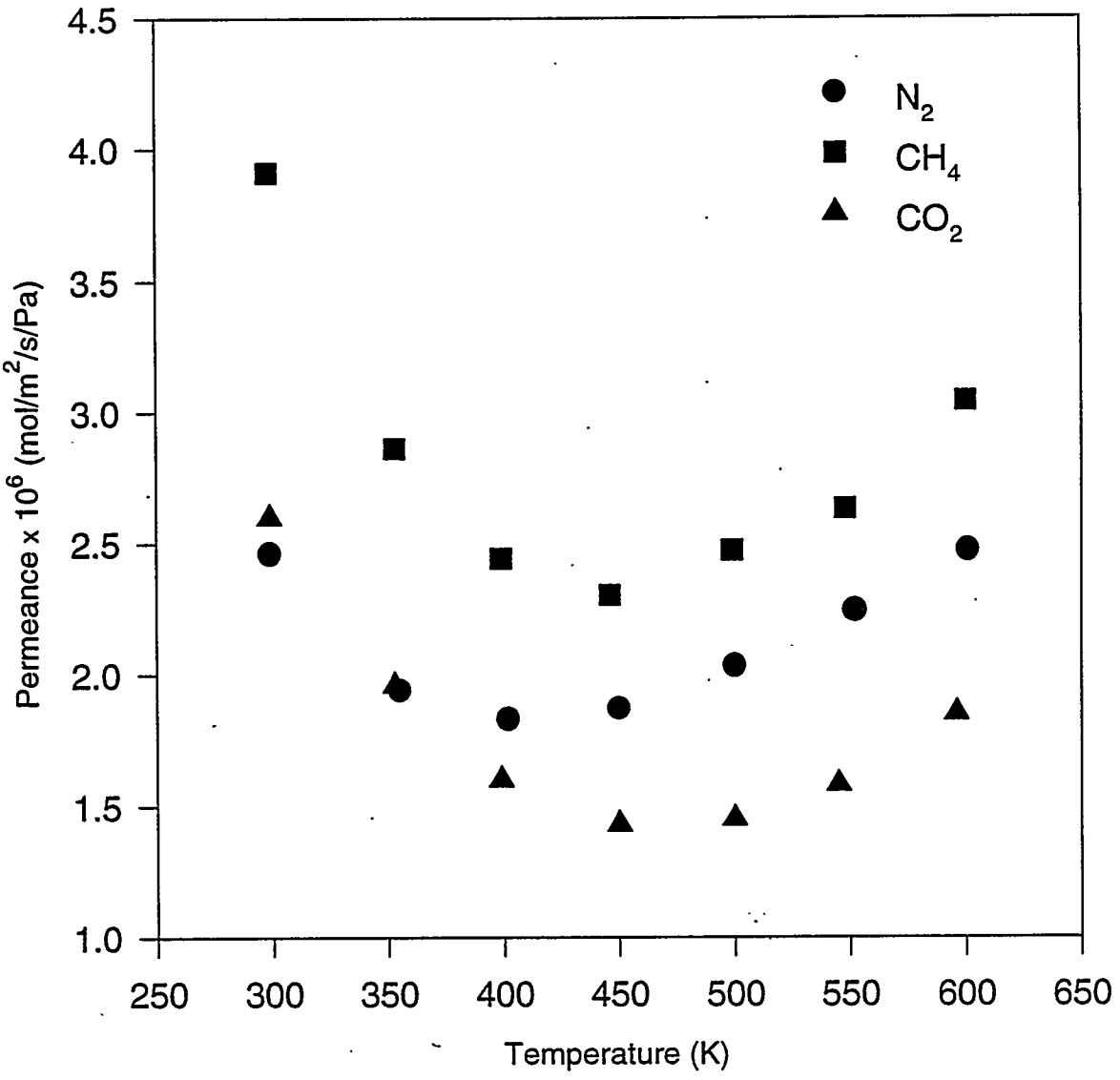

Figure 1. Single Gas Permeances Versus Temperature For A Silicalite-1 Membrane

Session 7

Drilling, Completion, and Stimulation

7.1 Steerable Percussion Air Drilling System

CONTRACT INFORMATION

Contract Number	DE-AC21-92MC28182
Contractor	Smith International, Inc. P.O. Box 60068 Houston, TX 77205-0068 (713) 233-5428 (713) 233-5205
Contract Project Manager	Huy D. Bui
Principal Investigators	Huy D. Bui Michael A. Gray Michael S. Oliver
METC Project Manager	Albert B. Yost II
Period of Performance	September 30, 1992 to May 31, 1995

Schedules and Milestones

FY95 Program Schedule

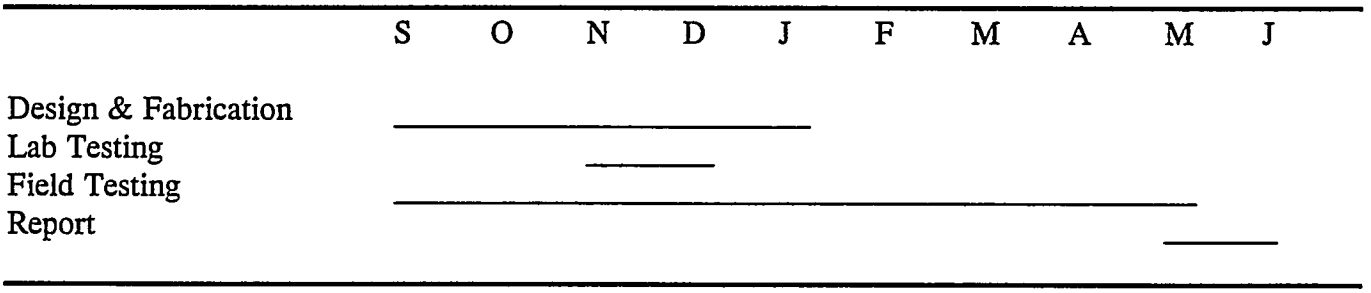

BACKGROUND INFORMATION

The Steerable Percussion Air Drilling System (SPADS) is an attempt to make possible for the first time the use of air percussion method to drill directionally in hard formations. Rock disintegration is accomplished as a result of the transfer of the percussive energy from the piston-to-bit impact on to the formation, as opposed to the constant crushing force applied by the collar weight of a large magnitude in conventional drilling [1].

The heart of SPADS is a rotational mechanism, that permits and induces the bit's rotational motion independently of the drill string's rotation. In contrast, the conventional percussion drilling tools employ an external rotational system located on the ground surface to rotate the *entire* drill string. Consequently, these tools suffer from an inherent limitation of permitting straight hole drilling only. SPADS on the other hand enables the capability for directional control of the well bore, since the entire drill string is not required to rotate with the bit [2].

As compared to mud or air powered PDM motors, the advantages offered by SPADS are: directional drilling at high penetration rate, reduced mud costs, negligible formation damage and an immediate indication of hole productivity [3] [4].

OBJECTIVES AND PROJECT DESCRIPTION

The cost-sharing contract between the U.S. Department of Energy and Smith International calls for the design, fabrication, and the laboratory and field testing of two complete prototypes as follows:

1. Rotational Hammer: Two downhole hammers with built-in rotational mechanism:
   Hammer OD: 6 3/4" to 6 7/8"
   Hammer Length: 5 to 7 feet
   Rotational Speed: 20 to 30 RPM
   Output Torque: 1,000 ft-lb max

2. Percussion Bits: Up to 14 Diamond Enhanced bits required to conduct field tests either 7 7/8", 8 1/2" or 8 3/4"

3. Bend Subs: Either fixed or adjustable angle bend subs, from 1/2 degree to 3 degrees

4. Stabilizers: Near-bits and other stabilizers required in the bottom hole assemblies.

The two prototypes shall undergo lab testing to optimize impact energy prior to the field test. The field test plan calls for:

1. Straight hole testing: to harden the system's capability of drilling through hard rock independently from the drill string rotation.

2. Directional hole testing: conduct three shallow directional field tests to evaluate build rates as a function of bend angles and placement of stabilizers, effects of side loads and reactive torques, and system reliability and mean time between failures.

3. System field testing: conduct up to three high angle or horizontal field tests to prove the system capability for commercialization.

In addition, the contract also calls for the evaluation of Geoscience Electronics Corporation's (GEC) electromagnetic MWD tool as a means to telemeter directional data.

RESULTS

1. Lab Testing

An in-house testing facility for SPADS was designed and built to enable the monitoring of change in performance as a result of changes in different design variables. The test facility is equipped with a flow loop, a data acquisition

system, and associated instrumentation to measure different parameters that will indicate the hammer performance.

During the testing, the following parameters were monitored:

(a) Impact Frequency
(b) Impact Velocity
(c) Instantaneous Pressures in the Upper and Lower Chambers
(d) Bit Rotation

As a result of this testing, appropriate modifications were incorporated into SPADS to fulfill the following objectives:

(i) Optimal sizing of the upper and lower chambers and control of the charging and discharging cycles for air from these chambers in order *to maximize the impact energy and the operating frequency*, and

(ii) Optimal distribution of the piston's kinetic energy between the linear and the rotational subsystems, in order *to ensure adequate bit rotation under extreme conditions of torque.*

2. Field Testing

A number of field tests were included under the scope of this project. The *initial* objective of the tests is to demonstrate the ability of the system to drill straight through hard rock at competitive penetration rates and independent of the drill string rotation.

During the year of 1994 a total of five field tests were conducted in West Virginia and West Texas to optimize and tool harden the rotational hammer itself. A number of problems ranging from tool design to operation procedures were encountered. The causes of failure and remedies adopted at the end of individual field tests are documented in Table 1.

While the drilling machine proved its ability to drill at a penetration rate (ROP) exceeding 90 feet per hour without rotating the drill string, it also showed its sensitivity to excessive weight on bit (WOB). Drilling at these straight hole field tests was halted after 40 to 110 feet during each test due to the stalling of the piston. This stalling is blamed mostly on the extreme rotational resistance torque which the bit has to overcome when too much weight is applied on the bit. A couple of new bit face designs are being implemented in an attempt to lower the torque under extremely high WOB conditions.

Additional lab testing was needed to better understand the magnitude of the torque required to rotate the bit during the drilling operation and to understand the associated circumstances which produce reasonably low torque at times and extraordinarily high torque at others, as observed in the field tests.

3. Additional Lab Testing

At Smith International, we rigged up a method for allowing us to actually drill on different formations. We drilled on hard rock (granite) as well as softer rock (limestone) using a forklift with an attempt to study the bottomhole patterns in different formations during drilling. The forks were loaded with collars of different weights to study the effect of WOB on the magnitude of the torque. A torque sub was designed and fabricated to measure the torque encountered during actual drilling conditions.

The study revealed that SPADS generates sufficient impact energy to drill in hard as well as soft rock; however under extreme conditions

Table 1. Results from the Field Testing

TEST #	FOOTAGE DRILLED	CAUSE OF FAILURE	REMEDY
Test 1	109 ft	Piston broke due to grinding cracks; Ceramic balls fractured due to sharp edges	Better quality control
Test 2	46 ft	Sand invasion	Install spring at check valve
Test 3	50 ft	Interference of bearing due to temperature gradient	Better thermal conducting material
Test 4	91 ft	Hammer stalled in dead band due to high torque	Divert more energy for rotation
Test 5	110 ft	High torque in formation changes	New low-torque bit designs

of loading, the hammer stalled as a result of a drastic increase in the torque on bit. The effect was especially notable in softer formations like limestone, where high WOB (approximately 8,000 lbs.) caused the bit to bury itself into the formation. The lack of a refined weight control technique prompted us to conduct additional testing at Sandvik Rock Tools, Inc.

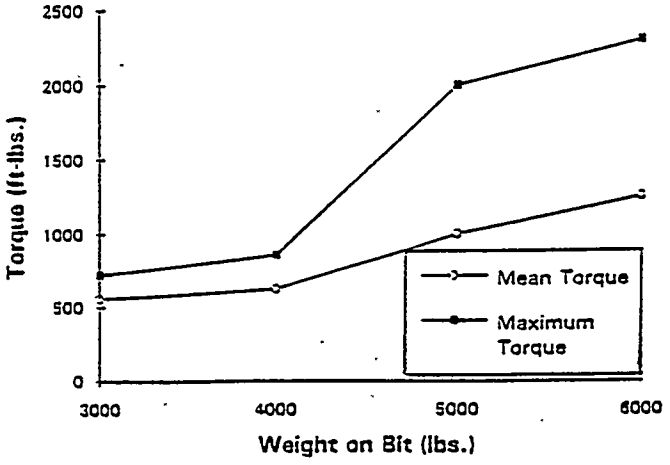

Figure 1. Effect of WOB on Torque

The facility at Sandvik is routinely employed for testing the performance of conventional down-the-hole hammers. The facility is equipped with a hydraulic hold down system that allows a better control of the WOB. A series of tests were conducted at Sandvik at different line pressures by varying the weight on the bit. Three different formations were tested viz., granite, limestone, and sandstone.

The results indicated that there is an optimum WOB at which the torque is reasonably low. If WOB is lower than the optimum value, the hammer has a tendency to remain open, causing a reduction in both frequency and ROP. On the other hand, an increase in WOB above the optimum is usually always accompanied by an increase in torque and a decrease in the ROP. With an increase in torque, more energy must be imparted to the rotary motion rather than the linear motion, causing a reduction in impact velocity and therefore also the ROP. The effect of WOB on the torque is shown in Figure 1. The optimum WOB in this case is in the range of 3,000-4,000 lbs, when the line pressure is 200 psi. Any increase in WOB results in a corresponding increase in the torque as well.

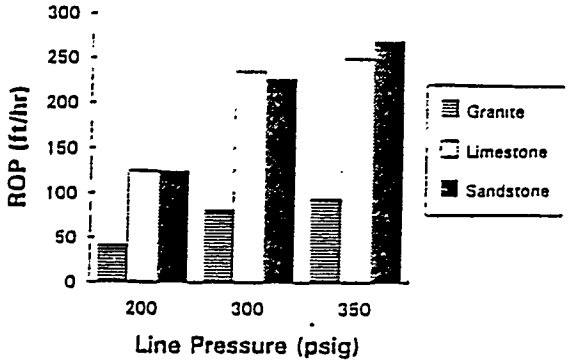

Figure 2. Hammer Performance in Different Formations

The performance of the hammer in different formations is shown in Figure 2. The tests were performed at three different line pressures viz., 200, 300, and 350 psig at the optimum WOB. There is a significant increase in the ROP in soft formations like limestone and sandstone. However, the torque encountered under identical conditions of line pressure and WOB is nearly the same in all the formations. Stalling of the hammer was not possible in these tests, since the maximum WOB that could be applied was limited to 6,000 lbs due to the capacity of the test rig.

FUTURE WORK

The following changes will be incorporated during the next straight hole field test scheduled for mid April:

(1) A better method of WOB control in the field tests e.g., pull down rigs

(2) Continuous monitoring of the WOB and torque

(3) Low torque bits to reduce the sensitivity of the hammer performance to WOB: redesign bit face to improve the rock to cutter interface. More and smaller diamond inserts are placed close together to provide better protection for the gage row.

REFERENCES

1. Bui, H. "Steerable Percussion Air Drilling System", Proceedings of the Natural Gas R&D Contractors Review Meeting, U.S. Department of Energy, DOE/METC-94/1002 (DE 94004065), November 16-18, 1993.

2. Bui, H., and Oliver, M., "Percussion Drilling Assembly", U.S. Patent No. 5,332,136, issued June 21, 1994.

3. Whitley, M., and England, W., "Air Drilling Operations Improved by Percussion Bit-Hammer Tool Tandem", SPE/IADC 13429, presented at the SPE/IADC Drilling Conference, New Orleans, LA, March 6-8, 1985.

4. Pratt, C., "Modifications to and Experience with Percussion Air Drilling", SPE/IADC 16166, presented at the SPE/IADC Drilling Conference, New Orleans, LA, March 15-18, 1987.

7.2 Development and Testing of Underbalanced Drilling Products

CONTRACT INFORMATION

Contract Number DE-AC21-94MC31197

Contractor

Maurer Engineering Inc.
2916 West T.C. Jester
Houston, Texas 77018-7098
(713) 683-8227 (telephone)
(713) 683-6418 (telefax)

Other Funding Sources None

Contractor Project Manager William C. Maurer

Principal Investigators William C. Maurer
George H. Medley, Jr.

METC Project Manager John R. Duda

Period of Performance September 30, 1994 to November 30, 1997

Schedule and Milestones::

TASKS	FY95												FY96												FY97	
	O	N	D	J	F	M	A	M	J	J	A	S	O	N	D	J	F	M	A	M	J	J	A	S	O	N
1. Research Existing Models	x	x	x																							
2. Develop Foam Model				x	x	x	x	x	x																	
3. Validate Model										x	x	x														
4. Study Market Potential	x	x	x	x	x	x	x	x	x	x	x	x														
5. Research LWSA	x	x	x	x	x	x	x	x	x	x																
6. Modify LWSA/Equipment									x	x																
7. Yard Test Additives & Equipment										x	x	x														
8. Test Plan													x	x												
9. Field Tests															x	x	x	x	x	x	x	x	x	x	x	x
10. Technology Transfer																	x					x				

Development and Testing of Underbalanced Drilling Products

OBJECTIVES:

The first objective of this project is to develop a user-friendly, PC, foam drilling computer model, FOAM, which will accurately predict frictional pressure drops, cuttings lifting velocity, foam quality, and other drilling variables. The model will allow operating and service companies to accurately predict pressures and flow rates required at the surface and downhole to efficiently drill oil and gas wells with foam systems.

The second objective of this project is to develop a lightweight drilling fluid that utilizes hollow glass spheres to reduce the density of the fluid and allow drilling underbalanced in low-pressure reservoirs. Since the resulting fluid will be incompressible, hydraulics calculations are greatly simplified, and expensive air compressors and booster pumps are eliminated. This lightweight fluid will also eliminate corrosion and downhole fire problems encountered with aerated fluids.

BACKGROUND INFORMATION

In the late 1940s, oil companies began air drilling to increase drilling rates in hard rock and to overcome severe loss circulation problems. Other benefits of air drilling include reduced formation damage and reduced differential sticking problems.

The most important benefit of underbalanced drilling is increased drilling rate due to reduced differential pressure at the hole bottom as shown in Figure 1.

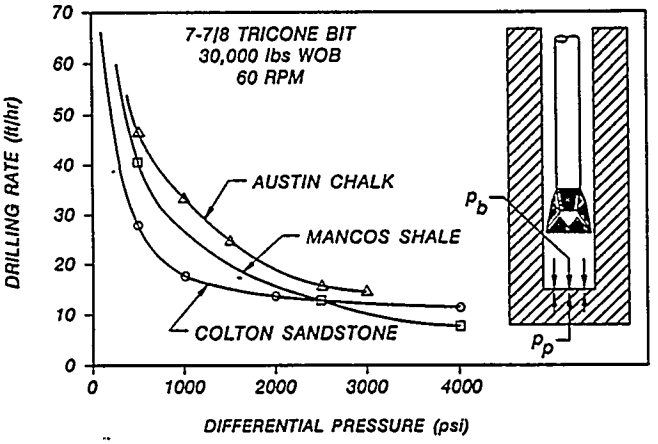

Figure 1. Effect of Differential Pressure on Drilling Rate (Moffitt, 1991)

The beneficial effect of reduced hydrostatic pressure occurs at all bit weights as shown in Figure 2.

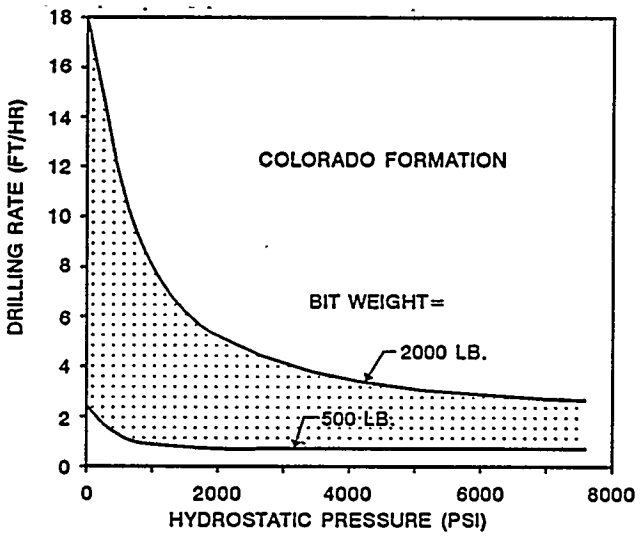

Figure 2. Effect of Hydrostatic Pressure on Drilling Rate (Murray & Cunningham, 1955)

Many tight-gas reservoirs in the United States are attractive targets for underbalanced drilling because they are located in hard-rock country where tight, low-permeability formations compound the effect of formation damage encountered with conventional drilling fluids.

Drilling underbalanced in under-pressured or depleted reservoirs requires fluids lighter than water (Sp. Gr. < 1). Many types of fluids systems are used, ranging from 100 percent air to 100 percent liquid, with all fluids having densities below 6.9 ppg (SG = 0.83) containing gas or air in some form (Figure 3).

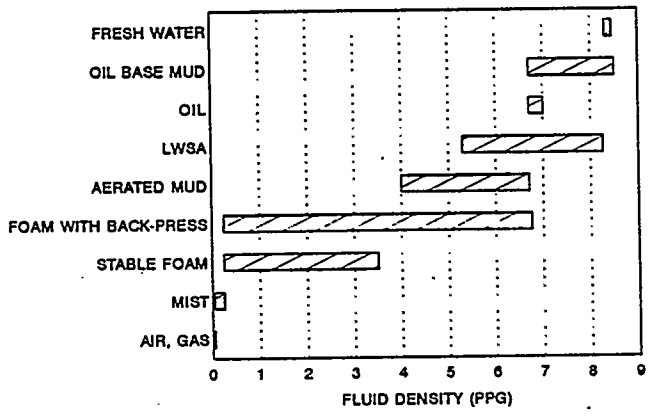

Figure 3. Fluid Density Range

During the 1950s and 1960s, drilling techniques expanded to include mist, foam, and aerated fluids, but the introduction of two-phase fluids increased the difficulty of predicting fluid flow parameters with these compressible fluids. All of the two-phase systems shown in Figure 4 have been used successfully for drilling during the past four decades.

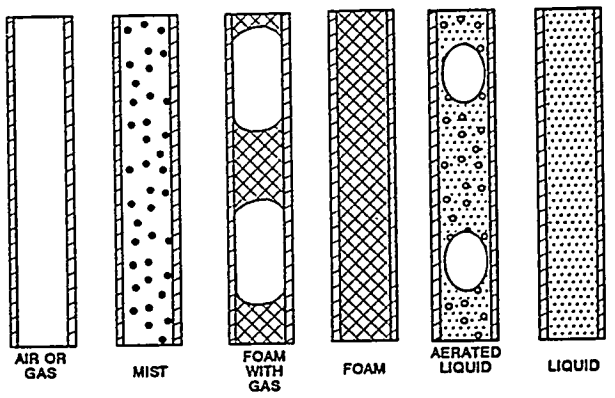

Figure 4. Types of Flow Regimes (Lorenz, 1980)

The hydraulics for 100 percent fluid is relatively easy to predict because this fluid is essentially incompressible. The 100 percent gas fluid is harder to model, due to its compressibility, even though it is still one continuous phase.

The hydraulics of mist and foam are much more difficult to model since they are compressible, and they are two phase fluids. Foam is generally defined as any two-phase fluid with liquid as the continuous phase (having a gas emulsified in it), while mist is defined as a two-phase fluid having gas as the continuous phase, as shown in Figure 5. Gas becomes the continuous phase at concentrations above 97-98 percent by volume.

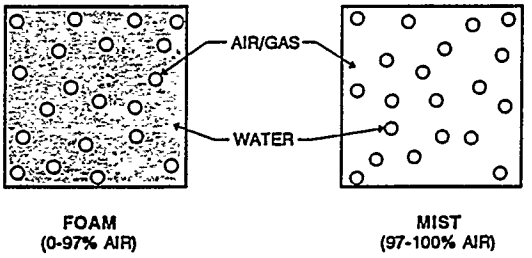

Figure 5. Fluid Phase Continuity

Advantages and disadvantages of different lightweight fluids are presented in Table I. The

major advantage of underbalanced fluids in increased ROP.

Table I. Advantages of Underbalanced Fluids

AIR/GAS/MIST	FOAM/LWSA
HIGH ROP	HANDLE WATER INFLUX
LOW CHEMICAL COST	IMPROVE HOLE STABILITY
EASY TO USE	EXCELLENT HOLE CLEANING
REDUCED ENVIRON-	REDUCE COMPRESSORS
MENTAL IMPACT	NO DOWNHOLE FIRES
	MUD PULSE MWD (LWSA)

Fluids having gas or air as the continuous phase have the advantage of simplicity, low additive cost, and minimal equipment requirements. They also produce less environmental damage since there is minimal liquid waste disposal.

Table II compares the disadvantages of the different underbalanced drilling fluids.

Table II. Disadvantages of Underbalanced Fluids

AIR/GAS/MIST	FOAM/LWSA
WATER INFLUX	ADDITIVE COST
HOLE EROSION	MEASUREMENT/CALCULATION
DOWNHOLE FIRES	COMPLEXITY
HOLE INSTABILITY	

The major disadvantage of air, gas or mist fluids is their inability to handle formation fluid influxes. When the influx becomes too great for air or mists to handle, the fluid system is usually switched to foam or aerated fluid.

Foam and the proposed Lightweight Solid Additive (LWSA) muds consisting of hollow glass spheres eliminate many of the problems associated with air, gas, and mist drilling fluids including borehole stability problems, excessive compressor requirements, and downhole fires and explosions. Their greatest advantage is their ability to handle large influxes of oil or water.

Foam has the additional advantage of increased cuttings carrying capacity. Figure 6 shows that as the foam quality increases (i.e. the percent air increases) the lifting force increases. The maximum lifting force is achieved with 2 to 5 percent liquid, just within the region defined as a foam.

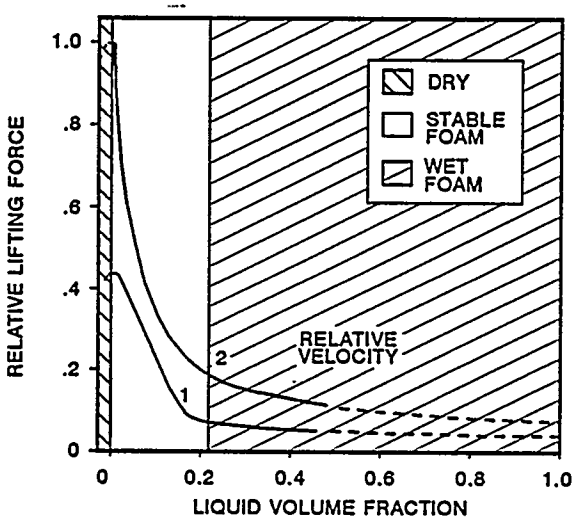

Figure 6. Foam Lifting Capacity (Beyer et al., SPE 3986)

As a foam becomes wetter, its viscosity decreases along with its ability to carry cuttings. As the fluid crosses over into a gas-continuous phase it lifts the cuttings well, but its ability to hold cuttings in suspension at very low velocities disappears.

Aerated fluid can either be circulated down the drill pipe from the surface, or injected at some point in the drill-string casing annulus through a "parasite" string strapped to the outside of the casing as shown in Figure 7. Air can also be injected down the annulus of dual wall drill pipe. The injected air reduces the pump pressure at the surface and lowers the hydrostatic head in the annulus.

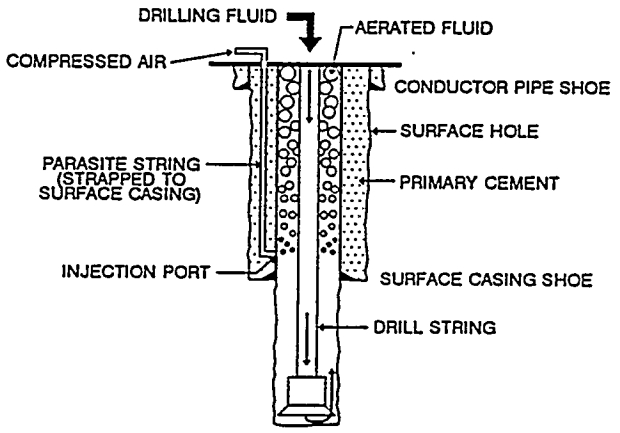

Figure 7. Typical Parasite String

Downhole fires and explosions are a problem when drilling with air, especially in long horizontal wells where days or weeks are spent drilling in oil or gas pay zones. Explosive mixtures of air and hydrocarbon gas are shown in Figure 8. If a flammable mixture of oxygen and natural gas or oil exists downhole, ignition can occur due to heat generated by friction or by sparks generated by the drill bit.

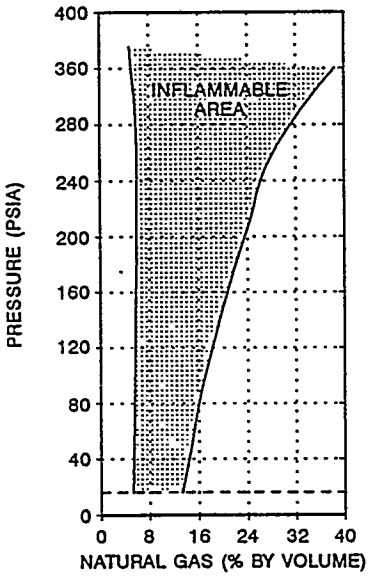

Figure 8. Explosive Mixtures (Hook et al., 1977)

Although foam or aerated muds eliminate the fire and explosion problem, they are hindered by the increasingly complex hydraulic calculations and the high cost of foam chemicals.

Prior to computers it was nearly impossible to accurately calculate circulating pressures for compressible fluids. The tedious manual calculations led to the development of nomographs and charts (Figure 9), rules-of-thumb, and correction factors which gave approximate answers and decreased the engineers' ability to scientifically use these fluids.

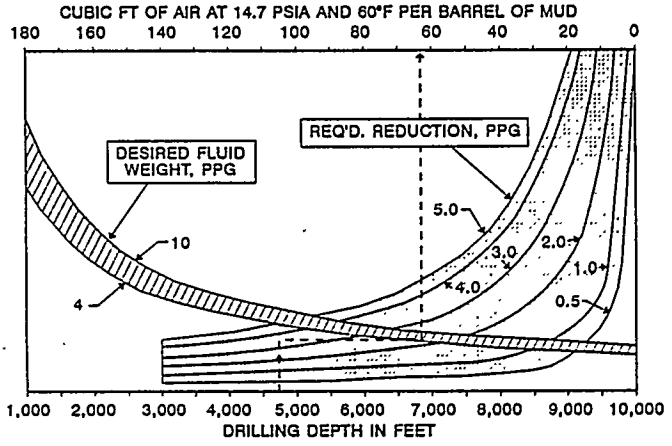

Figure 9. Volume Requirement Chart (Poettman, et al., 1995)

An accurate hydraulic model is needed for foam drilling to allow engineers to better plan and drill wells. Chevron developed a mainframe computer model for foam circulation in the early 1970s that was state -of-the-art at that time, but its availability to field engineers is limited.

Similarly, there is a need for incompressible drilling fluids that utilize solid additives (e.g., hollow glass spheres) to lighten the fluid. This type of fluid would overcome the severe fire, explosion, and corrosion associated with aerated drilling fluids.

In the late 1960s, the Russians tested lightweight fluids that utilized hollow glass spheres to reduce the fluid density. Data available on the Russian spheres are presented in Table III.

Table III. Russian Hollow Spheres

FIRST MANUFACTURED	—	1968
FIRST USE IN DRILLING	—	1970-71
MATERIAL	—	GLASS
COMPRESSIVE STRENGTH	—	3200-3600 PSI
SPECIFIC GRAVITY	—	0.26-0.36
AVERAGE DIAMETER	—	50-60 MICRONS

Oil-field service companies have used hollow glass spheres and other lightweight additives for years to reduce the density of cements and the hydrostatic head in lost circulation areas. To the best of our knowledge, hollow glass spheres were never used in lightweight drilling fluids outside of Russia until this DOE project.

A fluid incorporating lightweight solid additives (S.G.= 0.3 to 0.6) would have many advantages over aerated fluids as shown in Table IV

Table IV. Benefits of Hollow Sphere Mud

- ALLOWS USE OF MWD TOOLS
- ELIMINATES EXPENSIVE COMPRESSORS
- REDUCES CORROSION PROBLEMS
- ELIMINATES DOWNHOLE FIRES
- ELIMINATES NITROGEN
- IMPROVES MOTOR PERFORMANCE
- IMPROVES HOLE STABILITY
- SIMPLIFIES PRESSURE CALCULATIONS
- REDUCES DRILL-STRING VIBRATIONS

PROJECT DESCRIPTION

Phase I includes development of 1) a foam hydraulics model, FOAM, that will accurately calculate circulating pressures, cuttings lifting velocities, and compressor requirements, and 2) lightweight drilling fluids that utilize hollow glass spheres to reduce the fluid density.

Phase II includes field testing of the foam drilling computer model and the lightweight drilling fluids utilizing hollow glass spheres.

Foam Computer Model

A literature search was used to identify all available mathematic models related to the pressure and flow characteristics of foam fluids including calculation of downhole pressures, flow rates, volumes, foam quality, foam rheology and cuttings carrying capacity. In addition, unpublished laboratory tests and unpublished mathematical models provided by Chevron and other sources were reviewed.

The Chevron information was of significant value since Chevron spent many man-years and many millions of dollars developing foam computer models in the 1970s.

Air and foam drilling service companies were contacted to determine which computer models, if any, were in general use within the industry. Invariably, service companies either use the Chevron model under license, or models based on the Chevron model. One service company uses a proprietary spreadsheet model developed by a third party. These proprietary models are not generally available to the industry.

A PC-based model for foam fluids developed in conjunction with a Gas Research Institute contract, based on an "EXCEL" spreadsheet with no

graphics, was identified. A copy of this model was also obtained for comparison with the DOE foam model.

A PC-based, Windows foam drilling model is being developed on this DOE project using the best mathematical models in the industry. The model will be user-friendly, accurate, and available in a form compatible with rugged well-site usage. The program format will be similar to the twenty user-friendly PC programs developed by Maurer Engineering for the 120 DEA-44 Horizontal Well Technology Participants across the world.

During Phase I, the results generated by this foam hydraulics computer program will be validated by comparison with other foam models (e.g., Chevron model) and available laboratory and field data.

During Phase II, at least two field tests of the computer model will be conducted while wells are being drilled with foam. Surface and downhole data (e.g., pressures and temperatures) will be collected for comparison with the model's output.

Lightweight Solid Additives

Commercially available hollow glass spheres used as extenders in paints and other materials have been identified and the best candidates have been selected for laboratory and field testing. A Phase I test plan has been developed that includes laboratory and yard testing of drilling muds containing hollow spheres.

The laboratory tests include standard API drilling fluid tests such as density, filtration loss, and rheology of fluids composed of various concentrations of hollow glass spheres in water-base and oil-base muds.

Phase I yard testing will study the effectiveness of existing solids handling equipment on LWSA fluids with regard to both damage and recovery of the LWSA. Modifications of existing solids-control equipment will be carried out as required.

During Phase II, at least two field tests will be carried out using LWSA drilling fluids. Chevron and other operators have expressed high interest in field testing these fluids on their wells, because they see a major payout in their field operations if the DOE tests are successful.

Market Study

A market study for underbalanced drilling fluids in the United States will be carried out. Preliminary findings are that underbalanced drilling is expanding rapidly and will become a major factor worldwide within the next five years.

Reports

Topical reports covering Phase I and Phase II efforts will be prepared and the technology developed will be transferred to the industry via technical articles and forums.

RESULTS

Foam Computer Model

To date, all known, available mathematical foam models have been studied, and modified and improved as needed for inclusion in this DOE foam model. A prototype version of the program has been developed for demonstration. Beta versions of this program are being tested by air and foam drilling service companies. Work is continuing to complete an operational model by the end of Phase I.

The PC-based model runs under a WINDOWS environment, and is fully transportable to

the rig site where real-time adjustments to the operation can be made as conditions change.

Site specific input data includes basic project description, directional survey data, drill string and wellbore descriptions, and planned drilling parameters such as gas and liquid injection rates and properties, anticipated drilling rates, pore pressures, and fracture gradients.

The compiled output is in both tabular and enhanced graphics form with a series of graphs illustrating the different parameters required by the drilling engineer when planning or troubleshooting field wells.

The primary concern of drilling engineers is the circulating pressure throughout the well, as shown in Figure 10. This pressure profile is useful in determining the amount of compression needed at the surface and to ensure that downhole pressures do not fracture the formation, allow unwanted fluid influxes into the well, or allow the wellbore to collapse.

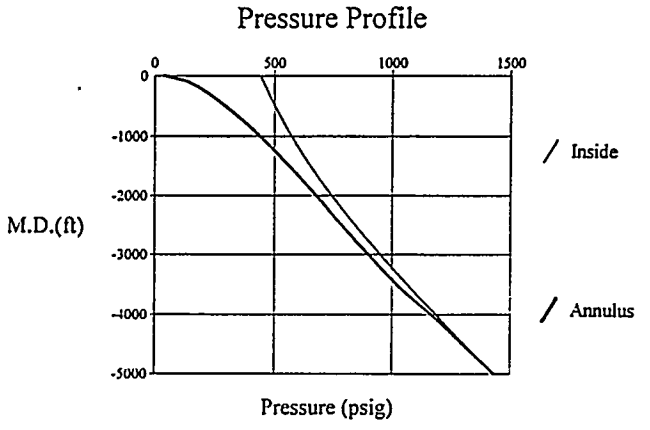

Figure 10. Pressure Profile

Foam density, plotted in Figure 11, is useful to the drilling engineer for various reasons including its effect on downhole motor performance in terms of cooling and lubrication.

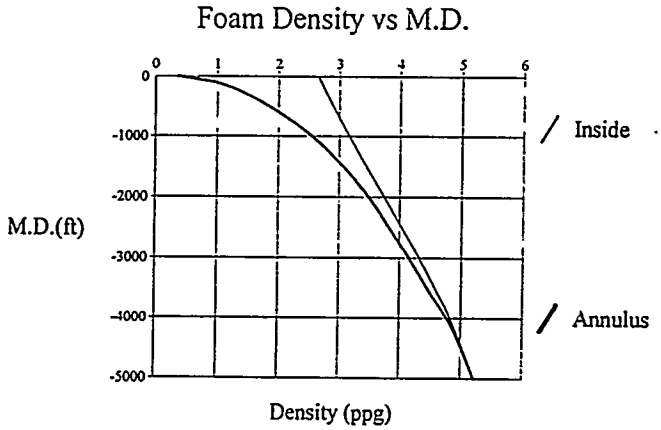

Figure 11. Foam Density

Foam quality, shown in Figure 12 relates to viscosity and the ability of foam to lift cuttings in the annulus. Drilling engineers use a rule of thumb that the foam quality should be above fifty-five percent to prevent the breakdown of foam into water or slug flow and to maintain adequate cuttings carrying capacity.

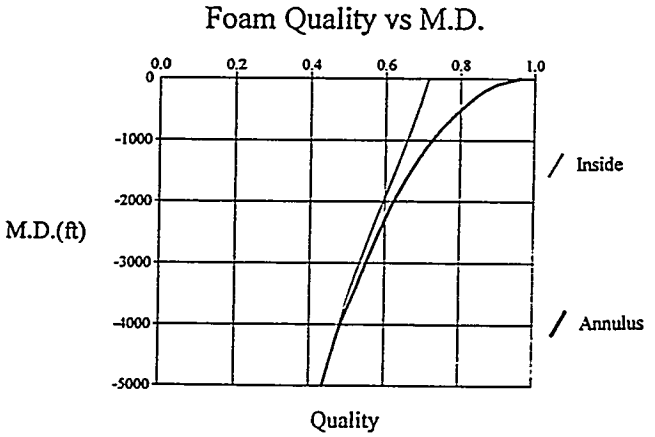

Figure 12. Foam Quality

Cuttings lifting velocity is one of the most important parameters since many field problems

(e.g., mud rings, downhole fires, stuck pipe, fishing jobs) occur because of inadequate hole cleaning.

Figure 13 shows an example where the cuttings lifting velocity is lowest at the top of the drill collars. In many air drilled wells, large cuttings remain at the top of the collars until they are reground to the point where they are small enough to be lifted to the surface.

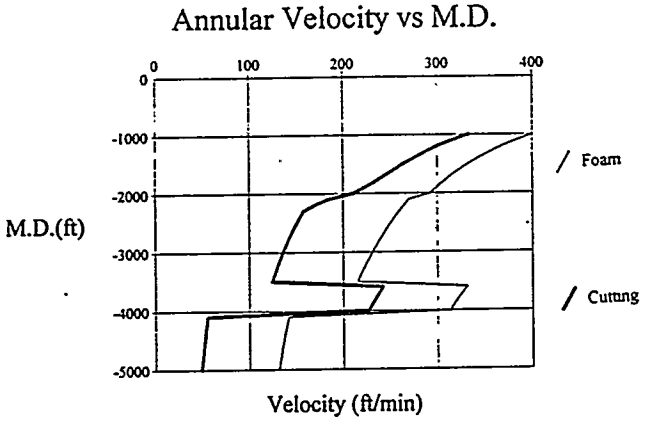

Figure 13. Cuttings Lifting Velocity

An additional feature of the program is the ability to design or troubleshoot field jobs by running sensitivity analyses on input parameters.

Figure 14 shows the total pressure and the cuttings lifting velocity at total depth for a given input case. Note that at higher gas injection rates, the bottom hole pressure exceeds the formation fracture gradient and loss of circulation would occur. At lower gas injection rates, the lifting velocity becomes negative, indicating an accumulation of cuttings at the bottom. This shows that some input modification is necessary to obtain a viable drilling scenario.

The effect of increasing the input liquid injection from 40 GPM to 100 GPM is illustrated in Figure 15. Both bottom-hole pressure and cutting lifting velocity move into satisfactory ranges for the given range of gas injection rate.

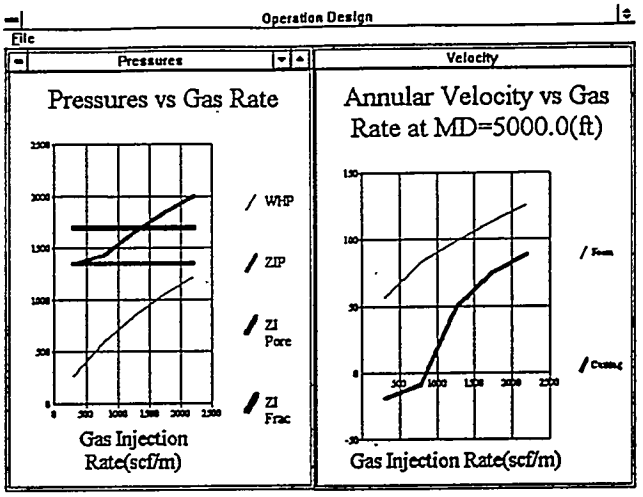

Figure 14. Initial Design Parameters

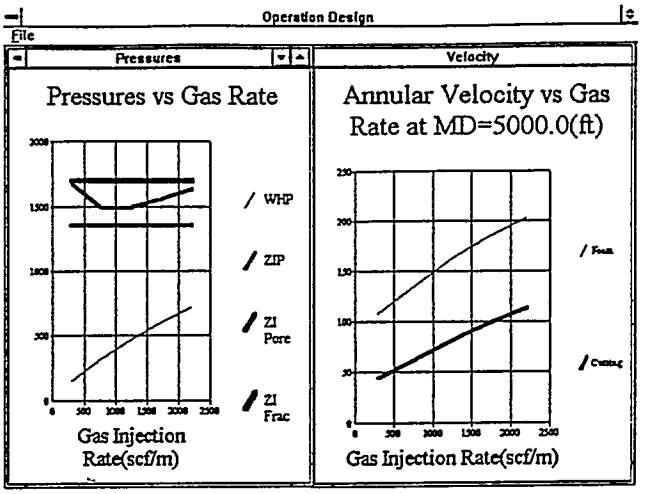

Figure 15. Design Improvement

Hollow Glass Spheres Fluids

Research into lightweight solids having a specific gravity of less than 1.0 led to the identification of several candidate hollow glass spheres (i.e., glass, ceramic, and plastic). Initial candidates include lightweight additives familiar to the industry such as

the crystalline-silica (commonly called Spherelite™) used in lightweight cements.

With cements, hollow glass spheres with specific gravities of 0.7 are adequate since they have a large effect on cements with specific gravities of 1.8 to 2.0. These spheres have minimal effect on water which has a specific gravity of 1.0. Therefore lighter spheres are required (i.e., Sp.Gr. = 0.35 to 0.40) in lightweight drilling fluids.

For example, the addition of 50 percent Spherelite™ by volume (Sp.Gr. = 0.7) would reduce the density of 8.5 ppg mud to only 7.7 ppg. This would not be adequate for most underbalanced drilling applications.

Hollow glass spheres with specific gravities of 0.38 and collapse pressures of 3000 to 4000 psi were found that can be used effectively in drilling fluids. These spheres, used commercially as extenders in paints, glues, and other liquids, are ideal for use in lightweight drilling fluids due to their low specific gravity (Figure 16).

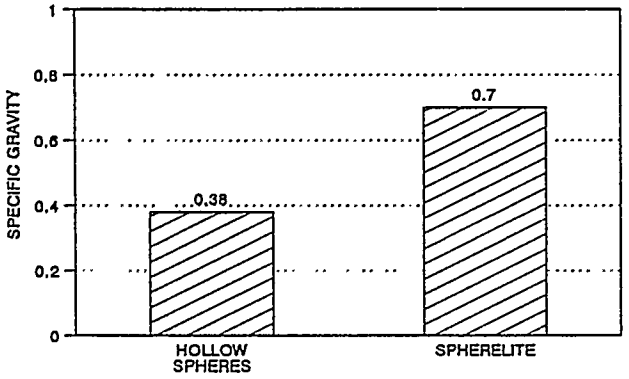

Figure 16. Specific Gravity

A 50-percent concentration of these hollow glass spheres (Sp.Gr. = 0.38) decreases the density of 8.5 ppg mud to 5.8 ppg as shown in Figure 17, which is sufficient for many field applications. These hollow glass spheres have the added benefit of being nearly incompressible.

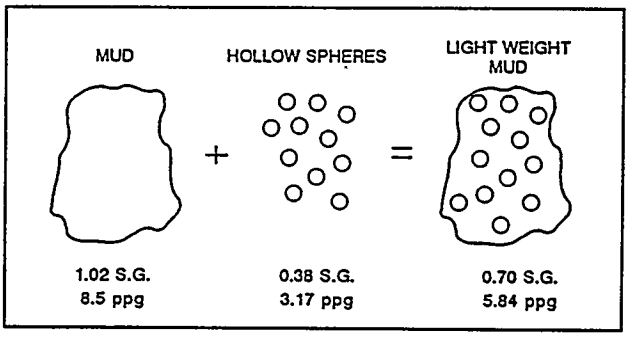

Figure 17. Lightweight Mud

The specific gravity of a sphere is a function of the ratio of its outer diameter to inner diameter (O.D./I.D.) (i.e., wall thickness) as shown in Figure 18.

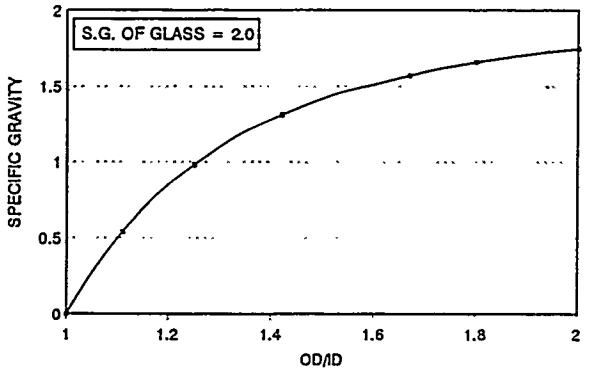

Figure 18. Specific Gravity

The most critical factor beside density is the collapse pressure of the spheres which is proportional to the O.D./I.D. ratio cubed as shown in Figure 19. It is critical that the spheres not collapse at the high fluid pressures existing at the hole bottom of gas wells since this will increase the mud density.

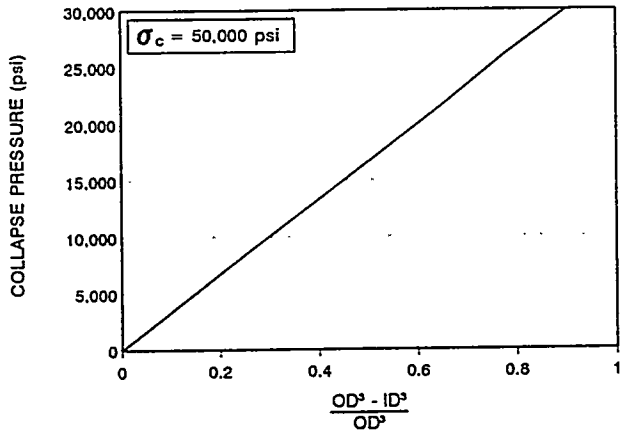

Figure 19. Collapse Pressure

Collapse tests were performed on four candidate, hollow sphere additives. The hollow spheres were mixed with water and placed in a pressure test cell as shown in Figure 20. The percent of "sinkers" was measured first with no pressure applied and then after 2000 psi was applied to the fluid for 24 hours. The collapse test results are shown in Table V.

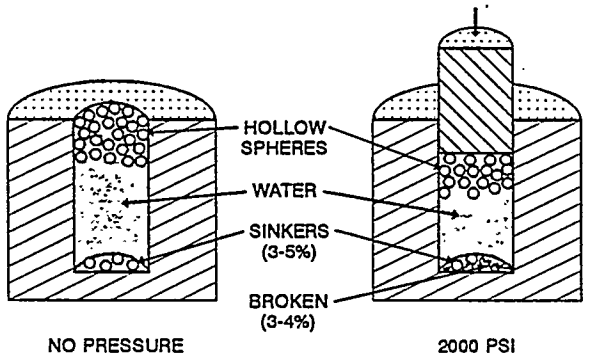

Figure 20. Collapse Pressure Test

Table V. Pressure Test Results on Hollow Spheres

Sphere Identity	Material	Average Specific Gravity (Water=1.0)	Advertised Compressive Strength, psi	Percent "Sinkers"
1	Glass	0.38	4,000	5
2	Glass	0.37	3,000	8
3	Plastic	0.02	2,000	15
4	Glass	0.28	2,000	20

Figure 21 shows how the volume of the mixture containing hollow spheres decreased as the pressure increased. The compressibility of the sphere/water mixture was 3.6 x 10^{-6} psi^{-1}, compared to 3.2 x 10^{-6} psi^{-1} for water alone, which indicated that the hollow spheres are essentially incompressible.

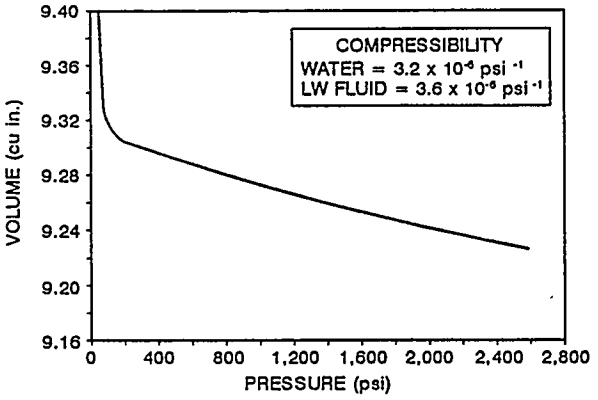

Figure 21. Lightweight Fluid Compressibility

Spheres 1 and 2 were selected for additional testing, because of their higher collapse strength and fewer of them broke and sank.

Table VI lists the standard API drilling fluid tests carried out on the candidate hollow glass spheres in water- and oil-base fluids.

TABLE VI. Hollow Sphere Mud Tests

- FLUID DENSITY
- RHEOLOGY
- FILTRATION
- CONTAMINATION
- HOT ROLLING
- HYDRAULICS

Water-base polymer mud systems containing up to 40 percent by volume of hollow spheres were tested.

Figure 22 shows that the density of 8.8 ppg mud decreased to 6.0 ppg as the concentration of hollow glass spheres (0.38 Sp.Gr.) increased from 0 to 50 percent.

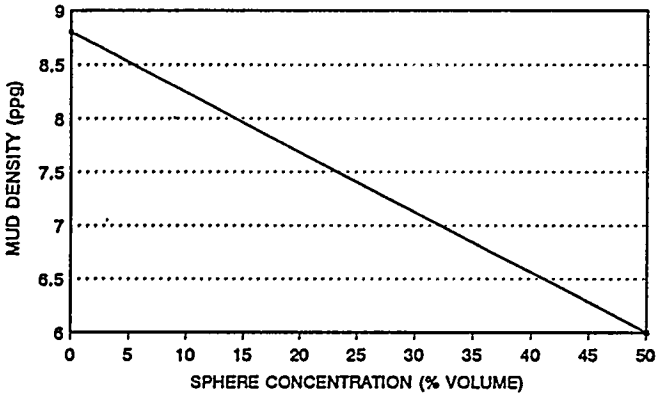

Figure 22. Mud Density

The rheology of lightweight fluids containing hollow glass spheres is similar to that of conventional drilling fluids (Figure 23). Plastic viscosity (PV) increases with increasing solids content in drilling muds. The PV of 60 at a sphere concentration of 40 percent is relatively high, but within acceptable limits for a drilling fluid.

Yield point (YP) is a measure of the fluid's capacity to suspend and carry cuttings. Figure 23 shows that YP increased, but remained within acceptable limits, as the solid concentration was increased to 40 percent.

Figures 24 and 25 show that the PV and YP of a lightweight fluid hot-rolled at 150 degrees F for 16 hours were slightly lower than the same lightweight mud tested at 120 degrees F. These hot-roll tests will be re-run to verify the plateau around 20 percent LWSA concentration.

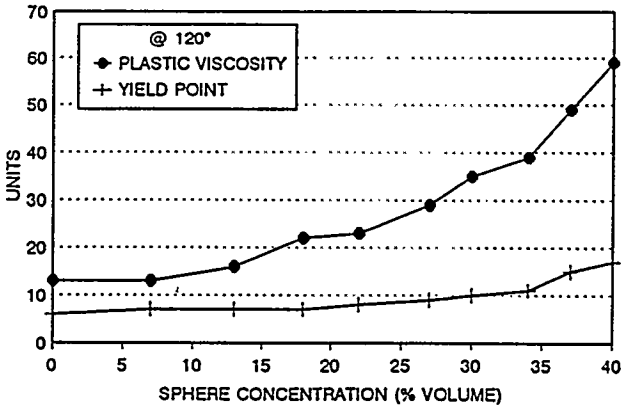

Figure 23. Lightweight Fluid Rheology

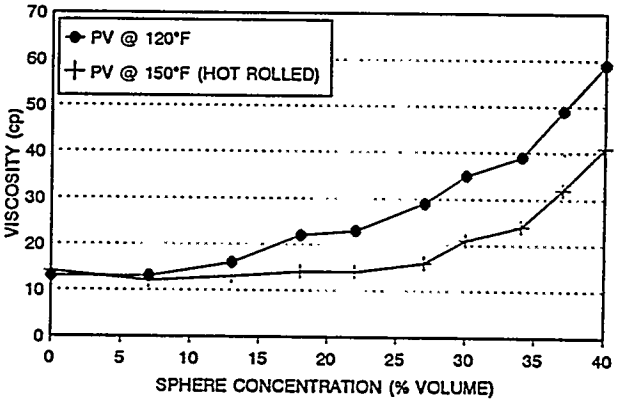

Figure 24. Plastic Viscosity

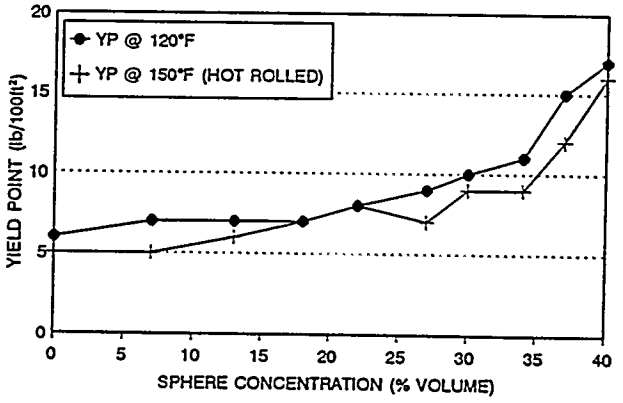

Figure 25. Yield Point

Figure 26 shows that the API filtration loss decreased from 8.3 to 6.2 cc/30 min as the hollow sphere concentration increased from 0 to 25 percent and then increased to 6.5 cc/30 min as the sphere concentration was increased to 40 percent. These filtration values are similar to those for conventional drilling fluids.

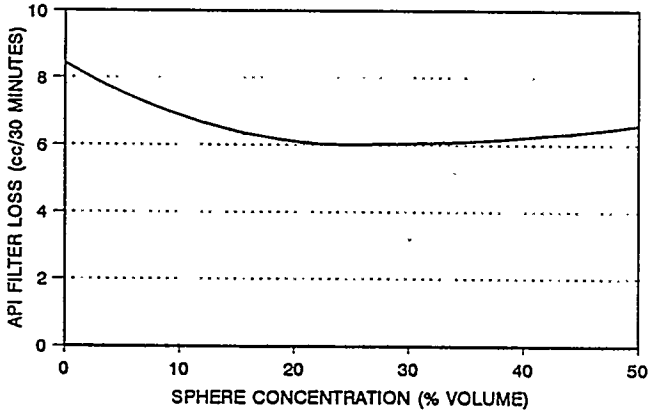

Figure 26. Filtration Loss

A solids control system consisting of a hydrocyclone and shale shaker has been assembled. Preliminary hollow glass sphere fluid testing through the hydrocyclone has started.

FUTURE WORK

Foam Computer Model

Development of the foam drilling computer model is well underway. Additional work still needed includes:

(1) Methods to handle influxes of gas, oil, or water;

(2) Adding jet subs, downhole motors, and other features to the model;

(3) Comparing foam model output with existing laboratory and field data,

(4) Phase II field verification of the model.

Lightweight Solid Additives

Tests to date have convinced experienced mud engineers that good lightweight drilling fluids can be constructed using hollow glass spheres.

Additional work remaining on lightweight solid additives includes:

(1) Formulating and testing the LWSA in oil-base and brine water muds,

(2) Testing the durability and recoverability of the LWSA with conventional solids control equipment,

(3) Testing the durability of the LWSAs with jet nozzles, pumps, and mixing equipment,

(4) Determining the effects of contamination on LWSA mud,

(5) Determining the economics of the LWSA fluid, and

(6) Phase II field testing of the lightweight fluid.

REFERENCES

Beyer, A.H., et al., 1972: "Flow Behavior of Foam as a Well Circulating Fluid," SPE 3986, AIME Meeting, San Antonio, Texas, October 8-11.

Cooper, Leonard W. et al., 1977: "Air Drilling Techniques," SPE 6435, presented at the Deep Drilling and Production Symposium, Amarillo, Texas, April 17-19.

Halliburton Services Company, *Cementing Technology Manual,* Section 12, p. 12-25, October, 1993.

Hook, R.A., Cooper, L.W., and Payne, B.R., 1977: "Part 2—Air, Mist and Foam Drilling: A Look at Latest Techniques." *World Oil*, May.

Lorenz, Howard, 1980: "Field Experience Pins Down Uses for Air Drilling Fluids," *Oil and Gas Journal*, May 12.

Moffitt, Stan, 1991: Personal Communications (Unpublished), Reed Tool Co. Data, Houston, Texas, September 5.

Murray, A.S., and Cunningham, R.A., 1955: "Effect of Mud Column Pressure on Drilling Rates," AIME 505-G, *Transactions* Volume 204, p. 196.

Poettman, F.H. and Begman, W.E., 1955: "Density of Drilling Muds Reduced by Air Injection," *World Oil*, August 1.

Westermark, R.V., 1986: "Drilling With a Parasite Aerating String in the Disturbed Belt, Gallatin County, Montana," IADC/SPE 14734, presented at the 1986 IADC/SPE Drilling Conference, Dallas, Texas, February 10-12.

7.3 DOE/GRI Development and Testing of a Downhole Pump for Jet-Assist Drilling

CONTRACT INFORMATION

Contract Number	DE-AC21-94MC31198
Contractor	FlowDril Corporation 21414 68th Ave. So. Kent, WA 98032 (206) 872-8500 (206) 872-9660
Other Funding Sources	Gas Research Institute (GRI)
Contractor Project Manager	Scott D. Veenhuizen
METC Project Manager	John R. Duda
Period of Performance	Sept. 30, 1994 to Nov. 30, 1996

Schedule and Milestone

FY95 Program Schedule

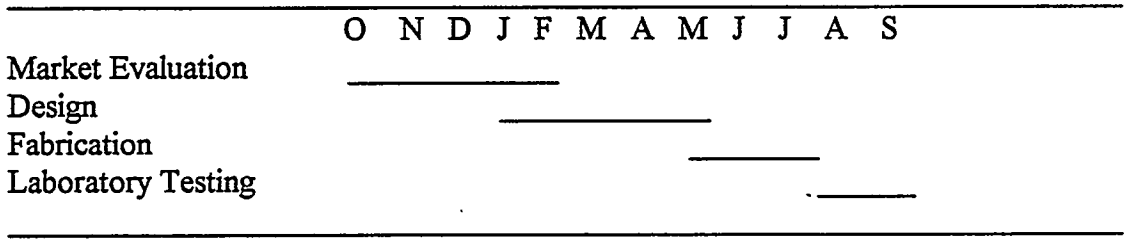

OBJECTIVES

The objective of this project is to accelerate development and commercialization of a high pressure downhole pump (DHP™) to be used for ultra-high pressure, jet-assisted drilling. The purpose of jet-assisted drilling is to increase the rate of penetration (ROP) in the drilling of deeper gas and oil wells where the rocks become harder and more difficult to drill. As a means to accomplishing this objective, a second generation commercial prototype of a DHP™ is to be designed, fabricated, tested in the laboratory, and eventually tested in the field.

BACKGROUND INFORMATION

During the late 1980s and early 1990s, FlowDril developed the FlowDril System®, a surface based high pressure pumping system with a dual conduit drill string for ultra-high pressure, 234 MPa (34,000 psi), jet-assisted drilling of gas and oil wells. The FlowDril System® has been described in part by Butler et al. (1990), Cure and

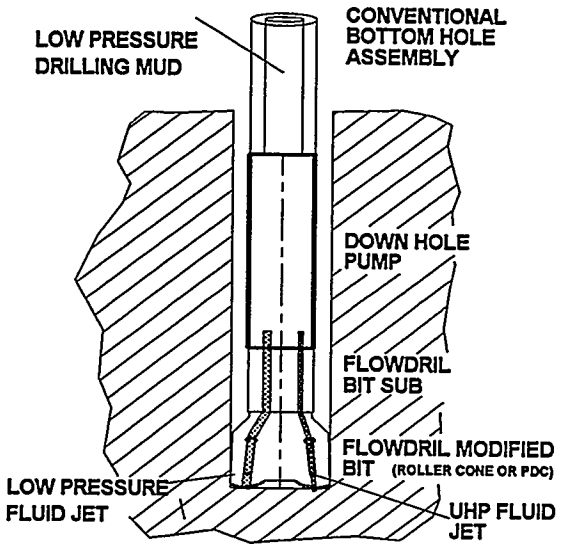

Figure 1. Jet-Assisted Drilling with a Downhole Pump

Fontana (1991), O'Connor and Scott (1991), and Veenhuizen et al. (1993). During field trials, this system was able to achieve reliable operation with ROP enhancements between 1.5 and 2.5 times conventional rates. However, due to the cost of the system, it had a limited market.

In late 1993, FlowDril and the Gas Research Institute (GRI), based on the technology developed in pumping and sealing high pressure drilling mud with the FlowDril System®, began development of a downhole high pressure pump (DHP™) for jet-assisted drilling. This approach is illustrated in Figure 1. The DHP™ is located in the conventional drill string just above the jet-assisted drill bit. The power to drive the DHP™ is provided from the mud stream pumped downhole through the drill string. Conventional flow rates are used but pressure at the rig pump is increased up to about 13.8 MPa (2,000 psi) above typical surface pressures. The size of the DHP™ is about the same as a conventional drill collar and is handled by the rig similar to a drill collar. An experimental field prototype DHP™ has been designed, fabricated, and has undergone testing in the laboratory. A market analysis indicated that the DHP™ should be sized for either 200 mm (7-7/8 inch) or 216 mm to 222 mm (8-1/2 inch to 8-3/4 inch) hole size. A 222 mm (8-3/4 inch) hole size was selected for the experimental prototype at the beginning of the design phase as it was thought that the technology would be easier to develop and demonstrate in the larger hole size and while still responding to a significant market segment.

The first field experiment with the DHP™ was conducted in January of this year at AMOCO's Catoosa Drilling Test Facility in Oklahoma. Photographs of it being picked up by the rig at Catoosa are shown in Figure 2 and Figure 3. The ultra-high pressure, jet-assisted drill bit used is shown in the photograph in Figure 4. The objective of this first experiment was to evaluate the dynamic wear and loading on various components within the DHP™ in a downhole environment. Particular interest was with centralizers in the pump and accumulator sections, and with the high pressure plungers under combined pressure and g-loads. Additional interest was in whether or not the pump operated normally when stressed

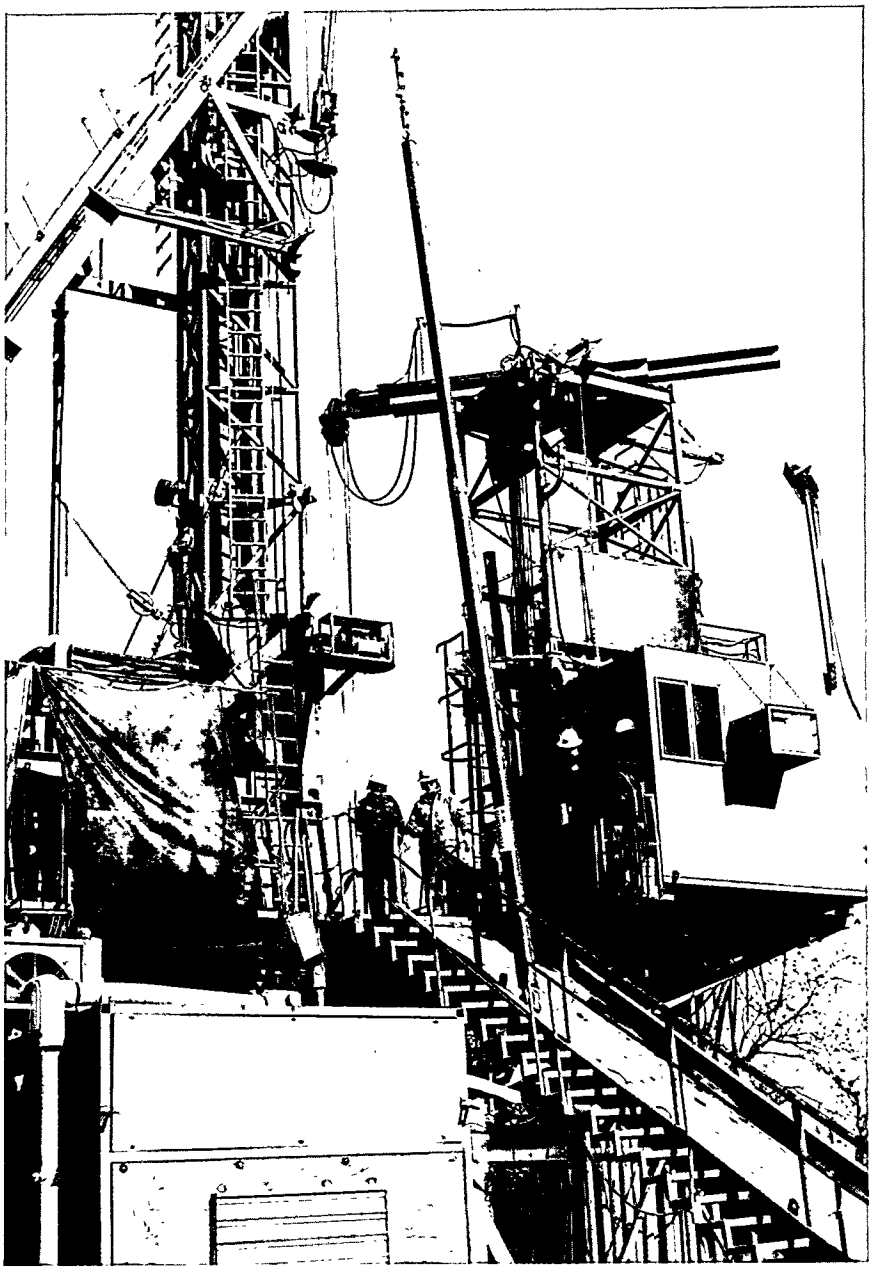

Figure 2. The FlowDril DHP™ Being Picked Up by the Rig During First Field Experiment, Catoosa, OK

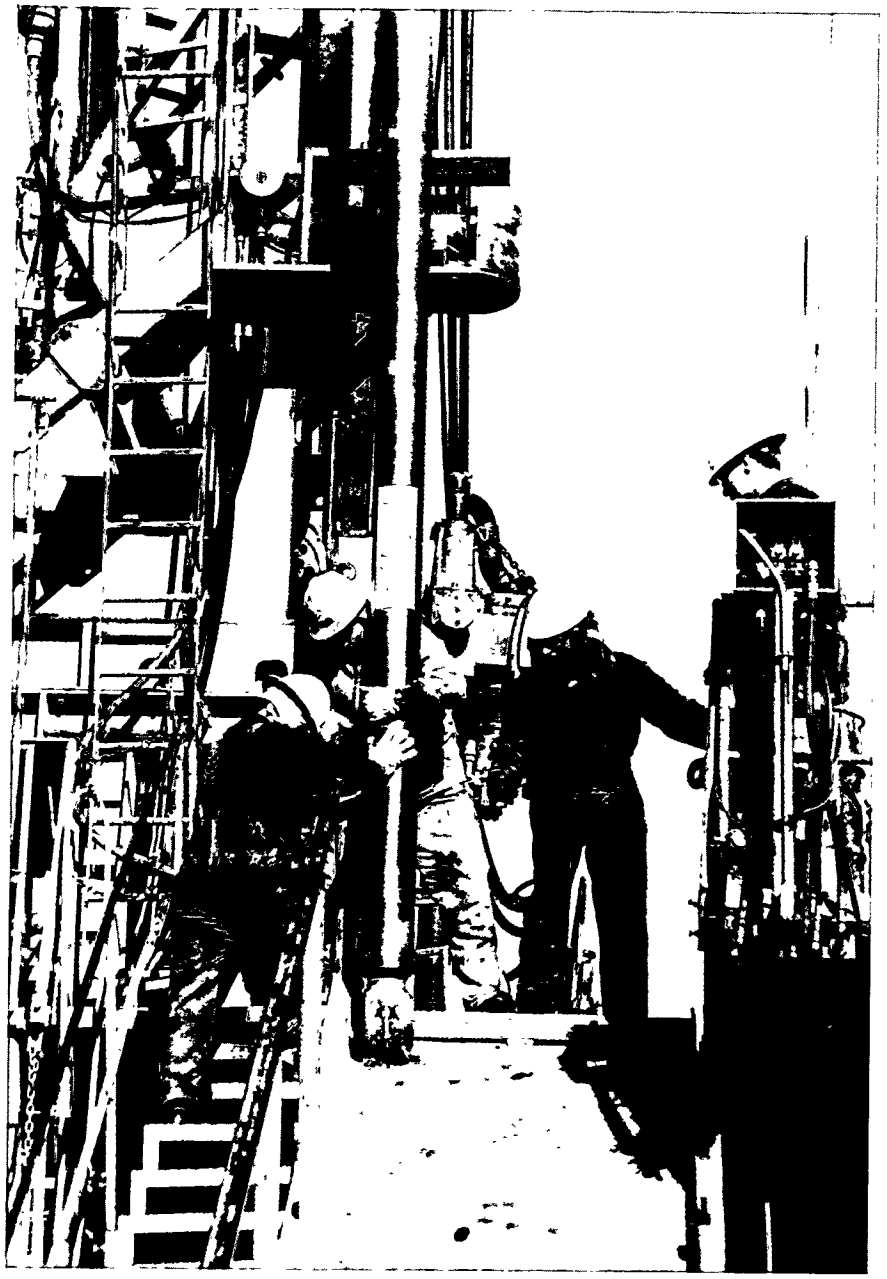

Figure 3. The FlowDril DHP™ Being Brought onto the Rig Floor

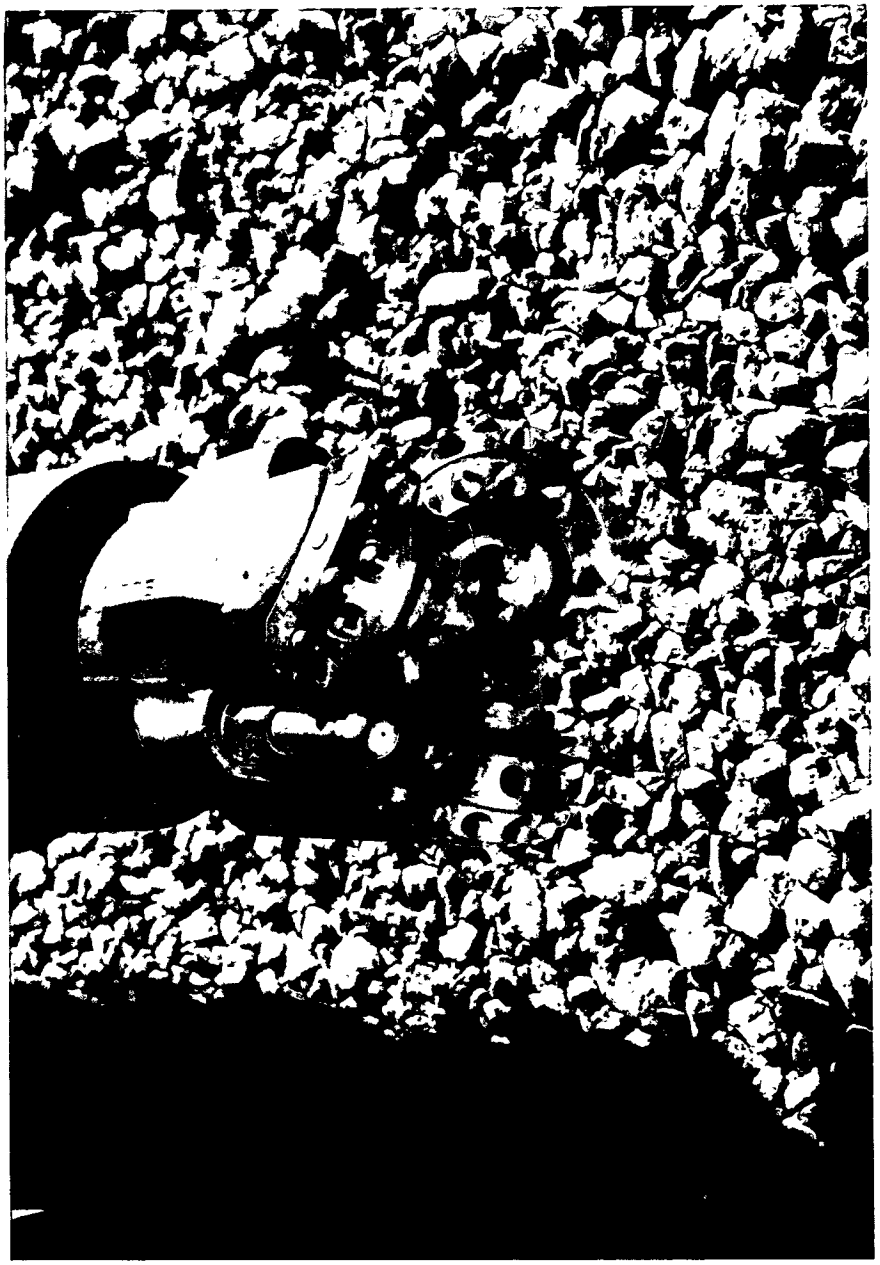

Figure 4. The FlowDril DHP™ Ultra-High Pressure Nozzle on Drill Bit

downhole with weight on the bit, and whether the by-pass valve would operate consistently and was compatible with rig and drilling operations.

Results of a thorough examination of the DHP™ in the laboratory after the experiment at Catoosa revealed that there was very little wear or vibration effect, and no apparent erosion on any of the pump components, with exception of those associated with a low pressure seal failure. The low pressure static seal that failed prevented operation of the pump at full output pressure after the first 45 meters (150 feet) of drilling. It was believed to have been damaged during assembly before being sent to the field. This problem had been experienced previously during laboratory testing and the design had been changed, but not implemented before the field experiment.

The by-pass valve, used to by-pass the pump section during circulating periods, operated consistently and satisfactorily throughout the experiment. Large drill cuttings were found inside the pump housing above the pump section, and inside the drive section of the pump. These are believed to have entered through the conventional bit nozzles during connections or during tripping, and can be prevented by using a conventional float valve in the drill string.

Although not part of the objectives of field experiments with the DHP™, ROP as well as drilling parameters were measured. A plot of these data for most of the period during which the DHP™ was capable of a full 200 MPa (29,000 psi) output pressure is shown in Figure 5. With ultra-high pressure jet-assist and the softer formation, the bit drilled the first 6 meters (20 feet) in 4 minutes, or an ROP of 91 m/h (300 fph). This is an ROP 2.6 times that of the offset hole, DM-2, drilled conventionally with a comparable bit with more than twice the bit weight. If adjustments for weight on bit and rpm are made, the jet-assist ROP was about four to five times the conventional ROP. This kind of ROP enhancement, it must be noted, is indicative of an ultra-high pressure jet that is cavitating because of the shallow depth and is therefore much more effective than would be expected at deeper well depths where cavitation does not occur. At deeper well depths where the DHP™ would normally operate, an ROP increase of 1.5 to 2.5 times conventional is to be expected. During the experiment, the fast ROP caused concern that the hole annulus was being over-loaded with drill cuttings and might cause sticking problems, and that the bit was being over-drilled and might cause hole deviation problems. As a consequence of these concerns, ROP was limited to about 46 m/h (150 fph) by controlling weight on bit for the remainder of the experiment.

Plans for the experimental field prototype DHP™ are for continued laboratory testing and additional field experimentation. A second field experiment is planned for March of this year. It will be in a 250 mm (9-7/8 inch) hole. It will be at a depth of about 1900 meters (6,200 feet) in an East Texas commercial gas well to be drilled for Union Pacific Resources. The objective of this field experiment will be to establish the strengths and weaknesses of the experimental field prototype DHP™ design as a basis for continued design improvements.

PROJECT DESCRIPTION

To accelerate development and commercialization of the DHP™ technology for ultra-high pressure, jet-assisted drilling, FlowDril has contracted with DOE to develop and test a commercial prototype DHP™. The DOE project is outlined by the following:

- Market Evaluation
- Design
- Fabrication
- Laboratory Testing
- Field Prototype Design and Fabrication
- Field Prototype Testing

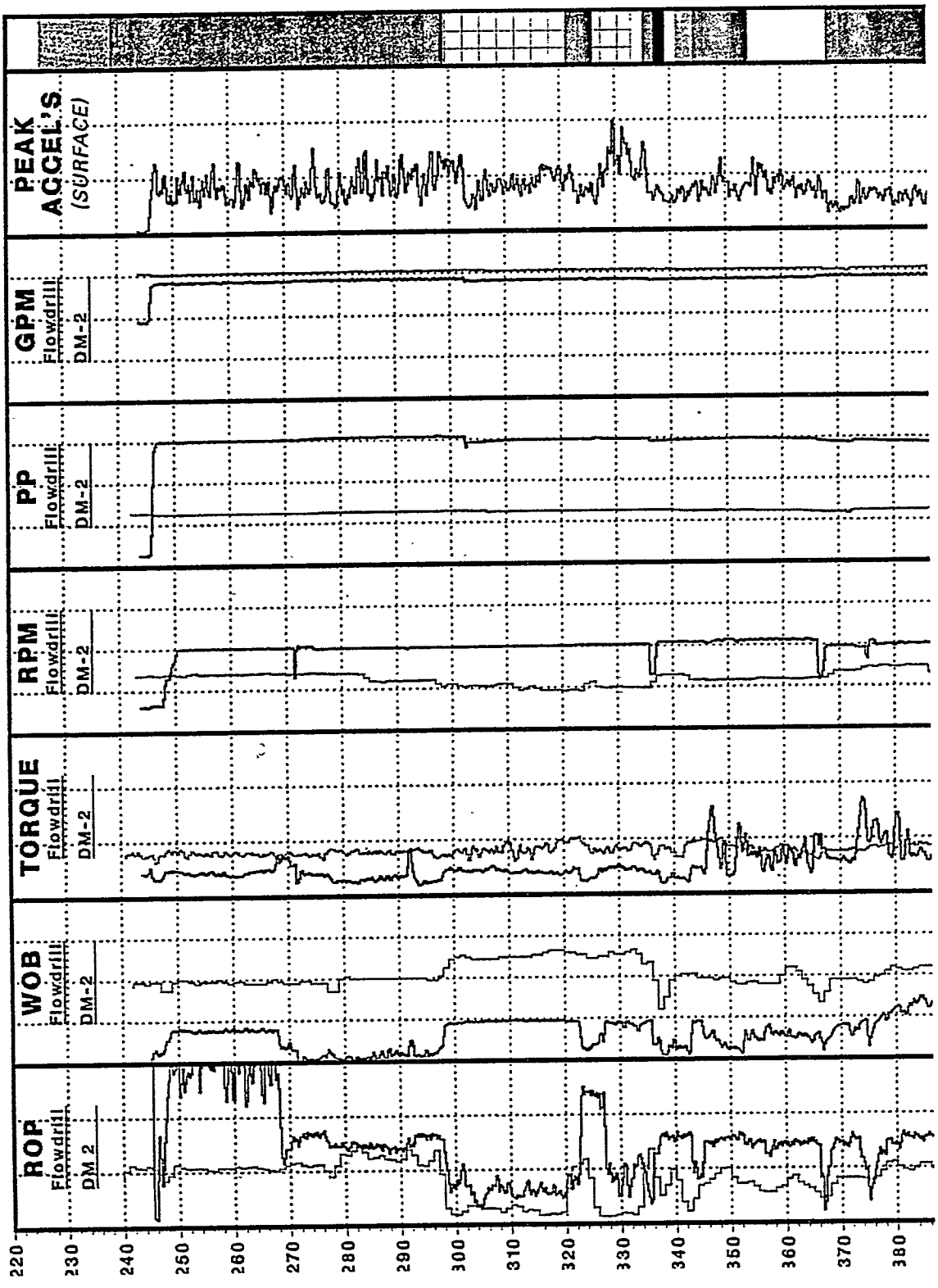

Figure 5. Drilling Parameters, First Field Experiment FlowDril DHP™, Catoosa, OK

Table 1.
U.S. DHP Market Size

Hole Size	DHP™ Annual Market Size(Revenue)
311 mm (12-1/4")	$12.4 million/yr.
240 - 250 mm (9-1/2" - 9-7/8")	$47.6 million/yr.
216 - 222 mm (8-1/2" - 8-3/4")	$58.0 million/yr.
200 mm (7-7/8")	$76.6 million/yr.
152 - 170 mm (6" - 6-3/4")	$11.4 million/yr.
120 mm (4-3/4")	$ 4.0 million/yr.

The purpose of the market evaluation is to define the hole size for the DOE commercial prototype DHP™ that best responds to the market place for domestic gas and oil well drilling. Hole sizes from 4-3/4 inch slim-hole size up through conventional surface hole sizes are considered. The detailed design is to be a commercial prototype design that is an improvement over the experimental prototype design. The DHP™ components designed and fabricated for testing in the laboratory will be field grade commercial prototype components, but only the actual pump section will be completed for laboratory testing. The remainder of the complete commercial prototype DHP™ to enable field testing is to be completed under field prototype design and fabrication which remains at the discretion of DOE pending results from laboratory testing.

RESULTS

A market analysis by Veenhuizen and O'Connor (1993) using 1992 data indicated that about a $200 million annual market exists for jet-assisted drilling using the DHP™ in the drilling of deeper gas, oil and dry wells in the US. For only gas wells, there is about a $74 million annual market. Estimated savings to the drilling industry, assuming a two times conventional rate of penetration, were $173 million and $42 million annually for all drilling and for only gas drilling, respectively. The hole size for which the largest DHP™ market was identified was 200 mm (7-7/8 inch), with 216 mm to 222 mm (8-1/2 inch to 8-3/4 inch) being the second largest.

The market analysis was revisited to re-assess market size by hole size. An emphasis was an examination of potential market for DHP™ jet-assist drilling at slim-hole sizes up to 6-1/8 inch sizes. Drilling smaller size holes with coiled tubing was included as a subset of slim-hole drilling. Results by hole size from the updated market analysis are tabulated in Table 1. The 6 inch to 6-3/4 inch hole size range consists primarily of 6-1/8 inch and 6-1/2 inch. The market size shown for 4-3/4 inch is all slim-hole drilling and is the estimated maximum market size for 1995. It is expected to grow to $8 million - $10 million by the year 2000, but still remain less than for other hole sizes.

As shown in Table 1, the largest market and corresponding savings to the drilling industry is expected to be for 200 mm (7-7/8 inch) hole size. Accordingly, with the experience from the experimental design, and to accelerate commercialization of the DHP™ technology, the DOE second generation commercial prototype DHP™ is sized for a 200 mm (7-7/8 inch) hole.

The DOE commercial prototype DHP™ will be based on the same concept as the

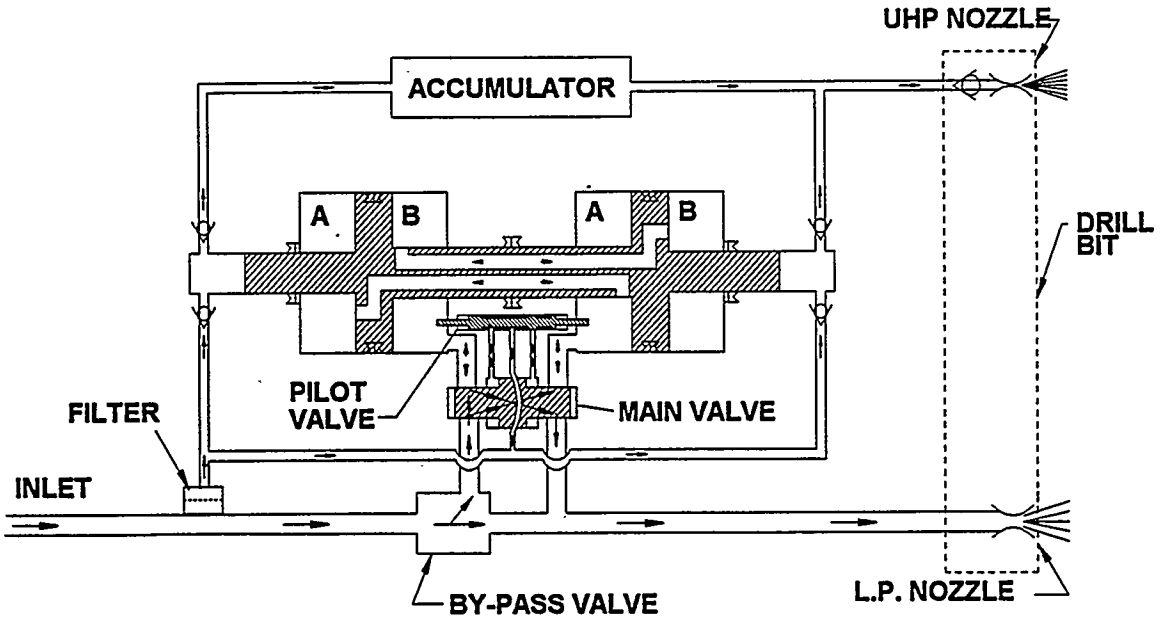

Figure 6. FlowDril Downhole Pump Concept

experimental prototype. The concept, illustrated in Figure 6, utilizes a reciprocating intensifier style high pressure pump. With the by-pass valve closed, the drive fluid passes through the main four-way directional control valve and is directed to either the "A" side or the "B" side of the low pressure drive pistons. The larger diameter drive pistons and the smaller diameter high pressure plungers are connected and form the main assembly that reciprocates back and forth in the pump. When the drive piston/plunger assembly reaches the end of its travel, a trigger mechanically activates the pilot valve, which in turn shifts the main valve, re-directing the drive fluid from "A" to "B", or "B" to "A", driving the drive piston/plunger assembly in the opposite direction. When the by-pass is closed, all of the fluid is directed into the drive section of the DHP™, except that which is drawn off through the self-cleaning filter to become the high pressure fluid output of the pump. The output pressure of the DHP™ is determined by the drive fluid pressure and the ratio of the area of the larger diameter drive pistons to the smaller diameter plungers.

During periods of circulating downhole, the by-pass is open and the pumping section does not generate high pressure. The purpose of the accumulator is to maintain flow of high pressure fluid through the ultra-high pressure (UHP) nozzle during the change in stroke direction when the drive piston/plunger assembly momentarily stops.

The arrangement of the basic components within the DOE commercial prototype design with four drive pistons is shown in Figure 7. To reduce the outer diameter to 171 mm (6-3/4 inch) for the smaller diameter hole requires increasing the number of low pressure drive pistons from three to four. The DOE design of the DHP™ will use the same internal fluid porting scheme, but the main valve will be an alternative design that reduces internal pressure losses through the pump. This will lead to a better overall pump efficiency. The pilot valve

will be of a more compact design, allowing more flexibility in space utilization within the control valve manifold. The housing will be a single piece that includes the accumulator and pump instead of the three piece design of the experimental design. Incorporating the accumulator into the upper end of the housing will allow the overall length to be shortened from 10 meters (33 feet) to about 7.6 meters (25 feet). The most notable differences will be a smaller outside diameter, shorter overall length, and the addition of a fourth drive piston in the low pressure drive section. The main features of the DOE design are summarized below.

- Outer Diameter 171 mm (6-3/4") for 200mm (7-7/8) Hole
- Drive Pistons 4 instead of 3
- 1-Piece Housing with Integral Accumlator instead of 3-Piece
- Overall length of 7.6 meters (25 feet) instead of 10 meters (33 feet)
- More Compact Pilot Valve
- Alternate Main Valve Design
- Fewer Parts, Fewer Seals
- Better Efficiency

The general specifications for the DOE and for the larger experimental design are shown in Table 2. Both are designed to produce an output pressure of 207 MPa (30,000 psi). Because a smaller hole size requires less flow of drilling fluid, the DOE design will produce less output flow than the pump for the larger hole size. The higher average efficiency for the DOE design is primarily the result of the fourth drive piston and a more hydraulically efficient main valve.

FUTURE WORK

The design of the DOE commercial prototype DHP™ is currently in progress. The layout of the complete DHP™ is expected to be completed by mid-April. Fabrication and laboratory experimentation is expected to be completed in September. Pending successful completion of the laboratory testing phase, the DOE commercial DHP™ should be ready for testing in the field by the end of the calendar year.

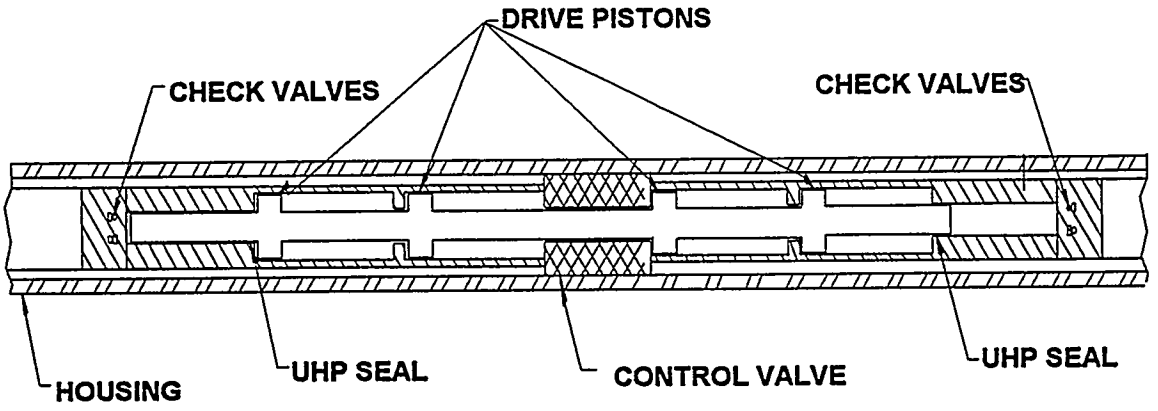

Figure 7. Arrangement of Basic Components within the DOE/FlowDril DHP™ Showing Four Drive Pistons

Table 2.
DOE/ FlowDril DHP™ Specifications

	DOE Tool	Experimental Tool
Bit Diameter	7-7/8"	8-3/4"
Length	25' 1-Piece	33' 3-Piece
DHP Outside Diameter	6-3/4"	7-5/8"
Area Ratio	14:1	14:1
Maximum Output Pressure*	30,000 psi	30,000 psi
Maximum Output Flow*	19.7 gpm	23.6 gpm
Average Efficiency*	72 %	69 %

* 10,000 feet, 45,000 lb WOB, 9.5 ppg mud

REFERENCES

Butler, T. J., Fontana, P., and Otta, R., "A Method for Combined Jet and Mechanical Drilling," SPE Paper 20460, 65th Annual Technical Conference and Exhibition, New Orleans, Sept. 23-26, 1990.

Cure, L. M., and Fontana, P., "Jet Assisted Drilling Nears Commercial Use," *Oil and Gas Journal*, March 11, 1991.

O'Connor, J. M., and Scott, L., "Dual Conduit System Speeds Drilling," *The American Oil and Gas Reporter*, Sept. 1991.

Veenhuizen, S. D., Butler, T. J., and Kelley, D. P., "Jet-Assisted Mechanical Drilling of Oil and Gas Wells," to be presented at the 7th American Water Jet Conference, Seattle, WA, August 28-31, 1993.

Veenhuizen, S. D. and O'Connor, J. M., "Market Analysis: Downhole Pump for Jet-Assisted Drilling," Topical Report GRI-94/0176, Gas Research Institute, April, 1994.

7.4 High-Power Slim-Hole Drilling System

CONTRACT INFORMATION

Contract Number

DE-AC21-94MC30088

Contractor

Maurer Engineering Inc.
2916 West T.C. Jester
Houston, Texas 77018
(713) 683-8227 (telephone)
(713) 683-6418 (telefax)

Other Funding Sources

None

Contractor Project Manager

William J. McDonald, Ph.D.

Principal Investigators

John H. Cohen

METC Project Manager

John R. Duda

Period of Performance

Sept. 30, 1994 to Sept 30, 1995

Schedule and Milestones

TASKS	FISCAL YEAR '95 PROGRAM SCHEDULE											
	O	N	D	J	F	M	A	M	J	J	A	S
1. Design Motor	x	x	x									
2. Fabricate Motor			x	x	x							
3. Motor Tests						x	x	x				
4. Design TSP Bits								x	x			
5. Fabricate Bits									x			
6. Drilling Tests										x	x	x

High-Power Slim-Hole Drilling System

OBJECTIVES:

The objective of this project is to implement new high-power slim-hole motors and bits into field gas well drilling applications. Development of improved motors and bits is critical because rotating time constitutes the major cost of drilling gas wells.

Conventional motors drill most formations 2 to 3 times faster than rotary continuous coring systems due to greater power transfer to the drill bit. New high-power motors and large-cutter TSP bits being developed by Maurer Engineering, Inc. (MEI) drill 2 to 3 times faster than conventional motors. These slim-hole high-power motors and bits, which are ready for field testing on this DOE project, should reduce drilling costs by 20 to 40 percent in many areas.

Phase I

The objective of Phase I is to design, manufacture and laboratory test improved high-power slim-hole motors and large-cutter TSP bits. This work will be done in preparation for Phase II field tests.

Phase II

The objective of Phase II will be to field test the high-power motors and bits in Amoco's Catoosa shallow-test well near Tulsa, OK, and in deep gas wells. The goal will be to drill 2 to 3 times faster than conventional motors and to reduce the drilling costs by 20 to 40 percent over the intervals drilled.

BACKGROUND INFORMATION:

In the late 1950s and 1960s, over 3000 slim holes were drilled in oil and gas fields worldwide. These slim holes reduced well costs by 20 to 50 percent in many areas, primarily due to reduced rig and tubular costs. Although significant cost savings were achieved, larger holes were used predominantly in the '70s and '80s due to 1) short life of small-diameter roller bits, 2) high oil prices, and 3) the misconception that large holes were needed everywhere. Many companies are now re-examining the use of slim-hole drilling because improved slim-hole drilling motors equipped with advanced TSP and PDC bits have potential for reducing well costs by 40 to 60 percent in many areas.

Basic Slim-Hole Drilling Systems

There are currently three basic slim-drilling systems (see Figure 1) being utilized or developed.

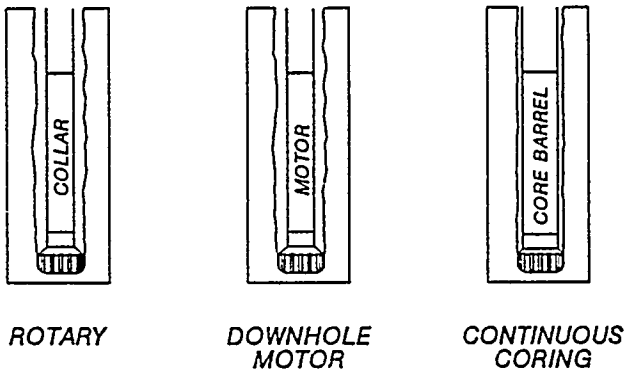

Figure 1. Basic Slim-Hole Drilling Systems

Rotary slim-hole rigs rotate small diameter drill pipe at speeds of 300 to 800 rpm. Twist-offs of the small-diameter drill pipe are a major problem with this system.

Downhole Motor systems utilize slim-hole motors to rotate bits at speeds of 800 to 2000 rpm. They drill at high rates and eliminate drill string twist-off problems by eliminating drill string rotation.

Continuous Coring systems use slim-hole mining core barrels to continuously core entire wells. They are used in new drilling areas where geologists need cores to define geology.

PROJECT DESCRIPTION:

Phase I — Design and Laboratory Tests

During Phase I, MEI is designing and testing a slim-hole high-power drilling system that includes a downhole multi-lobe Moineau motor and a large-cutter TSP bit.

The new 3⅜-in. multi-lobe motor, capable of delivering twice the power of conventional motors will be used to drill slim-holes with 4½- and 4¾-in. diameter bits. Figure 2 shows key improvements that will be made to the motor.

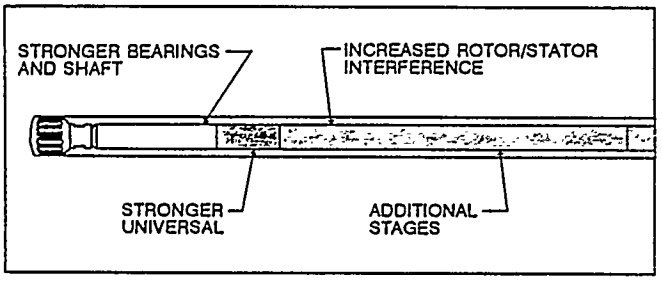

Figure 2. High-Power Motor Improvements

The power end of the motor will be manufactured from two standard Robbins & Myers (R&M) stators and a specially-machined, double-length rotor. The lobe configuration will be 4/5 as shown in Figure 3.

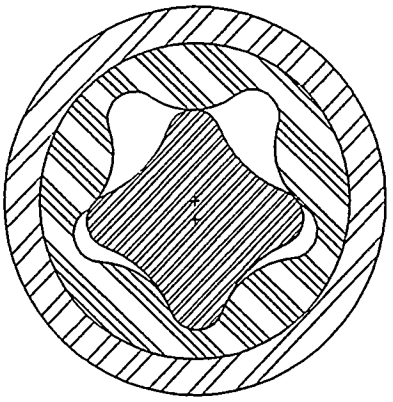

Figure 3. Motor Lobe Configuration

Due to its higher power, the motor must have a stronger bearing pack and stronger flex coupling. MEI will use the latest technologies to improve bearings and flex couplings for use in this motor.

The areas of improvement on the flex coupling include improved high-strength steels, lobe-cutting methods and a titanium flex shaft. MEI will select the best flex coupling for field testing.

The bearing pack improvements include improved high-strength steel for the drive shaft, metal-on-metal radial bearings and stronger thrust bearings. The improved drive shaft will have a large bore to decrease pressure losses through the drive shaft and to allow increased flow through the motor, resulting in higher rotary speed, increased power, and improved hole cleaning.

The extra Moineau stages will permit higher pressure drop across the motor section, resulting in increased torque, higher power, increased weight-on-

bit and increased drilling rate. The higher-than-normal bit loads will be absorbed by improved bearings in the bearing pack.

An engineering review will be conducted after the high-power slim-hole motor design drawings are completed. Problems found will be corrected and final manufacturing drawings will be prepared.

MEI will fabricate and test critical motor components to select the best design for use in the field motors. All manufactured components will be inspected for dimensional accuracy and material coupons will be used to insure correct heat treatment of all parts.

After all parts have been inspected, MEI will assemble and test the motor on the Drilling Research Center (DRC) motor dynamometer test stand shown in Figure 4.

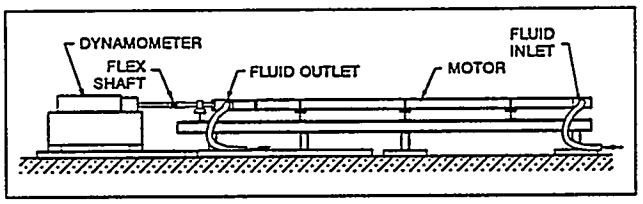

Figure 4. DRC Motor Dynamometer

Motor performance curves will be compared with theoretical calculations in preparation for field testing. The test stand will also be used to evaluate critical components such as flex couplings and flex shafts.

The second component of the slim-hole high-power drilling system is the large-cutter TSP (LC-TSP) BIT. An earlier study showed that the majority of time in drilling a well is spent rotating the bit and tripping; therefore, the greatest reductions in time and cost can be obtained by increasing the penetration rate. As a result, these advanced TSP bits were developed.

PDC bits have made a major improvement in oil and gas drilling during the past ten years, especially in softer shales where the PDC bits are very effective. However, the PDC cutters deteriorate and fail in hard rock due to severe temperature limitations. PDC cutters fail at 700° C, whereas TSP cutters operate effectively at temperatures up to 1200° C (Fig. 5).

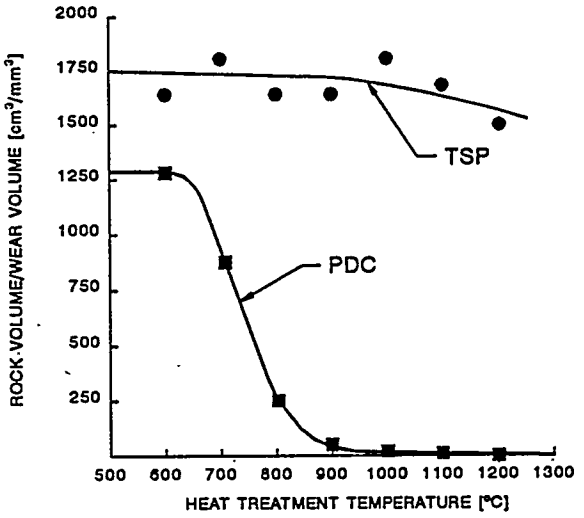

Figure 5. Temperature Effects on PDC and TSP Cutters (Clark et al., 1987)

This decrease in strength of the PDC cutters is due to differences in the thermal expansion of the diamond and the cobalt binder in the void spaces between the diamonds, as shown in Figure 6. As the cutters are heated, the cobalt binder expands more than the diamonds, causing thermal fracturing and failure of the PDC cutters.

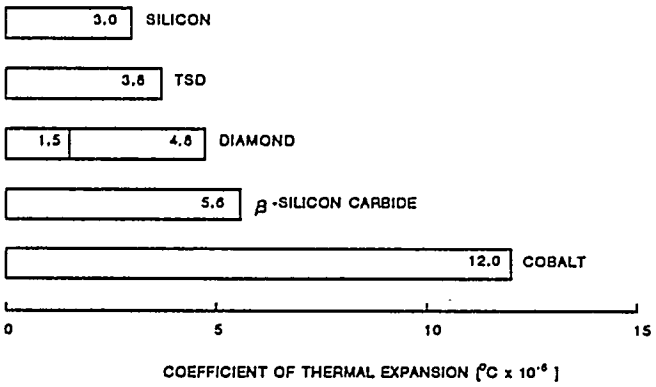

Figure 6. Thermal Coefficient of Expansion (Clark et al., 1987)

TSP cutters contain silicon instead of cobalt in the pore spacers between the diamonds. The silicone binder allows the PDC cutters to operate effectively at high temperatures because the thermal coefficient of expansion of silicon is similar to that of diamond. Consequently, TSP cutters can drill hard rock without excessive wear or breakage of the cutter as shown in Figure 7. In this test, a TSP bit drilled over 300 ft. in granite that is much harder than the sedimentary rocks normally encountered in gas wells.

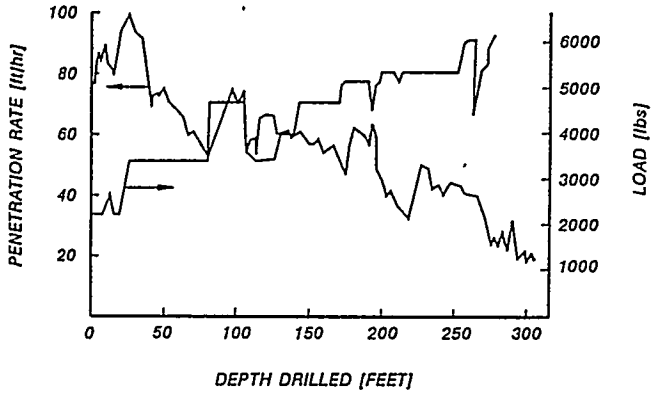

Figure 7. TSP Bit Drilling Granite (Clark et al., 1987)

MEI, in conjunction with The University of California at Berkeley, conducted numerous single cutter and laboratory bit tests varying the number, size, and configuration of TSP cutters. These tests showed that TSP bits utilizing large TSP cutters (7mm x 7mm x 5mm) drill much faster and further than conventional PDC and TSP bits. Figure 8 shows a large-cutter TSP bit that performed well in laboratory tests.

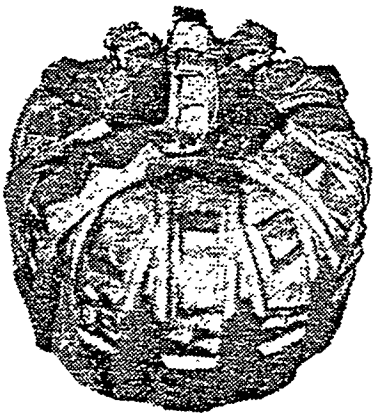

Figure 8. LC-TSP Bit

As part of Phase I, MEI will design LC-TSP bits with torque and speed characteristics that match the high-power motor characteristics, and the lithology of the area to be drilled.

The field motor and bits will be tested on the DRC motor drilling stand (Figure 9). Data from these tests will be used to determine the optimum field operating parameters for the slim-hole drilling system.

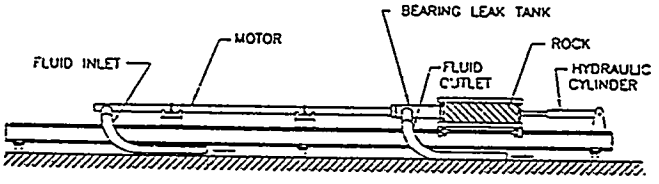

Figure 9.. Motor Drilling Stand

Phase II — Field Tests

During Phase II, shallow drilling tests (2500 ft) will be conducted at Amoco's Catoosa test site near Tulsa. The results of these shallow tests will be used to optimize the motors and bits prior to conducting full-scale field tests. The field system will then be laboratory tested on the DRC's dynamometer and drilling test stands prior to field tests.

Following the laboratory tests, the slim-hole system will be tested in slim-hole gas wells. A minimum of five tests will be conducted at locations where there is sufficient offset data to make comparisons between conventional drilling and the new high-power slim-hole system. The results of the laboratory and field tests will be submitted to the DOE in a final report.

RESULTS:

Design of the high-power motor is completed and the modified motor components are being manufactured. Alternative methods of manufacturing the flex high-strength coupling are being studied, including using high-pressure abrasive-jets to cut the lobes on flex coupling since this technique applies no heat to the part, thus eliminating thermal damage produced by flame cutting.

In preliminary tests, the abrasive jet penetrated the steel on the side opposite the cut, damaging the inside of the lobe cut (Figure 10). Attempts are being made to eliminate this problem since the use of this jet-cutting technique looks promising.

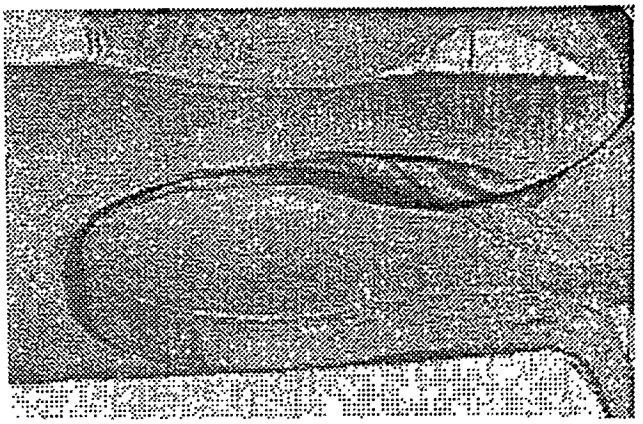

Figure 10. Water Jet Damage on Inside of Cut Coupling

Modifications to the lobe patterns used on these couplings is also being explored to increase the strength and wear resistance of these couplings.

MEI is also examining the use of titanium-flex shafts in place of standard-flex couplings. Robbins and Meyers ran a finite element analysis on a titanium-flex coupling for the high-power motor which shows the stresses for different length flex shafts (Table 1).

Table 1. Flex Shaft Stresses (Robbins & Meyers)

Assumptions:
1) Rotor Eccentricity = 0.165 in.
2) Flex due to motor bend = 2.5°
3) Maximum down thrust 5900 lbs
4) Maximum torque 1660 ft-lbs
5) Titanium bar, OD = 1.75 in.

Length	Bore	Max. Stress (PSI)
24 in.	None	108K
24 in.	.75 in.	112K
30 in.	None	70 K
30 in.	.75 in.	67K
36 in.	None	42K
36 in.	.75 in	38K

The endurance limit for titanium is 40 ksi so a shaft 1.75 in. x .75 in. diameter 36 in. long should give infinite life at the predicted maximum load conditions. The length added by the flex shaft is small compared to the newer length of the high-power motor.

FUTURE WORK:

The high-power motor will be assembled and tested as soon as all motor components are manufactured.

Torque tests of different design flex couplings will be conducted up to the failure load using a rotary torque machine. The best coupling design will be selected for laboratory testing in the high-power motor. Design of the flex shaft will be completed and manufacture begun. Prototype flex couplings and flex shafts will be tested on the dynamometer test stand to determine their effect on motor performance.

MEI will develop a test plan for the dynamometer and drilling tests while manufacture of the motor is completed. Dynamometer testing of the motor will be carried out to determine motor torque, speed, power output, and efficiency. The large-cutter TSP field bits will be designed and manufactured after the field sites are selected and the bit sizes and the lithology determined.

Drilling tests will be conducted with the high-power motors and LC-TSP bits before field tests are conducted.

REFERENCES:

Clark, I.E. and Shafto, G.R., 1987: "Core Drilling With SYNDAX3 PCD," *Industrial Diamond Review*, April.

Delpassand, Majid, 1995: Personal Communication, Moyno Oilfied Products (A Division of Robbins and Meyers, Inc.), Fairfield, California.

7.5 Fracturing Fluid Characterization Facility (FFCF): Recent Advances

CONTRACT INFORMATION

Cooperative Agreement Number	DE-FC21-92MC29077
Contractor	University of Oklahoma School of Petroleum and Geological Engineering 100 East Boyd, Room T301 Norman, Oklahoma 73019-0628 (405) 325-2921
Other Funding Sources	Gas Research Institute 8600 Bryn Mawr Avenue Chicago, Illinois 60631
Contract Project Manager	Subhash N. Shah
Principal Investigators	Subhash N. Shah John E. Fagan
METC Project Manager	Karl-Heinz Frohne
Period of Performance	September 1, 1993 to December 31, 1994
Schedule and Milestones	**See Table 1**

OBJECTIVES

The objectives of this project are:

1. Investigate fluid rheological behavior, dynamic fluid leak-off behavior, and proppant transport characteristics of various fracturing fluids used for stimulating oil and gas bearing formations.

2. Develop new information for characterizing the behavior of fracturing fluids under conditions more representative of the behavior in actual fractures.

3. Continue utilizing the advanced capabilities of the high pressure simulator (HPS) to perform near-term research and development activities and not to construct a large-scale simulator that was proposed originally.

BACKGROUND INFORMATION

Numerical simulators used today for simulating hydraulic fracturing treatments incorporate assumptions and approximations.[1,2] Evaluation of the consequences of these assumptions and approximations has not yet been conclusive because controlled experiments on a scale necessary for the evaluation have not been possible. In order to accurately design and control hydraulic fracturing treatments, gas producers and service companies must be able to characterize the performance of the fluids used in creating a fracture and placing the proppant. In addition, most fundamental data relating to fluid behavior and proppant transport in fractures have been obtained from laboratory-scale studies, and there is uncertainty about scaling data from such tests to field-scale applications.[3] To address and help resolve some of these issues, the Gas Research Institute (GRI), the U.S. Department of Energy (DOE), and The university of Oklahoma (OU) have jointly established a "Fracturing Fluid Characterization Facility (FFCF)" which is dedicated to the investigation of fracturing fluid flow behavior and proppant transport phenomena. Experience gained during construction and operation of the prototype simulator suggested that budgetary constraints would not allow a large-scale simulator to be built on these same operating principles as proposed originally. As a consequence, the former prototype simulator was re-designated the high pressure simulator (HPS) and is currently being used to the maximum extent possible to perform fracturing fluid research. Based on results obtained to-date, the HPS has come to be recognized as a considerable advancement over other industry fracture simulators. Therefore, it was decided to continue utilizing the advanced capabilities of the HPS to perform near-term research and development activities. During 1994, the FFCF project was, thus, refocused to accomplish this research effort. A revised research plan was developed keeping in mind the original goals of the FFCF project.

To date, a series of tests have been performed to confirm the operational readiness of the HPS to perform the many functions for which it was designed. The operations of the mechanical and instrumentation systems have been verified.[4-7] Utilizing the advanced capabilities of the HPS, extensive fluid testing has been conducted to investigate the major research areas of fluid rheology/fluid behavior, proppant transport, dynamic fluid loss, and perforation friction loss. The testing program has produced results that support some industry assumptions and contradict others. This paper describes equipment enhancements, data acquisition and instrumentation upgrades, R & D test results, and future research planned for the FFCF.

PROJECT DESCRIPTION

The main focus of the FFCF has been the design, fabrication, and construction of the high

pressure simulator to experimentally investigate the rheological behavior and proppant transport characteristics of various fracturing fluids under field-simulated conditions. The detailed description of the HPS as well as the auxiliary equipment, and data acquisition and control systems associated with the simulator has been provided earlier.[4,8] In the following, a brief description of the HPS and auxiliary equipment is provided. Also provided are the modifications to various equipment and instrumentation needed to accomplish the goals of the project.

High Pressure Simulator

The high pressure simulator (HPS) for characterization of fracturing fluids is a vertical, variable-width, parallel-plate flow cell capable of operating at elevated temperatures (250°F) and pressures (1200 psi). A photograph of the HPS is shown in Figure 1. The slot dimensions are 7 ft high and 9 1/3 ft long, formed by two faces, one fixed and the other movable by servo control. Slot width can be adjusted dynamically over the range of 0 to 1.25 in. by a system of 12 hydraulically actuated platens. Each platen is 28 inch square and the platens are laid out in a 3 by 4 matrix to form one face of the simulated fracture. The platen surfaces can be changed from smooth impermeable surfaces to rough permeable surfaces. Fluid enters the HPS through manifolds which simulate a wellbore with perforations. Behind each facing is a system of fluid collection channels which route fluid loss to a point outside the flow cell for measurement.

Inlet and exit manifolds are 2 3/4 in. in diameter and are equipped with 22 openings which are 3/4 in. in diameter and on 4-in. spacing. Using a series of blank and sized inserts, the inlet manifold can be easily modified to simulate perforated intervals of different size and distribution.

The fiber optic vision system and the Laser Doppler Velocimetry (LDV) system of the flow cell facilitate the visualization and accurate measurement of flow behavior of fracturing fluids with or without proppant.

The HPS has many unique features:

1. The use of simulated wellbore and perforations that allow fluid entry into the slot geometry.
2. Flexibility of varying perforation size and distribution.
3. The dynamic variation of gap width of the fracture slot.
4. Measurement at high pressure (1200 psi) and temperature (250°F).
5. The use of either synthetic or natural rock facing as the fracture surface.
6. Measurements of point velocities and velocity profiles across the slot width with the LDV.
7. A state-of-the-art fiber optics system for fluid and proppant flow visualization inside the slot.
8. Field-size equipment for fluid preconditioning to represent the same shear and temperature histories encountered in the field.

Auxiliary Equipment and Instrumentation

Auxiliary equipment for the HPS consists of equipment for mixing and pumping fluids and slurries through the HPS and equipment for heating the fluid. Low pressure pumping equipment consists of Moyno pump and a centrifugal pump. The centrifugal pump serves to boost the suction of the Moyno pump, as an aid in fluid preparation, and as a point of crosslinker

injection for crosslinked and proppant-laden crosslinked fluids. Two ISCO syringe pumps are available to inject the crosslinker into the suction of the centrifugal pump.

High pressure pumping equipment consists of a triplex pump and a Galigher centrifugal pump. The centrifugal pump is used to boost the suction of the triplex pump, as an aid in fluid mixing, and as an injection point for the crosslinker. A special flow-over-poppet throttling valve with fuzzy logic control is installed to the exit line of the HPS for the purpose of holding up to 1000 psi back pressure on the flow cell.

Fluid mixing and storage vessels include a 55 gal stainless steel tank equipped with a three-bladed air mixer, a 200 gal ribbon blender, and a 1000 gal polyethylene storage tank. Also, available are the two 50-bbl fluid mixing and storage tanks on a trailer unit. Each tank is equipped with an individually-controlled, hydraulically-driven agitator. Two 330-sack bulk sand-storage tanks are located on a second trailer. Sand can be transferred pneumatically from these tanks to the 50-bbl fluid mixing tanks to prepare slurries.

The instrumentation system of the HPS is capable of real time monitoring of temperature, pressure (both system and differential pressure across various positions along the length of the flow cell), adjustable gap width at different locations, flow rate and density. The leak-off through the permeable surfaces can also be measured to characterize dynamic fluid loss behavior of the fluids. Additional information about the equipment and instrumentation can be found elsewhere.[5,6,9]

Equipment Enhancements

Several HPS upgrade modifications are made to make the HPS much more user friendly. The improved modification of the light pipe assembly for the vision system was done to increase the light transmission across the simulated fracture and improve the image production from the receiver side of the HPS. The improved vision camera brackets are made so that more precise camera alignment can be obtained between the camera and the image conduit. A hydraulic slave cylinder has been adapted to the HPS to open and close the HPS more smoothly and safely. The exit manifold of the HPS has been improved with high pressure piping which gives the capability to run low or high pressure tests and maintain uniform flow through the simulated fracture. A new method of HPS crack calibration and tuning the HPS alignment has been developed which allows a more accurate crack determination.

The new fluid pre-conditioning system has now been installed at the FFCF. This system implements the use of a low-shear heat exchanger and steel coil tubing which allows high-shear history simulation. The target shear rate is 1350 sec^{-1} with a residence time of 5 minutes. The total length of the coil tubing is 5000 ft and using a pump rate of 60 gal/min through this tubing will provide a shear rate of 1400 sec^{-1} and a residence time of 4.8 minutes. The tubing has been placed on three spools of 1000, 2000, and 2000 ft, which allows the opportunity to study the effect of residence time on fluid properties at various levels of shear.

Data Acquisition and Instrumentation Upgrades

The data acquisition and instrumentation systems are enhanced to provide data more attune to the needs of the project while providing a reduction in system operating cost. The pressure, temperature, and simulator data acquisition has been replaced by a Fluke Hydra system. The new system offers increased reliability, and accuracy over the Data Translation system, as well as providing improved data display and logging. The new system also provides greatly decreased reoccurring cost for temperature measurements in the HPS. The new system is designed to replace the existing IBM/RISC as well as the Data

Translation system.

The Laser Doppler Velocimetry (LDV) system has had rotational and translation systems installed on three of the nine stations. These three stations can be moved easily to any one of the nine LDV locations on the HPS. This rotation and translation capability allows the user to gain more precise velocity profile data within the slot as well as gain information on the vertical velocity component. In addition to the rotation and translation, the LDV windows are modified to move the LDV probe closer to the slot flow. This movement will give the LDV system increased sensitivity, increased penetration of opaque fluids, a reduced probe volume for near wall studies, and a better signal to noise ratio for obtaining overall velocity profiles.

The vision system has undergone improvement towards the gaining of spot proppant concentration data of the HPS slot flow. A method of determining the spot concentration in transparent slot flow has been developed. This transparent slot flow methodology is being adapted to video data from the HPS, thus allowing the determination of spot proppant concentration measurements in the HPS. The improvements in lighting, fibers, and vision sensors have also been made.

An improvement in the reliability of the system, as well as improved throughput and maintenance have resulted from these changes in the instrumentation system.

Procedure

High Pressure Fluid Rheology. The purposes of these tests were: (1) to evaluate the operation of the apparatus and associated mechanical and instrumentation systems at elevated pressure with non-Newtonian fluids, and the operation of the field-size equipment and the throttling valve; (2) to acquire the rheological properties of non-Newtonian fluids; and (3) to evaluate the effect of high pressure on the rheology of these fluids.

A 60 lb/Mgal linear hydroxypropyl guar (HPG) solution was mixed at room temperature and tested in a recirculating mode employing the triplex plunger pump. Flow data were gathered at several different gap widths using a series of flow rates for each gap width. Cooling fluid circulated through a double-pipe heat exchanger kept the test fluid at constant temperature. The test was performed at ambient temperature and with all perforations open. Steady-state differential pressure data were acquired at each constant flow rate. Figure 2 provides the designation and location of all differential pressure transducers used on the flow cell. The fluid samples were also evaluated on model 35 Fann viscometer for later comparison with the HPS slot data.

High Temperature Fluid Rheology. The objective of these experiments was to verify the operation of the HPS mechanical and instrumentation systems at elevated temperature and to provide rheological data of linear solutions at elevated temperature.

Flow data with a 150 lb HPG/Mgal polymer solution were obtained at temperatures of approximately 200°F and 225°F with a gap width of 0.50 inch. A 150 lb HPG/Mgal fluid was selected to provide a measurable level of differential pressure at these temperatures and to also provide a fluid which can be easily characterized with a model 50 Fann viscometer for comparison. The tap water was initially heated to approximately 120°F by recirculating from both mixing tanks and through the flow cell using a leased hot oil unit. At this point, polymer solution was mixed in one tank. The temperature of the polymer solution and flow cell was elevated to approximately 200°F by recirculating the one gel tank. The remaining tank of hot water was reserved as a flush fluid to minimize thermal shock of the HPS and its facings. Flow data were collected at approximately 200°F by recirculating through the flow cell using the hot oil unit at rates of 20, 30, 40, 50, and 60 gal/min. At the end of this flow rate sweep, the temperature was elevated

to approximately 225°F where another flow rate sweep was made.

Slurry Rheology. The objective was to evaluate the effect of proppant concentration on slurry rheology, and to establish operational procedure for future slurry rheology tests.

The test fluids were 60 lb HPG/Mgal containing 0, 2, 4, 6, 8, and 10 lb/gal 20/40 mesh sand. 1000 gallons of linear HPG was prepared and batches of approximately 200 gallons were transferred to the ribbon blender to prepare slurries. Slurries with different proppant concentrations were prepared from fresh batches of clean gel transferred from the 1000 gallon tank. The flow rates were maintained high enough to minimize any settling from the fluid. The experiment was monitored with the fiber optic vision system to detect settling and any other abnormal phenomena.

Crosslinked Fluid Rheology. The purpose of this test was to evaluate the operation of the apparatus with crosslinked gel and also to acquire the rheological properties of crosslinked fluids.

A 60 lb/Mgal HPG polymer solution was first mixed in a 1000 gal capacity mixing tank. Some of the solution was then transferred into a 200 gallon capacity ribbon blender and a batch of titanium-crosslinked gel was prepared batch-wise. The crosslinked 60 lb/Mgal HPG gel was pumped single-pass at 20, 30, 40, and 60 gal/min in 0.375 inch gap width. All perforations were open for this test. Differential pressure versus flow rate data were acquired.

Wall Slippage Phenomena. The objective of this study was to evaluate the flow behavior of crosslinked fluids to determine if wall slip is present during flow through the simulated fracture geometry of the HPS.

All early observations of anomalous flow behavior was assumed to be the results of the fluid being batch-mixed rather than continuously-mixed as occurs in the field operations. Several experiments were designed and performed in an attempt to discover the phenomena responsible. As a result of that effort, an experimental approach was developed to assess the influence of wall slippage on the rheological response. These "wall slippage" experiments were performed with a titanium-crosslinked 60 lb HPG/Mgal fluid.

With the HPS, conventional continuous crosslink fluid flow experiments could be performed in one of two ways. In the first method, an initial gap width was set and the continuously crosslinked fluid was pumped at various flow rates in a single pass through the HPS slot. A new gap width was then set and the same variation in flow rate was followed. This procedure was repeated for a range of fixed gap width to provide shear stress versus shear rate data. In the second method, an initial flow rate was set. and gap width was varied while the continuously crosslinked fluid was pumped single-pass through the HPS slot. A new flow rate was then set and the same variation in gap width was followed. This procedure was repeated for a range of fixed flow rate values to provide shear stress versus shear rate data. The experiments with a titanium-crosslinked 60 lb HPG/Mgal fluid showed that both conventional testing methods provided equivalent results.

The "wall slippage" test was based on maintaining a constant mixing and crosslinking flow rate while simultaneously varying gap width and slot flow rate to achieve a fixed level of shear rate. In the current experiments, a constant mixing and crosslinking flow rate of 60 gal/min formed a base from which preselected flows were diverted through the simulator to provide the same nominal shear rate at four different gap widths.

Dynamic Fluid Loss. The objective of these experiments was to develop a dynamic fluid loss measurement capability in the HPS.

The first experiment performed used three permeable facings, graduated cylinders, and stopwatches to capture cumulative leak off volume as a function of time. These facings were

positioned to a wall as horizontal stripes through the center. The permeability of each facing was determined individually with tapwater at approximately 200 psi. The dynamic fluid loss test was then started by using the high pressure pumping equipment to deliver a 60 lb HPG/Mgal polymer solution at 1000 psi in a single pass through the flow cell. During the second experiment, permeability to water for each facing was determined at 930 psi. A dynamic fluid loss test at approximately 1000 psi then followed using a 60 lb HPG/Mgal polymer solution containing 50 lb silica flour/Mgal as a fluid loss control additive.

Perforation Pressure Loss. The objective of these tests was to evaluate the effect of system pressure on perforation pressure losses.

Fluids investigated were a 60 lb/Mgal HPG solution and titanium-crosslinked 60 lb HPG/Mgal gel. The experiments were designed to provide the realistic flow conditions associated with a perforation tunnel and a simulated fracture downstream. The perforation pattern installed in the HPS for these tests simulated four 3/8 inch shots on 1 ft spacing. The perforations were positioned at 24, 36, 48, and 60 inch from the bottom of the simulator. The fluid was crosslinked in a single pass at a constant flow rate of 60 gal/min and portions of the total flow were diverted to the HPS for the measurement of perforation pressure loss at various flow rates.

RESULTS

High Pressure Fluid Rheology

To evaluate the performance of the instrumentation system with a triplex pump, flow data were gathered with a 60 lb/Mgal HPG polymer solution. Comparing these data to similar data obtained earlier with a Moyno pump revealed that triplex pump pulsations were not detrimental to the data acquisition.

The differential pressure versus flow rate data were converted to obtain wall shear stress and nominal shear rate. From these quantities, apparent viscosity (ratio of shear stress to shear rate) values were calculated. Data from a model 35 Fann viscometer were also analyzed in terms of shear stress and shear rate, and the power law constants n and K_v were determined. To compare slot data with data from Fann viscometer, the K_v of the viscometer was converted to K_a for slot.[5] Figure 3 depicts the apparent viscosity versus shear rate data for a 60 lb HPG/Mgal polymer solution at ambient pressure. It is evident from the data in this figure that the 60 lb HPG/Mgal solution can adequately be described by a simple power law rheological model ($\tau = K\gamma^n$). It shows that all slot viscosity values are well within the ±10% bounds of the rotational viscometer data for this fluid. The regression of slot data provided $n = 0.311$ and $K_a = 0.132$ $lb_f.sec^n/ft^2$ for a 60 lb HPG/Mgal fluid.

To evaluate the performance of the throttling valve and investigate the effect of system pressure on the rheology of fluid, two identical tests were conducted using a 60 lb HPG/Mgal polymer solution. During the first test the throttling valve was in the system but it was fully open. A second test was conducted in which approximately 700 psi back pressure was applied to the fluid at each flow rate by controlling the throttling valve. Actually, the test was designed to provide 1000 psi, but due to an electronic problem during the test, only 700 psi was obtained. All other conditions remained the same as before. Regression of the 700 psi slot data produced $n = 0.292$ and $K_a = 0.138$ $lb_f.sec^n/ft^2$ which are very similar to the parameters obtained from the test without any back pressure. Again, slot viscosities matched well with the rotational viscometer data.

Figure 4 presents a comparison of all rheological data obtained with 60 lb HPG fluid. From this figure, it can be seen that the data with backpressure are slightly lower than the data without back pressure. The fluid temperature while testing without back pressure was almost

constant (69°F) while it increased from 80°F to 85°F under pressure testing. Thus, the fluid viscosity would be lower at higher temperature which could explain the slightly lower response in Figure 4. Further, considering three different tests, which means three different batches of fluid mix, there is a good agreement among the data. Similar observations were also derived from testing 40 lb HPG/Mgal polymer solution.

Later, two tests with 60 lb HPG/Mgal fluid, one at atmospheric pressure and the other at 1000 psi, were performed. Similar conclusions, as mentioned above, were drawn: i.e., (1) the elevated pressure did not alter instrumentation response when using a triplex pump, (2) slot data agreed with the laboratory viscometric data, and (3) results obtained from low pressure pumping equipment were comparable to the results obtained with the high pressure pump.

High Temperature Fluid Rheology

Figure 5 presents the apparent viscosity versus shear rate data for a 150 lb HPG/Mgal polymer solution at 200°F in the HPS. The rheological data for this fluid fit the power law model adequately with n = 0.29 and K_a = 0.304 $lb_f.sec^n/ft^2$. The slot data again agree within ±10% of the rotational viscometer data. Similar rheological data for the same fluid but at 225°F also showed a good agreement with the model 50 Fann viscometer. Thus, the satisfactory agreement within ±10% lines from the Fann viscometer data verifies proper functioning of HPS mechanical systems and instrumentation at elevated temperature.

Slurry Rheology

Figure 6 depicts the apparent viscosity versus shear rate data for 60 lb HPG/Mgal fluid containing 10 lb/gal 20/40 sand. It can be seen that slurry has higher apparent viscosity when compared to the viscosity of the corresponding clean gel. The data can adequately be fitted with the power law model with n = 0.17 and K_a = 0.30 $lb_f.sec^n/ft^2$. Similar results were obtained at other proppant concentrations. The experimental conditions covered a wide range of shear rate and, from this, it was concluded that the consistency index of power law increases while the flow behavior index decreases with increasing proppant concentration.

Crosslinked Fluid Rheology

Since the first use of crosslinked fluids for fracture stimulation more than 20 years ago, the industry has been struggling to find a way to use viscometric data to describe the rheological behavior of these fluids in a fracture. The standard R1B1 viscometer configuration was found to have two major limitations. First, the extremely viscous nature of these fluids made it virtually impossible to fill the narrow gap between the R1 rotor and B1 bob (see Table 2). Second, when it was possible to fill the gap, these highly viscoelastic fluids would extrude from the gap, even at low RPM, producing erroneous readings. To combat these two problems, the industry chose to use wide gap configurations such as the R1B2. However, the wide gap viscometer was found to produce viscosities much larger than anticipated. Over the past few years, the industry has moved to a configuration which is intermediate to narrow and wide gap geometries. As an example, the API Subcommittee on Crosslinked Fracturing Fluid Rheology is advocating the use of the R1B5X configuration. This viscometer configuration overcomes the limitations of an extremely narrow gap and yet provides viscosity values more in line with industry expectations. Where possible, flow data from the HPS were compared to viscometric data collected with wide gap R1B2M and intermediate gap R1B5X configurations.

Results obtained with a titanium-crosslinked 60 lb HPG gel are presented in

Figure 7. As mentioned earlier, the fluid was crosslinked batch wise and pumped in a single pass. The apparent viscosity versus shear rate data in Figure 7 show that this crosslinked fluid is highly non-Newtonian with n = 0.072 and K_a = 0.451 $lb_f.sec^n/ft^2$. The slot results are compared with the data obtained from a wide gap (B2M bob with standard sleeve) model 39 Fann viscometer. The viscosity values obtained from the slot model are significantly lower than the rotational viscometer equipped with B2M bob.

Similar comparison of slot data with data from an intermediate gap model 39 Fann viscometer is shown in Figure 8. Again, the viscosity values obtained from the slot model are closer but still significantly lower than the rotational viscometer equipped with B5X bob. At 100 sec^{-1} shear rate, R1B2M and R1B5X are 256% and 200% above the HPS data, respectively, as shown in Figures 7 and 8.

Wall Slippage

An unusual and previously unexplained flow behavior has been observed in the HPS with crosslinked fracturing fluids. Data from all gap widths failed to converge to a single line, indicating the presence of slip-like phenomena. Observation of these complex phenomena is possible only in a device, such as the HPS, which can be adjusted dynamically during an experiment to different gap widths.

The slot flow data collected for titanium-crosslinked 60 lb HPG/Mgal gel at various flow rates at a fixed gap width are depicted in Figure 9. The shear stress versus shear rate plot of Figure 9 shows individual lines for each gap width rather than the expected single line.

Consider the likely scenario that two laboratories using different-width, slot flow devices are developing shear stress versus shear rate plots for analysis with the power law model. They are using continuous crosslinking at various rates to formulate their fluids. While the n values (slopes) are similar (see Figure 9), the K_a values (Y-intercepts) vary more than 166%. With this variation in power law parameters, a variation in apparent viscosity of 171% would be generated at a shear rate of 100 sec^{-1}.

Slot flow data collected for titanium-crosslinked 60 lb HPG/Mgal gel using a constant crosslinking rate while varying gap width are shown in Figure 10. It is evident from the results in Figure 10 that this method also produced results similar to results obtained using the conventional testing procedure.

Now consider a second scenario in which both laboratories now realize that they must use the FFCF procedure which requires constant rate, continuous crosslinking, with flow diversion to achieve various shear rates in the slot. The laboratories use different equipment for mixing and fluid preparation. A likely result from their efforts is shown in Figure 10. They once again obtain a wide variation in power law parameters which is the result of creating different fluids in different mixing equipment. Once again, n values are similar, but K_a values vary more than 131%. With this variation in power law parameters, a variation in apparent viscosity of 159% would be generated at a shear rate of 100 sec^{-1}.

Slot flow data gathered for titanium-crosslinked 60 lb HPG/Mgal gel using a constant crosslinking rate with preselected flows diverted through the simulator to provide the same nominal shear rate at several gap widths are shown in Figure 11. As evident from the results shown in this figure, the same wall shear stress was observed at the same nominal shear rate in various gap widths. This is a confirmation of the absence of slippage. The slight variation at low shear rates could be the result of experimental artifacts since the crosslinked fluid data are difficult to collect under these conditions.

Dynamic Fluid Loss

The initial fluid loss experiments with

eight synthetic permeable facings produced some puzzling results. During the initial determination of permeability to water at 200 psi, a complete shut-off in fluid leakage occurred at a number of the facings. it was speculated that rust particles and other contaminants in the water served as very effective fluid loss control agents. Although very little fluid loss was expected from the damaged facings, during the fluid loss test using 60 lb HPG/Mgal solution at 1000 psi, a surprisingly large volume of linear solution was found exiting the fluid loss ports and the flow did not diminish significantly with time. Because the initial permeability to water was very small to non-existent, the source of linear polymer solution leak-off was believed to be around the facing seal. At this point various facing seal schemes were evaluated and it was concluded that there was no evidence of polymer invasion around the facing seals. Later, during a second fluid loss test at 1000 psi with 60 lb HPG/Mgal solution, a similar result to that experienced in the first test was observed, i.e., no fluid loss control.

A dynamic fluid loss test with three synthetic permeable facings at approximately 1000 psi was then conducted using a 60 lb HPG/Mgal polymer solution containing 50 lb silica flour/Mgal as a fluid loss control additive. An initial permeability to water at 930 psi, showed that the three facings had permeabilities of 0.0522, 0.366, and 0.653 md. Excellent fluid loss control was achieved for the first time. The filtrate was water thin and the rate of efflux diminished with time. Cumulative volume data collected as a function of time were treated in the standard manner for fluid loss tests. Figure 12 presents the cumulative volume versus square-root-of-time data from one of the facings. A linear regression of these data and similar data from the other facings, provided C_w values of 0.00023, 0.00038, and 0.00029 ft/min$^{1/2}$. The corresponding spurt loss values were 0.0260, 0.0422, and 0.0359 gal/ft^2, respectively.

To compare dynamic fluid loss results obtained in the HPS with those from scaled experiments, samples of the HPS facing material were used in the laboratory to obtain fluid loss data with the same fluid used in the HPS. Surface area of the 1.5 inch diameter laboratory sample was 11.4 cm^2 while surface area of the FFCF facing was 3912.2 cm^2. Figure 13 presents the cumulative volume versus square-root-of-time data for dynamic fluid loss test performed with 60 lb HPG/Mgal solution containing 50 lb silica flour/Mgal. Test was performed at 50 sec^{-1} shear rate and 1000 psi in the laboratory. Fluid loss coefficient, C_w and spurt loss values were calculated from the data.

C_w values from both sources (Figures 12 and 13) are essentially the same, 0.00029 and 0.00030 ft/min$^{1/2}$, from HPS and laboratory experiments, respectively. Spurt loss values of 0.0359 and 0.11 gal/ft^2 from HPS and laboratory experiments, respectively, varied as expected based on HPS facing and laboratory sample permeabilities of 0.653 and 1.56 md, respectively.

Perforation Friction Loss

Recently Lord et al.[10] have presented correlations to describe the perforation pressure-loss behavior of polymer solutions as well as crosslinked polymer gels. Predictions of these correlations are shown to differ significantly from those made by conventional orifice-type equations. In the new correlations, pressure drop is shown to be dependent on fluid type, viscosity, and perforation size in addition to the conventional dependence on fluid density. However, all tests were conducted only at system pressure. The effect of elevated pressure on perforation pressure loss was not included in the investigation. Some industry critics felt that elevated pressure could have a significant effect, particularly, on perforation pressure loss of crosslinked fluids.

Therefore, tests were conducted to study the effect of elevated pressure on perforation pressure loss. Figure 14 presents the perforation pressure loss versus flow rate squared data for the

flow of a titanium-crosslinked 60 lb HPG/Mgal polymer gel through four 3/8 inch perforations on 1 ft spacing. Two sets of data, one with and the other without back pressure, are shown. It is evident that elevated pressure does not have any effect whatsoever, on the perforation pressure loss for crosslinked gels. A similar conclusion was also drawn from the data with linear polymer solutions. As expected, crosslinked fluids exhibit a linear relationship between the perforation pressure loss and the square of flow rate with a Y-intercept which can be attributed to the excess entrance losses. The regression analysis of the data depicted in Figure 14 produced C'_d of 0.66 and Y-intercept of 4.0 psi which agree well with the previously reported results.[10]

FUTURE RESEARCH

As mentioned earlier, the FFCF project was refocused to accomplish near-term research results. The Research and Development Plan for the next four years have been developed.

The R&D Plan is divided into three phases: Phases I and II are for 18 months while Phase III is for 12 month period. Testing under each phase considers conducting research in the four major research areas: fluid rheology, proppant transport, dynamic fluid loss, and perforation pressure losses. Phase I deals with the acquisition of new equipment and instruments as well as the enhancements of existing instrumentation. Furthermore, it also includes the Technical Advisory Group's (TAG) target fluid testing and evaluation. Phase II consists of additional testing and evaluation with the TAG's target fluid, model fluids, and other fluid systems that are most commonly employed in hydraulic fracturing treatments today. This phase also includes the development of new techniques for testing various fracturing fluids. Under Phase III, further testing and evaluation of model fluids and other fracturing fluid systems will be continued. It also addresses the development of new techniques for testing foam fluids, foam fluid leakoff measurement device, and foam texture measurement device. Various nitrogen foam fluids will also be tested and evaluated.

CONCLUSIONS

The following conclusions have been drawn as a result of testing conducted using the high pressure simulator:

1. Verification tests, performed in the large-scale, high pressure fracture-simulator, confirmed the proper functioning of instrumentation and control systems under a wide range of operating conditions.

2. Industry standard Couette viscometers (model 35 and model 50 Fann viscometers) can be used to characterize the rheological behavior of linear polymer solutions in fractures.

3. Industry standard Couette viscometers cannot be used to reliably characterize the rheological behavior of crosslinked polymer solutions in fractures. This conclusion was reached after observing the failure of viscometric data to predict crosslinked fluid behavior in the FFCF HPS.

4. As investigation of proppant-laden slurry rheology revealed that increased proppant loading decreases the power law index and increases the consistency index. The results confirmed previously published information from small laboratory devices.

5. An investigation of flow through perforations showed that perforation size and fluid viscosity must be considered when selecting a coefficient for use in the standard pressure loss equation. The

industry practice of selecting a single coefficient value independent of perforation size and fluid viscosity can lead to errors in excess of 222% when predicting pressure loss. Further, an investigation of flow through perforations using the HPS has revealed that elevated system pressure has no significant effect on the perforation pressure loss.

6. Unusual and previously undocumented flow behavior has been observed in the HPS with crosslinked fracturing fluids. Whenever flow data from various gap widths failed to converge to a single line, the initial speculation was that wall slip was occurring. A constant mixing rate experiment with flow diversion technique to achieve the same shear rate in various gap widths proved that this was not the case. This latter procedure provided very low n values, which is indicative of a wall-dominated, plug-like flow.

7. A technique was developed for preparing and installing Berea sandstone facings in the HPS. Fluid loss tests performed using these natural rock facings provided the first evidence of filter-cake buildup in the HPS. Calculated fluid loss parameters compared favorably with laboratory results from much smaller samples of the same material.

8. As part of the fluid pre-conditioning system, a low shear heat exchanger was designed, assembled, and evaluated. It was found that the designed heat exchanger is capable of heating crosslinked gels and slurries, at 40 gal/min, to 200°F.

9. The data acquisition and instrumentation systems were enhanced to provide data more attune to the needs of the project while providing a reduction in system operating cost. An improvement in the reliability of the system, as well as improved throughput and maintenance have resulted from these changes in the instrumentation system.

NOMENCLATURE

C'_d = discharge coefficient for crosslinked polymer fluids

C_w = wall building fluid loss coefficient

K = consistency index of power law fluid model

K_a = fracture consistency index of power law fluid model

K_v = viscometer consistency index of power law fluid model

n = flow behavior index of power law fluid model

Δp_{pf} = perforation pressure loss

q = flow rate per perforation

t = time

V = cumulative fluid volume

γ = nominal shear rate

τ_w = wall shear stress

ACKNOWLEDGEMENTS

The authors wish to thank the Gas Research Institute, the U.S. Department of Energy, and the University of Oklahoma for funding this project and permission to publish this work.

MTS Systems Corporation designed, built, and installed the apparatus and has participated in the project since its inception.

Halliburton Energy Services has also participated in the project since its inception, has supplied the auxiliary equipment, and its employees have provided many valuable suggestions and much valuable assistance.

REFERENCES

1. Gidley, J. L., Holditch, S. A., Nierode, D. E., and Veatch, R. W. Jr.: Recent Advances in Hydraulic Fracturing, Society of Petroleum Engineers, Richardson, TX, 1989, chapters 4 and 5.

2. Warpinski, N. R., Moschovidis, Z. A., Parker, C. D., and Abou-Sayed, I. S.: "Comparison Study of Hydraulic Fracturing Models: Test Case-GRI Staged Field Experiment No. 3," SPE 25890, Denver, CO, April 1993.

3. Medlin, W. L., Sexton, J. H., and Zumwalt, G. L.: "Sand Transport Experiments in Thin Fluids," SPE 14469, Las Vegas, NV, September 1985.

4. Evans, R. D.: "Fracturing Fluid Characterization Facility," paper presented at the DOE Fuels Technology Contractors Review Meeting, Morgantown, WV, November 16-18, 1993.

5. Rein, R. G. Jr., Lord, D. L., and Shah, S. N.: "Description of a Large, High Pressure, Slot Flow Apparatus for Characterizing Fracturing Fluids," paper SPE 26524 presented at the 1993 Annual Technical Conference and Exhibition, Houston, TX, October 3-6.

6. Mears, R. B., Sluss, J. J. Jr., Fagan, J. E., and Menon, R. K.: "The Use of Laser Doppler Velocimetry (LDV) for the Measurement of Fracturing Fluid Flow in the FFCF Simulator," paper SPE 26619 presented at the 1993 Annual Technical Conference and Exhibition, Houston, TX, October 3-6.

7. Shah, S. N. and Lord, D. L.: "Tests Confirm Operational Status of a Large-Slot Flow Apparatus for Characterizing Fracturing Fluids," paper SPE 29499 presented at the Production Operations Symposium, Oklahoma City, OK, April 2-4, 1995.

8. Vinod, P. S.: "Functional Capabilities of the High Pressure Simulator for Fracturing Fluid Characterization," Topical Report, GRI-94/0438, December 1994.

9. Rivera, V. P. and Farabee, L. M.: "Fuzzy Logic Controls Pressure in OU/GRI/DOE Fracturing Fluid Characterization Facility," paper SPE 28239 presented at the 1994 SPE Petroleum Computer Conference, Dallas, TX, July 31 - August 3.

10. Lord, D. L., Shah, S. N., Rein, R. G. Jr., and Lawson, J. T. III: "Study of Perforation Friction pressure Employing a large-scale Fracturing Flow Simulator," paper SPE 28508 presented at the 1994 Annual Technical Conference and Exhibition, New Orleans, LA, September 25-28.

Table 1. Schedule and Milestones: October 1, 1994-March 31, 1996

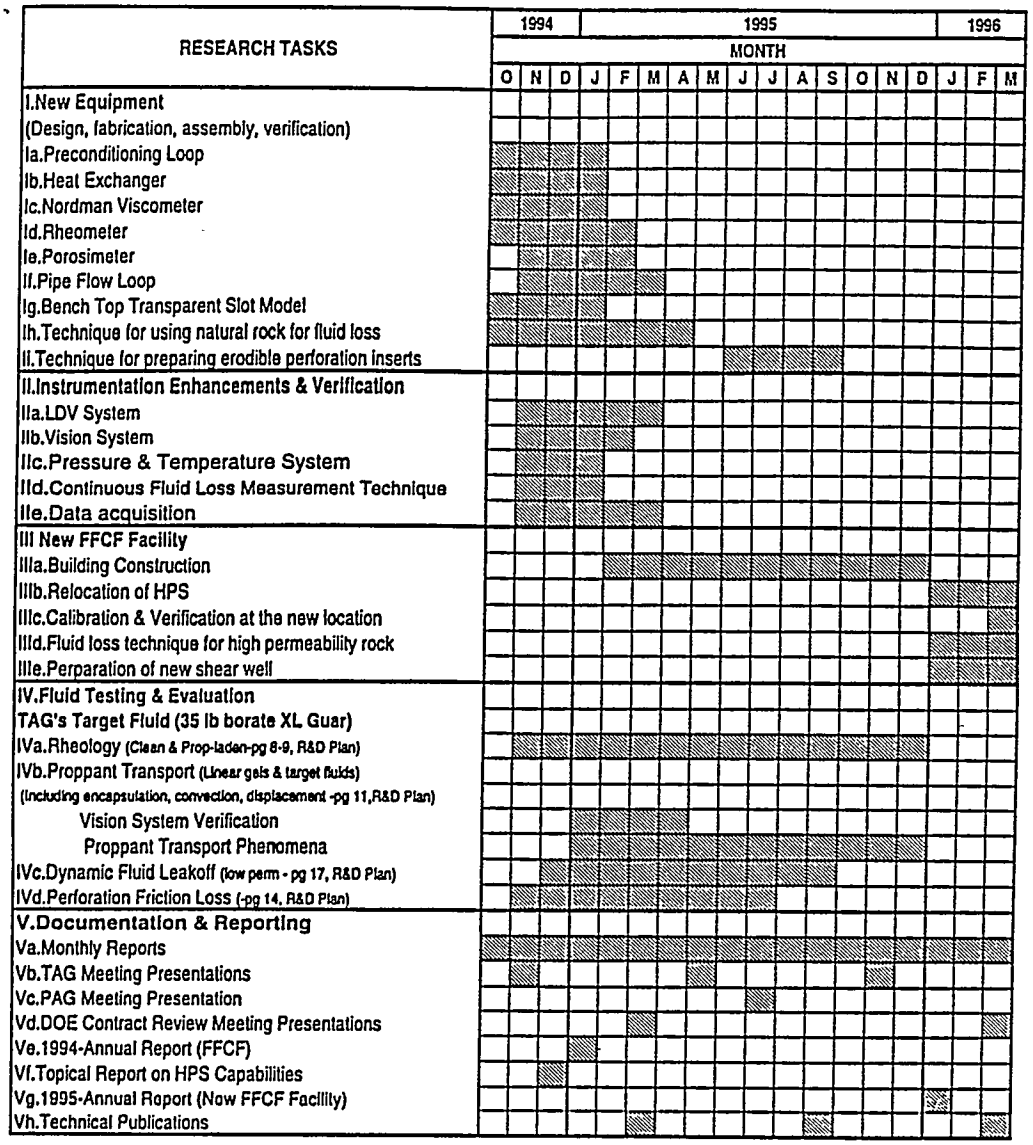

Table 2. Fann Viscometer - Bob Combinations

Viscometer Configuration	Cup Internal Radius (mm)	Bob Outside Radius (mm)	Bob Length (mm)
R1B1	18.42	17.25	76.20
R1B2	18.42	12.28	76.20
R1B2M	18.42	12.28	63.50
R1B2M	18.42	16.00	87.28

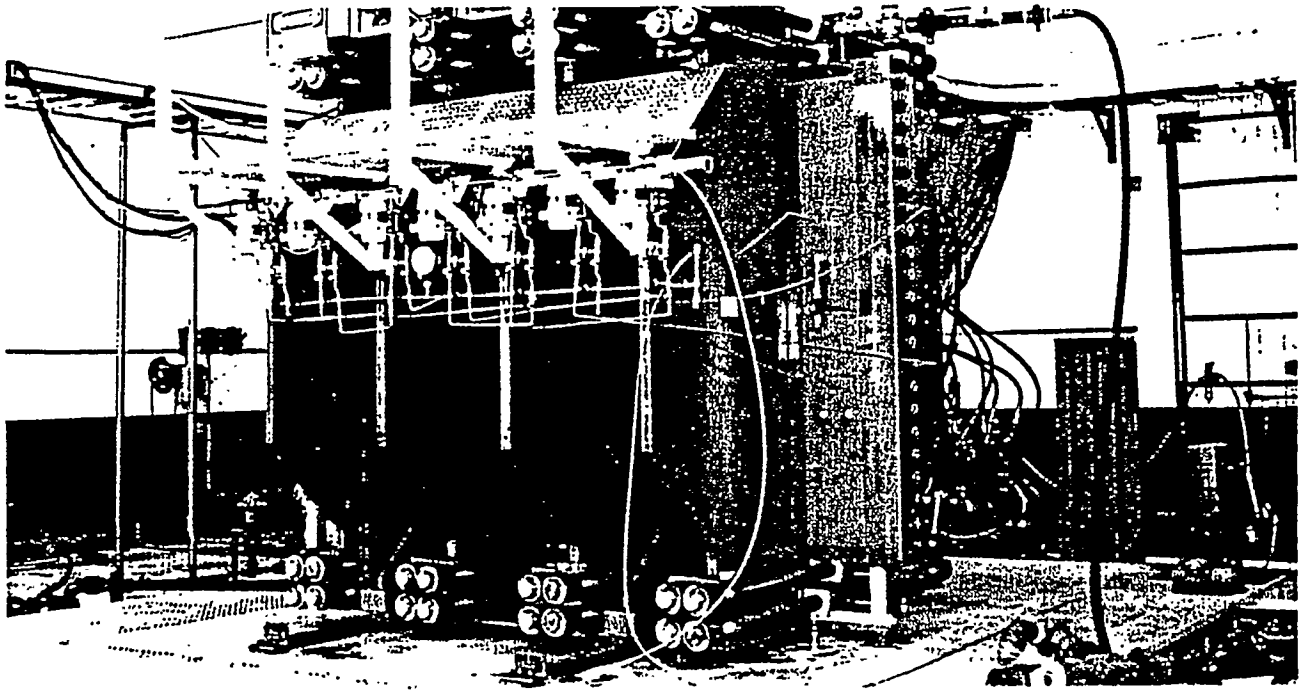

Figure 1. High Pressure Simulator at the Fracturing Fluid Characterization Facility

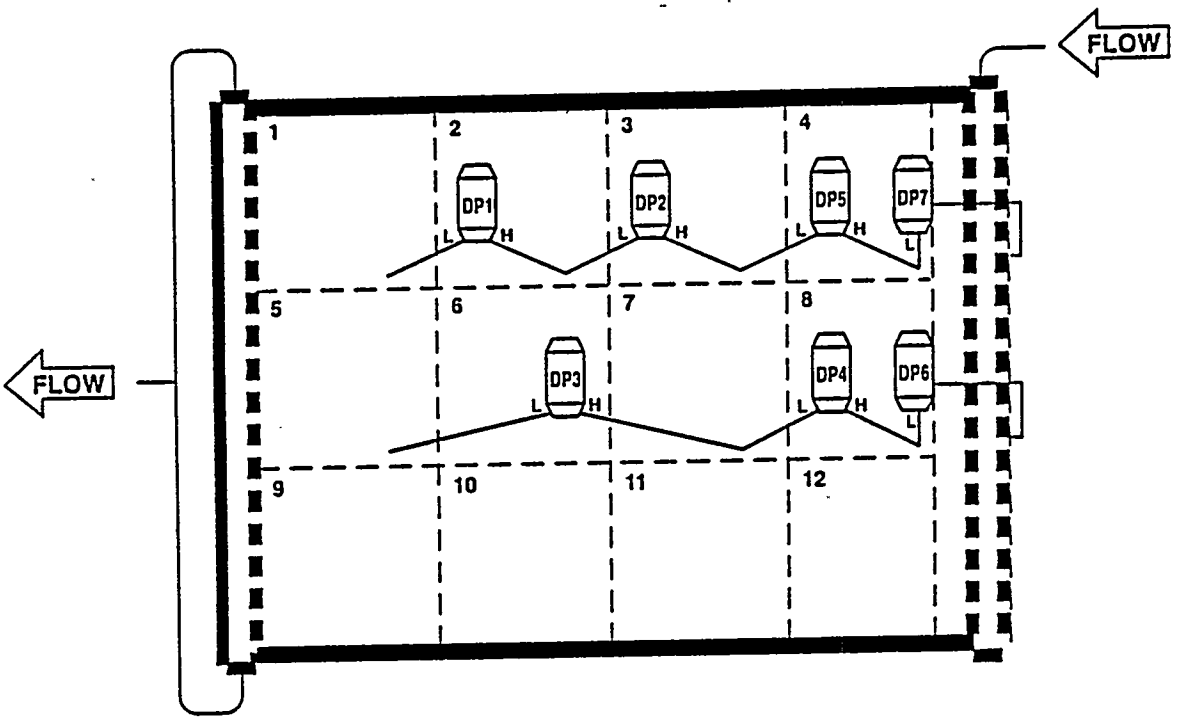

Figure 2. HPS Platen Identification And Differential Pressure (DP) Transducer Tap Locations

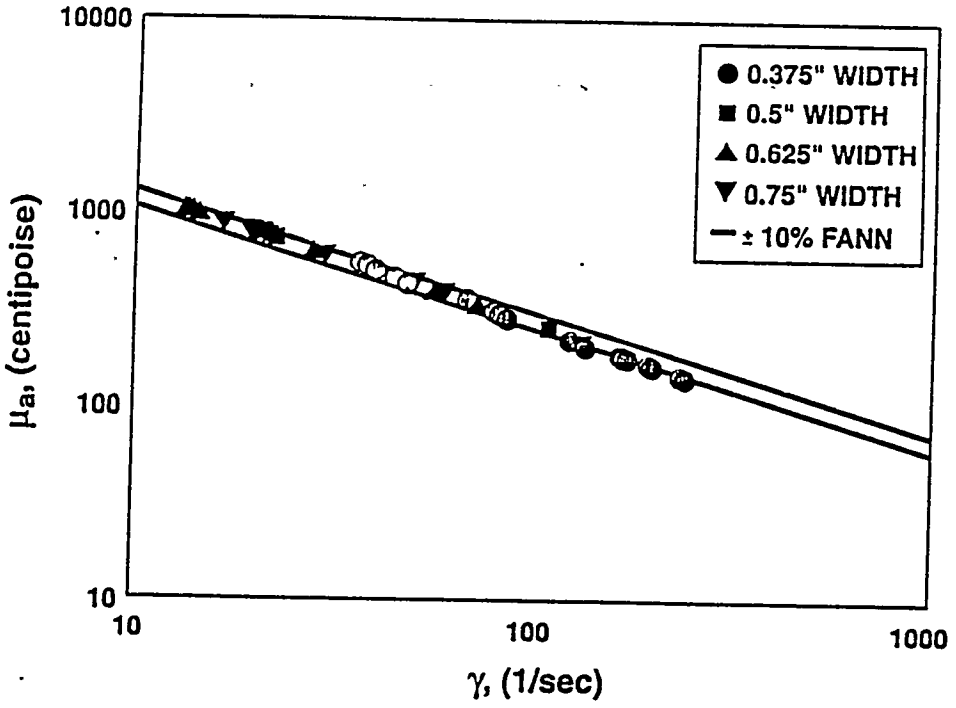

Figure 3. Apparent Viscosity Versus Shear Rate For A 60 lb HPG/Mgal Polymer Solution In Various HPS Gap Widths And In A Model 35 Fann Viscometer For Comparison

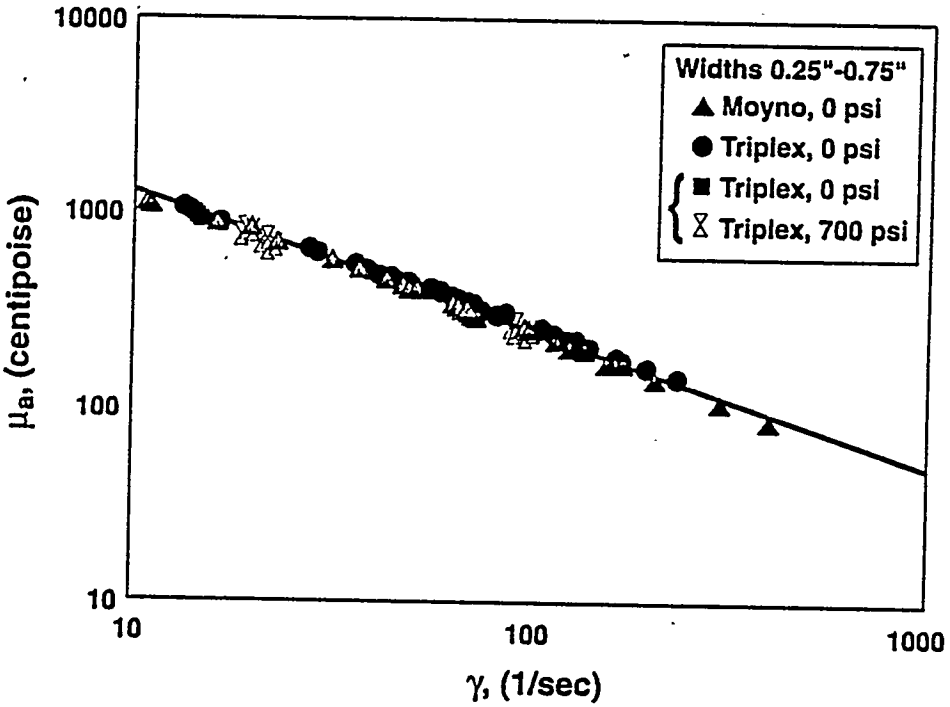

Figure 4. Apparent Viscosity Versus Shear Rate For A 60 lb HPG/Mgal Polymer Solution In Various Gap Widths At Ambient And Elevated Pressure Using Laboratory And Field Size Pumping Equipment

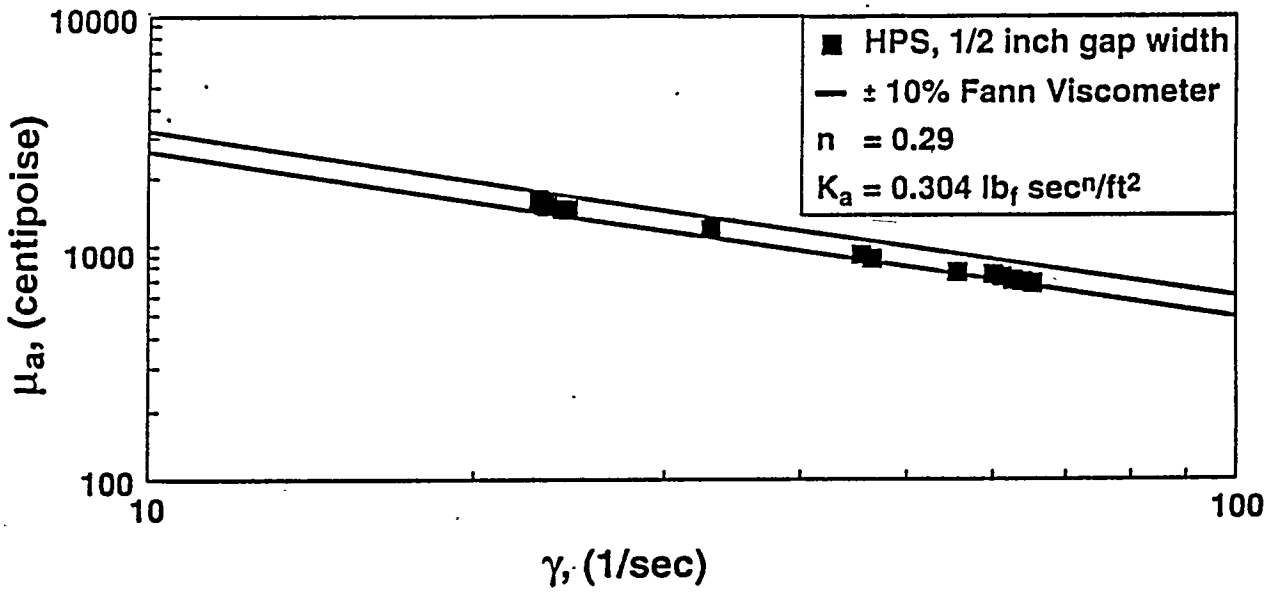

Figure 5. Apparent Viscosity Versus Shear Rate For A 150 lb HPG/Mgal Polymer Solution At 200°F In The HPS And In A Model 50 Fann Viscometer For Comparison

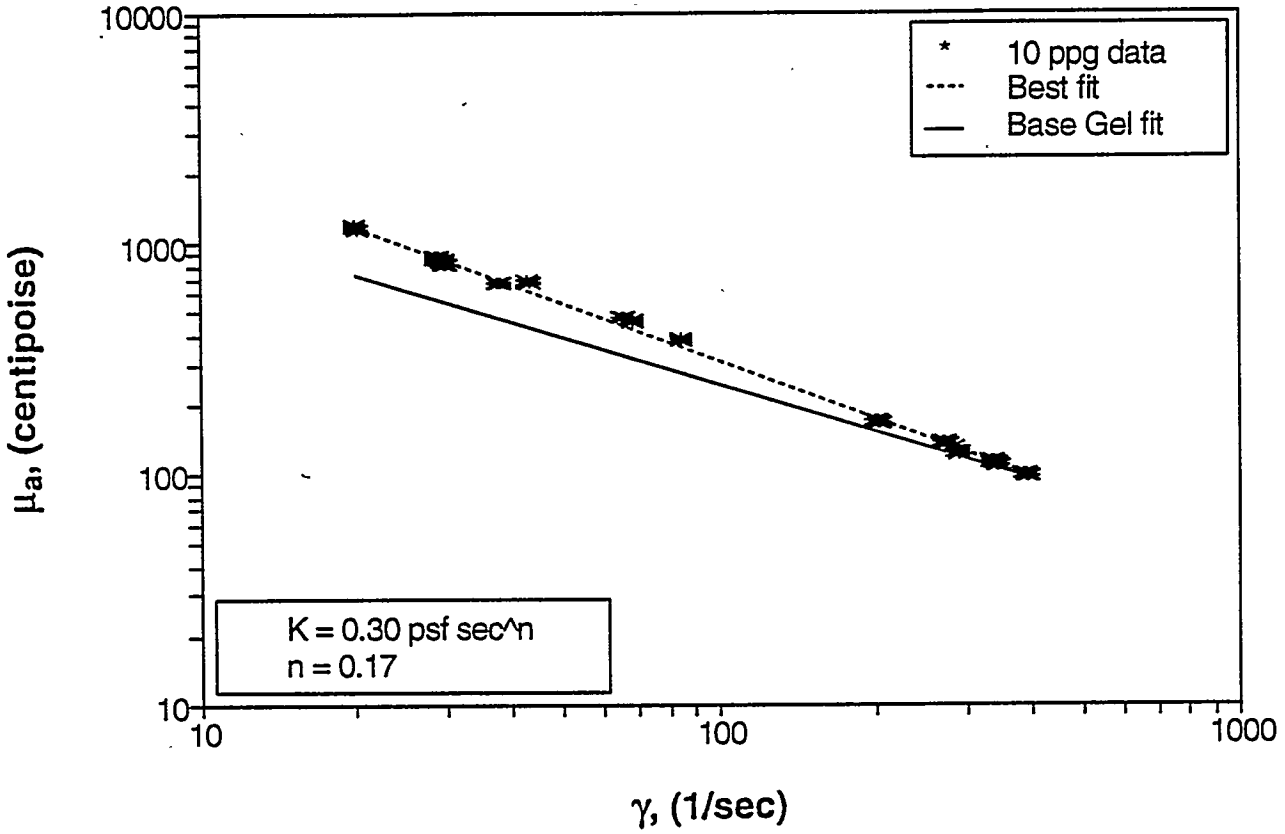

Figure 6. Apparent Viscosity Versus Shear Rate For A 60 lb HPG/Mgal Polymer Solution Containing 10 lb/gal 20/40 Mesh Sand.

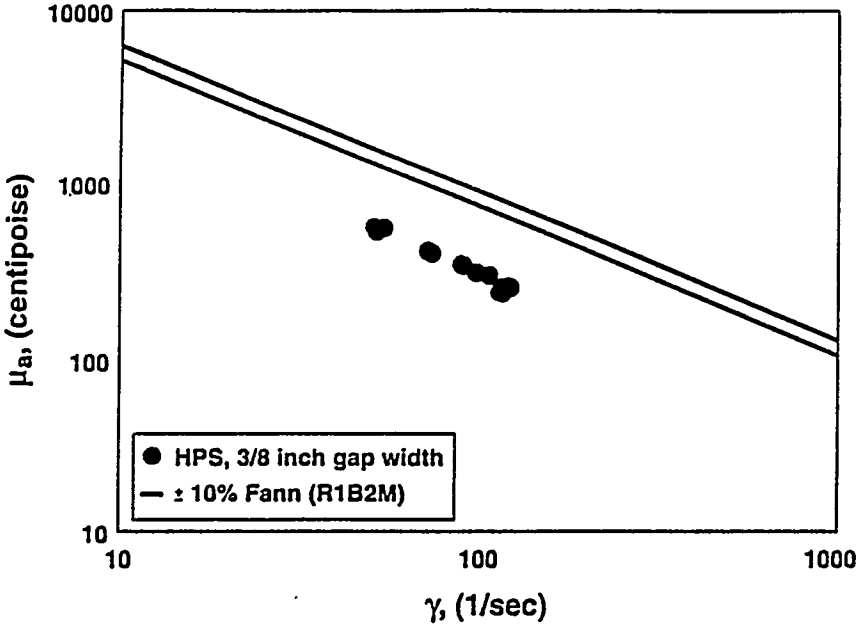

Figure 7. Apparent Viscosity Versus Shear Rate For A Titanium-Crosslinked 60lb HPG/Mgal Gel. Comparison Of Data From The HPS With Measurements In A Wide Gap Model 39 Fann Viscometer.

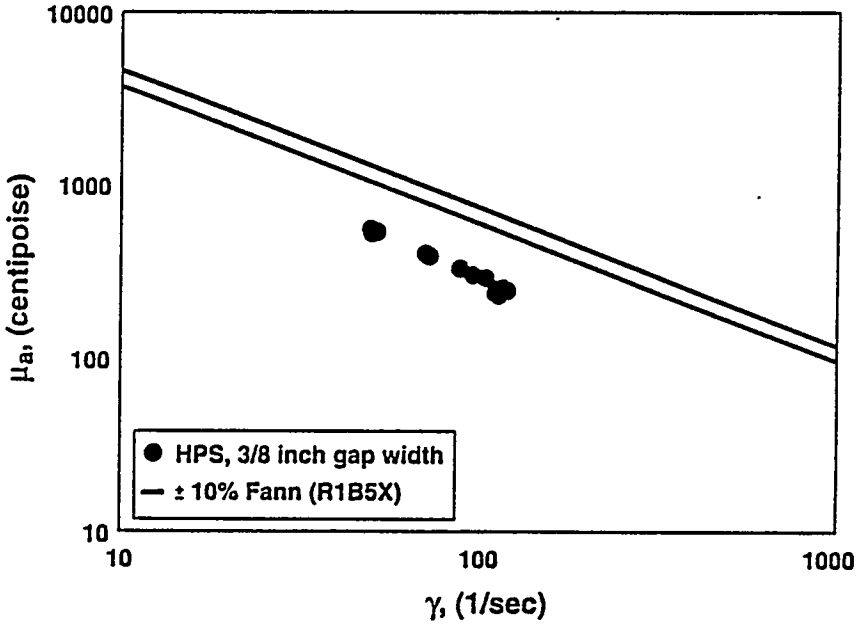

Figure 8. Apparent Viscosity Versus Shear Rate For A Titanium-Crosslinked 60 lb HPG/Mgal Gel. Comparison Of Data From The HPS With Measurements In An Intermediate Gap Model 39 Fann Viscometer.

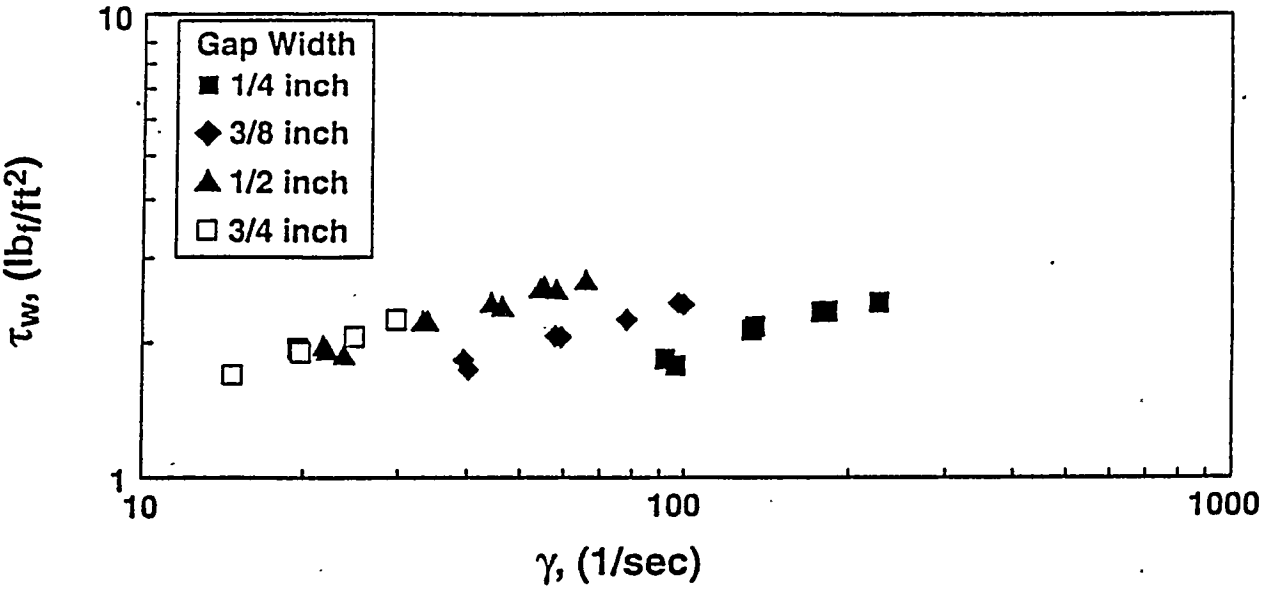

Figure 9. Shear Stress Versus Shear Rate For A Titanium-Crosslinked 60 lb HPG/Mgal Gel. Flow Rate Varied At A Fixed Gap Width To Generate The Data Shown.

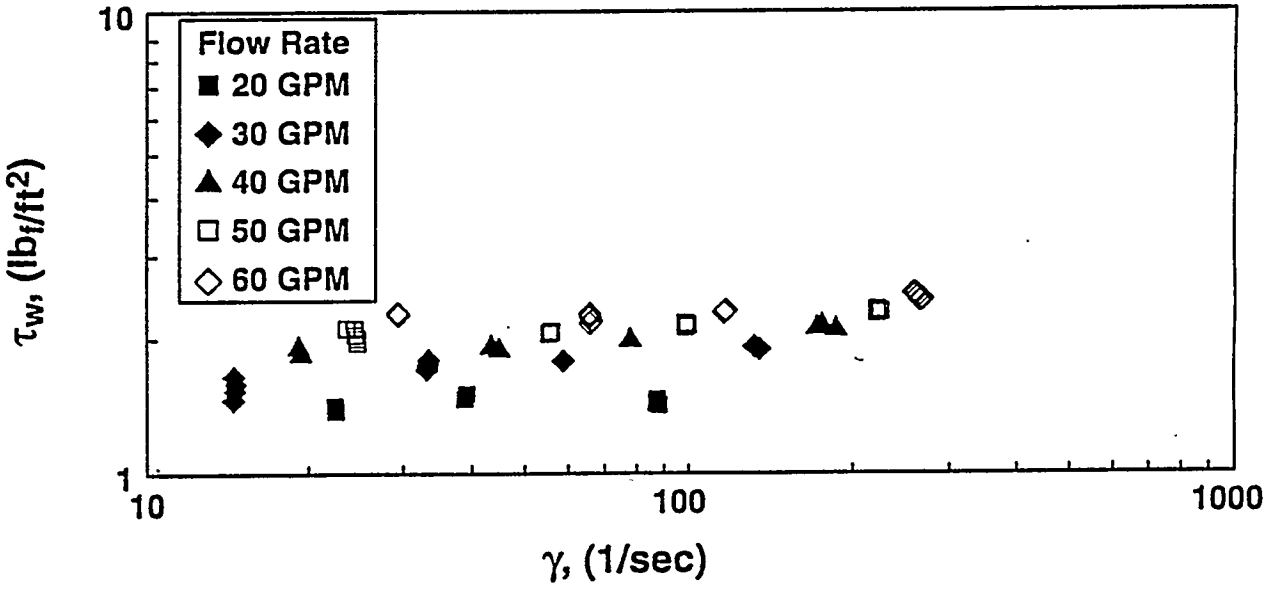

Figure 10. Shear Stress Versus Shear Rate For A Titanium-Crosslinked 60 lb HPG/Mgal Gel. Gap Width Varied At Constant Flow Rate To Generate The Data Shown.

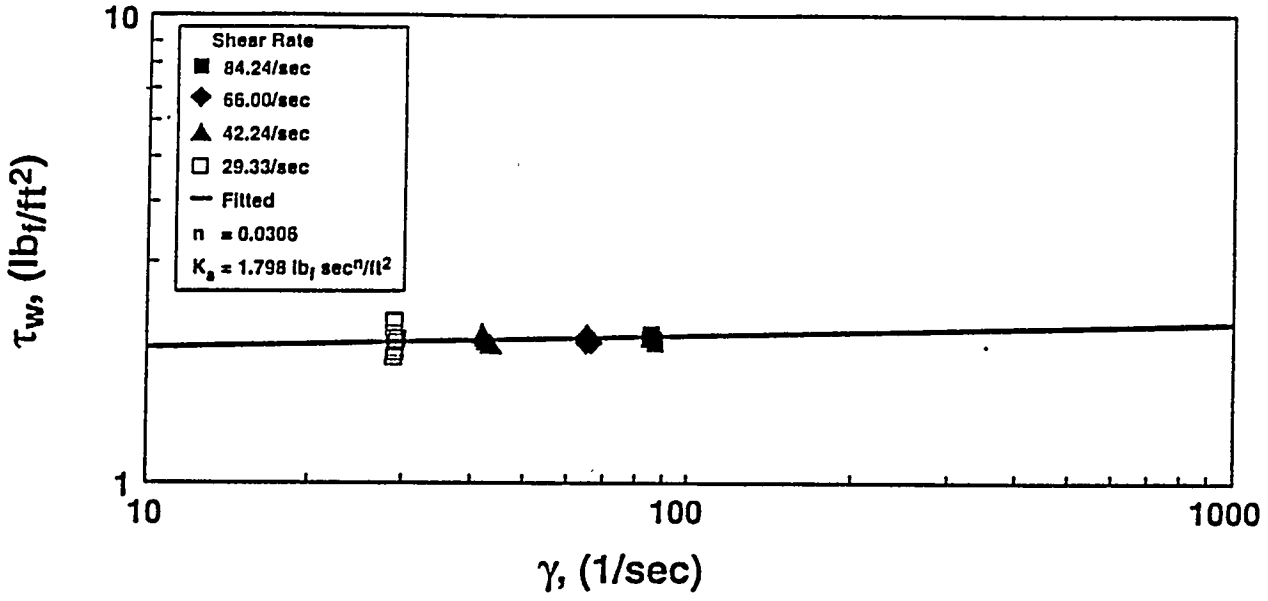

Figure 11. Shear Stress Versus Shear Rate For A Titanium-Crosslinked 60 lb HPG/Mgal Gel. Data Generated By Continuous Crosslinking At A Fixed Flow Rate With Diversion Of Portions Of The Flow Into Various Gap Widths To Provide The Data Shown.

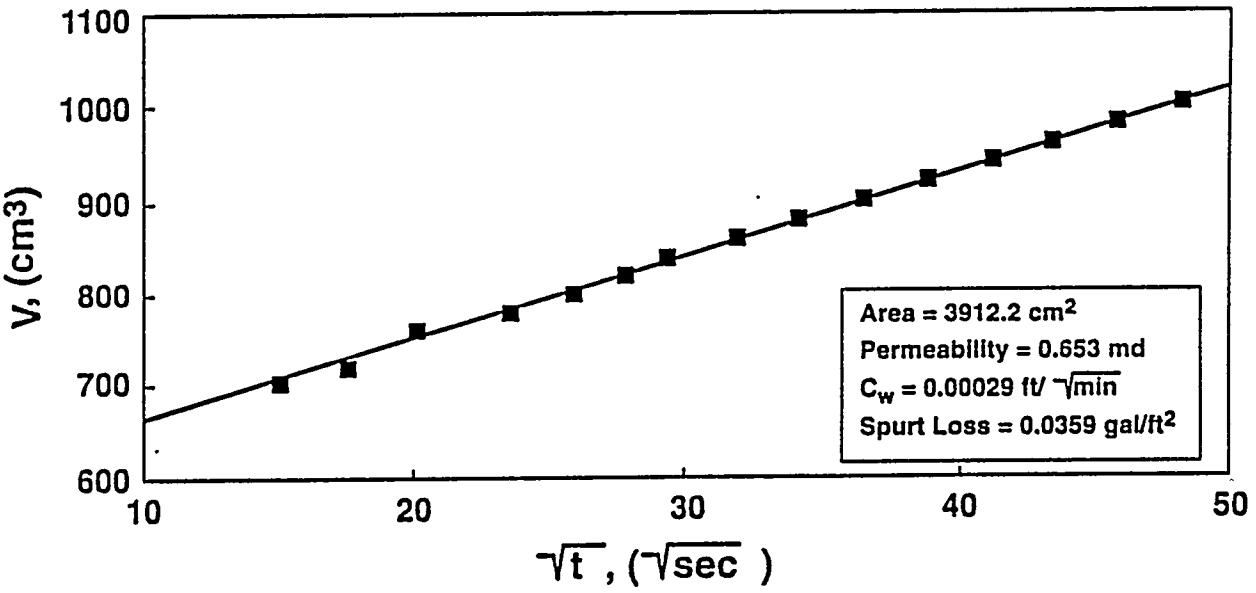

Figure 12. Cumulative Volume Versus Square-Root-Of-Time For Dynamic Fluid Loss Test With 60 lb HPG/Mgal Polymer Solution Containing 50 lb Silica Flour/Mgal. Test Performed At 55/sec Shear Rate And 1000 psi Pressure In The HPS.

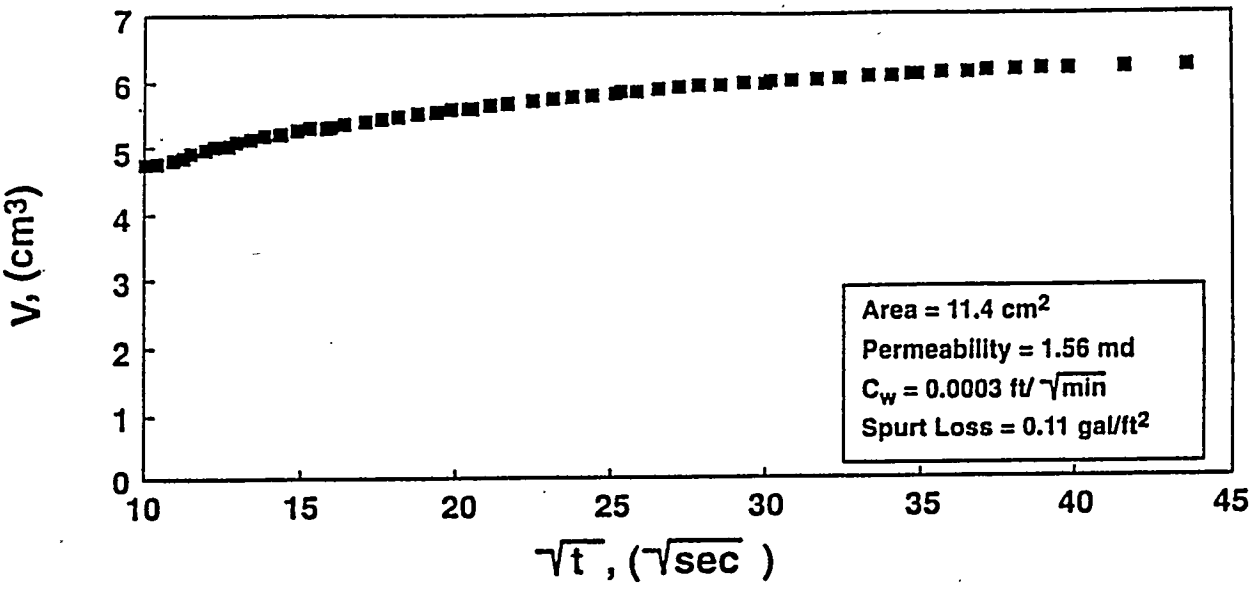

Figure 13. Cumulative Volume Versus Square-Root-Of-Time For Dynamic Fluid Loss Test With 60 lb HPG/Mgal Polymer Solution Containing 50 lb Silica Flour/Mgal. Test Performed at 50/sec Shear Rate and 1000 psi Pressure In The Laboratory.

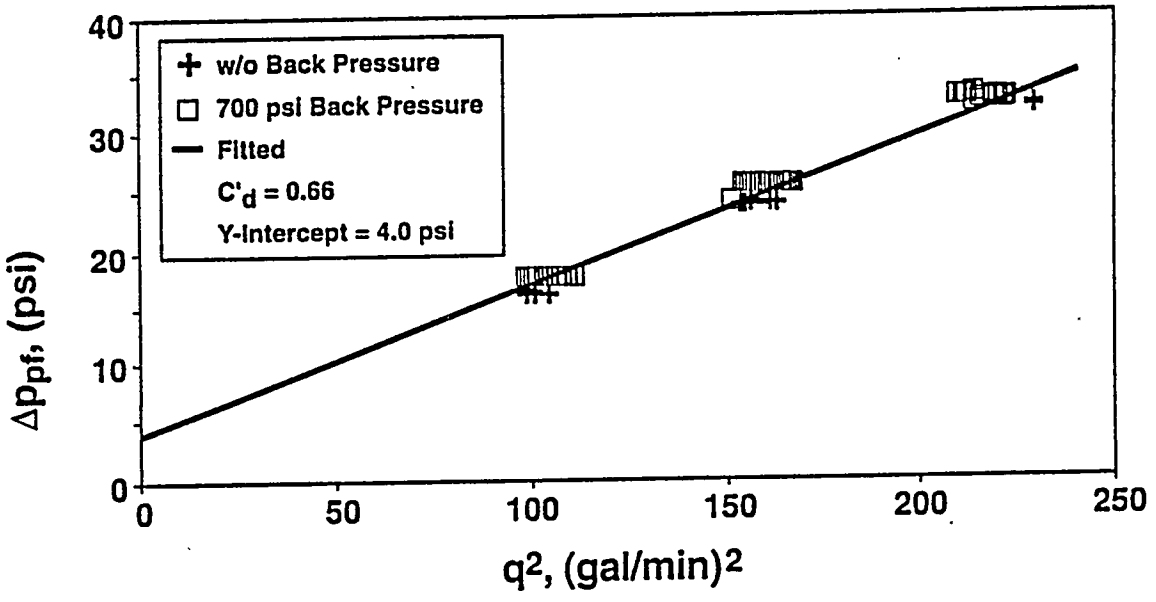

Figure 14. Perforation Pressure Loss Versus Flow Rate Squared For The Flow Of A Titanium-Crosslinked 60 lb HPG/Mgal Gel Through Four 3/8 Inch Perforations On 1 ft Spacing.

7.6 Application of Microseismic Technology to Hydraulic Fracture Diagnostics: GRI/DOE Field Fracturing Multi-Sites Project

CONTRACT INFORMATION

Cooperative Agreement Number	DE-FC21-93MC30070
Contractor	CER Corporation 955 Grier Drive, Suite A Las Vegas, NV 89119 (702) 361-2700 voice (702) 361-7653 fax
Other Funding Sources	Gas Research Institute Contract No. 5093-221-2553
Contractor Project Manager	Richard E. Peterson
Principal Investigators	Roy Wilmer, CER Norman R. Warpinski, Sandia National Laboratories Timothy B. Wright, Resources Engineering Systems Paul T. Branagan, Branagan & Associates James E. Fix, Fix & Associates
METC Project Manager	Karl H. Frohne
Period of Performance	July 28, 1993, to July 27, 1996

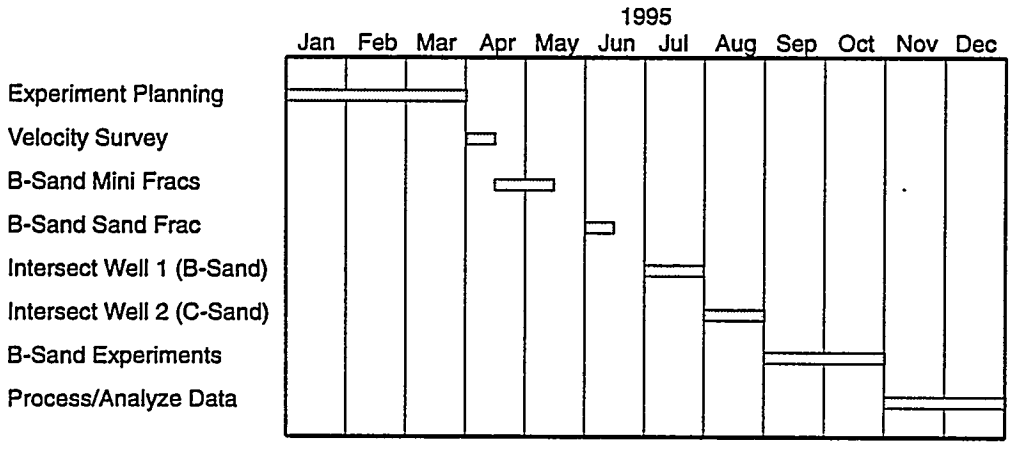

OVERALL OBJECTIVE OF THE PROJECT

The objective of the Field Fracturing Multi-Sites Project (M-Site) is to conduct field experiments and analyze data that will result in definitive determinations of hydraulic fracture dimensions using remote well and treatment well diagnostic techniques. In addition, experiments will be conducted to provide data that will resolve significant unknowns with regard to hydraulic fracture modeling, fracture fluid rheology and fracture treatment design. These experiments will be supported by a well-characterized subsurface environment as well as surface facilities and equipment conducive to acquiring high-quality data. It is anticipated that the project's research advancements will provide a foundation for a fracture diagnostic service industry and hydraulic fracture optimization based on measured fracture response.

BACKGROUND INFORMATION

The M-Site Project is jointly sponsored by the Gas Research Institute (GRI) and the U.S. Department of Energy (DOE). The site developed for M-Site hydraulic fracture experimentation is the former DOE Multiwell Experiment (MWX) site located near Rifle, Colorado, as shown in Figure 1. The MWX project drilled three closely-spaced wells (MWX-1, MWX-2 and MWX-3) which were the basis for extensive reservoir analyses and tight gas sand characterizations in the blanket and lenticular sandstone bodies of the Mesaverde Group. The research results and background knowledge gained from the MWX project are directly applicable to research in the current M-Site Project. The contractor team organized by GRI and DOE to execute the M-Site Project includes CER, Sandia National Laboratories, Resources Engineering Systems, Branagan & Associates, and James E. Fix & Associates.

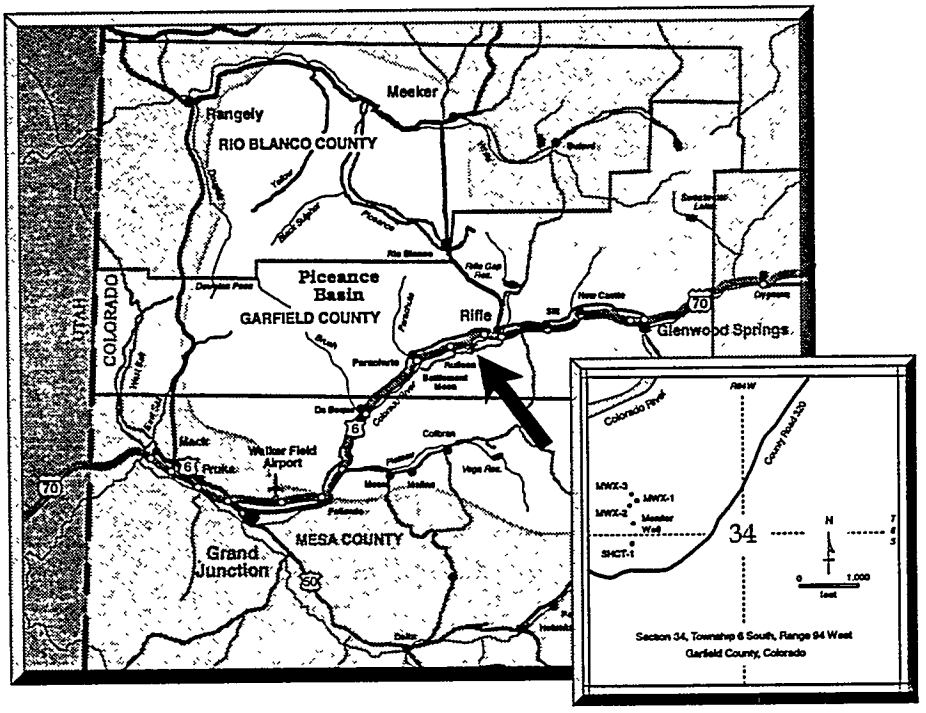

Figure 1 Location of the Field Fracturing Multi-Sites Project

All of the proposed M-Site experimentation is occurring in several sandstone units, shown in Figure 2 and informally referred to as the A, B and C Sands, which are present in the upper Mesaverde Group between 4,100 and 5,000 ft. The B and C Sand units at the M-Site have the following characteristics:

- paralic depositional environment which resulted in relatively thick and widely continuous sand bodies;
- normal pressure gradient;
- core-sample permeability averaging 0.02 md and porosity averaging 6.1 percent; and
- high water saturations averaging 80 to 90 percent.

The deeper A Sand interval is within the fluvial transition zone of the Mesaverde and, therefore is laterally discontinuous, slightly over-pressured, and capable of gas production.

TECHNICAL APPROACH TO M-SITE FIELD OPERATIONS AND RESEARCH ACTIVITIES

The M-Site field operations and research activities described in this document occurred during the period from October 1993 to October 1994 and include the following primary activities:

- fracture diagnostics experiments in the A Sand interval; and
- drilling and instrumentation of Monitor Well No. 1.

These activities are consistent with a "staged approach" wherein each project phase builds upon the previous to result in more comprehensive experiments and data acquisition. A more complete description of the technical approach to the above two activities is included in the following sections.

Fracture Diagnostics Experiments In The A Sand Interval

A series of A Sand data acquisition operations and experiments were planned interval to accomplish the following objectives:

Characterization of the A-Sand Velocity Structure. The stratigraphy of the upper Mesaverde section is characterized by layered sandstone, siltstone and mudstone lithologies. Processing of seismic data in subsequent experiments (i.e., accurate location of remotely-detected microseismic events which occur as a result of hydraulic fracturing) to be conducted at the M-Site requires that the velocity structure of the A-Sand interval be well characterized. Therefore, a crosswell velocity survey was planned using the MWX-2 well to emplace a five-level borehole accelerometer package and the MWX-3 well for emplacing an airgun seismic source.

Remote-Well Seismic Data Acquisition with Multi-Level Accelerometers. The objectives of the fracture diagnostic experiments in the A Sand were to use multiple seismic receivers (triaxial accelerometers) in a remote observation well to: a) develop fielding techniques for the more comprehensive accelerometer array to be installed in the Monitor Well No. 1; and b) to substantially reduce vertical wavefield errors thereby providing data for more accurate location of microseismic events. To accomplish this goal, four mini-fracs were to be pumped during which a multi-level accelerometer array, placed in the borehole on a fiber optics wireline, would detect microseisms and transmit these data to surface recording systems. Three of the mini-fracs were planned to be fluid only. The fourth mini-frac

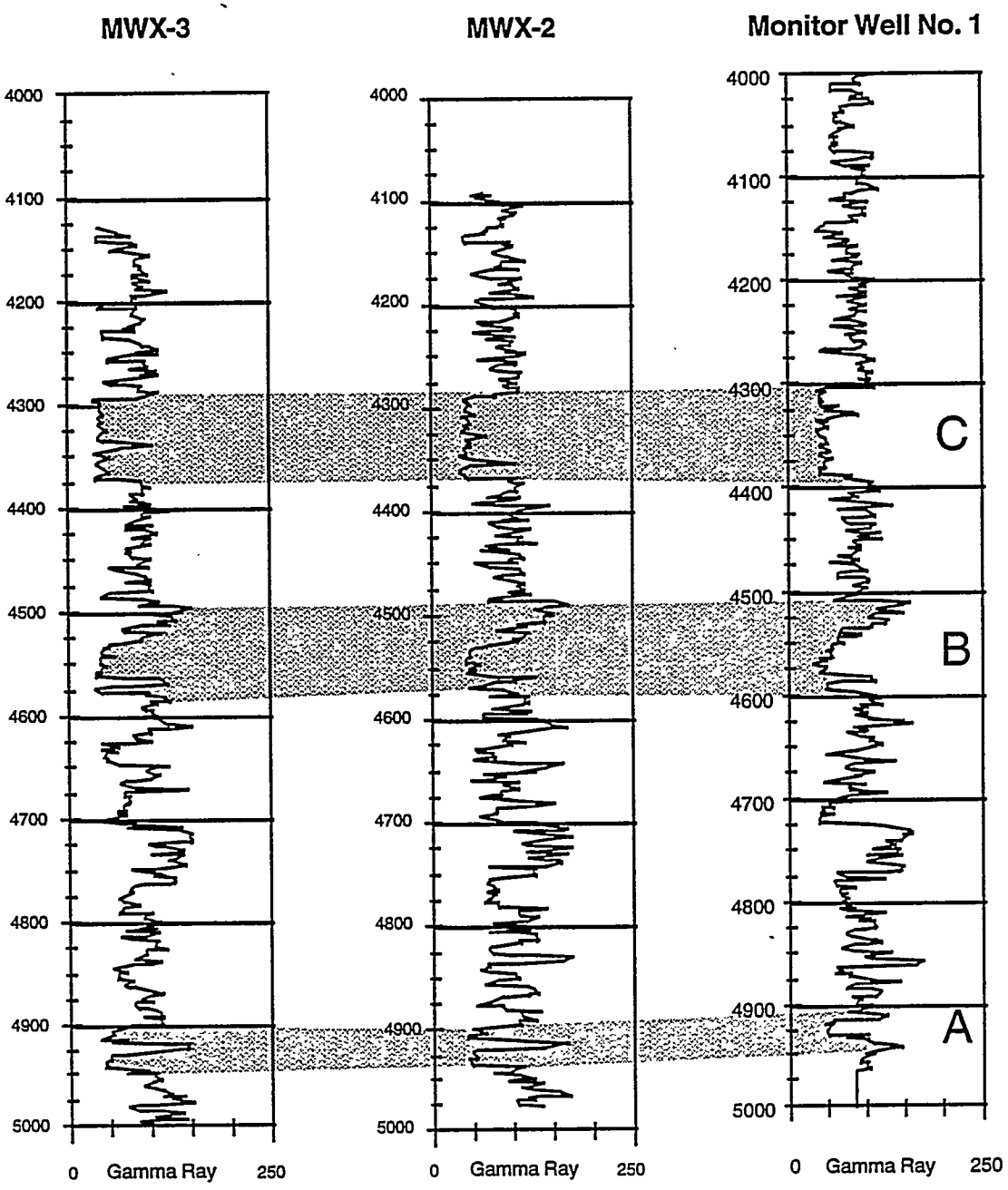

Figure 2 Upper Mesaverde Sandstone Units Targeted for Research in the Multi-Sites Project

would include proppant, thereby providing an opportunity to contrast the character of microseismic events from the two types of treatments.

Development of Event Detection and Data Processing Capabilities. The overall diagnostic strategy at the M-Site is to automate all of the seismic processing to avoid the time spent searching for and capturing microseismic events from taped data. Thus, microseisms which occur as a result of the A Sand fracture treatments will provide data that can be processed and used to develop the automatic techniques for rapidly defining the location of microseismic events.

Verification of Treatment Well Fracture Diagnostic Techniques. The objective of this set of experiments was to use the new borehole accelerometer technology to independently validate the H/Z technique for determining fracture height and azimuth. Verification would be achieved by comparing the fracture height results determined from the remote-well multilevel seismic array with the H/Z data.

Assessment of Convective Processes During Hydraulic Fracturing. An experiment was designed to improve the understanding of factors related to effective placement of proppant in a hydraulic fracture and fluid convective processes which may redistribute this proppant in the fracture and/or the wellbore. The basic strategy was to pump a propped frac (Propped Frac No. 4-A) in which the fluid and proppant have been tagged with three different radioactive tracers. Wireline logging runs with a spectral gamma ray tool would then be performed to monitor the location of these tracers in and around the wellbore.

Drilling and Instrumentation of Monitor Well No. 1

Comprehensive seismic experimentation which has the potential for clearly defining the dimensions of a hydraulic fracture requires an instrumentation array beyond that which can be fielded on a wireline retrievable system. Therefore, the objective of this phase of the M-Site Project was to execute the following operations:

Drill and Case a Specially Designed Wellbore. The design of Monitor Well No. 1 was driven by the need to cement instrumentation arrays in a downhole environment where they are likely to function for a long time. Thus, this design required a 12-1/4-in. borehole drilled to 5,000 ft with a minimum of borehole deviation; 9-5/8-in. casing would then be set and cemented.

Acquire and Analyze Select Data Sets. In the process of drilling Monitor Well No. 1, additional opportunities would be presented to acquire data in the A, B and C sand intervals. Thus, coring, core analysis and wireline logging programs were designed to selectively evaluate reservoir character and stress magnitude/direction.

Emplace Seismic and Earth-Tilt Instrumentation. Of primary importance to M-Site fracture diagnostics experiments would be the successful emplacement of 30 accelerometers, 6 inclinometers and their respective cabling in the 4,000- to 4,900-ft interval of Monitor Well No. 1. Thus, special procedures and precautions were designed to secure the instruments to a tubing string and cement this assembly in place.

RESULTS

The results of the two primary research activities described in this document are provided in the following sections.

Fracture Diagnostics Experiments in the A Sand Interval

A series of experiments and data acquisition operations were designed and executed between October 25 and November 5, 1993, in the A Sand interval of the Mesaverde section. The primary experiments were performed in conjunction with a series of small hydraulic fracturing treatments in MWX-3 while simultaneously collecting seismic data in both the treatment well (MWX-3) and a remote observation well (MWX-2). As shown in Figure 3, MWX-3 was perforated in the A Sand at 4,900-20 ft and 4,930-46 ft with 72 holes (0.4 inches) at 2 shots per foot (SPF) and 120° phasing. Figure 3 also shows the wellbore configuration of the MWX-2 well, as a seismic monitor well, during the mini-frac testing. Three separate fluid-only mini-frac treatments were performed and one propped treatment was performed in this effort. Tables 1 and 2 summarize the salient details of these treatments. Detailed results of these operations and research results are found in CER and others, 1995a. These results of these activities are summarized as follows:

Crosswell Tomography. The initial phase of field data acquisition which occurred prior to the mini-fracs involved a comprehensive crosswell tomographic survey to characterize the velocity structure of the gross interval between 4,500 and 5,200 ft. The A-Sand interval was completely covered in the crosswell tomography survey by varying the depth interval that the accelerometer array was locked into and by varying the depth of the airgun source. Receivers were moved at 10-ft increments between 4,500 and 5,000 ft, while airgun shots were positioned at 5-ft intervals between 4,500 and 5,200 ft. The crosswell survey used MWX-3 for emplacement of the seismic source and MWX-2 for emplacement of the borehole accelerometer array.

The data from the tomographic survey are high quality, with clear p-wave arrivals. Generally, there are good signal-to-noise ratios for these traces with excellent p-wave first-arrival standout and visible waves.

Analysis of the p-wave arrival first breaks were completed first, as p-wave data required considerably less processing than the s-wave results. Several test tomographic inversion runs were performed to determine proper processing parameters and to winnow poor quality first-arrival picks. In the final tomographic inversion, a starting velocity model was constructed with sonic log data from MWX-2 and MWX-3. Best results were obtained by allowing inversion to proceed with velocities constrained to fit the starting model at the top and bottom of the tomogram. In these areas, pixel velocities are poorly resolved because of the limited ray path coverage. Global velocity constraints were applied to keep topographic velocities within a few percent of the sonic log velocities. Figure 4 shows a black and white representation of the inversion results. The higher velocity A Sand at 4,940 ft and B sand at 4,530 ft can be clearly seen.

Fracture Dimensions Based on Remote-Well Microseismics. Remote well (MWX-2) seismic monitoring was performed during each of the four mini-frac treatments using a multi-level downhole seismic receiver array, fiber optic wireline and surface data acquisition system. The receiver array, configured to obtain the widest possible aperture, consisted of three receivers spaced at 10-ft intervals and a fourth receiver 50 ft below the third. The receivers were clamped and oriented in the cased wellbore between 4,885 and

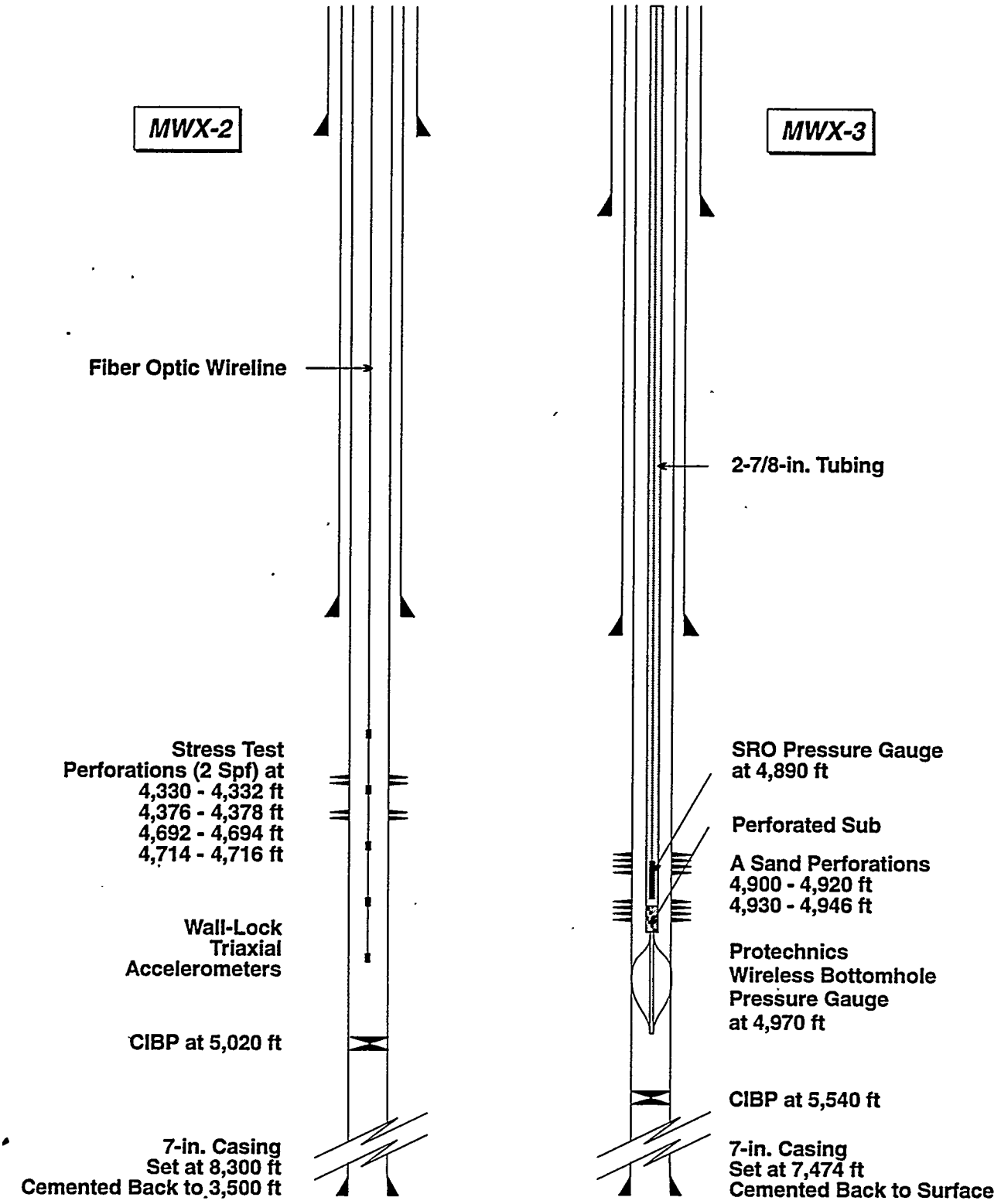

Figure 3 Configurations of the MWX-2 Observation Well and the MWX-3 Treatment Well for A Sand Mini-Fracs

Table 1. Treatment Volumes for Mini-Fracs No. 1-A to 3-A

	Treatment Volume	Injection Rate	Fluid Type
Mini-Frac No. 1-A	450 bbl	25.0 bpm	40 lb/Mgal linear gel
Mini-Frac No. 2-A	400 bbl	15.1 bpm	40 lb/Mgal linear gel
Mini-Frac No. 3-A	434 bbl	20.4 bpm	40 lb/Mgal linear gel

Table 2. Pump Schedule for Propped Frac No. 4-A

Stage	Slurry Volume, bbl	Slurry Rate, bpm	Stage Sand, lb	Comments
1	75	20	---	Pad (40 lb/Mgal linear)
2	52	20	4,400[1]	2 ppg proppant
3	51	20	---	Start flush
4	---	---	---	Shutdown for ISIP
5	80	20	---	Underdisplace
6	---	---	---	Run RA log
7	90	20	---	Overdisplace
9	72	20	---	Pad (40 lb/Mgal X-link)
10	84	20	12,500[2]	4 ppg proppant
11	36	15	---	Flush (40 lb/Mgal linear)
12	---	---	---	Shutdown for ISIP
13	104	17	---	Flushed to top perf
14	---	---	---	Run RA log

[1]Proppant tagged with ^{192}Ir Zero Wash
[2]Proppant tagged with ^{124}Sb Zero Wash

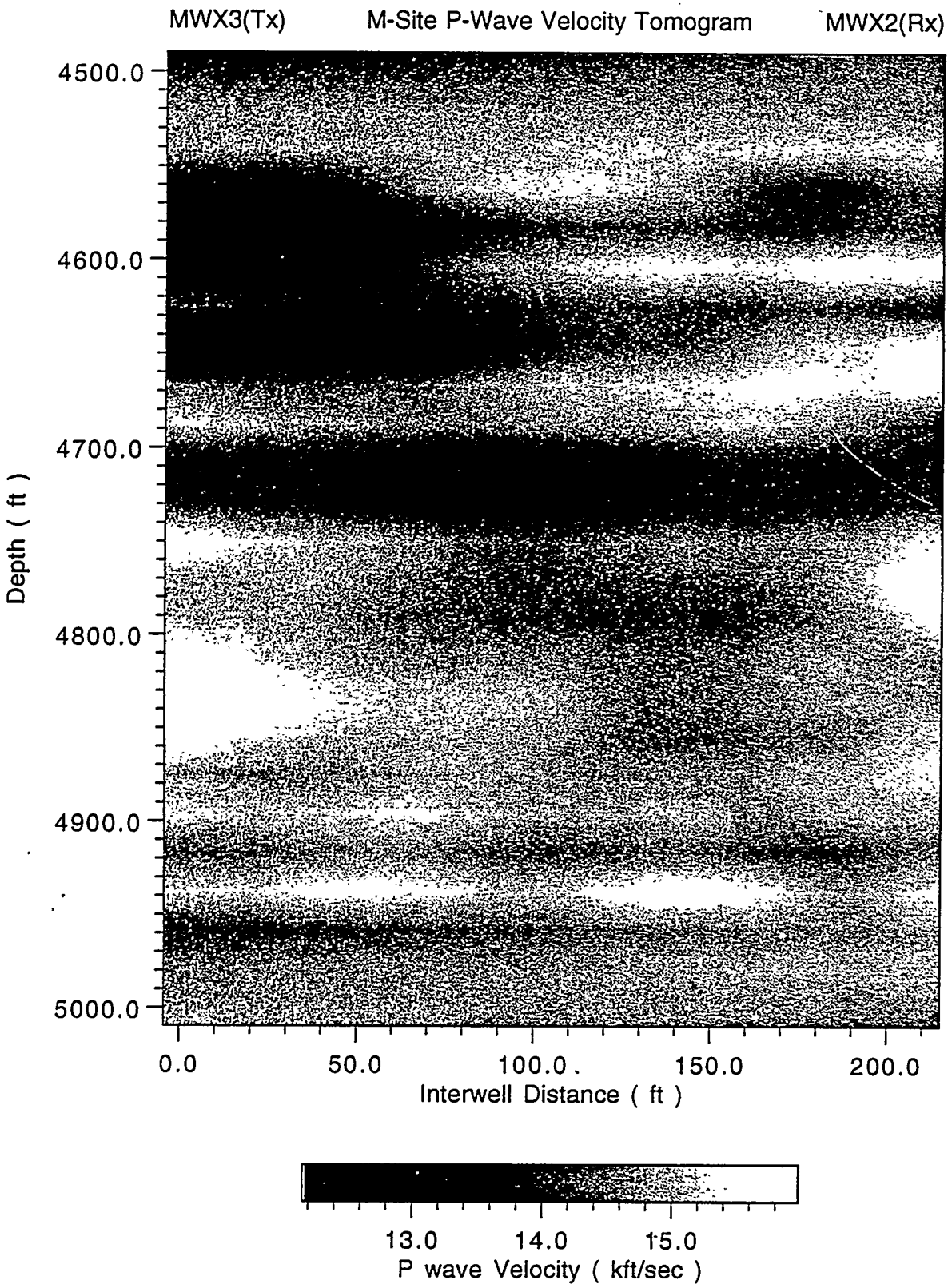

Figure 4 Black and White Representation of the Tomographic Inversion

4,955 ft. In addition to collecting raw data, microseismic event detection capabilities were developed based on amplitude triggering. The event detection compares a moving-amplitude window with a resettable threshold for each channel to determine if events have been recorded. The system incorporates flexibility in being able to turn off noisy channels, to change the threshold when conditions are noisy (e.g., during pumping), or to bias the search for signals by choosing particular channels.

Figure 5 shows a correlated plot of bottom-hole pressure with microseismic events triggered by the event detector for Mini-Frac No. 1-A. Initially, the event-detector threshold was set high to minimize pump-noise events, and, thus, few events were triggered when pumping started The threshold was subsequently lowered and approximately 5 minutes into the treatment, events were being detected at an average rate of about 5 per 2-minute interval. While the number of events jumped at shut-in, they rapidly declined after shut-in to fewer than one event per minute.

Seventy-eight of these seismic events were subsequently analyzed to determine their locations. Figure 5 also illustrates a plan and profile view of the final plot of event locations using the most accurate imaging analysis possible with the 4-level array. As shown in this figure, the final plot illustrates a fracture-wing asymmetry of 2:1. This plot, however, does not adequately portray the development of fracture geometry with time. This fracture growth with time is interpreted as follows:

- After only 12 minutes of pumping, the fracture reached its total length extent with very little height growth.
- Seven minutes later, some upward and downward height growth are noted which correlates to a decrease in the treating pressure.
- At the shut-in time at 30 minutes, there is some additional height growth and an increasing width of signals in the horizontal plane.
- Upward and downward growth continue for about 9 minutes after shut-in.

Microseismic events occurring as a result of Mini-Frac No. 2-A were also analyzed and indicate that the fracture is asymmetric (but to a lesser degree than that observed in the Mini-Frac No. 1-A) and the band of microseisms is wider possibly because of leakoff-induced microseisms. Mini-Frac No. 3-A also shows a tendency for greater width of the signal zone. The fourth mini-frac, which included a proppant stage, was notable for its excessive amount of non-microseismic signals.

Fracture Dimensions Based on Treatment Well Microseismics. Treatment well diagnostics for fracture top and bottom were conducted as a part of the Mini-Frac No. 3-A experiment design and used a single 3-component receiver in the MWX-3 treatment well. The H/Z fracture height determination technique was applied and is based on Continuous Microseismic Radiation, i.e., the continuum of small background earth motion events which occur following a hydraulic stimulation. The background motion data are formed into its two vector components: the horizontal component H and the vertical component Z. The top and bottom of the hydraulic fracture is interpreted to occur where the H/Z ratio inverts from a vertical dominance to a horizontal dominance.

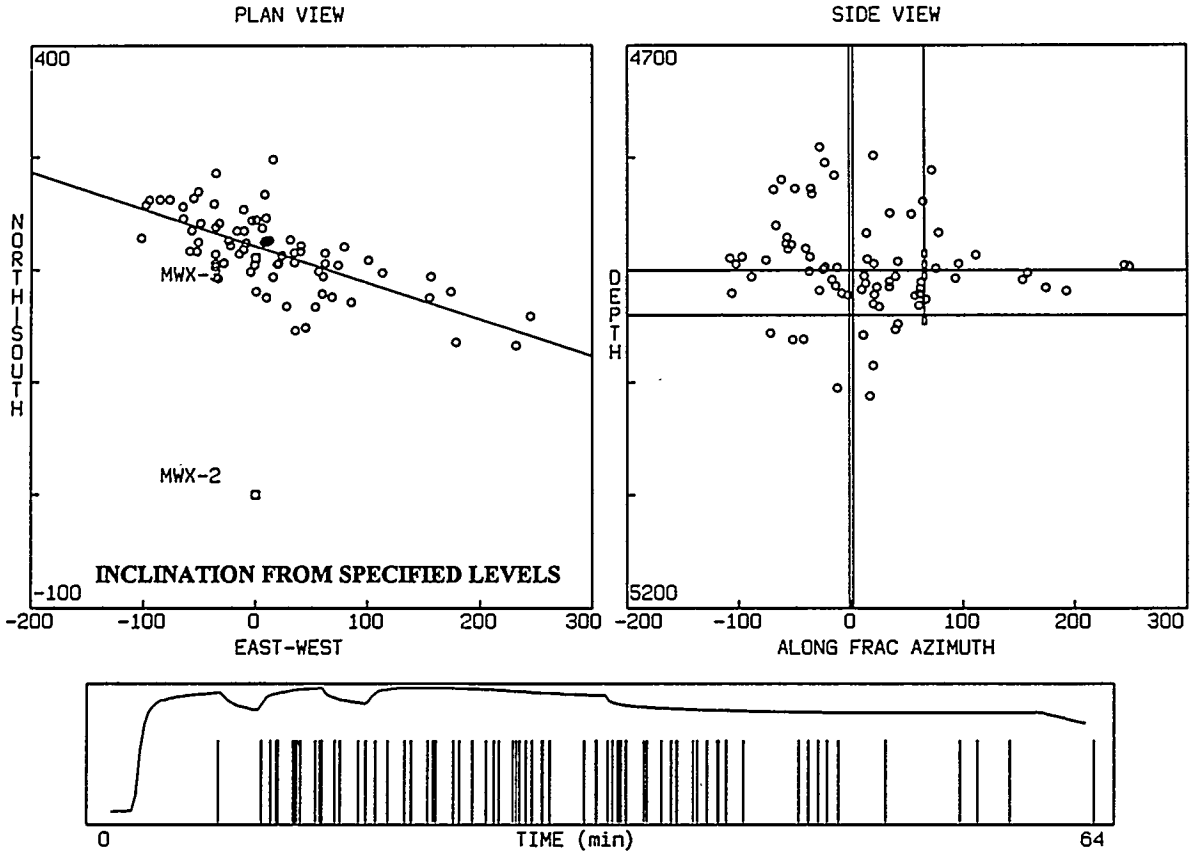

Figure 5 Correlated Plot of Bottomhole Pressure With Seismic Events and a Plan and Profile View of Microseismic Event Locations for Mini-Frac No. 1-A

Following Mini-Frac No. 3-A, 17 depth stations were occupied between 4,900 and 5,300 ft. The results of the fracture height processing, as shown in Figure 6, indicate that the top of the fracture is at 4,725 ft and the bottom of the fracture is at 4,975 ft for an overall height of 250 ft.

Fracture Dimensions Based on 3D Fracture Modeling. The 3-D hydraulic fracture model FRACPRO, developed for GRI by Resources Engineering Systems, was used to record and analyze the pressure and flow data in real time during all four injections. Data were collected via a serial connection to a data acquisition computer which was receiving data from the fracturing service company. For treatments where it was not directly measured, surface pressures were used by the wellbore model to estimate bottomhole pressure. The closure stress profile used for these analyses were the same as used for previous analyses of the four mini-fracs conducted in 1992 (CER and others, 1992). Similarly, the three-layer modulus model and leakoff properties are the same as for the 1992 tests. While model results were developed for all four injections, only those results for Mini-Frac No. 1-A are reported here.

Mini-Frac No. 1-A consisted of pumping 450 bbl of 40 ppg linear gel (circulated to the perforations before fracturing) in several stages and flushed with KCl water. The intermediate shut-ins were useful for matching fall-off behavior. Analysis of the first mini-frac benefited from the use of the bottomhole pressure data

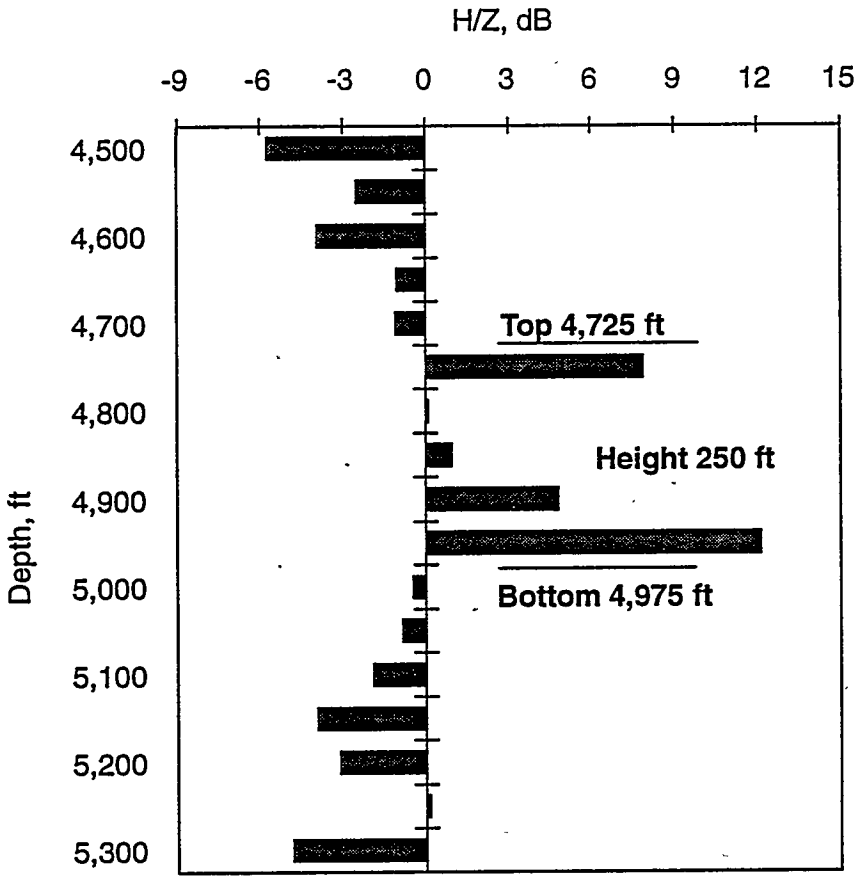

Figure 6 Fracture Height as Determined by H/Z Analysis

which was used to correlate the model pressures with the observed net. Two quick shutdowns also assisted in evaluating the degree of near-wellbore friction. The treatment data and net pressure match are shown in Figure 7. Perforation/tortuosity pressure losses were estimated to be approximately 150 psi at 26 BPM, which agrees with previous and subsequent injections. Figure 8, which shows a schematic of one wing of the fracture at shut-in, also shows the net pressure predicted by FRACPRO. Efficiency was estimated to be about 56 percent at shut-in. Fracture containment was minimal, and the resulting fracture geometry was estimated to be essentially radial.

Fracture Dimensions and Convective Processes Based on Tracer Investigations. A series of investigations employing radioactive (RA) tracers were undertaken as a part of Mini-Frac No. 4-A. The objectives of these tracer investigations were to 1) assess slurry convection processes which may redistribute the proppant; and 2) evaluate early and final proppant and frac fluid placement (frac height). The strategy used to achieve these investigative objectives involved three different short-lived RA tracers to tag each of the fracture treatment component (i.e., gelled frac fluid and the two stages of proppant) and monitor the location of these tracers in and around the wellbore using multiple logging surveys with gamma ray (GR) and spectral GR detector logging tools.

The observations of wellbore RA activity suggests that large-scale convection failed to

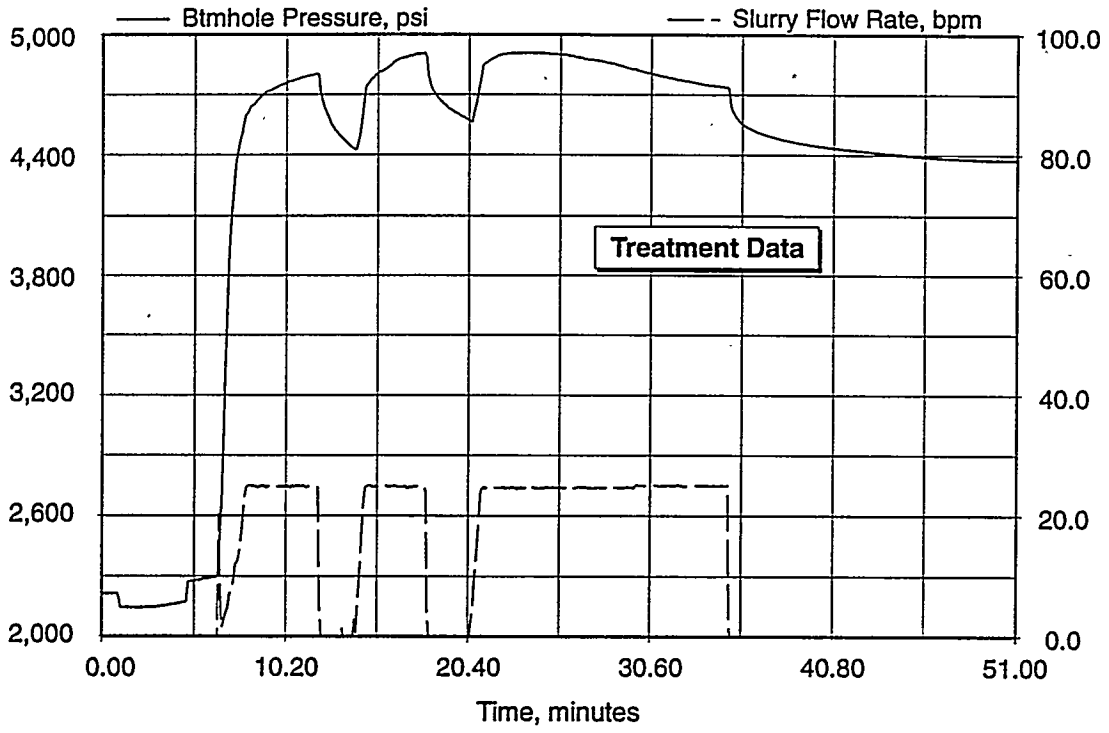

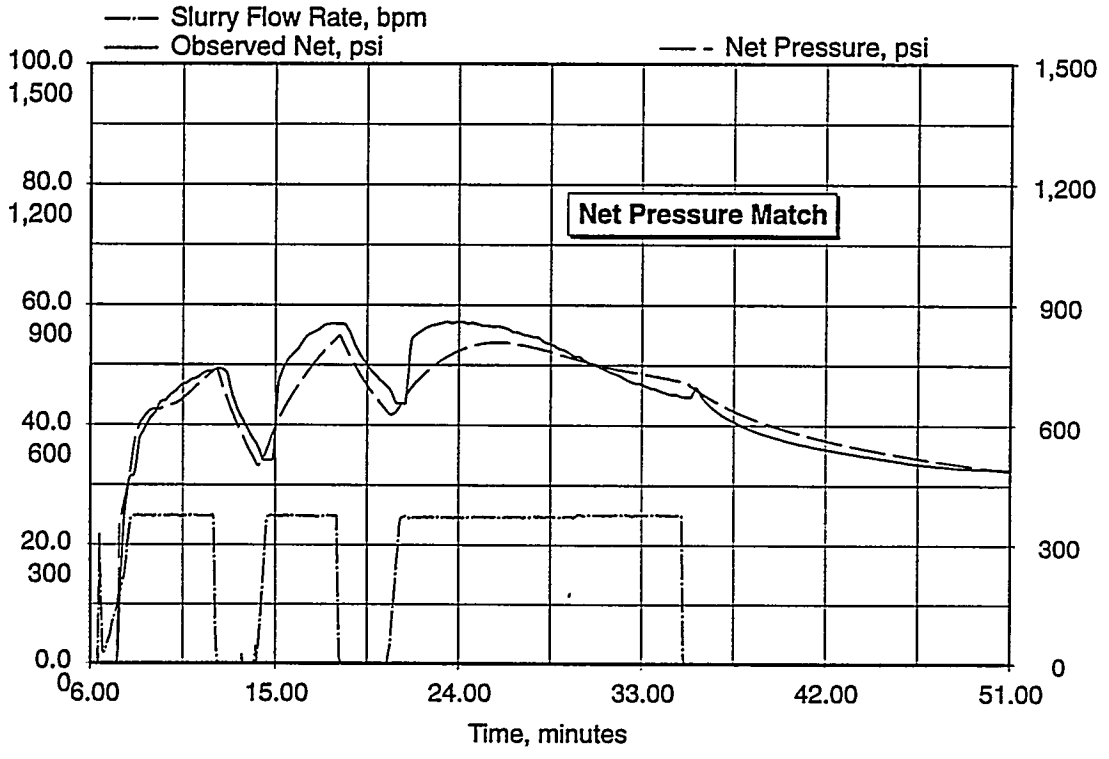

Figure 7 Treatment Data and Net Pressure Match from Mini-Frac No. 1-A

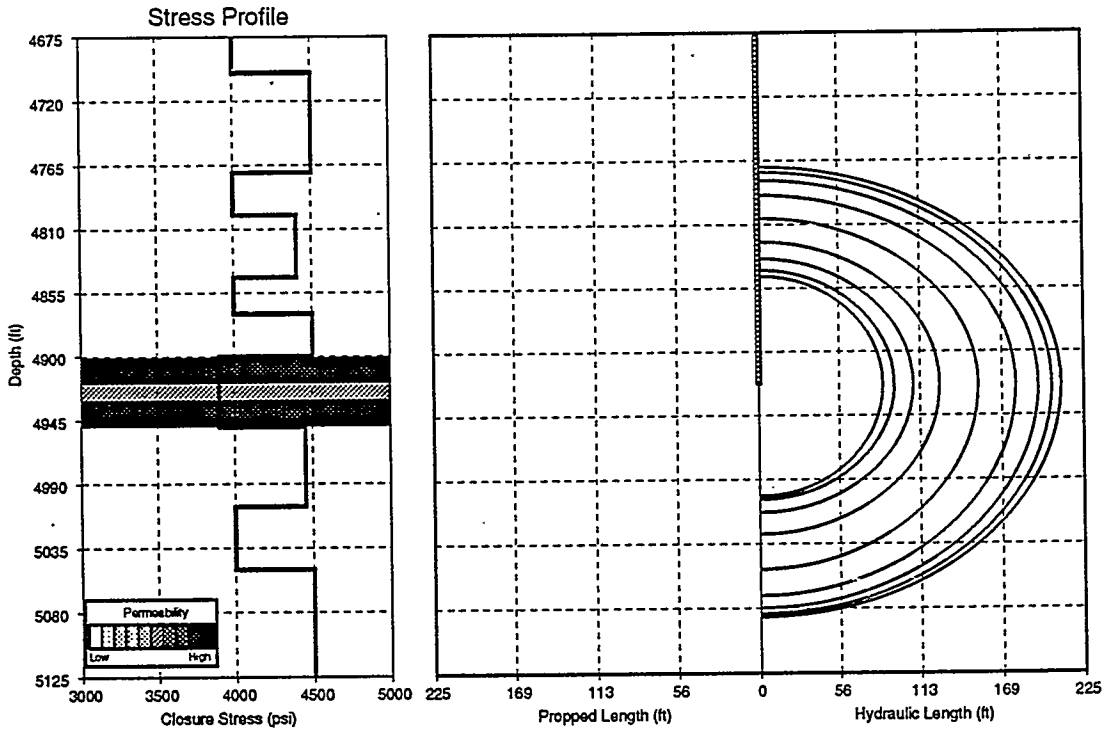

Figure 8 Mini-Frac No. 1 Geometry as Determined by 3-D Modeling

occur, at least not within the available open wellbore area or between the wellbore and frac. Although some of the RA material appears in the "rat hole" below the perfs, it may have been dragged there, viscously or otherwise, during the descent of the logging tool to bottom prior to initiating the actual GR surveys. Further, the quantities of RA found below the perfs are rather minor amounting to about 3 percent of the total wellbore activity. Had unimpeded density convection occurred in the wellbore, almost 200 ft of RA tagged slurry initially located above the base of the perfs could be expected to be found lying on the well bottom (±5,300 to 5,500 ft) after having displaced the less dense water. Although some loss of RA material from the wellbore is evident, these losses could easily be explained by fracture leakoff coupled with wellbore decompression; thus, these data and observations do not suggest any gross occurrence of convection and/or settling.

The first proppant stage (4,400 lb of 20/40 sand at 2 ppg) of Mini-Frac No. 4-A was tagged with the RA tracer ^{192}Ir. The second proppant stage (12,500 lb of 20/40 sand at 4 ppg) was tagged with ^{124}Sb. The 3,024 gal of x-linked gelled frac fluid that constituted the fluid stage of the 4 ppg slurry was tagged with ^{46}Sc. Spectral GR logging surveys then provided data regarding the spacial position of these three different tracers, thereby identifying the corresponding location of each stage of the fracturing treatment.

The final measured near-wellbore location of the second 4 ppg proppant stage and attendant frac gel fluid were defined during the post-frac spectral GR survey. It was noted earlier that the 4 ppg stage was tagged with ^{124}Sb while the x-link gel was tagged with ^{46}Sc and that these GR activity values represent those sources of activity located behind pipe. Activity values for the 4 ppg proppant stage are considerably diminished above

4,825 ft and below 5,050 ft, while activity from the x-link gel appears to fall off similarly below 5,050 ft but remains high up to the top of the survey at 4,750 ft. This suggests that the unpropped frac height may have grown above 4,750 ft.

To assist in defining propped frac height, the ^{124}Sb spectral activity was accumulated and then normalized. The results are as shown in Figure 9 where this normalized activity for the 4 ppg proppant stage is displayed as a function of depth. Propped frac height was then interpreted to correspond to a depth range of 4,800 to 5,010 ft.

Discussion of A Sand Experiment Results. The primary reasons for developing fracture diagnostic technology are 1) to optimize the fracture process by understanding fracture growth in a particular reservoir, and 2) to validate and improve fracture models. The first reason is not applicable at M-Site because there is no attempt to produce these reservoirs. The second objective is, however, of particular interest because of the wealth of high-quality data. With accurate bottomhole pressure measurement, the pressure history-match model runs have provided state-of-the-art calculations of fracture size.

Figure 10 shows a combined plot of the Mini-Frac No. 1-A (fluid only) fracture geometry as determined from 3D fracture modeling and the loci of microseismic events detected by the 4-level remote-well accelerometer array. For reference, the Mini-Frac No. 3-A (fluid only) fracture height as determined by H/Z seismic monitoring in the treatment well and the Propped Frac No. 4-A near-wellbore fracture height determined from GR logging of the RA-tagged proppant are also shown on the composite plot.

Mini-Frac 1-A, common to both the 3D fracture modeling and the microseismic event locations, has an obvious disagreement in the fracture wing symmetry. On one wing, the microseisms extend somewhat farther than the model predicts, and on the other wing, the measured fracture length is considerably less. Such asymmetry, however, is one facet of fracture growth that cannot be handled by any fracture model unless data on the stress or lithology factors that have limited the growth on one wing can be measured and factored into the models. If not for the asymmetry, it is likely that the calculated and measured wing lengths would have been reasonably close.

Upward fracture growth is one feature that found agreement between the 3D modeling and the microseismic event locations. Fracture growth downward found more of a difference between the diagnostics and the fracture model calculations. This discrepancy may have been due to any of four factors: 1) inaccurate stress data below the fracture; 2) inaccurate model prediction; 3) insufficient understanding of the correct interpretation of the microseismic data; or 4) inaccurate microseism locations due to layering.

Since only limited stress data were available around this sand, and those data were used to calibrate a sonic-based stress log, it is possible that high stress zones exist below the A Sand and were not detected or used for modeling purposes. Such high stress layers would have reduced fracture growth downward and brought the two techniques into agreement.

Drilling And Instrumentation Of Monitor Well No. 1

A significant accomplishment of the M-Site research program has been the emplacement of a comprehensive seismic and earth-tilt instrumentation array in a new well drilled on the M-Site location. The location of this well, in relation to the

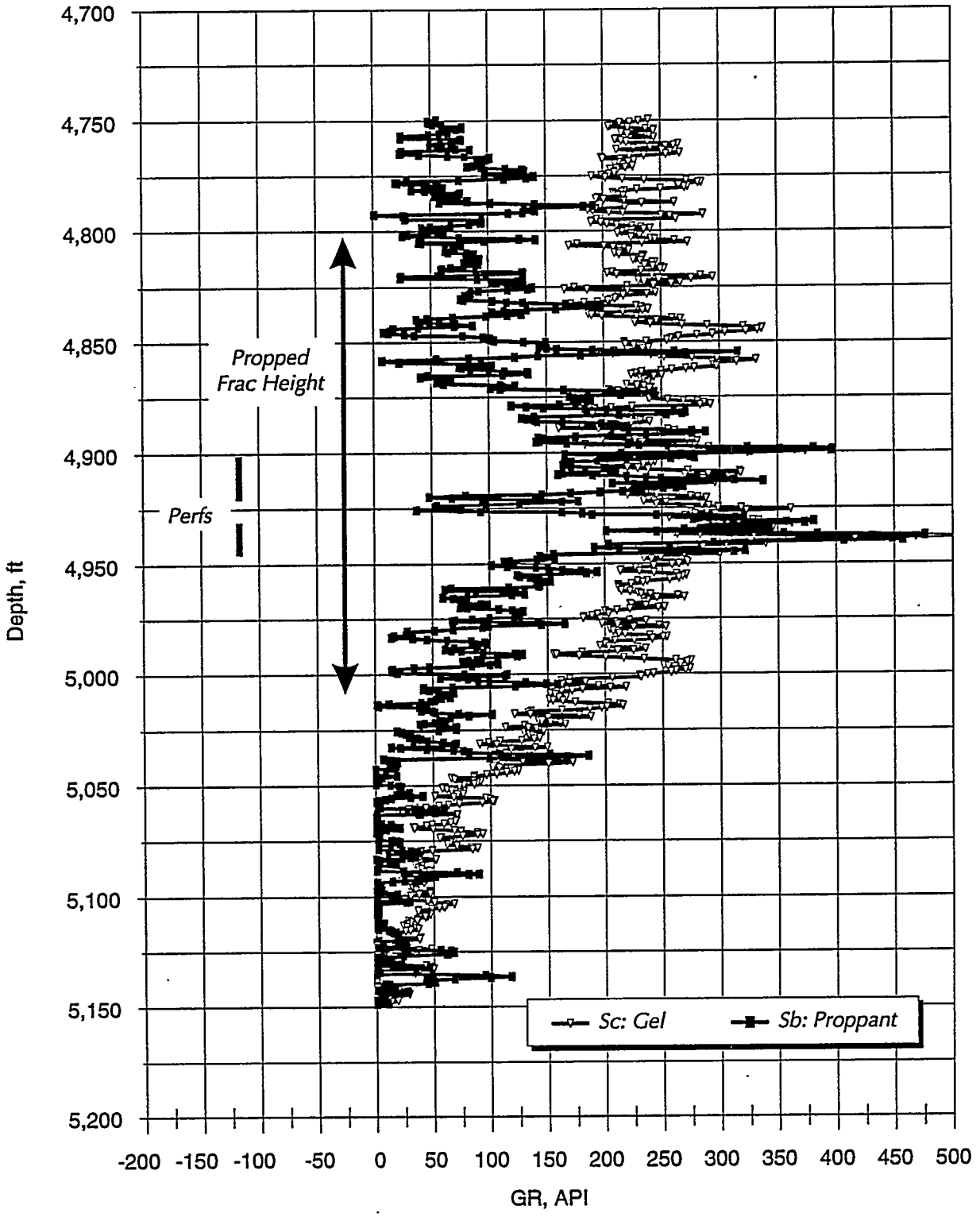

Figure 9 RA Activity for the 4ppg proppant Stage Showing Frac Height at the Wellbore

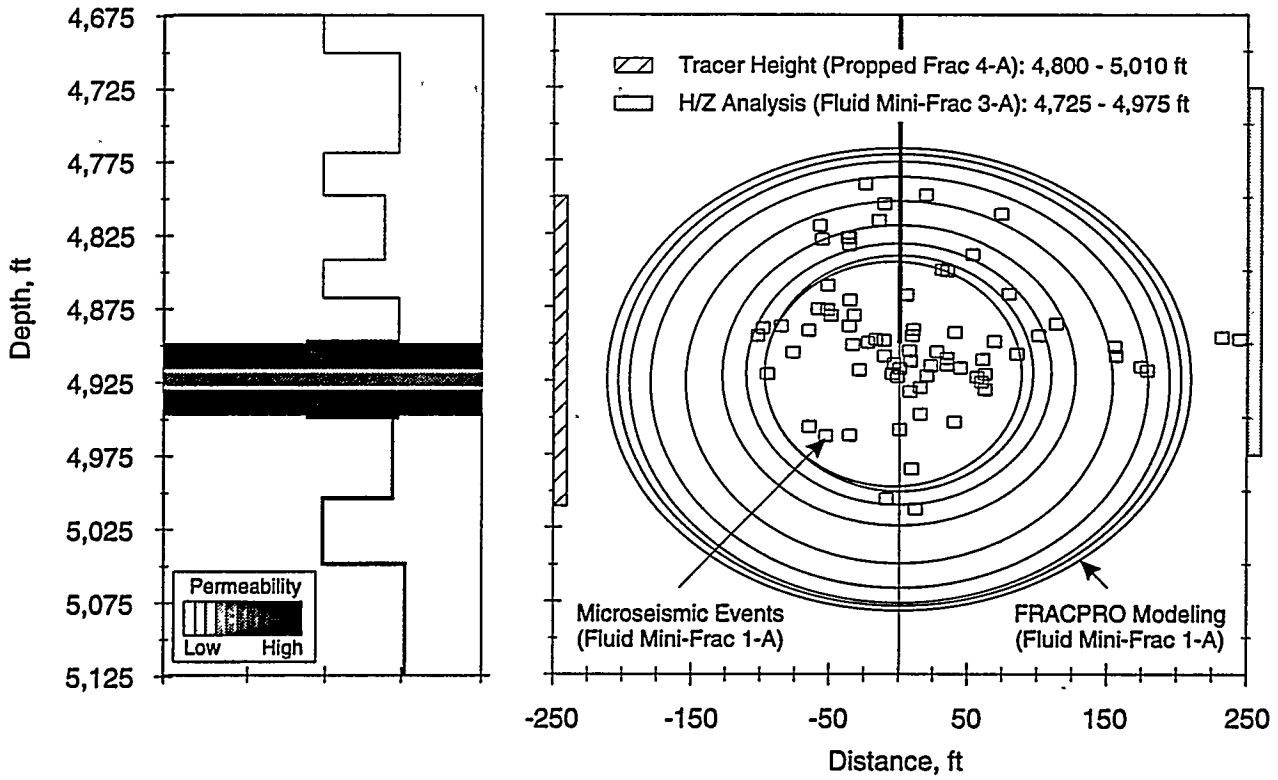

Figure 10 Composite Plot of the A Sand Fracture Geometry from all Available Techniques

MWX wells, is shown in Figure 11. The Monitor Well No. 1 was drilled in February and March 1994 to a total depth of 5,000 ft; 9-5/8-in. casing was subsequently run to TD and cemented to 2,120 ft (CER and others, 1995b). In the drilling phase of the Monitor Well, a focused dataset was acquired and used to further characterize the C and B Sand intervals. A total of 103 ft of core and log data were acquired for characterization of natural and induced fractures, assessment of reservoir fluids and porosities, and development of a mechanical properties/stress profile. These data were analyzed and used to confirm that the C and B sand intervals are thick and relatively homogenous, appear to be unfractured, have high water saturations, and have low permeability. Special core analyses (e.g., circumferential velocity analysis) were performed which indicate that the general stress orientation appears to be ESE-WNW which is in agreement with previous data from this site.

In October 1994, an instrumentation array composed of 30 accelerometers, 6 inclinometers and their respective cabling systems was secured to a tubing string and run in the wellbore to the approximate depth interval between 4,014 and 4,882 ft. The tubing and attached instrumentation cabling were cemented in place, thereby allowing comprehensive fracture diagnostics experiments to be implemented in the 1995 research program. Figure 12 illustrates the configuration of this instrumentation array.

FUTURE WORK

Field operations and experiments are planned for 1995 according to the project schedule shown in the Contract Information section. These experiments will be conducted using MWX-2 as the treatment well, MWX-3 as an observation well for wireline seismic instruments, and the Monitor Well No. 1 for acquisition of comprehensive

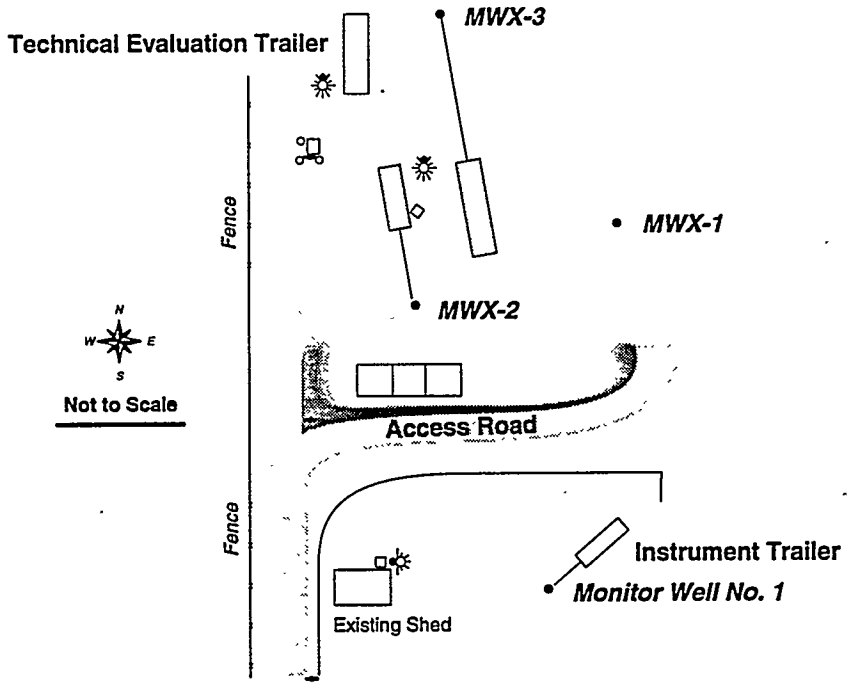

Figure 11 Location of Monitor Well No. 1 and the MWX Wells

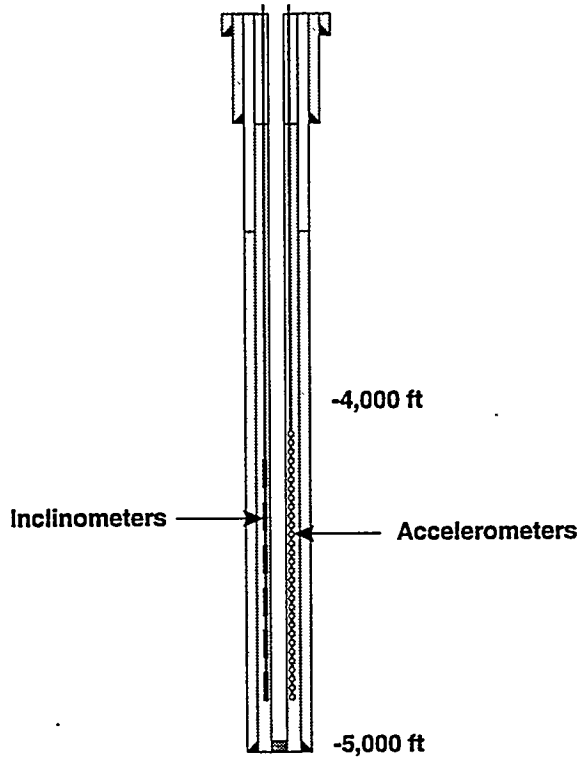

Figure 12 Configuration of the Monitor Well Instrumentation Array

seismic and earth-tilt data. The experiments planned to be conducted in 1995 are summarized as follows:

B Sand Experiments

The initial data acquisition activity to be performed in the B Sand interval will be a velocity survey to more completely characterize the seismic velocity structure in this interval. Subsequently, a series of fluid-only mini-fracs and a propped frac treatment will be executed to accomplish the following research objectives:

a) Acquire comprehensive seismic data during sequential hydraulic fracture treatments. These data will allow a comparison of seismic responses in un-fractured rock and re-fractured rock.

b) Compare fracture mapping results using redundant seismic instrumentation systems (30 level in Monitor Well, 5 level in MWX-3, 1 level in MWX-2) that will allow comparison of fracture mapping results.

c) Assess fracture opening and closure resulting from the mini-frac using the Monitor Well No. 1 inclinometers.

d) Pump multiple mini-frac treatments that are tagged with unique radioactive, chemical or color tags for assessment of multiple crack generation during the intersecting well phase of the project.

e) Acquire bottomhole pressure data for 3-D fracture modeling.

One of the potential seismic experiments to be conducted in the B Sand will be to map the extent of the shear-wave shadow. Shear-wave shadow experiments could be performed using MWX-3 for deployment of a downhole seismic source and the Monitor Well as the seismic-signal receiver well. Execution of this seismic experiment would provide additional interpretation of hydraulic fracture length and height. The last fracture treatment to be pumped in the B Sand would include proppant for additional fracture diagnostics experiments and for fracture technology research to be conducted in the next phase of the project.

B Sand Intersecting Well

The goal of this phase of the project is to a) drill a new wellbore which will intersect the propped hydraulic fracture created in the last B Sand injection; and b) perform hydraulic fracture conductivity tests between the treatment well and the intersection well. The goals of the intersecting well phase of the project are described as follows:

a) Verify hydraulic fracture orientation by coring through the hydraulic fracture at a known remote location and subsequent spectral gamma ray logging through the open-hole interval.

b) Determine if there are multiple fractures and re-create their generation through visual inspections of the core and RA tracer logging on recovered core.

c) Measure proppant distribution within a fracture by cutting and recovering core at several points across the plane of the fracture thereby allowing proppant concentrations to be assessed and compared to model-predicted values.

d) Measure conductivity within the fracture by injecting fluids in the treatment well and recovering them in the intersect well.

C Sand Intersecting Well

A second deviated wellbore is planned for the C Sand interval. This borehole, however, would

cut across the C Sand and would be in place *prior* to initiation of hydraulic fracture treatments in the C Sand. The intent of this experiment would be to 1) measure the hydraulic pressure at the leading edge of the fracture; 2) provide a direct indication of the horizontal growth rate of the fracture wing and, thus, provide comparisons of fracture length determined from seismic and net pressure calculations; and 3) provide estimates of fracture width. It is anticipated that emplacement of the C Sand wellbore will be accomplished in 1995 and that the experiments would be conducted in 1996.

REFERENCES

CER Corporation, Sandia National Laboratories, and Resources Engineering Systems, 1992: "Multi-Site Project Seismic Verification Experiment and Assessment of Site Suitability," GRI Topical Report No. GRI-93/0050 prepared under contract No. 5092-221-2130, February.

CER Corporation, Sandia National Laboratories, Resources Engineering Systems, Branagan & Associates, Fix & Associates, 1995a: "Results of Multi-Site Experimentation in the A-Sand Interval: Fracture Diagnostics, Fracture Modeling and Crosswell Tomography," GRI Topical Report No. GRI-95/0066, prepared under Contract No. 5093-221-2553, March.

CER Corporation, Sandia National Laboratories, Resources Engineering Systems, Branagan & Associates, Fix & Associates, 1995b: "GRI/DOE Multi-Sites Fracture Diagnostics Project: Monitor Well No. 1 Drilling, Data Analysis and Instrument Emplacement," GRI Topical Report No. GRI-95/0045 prepared under Contract No. 5093-221-2553, March.

7.7 Liquid-Free CO_2/Sand Fracturing in Low Permeability Reservoirs

CONTRACT INFORMATION

Contract Number	DE-AC21-90MC26025 Production Verification Tests
Contractor	Petroleum Consulting Services P. O. Box 35833 Canton, Ohio 44735 (216) 499-3823
Contractor Project Manager	Raymond L. Mazza
Principal Investigators	Raymond L. Mazza James B. Gehr
METC Project Manager	Albert B. Yost II
Period of Performance	May 5, 1990 to November 10, 1995

Schedule and Milestones

FY95/96 Program Schedule

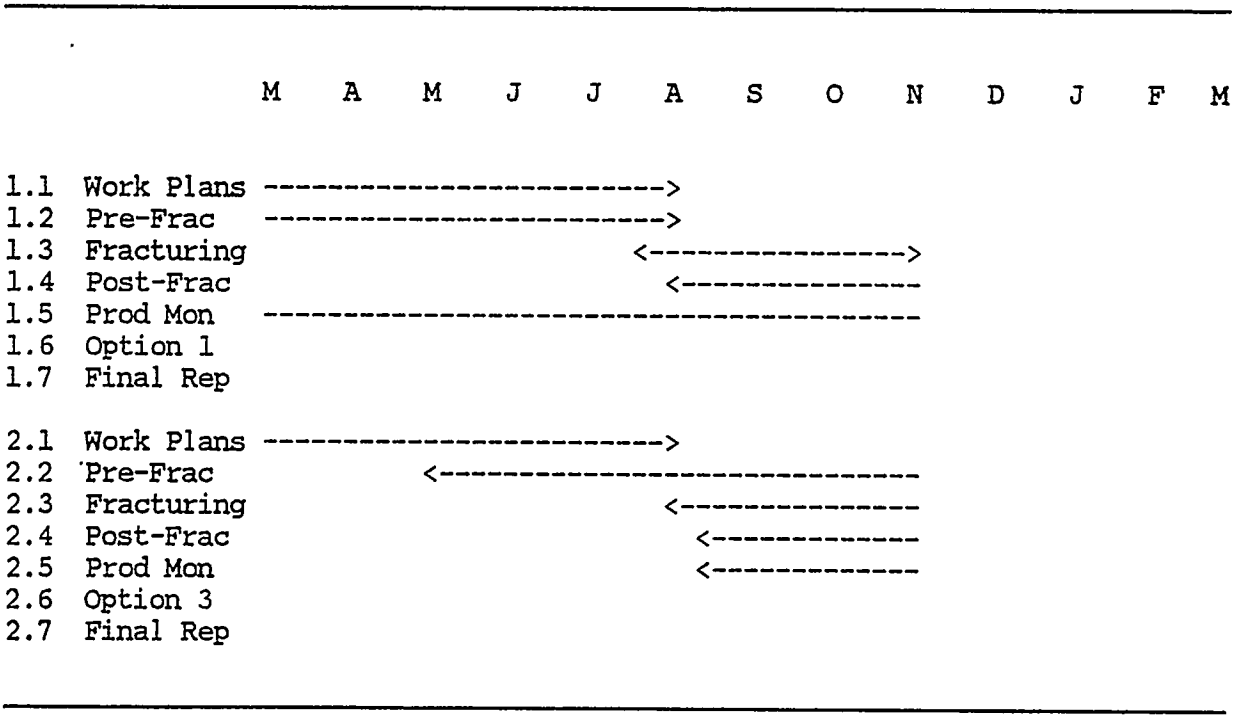

OBJECTIVES

* To demonstrate the effectiveness of a non-damaging liquid, carbon dioxide (CO_2) in creating sand-propped hydraulic fractures in "tight" gas bearing formations within the Appalachian Basin.

* To compare and rank the gas production responses from wells treated with liquid CO_2 with other types of treatments (shooting, water based, nitrogen, etc.).

BACKGROUND INFORMATION

From a historical perspective, discussion in the public literature concerning the application of sand fracturing with CO_2 first appeared in 1982. It was reported that over 40 liquid CO_2\sand treatments had been performed by American FracMaster in the U.S. by 1982. Early results were encouraging, but frac equipment was moved out of the U.S. shortly thereafter eliminating the opportunity for operators to continue to test the fracturing process in the U.S. Of those 40 treatments, 60 percent were successful in gas wells, 25 percent were successful in oil wells, and 15 percent were considered noncommercial. Concurrently, during the early 1980's, more than 40 frac treatments were performed in Canada using gelled liquid CO_2\sand fracs. Early test results indicated a 50 percent increase in production response. Laboratory research proceeded in 1983 toward evaluation of different proppant mesh sizes using a proprietary gelling agent that added viscosity to the liquid CO_2. Subsequently, the continued use of viscous chemicals was suspended in future jobs executed in Canada. Research continued on understanding the mechanics of the CO_2 fracturing process and development of a suitable way to improve the rheology of liquid CO_2. Hydrocarbon based gelling agents were tested that would yield over a 2 centipoise viscosity.

During 1985, numerical simulation models were developed for proppant transport that included flow turbulency and its effect on proppant settlement and pressures in the fracture. These numerical simulation models for CO_2\sand fracturing are quite different from conventional stimulation models.

During 1987, additional efforts were focused on a method to create viscosity in the presence of liquid CO_2, which resulted in the testing of a blend of high molecular weight fatty alcohol, a sorbitan fatty acid ester and diesel oil representing 2 percent by volume. This component was then combined with liquid CO_2 to create a viscous emulsion. A selective number of stimulations were performed in Canada using this emulsion system with mixed results. Shortly thereafter, the use of viscous agents was abandoned in favor of injecting proppant into 10 percent liquid CO_2. The obvious benefit was the elimination of residue and formation compatibility associated with the hydrocarbon-based viscous agents. By late 1987, it was reported that more than 450 100-percent liquid CO_2\sand fracs had been performed primarily in Canada. Over 95 percent of the wells were gas wells at depths less than 8200 feet with the largest sand volumes used at approximately 44 tons. Typical sand volumes pumped ranged from approximately 10 to 22 tons.

INTRODUCTION

Review of the literature indicated that the technology was available to the U.S. operators for a short period of time in the early 1980's but has since remained outside the U.S. and not available

as a commercial service inside the U.S. In an effort to re-introduce this technology to U.S. operators and test the effectiveness of this stimulation technique in various geologic settings, a contract was developed with Petroleum Consulting Services to stimulate and test up to 27 wells using the CO_2\sand fracturing methods in the Appalachian Basin.

WELL SELECTION CRITERIA

A candidate well selection methodology was developed to improve the confidence in comparing technology results in various geologic settings. As a minimum requirement, emphasis was placed on providing an established background of production data from control wells to which the production responses from the candidate wells would be compared and an assessment made.

The candidate well selection criteria includes--

1. That the wells are located in accepted areas of legitimate, cost-effective, gas production.

2. That sufficient nearby background production information is available to enable the results of the procedure to be evaluated.

3. That any sand be removed from the wellbore immediately following the stimulation.

4. That the wells be turned in line no later than 30 days after treatment, and that the merits of using this technology be measured from production responses into the pipeline rather than interrupting operator plans for production by conducting an elaborate welltesting effort and forecasting indirect indicators of response.

PROCEDURE - FIELD EQUIPMENT

Sand proppant is combined with liquid CO_2 in a pressurized blender to generate a sand/liquid CO_2 slurry. The blender is operated at a pressure of approximately 300 psi, and, as presently configured, can store up to 47,000 pounds of sand. It can develop CO_2\sand slurries with densities of up to 5 pounds per gallon at outputs of 55 barrels per minute.

The slurry is discharged directly into the suction side of conventional pump trucks which increase the sand-laden CO_2 slurry to wellhead treating pressures and inject it into the wells.

The liquid CO_2 is stored in two (2) 60-ton portable storage trailers which discharge directly into the blender. They are filled via 20-ton transport trailers prior to these treatments.

During the treatment, the CO_2 is displaced from the CO_2 storage vessels and into the blender with gaseous nitrogen, which allows a constant pressure to be maintained.

The sand concentration is monitored with a densimeter throughout the treatment and is adjusted to create the desired sand schedule.

Following the treatment, the well is flowed back on a choke. Care is exercised to allow the formation stresses to close on the sand pack and for the CO_2 to change to a gaseous phase. Flowbacks generally require two (2) to three (3) days immediately following the treatment.

JOB EXECUTION

To date, thirteen (13) wells have been stimulated, four (4) have been treated with CO_2\sand in two (2) stages. Eleven (11) wells are situated in eastern Kentucky and the other three (3) in western New York.

The three (3) Chautauqua County, New York wells were treated in the Silurian Age Whirlpool Sandstone, and turned in line in July, 1994. The operator has not furnished production data. The remaining wells were treated in the Devonian Shale. Six (6) wells were treated as single stage treatments and the remaining four (4) were treated with two (2) stage stimulations, as is the local practice.

The project, as originally proposed, included only single stage treatments but has been altered to accommodate local practices. These four (4) two (2) stage wells were compared with nearby wells which were hydraulically fractured with two (2) stages of either nitrogen gas and no proppant, or with nitrogen foam with proppant.

Fourteen (14) additional stimulations are planned in the Appalachian Basin over the next year. The treatment program has been temporarily delayed because the closed system blender necessary for these treatments has been unavailable for the past thirteen (13) months. Plans are underway to have a unit manufactured exclusively for U.S. operations and delivery is anticipated in July, 1995.

The concept of transporting sand in a closed pressure vessel has been under development outside the U.S. since 1981. Although the concept of hydraulic fracturing underground gas formations is not new, the equipment requirements have changed drastically over the years. The CO_2\sand fracturing process differs substantially from conventional treatments in that job execution requires a pressurized blender that can combine liquid CO_2 with proppants under pressure.

DISCUSSION

Stimulation Treatments

There were three (3) types of stimulation treatments involved in a fifteen (15) well 2-stage Devonian Shale study group. Four (4) wells were stimulated with CO_2\sand, seven (7) with nitrogen, and four (4) with nitrogen foam.

All fifteen (15) wells were stimulated with two (2) stages across the entire Devonian Shale interval to provide a common basis for comparison. The CO_2\sand candidate well locations were selected to be close to wells with other types of stimulation to provide a comparison of production responses between CO_2\sand treatments with those from other stimulation types.

The CO_2\sand stimulations in all four (4) involved 120 tons of CO_2 per stage and up to 47,500 pounds of sand.

One (1) of the four (4) wells, FH179, differed significantly from the other fourteen (14) wells in the study area group because of the apparent high stress state which resulted in high breakdown and treating pressures, limited ability to increase sand concentration, and later associated liquid production. The first stage treatment was aborted, and the interval was reperforated with fresh acid which was subsequently swabbed and replaced with another volume of fresh acid prior to reinitiating the first stage treatment. The second attempt at treating the first stage

also experienced high treating pressures, which limited the rate and sand volume. These behaviors were non-typical and considered to be the result of an anomalous geologic environment. The second stage responded similarly and a reduced sand volume was placed.

Sand volumes ranged from 35,000-47,500 pounds for the other six (6) treatment stages (three (3) wells) - averaging 43,300 pounds per stage. Maximum pump rates ranged from 44.6 to 53.5 barrels per minute, averaging 50.7. The pad volumes were all 100 barrels (19.2T) and the average sand concentrations ranged from 2.1 to 2.8 pounds per gallon, the maximum sand concentrations ranged from 4.0 to 5.2 pounds per gallon, averaging 4.7.

Nitrogen Gas

The nitrogen treatments were all executed at 100 Mscf per minute with a total of 1.0 MMcf per stage. There was no proppant conveyed.

Nitrogen Foam

The nitrogen foam treatments ranged from 75 to 90 quality and from 50,000 to 120,000 pounds of sand were placed.

PRODUCTION COMPARISON

The four (4) 2-stage CO_2\sand stimulated wells have been on production for sixteen (16) months. Cumulative production are compared on an individual group basis as well as a composite basis.

Production results from these fifteen (15) wells are compared and after sixteen (16) months of production, CO_2\sand fractured wells in the Pike County, Kentucky study area are nearly twice as productive as nitrogen gas fraced wells and greater than five (5) times better than the foam fraced wells in the study group. The per well incremental gas production after sixteen (16) months ranged from 21.9-33.1 MMcf for nitrogen gas and foam fraced wells, respectively.

CONCLUSIONS

1. After 16 months of production, CO_2\sand fractured wells in the Pike County, Kentucky, study area produce 2.0 times more gas than nitrogen gas treated wells and produce 21.9 MMcf additional gas per well.

2. After 16 months of production, CO_2\sand fractured wells in the Pike County, Kentucky, study area produce 4.4 times more gas than nitrogen foam treated wells and produce 33.1 MMcf additional gas per well.

3. For the Pike County, Kentucky, study area, payout times for the incremental cost of stimulation is estimated conservatively at less than 9 months.

4. Both groups of wells in the Pike County, Kentucky, study area show consistent relative production improvements compared to the overall study area results.

7.8 Advanced Drilling Systems Study

CONTRACT INFORMATION

Contract Number	DE-AC04-94AL85000
Contractor	Sandia National Laboratories P.O. Box 5800 Albuquerque, NM 87185-0419
Other Funding Sources	U. S. Department of Energy Geothermal Division EE-122 Energy Efficiency and Renewable Energy 1000 Independence Ave. Washington, DC 20585
Contractor Project Manager	James C. Dunn
Principal Investigators	Kenneth G. Pierce Billy J. Livesay, Livesay Consultants
METC Project Manager	Albert B. Yost II
Period of Performance	September 1994 to Spring 1995

INTRODUCTION

This work was initiated as part of the National Advanced Drilling and Excavation Technologies (NADET) Program. It is being performed through joint funding from the Department of Energy Geothermal Division and the Natural Gas Technology Branch, Morgantown Energy Technology Center.

Interest in advanced drilling systems is high. The Geothermal Division of the Department of Energy has initiated a multi-year effort in the development of advanced drilling systems; the National Research Council completed a study of drilling and excavation technologies last year; and the MIT Energy Laboratory recently submitted a proposal for a national initiative in advanced drilling and excavation research. The primary reasons for this interest are financial. Worldwide expenditures on oil and gas drilling approach $75 billion per year. Also, drilling and well completion account for 25% to 50% of the cost of producing electricity from geothermal energy. There is incentive to search for methods to reduce the cost of drilling.

Work on ideas to improve or replace rotary drilling technology dates back at least to the 1930's. There was a significant amount of work in this area in the 1960's and 1970's; and there has been some continued effort through the 1980's. Bill Maurer documented much of this effort in two books: *Novel Drilling Techniques*, published in 1968 (ref. 1), and *Advanced Drilling Techniques*, published in 1980 (ref. 2).

Undoubtedly there are concepts for advanced drilling systems that have yet to be studied; however, it is almost certain that new efforts to initiate work on advanced drilling systems will build on an idea or a variation of an idea that has already been investigated. Therefore, a review of previous efforts coupled with a characterization of viable advanced drilling systems and the current state of technology as it applies to those systems provide the basis for the current study of advanced drilling.

A SYSTEMS APPROACH

Nearly all studies of advanced drilling systems concentrate on methods of reducing rock. There is often little or no discussion of how these methods would fit into the full system necessary to drill, maintain, and complete a well. Unless the entire system is considered, much effort and money could be spent improving specific aspects of drilling technology only to discover that other facets of the problem prevent successful deployment of the system. Consequently, this study has not just investigated novel methods for reducing rock, but has examined all aspects of drilling systems necessary to make and complete a well.

Table 1 identifies six basic functions that must be performed by all drilling systems. The last function, preservation of the borehole, includes completion, i.e. casing and cement. This is not a necessary function in the sense that a well could be drilled without completion. However, completion is considered a basic function for two reasons:

1. Completion is necessary for a well to be of any use, and

2. Completion is a significant well cost.

In addition to the functions listed in Table 1, there are a number of constraints imposed on all viable drilling systems. For instance, environmental impact must be considered. The system footprint, any emissions to the local environment, and the control of hazardous materials cannot be ignored. Similarly, operational safety must be weighed. Also, all viable systems must be capable of directional control and must have some capability for sensing and communication with the operator. These constraints are summarized in Table 2.

Table 1. Basic Drilling Functions

- Transmission of energy to the system-rock interface
- Reduction of the rock
- Removal of the rock
- Maintenance of the borehole
- Control of formation fluids
- Preservation of the borehole

Table 2. Drilling System Constraints

- Environmental impact
- Operational safety
- Directional drilling and control
- Sensing and communication

While we have classified drilling systems according to cutting mechanism in this study, we have analyzed the systems according to how they perform the functions listed in Table 1 under the constraints given in Table 2.

STUDY GOALS

The purposes of this study are to provide information that will help policy makers and project managers make decisions concerning the development of advanced drilling systems, and to update the history and determine the current status of research in advanced drilling. To accomplish these purposes, the objectives listed in Table 3 have been identified.

Table 3. Study Objectives

- Provide system descriptions
- Estimate capital and operating costs
- Assess system performance
- Identify common problems
- Outline possible development programs

In addition to the basic description defined by the drilling functions and constraints, particular capabilities and advantages of various systems have been identified, and technical as well as financial limitations have been studied for each system.

The development of estimates of the capital and operating costs is ongoing. Estimating the cost of equipment that exists in concept only is an uncertain operation at best. However, much of the equipment associated with advanced drilling systems is common to current technology. This commonality will have the effect of reducing the uncertainty in the overall system cost estimates.

Performance assessment for most systems is difficult. The stage of development varies dramatically from concept to concept. There is little data, other than that collected in laboratory bench tests, associated with many of the concepts that are under consideration. It is neither easy nor accurate to extrapolate expected performance characteristics from such data. For many concepts, the best that can be done is an order-of-magnitude estimate of the expected rate-of-penetration (ROP). Performance assessment for some systems consists of an estimate of the necessary performance in order for the system to compete with current technology.

Because of the systems approach taken in this study, we have identified a number of problems and needs that are common to several advanced drilling systems. These are discussed later in this paper.

The last objective listed in Table 3 is to identify the technical problems and needs of the various concepts and assess the likelihood of successfully solving these problems.

STUDY PROGRESS

In consultation with the sponsors, we have determined the systems and concepts for study and have developed system descriptions. We have defined the equipment and material requirements for each system by function as well as by source (i.e. capital, rental, service, expendable).

We have also conducted a survey of the industry. The discussions in this survey consisted of one or more of the following topics:

1. Study direction and organization,

2. Previous work performed on advanced drilling in general or one of the concepts in particular, and

3. Ongoing efforts in the area of drilling research.

We have collected a significant amount data concerning the capital and operating costs associated with drilling. The analysis of these data is ongoing.

DRILLING CONCEPTS

Table 4 lists the concepts, sorted by cutting mechanism, that have been studied. This list was developed to cover the range from current technology, through ongoing efforts in drilling research, to highly speculative concepts. Included are cutting mechanisms that induce stress mechanically, hydraulically, and thermally.

The initial analyses of rig capital and operating costs indicate that it is not possible to build a new rig and operate at a profit given current rates. Rig rates today are artificially low

Table 4. Systems and Concepts: Sorted by Cutting Mechanism

- Baseline technology
- Emerging technology
- Rotary-assisted drilling
  - → jet-assist
  - → projectile-assist
  - → spark-assist
  - → thermal-assist (microwave)
- Mud hammer
- Thermal spallation jet
- High-pressure jet
  - → abrasive jet
- Spark
- Explosive
- Pulsed-laser water-jet
- Plasma arc
- E-beam
- Laser thermal
- Subterrene (rock melting)

due to excess equipment and low demand. Thus, it is necessary to estimate the true costs of current and emerging technology, and the resultant day rates, as a basis for equitable comparisons to the expected day rates of other systems.

Most, if not all, of the concepts listed in Table 4 will be familiar to anyone who has followed the efforts in the development of novel drilling systems. The only concept less than twenty years old is the pulsed-laser water-jet that is being developed by Powerpulse Systems of Lakewood, CO (ref. 3). An unusual aspect of this system is the use of the laser. We generally think of lasers as thermal sources. However, with this system, the laser is being used to impart a mechanical impulse to the rock.

Many of the concepts listed in Table 4 are currently being studied or developed. At least three companies; FlowDril in Kent, WA (refs. 4 through 9), Maurer Engineering in Houston, TX, and Drilling Technology in Plano, TX (refs. 10 and 11); are actively pursuing jet-assisted drilling. Tround International of Washington, DC, has an operational projectile-assisted drilling system (refs. 12 and 13). Both Tetra Corporation (ref. 14) in Albuquerque, NM, and the Twin Cities Research Center of the U.S. Bureau of Mines in Minneapolis, MN, are studying the use of spark discharge for reducing rock. The Twin Cities Research Center also has recently been active in the following areas:

1. The use of lasers for cutting kerfs,

2. The use of microwave energy to alter properties and aid the mechanical destruction of rock (ref. 15), and

3. The use of chemicals for modification of rock properties.

Novatek in Provo, UT, has an operational mud hammer (ref. 16). In conjunction with MIT, Los Alamos National Laboratory in Los Alamos, NM, has been studying thermal spallation under a full column of liquid (ref. 17). Los Alamos National Laboratory also has a program studying the use of a rock melting system for environmental drilling (ref. 18).

In addition to systems built around the rock-cutting mechanisms listed in Table 4, we have also looked at the capability of other approaches to reduce drilling costs. Included are underbalanced drilling, coiled tubing, reduced casing sizes, and chemical modification of rock properties.

COMMON PROBLEMS

This study has taken a systems approach to avoid overlooking some facet of the problem that would prevent successful deployment of the system. However, there has been another consequence of the systems approach: we have identified a number of common problems that run

across multiple systems. Table 5 lists some of these common problems and needs in two groups.

Table 5. Common Problems and Needs

- Multi-channel conduit (gas/liquid/electrical)
- Electric conduit downhole
- Maintenance of the borehole gage
- Controllable thruster/retractor/director for the drilling head

- Reduced rate-of-penetration with depth
- Well control and wellbore stability in the absence of liquids
- Methods to reduce the size of the surface system

The first group might be considered engineering problems; since, in many cases, technical solutions have been found, but these solutions have proven impractical. The second group is more fundamental in nature.

ENGINEERING PROBLEMS

A number of the systems under consideration require multiple conduits for the transmission of different fluids and/or electrical energy. Multi-conduit pipe can be manufactured. However, when compared to standard drill pipe, it is both heavy and expensive.

Problems with transmission of electrical energy downhole was one reason Sandia Laboratories quit working on spark drills twenty years ago. A number of systems would benefit from cheap and reliable methods to transmit electricity to the drill head. This is especially true of the high-energy systems listed in Table 4. Even rotary technology would benefit from such a development. A power cable would allow the use of electric motors as well as other tools that need electric power. A major impediment to the expansion of measurement-while-drilling systems is data transmission rate. The development of fast, reliable telemetry would allow not only the use of current downhole sensors such as pressure, temperature, and formation evaluation tools; but also the development and use of systems to evaluate the condition of the bit, to detect kicks almost instantaneously, and to provide data for real-time analyses of downhole conditions. An electric cable would provide the necessary transmission capability for diagnostic, look-ahead, and other smart sensors.

While no practical method has been developed to make electrical connections at each joint when using drill pipe, electric cables can be run in coiled tubing. Coiled tubing sizes to 3.5-inch OD are currently available with 4.5-inch to 5-inch tubing expected in the near future. However, because of fatigue strength limitations, coiled tubing for drill pipe is currently restricted to about 2.375-inch OD. This size limits fluid flow and, hence, maximum hole size. The use of coiled tubing also requires the use of a mud motor which significantly increases the cost of operations. The inability to turn from the surface results in other disadvantages for coiled tubing.

Maintenance of borehole gage is a concern for nearly all of the system concepts that are not rotary hybrids. For a given set of conditions, the diameter of the hole created with high-pressure jets and thermal systems will depend largely on the advance rate of the drilling head. There is a minimum hole diameter needed for running casing. Above this minimum, though, excessive variation will cause problems when cementing the casing.

A number of systems require some type of downhole mount for the drilling head. This mount needs to be capable of controlling both rate and direction of advance of the drilling head. As with other problems listed in Table 5, the development of such a device would not only solve problems for novel rock reduction mechanisms, but would also be beneficial to rotary cutting technology.

FUNDAMENTAL PROBLEMS

While studying past efforts to develop novel drilling concepts, we have discovered instances where engineers claim that programs were terminated at least partially because of reduced cutting effectiveness at depth. These instances include the efforts with spark drills at Sandia Laboratories, the efforts with mud hammers at Amoco, and the efforts with high-pressure jets at Exxon. This suggests that there is still a need for better understanding of the effects of depth and fluid pressure on rock properties as they apply to drilling. But more importantly, it is clear that a first step in the development of any new drilling system should be to test the performance of the concept at depth. There are facilities capable of independently simulating pore pressure, rock stress, and borehole fluid pressure at depth. Unconventional rock-cutting concepts should be tested at one of these facilities prior to the expenditure of significant resources on system development.

A number of the concepts listed in Table 4 are unable to operate under a full column of liquid. While cuttings can be removed with air, the absence of drilling mud greatly inhibits the ability to control formation fluids and maintain borehole stability. Thus the applicability of any system that cannot operate in the presence of drilling mud is greatly diminished. The development of concepts such as temporary borehole lining, casing-while-drilling, or other methods to control formation fluids and maintain borehole stability in the absence of drilling mud would increase the viability of many concepts.

The last item in Table 5, methods to reduce the size of the surface system, is rather deceptively worded. For a land-based rig, the capital investment in the surface system is on the order of ten-million dollars. Investigation of the surface system reveals that little of it is dependent on the way rock is cut.

The sizes and specifications for the mast, substructure, and drawworks are determined by the need to handle casing, not by how the rock is cut. The requirements of the mud pumps, pits, and mud-cleaning equipment are determined by the need to remove the cuttings, not by how the cuttings are produced. Eliminating rotary drilling could reduce the load on the diesel-electric generators. However, energy must be supplied in some form for any rock-cutting system.

About the only equipment that depends on how we cut rock is the bottom hole assembly. It is doubtful that any novel rock cutting mechanism will cost less than drill collars, stabilizers, and bits. Overall, it is unlikely that significant savings in materials and equipment can be achieved by simply changing the way we cut the rock.

Similar conclusions are reached when daily operational costs are considered. The numbers and skills of the crew are determined by the surface equipment. Rig insurance is determined by capital investment; liability insurance and workman's compensation costs are dependent on payroll. Fuel charges vary with energy consumption.

Reduction of drilling costs can occur only by changing the nature of the surface system or increasing the rate of penetration. Neither capital investment nor daily operational costs are significantly affected by the way we cut rock. Any increase in capital or operating costs must be offset by a commensurate increase in penetration rate. Unconventional rock-cutting mechanisms can reduce costs only if they can increase the rate of penetration.

CONCLUSIONS

This study of advanced drilling systems is ongoing. The discussion in this paper summarizes the efforts to date. We have investigated a number of drilling concepts from a systems

perspective. We have achieved some preliminary insights particularly concerning common problems and requirements.

Preliminary analyses indicate that little of the cost of drilling is due to the way we cut rock. A large part of the capital and operating costs associated with drilling are determined by the nature and size of the surface system. Changes to the surface system to reduce these costs will not only help novel cutting mechanisms, but will also reduce the cost of drilling with current cutting technology. In addition to reductions in surface system, increasing rate of penetration can also reduce overall well costs. Novel cutting mechanisms that dramatically increase the rate-of-penetration may be beneficial, especially in hard-rock drilling.

It is emphasized that the results and discussions presented here are preliminary. A final report will be issued after completion of the cost and performance analyses.

Note: Work performed at Sandia National Laboratories is supported by the U.S. Department of Energy under contract DE-AC04-94AL8500

REFERENCES

1. William C. Maurer, *Novel Drilling Techniques*, Pergamon Press, Library of Congress No. 68-17738, 1968

2. William C. Maurer, *Advanced Drilling Techniques*, Petroleum Publishing Company, Tulsa, OK, ISBN 0-87814-117-0, 1980

3. John G. Sellar, *Rock Excavation Using a Pulsing Laser-Water Jet*, report prepared for the EPRI Center for Materials Production, Pittsburgh, PA, CMP report number 93-7, November 1993

4. Jeff Littleton, editor, *Jet Drilling Technology Advances*, Drilling, November/December 1987

5. Rich McNally, associate editor, *Increasing Penetration Rates with High-Pressure Mud*, Petroleum Engineer International, December 1987

6. Mike Killalea, editor, *High Pressure Drilling System Triples ROPS, Stymies Bit Wear*, Drilling, March/April, 1989

7. T. Butler, P. Fontana, and R. Otta, FlowDril Corp., *A Method for Combined Jet and Mechanical Drilling*, SPE paper 20460, September 1990

8. Mike Cure, Grace Drilling Co., and Pete Fontana, FlowDril Corp., *Jet-Assisted Drilling Nears Commercial Use*, Oil & Gas Journal, March 11, 1991

9. J. J. Kolle, QUEST Integrated Inc., and R. Otta and D. L. Stang, FlowDril Corp., *Laboratory and Field Testing of an Ultra-High-Pressure, Jet-Assisted Drilling System*, SPE paper 22000, March 1991

10. Frank J. Schuh, *MultiCon™ Drilling System Potential*, Drilling Technology, Inc., Plano, TX, February 1994

11. Frank J. Schuh, *MultiCon™ Drilling System Economics*, Drilling Technology, Inc., Plano, TX, January 1995

12. Robert J. Regan, *Mining Cannon is a Real Rockbuster*, Iron Age, June 24, 1983

13. Allen Howland, *Machine Gun Bit Speeds Air Drilling*, Drilling Technology, August 1984

REFERENCES (cont)

14. William M. Moeny and James G. Small, *Focused Shock Spark Discharge Using Multiple Electrodes*, U.S. Patent #4,741,405, May 1988

15. D. P. Lindroth, W. R. Berglund, R. J. Morrell, and J. R. Blair, U. S . Bureau of Mines, Minneapolis, MN, *Microwave-Assisted Drilling in Hard Rock*, SME nonmeeting paper 91-224, Mining Engineering, September 1992

16. David S. Pixton, Yu Xiangguang, Vance I. Fryer, Steven J. Payne, David R. Hall, *A New Generation Mud Driven Rotary Percussion Tool: Summary of Current Research and Development Efforts*, Second Ed., Novatek, Provo, UT, February 1990

17. Worldrill Corporation, *Improvements in or Relating to Drilling with Centrifuge/Vortex Combustion Jet Spallation*, British and Foreign Patent Application, continuation of patent application PCT/GB94/00515

18. Sue J. Goff, Gilles Y. Bussod, Kenneth Wohletz, Aaron Dick, and John C. Rowley, *Rock Melting: A Specialty Drilling System for Improved Hole Stability in Geothermal Wells*, Los Alamos National Laboratory, Los Alamos, NM

Appendices

Appendix A

NATURAL GAS RD&D
CONTRACTORS REVIEW MEETING
April 4 - 6, 1995

Southern University
Baton Rouge, LA

TUESDAY, APRIL 4, 1995

8:00 a.m. REGISTRATION
F. G. Clark Activity Center

DOE/GRI/MMS NATURAL GAS ATLAS SERIES SEMINAR
F. G. Clark Activity Center

8:45 a.m. *Opening Remarks*
Harold D. Shoemaker

9:00 a.m. *Northern Gulf of Mexico Oil and Gas Atlas Seminar*
Steven J. Seni, Bureau of Economic Geology
University of Texas at Austin
Gary Lore, Mineral Management Service
U.S. Department of the Interior

12:00 p.m. LUNCH
Mayberry Dining Hall

SESSION 1 -- PLENARY SESSION
F.G. Clark Activity Center

Chairperson: Rodney D. Malone

1:30 p.m. 1.1 *Welcome*
William Moore
Southern University

1:50 p.m. 1.2 *Keynote Speaker*
Patricia Godley
Office of Fossil Energy

2:20 p.m. 1.3 *Natural Gas Technology Summary and Opening Remarks*
Thomas W. Keech
Morgantown Energy Technology Center

2:50 p.m.	1.4	*Gas Research Institute Gas Program Summary* Myron Gottlieb Gas Research Institute
3:20 p.m.		BREAK
3:35 p.m.	1.5	*Summary-Natural Gas Fuel Cells and Natural Gas Turbines* Rita Bajura Morgantown Energy Technology Center
4:05 p.m.	1.6	*Summary of Petroleum Technology Transfer Council Activities* Deborah Rowell Petroleum Technology Transfer Council
4:35 p.m.	1.7	*Summary of Department of Energy Oil Program* Betty Felber U.S. Department of Energy Bartlesville Project Office
5:05 p.m.		ADJOURN
5:30 p.m.		Social Mayberry Dining Hall Lawn
6:00-8:00 p.m.		Cajun Barbecue Mayberry Dining Hall Lawn

WEDNESDAY, APRIL 5, 1995

7:30 a.m. REGISTRATION
F. G. Clark Activity Center

Concurrent Session A - F. G. Clark Activity Center

SESSION 2A
RESOURCE & RESERVES -- Resource Characterization

Chairperson: Charles W. Byrer - Welcome Announcements

8:00 a.m.	2A.1	*Reserves in Western Basins* Mark Cocker The Scotia Group, Inc.

8:30 a.m. 2A.2 *Secondary Natural Gas Recovery--Infield Reserve Growth Joint-Venture: Applications in Mid-Continent Sandstones*
Robert J. Finley
Bureau of Economic Geology
The University of Texas at Austin

SESSION 3A
RESOURCE & RESERVES -- Modeling and Data Bases

Chairperson: Anthony M. Zammerilli

9:00 a.m. 3A.1 *Development of the Gas Systems Analysis Model (GSAM)*
Michael L. Godec
ICF Resources, Inc.

9:30 a.m. 3A.2 *Development of the DOE Gas Information System (GASIS)*
Robert H. Hugman
Energy and Environmental Analysis, Inc.

10:00 a.m. BREAK

SESSION 4A
LOW PERMEABILITY RESERVOIRS -- Low Permeability Reservoir Characterization

Chairperson: Karl-Heinz Frohne

10:15 a.m. 4A.1 *Multistrata Exploration and Production Study*
John Maestas
The College of West Virginia

10:45 a.m. 4A.2 *Brine Disposal Process for Morcinek Coal Mine*
H. Brandt
Aquatech Services, Inc.

11:15 a.m. 4A.3 *Geologic Analysis of Upper Cretaceous and Lower Tertiary Low-Permeability (Tight) Gas-Bearing Rocks in the Wind River Basin, Wyoming--A Prelude to an Estimate of In-Place Gas Resources*
Ronald C. Johnson
U.S. Geological Survey

11:45 a.m. 4A.4 *Geotechnology for Low Permeability Gas Reservoirs, 1995*
W. R. Wawersik
Sandia National Laboratories

12:15 p.m. LUNCH
Mayberry Dining Hall

SESSION 5A
LOW PERMEABILITY RESERVOIRS -- Natural Fracture Detection

Chairperson: Royal J. Watts

1:45 p.m. 5A.1 *LBL/Industry Heterogeneous Reservoir Performance Definition Project*
Ernest L. Majer and Jane C. S. Long
Lawrence Berkeley Laboratory

2:15 p.m. 5A.2 *Fracture Detection, Mapping, and Analysis of Naturally Fractured Gas Reservoirs Using Seismic Technology*
Heloise Lynn
Lynn, Inc.

2:45 p.m. 5A.3 *Naturally Fractured Tight Gas Reservoir Detection Optimization*
David Decker
Advanced Resources International, Inc.

3:15 p.m. BREAK

3:30 p.m. 5A.4 *Naturally Fractured Tight Gas Reservoir Detection Optimization*
Heloise Lynn
Lynn, Inc.

SESSION 6A
DRILLING, COMPLETION, AND STIMULATION

Chairperson: John R. Duda

4:00 p.m. 6A.1 *Development of a Near-Bit MWD System*
William J. McDonald
Maurer Engineering, Inc.

4:30 p.m. 6A.2 *Measurement-While-Drilling (MWD) Systems for Underbalanced Drilling*
William H. Harrison
Geoscience Electronics Corporation

5:00 p.m. ADJOURN

WEDNESDAY, APRIL 5, 1995

Concurrent Session B - Nursing School

SESSION 2B
NATURAL GAS UPGRADING -- Gas-to-Liquids Conversion

Chairperson - Rodney D. Malone

8:00 a.m.	2B.1	*Catalytic Conversion of Light Alkanes: Proof-of-Concept* James E. Lyons Sun Company, Inc.
8:30 a.m.	2B.2	*Selective Methane Oxidation Over Promoted Oxide Catalysts* Richard G. Herman Lehigh University
9:00 a.m.	2B.3	*Enhancement of Methane Conversion Using Electric Fields* Richard Mallinson University of Oklahoma
9:30 a.m.	2B.4	*Conversion Economics for Alaska North Slope Natural Gas* Charles P. Thomas Idaho National Engineering Laboratory
10:00 a.m.		BREAK
10:15 a.m.	2B.5	*Economics of Natural Gas Upgrading* John H. Hackworth K&M Engineering & Consulting
10:45 p.m.	2B.6	*An Overview of PETC's Gas-to-Liquids Technology R&D Program* Gary J. Stiegel/Arun C. Bose Pittsburgh Energy Technology Center

SESSION 3B

NATURAL GAS UPGRADING -- Low-Quality Natural Gas

Chairperson: Harold D. Shoemaker

11:15 a.m.	3B.1	*Upgrading Low-Quality Natural Gas by Means of Highly Performing Polymer Membranes* B. Krishnakumar Syracuse University
11:45 a.m.	3B.2	*Evaluation of High Efficiency Gas-Liquid Contactors for Natural Gas Processing* Dharam Punwani Institute of Gas Technology
12:15 p.m.		LUNCH Mayberry Dining Hall
1:45 p.m.	3B.3	*Membrane Processes for Separation of H_2S from Natural Gas* Kaaeid A. Lokhandwala Membrane Technology and Research, Inc.
2:15 p.m.	3B.4	*Low-Quality Natural Gas Sulfur Removal/Recovery* W. Jeffrey Cook Acrion Technologies, Inc.
2:45 p.m.	3B.5	*Microbially-Enhanced Redox Solution Reoxidation for Sweetening Sour Natural Gas* Martin Taylor Texas A&M University
3:15 p.m.		BREAK

SESSION 4B
NATURAL GAS STORAGE

Chairperson: Albert B. Yost, II

3:30 p.m.	4B.1	*Natural Gas Storage--End-User Interaction* Leonard R. Crook, Jr. ICF Resources, Inc.

4:00 p.m. 4B.2 *Field Verification of New and Novel Fracture Stimulation Technologies for the Revitalization of Existing Underground Gas Storage Wells; Project Description and Status (April 1995)*
Scott R. Reeves
Advanced Resources International, Inc.

4:30 p.m. 4B.3 *Underground Natural Gas Storage Reservoir Management*
Isaias Ortiz
United Energy Development Consultants, Inc.

5:00 p.m. ADJOURN

POSTER SESSION
Hilton Hotel "Le Grande" Salon

6:00 - 7:30 p.m.

P1 *Inorganic Polymer-Derived Ceramic Membranes*
Rakesh Sehgal
University of New Mexico

P2 *Atlas of Major Appalachian Basin Gas Plays*
Douglas G. Patchen
Appalachian Oil and Natural Gas Research Consortium

P3 *Atlas of Northern Gulf of Mexico Gas and Oil Reservoirs-- Chronostratigraphic Plays and Depositional Styles*
Steven J. Seni
Bureau of Economic Geology
The University of Texas at Austin

P4 *Natural Gas Supply SBIR Program*
Harold D. Shoemaker/William J. Gwilliam
Morgantown Energy Technology Center

P5 *Methodology for Optimizing the Development and Operation of Gas Storage Fields*
James C. Mercer, James R. Ammer and Thomas H. Mroz
Morgantown Energy Technology Center

P6 *The Synthesis and Characterization of New Iron Coordination Complexes Utilizing an Asymmetric Coordinating Chelate Ligand*
Bruce Watkins
Lawrence Livermore National Laboratory

P7 *GASIS Demonstration*
E. Harry Vidas/Robert H. Hugman
Energy and Environmental Analysis, Inc.
Harold D. Shoemaker
Morgantown Energy Technology Center

P8 *Development of the Gas Systems Analysis Model (GSAM)*
Alan B. Becker
ICF Resources, Inc.

P9 *Feasibility Study to Evaluate Plasma Quench Process for Natural Gas Conversion Applications*
Peter C. Kong and Brent A. Detering
Idaho National Engineering Laboratory
Lockheed Technologies, Inc.

P10 *Steady-State and Transient Catalytic Oxidation and Coupling of Methane*
Richard Borry
Lawrence Berkeley Laboratory

P11 *Thermoacoustic Natural Gas Liquefier*
Greg Swift
Los Alamos National Lab

P12 *Fractal Modeling of Natural Fracture Networks*
Martin V. Ferer
West Virginia University

P13 *Environmental Contractor's Posters (MSO)*
Thomas J. Kulp
Sandia National Laboratories

P14 *Zeolite Membranes for Gas Separations*
Yogeshwar V. Gokhale
University of Colorado at Boulder

THURSDAY, APRIL 6, 1995

7:30 a.m. REGISTRATION
F. G. Clark Activity Center

SESSION 7 -- DRILLING, COMPLETION, AND STIMULATION

Chairperson: John R. Duda - Welcome Announcements

8:00 a.m. 7.1 *Steerable Percussion Air Drilling System*
Huy D. Bui
Smith International, Inc.

8:30 a.m. 7.2 *Development and Testing of Underbalanced Drilling Products*
George H. Medley, Jr.
Maurer Engineering, Inc.

9:00 a.m. 7.3 *DOE/GRI Development and Testing of a Downhole Pump for Jet-Assist Drilling*
Scott D. Veenhuizen
FlowDril Corporation

9:30 a.m. 7.4 *Development and Testing of a High Power Slim-Hole Drilling System*
John H. Cohen
Maurer Engineering, Inc.

10:00 a.m. BREAK

10:15 a.m. 7.5 *Fracturing Fluid Characterization Facility (FFCF)*:
Recent Advances
Subhash N. Shah
University of Oklahoma

10:45 a.m. 7.6 *Application of Microseismic Technology to Hydraulic Fracture Diagnostics: GRI//DOE Field Fracturing Multi-Sites Project*
Richard E. Peterson
CER Corporation

11:15 a.m. 7.7 *Liquid-Free CO_2/Sand Fracturing in Low Permeability Reservoirs*
Raymond L. Mazza
Petroleum Consulting Services

11:45 a.m. 7.8 *Advanced Drilling Systems Study*
Kenneth G. Pierce
Sandia National Laboratories

12:15 p.m. ADJOURN

CONFERENCE EXHIBITS

E1 *Natural Gas Display*
Rodney D. Malone and Charles W. Byrer
Morgantown Energy Technology Center

E2 *Gas Exhibit*
Brian Gahan
Gas Research Institute

E3 *Gas Exhibit*
Gary Kapp
American Gas Association

E4 *Oil Exhibit*
Thomas Wesson
Bartlesville Project Office

E5 *METC Natural Gas and Fuel Cells Exhibit*
Rodney D. Malone
Morgantown Energy Technology Center

E6 *Bureau of Economic Geology (BEG)*
Robert J. Finley
The University of Texas at Austin

Meeting Participants

James N. Albright
Geoengineer/Group Leader
Los Alamos National Laboratory
P.O. Box 1663, EES-4, MS D443
Los Alamos, NM 87545
505-667-4318, (FAX) 505-667-8487
ALBRIGHT@LANL.GOV

Jon B. Anderson
Director of Marketing
UTD Incorporated
8560 Cinderbed Road
Suite 1300, P.O. Box 8560
Newington, VA 22122
703-339-0800, (FAX) 703-339-6519

Ralph Avellanet
Program Manager, Gas Processing
U.S. Department of Energy
1000 Independence Avenue, S.W.
FE-32, 3E-028
Washington, DC 20585
202-586-8499, (FAX) 202-586-6221

Rita A. Bajura
Associate Director, OPTM
U.S. DOE/METC
P.O. Box 880, MS B06
Morgantown, WV 26507-0880
304-285-4109, (FAX) 304-285-4292
RBAJUR@METC.DOE.GOV

Eric Batchelder
Geologist
Minerals Management Services
1201 Elmwood Park Boulevard
New Orleans, LA 70123-2394
504-736-2683, (FAX) 504-736-2905

C. Richard Bates
Geophysicist
Coleman Research Corporation
301 Commercial Road, #B
Golden, CO 80401
303-278-8700, (FAX) 303-278-0789

Thomas F. Bechtel
Director
U.S. DOE/METC
P.O. Box 880, MS C02
Morgantown, WV 26507-0880
304-285-4931, (FAX) 304-285-4292
TBECHT@METC.DOE.GOV

Al Becker
Senior Consultant
ICF Consulting
9300 Lee Highway
Fairfax, VA 22031
703-934-3860, (FAX) 703-691-3349

Robert Beham
Senior Geography Advisor
Conoco, Inc.
400 East Kaliste Saloom Road
LaFayette, LA 70508
318-269-3341

John H. Benton
Project Manager
Petroleum Technology Transfer
1801 Broadway, Suite 1120
Denver, CO 80202
303-293-9933, (FAX) 303-295-0065

Stephanie Bialobok
Consulting Geologist
Lourie Consultants
3924 Hadden Street
Metairie, LA 70002
504-887-5531, (FAX) 504-888-1994

Richard Borry
Graduate Student
University of California at Berkeley
201 Gilman Hall
Berkeley, CA 94720
510-642-6892, (FAX) 510-642-4778
RBORRY@VIOLET.BERKELEY.EDU

Ray M. Boswell
Geologist
EG&G/TSWV
P.O. Box 880, MS M06
Morgantown, WV 26507-0880
304-285-4541, (FAX) 304-285-4403
RBOSWE@METC.DOE.GOV

Kent A. Bowker
Area Manager
Chevron USA
P.O. Box 1635
Houston, TX 77251
713-754-7615, (FAX) 713-754-3891
KABO@CHEVRON.COM

Paul Branagan
Senior Scientist
Branagan & Associates
4341 Soria Way
Las Vegas, NV 89121
702-454-3394

Harry Brandt
Technical Director
Aquatech Services, Inc.
P.O. Box 946
Fair Oaks, CA 95628
916-723-5107, (FAX) 916-723-6709

Jerlene A. Bright
Director, DPDS
Dwight's Energy Data, Inc.
4350 Will Rogers Parkway, #207
Oklahoma City, OK 73108
405-948-4523, (FAX) 405-948-8619

Huy D. Bui
Project General Manager
Smith International, Inc.
16740 Hardy Street
Houston, TX 77032
713-233-5428, (FAX) 713-233-5205

Robert C. Burruss
Program Coordinator - Energy
U.S. Geological Survey
National Center, MS 915
Reston, VA 22092
703-648-6472, (FAX) 703-648-5464
BURRUSS@BPGSUV.CR.USGS.GOV

Talmage P. Bursh
Professor of Chemistry
Southern University
212 Lee Hall
Baton Rouge, LA 70813
504-771-3990, (FAX) 504-771-4722

Charles W. Byrer
Project Manager
U.S. DOE/METC
P.O. Box 880, MS E06
Morgantown, WV 26507-0880
304-285-4547, (FAX) 304-285-4469
CBYRER@METC.DOE.GOV

Robert H. Caldwell
Partner
The Scotia Group
4849 Greenville, Suite 1150
Dallas, TX 75206
214-987-1042, (FAX) 214-987-1047
76550.1241@COMPUSERVE.COM

Robert Chatelain
Manager
American Technologies, Inc.
1215 Avenue H, Suite 3
Westwego, LA 70118
504-348-7214, (FAX) 504-348-4107

Derald Chriss
Assistant Professor
Southern University
P.O. Box 10572
Baton Rouge, LA 70813
504-771-3990, (FAX) 504-771-4722

Mark Cocker
Vice President, Geology
The Scotia Group
4849 Greenville, Suite 1150
Dallas, TX 75206
214-987-1042, (FAX) 214-987-1047

John H. Cohen
Vice President
Maurer Engineering, Inc.
2916 West T. C. Jester
Houston, TX 77018-7098
713-683-8227, (FAX) 713-683-6418

Jeff Cook
Chemical Engineer
Acrion Technologies, Inc.
9099 Bank Street
Cleveland, OH 44125
216-573-1186, (FAX) 216-573-1186

Peter Cover
Director
Natural Gas Strategic Planning
U.S. Department of Energy
1000 Independence Avenue, S.W.
Washington, DC 20585
202-586-7297, (FAX) 202-586-1188

Alex Crawley
Program Coordinator
U.S. Department of Energy
P.O. Box 1398
Bartlesville, OK 74005
918-337-4406, (FAX) 918-337-4418

Leonard R. Crook
Vice President
ICF Consulting
9300 Lee Highway
Fairfax, VA 22031
703-934-3371, (FAX) 703-691-3349

A.S. Damle
Research Chemical Engineer
SRI International
333 Ravenswood Avenue
Menlo Park, CA 94025
415-859-5458, (FAX) 415-859-2813

David A. Damon
Research Manager
Consolidated Natural Gas
625 Liberty Avenue, 23rd Floor
Pittsburgh, PA 15222-3199
412-227-1464, (FAX) 412-456-7603
DADAMON@TELERAMA.LM.COM

Ken E. Davis
Principal Staff Consultant
Envirocorp Services and Tech.
7020 Portwest Drive, Suite 100
Houston, TX 77024
713-880-4640, (FAX) 713-880-3248

Bruce Dean
Research Assistant
West Virginia University
P.O. Box 6315
Physics Department
Morgantown, WV 26506-6315
304-293-3422, (FAX) 304-293-5732

David Decker
Vice President
Advanced Resources International
165 S. Union Boulevard
Denver, CO 80228
303-986-2121, (FAX) 303-986-8017

Brent A. Detering
Scientist
Idaho National Engineering Lab
P.O. Box 1625, MS 2210
Idaho Falls, ID 83415-2210
208-526-1720, (FAX) 208-526-0690
BAD@INEL.GOV

John R. Duda
Project Manager
U.S. DOE/METC
P.O. Box 880, MS E06
Morgantown, WV 26507-0880
304-285-4217, (FAX) 304-285-4469
JDUDA@METC.DOE.GOV

Eric R. Evitt
Director, New Technology
Catalytica, Inc.
430 Ferguson Drive
Mountain View, CA 94043
415-940-6330, (FAX) 415-968-7129

F. Farshad
Associate Professor
University of Southwestern LA
P.O. Box 44130
LaFayette, LA 70504-4130
318-482-5862, (FAX) 318-988-0119

Tim Fasnacht
Technology Manager
Gas Research Institute
8600 W. Bryn Mawr Avenue
Chicago, IL 60631
312-399-8221, (FAX) 312-399-4609
TFASNACH@GRI.ORG

Tom Fate
Project Manager
Gas Research Institute
8600 W. Bryn Mawr
Chicago, IL 60631
312-399-4601, (FAX) 312-399-4609
TFATE@GRI.ORG

Betty Felber
Program Coordinator
U.S. Department of Energy
P.O. Box 1398
Bartlesville, OK 74005
918-337-4400, (FAX) 918-337-4418

Martin V. Ferer
Professor of Physics
West Virginia University
P.O. Box 6315
Physics Department
Morgantown, WV 26506-6315
304-293-3422, (FAX) 304-293-5732
FERER@WVNVMS.WVNET.EDU

Robert J. Finley
Associate Director
Bureau of Economic Geology
Box X, University Station
Austin, TX 78713
512-471-1534, (FAX) 512-471-0140
FINLEYR@BEGV.BEG.UTEXAS.EDU

Robert L. Ford
Executive Director, C.E.E.S.
Southern University
Cottage 8, R. E. Smith Boulevard
Baton Rouge, LA 70813
504-771-4723, (FAX) 504-771-4722
ROBERT.FORD@EM.DOE.GOV

Raymond Fortuna
Program Manager, Geothermal Division
U.S. Department of Energy
1000 Independence Avenue, S.W.
EE-122
Washington, DC 20585
202-586-1711, (FAX) 202-586-8185

Christopher J. Freitas
Program Manager
U.S. Department of Energy
1000 Independence Avenue, S.W.
Room 3E028, FE-32
Washington, DC 20585
202-586-1657, (FAX) 202-586-6221
CHRISTOPHER.FREITAS@HQ.DOE.GOV

Karl-Heinz Frohne
Project Manager
U.S. DOE/METC
P.O. Box 880, MS E06
Morgantown, WV 26507-0880
304-285-4412, (FAX) 304-285-4403
KFROHN@METC.DOE.GOV

Brian Gahan
Technology Manager
Gas Research Institute
8600 W. Bryn Mawr Avenue
Chicago, IL 60631
312-399-5481, (FAX) 312-399-4609
BGAHAN@GRI.ORG

Daniel D. Gleitman
Program Manager
Sperry-Sun Drilling Services
3000 N. Sam Houston Parkway, E.
Houston, TX 77032
713-987-6146, (FAX) 713-987-5369

Michael L. Godec
Vice President
ICF Consulting
9300 Lee Highway
Fairfax, VA 22031-1207
703-934-3869, (FAX) 703-691-3349

Patricia Godley
Assistant Secretary, FE
U.S. Department of Energy
Office of Fossil Energy, FE-1
1000 Independence Avenue, S.W.
Washington, DC 20585
202-586-6660, (FAX) 202-586-7847

Yogeshwar V. Gokhale
Graduate Student
University of Colorado
Dept. of Chemical Engineering
Boulder, CO 80309-0424
303-492-7471, (FAX) 303-492-4341
GOKHALE@SPOT.COLORADO.EDU

Michael Gondouin
Executive Vice President
S-Cal Research Corporation
32 San Marino Drive
San Rafael, CA 94901
415-456-8237, (FAX) 415-456-8237

Myron Gottlieb
Vice President, Natural Gas Supply
Gas Research Institute
8600 W. Bryn Mawr Avenue
Chicago, IL 60631
312-399-8266, (FAX) 312-399-8170

Leonard E. Graham
Associate Director, TBD
U.S. DOE/METC
P.O. Box 880, MS E06
Morgantown, WV 26507-0880
304-285-4473, (FAX) 304-285-4292
LGRAHA@METC.DOE.GOV

Hugh D. Guthrie
Product Manager
U.S. DOE/METC
P.O. Box 880, MS B06
Morgantown, WV 26507-0880
304-285-4632, (FAX) 304-285-4469
HGUTHR@METC.DOE.GOV

W. J. (Bill) Gwilliam
Project Manager
U.S. DOE/METC
P.O. Box 880, MS E06
Morgantown, WV 26507-0880
304-285-4401, (FAX) 304-285-4403
WGWILL@METC.DOE.GOV

John Hackworth
Senior Associate
K&M Engineering & Consultants
583 Allegheny Avenue
Oakmont, PA 15139
412-826-1661, (FAX) 412-826-1662

Brian J. Harder
Research Engineer
Basin Research Institute
Louisiana State University
208 Howe Russell Geoscience
Baton Rouge, LA 70803-4101
504-388-8533, (FAX) 504-388-3662

William H. Harrison
Vice President
Geoscience Electronics Corporation
725-B Lakefield Road
Westlake Village, CA 91301
805-496-0300, (FAX) 805-495-1889
HARRISON@SPERRY-SUN.HOU.COM

Richard G. Herman
Principal Research Scientist
Lehigh University
Sinclair Laboratory
7 Asa Drive
Bethlehem, PA 18015
610-758-3486, (FAX) 610-758-6555
RGH1@LEHIGH.EDU

John L. Hill
Vice President
UTD Incorporated
8560 Cinderbed Road
Suite 1300, P.O. Box 8560
Newington, VA 22122
703-339-0800, (FAX) 703-339-6519

Barry Hoffman
Process Engineer
Mobil
13777 Midway Road
Dallas, TX 75244
214-851-8458, (FAX) 214-851-8349

Robert H. Hugman
Manager, Resources Analysis
Energy & Environ. Analysis
1655 N. Fort Myer Drive
Suite 600
Arlington, VA 22209
703-528-1900, (FAX) 703-528-5106

Shamsuddin Ilias
Assistant Professor
NC AT&T State University
Chemical Engineering Department
Greensboro, NC 27411
910-334-7564, (FAX) 910-334-7904
ILIAS@GARFIELD.NCAT.EDU

Chacko J. John
Director
Basin Research Institute
Louisiana State University
208 Howe Russell Geoscience
Baton Rouge, LA 70803-4101
504-388-8681, (FAX) 504-388-3662

Michael H. Johnson
Director of Research
Baker Hughes Inteq
P.O. Box 670968
Houston, TX 77073
713-625-4703, (FAX) 713-625-5703

Ronald C. Johnson
Geologist
U.S. Geological Survey
Box 25046, MS 939
Denver Federal Center
Denver, CO 80225-0046
303-236-5546, (FAX) 303-236-0459
RJOHNSON@SEDPROC.CR.USGS.GOV

Gary S. Kapp
Director, Sales and Marketing
American Gas Assoc. Labs
8501 E. Pleasant Valley Road
Independence, OH 44131
216-328-8111, (FAX) 216-328-8101

Thomas W. Keech
Division Director, Fuels Resources
U.S. DOE/METC
P.O. Box 880, MS D04
Morgantown, WV 26507-0880
304-285-4291, (FAX) 304-285-4403
TKEECH@METC.DOE.GOV

Stephen L. Kelly
Regional Manager
Envirocorp Services and Tech.
11800 Industriplex Boulevard
Suite 15
Baton Rouge, LA 70809
504-753-2561, (FAX) 504-751-5402

John R. Kleist
Technology Representative
Chevron Petroleum Tech. Company
1301 McKinney
Houston, TX 77010
713-754-7625, (FAX) 713-754-7631

Charles A. Komar
Staff Manager
U.S. DOE/METC
P.O. Box 880, MS B05
Morgantown, WV 26507-0880
304-285-4107, (FAX) 304-285-4403
CKOMAR@METC.DOE.GOV

Michael Koplow
Senior Consultant
Arthur D. Little, Inc.
Acorn Park
Cambridge, MA 02140-2390
617-498-6122, (FAX) 617-498-5000

B. Krishnakumar
Research Associate
Syracuse University
Chemical Engineering
320 Hinds Hall
Syracuse, NY 13244-1190
315-443-2557, (FAX) 315-443-2559
1JJANSEN@SUADMIN.SYR.EDU

Larry Kuehn
Process Engineer
Bovar Corporation
3130 Rogerdale, Suite 110
Houston, TX 77042
713-789-1084, (FAX) 713-789-0029

Damian Kulas
Mechanical Engineer
American Technologies, Inc.
1215 Avenue H, Suite 3
Westwego, LA 70118
504-348-7214, (FAX) 504-348-4107

Thomas J. Kulp
Senior Member Technical Staff
Sandia National Laboratories
P.O. Box 969, MS 9057
Livermore, CA 94551-0969
510-294-3676, (FAX) 510-294-2276

Vello Kuuskraa
President
Advanced Resources International
1110 N. Glebe Road, Suite 600
Arlington, VA 22201
703-528-8420, (FAX) 703-528-0439

William F. Lawson
Division Director, Tech. Base Program
U.S. DOE/METC
P.O. Box 880, MS B05
Morgantown, WV 26507-0880
304-285-4173, (FAX) 304-285-4403
WLAWSO@METC.DOE.GOV

James L. LeBlanc
Professor
University of Southwestern LA
P.O. Box 44690
LaFayette, LA 70504
318-482-6555, (FAX) 318-482-6688

Thomas T. Leuchtenburg
Group Manager, Government Relations
Gas Research Institute
1331 Pennsylvania Avenue, N.W.
Suite 730 N
Washington, DC 20004
202-662-8980, (FAX) 202-347-6925

B. J. Livesay
Consultant
Livesay Consultants
126 Countrywood Lane
Encinitas, CA 92024
619-436-1307, (FAX) 619-942-8375

Kaaeid Lokhandwala
Research Scientist
Membrane Technology and Research
1360 Willow Road, No. 103
Menlo Park, CA 94025
415-328-2228, (FAX) 415-328-6580

Jane C. S. Long
Department Head, Energy Resources
Lawrence Berkeley Laboratory
1 Cyclotron Road
Berkeley, CA 94720
510-486-6697, (FAX) 510-486-5686

John C. Lorenz
Senior Member Technical Staff
Sandia National Laboratories
Geotechnology Research
Division 6253
Albuquerque, NM 87185-5800
505-844-3695, (FAX) 505-844-7354

Heloise Lynn
Geophysicist/President
Lynn Incorporated
1646 Fall Valley Road
Houston, TX 77077
713-496-5358, (FAX) 713-497-6250

James E. Lyons
Senior Principal Scientist
Sun Company, Inc.
Research and Development Dept.
P.O. Box 1135
Marcus Hook, PA 19061
610-859-1731, (FAX) 610-859-5980

John R. Maestas
Vice President
Institutional Advancement
The College of West Virginia
P.O. Box AG
Beckley, WV 25802-2830
304-253-7351, (FAX) 304-253-3463

Ernest L. Majer
Department Head, Geosciences
Lawrence Berkeley Laboratory
University of California
1 Cyclotron Road, MS 50-E
Berkeley, CA 94720
510-486-6709, (FAX) 510-486-5686

Richard G. Mallinson
Chemical Engineer
University of Oklahoma
100 E. Boyd, Room T335
School of Chemical Engineering
Norman, OK 73019
405-325-4378, (FAX) 405-325-5813
RMALLINSON@UOKNOR.EDU

Rodney D. Malone
Project Manager
U.S. DOE/METC
P.O. Box 880
Morgantown, WV 26507-0880
304-599-1968, (FAX) 304-285-4403
RMALON@METC.DOE.GOV

Bernard Manowitz
Senior Chemical Engineer
Brookhaven National Laboratory
Building 801
Upton, NY 11973
516-282-2458, (FAX) 516-282-5526

David Marin
Geologist
Minerals Management Services
1201 Elmwood Park Boulevard
New Orleans, LA 70123
504-736-2671, (FAX) 504-736-2905

Kenneth E. Markel
Associate Director, OPM
U.S. DOE/METC
P.O. Box 880, MS D01
Morgantown, WV 26507-0880
304-285-4364, (FAX) 304-285-4292
KMARKE@METC.DOE.GOV

Alan (Jack) Marshall
Field Test Coordinator
Smith International, Inc.
Old Rt. 33, W. Mudlick Road
Route 3, Box 392
Buckhannon, WV 26201
304-472-2298, (FAX) 304-472-2332

Bobby Mayweather
President
BJM & Associates
2428 Germantown Drive
Baton Rouge, LA 70815
504-926-0432, (FAX) 504-771-4722

Ray Mazza
President
Petroleum Consulting Services
P.O. Box 35833
Canton, OH 44735
216-499-3823, (FAX) 216-499-2280

William J. McDonald
Executive Vice President
Maurer Engineering, Inc.
2916 West T. C. Jester
Houston, TX 77018-7098
713-683-8227, (FAX) 713-683-6418

K. Evans McIntyre, Jr.
Senior Geologist
Envirocorp Services and Tech.
11800 Industriplex Boulevard, Suite 15
Baton Rouge, LA 70809
504-753-2561, (FAX) 504-751-5402

George Medley
Senior Drilling Engineer
Maurer Engineering, Inc.
2916 West T. C. Jester
Houston, TX 77018-7098
713-683-8227, (FAX) 713-683-6418

Yuv R. Mehra
President
Advanced Extraction Tech
2 Northpoint Drive, Suite 820
Houston, TX 77060
713-447-0571, (FAX) 713-447-5601

Howard S. Meyer
Principal Technology Manager
Gas Research Institute
8600 West Bryn Avenue
Chicago, IL 60631-3562
312-399-8230, (FAX) 312-399-8170

Dodd Miller
Consultant
Westbay Instruments, Inc.
111 Woodhaven Lane
Seabrook, TX 77586
713-326-3267, (FAX) 713-326-5281

Robert L. Miller
Resource Manager
Southern University
Cottage 8, R. E. Smith Boulevard
Baton Rouge, LA 70813
504-771-4724, (FAX) 504-771-4722
ROBERT.MILLER@EM.DOE.GOV

Robert N. Miller
Senior Contract Manager
Air Products & Chemicals, Inc.
7201 Hamilton Boulevard
Allentown, PA 18195
610-481-4780, (FAX) 610-481-2576

William E. Moore
Vice Chancellor, Academic Affairs
Southern University
P.O. Box 9818
Baton Rouge, LA 70813
504-771-2360, (FAX) 504-774-9252

Thomas H. Mroz
Geologist
U.S. DOE/METC
P.O. Box 880, MS A04
Morgantown, WV 26507-0880
304-285-4071, (FAX) 304-285-4469
TMROZ@METC.DOE.GOV

Vito F. Nuccio
Geologist
U.S. Geological Survey
Box 25046, MS 939
Denver, CO 80225
303-236-1654, (FAX) 303-236-5734

Christian U. Okoye
Professor
University of Southwestern LA
Petroleum Engineering Department
P.O. Box 44690
LaFayette, LA 70504
318-482-6557, (FAX) 318-482-6688

Isaias Ortiz
President
UEDC
2301 Duss Avenue, Suite 12
Ambridge, PA 15003
412-266-8833, (FAX) 412-266-9002

R. Patrick Parsons
Consultant - P.E.
The College of West Virginia
P.O. Box AG
Beckley, WV 25802
304-253-7351, (FAX) 304-253-3463

Douglas G. Patchen
Program Coordinator
Appalachian Oil and Natural Gas
P.O. Box 6064
Morgantown, WV 26506-6064
304-293-2867, (FAX) 304-293-3749
U0A7E@WVNVM.WVNET.EDU

Gene D. Pauling
Petroleum Engineer
U.S. Department of Energy
Metairie Site Office
900 Commerce Road, E.
New Orleans, LA 70123
504-734-4131, (FAX) 504-734-4909

Lawrence J. Pekot
Principal Consultant
Scan Power, Inc.
11111 Wilcrest Green, Suite 250
Houston, TX 77042
713-260-7029, (FAX) 713-260-7199

Richard E. Peterson
Project Manager
CER Corporation
955 Grier Drive, Suite A
Las Vegas, NV 89119
702-361-2700, (FAX) 702-361-7653

Kenneth G. Pierce
Senior Member Technical Staff
Sandia National Laboratories
P.O. Box 5800, MS 0419
Albuquerque, NM 87185-0419
505-844-9176, (FAX) 505-844-9293

Dharam V. Punwani
Vice President, Technology Development
Institute of Gas Technology
1700 S. Mt. Prospect Road
Des Plaines, IL 60018
708-768-0523, (FAX) 708-768-0546
PUNWANI@IGT.ORG

Scott R. Reeves
Senior Project Manager
Advanced Resources International
1110 N. Glebe Road, Suite 600
Arlington, VA 22201
703-528-8420, (FAX) 703-528-0439

Herman H. Rieke
Professor and Department Head
University of Southwestern LA
P.O. Box 44690
LaFayette, LA 70504
318-482-6555, (FAX) 318-482-6688

Deborah Rowell
Executive Director
Petroleum Technology Transfer
1101 16th Street, N.W.
Suite 1-C
Washington, DC 20036-4803
202-785-2225, (FAX) 202-785-2240
DROWELL@PTTC.ORG

S. Phillip Salamy
Petroleum Engineer
BDM Oklahoma
220 N. Virginia Avenue
Bartlesville, OK 74003
918-337-4579, (FAX) 918-337-4365

Rakesh Sehgal
Research Assistant
University of New Mexico
Advanced Materials Lab
1001 University Boulevard, S.E.
Albuquerque, NM 87106
505-272-7135, (FAX) 505-272-7304
CN0GR8AA@UNM.EDU

Dominic Seneviratne
Application Programmer
Southern University
Cottage 8, R. E. Smith Boulevard
Baton Rouge, LA 70813
504-771-3723, (FAX) 504-771-4722

Steven J. Seni
Research Scientist
Bureau of Economic Geology
University of Texas at Austin
University Station, Box X
Austin, TX 78713
512-471-7721, (FAX) 512-471-0140
SENIS@BEGV.BEG.UTEXAS.EDU

Subhash N. Shah
Professor and Director, FFCF Project
University of Oklahoma
100 East Boyd, Room T301
Norman, OK 73019
405-325-1105, (FAX) 405-325-2958
SUBHASH@RMG.UOKNOR.EDU

Harold D. Shoemaker
Project Manager
U.S. DOE/METC
P.O. Box 880, MS E06
Morgantown, WV 26507-0880
304-285-4715, (FAX) 304-285-4469
HSHOEM@METC.DOE.GOV

Paul W. Smith
Senior Geologist
Dwight's Energy Data, Inc.
4350 Will Rogers Parkway, No. 207
Oklahoma City, OK 73108
405-948-4551, (FAX) 405-948-8619

Peet M. Soot
President
Northwest Fuel Development
4064 Orchard Drive
Lake Oswego, OR 97035
503-699-9836, (FAX) 503-699-9847

Peter S. Springer
Senior Analyst
Energy and Environ. Analysis
1655 N. Fort Myer Drive, Suite 600
Arlington, VA 22209
703-528-1900, (FAX) 703-528-5106

Gary J. Stiegel
Program Coordinator
Pittsburgh Energy Technology Center
P.O. Box 10940
Pittsburgh, PA 15236
412-892-4499, (FAX) 412-892-4604
STIEGEL@PETC.DOE.GOV

Elena Subia Melchert
Petroleum Engineer
U.S. Department of Energy
1000 Independence Avenue, S.W.
Washington, DC 20585
202-586-5095, (FAX) 202-586-6221
ELENA.MELCHERT@DOE.GOV

Gregory W. Swift
Technical Staff Member
Los Alamos National Laboratory
Mail Stop K764
Los Alamos, NM 87545
505-665-0640, (FAX) 505-665-7652
SWIFT@LANL.GOV

Martin Taylor
Research Assistant
Texas A&M University
Chemical and Natural Gas Engineering
Campus Box 193
Kingsville, TX 78363
512-595-2002, (FAX) 512-595-2106

Charles P. Thomas
Principal Engineer
Idaho National Engineering Lab
P.O. Box 1625, MS 2213
Idaho Falls, ID 83415-2213
208-526-0165, (FAX) 208-526-0603
CPT@INEL.GOV

Donald C. Thomas
Chemical Engineer
Independent
141 Valleybrook Circle
Hixson, TN 37343
615-842-7364, (FAX) 615-843-1591

Thomas A. Tremblay
Research Scientist Associate
Bureau of Economic Geology
University of Texas
Box X, University Station
Austin, TX 78713
512-471-1534, (FAX) 512-471-0140

Scott D. Veenhuizen
Senior Research Scientist
Flowdril Corporation
21414 68th Avenue, South
Kent, WA 98032
206-872-8500, (FAX) 206-872-9660

Bruce Watkins
Lawrence Livermore National Lab
P.O. Box 808, L-282
Livermore, CA 94550
510-423-5188, (FAX) 510-422-2382

Royal J. Watts
Project Manager
U.S. DOE/METC
P.O. Box 880, MS E06
Morgantown, WV 26507-0880
304-285-4218, (FAX) 304-285-4403
RWATTS@METC.DOE.GOV

Wolfgang R. Wawersik
Manager
Sandia National Laboratories
Geomechanics Department
P.O. Box 5800, MS 0751
Albuquerque, NM 87185
505-844-4342, (FAX) 505-844-7354
WRWAWER@SANDIA.GOV

Jing-Fong Wei
Associate Professor
Southern University
P.O. Box 10572
Baton Rouge, LA 70813
504-771-3990, (FAX) 504-771-4722

William W. Weiss
Field Petroleum Engineer
NM PRRC
NM Institute of Mining and Technology
Socorro, NM 87801
505-835-5220, (FAX) 505-835-6031
WEISS@BAERVAN.NMT.EDU

Donald E. Wicks
Executive Vice President
Advanced Resources International
165 S. Union Boulevard, Suite 800
Denver, CO 80228
303-986-2121, (FAX) 303-986-8017

Paul R. Wieber
Associate Director, Institutional Dev.
U.S. DOE/METC
P.O. Box 880, MS B05
Morgantown, WV 26507-0880
304-285-4544, (FAX) 304-285-4292
PWIEBE@DOE.METC.GOV

Aubrey Williams
Graduate Assistant
Southern University
P.O. Box 10572
Baton Rouge, LA 70813
504-771-3990, (FAX) 504-771-4722

Ching Wu
Professor
Texas A&M University
Petroleum Engineering Department
College Station, TX 77843-3116
409-845-8401, (FAX) 409-845-1307
WU@SPINDLETOP.TAMU.EDU

Albert B. Yost
Project Manager
U.S. DOE/METC
P.O. Box 880, MS E06
Morgantown, WV 26507-0880
304-285-4479, (FAX) 304-285-4469
AYOST@METC.DOE.GOV

Anthony Zammerilli
Petroleum Engineer
U.S. DOE/METC
P.O. Box 880, MS E06
Morgantown, WV 26507-0880
304-285-4641, (FAX) 304-285-4403
AZAMME@METC.DOE.GOV

Author Index

Organization Index

L

M

P

R

S

T

U

*U.S. Government Printing Office 1995 609-544

This cover stock is 30% post-consumer waste
and 30% pre-consumer waste, and is recyclable.